Volume 136 No. 5 Pp. 667–874

ANESTHESIOLOGY

MAY 2022

ANESTHESIOLOGY®
Trusted Evidence: Discovery to Practice®
2022
May

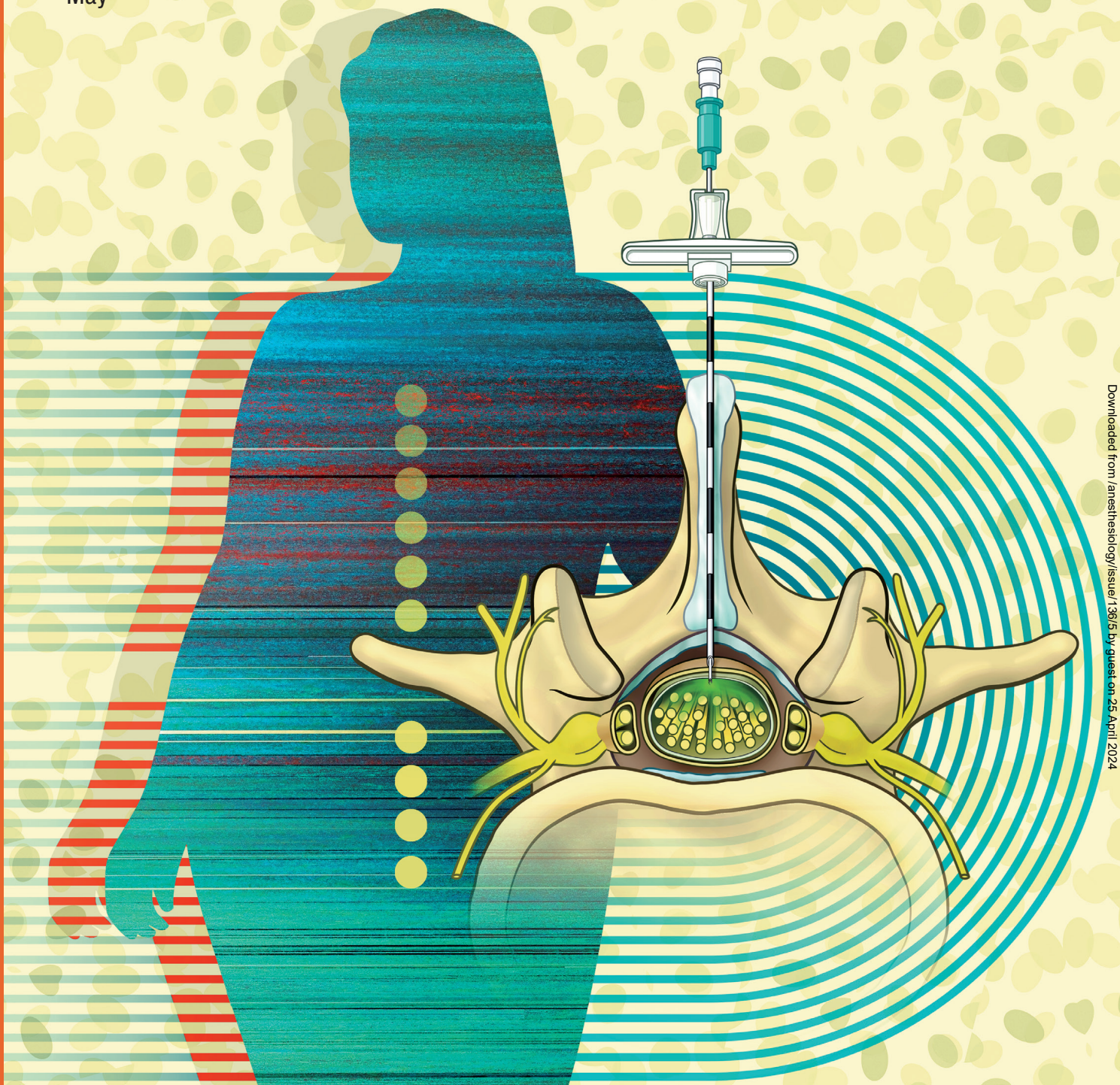

Quality of Labor Analgesia with Dural Puncture Epidural *versus* Standard Epidural Technique in Obese Parturients

Volume 136
Number 5
anesthesiology.org

The Official Journal of the American Society of Anesthesiologists

THIS MONTH IN ANESTHESIOLOGY

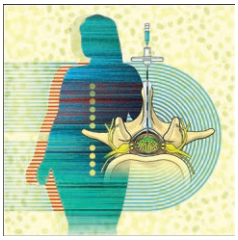

678 Quality of Labor Analgesia with Dural Puncture Epidural *versus* Standard Epidural Technique in Obese Parturients: A Double-blind Randomized Controlled Study

The dural puncture epidural analgesia technique for labor pain relief may offer advantages over the standard epidural technique by indirectly confirming correct identification of the epidural space and enhancing transfer of epidurally administered medications into the intrathecal space. Parturients who are obese have an increased risk of block failure and could benefit from these potential advantages. The hypothesis that the dural puncture epidural technique will be associated with improved quality of labor analgesia compared to the standard epidural technique was tested in a double-blind randomized controlled study of 132 obese parturients. The primary outcome was the quality of labor analgesia defined as a composite of five components, including asymmetrical block and epidural top-ups, the presence of one or more of which was considered positive for the outcome. The primary outcome was observed in 34 of 66 (52%) patients in the dural puncture epidural group and 32 of 66 (49%) patients in the standard epidural group, for an odds ratio (95% CI) of 1.1 (0.5 to 2.4) when adjusted for baseline characteristics. *See the accompanying Editorial on* ***page 667****. (Summary: M. J. Avram. Image: A. Johnson, Vivo Visuals Studio.)*

688 Self-reported Race/Ethnicity and Intraoperative Occult Hypoxemia: A Retrospective Cohort Study

Although measurement of blood oxygen saturation by pulse oximetry (Spo_2) is generally a reliable noninvasive measure of arterial oxygenation (Sao_2), skin pigmentation may interfere with its accuracy. The hypothesis that there is a greater prevalence of occult hypoxemia in patients whose self-reported race/ethnicity as a surrogate for skin pigmentation is other than White was tested in a retrospective study of 46,253 patients receiving an anesthetic, including at least one arterial blood gas measurement. Occult hypoxemia, defined as Sao_2 less than 88% despite Spo_2 more than 92%, was present in 2,016 of 151,070 (1.3%) paired Sao_2–Spo_2 readings. The prevalence of occult hypoxemia was 1.1% (791 of 70,722 paired readings) in Whites, 2.1% (339 of 16,011 paired readings) in Blacks, and 1.8% (383 of 21,223 paired readings) in Hispanics. The prevalence in Asians and Other race/ethnicity patients was similar to that of Whites. The odds ratio (95% CI) for occult hypoxemia relative to Whites was 1.44 (1.11 to 1.87) for Blacks and 1.31 (1.03 to 1.68) for Hispanics. *See the accompanying Editorial on* ***page 670****. (Summary: M. J. Avram. Image: Adobe Stock.)*

732 Extracorporeal Membrane Oxygenation for Respiratory Failure Related to COVID-19: A Nationwide Cohort Study

Extracorporeal membrane oxygenation (ECMO) support has been reported to improve both morbidity and mortality in severe acute respiratory distress syndrome (ARDS) patients. Severe manifestations of COVID-19 such as ARDS and acute myocardial injury suggest a possible role for ECMO support. This study determined in-hospital mortality of 429 patients in 47 centers in France with a diagnosis of COVID-19 supported by venovenous ECMO for respiratory failure with a minimum follow-up of 28 days after ECMO cannulation up to October 25, 2020. In-hospital mortality was 51% (219 of 429), with a median (interquartile range) follow-up of 49 days (33 to 70 days). Mortality at day 28 and at day 90 were 42% (180 of 429) and 60% (215 of 357), respectively. Variables associated with in-hospital mortality in multivariable analysis included older age, total bilirubin of 6.0 mg/dl or more at ECMO cannulation, and ventilation for more than 7 days before ECMO cannulation. The authors suggest venovenous ECMO support should be considered early within the first week of initiation of mechanical ventilation. *(Summary: M. J. Avram. Image: J. P. Rathmell.)*

697 Frequency and Risk Factors for Difficult Intubation in Women Undergoing General Anesthesia for Cesarean Delivery: A Multicenter Retrospective Cohort Analysis

Estimates of the frequencies of difficult and failed intubation in the obstetric population are several-fold higher than those reported for the general surgical population. The purpose of this retrospective study was to provide contemporary estimates of the frequencies of difficult and failed intubation in women undergoing general anesthesia for cesarean delivery in the United States between 2004 and 2019 using data from 45 Multicenter Perioperative Outcomes Group sites. Difficult intubation was defined as difficult laryngoscopy (Cormack-Lehane view of 3 or more), three or more intubation attempts, flexible scope intubation after failed laryngoscopy, rescue supraglottic airway, or surgical airway. Failed intubation was defined as any attempt at intubation without successful endotracheal tube placement. Difficult intubation was identified in 295 of 14,537 cases (2.0% [95% CI, 1.8 to 2.3%]) and there were 18 cases of failed intubation (0.1% [95% CI, 0.1 to 0.2%]). Most factors strongly associated with difficult intubation were nonobstetric in nature and were related to patient or airway characteristics. *(Summary: M. J. Avram. Image: J. P. Rathmell.)*

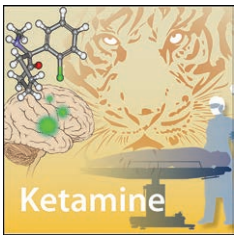

792 Ketamine Psychedelic and Antinociceptive Effects Are Connected

Ketamine produces analgesia as well as psychedelic effects related to its dissociative properties at subanesthetic doses. It has been suggested that ketamine analgesia may be generated by its dissociative effects, although there is evidence that suggests the two endpoints are independent and not connected. This was a planned secondary analysis of a study in which subjects received increasing doses of racemic ketamine and S-ketamine on different occasions and were tested for pain relief to a pressure pain stimulus and alterations in perception of external stimuli, a measure of psychotropic effect. A population pharmacokinetic–pharmacodynamic model and was developed to describe the relationship between effect site concentrations of S- and R-ketamine and their norketamine metabolites and pressure pain threshold and change in external perception. The pharmacodynamics of S-ketamine did not differ for antinociception and external perception, which had the same potency parameter (C50) and plasma-effect site equilibration half-time whether administered as racemic ketamine or S-ketamine. R-ketamine did not contribute to either endpoint while S-norketamine had a small antagonistic effect for both endpoints. *See the accompanying Editorial on* ***page 675****. (Summary: M. J. Avram. Image: A. Johnson, Vivo Visuals Studio.)*

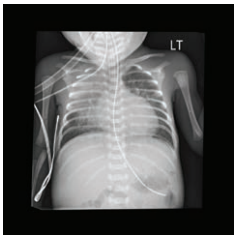

749 Early Restrictive Fluid Strategy Impairs the Diaphragm Force in Lambs with Acute Respiratory Distress Syndrome

Critical illness–associated diaphragm weakness develops in most mechanically ventilated critically ill patients. The hypothesis that a liberal fluid strategy induces diaphragm muscle fiber edema leading to a reduction in diaphragmatic force-generating capacity was tested in 19 female lambs with experimental pediatric acute respiratory distress syndrome (ARDS). The animals were randomized to receive either a restrictive (60 ml/kg per day) or liberal (120 ml/kg per day) fluid regime throughout a 6-h period of mechanical ventilation. Contrary to the hypothesis, a liberal fluid regimen did not lead to diaphragm muscle fiber edema and early fluid restriction decreased the force generating capacity of the diaphragm. The estimated marginal mean (95% CI) decreases in the pressure generating capacity of the diaphragm during application of 5 cmH_2O positive end-expiratory pressure (PEEP) and 10 cmH_2O PEEP after 6 h of mechanical ventilation were –9.6 cmH_2O (–14.4 to –4.8 cmH_2O) and –10.3 cmH_2O (–15.2 to –5.4 cmH_2O), respectively, in the restrictive group, and –0.8 cmH_2O (–5.8 to 4.3 cmH_2O) and –2.8 cmH_2O (–8.0 to 2.3 cmH_2O), respectively, in the liberal group. *See the accompanying Editorial on* ***page 672****. (Summary: M. J. Avram. Image: J. P. Rathmell.)*

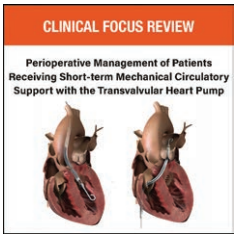

829 Perioperative Management of Patients Receiving Short-term Mechanical Circulatory Support with the Transvalvular Heart Pump (Clinical Focus Review)

The first line treatment for cardiogenic shock includes optimization of volume status and administration of vasopressors and inotropic medications. However, medical therapy alone may not provide adequate circulatory support and may increase myocardial oxygen consumption. When medical therapy alone does not provide adequate circulatory support, short-term mechanical circulatory support, such as that provided by the transvalvular heart pump, should be considered. The transvalvular heart pump can augment systemic blood flow while reducing myocardial oxygen consumption. The present review provides anesthesiologists with an overview of the transvalvular heart pump, including its mechanics and hemodynamic effects, as well as considerations for perioperative management for device placement and initial optimization to allow them to provide optimal patient care and contribute to the perioperative decision-making process. It also discusses the timing and management of weaning from transvalvular heart pump support and subsequent pump explantation. An overview of major studies evaluating transvalvular heart pump use in cardiogenic shock is provided. *(Summary: M. J. Avram. Image: From original article.)*

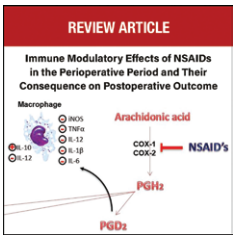

843 Immune Modulatory Effects of Nonsteroidal Anti-inflammatory Drugs in the Perioperative Period and Their Consequence on Postoperative Outcome (Review Article)

Nonsteroidal anti-inflammatory drugs (NSAIDs) inhibit cyclooxygenase-1 and -2, key enzymes involved in prostaglandin synthesis, to varying degrees thereby producing analgesia, antipyresis, and immune modulation. They are administered in the perioperative period to facilitate pain management but may affect postoperative outcomes in beneficial or harmful ways due to their effects on the inflammatory response elicited by surgery. This narrative review evaluates the evidence available from *in vitro* studies and randomized controlled animal and human trials, systematic reviews, and meta-analyses of potential immune system-related consequences of perioperative NSAID administration. These include effects on systemic inflammatory response syndrome (SIRS), acute respiratory distress syndrome (ARDS), immediate and persistent postoperative pain, oncological and neurological outcome, and wound, anastomotic, and bone healing. It concludes that NSAIDs have been shown to have immune modulatory effects in cellular and animal models and affect various outcomes in these models but the immune modulatory effects of these drugs on perioperative outcomes in clinical studies are much less clear. *(Summary: M. J. Avram. Image: From original article.)*

 DOI: 10.1097/ALN.0000000000004210

TABLE OF CONTENTS

ANESTHESIOLOGY

Volume 136
Issue 5
May 2022

◇ *Refers to This Month in ANESTHESIOLOGY*
◆ *Refers to Editorial*
This article has an Audio Podcast
See Supplemental Digital Content
CME Article
This article has a Video Abstract
Readers' Toolbox
This article has a Visual Abstract
OPEN *This article is Open Access*

ON THE COVER: The dural puncture epidural technique may improve analgesia quality by confirming midline placement and increasing intrathecal translocation of epidural medications. This would be advantageous in obese parturients with increased risk of block failure. In this issue of ANESTHESIOLOGY, Tan *et al.* test the hypothesis that quality of labor analgesia will be improved with dural puncture epidural compared to standard epidural technique in obese parturients. In an accompanying editorial, Segal and Pan describe the evolution of the dural puncture epidural technique and conclude that the overall impact of this technique on the quality of labor analgesia is modest at best. Cover Illustration: A. Johnson, Vivo Visuals Studio.

- Tan *et al.*: Quality of Labor Analgesia with Dural Puncture Epidural *versus* Standard Epidural Technique in Obese Parturients: A Double-blind Randomized Controlled Study, p. 678
- Segal and Pan: Dural Puncture Epidural for Labor Analgesia: Is It Really an Improvement over Conventional Labor Epidural Analgesia? p. 667

ANESTHESIOLOGY (ISSN 0003-3022) is published monthly by Wolters Kluwer Health, Inc., 1800 Dual Highway, Suite 201, Hagerstown, MD 21740-6636. Periodicals postage paid at Hagerstown, MD, and at additional mailing offices. Postmaster: Send address changes to ANESTHESIOLOGY, P.O. BOX 1610, Hagerstown, MD 21740.

body mass index, Mallampati score III or IV, small hyoid-to-mentum distance, limited jaw protrusion, limited mouth opening, and cervical spine limitations.

BASIC SCIENCE

A Neural Circuit from the Paraventricular Thalamus to the Bed Nucleus of the Stria Terminalis for the Regulation of States of Consciousness during Sevoflurane Anesthesia in Mice

J.-Y. Li, S.-J. Gao, R.-R. Li, W. Wang, J. Sun, L.-Q. Zhang, J.-Y. Wu, D.-Q. Liu, P. Zhang, B. Tian, W. Mei 709

Chemogenetic inhibition of paraventricular glutamatergic neurons in the mouse thalamus projecting to the bed nucleus of the stria terminalis reduced induction time and prolonged emergence from sevoflurane anesthesia, while activation of this pathway had opposite effects. These observations suggest that glutamatergic neurons of the paraventricular thalamus contribute to the mechanisms of actions of sevoflurane anesthesia *via* their projections to the bed nucleus of the stria terminalis. *SUPPLEMENTAL DIGITAL CONTENT IS AVAILABLE IN THE TEXT*

Critical Care Medicine

CLINICAL SCIENCE

Extracorporeal Membrane Oxygenation for Respiratory Failure Related to COVID-19: A Nationwide Cohort Study

N. Nesseler, G. Fadel, A. Mansour, M. Para, P.-E. Falcoz, N. Mongardon, A. Porto, A. Bertier, B. Levy, C. Cadoz, P.-G. Guinot, O. Fouquet, J.-L. Fellahi, A. Ouattara, J. Guihaire, V.-G. Ruggieri, P. Gaudard, F. Labaste, T. Clavier, K. Brini, N. Allou, C. Lacroix, J. Chommeloux, G. Lebreton, M. A. Matthay, S. Provenchere, E. Flécher, A. Vincentelli, for the ECMOSARS Investigators.....732

In this investigation, most patients were cannulated by a mobile extracorporeal membrane oxygenation unit without a negative impact on mortality. Based on this report, venovenous extracorporeal membrane oxygenation support should be considered within the first week of mechanical ventilation initiation for optimal outcomes. *SUPPLEMENTAL DIGITAL CONTENT IS AVAILABLE IN THE TEXT*

BASIC SCIENCE

Early Restrictive Fluid Strategy Impairs the Diaphragm Force in Lambs with Acute Respiratory Distress Syndrome

M. M. Ijland, S. A. Ingelse, L. M. van Loon, M. van Erp, B. Kusters, C. A. C. Ottenheijm, M. Kox, J. G. van der Hoeven, L. M. A. Heunks, J. Lemson 749

Using an ovine model of pediatric acute respiratory distress syndrome with lung-protective ventilation, the authors compared a strict restrictive fluid strategy with norepinephrine to a liberal fluid strategy over a 6-h period evaluating transdiaphragmatic pressure over a wide range of positive end-expiratory pressure levels along with evaluation of diaphragm microcirculation, histology, and biomarkers reflective of inflammation and oxidative stress. Baseline measurements of transdiaphragmatic pressures before lung injury showed an inverse relationship with increasing positive end-expiratory pressure. Fluid restriction significantly reduced transdiaphragmatic pressures at positive end-expiratory pressure levels of 5 and 10 cm H2O but not at 15 or 20 cm H2O. Microvessel density was significantly reduced, although the histology and markers of inflammation and oxidative stress were not affected. *SUPPLEMENTAL DIGITAL CONTENT IS AVAILABLE IN THE TEXT*

Phrenic Nerve Block and Respiratory Effort in Pigs and Critically Ill Patients with Acute Lung Injury

S. M. Pereira, B. E. Sinedino, E. L. V. Costa, C. C. A. Morais, M. C. Sklar, C. Adkson Sales Lima, M. A. M. Nakamura, O. T. Ranzani, E. C. Goligher, M. R. Tucci, Y.-L. Ho, L. U. Taniguchi, J. E. Vieira, L. Brochard, M. B. P. Amato 763

The authors evaluated the effects of phrenic nerve block in a porcine model of acute respiratory distress syndrome and in nine patients with excessive inspiratory effort with acute respiratory distress syndrome on mechanical ventilation evaluating transdiaphragmatic pressures and electrical activity, as well as distribution of ventilation by electrical impedance tomography. In both groups, tidal volume, driving pressure, peak transpulmonary pressure, and electrical activity of the diaphragm decreased significantly with phrenic nerve block, with a slight decrease in dependent ventilation, while the respiratory rate was unchanged. Duration of the block was approximately 12 h. *SUPPLEMENTAL DIGITAL CONTENT IS AVAILABLE IN THE TEXT*

Prone Position Minimizes the Exacerbation of Effort-dependent Lung Injury: Exploring the Mechanism in Pigs and Evaluating Injury in Rabbits

T. Yoshida, D. Engelberts, H. Chen, X. Li, B. H. Katira, G. Otulakowski, Y. Fujino.....779

The authors utilized porcine and rabbit models of lung injury to evaluate pulmonary mechanics, distribution of ventilation, and biochemical and histologic effects on lung injury with varying positive end-expiratory pressure levels. Independent of positive end-expiratory pressure levels, prone positioning reduced maldistribution of lung stress and reduced effort-dependent evidence of lung injury. *SUPPLEMENTAL DIGITAL CONTENT IS AVAILABLE IN THE TEXT*

Pain Medicine

CLINICAL SCIENCE

Ketamine Psychedelic and Antinociceptive Effects Are Connected

E. Olofsen, J. Kamp, T. K. Henthorn, M. van Velzen, M. Niesters, E. Sarton, A. Dahan 792

In a planned secondary analysis, a population pharmacokinetic–pharmacodynamic model of ketamine and its metabolite norketamine was developed to describe the relationship between effect site concentrations of *S*- and *R*-ketamine and their metabolites and pressure pain threshold

and the change in external perception as a measure of ketamine psychotropic effect. The pharmacodynamics of *S*-ketamine did not differ for antinociception and external perception, which had the same potency parameter (C_{50}) and plasma-effect site equilibration half-time whether administered as racemic ketamine or *S*-ketamine. *R*-ketamine did not contribute to either endpoint, while *S*-norketamine had a small antagonistic effect for both endpoints.

BASIC SCIENCE

Using male and female mouse models, it was observed that Slick reduces responses to noxious thermal and chemical stimulation. Conversely, Slick expressed on spinal interneurons facilitates somatostatin-induced itch. Analgesics targeting Slick channels may decrease pain but could increase itching if they reach the central nervous system. *SUPPLEMENTAL DIGITAL CONTENT IS AVAILABLE IN THE TEXT*

Education

CLASSIC PAPERS REVISITED

IMAGES IN ANESTHESIOLOGY

CLINICAL FOCUS REVIEW

Use of the transvalvular heart pump to provide short-term circulatory support in the perioperative setting is growing. The considerations for the perioperative management of patients receiving transvalvular heart pump support are reviewed for the anesthesiologist.

REVIEW ARTICLE

Nonsteroidal anti-inflammatory drugs have immune modulatory effects in animal models and significantly affect outcome. In clinical studies, however, the immune-modulating effects of these drugs on perioperative outcome are much less evident.

MIND TO MIND

CORRESPONDENCE

Anesthesiology Reflections from the Wood Library-Museum

INSTRUCTIONS FOR AUTHORS

The most recently updated version of the Instructions for Authors is available at www.anesthesiology.org. Please refer to the Instructions for the preparation of any material for submission to ANESTHESIOLOGY.

Manuscripts submitted for consideration for publication must be submitted in electronic format *via* Editorial Manager (https://www.editorialmanager.com/aln). Detailed directions for submission and the most recent version of the Instructions for Authors can be found on the Journal's Web site (http://www.anesthesiology.org). Books and educational materials for review should be sent to Alan Jay Schwartz, M.D., M.S.Ed., Director of Education, Department of Anesthesiology and Critical Care Medicine, The Children's Hospital of Philadelphia, 34th Street and Civic Center Blvd., Room 9327, Philadelphia, Pennsylvania 19104-4399. Article-specific permission requests are managed with Copyright Clearance Center's Rightslink service. Information can be accessed directly from articles on the journal Web site. More information is available at http://anesthesiology.pubs.asahq.org/public/rightsandpermissions.aspx. For questions about the Rightslink service, e-mail customercare@copyright.com or call 877-622-5543 (U.S. only) or 978-777-9929. Advertising and related correspondence should be addressed to Advertising Manager, ANESTHESIOLOGY, Wolters Kluwer Health, Inc., Two Commerce Square, 2001 Market Street, Philadelphia, Pennsylvania 19103 (Web site: http://www.wkadcenter.com/). Publication of an advertisement in ANESTHESIOLOGY does not constitute endorsement by the Society or Wolters Kluwer Health, Inc. of the product or service described therein or of any representations made by the advertiser with respect to the product or service.

ANESTHESIOLOGY (ISSN 0003–3022) is published monthly by Wolters Kluwer Health, Inc., 1800 Dual Highway, Suite 201, Hagerstown, MD 21740-6636. Business office: Two Commerce Square, 2001 Market Street, Philadelphia, PA 19103. Periodicals postage paid at Hagerstown, MD, and at additional mailing offices.

Annual Subscription Rates: *United States*—$1125 Individual, $2904 Institution, $442 In-training. *Rest of World*—$1186 Individual, $3224 Institution, $442 In-training. Single copy rate $288. Subscriptions outside of North America must add $58 for airfreight delivery. Add state sales tax, where applicable. The GST tax of 7% must be added to all orders shipped to Canada (Wolters Kluwer Health, Inc.'s GST Identification #895524239, Publications Mail Agreement #1119672). Indicate in-training status and name of institution. Institution rates apply to libraries, hospitals, corporations, and partnerships of three or more individuals. Subscription prices outside the United States must be prepaid. Prices subject to change without notice. Subscriptions will begin with currently available issue unless otherwise requested. Visit us online at www.lww.com.

Individual and in-training subscription rates include print and access to the online version. Online-only subscriptions for individuals ($372) and persons in training ($372) are available to nonmembers and may be ordered by downloading a copy of the Online Subscription FAXback Form from the Web site, completing the information requested, and faxing the completed form to 301-223-2400. Institutional rates are for print only; online subscriptions are available *via* Ovid. Institutions can choose to purchase a print and online subscription together for a discounted rate. Institutions that wish to purchase a print subscription, please contact Wolters Kluwer Health, Inc., 1800 Dual Highway, Suite 201, Hagerstown, MD 21740-6636; phone: 800-638-3030; fax: 301-223-2400. Institutions that wish to purchase an online subscription or online with print, please contact the Ovid Regional Sales Office near you or visit www.ovid.com/site/index.jsp and select Contact and Locations.

Address for non-member subscription information, orders, or change of address: Wolters Kluwer Health, Inc., 1800 Dual Highway, Suite 201, Hagerstown, MD 21740-6636; phone: 800-638-3030; fax: 301-223-2400.

Address for member subscription information, orders, or change of address: Members of the American Society of Anesthesiologists receive the print and online journal with their membership. To become a member or provide a change of address, please contact the American Society of Anesthesiologists, 1061 American Lane, Schaumburg, Illinois 60173-4973; phone: 847-825-5586; fax: 847-825-1692; e-mail: membership@ASAhq.org. For all other membership inquiries, contact Wolters Kluwer Health, Inc., Customer Service Department, P.O. Box 1610, Hagerstown, MD 21740; phone: 800-638-3030; fax: 301-223-2400.

Postmaster: Send address changes to ANESTHESIOLOGY, P.O. BOX 1610, Hagerstown, MD 21740.

ANESTHESIOLOGY

Trusted Evidence: Discovery to Practice®

The Official Journal of the American Society of Anesthesiologists anesthesiology.org

Mission: Promoting scientific discovery and knowledge in perioperative, critical care, and pain medicine to advance patient care.

For reprint inquiries and purchases, please contact *reprintsolutions@wolterskluwer.com* in North America, and *healthlicensing@wolterskluwer.com* for rest of world.

Anesthesiology is abstracted or indexed in Index Medicus/MEDLINE, Science Citation Index/SciSearch, Current Contents/Clinical Medicine, Current Contents/Life Sciences, Reference Update, EMBASE/Excerpta Medica, Biological Abstracts (BIOSIS), Chemical Abstracts, Hospital Literature Index, and Comprehensive Index to Nursing and Allied Health Literature (CINAHL).

The affiliations, areas of expertise, and conflict-of-interest disclosure statements for each Editor and Associate Editor can be found on the Journal's Web site (www.anesthesiology.org).

ANESTHESIOLOGY

Trusted Evidence: Discovery to Practice®

The Official Journal of the American Society of Anesthesiologists anesthesiology.org

Mission: Promoting scientific discovery and knowledge in perioperative, critical care, and pain medicine to advance patient care.

ANESTHESIOLOGY

Trusted Evidence: Discovery to Practice®

The Official Journal of the American Society of Anesthesiologists anesthesiology.org

Mission: Promoting scientific discovery and knowledge in perioperative, critical care, and pain medicine to advance patient care.

Instructions for Obtaining ANESTHESIOLOGY Continuing Medical Education (CME) Credit

CME Editors: Leslie C. Jameson, M.D., and Dan J. Kopacz, M.D.

ANESTHESIOLOGY's Journal CME is open to all readers. To take part in ANESTHESIOLOGY Journal-based CME, complete the following steps:

1. Read the accreditation information presented on this page.
2. Read this month's articles designated for credit (listed below) in either the print or online edition.
3. Register at http://www.asahq.org/shop-asa. In the category, search for Journal CME. Nonmembers will need to provide payment.
4. Complete the activity posttest and course evaluation.
5. Claim a maximum of 1 *AMA PRA Category 1 Credit™* by the credit claiming deadline.

Accreditation Information

Purpose: The focus of ANESTHESIOLOGY Journal-based CME is to educate readers on current developments in the science and clinical practice of anesthesiology.

Target Audience: ANESTHESIOLOGY Journal-based CME is intended for anesthesiologists. Researchers and other healthcare professionals with an interest in anesthesiology may also participate.

Accreditation and Designation Statements: The American Society of Anesthesiologists is accredited by the Accreditation Council for Continuing Medical Education to provide continuing medical education for physicians.

The American Society of Anesthesiologists designates this journal-based activity for a maximum of 1 *AMA PRA Category 1 Credits*™. Physicians should claim only the credit commensurate with the extent of their participation in the activity.

Maintenance of Certification in Anesthesiology™ program and MOCA® are registered trademarks of the American Board of Anesthesiology®. MOCA 2.0® is a trademark of the American Board of Anesthesiology®.

This activity contributes to the CME component of the American Board of Anesthesiology's redesigned Maintenance of Certification in Anesthesiology™ (MOCA®) program, known as MOCA 2.0®. Please consult the ABA website, http://www.theABA.org, for a list of all MOCA 2.0 requirements.

Rates

Two options are available:

	ASA Member	Non-member
Annual Fee	$0	$120

Payment may be made using Visa or MasterCard.
Please direct any questions about Journal-based CME to: EducationCenter@asahq.org

Date of Release: April 2022
Expiration Date: April 2025

This Month's ANESTHESIOLOGY Journal-based CME Article

Read the article by Nesseler *et al.* entitled "Extracorporeal Membrane Oxygenation for Respiratory Failure Related to COVID-19: A Nationwide Cohort Study" on page 732.

Learning Objectives

After successfully completing this activity, the learner will be able to anticipate the clinical course after initiation of extracorporeal membrane oxygenation (ECMO) in COVID-19 patients, determine which pre-ECMO variables are associated with a greater risk of mortality, and recognize the most common complications of ECMO therapy.

Disclosures

This journal article has been selected for and planned as a journal CME activity, which is designated for *AMA PRA Category 1 Credit*™. The authors disclosed relationships in keeping with ANESTHESIOLOGY's requirements for all journal submissions. All relationships journal authors disclosed to ANESTHESIOLOGY are disclosed to learners, even those relationships that are not relevant financial relationships, per the ACCME's requirements for CME activities.

Editor-in-Chief: Evan D. Kharasch, M.D., Ph.D., has disclosed no relevant financial relationships with commercial interests.

CME Editors: Leslie C. Jameson, M.D., has disclosed no relevant financial relationships with commercial interests. Dan J. Kopacz, M.D., has disclosed holding an equity position with Solo-Dex, Inc.

ASA Staff: Kari Lee and Anne Farace have disclosed no relevant financial relationships with commercial interests.

Disclaimer

The information provided in this activity is for continuing education purposes only and is not meant to substitute for the independent medical judgment of a healthcare provider relative to diagnostic and treatment options of a specific patient's medical condition.

DOI: 10.1097/ALN.0000000000004212

SCIENCE, MEDICINE, AND THE ANESTHESIOLOGIST
ANESTHESIOLOGY
Martin J. London, M.D., Editor
Key Papers from the Most Recent Literature Relevant to Anesthesiologists

Point-of-care screening for heart failure with reduced ejection fraction using artificial intelligence during ECG-enabled stethoscope examination in London, UK: A prospective, observational, multicentre study. Lancet Digit Health 2022; 4:e117–25. PMID: 34998740.

Better detection of heart failure with reduced ejection fraction, particularly in the outpatient setting, may improve long-term outcome. Previous research using a neural network (named AI-ECG) trained on the 12-lead electrocardiogram (ECG) has demonstrated useful sensitivity and specificity for detection of reduced ejection fraction. This observational, prospective, multicenter UK study used the AI-ECG algorithm retrained to interpret single-lead ECG input alone *via* two electrodes mounted on a stethoscope capable of wireless transmission. Fifteen seconds of supine ECG were recorded at four anatomical positions for cardiac auscultation, plus one additional position, comparing data to echocardiogram-derived ejection fraction. The primary outcome was performance of AI-ECG at classifying reduced left ventricular ejection fraction (40% or lower) using the area under the receiver operating characteristic curve (ROC). The cohort included 1,050 patients (mean age 62 yr, 51% male, 41% non-White), 10% with ejection fraction 40% or lower. ECG signal quality was best at the pulmonary position (93%). Quality was lowest for the aortic position (81%). AI-ECG performed best at the pulmonary valve position ($P = 0.02$), with a ROC area of 0.85 (95% CI, 0.81 to 0.89), sensitivity of 84.8% (76.2 to 91.3), and specificity of 69.5% (66.4 to 72.6). Diagnostic odds ratios did not differ by age, sex, or non-White ethnicity. Further improvements in ROC area were noted using two positions as well as a weighted logistic regression approach. *(Article Selection: Martin J. London, M.D. Image: Adobe Stock.)*

Take home message: Single-lead ECG tracings obtained using a specially designed stethoscope and processed using a neural network algorithm facilitated detection of left ventricular ejection fraction of 40% or lower in ambulatory primary care subjects.

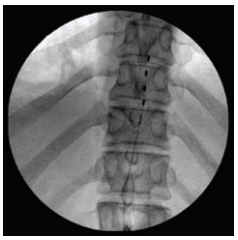

Association of spinal cord stimulator implantation with persistent opioid use in patients with postlaminectomy syndrome. JAMA Netw Open 2022; 5:e2145876. PMID: 35099546.

The results of spinal cord stimulation studies vary tremendously, with concerns of bias in the mostly industry-sponsored trials. The controversy around the therapeutic effect of spinal cord stimulation has led to an emphasis on objective measures of effectiveness such as requirement for supplemental opioid utilization. This case-control study included 552,937 patients with previous spine surgery and compared the incidence of chronic opioid therapy over a 12-month period after implantation (4.7% of the cohort) or a matched index date, in those without spinal cord stimulation in opioid-naïve patients or those on chronic opioid therapy. In the study period, similar proportions in the spinal cord stimulation and non–spinal cord stimulation groups receiving baseline opioid therapy remained on opioids (70.3% *vs.* 69.2%). In opioid-naïve patients, spinal cord stimulation was associated with a statistically lower likelihood of patients receiving subsequent opioid therapy (7.6% *vs.* 7.0%, $P = 0.003$). In multivariable analysis, spinal cord stimulation was associated with a greater likelihood of not being on opioids in both opioid-naïve (adjusted odds ratio 0.90; 95% CI, 0.85 to 0.96; $P < 0.001$) and chronic opioid therapy patients (adjusted odds ratio 0.93; 95% CI, 0.88 to 0.99; $P = 0.02$). *(Article Selection: Steven Cohen, M.D. Image: J. P. Rathmell.)*

Take home message: In a large case-control study, spinal cord stimulation in patients with previous spinal surgery is associated with a clinically questionable reduction in chronic opioid therapy in opioid-naïve patients, but not in individuals already on chronic opioid therapy.

Effect of anticoagulant therapy for 6 weeks vs 3 months on recurrence and bleeding events in patients younger than 21 years of age with provoked venous thromboembolism: The Kids-DOTT Randomized Clinical Trial. JAMA 2022; 327:129–37. PMID: 35015038.

Standard of care for the duration of anticoagulation after a first episode of venous thromboembolism in patients younger than 21 yr is a 3-month course of anticoagulation. However, recent practice has shifted toward a 6-week course. The Kids-DOTT Randomized Clinical Trial enrolled 417 patients younger than 21 yr with acute provoked venous thromboembolism at 42 centers in five countries between 2008 and 2021 comparing the two strategies. The primary therapeutic and safety endpoints were symptomatic recurrent venous thromboembolism and clinically relevant bleeding events within 1 yr of treatment initiation. The choice of anticoagulant was left at the discretion of the physician. Among 417 randomized patients, 297 (median age, 8 yr) met criteria for the primary per-protocol population analysis. The Kaplan-Meier estimate for the 1-yr cumulative incidence of the primary therapeutic outcome was 0.66% (95% CI, 0 to 1.95%) in the 6-week therapy group and 0.70% (95% CI, 0 to 2.07%) in the 3-month therapy group. For the primary safety outcome, the incidence was 0.65% (95% CI, 0 to 1.91%) and 0.70% (95% CI, 0 to 2.06%). *(Article Selection: David Faraoni, M.D., Ph.D. Image: Adobe Stock.)*

Take home message: Among patients younger than 21 yr with provoked venous thromboembolism, anticoagulant therapy for 6 weeks was noninferior to anticoagulant therapy for 3 months for the therapeutic endpoint of recurrent venous thromboembolism and the safety endpoint of bleeding episodes.

Association of surgeon–patient sex concordance with postoperative outcomes. JAMA Surg 2022; 157:146–56. PMID: 34878511.

Sex discordance between physicians and patients has been associated with worse clinical outcomes in primary care and acute cardiac care, particularly for male physicians treating female patients. This population-based, retrospective cohort study conducted in Ontario was designed to evaluate the effect of sex discordance between surgeons and patients in perioperative care. It focused on adults undergoing one of 21 common elective or emergency surgeries. The primary outcome was a composite of death, readmission, or complication within 30 days after surgery. Among 1,320,108 patients who underwent surgery by one of 2,937 surgeons in Ontario between January 2007 and December 2019, 602,560 (46%) were sex concordant with their surgeon and 717,548 (54%) were sex discordant. Sex discordance was associated with a greater likelihood of the primary outcome (adjusted odds ratio 1.07; 95% CI, 1.04 to 1.09). This association was different for male *versus* female patients: sex discordance was associated with worse outcomes for female patients (adjusted odds ratio, 1.11; 95% CI, 1.06 to 1.16) and better outcomes for male patients (adjusted odds ratio, 0.96; 95% CI, 0.93 to 0.99; *P* for interaction = 0.004). This effect was consistent across all surgical subspecialties and robust to subgroup analyses assessing procedure-, patient-, physician-, and hospital-level characteristics. *(Article Selection: Meghan Prin, M.D. Image: Adobe Stock.)*

Take home message: Sex discordance between patients and surgeons, primarily when female patients are treated by male surgeons, may play a role in worse surgical outcomes.

Multiple early factors anticipate post-acute COVID-19 sequelae. Cell 2022; 185:881–95.e20. PMID: 35216672.

Up to two thirds of COVID-19 patients develop "post-acute sequelae of COVID-19," also known as long COVID. These terms refer to health problems that persist for more than a month after an initial SARS-CoV-2 infection, such as fatigue, memory loss, gastrointestinal distress, and dyspnea. Long COVID is a poorly understood, heterogeneous condition, and generally symptoms cluster into one of four systems: neurological, gastrointestinal, respiratory, or nasal. A better understanding of this condition may allow for early intervention or prevention. In this longitudinal study of 309 COVID-19 patients (primary cohort n = 209; independent validation cohort n = 100) followed from initial diagnosis for 2 to 3 months and compared with 457 healthy controls, a systems biology approach was undertaken to elucidate, quantify, and immunologically characterize biological associations that may predict the development of long COVID. Four risk factors at initial COVID-19 diagnosis were identified: type 2 diabetes, Epstein-Barr viremia, SARS-CoV-2 RNAemia, and specific autoantibodies. Analyses of immune-transcriptomes revealed four convalescent immunological endotypes that were associated with varying acute disease severity and long COVID subtype. All four long COVID risk factors are detectable at initial COVID-19 diagnosis, which highlights the importance of prompt and thorough assessments and may allow for risk stratification. *(Article Selection: Meghan Prin, M.D. Image: Adobe Stock.)*

Take home message: Long COVID is common and may be associated with risk factors that are easily identifiable at initial COVID-19 diagnosis, allowing for early risk stratification and more precise treatment plans.

Why postmortems fail. Proc Natl Acad Sci USA 2022; 119:e2116638118. PMID: 35027455.

There is almost always an investigation after high-profile public disasters. The expectation is that, by uncovering early warning signs, we might prevent a recurrence of the disaster and make us safer. Unfortunately, the process of the inquiry usually just replicates the same political pressures and poor social science methods that originally led to the occurrence of the disaster in the first place, leading inevitably to biased and misleading conclusions. It is necessary to recognize that there is not a perfect correlation between the process and the outcome. From which it follows that terrible outcomes can sometimes arise from correct judgements in the presence of incomplete knowledge. People can be wrong for the right reasons. To avoid arriving at flawed conclusions, the subsequent inquiry has to have the humility to recognize: the difference between necessary and sufficient causation; the cost of false positives; the dangers of cherry-picking ideas; the problem that there are many "dots" that can be connected in many different ways; and at least considering whether the facts were also consistent with alternative explanations. *(Article Selection: Jamie Sleigh, M.D. Image: Space Shuttle Challenger, NASA [public domain].)*

Take home message: Although derived from the political and social sphere, these principles clearly also apply to the investigation of medical disasters.

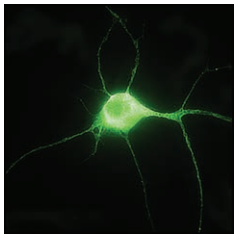

Skin-resident dendritic cells mediate postoperative pain via CCR4 on sensory neurons. Proc Natl Acad Sci USA 2022; 119:e2118238119. PMID: 35046040.

The chemokine receptor CCR4 has several ligands, including CCL2, CCL5, CCL17, and CCL22. This study investigated the role of dendritic cells and CCR4 in postoperative pain in a mouse model of plantar incision. Several interesting findings were reported. First, paw incision increased the expression of CCL17 and CCL22 in skin-resident dendritic and Langerhans cells. Second, exogenous injection of CCL17 and CCL22 was sufficient to induce acute mechanical and thermal hypersensitivity when administered subcutaneously; however, this behavioral response is abrogated by pharmacological blockade or genetic silencing of CCR4, suggesting that CCR4 is required for producing mechanical and thermal nociception elicited by these two cytokines. Third, electrophysiological assessment of dissociated sensory neurons from naïve and postoperative mice revealed that CCL22 was able to directly activate sensory neurons and enhance their excitability after injury. Fourth, postoperative nociception is reduced in mice lacking CCR4 or in wild-type animals treated with CCR4 antagonist. Finally, postoperative nociception is reduced in transgenic mice depleted of dendritic cells. *(Article Selection: Ru-Rong Ji, Ph.D. Image: J. P. Rathmell.)*

Take home message: This study demonstrates an essential role of dendritic cells in postoperative nociception in animals and reveals CCR4 as a potential drug target for the development of new pain therapeutics.

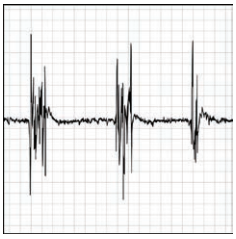

Brain responses to propofol in advance of recovery from coma and disorders of consciousness: A preliminary study. Am J Respir Crit Care Med 2022; 205:171–82. PMID: 34748722.

Prognosis of recovery in unresponsive, brain-injured patients is of utmost clinical importance but definitive clinical tools for prognostication are lacking. Propofol induces distinctive neural network reconfiguration in the healthy brain as consciousness is lost, such as anteriorization of a network hubs and neutralization of feedback-dominant connectivity. This case series utilized an adaptive reconfiguration index, metrics of a network hubs and directed functional connectivity, to predict patients who would regain full consciousness within 3 months. High-density electroencephalograms (EEGs) were recorded before, during, and after the administration of propofol at a target effect site concentration of 2 ug/min in 12 adult patients, 7 with acute (less than 6 months) and 5 with chronic (more than 6 months) unconsciousness. The chronic patients were considered as negative controls since a low adaptive reconfiguration index was predicted reflecting a low likelihood of recovery of consciousness. In 3 of the 6 acute patients who recovered consciousness by 3 months, the network hub topography and the directed functional connectivity patterns paralleled those of healthy subjects who receive propofol. The three acute patients who completed the study and did not recover consciousness at 3 months demonstrated minimal hub reconfiguration during propofol exposure and little to no reconfiguration in directed functional connectivity. *(Article Selection: Charles Emala, Sr., M.D., M.S. Image: J. P. Rathmell.)*

Take home message: In this small case series, the propofol-induced adaptive reconfiguration index, an EEG measured alteration of a network hubs and directed functional connectivity, was predictive of those unresponsive brain-injured patients who regained consciousness within 3 months.

Balanced multielectrolyte solution versus saline in critically ill adults. N Engl J Med 2022; 386:815–26. PMID: 35041780.

In critically ill patients, the optimal type and composition of intravenous fluids remain controversial with balanced multi electrolyte solutions increasingly preferred over saline. Critically ill patients were randomized to receive either a balanced multielectrolyte solution or 0.9% sodium chloride for fluid therapy in the intensive care unit (ICU) for up to 90 days after randomization. The primary endpoint was the incidence of 90-day all-cause mortality. Secondary endpoints included new renal-replacement therapy and the maximum increase in creatinine concentration. Among the 5,037 patients recruited from 53 ICUs in Australia and New Zealand, 2,515 patients were assigned to the balanced multielectrolyte solution group and 2,522 to the 0.9% sodium chloride group. Death within 90 days after randomization occurred in 21.8% of the patients treated with balanced multielectrolyte solution and in 22.0% of the patients treated with 0.9% sodium chloride (difference of −0.15 percentage points [95% CI, −3.60 to 3.30]). The incidence of new renal-replacement therapy was 12.7% in the balanced multielectrolyte solution group and 12.9% in the saline group (difference of −0.20 percentage points [95% CI, −2.96 to 2.56]). No difference was reported in the mean increase in creatinine concentrations between the two groups. *(Article Selection: David Faraoni, M.D., Ph.D. Image: J. P. Rathmell.)*

Take home message: In this randomized study of critically ill adults who received fluid therapy with a balanced multielectrolyte solution for up to 90 days, there was no difference in the risk of mortality or acute kidney injury when compared to 0.9% sodium chloride.

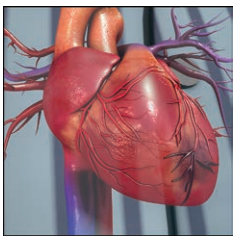

Cardiomyocytes disrupt pyrimidine biosynthesis in nonmyocytes to regulate heart repair. J Clin Invest 2022; 132:e149711. PMID: 34813507.

Myocardial infarction (MI) is a major cause of heart failure. Although fibroblasts, macrophages, and endothelial cells play a pivotal role in postischemic regeneration, the role of cardiomyocytes in wound healing is poorly understood. Using a murine model of ischemic cardiac injury and an arsenal of pharmacological and genetic approaches, the critical role of the ectonucleotidase (ENPP1) in the process of myocardial regeneration was identified. Cardiac damage increased expression of ENPP1 selectively in nonmyocytes, namely fibroblasts, macrophages, and endothelial cells, which was found to metabolize adenosine triphosphate (ATP) derived from cardiomyocytes to adenosine monophosphate (AMP). Cardiomyocytes in response to AMP released adenine and other purine nucleosides, which inhibited the cell cycle and induced apoptotic cell death in cycling nonmyocytes by blocking pyrimidine biosynthesis (UMP synthase) and upregulating the p53-signaling pathway. A knockout model for ENPP1 showed improved cardiac function and decreased chamber size after permanent ligation of the coronary artery. Only 6% of mice in the ENPP1 knockout group showed ejection fractions less than 20%, compared with 50% in control littermates. Peri-infarct histology exhibited increased capillary density and reduced scar formation. By screening a library of 200,000 compounds, a polyphenolic flavonoid named myricetin was identified as potent ENPP1 inhibitor, which also improved post-MI outcome in mice. *(Article Selection: Michael Zaugg, M.D., M.B.A. Image: J. P. Rathmell.)*

Take home message: The discovery of a key cardiomyocyte–nonmyocyte crosstalk, which disrupts nonmyocyte cell function and deteriorates post ischemic wound healing, has potential implications as a newly identified small molecular inhibitor of ENPP1 to improve post-MI outcomes in mice.

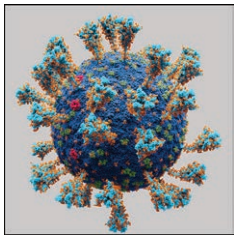

Evidence for a mouse origin of the SARS-CoV-2 Omicron variant. J Genet Genomics 2021; 48: 1111–21. PMID: 34954396.

The rapid and diverse accrual of mutations in the Omicron variant of SARS-CoV-2 has raised the question of whether its origin occurred in humans or an alternative mammalian host. Three hypotheses have been proposed for Omicron's many and divergent mutations compared to previous variants: (1) it circulated in a human population with insufficient viral surveillance and sequencing; (2) it evolved in a chronically infected and immunocompromised human host allowing for long-term intra-host viral interactions; (3) it evolved in a nonhuman host and jumped species to humans. Results demonstrate that the Omicron spike protein was subjected to stronger positive selection than any previously reported variants and that the molecular spectrum of the mutations was different from those mutations previously acquired by other viruses in humans. This is based on previous research demonstrating that the patterns of mutations in RNA viruses are highly dependent on host-specific cellular environments and that the pattern of mutations in Omicron more closely resembled virus evolution in a murine host. Moreover, molecular docking experiments predicted that the acquired mutations resulted in a higher binding affinity of Omicron for the mouse ACE2 than the receptor binding domains of the reference SARS-CoV-2 genome. *(Article Selection: Charles Emala, Sr., M.D., M.S. Image: Alexey Solodovnikov [Idea, Producer, CG, Editor], Valeria Arkhipova [Scientific Consultant], CC BY-SA 4.0,* via *Wikimedia Commons.)*

Take home message: The molecular spectrum of pre-outbreak mutations of the SARS-CoV-2 Omicron variant is inconsistent with evolution in humans but is more consistent with mutations accumulating in murine hosts for more than 1 yr before jumping back to humans.

Factors associated with opioid overdose after an initial opioid prescription. JAMA Netw Open 2022; 5:e2145691. PMID: 35089351.

Identifying patients at risk for opioid-related overdose remains a critical priority. In this retrospective, observational cohort study, data from the Oregon Comprehensive Risk Registry containing linked all payer claims with other health data were used to assess risk factors associated with overdose after the first (index) opioid prescription. Of the 236,921 patients, 667 (0.3%) experienced opioid overdose. Risk of overdose was highest among individuals 75 yr or older (adjusted hazard ratio, 3.22; 95% CI, 1.94 to 5.36) compared with young age groups; male sex (adjusted hazard ratio, 1.29; 95% CI, 1.10 to 1.51); dual eligible Medicare/Medicaid beneficiaries (adjusted hazard ratio, 4.37; 95% CI, 3.09 to 6.18), Medicaid (adjusted hazard ratio, 3.77; 95% CI, 2.97 to 4.80), or Medicare Advantage (adjusted hazard ratio, 2.18; 95% CI, 1.44 to 3.31) compared with commercial insurance; those with comorbid substance use disorder (adjusted hazard ratio, 2.74; 95% CI, 2.15 to 3.50), with depression (adjusted hazard ratio, 1.26; 95% CI, 1.03 to 1.55), or with one to two comorbidities (adjusted hazard ratio, 1.32; 95% CI, 1.08 to 1.62) or three or more comorbidities (adjusted hazard ratio, 1.90; 95% CI, 1.42 to 2.53) compared with none. Patients were at a greater overdose risk if they filled oxycodone (adjusted hazard ratio, 1.70; 95% CI, 1.04 to 2.77) or tramadol (adjusted hazard ratio, 2.80; 95% CI, 1.34 to 5.84) compared with codeine; used benzodiazepines (adjusted hazard ratio, 1.06; 95% CI, 1.01 to 1.11); used concurrent opioids and benzodiazepines (adjusted hazard ratio, 2.11; 95% CI, 1.70 to 2.62); or filled opioids from three or more pharmacies over 6 months (adjusted hazard ratio, 1.38; 95% CI, 1.09 to 1.75). *(Article Selection: Chad Brummett, M.D. Image: Adobe Stock.)*

Take home message: Although opioid overdose is uncommon after first prescriptions, there are patient and prescribing factors associated with overdose that may aid in medical decision making and patient education.

TO PUNCTURE OR NOT TO PUNCTURE

Dural Puncture Epidural VS. Standard Epidural

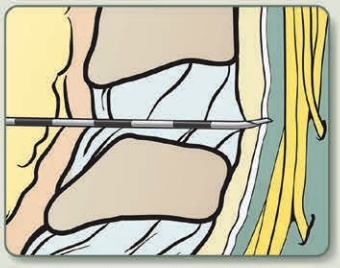

Dural puncture epidural (DPE) involves insertion of a spinal needle through the Tuohy needle during epidural placement, confirming CSF flow.

Possible advantages:

- Confirm midline placement
- Transfer of medications *via* puncture

In this issue, Tan *et al.*[1] evaluate whether DPE improves the quality of labor analgesia compared to standard epidural in *obese parturients*.

No difference in:

Primary composite outcome

1. Asymmetric block
2. Epidural top-ups
3. Catheter adjustments
4. Catheter replacement
5. Failed conversion for cesarean delivery

Timeline of DPE Studies[1,2]

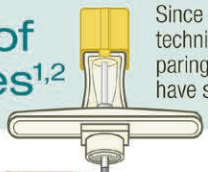

Since the first description of the technique in 1996, studies comparing DPE to standard epidural have shown varying results.

Suzuki *et al.* 1996
- Faster sacral spread

2005 Thomas *et al.*
- Sacral spread
- Asymmetric block
- Top-ups
- Catheter manipulation
- Catheter replacement

Cappiello *et al.* 2008
- Faster analgesic onset
- Faster sacral spread
- Fewer asymmetric blocks

2017 Chau *et al.*
- Faster sacral spread
- Fewer asymmetric blocks
- Fewer top-ups
- Analgesic onset

2018 Yadev *et al.*
- Faster analgesic onset

Heesen *et al.* (Sys Rev) 2019
- Faster analgesic onset
- Faster sacral spread
- Fewer top-ups
- Catheter manipulation
- Catheter replacement
- Asymmetric block

Wilson *et al.*
- Faster analgesic onset

2020 Lu *et al.*
- Faster analgesic onset

Layera *et al.* (Sys Rev)
- Faster analgesic onset
- Faster sacral spread
- Fewer asymmetric blocks

2021 Song *et al.*
- Faster analgesic onset

Wang *et al.*
- Faster analgesic onset

Benefits of DPE in the general pregnant population are modest, and the current study highlights the lack of differences for obese parturients. Individual clinician judgement is still necessary to determine appropriate indications for DPE.

CSF, cerebral spinal fluid.

Infographic created by Holly B. Ende, Vanderbilt University Medical Center; James P. Rathmell, Brigham and Women's Health Care/Harvard Medical School; and Jonathan P. Wanderer, Vanderbilt University Medical Center. Illustration by Annemarie Johnson, Vivo Visuals Studio. Address correspondence to Dr. Ende: holly.ende@vumc.org.

1. Tan HS, Reed SE, Mehdiratta JE, Diomede OI, Landreth R, Gatta LA, Weikel D, Habib AS: Quality of labor analgesia with dural puncture epidural versus standard epidural technique in obese parturients: A double-blind randomized controlled study. ANESTHESIOLOGY 2022; 136:678–87
2. Segal S, Pan PH: Dural puncture epidural for labor analgesia: Is it really an improvement over conventional labor epidural analgesia? ANESTHESIOLOGY 2022; 136:667–9

Anesthesia **SimSTAT**

TRAUMA | ROBOTIC SURGERY | PACU | L&D | APPENDECTOMY

Bringing simulation to you

Polish your clinical performance through a powerful online experience featuring the sights, sounds, and controls of a real O.R. Participate in a series of high fidelity simulation scenarios within a virtual environment on your time.

Get all five modules in a discounted bundle, or purchase the modules you need on their own.

MOCA®

Maintenance of Certification in Anesthesiology℠ program and MOCA® are registered trademarks of The American Board of Anesthesiology®. MOCA 2.0® is a trademark of The American Board of Anesthesiology®.

American Society of Anesthesiologists®

CAE

Participate in powerful simulation training online
asahq.org/simulation

Dural Puncture Epidural for Labor Analgesia: Is It Really an Improvement over Conventional Labor Epidural Analgesia?

Scott Segal, M.D., M.H.C.M., Peter H. Pan, M.D., M.S.E.E.

Neuraxial analgesia is considered the definitive standard for labor pain relief, utilized by more than 73% of laboring women in the United States, with growing popularity over time.[1] This is perhaps unsurprising given its analgesic effectiveness, titratability, relative lack of serious side effects, and acceptance by most obstetric clinicians. During the last several decades, various refinements to neuraxial labor analgesia have included the use of continuous infusions of local anesthetic, addition of lipophilic opioids to epidural injectates, use of higher-volume and lower-concentration local anesthetic solutions, patient-controlled epidural analgesia, programmed intermittent epidural bolus, combined spinal–epidural analgesia, and dural puncture epidural analgesia. In combined spinal–epidural and dural puncture epidural, a spinal needle is passed through the epidural needle, and in combined spinal–epidural, small doses of opioid, usually combined with very small doses of local anesthetic, are injected intrathecally at the time of epidural initiation. In dural puncture epidural, no drug is injected. In this issue of Anesthesiology, Tan *et al.*[2] report the results of a randomized clinical trial of dural puncture epidural compared to conventional epidural in obese parturients, hypothesizing that in this relatively high-risk group, dural puncture epidural would improve analgesia and lessen epidural failures.

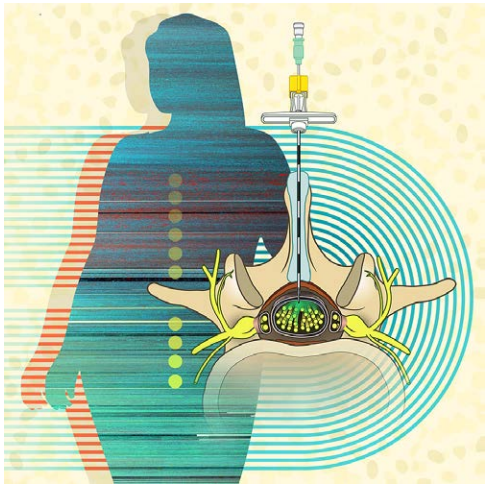

"Dural puncture epidural appears to be a clever idea in search of an indication."

Despite multiple features designed to demonstrate a clinically meaningful difference between dural puncture epidural and conventional epidural techniques, the authors found none (52% *vs.* 49% for the primary outcome, a composite of several measures of inadequate analgesia). Removing the very common outcome of clinician top-up did not change the conclusion (30% *vs.* 26%). No individual secondary outcomes appeared to differ, the time to effective analgesia was similar, and there were no differences in adverse events for the mothers or the babies.

The purported advantages of the combined spinal–epidural technique are faster onset of analgesia, especially in sacral dermatomes, less motor blockade and greater patient mobility, more positive identification of the epidural space by detection of cerebrospinal fluid (CSF), fewer epidural catheter failures and replacements, faster cervical dilation, greater patient satisfaction, and facilitation of use of more dilute epidural local anesthetic solutions. The possible disadvantages of the technique (although several have been largely disproven) include more pruritus, more frequent fetal heart rate changes including fetal bradycardia, increase in postdural puncture headache, and uncertainty regarding epidural functionality due to masking by the initial intrathecal medication. Importantly, continued innovation in conventional epidural analgesia has narrowed some of the advantages of the combined spinal–epidural technique observed in early studies.[3]

The dural puncture epidural technique attempts to have the best of both worlds, in principle, by providing the advantages of a modern low-dose labor epidural analgesic while avoiding the intrathecal opioid-induced pruritus and fetal bradycardia associated with combined spinal–epidural. Because there is affirmative observation of CSF before catheter insertion, dural puncture epidural (like combined spinal–epidural) may offer greater certainty of proper epidural needle placement. Finally, because the dural puncture might allow partial transdural passage of

Image: A. Johnson, Vivo Visuals Studio.

Accepted for publication February 17, 2022. Published online first on March 23, 2022. This editorial accompanies the article on p. 678.

Scott Segal, M.D., M.H.C.M.: Department of Anesthesiology, Wake Forest School of Medicine, Winston-Salem, North Carolina.

Peter H. Pan, M.D., M.S.E.E.: Department of Anesthesiology, Wake Forest School of Medicine, Winston-Salem, North Carolina.

 Anesthesiology 2022; 136:667–9. DOI: 10.1097/ALN.0000000000004187

<zdoi;. DOI: 10.1097/ALN.0000000000004187>

local anesthetic and opioid, some of the benefits of combined spinal–epidural may be observed, particularly the more rapid onset of sacral and perhaps overall analgesia. Conversely, because a dural puncture is still intentionally made, a potential, but likely small, risk of postdural puncture headache would remain.

Unfortunately, these theoretical benefits have not been consistently documented. The initial report of dural puncture epidural showed faster onset of sacral analgesia, a higher incidence of visual analog scale pain scores of less than 10 of 100 at 20 min, and fewer asymmetric blocks.[4] This study was criticized on statistical grounds;[5] in a subsequent study, the same institution found similar beneficial effects over the conventional epidural technique and fewer side effects than combined spinal–epidural,[6] but again, there were methodologic concerns.[7] Other groups found no or minimal differences between dural puncture epidural and conventional epidural blocks, and two meta-analyses published in 2019 concluded the differences were minor at best.[8,9] Subsequently, published studies from several international groups once again found slightly faster onset of adequate analgesia with dural puncture epidural,[10–12] but other studies found trivial or no differences.[13] While it is unclear why such disparate results have been observed, variations in spinal needle size, epidural drug administered, patient population studied, method of analgesia assessment, and other unknown confounders or random variation may be responsible. It is also certainly possible that some patients could benefit much more than others from the use of the dural puncture epidural technique but that in the parturient population as a whole, these benefits are obscured.

The study by Tan *et al.*[2] features a design well poised to help detect a difference between techniques. Obese women are often thought to present more difficult anatomy for identification of the epidural space and would thus potentially benefit more from the observation of CSF during dural puncture epidural, which would help the operator confirm midline placement of the epidural needle and reject a false loss of resistance. The investigators used a 25-gauge Whitacre spinal needle, which might increase transdural transfer of local anesthetic compared to finer needles. They utilized the programmed intermittent epidural bolus and patient-controlled epidural analgesia techniques for the subsequent epidural analgesia. The higher pressures achieved during such injections compared to continuous infusion might also increase transfer of drug to the intrathecal space. Finally, they measured a composite outcome of block inadequacy that included one or more of the following: the need for physician top-ups, asymmetric block, catheter adjustment or replacement, and failed conversion to surgical anesthesia for cesarean delivery. This primary outcome occurred in more than half the participants; use of a such a commonly observed event class increases the power of the study to detect a difference, compared to rarer outcomes. The study was adequately powered to detect a fairly large difference in the primary outcome (62% reduction, as has been observed in epidural *vs.* combined spinal–epidural studies). Careful attention to randomization and observer blinding was achieved, and randomly observed baseline differences between the groups were controlled for in the analyses.

Despite this study design, Tan *et al.*[2] found no advantage of the dural puncture epidural technique. They acknowledged that use of a very dilute epidural solution might have lessened the effect of transdural drug passage. Use of programmed intermittent epidural bolus and patient-controlled epidural analgesia may have made the epidural group function better than older techniques and lessened the possibility of showing an advantage of dural puncture epidural. In addition, several of their secondary outcomes had wide CI ranges that included clinically meaningful differences, even though the point estimate showed none. Furthermore, the study was powered to detect a greater than 60% difference in the composite outcome, which might have missed smaller differences in the composite or individual outcomes that could still be relevant.

Where does the current study leave the field? Dural puncture epidural appears to be a clever idea in search of an indication. In the general parturient population, the overall effect seems to be quite modest at best. In the higher-risk population studied by Tan *et al.*,[2] there were no significant advantages. It may still be possible to identify patients who could benefit (for example, those in whom equivocal loss of resistance is encountered). However, randomized clinical trials studying such narrow subgroups are unlikely to be performed, and individual clinician judgment will probably guide the development of a home, if any, for the dural puncture epidural technique.

Research Support

Supported by National Institute of Biomedical Imaging and Bioengineering, National Institutes of Health (Bethesda, Maryland) grant No. 1 R21 EB029493-01A1, Wake Forest Clinical and Translational Science Institute (Winston-Salem, North Carolina) grant No. UL1TR001420, and funds from the Anesthesia Patient Safety Foundation (Rochester, Minnesota; to Dr. Segal).

Competing Interests

The authors are not supported by, nor maintain any financial interest in, any commercial activity that may be associated with the topic of this article.

Correspondence

Address correspondence to Dr. Segal: bsegal@wakehealth.edu

References

1. Butwick AJ, Bentley J, Wong CA, Snowden JM, Sun E, Guo N: United States state-level variation in the use of

neuraxial analgesia during labor for pregnant women. JAMA Netw Open 2018; 1:e186567
2. Tan HS, Reed SE, Mehdiratta JE, Diomede OI, Landreth R, Gatta LA, Weikel D, Habib AS: Quality of labor analgesia with dural puncture epidural *versus* standard epidural technique in obese parturients: A double-blind randomized controlled study. Anesthesiology 2022; 136:678–87
3. Simmons SW, Taghizadeh N, Dennis AT, Hughes D, Cyna AM: Combined spinal–epidural *versus* epidural analgesia in labour. Cochrane Database Syst Rev 2012; 10:CD003401
4. Cappiello E, O'Rourke N, Segal S, Tsen LC: A randomized trial of dural puncture epidural technique compared with the standard epidural technique for labor analgesia. Anesth Analg 2008; 107:1646–51
5. Duzenmas D: Are the conclusions supported by the statistics? Anesth Analg 2010; 110:969; author reply 969
6. Chau A, Bibbo C, Huang CC, Elterman KG, Cappiello EC, Robinson JN, Tsen LC: Dural puncture epidural technique improves labor analgesia quality with fewer side effects compared with epidural and combined spinal epidural techniques: A randomized clinical trial. Anesth Analg 2017; 124:560–9
7. Richardson MG, Baysinger CL: Dural puncture epidural technique: Not so fast. Anesth Analg 2017; 125:700
8. Heesen M, Rijs K, Rossaint R, Klimek M: Dural puncture epidural *versus* conventional epidural block for labor analgesia: A systematic review of randomized controlled trials. Int J Obstet Anesth 2019; 40:24–31
9. Layera S, Bravo D, Aliste J, Tran DQ: A systematic review of DURAL puncture epidural analgesia for labor. J Clin Anesth 2019; 53:5–10
10. Lu YY, Cai JJ, Jin SW, Wang CH, Zhou YF, Hu MP, Li J: Application of dural puncture epidural technique for labor analgesia (translated from Chinese). Zhonghua Yi Xue Za Zhi 2020; 100:363–6
11. Song Y, Du W, Zhou S, Zhou Y, Yu Y, Xu Z, Liu Z: Effect of dural puncture epidural technique combined with programmed intermittent epidural bolus on labor analgesia onset and maintenance: A randomized controlled trial. Anesth Analg 2021; 132:971–8
12. Wang J, Zhang L, Zheng L, Xiao P, Wang Y, Zhang L, Zhou M: A randomized trial of the dural puncture epidural technique combined with programmed intermittent epidural boluses for labor analgesia. Ann Palliat Med 2021; 10:404–14
13. Wilson SH, Wolf BJ, Bingham K, Scotland QS, Fox JM, Woltz EM, Hebbar L: Labor analgesia onset with dural puncture epidural *versus* traditional epidural using a 26-gauge Whitacre needle and 0.125% bupivacaine bolus: A randomized clinical trial. Anesth Analg 2018; 126:545–51

The Pulse Oximeter Is Amazing, but Not Perfect

Philip Bickler, M.D., Ph.D., Kevin K. Tremper, Ph.D., M.D.

It is amazing to think that a device developed for aviation research during World War II and implemented into anesthesia care in the mid-1980s is now likely the most common medical device on Earth—with the possible exception of the thermometer. In the 1940s, Glenn Allen Millikan developed an ear oximeter to estimate hemoglobin saturation for determination of when high-altitude World War II fighter and bomber pilots required supplemental oxygen.[1] The Millikan oximeter required cumbersome calibration and so remained a research device for the next 30 yr. It was the ingenious observation of Takou Aoyagi in 1974 that the arterial signal could be obtained without calibration, if you assume that the only pulsatile absorber in the tissue is the pulsing arterial blood. Aoyagi's pulse oximeter involved a relatively simple device of light-emitting diodes and photodiode detectors and used the pulsatile absorbance signal to estimate arterial hemoglobin saturation. Once an empiric calibration for this approach was established for human subjects in controlled laboratory hypoxia conditions, no further calibration of pulse oximeters is needed. For the most part, the device today is the same as the original pulse oximeters of the 1980s.

"How does nonpulsatile skin pigmentation affect the pulse oximeter accuracy…?"

Before the pulse oximeter, clinicians relied on observed cyanosis to detect hypoxemia. Julius Comroe at the University of California, San Francisco (San Francisco, California), conducted volunteer studies in the 1940s using a Millikan oximeter to assess the accuracy of clinicians' ability to detect clinical cyanosis.[2] He demonstrated that these observations were unreliable until saturation was less than 80% and still highly variable between subjects and observers. This study was conducted in a well-lit setting in White subjects, recognizing that darker skin would make the detection of anoxemia more difficult, hence, the need for and rapid adoption of pulse oximetry as a standard of care.

In this issue of Anesthesiology, Burnett *et al.* analyze the accuracy of pulse oximeters in a large retrospective cohort of anesthetized patients with varying degrees of skin pigmentation.[3] It was noted in previous studies of volunteer subjects and intensive care unit patients that pulse oximeter readings were erroneously higher at lower saturations in patients with darker skin.[4] This current operating room study analyzed 11 yr of data from 46,000 patients under anesthesia. Their surrogate marker for skin pigmentation was self-reported race in the categories of White, Black, Hispanic, Asian, and Other. They estimated arterial oxygen saturation (Sa_{O_2}) by calculating saturation from blood gas data. The traditional way of assessing the accuracy of two methods of measuring a variable (*e.g.*, oxygen saturation measured by pulse oximetry [Sp_{O_2}] *vs.* Sa_{O_2}) is by a bias analysis—that is, the mean difference between the two measures and the SD of those differences. The bias being the average difference is the systematic error, and the SD of differences (or precision, as it is sometimes called) the random error.

In addition to determining the bias and precision by skin pigmentation groups, they also chose a clinical measure of the incidence of unrecognized hypoxemia defined as a saturation Sa_{O_2} less than 88% when the Sp_{O_2} reading was greater than 92 to 96%. In this analysis, they found that the incidence of occult hypoxemia differed with skin pigmentation (*e.g.*, White, 1.1%; Hispanic, 1.8%; and Black, 2.1%). The good news is this is a low incidence; the better news is that for the group with Sp_{O_2} greater than 96%, incidence was rare, and there were no differences among racial/ethnic groups. So, the clinical bottom line is to keep the Sp_{O_2} greater than 96%. If that cannot be achieved by increasing fraction of inspired oxygen or modifying positive

Image: Adobe Stock.

Accepted for publication February 11, 2022. Published online first on March 18, 2022. This editorial accompanies the article on p. 688.

Philip Bickler, M.D., Ph.D.: Department of Anesthesiology, University of California, San Francisco, San Francisco, California.

Kevin K. Tremper, Ph.D., M.D.: Department of Anesthesiology, University of Michigan, Ann Arbor, Michigan.

 Anesthesiology 2022; 136:670–1. DOI: 10.1097/ALN.0000000000004171

end-expiratory pressure, an invasive blood sample may be considered.

Several comments and questions related to the conclusions of the work from Burnett *et al.* are appropriate. Pulse oximeter errors and bias can be caused by motion (shivering), interfering substances (carboxyhemoglobin, methemoglobin), mistiming of blood draws and oximeter readings, optical interference, probe misplacement, and low perfusion. In the case of low perfusion, reductions in the pulse oximeter signal are compounded by light absorption by melanin. In the study by Burnett *et al.*, none of these factors were controlled. In addition, Black patients were older on average (62 *vs.* 52 yr) and had a greater incidence of kidney failure and diabetes than White patients. Could these disparities have contributed to lower perfusion, and amplified the calibration error? Further study is needed.

During the early years of pulse oximetry, it is likely that the in-human testing of pulse oximeters involved almost all White patients. It was not until 2005 that the limitations of this approach were identified.[4] It was noted that darker skin pigmentation caused a positive bias—that is, the pulse oximeter reading was higher than the actual saturation measured on a blood sample. The error was greater in saturation ranges that were less than 80%, but some bias existed at higher ranges as well. A recent controlled laboratory study, with multiple types of good-quality oximeters for sale in 2017 to 2020, found that oximeters *still* read 1 to 2% too high in patients with darker skin who were near the critical 90% hypoxia threshold.[5]

How does nonpulsatile skin pigmentation affect the pulse oximeter accuracy, particularly in producing a positive bias that might cause hypoxemia to be missed? The pulse oximeter measures the ratio of the pulse's added absorbance in red and infrared light transmitted through the tissue. The ratio (R) is then empirically calibrated with human volunteer data to produce an "R calibration curve," (*e.g.*, $R = 3.4$, $Spo_2 = 100\%$; $R = 1.0$, $Spo_2 = 85\%$). If the pigment acts as a variable light filter for the transmitted light frequency, the peak frequency could slightly change and produce a slightly changed R and slightly altered Spo_2 value. The red light-emitting diodes used in pulse oximeters do not produce a single wavelength of red light, but rather a bell curve distribution of wavelengths, and the shorter wavelengths of this distribution are more heavily absorbed by melanin than the longer. In effect, the R curve for patients with darker skin pigmentation needs to be different than that for White patients.

Another unanswered important clinical question is regarding patients who live in the low saturation ranges. The current study provides reassurance when Spo_2 is greater than 96%, but what about children with cyanotic heart disease? These patients live in the most error-prone range of Spo_2. During general anesthesia, it is rare to have patients with sustained saturations in the low 90s or 80s, but it is part of the treatment plan for patients with cyanotic heart disease. This population needs further study.

Overall, the work of Burnett *et al.* provides clinical context to errors in a device that we depend on every day. It gives us new targets for saturation ranges to be safe for all patients. The pulse oximeter is incredibly useful and reliable for medical monitoring, and it works on a tremendous range of patients. Even in the very low ranges of saturation where there are few to no calibration data, its directional trends are very useful. We should give thanks to the ingenuity of Takuo Aoyagi every day when we are reassured by that *beep, beep, beep*.

Competing Interests

The authors are not supported by, nor maintain any financial interest in, any commercial activity that may be associated with the topic of this article.

Correspondence

Address correspondence to Dr. Tremper: ktremper@umich.edu

References

1. Tremper KK, Barker SJ: Pulse oximetry. Anesthesiology 1989; 70:98–108
2. Comroe JH Jr, Botelho S: The unreliability of cyanosis in the recognition of arterial anoxemia. Am J Med Sci 1947; 124:1–6
3. Burnett GW, Stannard B, Wax DB, Lin H-M, Pyram-Vincent C, DeMaria S Jr, Levin MA: Self-reported race/ethnicity and intraoperative occult hypoxemia: A retrospective cohort study. Anesthesiology 2022; 136:688–96
4. Bickler PE, Feiner JR, Severinghaus JW: Effects of skin pigmentation on pulse oximeter accuracy at low saturation. Anesthesiology 2005; 102:715–9
5. Okunlola OE, Lipnick MS, Batchelder PB, Bernstein M, Feiner JR, Bickler PE: Pulse oximeter performance, racial inequity, and the work ahead. Respir Care 2022; 67:252–7

Fluid Balance: Another Variable to Consider with Diaphragm Dysfunction?

Robinder G. Khemani, M.D., M.S.C.I.

While mechanical ventilation is lifesaving for children with acute respiratory distress syndrome (ARDS), it has become clear that it can lead to significant harm from ventilator-induced lung injury, patient self-inflicted lung injury, and ventilator-induced diaphragm dysfunction.[1] To that end, therapeutic strategies that try to balance lung and diaphragm protection have become a priority in both pediatric and adult ARDS.[2] In this month's issue, Ijland *et al.*[3] provide provocative results evaluating the effect of fluid strategies on diaphragm function in an experimental model of pediatric ARDS. The results highlight that fluid management can have potentially competing effects on the lung and the diaphragm.

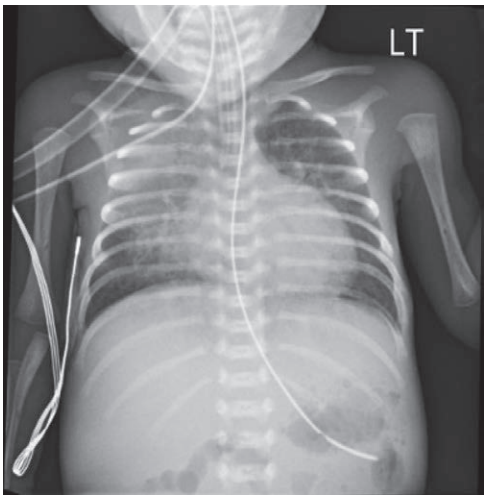

"…fluid management can have potentially competing effects on the lung and the diaphragm."

The authors should be commended for an elegant and comprehensive controlled study, conducted in 19 lambs with on average moderate ARDS. The authors hypothesized that lambs managed with a liberal fluid strategy would have more impairment in diaphragm strength, because the liberal strategy would promote more edema in diaphragm myofibrils, impairing force-generating capacity. They found, in contrast to their hypothesis, that lambs managed with a restrictive fluid strategy with use of norepinephrine to maintain blood pressure and cardiac output had a nearly 10 cm H_2O loss in contractile activity of the diaphragm with electrical stimulation, while the liberal fluid strategy group had minimal noticeable change in diaphragm function. Mechanistically, the study found no clear differences in histopathologic findings of size or shape of type I or II myofibrils in the diaphragm between groups and no difference in markers of inflammation or oxidative stress. The authors speculate that potential mechanisms for this observed difference may relate to restrictions in microvascular circulation with the use of norepinephrine and restrictive fluids or disturbances at the level of the neuromuscular junction. While they were unable to test the latter hypothesis, the restrictive fluid group may have had lower density of microvessels, although this was not statistically significant and possibly underpowered for a meaningful effect.

In addition, the authors describe a novel finding related to positive end-expiratory pressure (PEEP) levels and the force-generating ability of the diaphragm. The authors found that as PEEP was increased from 5 to 10, 15, and 20 cm H_2O, there was a dose-dependent reduction in the force-generating capacity of the diaphragm, and this PEEP effect was more important than the impact of fluids when PEEP levels were very high (*i.e.*, 15 to 20 cm H_2O). Certainly, it is highly plausible that the force-generating capacity of the diaphragm will decrease as PEEP is increased if it results in more flattening and elongation of the diaphragm at rest. These higher levels of PEEP may put the diaphragm at more of a mechanical disadvantage, which thereby results in less force. In this experiment, the force was measured with electrical stimulation of the phrenic nerves directly, but these findings corroborate previous investigations in spontaneously breathing adults with vigorous effort where increasing PEEP results in a reduction in large swings in esophageal pressure.[4] There are other potential mechanisms through which increasing PEEP may decrease respiratory effort in spontaneously breathing patients such as lung recruitment and Hering–Breuer reflexes, but the findings from this study highlight the potential impact that diaphragmatic elongation and location have on force generation. This implies that we should be standardizing PEEP levels when measuring the force-generating capacity of the

Image: J. P. Rathmell.

Accepted for publication February 23, 2022. Published online first on March 24, 2022. This editorial accompanies the article on p. 749.

Robinder G. Khemani, M.D., M.S.C.I.: Department of Anesthesiology and Critical Care Medicine, Children's Hospital Los Angeles, Los Angeles, California; Department of Pediatrics, University of Southern California Keck School of Medicine, Los Angeles, California.

 Anesthesiology 2022; 136:672–4. DOI: 10.1097/ALN.0000000000004191

diaphragm, regardless of the method (*i.e.*, electrical stimulation, maximal effort maneuvers during airway occlusion, or noninvasive measurements such as ultrasound). We certainly need more mechanistic and clinical studies focused on the interaction between PEEP and diaphragm function in mechanically ventilated adults and children.

So, how can we use these findings to help us at the bedside? Given that these are preclinical data, we certainly should not be changing clinical practice based on these results. However, this study highlights that fluid management is yet another variable that we need to carefully consider as we are investigating risk factors for ventilator-induced diaphragm dysfunction and devising treatment strategies. Controlled trials in adults with ARDS and multiple observational studies in pediatric ARDS have demonstrated improved oxygenation and potential improvements in short-term clinical outcomes when ARDS patients are managed with a restrictive fluid strategy.[5–7] These benefits are likely coming from improved respiratory compliance and oxygenation, leading to less lung stress, and lowering the risk of ventilator-induced lung injury. However, findings from this study have highlighted that these restrictive strategies that try to protect the lung may harm the diaphragm. This is, of course, not the first time that therapeutic strategies developed to protect the lung have had negative consequences on the diaphragm. Controlled ventilation with sedation or neuromuscular blockade is extremely common in adults and children with ARDS, to prevent progression of ventilator-induced lung injury. However, this leads to subphysiologic levels of patient effort, which can lead to overassistance myotrauma of the diaphragm, with atrophy and loss of force-generating capacity.[1] Certainly, protecting the lung should take priority, as ventilator-induced lung injury is clearly associated with multiple organ dysfunction and death. However, as our strategies to prevent ventilator-induced lung injury improve with time, we have an opportunity to try to simultaneously prevent diaphragmatic dysfunction. While some elements of diaphragmatic dysfunction are evident during the acute phase of ventilation (*i.e.*, prolonged weaning, extubation failure), there are longer-term impacts on post–intensive care unit health-related quality of life, respiratory health, and even mortality.[8] Hence, preventing diaphragm dysfunction should be a priority for us at the bedside.

In conclusion, the work by Ijland *et al.*[3] has provided provocative insights into the potential role that fluid balance and management strategies may have on the development of diaphragm dysfunction in ARDS. While this study was conducted in lambs, which are meant to represent pediatric-size patients, the findings are likely applicable more broadly. While these data do not warrant a change in clinical practice, they highlight that we must systematically evaluate the impact of fluid management strategies in all investigations related to ventilator-induced diaphragm dysfunction. Moreover, this study has also highlighted that PEEP levels should be standardized when performing measurements of diaphragmatic strength.

Research Support

Supported by National Institutes of Health (Bethesda, Maryland) grant Nos. 1RO11HL134666-01, 3R01HL134666-04S1, 1R13HD102137-01, 1RL1HD107785-01, 1R44HD103566-01, and 1R44HL150926-01 and by the Thrasher Foundation (Salt Lake City, Utah) and the Department of Anesthesiology and Critical Care Medicine at Children's Hospital Los Angeles (Los Angeles, California).

Competing Interests

The author is not supported by, nor maintains any financial interest in, any commercial activity that may be associated with the topic of this article.

Correspondence

Address correspondence to Dr. Khemani: rkhemani@chla.usc.edu

References

1. Goligher EC, Dres M, Patel BK, Sahetya SK, Beitler JR, Telias I, Yoshida T, Vaporidi K, Grieco DL, Schepens T, Grasselli G, Spadaro S, Dianti J, Amato M, Bellani G, Demoule A, Fan E, Ferguson ND, Georgopoulos D, Guérin C, Khemani RG, Laghi F, Mercat A, Mojoli F, Ottenheijm CAC, Jaber S, Heunks L, Mancebo J, Mauri T, Pesenti A, Brochard L: Lung- and diaphragm-protective ventilation. Am J Respir Crit Care Med 2020; 202:950–61
2. Khemani RG, Hotz JC, Klein MJ, Kwok J, Park C, Lane C, Smith E, Kohler K, Suresh A, Bornstein D, Elkunovich M, Ross PA, Deakers T, Beltramo F, Nelson L, Shah S, Bhalla A, Curley MAQ, Newth CJL: A phase II randomized controlled trial for lung and diaphragm protective ventilation (Real-time Effort Driven VENTilator management). Contemp Clin Trials 2020; 88:105893
3. Ijland MM, Ingelse SA, van Loon LM, van Erp M, Kusters B, Ottenheijm CAC, Kox M, van der Hoeven JG, Heunks LMA, Lemson J: Early restrictive fluid strategy impairs the diaphragm force in lambs with acute respiratory distress syndrome. Anesthesiology 2022; 136:749–62
4. Yoshida T, Grieco DL, Brochard L, Fujino Y: Patient self-inflicted lung injury and positive end-expiratory pressure for safe spontaneous breathing. Curr Opin Crit Care 2020; 26:59–65
5. Yehya N, Harhay MO, Klein MJ, Shein SL, Piñeres-Olave BE, Izquierdo L, Sapru A, Emeriaud G, Spinella PC, Flori HR, Dahmer MK, Maddux AB, Lopez-Fernandez YM, Haileselassie B, Hsing DD, Chima

RS, Hassinger AB, Valentine SL, Rowan CM, Kneyber MCJ, Smith LS, Khemani RG, Thomas NJ; Pediatric Acute Respiratory Distress Syndrome Incidence and Epidemiology (PARDIE) V1 Investigators and the Pediatric Acute Lung Injury and Sepsis Investigators (PALISI) Network. Predicting mortality in children with pediatric acute respiratory distress syndrome: A pediatric acute respiratory distress syndrome incidence and epidemiology study. Crit Care Med 2020; 48:e514–22

6. Valentine SL, Nadkarni VM, Curley MA; Pediatric Acute Lung Injury Consensus Conference Group: Nonpulmonary treatments for pediatric acute respiratory distress syndrome: Proceedings from the Pediatric Acute Lung Injury Consensus Conference. Pediatr Crit Care Med 2015; 16(5 suppl 1):S73–85
7. Wiedemann HP, Wheeler AP, Bernard GR, Thompson BT, Hayden D, deBoisblanc B, Connors AF, Hite RD, Harabin AL; National Heart Lung, and Blood Institute Acute Respiratory Distress Syndrome (ARDS) Clinical Trials Network: Comparison of two fluid-management strategies in acute lung injury. N Engl J Med 2006; 354:2564–75
8. Medrinal C, Prieur G, Frenoy É, Robledo Quesada A, Poncet A, Bonnevie T, Gravier FE, Lamia B, Contal O: Respiratory weakness after mechanical ventilation is associated with one-year mortality: A prospective study. Crit Care 2016; 20:231

Ketamine Analgesia and Psychedelia: Can We Dissociate Dissociation?

George A. Mashour, M.D., Ph.D.

Ketamine is arguably the most interesting drug in our armamentarium. Depending on the dose and setting, ketamine can be used as an anesthetic, analgesic, antidepressant, psychedelic, or psychotomimetic (*e.g.*, to model psychiatric disorders such as schizophrenia). But what is the interrelationship of these psychoactive properties? Are they all reducible to a single and fundamental cause? Or do they represent a constellation of dissociable traits with distinct underlying mechanisms? In this issue of Anesthesiology, Olofsen *et al.* report a study that attempts to dissect the antinociceptive and psychedelic effects of ketamine.[1]

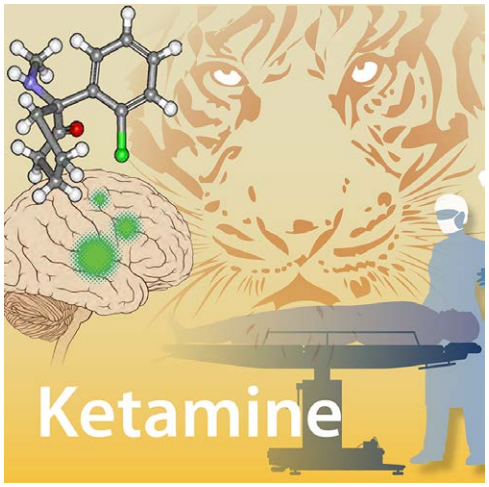

"… if [ketamine] works, who cares whether the analgesic and psychedelic effects are mechanistically distinct?"

The story of ketamine (or CI-581, as it was then known) began in the 1960s, when it was synthesized as an analog to mitigate the profound and prolonged emergence of delirium associated with phencyclidine. Clinical pharmacologist Dr. Edward Domino and anesthesiologist Dr. Guenter Corssen, two faculty members at the University of Michigan Medical School (Ann Arbor, Michigan), were the first to study ketamine in human patients.[2] After hearing of the unusual disconnection from the environment induced by ketamine, Domino's wife suggested that it be described as a "dissociative anesthetic." This phrase appeared in the first publication describing the clinical effects of ketamine anesthesia[3] and continues to be used today. Focusing on the dissociative effects of this drug is warranted because, although ketamine evokes numerous canonical traits of the psychedelic experience, the intensity of the dissociative experience far exceeds that induced by serotonergic counterparts such as psilocybin.[4]

Another reason it is important to highlight this signature feature of dissociation is that it could account for the other observed effects of ketamine. Perhaps pain, for example, is attenuated during exposure to ketamine because the self does not feel connected to the body that might be encountering the noxious stimulus. But if it works, who cares whether the analgesic and psychedelic effects are mechanistically distinct? The answer is that if these effects can be mechanistically differentiated, then it might be possible to design new drugs that can accomplish the analgesic (or antidepressant) actions of ketamine without the psychedelic and dissociative effects, which can be dysphoric for many. Along these lines, a laboratory study of methylenedioxymethamphetamine (commonly referred to as "MDMA" and colloquially known as "ecstasy") showed that the neural mediators responsible for pro-social effects and drug reward effects were distinct.[5] Incidentally, we, as a field, should be proud that an anesthesiologist, Dr. Boris Heifets from Stanford University (Stanford, California), conducted that study. In sum: understanding the dissociative effects of ketamine is of central importance to its neuropharmacology, and determining if dissociation and analgesia (or other effects) are mechanistically distinct is important for future drug discovery.

The approach of Olofsen *et al.* to address this question was to reanalyze a study of ketamine in 17 males.[1] The original study was a four-armed randomized trial,[6] but for this *post hoc* analysis, only two groups were investigated. One group received racemic ketamine, and another received S-ketamine, both with escalating infusion rates. During infusion, investigators assessed pain thresholds (antinociceptive effects) and perceptual disturbances (psychedelic effects). Blood drawn from an arterial catheter was used to measure plasma concentrations of ketamine and its metabolite norketamine; pharmacokinetic/pharmacodynamic models were generated. The overall goal was to identify the

Image: A. Johnson, Vivo Visuals Studio.

Accepted for publication February 11, 2022. Published online first on March 18, 2022. This editorial accompanies the article on p. 792.

George A. Mashour, M.D., Ph.D.: Department of Anesthesiology, University of Michigan Medical School, Ann Arbor, Michigan.

 Anesthesiology 2022; 136:675–7. DOI: 10.1097/ALN.0000000000004172

<zdoi;. DOI: 10.1097/ALN.0000000000004172>

effect-site drug concentration at which antinociceptive or psychedelic effects appeared. What the investigators found was that the model for the antinociceptive effect of ketamine and the model for the psychedelic effect of ketamine were not statistically distinguishable. Furthermore, including both endpoints in the same model improved its performance. The conclusion was that the antinociceptive and psychedelic effects of ketamine co-appear, suggesting interdependence and a common underlying mechanism. These findings, however, are not consistent with the results of previous work, including that from the authors. For example, Gitlin *et al.*[7] administered 2 mg/kg IV ketamine to 15 healthy volunteers and identified distinct models for analgesia and dissociative effects, suggesting independence and distinct underlying mechanisms. The Discussion section in the article from Olofsen *et al.*[1] appropriately addresses the many methodologic differences between their work and that of others as a way of accounting for the divergent findings.

So, what is the next stop on the ketamine trip? First, back to the laboratory. The most definitive way to address whether the psychedelic and analgesic effects of ketamine have distinct mechanisms is to dissect them based on receptors and/or neural circuits. As noted, the work on methylenedioxymethamphetamine is an encouraging precedent.[5] Furthermore, since the onset time for analgesic and psychedelic effects is important for investigations in humans, it is important to remember that ketamine has complex and fast dynamics in the human cortex. For example, ketamine anesthesia is associated with rapid alternation of low-frequency and high-frequency electroencephalographic signals, accompanied by shifts in complexity and functional connectivity.[8–10] Last, for those who are wondering how to assess psychedelic effects in animal or translational models, neurophysiologic findings such as increased complexity or altered cortical oscillations that correlate with psychedelic phenomenology in humans can also be identified in the rodent brain during exposure to subanesthetic ketamine.[11] Collectively, this line of investigation can yield important scientific contributions and is aligned with a wider trend of synthesizing nonhallucinogenic analogs of psychedelic drugs that have therapeutic potential, as has been recently done with ibogaine[12] and lysergic acid diethylamide (known widely as "LSD").[13]

In conclusion, the work of Olofsen *et al.*[1] challenges us to take the next step in basic, translational, and clinical research. Importantly, the healthy controversy surrounding ketamine in our field is connected to a much broader and more intense dialog of whether the apparent therapeutic effects of psychedelic drugs such as psilocybin or dimethyltryptamine are necessarily linked to altered states of consciousness *per se*, or whether therapeutic benefit can ultimately be dissociated from dissociation and other dimensions of the psychedelic experience.

Research Support

Dr. Mashour is supported by R01GM111293 from the National Institutes of Health (Bethesda, Maryland).

Competing Interests

Dr. Mashour is a consultant for TRYP Therapeutics (San Diego, California); however, his consulting is not related to ketamine.

Correspondence

Address correspondence to Dr. Mashour: gmashour@med.umich.edu

References

1. Olofsen E, Kamp J, Henthorn TK, van Velzen M, Niesters M, Sarton E, Dahan A: Ketamine psychedelic and antinociceptive effects are connected. Anesthesiology 2022; 136:792–801
2. Domino EF: Taming the ketamine tiger. Anesthesiology 2010; 113:678–84
3. Corssen G, Domino EF: Dissociative anesthesia: Further pharmacologic studies and first clinical experience with the phencyclidine derivative CI-581. Anesth Analg 1966; 45:29–40
4. Studerus E, Gamma A, Vollenweider FX: Psychometric evaluation of the altered states of consciousness rating scale (OAV). PLoS One 2010; 5:e12412
5. Heifets BD, Salgado JS, Taylor MD, Hoerbelt P, Cardozo Pinto DF, Steinberg EE, Walsh JJ, Sze JY, Malenka RC: Distinct neural mechanisms for the prosocial and rewarding properties of MDMA. Sci Transl Med 2019; 11:eaaw6435
6. Jonkman K, van der Schrier R, van Velzen M, Aarts L, Olofsen E, Sarton E, Niesters M, Dahan A: Differential role of nitric oxide in the psychedelic symptoms induced by racemic ketamine and esketamine in human volunteers. Br J Anaesth 2018; 120:1009–18
7. Gitlin J, Chamadia S, Locascio JJ, Ethridge BR, Pedemonte JC, Hahm EY, Ibala R, Mekonnen J, Colon KM, Qu J, Akeju O: Dissociative and analgesic properties of ketamine are independent. Anesthesiology 2020; 133:1021–8
8. Akeju O, Song AH, Hamilos AE, Pavone KJ, Flores FJ, Brown EN, Purdon PL: Electroencephalogram signatures of ketamine anesthesia-induced unconsciousness. Clin Neurophysiol 2016; 127:2414–22
9. Li D, Mashour GA: Cortical dynamics during psychedelic and anesthetized states induced by ketamine. Neuroimage 2019; 196:32–40
10. Li D, Vlisides PE, Mashour GA: Dynamic reconfiguration of frequency-specific cortical coactivation patterns during psychedelic and anesthetized states induced by ketamine. Neuroimage 2022; 249:118891

11. Brito MA, Li D, Fields CW, Rybicki-Kler C, Dean JG, Liu T, Mashour GA, Pal D: Cortical acetylcholine levels correlate with neurophysiologic complexity during subanesthetic ketamine and nitrous oxide exposure in rats. Anesth Analg 2021 [Epub ahead of print]
12. Cameron LP, Tombari RJ, Lu J, Pell AJ, Hurley ZQ, Ehinger Y, Vargas MV, McCarroll MN, Taylor JC, Myers-Turnbull D, Liu T, Yaghoobi B, Laskowski LJ, Anderson EI, Zhang G, Viswanathan J, Brown BM, Tjia M, Dunlap LE, Rabow ZT, Fiehn O, Wulff H, McCorvy JD, Lein PJ, Kokel D, Ron D, Peters J, Zuo Y, Olson DE: A non-hallucinogenic psychedelic analogue with therapeutic potential. Nature 2021; 589:474–9
13. Cao D, Yu J, Wang H, Luo Z, Liu X, He L, Qi J, Fan L, Tang L, Chen Z, Li J, Cheng J, Wang S: Structure-based discovery of nonhallucinogenic psychedelic analogs. Science 2022; 375:403–11

ANESTHESIOLOGY

Quality of Labor Analgesia with Dural Puncture Epidural *versus* Standard Epidural Technique in Obese Parturients: A Double-blind Randomized Controlled Study

Hon Sen Tan, M.D., M.Med., M.H.Sc.,
Sydney E. Reed, M.D., Jennifer E. Mehdiratta, M.D., M.P.H.,
Olga I. Diomede, M.D., M.S., Riley Landreth, M.D.,
Luke A. Gatta, M.D., Daniel Weikel, M.Sc.,
Ashraf S. Habib, M.B.B.Ch., M.Sc., M.H.Sc., F.R.C.A.

ANESTHESIOLOGY 2022; 136:678–87

EDITOR'S PERSPECTIVE

What We Already Know about This Topic

- The "dural puncture epidural technique" is performed by puncturing the dura with a spinal needle but without injecting medications intrathecally.
- Dural puncture epidural has been suggested to improve the efficacy of labor epidural analgesia, potentially by increasing the likelihood of midline placement or by facilitating the translocation of medication from the epidural to intrathecal space. However, data regarding the efficacy of this technique are mixed.
- Obese patients are at higher risk for epidural failure, so the dural puncture technique may have particular utility in this population.

What This Article Tells Us That Is New

- A total of 132 term parturients with body mass index of 35 kg · m^{-2} or greater were randomized to either a dural puncture epidural using a 25-gauge Whitacre needle or a standardized epidural technique. This was followed, in both groups, by maintenance with programed intermittent boluses and patient-controlled epidural analgesia.
- The primary outcome was a composite of five outcomes indicating lower quality of labor analgesia. There was no meaningful difference between the two groups (52 *vs.* 49%; absolute risk difference, 3.0%; 95% CI, –14.0 to 20.1%) in the primary outcome or the secondary outcomes assessed.
- The study excludes a large benefit for dural puncture epidural in improving labor analgesia in obese parturients, although CI ranges for the primary outcome were wide and do not fully exclude the potential for a clinically meaningful effect.

ABSTRACT

Background: The dural puncture epidural technique may improve analgesia quality by confirming midline placement and increasing intrathecal translocation of epidural medications. This would be advantageous in obese parturients with increased risk of block failure. This study hypothesizes that quality of labor analgesia will be improved with dural puncture epidural compared to standard epidural technique in obese parturients.

Methods: Term parturients with body mass index greater than or equal to 35 kg · m^{-2}, cervical dilation of 2 to 7 cm, and pain score of greater than 4 (where 0 indicates no pain and 10 indicates the worst pain imaginable) were randomized to dural puncture epidural (using 25-gauge Whitacre needle) or standard epidural techniques. Analgesia was initiated with 15 ml of 0.1% ropivacaine with 2 μg · ml^{-1} fentanyl, followed by programed intermittent boluses (6 ml every 45 min), with patient-controlled epidural analgesia. Parturients were blinded to group allocation. The data were collected by blinded investigators every 3 min for 30 min and then every 2 h until delivery. The primary outcome was a composite of (1) asymmetrical block, (2) epidural top-ups, (3) catheter adjustments, (4) catheter replacement, and (5) failed conversion to regional anesthesia for cesarean delivery. Secondary outcomes included time to a pain score of 1 or less, sensory levels at 30 min, motor block, maximum pain score, patient-controlled epidural analgesia use, epidural medication consumption, duration of second stage of labor, delivery mode, fetal heart tones changes, Apgar scores, maternal adverse events, and satisfaction with analgesia.

Results: Of 141 parturients randomized, 66 per group were included in the analysis. There were no statistically or clinically significant differences between the dural puncture epidural and standard epidural groups in the primary composite outcome (34 of 66, 52% *vs.* 32 of 66, 49%; odds ratio, 1.1 [0.5 to 2.4]; $P = 0.766$), its individual components, or any of the secondary outcomes.

Conclusions: A lack of differences in quality of labor analgesia between the two techniques in this study does not support routine use of the dural puncture epidural technique in obese parturients.

(ANESTHESIOLOGY 2022; 136:678–87)

Neuraxial analgesia is considered the accepted standard technique for labor pain relief, owing to its excellent efficacy and low risk of adverse effects.[1] Dural puncture epidural involves dural puncture with a spinal needle but without administration of intrathecal drugs. Neuraxial analgesia is then initiated by medications given through an epidural catheter.[2] The purported advantages of dural puncture epidural over the standard epidural technique stem from a clear and definitive endpoint of cerebrospinal fluid (CSF) return *via* the spinal needle. This confirms midline placement of the Tuohy needle and may increase transfer of epidural medications through the dural puncture into the intrathecal space, thereby hastening analgesic onset and improving the quality of analgesia.[2–5] However, available data comparing dural puncture epidural and standard epidural techniques

 Anesthesiology 2022; 136:678–87. DOI: 10.1097/ALN.0000000000004137

are sparse, with two recent systematic reviews reporting no clear evidence of clinical benefit associated with the dural puncture epidural technique.[3,4]

The ostensible advantages of the dural puncture epidural technique would especially benefit obese parturients, in whom difficulty with palpating anatomical landmarks and possible false loss of resistance from increased adipose tissue may make neuraxial placement challenging and increase the epidural catheter failure rate.[6] Moreover, obese parturients are at higher risk of intrapartum cesarean delivery,[7] during which a well-functioning epidural catheter can be used to administer regional anesthesia. This would avoid general anesthesia and its associated risks, such as failed intubation and pulmonary aspiration of gastric contents, which are of particular relevance in obese parturients.[8,9] Hence, we performed this double-blind randomized controlled study to compare dural puncture and standard epidural techniques for neuraxial analgesia in obese parturients, with the hypothesis that the dural puncture epidural technique will be associated with improved quality of labor analgesia compared to the standard epidural technique.

Materials and Methods

After approval by the Duke University Institutional Review Board (Durham, North Carolina; approval No. PRO00079368) and registration on Clinicaltrials.gov (NCT03074695, posted on March 9, 2017; Principal Investigator, Ashraf Habib), this superiority, parallel group, randomized controlled study was conducted from April 2017 to November 2020 at Duke University Medical Center. Written informed consent was obtained from all enrolled parturients.

A convenience sample of women admitted for spontaneous or induced labor was screened for enrollment and approached by investigators. We included English-speaking, nulliparous or multiparous, obese (body mass index greater than or equal to 35 $kg \cdot m^{-2}$) adult parturients (age, 18 to 45 yr) with singleton vertex fetuses at 37 to 41 weeks' gestation, cervical dilation 2 to 7 cm, and with numeric rating scale (0 to 10, where 0 indicates no pain and 10 indicates the worst pain imaginable) pain score greater than 4. We excluded parturients with major cardiac disease, chronic pain, chronic opioid use, previous cesarean delivery, and maternal pelvic/hip disease. The protocol was amended after initiation of the study to allow inclusion of parturients with body mass index greater or equal to 35 $kg \cdot m^{-2}$, whereas the original protocol was limited to parturients with body mass index greater or equal to 40 $kg \cdot m^{-2}$.

One of the study investigators evaluated eligibility, obtained informed consent, and enrolled the participants. After signing the written informed consent, parturients were randomized (1:1 ratio) to receive the dural puncture epidural or standard epidural technique using a computer-generated random number generator, stratified by class of obesity (body mass index 35 to 39.9, 40 to 49.9, and greater or equal to 50 $kg \cdot m^{-2}$) and by parity (nulliparous or multiparous). The allocation sequence was created by the study statistician. Allocation was concealed using sequentially numbered opaque sealed envelopes. Upon request for labor analgesia, the proceduralist opened the envelope containing the group allocation. Parturients, obstetricians, nurses, and anesthesia providers involved in labor analgesia management and data collection were blinded to the group allocation. Neuraxial procedures were performed by the attending anesthesiologist or by senior residents, fellows, or certified registered nurse anesthetists under the supervision of an attending anesthesiologist. The proceduralist and supervising attending anesthesiologist (if applicable) were not involved in subsequent management of labor analgesia.

Parturients received 500 to 1,000 ml of intravenous crystalloid hydration, and a 17-gauge Tuohy needle was sited at the estimated L3–L4 or L4–L5 interspace using loss of resistance to saline, with the parturients in the sitting flexed position. Preprocedure ultrasound was allowed at the discretion of the anesthesiologist. In the dural puncture epidural group, dural puncture with a 25-gauge Whitacre needle was performed using the needle-through-needle technique, and the spinal needle was withdrawn after confirmation of free-flowing CSF. A second attempt would be made, either at the same or at a different space, if CSF return was not observed. In both groups, a 19-gauge Duraflex wire-reinforced multiport catheter (Smith Medical, USA) was threaded 5 cm into the epidural space and secured in the sitting upright position with Tegaderm clear occlusive dressing (3M, USA). After negative aspiration for blood or

This article is featured in "This Month in Anesthesiology," page A1. This article is accompanied by an editorial on p. 667. Supplemental Digital Content is available for this article. Direct URL citations appear in the printed text and are available in both the HTML and PDF versions of this article. Links to the digital files are provided in the HTML text of this article on the Journal's Web site (www.anesthesiology.org). This article has an audio podcast. This article has a visual abstract available in the online version. Part of the work presented in this article has been presented at the Society for Obstetric Anesthesia and Perinatology 53rd Annual Meeting held virtually, May 12, 2021.

Submitted for publication July 22, 2021. Accepted for publication January 4, 2022. Published online first on February 14, 2022.

Hon Sen Tan, M.D., M.Med., M.H.Sc.: The Department of Women's Anesthesia, KK Women's and Children's Hospital, Singapore.

Sydney E. Reed, M.D.: The Divisions of Women's Anesthesia, Department of Anesthesiology, Duke University Medical Center, Durham, North Carolina.

Jennifer E. Mehdiratta, M.D., M.P.H.: The Divisions of Women's Anesthesia, Department of Anesthesiology, Duke University Medical Center, Durham, North Carolina.

Olga I. Diomede, M.D., M.S.: The Divisions of Women's Anesthesia, Department of Anesthesiology, Duke University Medical Center, Durham, North Carolina.

Riley Landreth, M.D.: The Divisions of Women's Anesthesia, Department of Anesthesiology, Duke University Medical Center, Durham, North Carolina.

Luke A. Gatta, M.D.: Department of Obstetrics and Gynecology, Duke University Medical Center, Durham, North Carolina.

Daniel Weikel, M.Sc.: Biostatistics and Bioinformatics, Department of Anesthesiology, Duke University Medical Center, Durham, North Carolina.

Ashraf S. Habib, M.B.B.Ch., M.Sc., M.H.Sc., F.R.C.A.: The Divisions of Women's Anesthesia, Department of Anesthesiology, Duke University Medical Center, Durham, North Carolina.

CSF, analgesia was initiated with divided doses of 15 ml of epidural medication (0.1% ropivacaine with 2 μg · ml^{-1} fentanyl) over 6 min as per standard practice. The end of administration of the loading dose was time zero. At that time, the blinded investigator was called into the room to start data collection. Pain with the preceding contraction was assessed at 3-min intervals for 30 min or until a pain score of 1 or less was achieved. At 30 min, the upper and lower sensory levels were assessed bilaterally using temperature discrimination to ice (defined as the dermatomal level at which the parturient reported the same cold sensation to ice compared to the shoulder), along with the modified Bromage score. Subsequently, pain scores and modified Bromage scores were collected every 2 h until delivery. Thoracic dermatomal sensory levels were assessed along the midclavicular line, in addition to the inguinal crease (L1), anterior thigh (L2), medial knee (L3), medial malleolus (L4), between the great and second toe (L5), lateral heel (S1), and medial popliteal fossa (S2), bilaterally. Motor block was assessed using the modified Bromage score (where 1 indicates unable to flex feet or knees, 2 indicates able to flex feet only, 3 indicates able to flex knees, 4 indicates detectable weakness in hip flexion, and 5 indicates no weakness with hip flexion).[10]

Labor analgesia was maintained with programed intermittent boluses of 6 ml of epidural medication every 45 min initiated 30 min after the loading dose, with the addition of patient-controlled epidural analgesia set at 8 ml per demand dose, lockout for 10 min, and maximum dose of 45 ml · h^{-1}. Breakthrough pain (defined as parturient request for supplemental analgesia beyond self-administered boluses) was managed as follows: asymmetric sensory levels (difference of more than 2 dermatomal levels) were treated by withdrawing the catheter 1 cm, administration of 5 ml of epidural medication, and repositioning of the parturient lateral with the lower sensory block side in the dependent position. Parturients with inadequate block height (bilateral sensory levels below T10) were given 5 ml of epidural medication, with up to 15 ml permitted over 15 min. Parturients with breakthrough pain despite adequate sensory levels (above T10 bilaterally) were treated with 100 μg of epidural fentanyl. Last, breakthrough pain persisting despite these interventions was assessed by the attending anesthesiologist for subsequent management.

In addition to pain scores, sensory levels, and modified Bromage scores, the following data were recorded every 2 h until delivery: presence of hypotension (systolic blood pressure less than 20% from admission blood pressure of less 90 mmHg), nausea, pruritus, asymmetric sensory block, need for epidural top-up, and catheter adjustment or replacement. On postpartum day 1, parturients were assessed for postdural puncture headache and were asked about their satisfaction with labor analgesia (where 0 indicates very dissatisfied and 10 indicates very satisfied). An obstetrician blinded to group assignments reviewed tocometry and continuous fetal monitoring stored on the hospital electronic medical system. Uterine contraction and fetal heart rate monitoring patterns were extracted in 10-min epochs, for the periods of 1 h before and 1 h after initial dosing of epidural analgesia. Baseline heart rate was the mean of the six 10-min epochs before and after epidural catheter placement. Quantitative assessment of fetal heart tracings also included variability (minimal, moderate, or marked) and decelerations (late or variable). The obstetrician also assigned a category to the fetal heart tracings before and after the epidural catheter placement based on the three-tier National Institute of Child Health and Human Development (Bethesda, Maryland) system.[11]

The primary outcome of the study was the quality of labor analgesia defined as a composite of (1) asymmetrical block (difference in sensory level of more than 2 dermatomes), (2) epidural top-ups, (3) catheter adjustments, (4) catheter replacement, and (5) failed conversion to regional anesthesia requiring general anesthesia or replacement neuraxial anesthesia in the event of cesarean delivery. All components of the primary composite outcome were treated as binary measures, and the presence of one or more of these components was considered positive for the primary composite outcome. Secondary outcomes included time to adequate analgesia (pain score less than or equal to 1), upper and lower sensory block levels at 30 min, modified Bromage score at 30 min and during labor, maximum pain score during labor, number of patient-controlled epidural analgesia demand and successful boluses, duration of neuraxial analgesia, total epidural medication consumption per hour, duration of second stage of labor, mode of delivery, fetal heart tones (heart rate, decelerations, variability, and National Institute of Child Health and Human Development system classification), Apgar scores at 1 and 5 min, maternal adverse events (hypotension, nausea, pruritus, and postdural puncture headache), and maternal satisfaction with labor analgesia.

Statistical Analysis

Based on a retrospective study by our group,[12] we anticipated that our primary outcome will occur in 35% of parturients assigned to the standard epidural group. Based on the findings by Hess *et al.*[13] of a 62% relative reduction in breakthrough pain with the combined spinal–epidural compared to the standard epidural technique, we defined a clinically meaningful effect as a similar reduction in the composite outcome to 14% in the dural puncture epidural group, which corresponds to an odds ratio of 0.30. A two-sided chi-square test for the difference in primary outcome incidence at an α level of 0.05 had 80% power to detect an odds ratio of 0.30 comparing the dural puncture epidural to the epidural technique in a study of 130 patients (65 per group). We planned to enroll up to 150 parturients to account for possible dropouts, with a goal to stop enrollment once our target sample size was achieved.

The data are reported as median [interquartile range] or number (%) as appropriate. Baseline characteristics were compared between groups using standardized mean difference. The primary composite outcome was analyzed using univariate logistic regression with *post hoc* sensitivity multivariable logistic regression analysis. The multivariable logistic regression included adjustment terms for baseline demographics and obstetric characteristics with standardized mean differences of more than 0.2 between the two groups. Secondary outcomes, such as time to adequate analgesia, sensory block levels, modified Bromage score, maximum pain score during labor, number of patient-controlled epidural analgesia demand and successful boluses, duration of neuraxial analgesia, total epidural medication consumption per hour, duration of second stage of labor, mode of delivery, fetal heart tones, Apgar scores, maternal adverse events, and maternal satisfaction were assessed using Fisher exact tests with associated risk differences for categorical measures and Mann–Whitney U tests with Hodges–Lehman shift for continuous measures. We report group differences with 95% CI, univariable directly calculated, and multivariable based on bootstrapping, in addition to *P* values. A *post hoc* sensitivity analysis excluding epidural top-ups from the composite outcome definition was conducted to explore the impact of including epidural top-ups on the overall study conclusions.

The data were analyzed on an intention-to-treat basis. All *P* values for the secondary outcomes were adjusted for multiple comparisons using the false discovery rate method, and the resulting Q values are presented. Additionally, time to adequate analgesia was compared between the groups *via* Kaplan–Meier estimates and log-rank tests. *P* values and adjusted Q values of less than 0.05 were considered statistically significant. Analysis was performed using *R* 4.0.0, with power calculations performed using NQuery. The detailed trial protocol can be obtained from the corresponding author upon request.

Results

A total of 204 parturients were screened for eligibility, of whom 141 were enrolled. Enrollment ceased after achieving our target sample size. Of the 141 parturients enrolled, 9 patients were excluded due to cesarean delivery before receipt of labor analgesia (n = 2), nonreceipt of labor analgesia (n = 4), or unavailability of research staff (n = 3). In total, 132 parturients completed the study, with 66 randomized to receive dural puncture epidural and 66 to receive standard epidural technique (fig. 1). CSF return was successfully confirmed in all parturients receiving the dural puncture epidural technique. Preprocedure ultrasound was utilized in three patients in the standard epidural group and none of the patients in the dural puncture epidural group. There were no missing data except for fetal heart tones as highlighted in tables 1 and 2. Baseline parturient and obstetric characteristics are summarized in table 1. The dural puncture epidural group had a greater proportion of self-identified Hispanic/Latino parturients, parturients who underwent induction of labor, and taller parturients compared to the standard epidural group.

There were no significant differences between the dural puncture epidural and standard epidural groups in our primary composite outcome of quality of analgesia (34 of 66, 52% *vs*. 32 of 66, 49%; absolute risk difference [95% CI], 3.0% [–14.0 to 20.1%]; odds ratio [95% CI], 1.1 [0.5 to 2.4]; $P = 0.766$, when adjusted for baseline characteristics with a standardized mean difference of more than 0.2 [parturient race, ethnicity, height, and induction status]). A *post hoc* sensitivity analysis excluding epidural top-ups from the primary composite outcome also revealed no significant differences between the groups (20 of 66, 30% *vs.* 17 of 66, 26%; odds ratio [95% CI], 1.09 [0.53 to 2.37]; $P = 0.846$). Details of the primary composite outcome and breakdown of its individual components are summarized in figure 2 and the Supplemental Digital Content (http://links.lww.com/ALN/C788). During labor, three catheters in the dural puncture epidural group needed replacement due to ineffective analgesia, whereas in the standard epidural group, two catheters were replaced due to ineffective analgesia, one catheter was replaced due to asymmetric block, one catheter migrated out of the epidural space, and one catheter was replaced due to disconnection. In both groups, two catheters were replaced for cesarean delivery, with each group having one catheter replaced with another neuraxial block and one converted to general anesthesia. Our secondary outcomes are summarized in table 2. There were no significant intergroup differences in upper and lower sensory block levels at 30 min, modified Bromage score at 30 min or during labor, maximum pain score during labor, number of patient-controlled epidural analgesia demand and successful boluses, duration of neuraxial analgesia, total epidural medication consumption per hour, duration of second stage of labor, mode of delivery, fetal heart tones, Apgar scores at 1 and 5 min, maternal adverse events, and maternal satisfaction with labor analgesia. A log-rank test analyzing the time to pain score 1 or lower showed no significant differences between the groups ($P = 0.650$; data not shown).

Discussion

In this randomized study, we compared the dural puncture epidural and standard epidural techniques for the initiation of neuraxial labor analgesia in obese parturients and found no significant differences in quality of analgesia between the two techniques. Unlike the standard epidural technique, dural puncture epidural involves dural puncture and confirmation of CSF return through the spinal needle. Purportedly, this indirectly confirms correct identification of the epidural space, increases the likelihood of midline Tuohy needle placement, and enhances the transfer of epidural medications into the intrathecal space. However, previous studies comparing dural puncture epidural *versus*

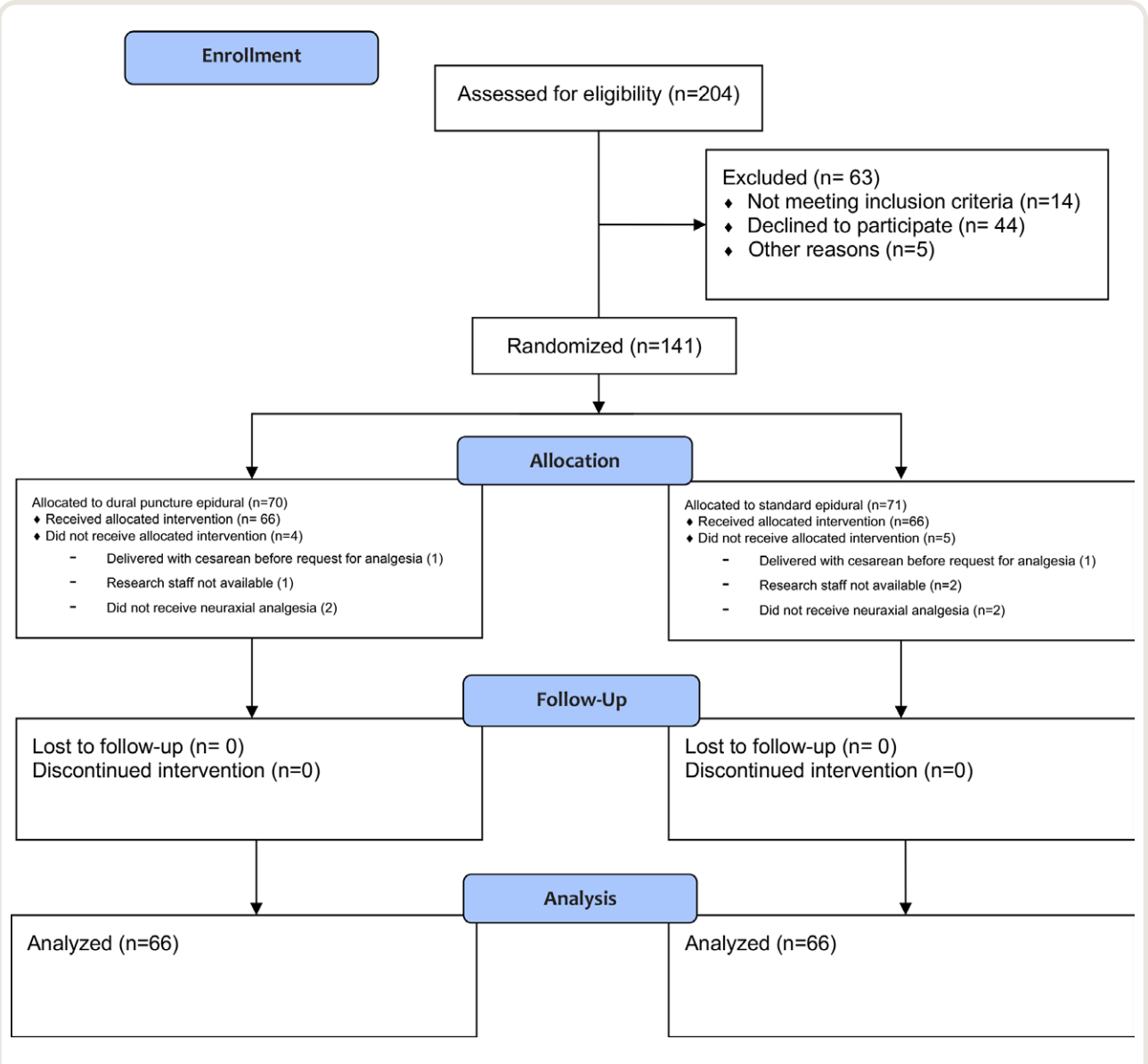

Fig. 1. Consolidated Standards of Reporting Trials flow diagram.

standard epidural techniques for labor analgesia reported conflicting results. Compared to the standard epidural technique, dural puncture epidural with 27-gauge spinal needles did not significantly alter the incidence of catheter manipulation or replacement, sacral block sparing, asymmetrical block, or the need for epidural top-up in one study,[14] while another study also using a 27-gauge spinal needle reported lower pain scores within the first 10 min and faster time to onset of analgesia with the dural puncture epidural compared to standard epidural technique.[15] With 26-gauge spinal needles, dural puncture epidural was associated with faster analgesic onset compared to the standard epidural technique.[16] Using larger 25-gauge spinal needles, both Cappiello *et al.*[17] and Chau *et al.*[5] reported lower incidence of sacral block sparing and asymmetric block with dural puncture epidural compared to the standard epidural technique but detected no significant difference in the time to onset of analgesia. Additionally, Chau *et al.*[5] noted that dural puncture epidural was associated with lower need for epidural top-ups than the standard epidural technique.

Notably, none of these studies specifically investigated the use of the dural puncture epidural technique in obese parturients. Those parturients would particularly benefit from indirect confirmation of Tuohy needle placement within the epidural space, given the increased difficulty in palpating anatomical landmarks and potential for false loss

Table 1. Baseline Demographic and Obstetric Characteristics

Characteristic	Dural Puncture Epidural (n = 66)	Standard Epidural (n = 66)	Standardized Mean Difference
Age, yr (median [interquartile range])	29 [25–34]	30 [25–34]	0.066
Height, cm (median [interquartile range])	165 [160–168]	162 [158–168]	0.212
Weight, kg (median [interquartile range])	115 [104–132]	112 [102–130]	0.007
Body mass index, kg · m^{-2} (median [interquartile range])	41 [39–48]	42 [38–46]	0.132
Body mass index strata			0.054
35–39.9 kg · m^{-2} nulliparous, n (%)	11 (17)	11 (17)	
35–39.9 kg · m^{-2} multiparous, n (%)	11 (17)	12 (18)	
40–49.9 kg · m^{-2} nulliparous, n (%)	19 (29)	19 (29)	
40–49.9 kg · m^{-2} multiparous, n (%)	11 (17)	11 (17)	
≥ 50 kg · m^{-2} nulliparous, n (%)	10 (15)	9 (14)	
≥ 50 kg · m^{-2} multiparous, n (%)	4 (6)	4 (6)	
Race			0.377
White, n (%)	26 (39)	26 (39)	
Black, n (%)	22 (33)	31 (47)	
Other, n (%)	17 (26)	9 (14)	
Ethnicity			0.527
Hispanic or Latino, n (%)	10 (15)	1 (2)	
Non-Hispanic, n (%)	50 (77)	61 (92)	
Unknown, n (%)	6 (8)	4 (6)	
Gravida (median [interquartile range])	2 [1–3]	2 [1–3]	0.106
Parity (median [interquartile range])	0 [0–1]	0 [0–1]	0.031
Nulliparous, n (%)	39 (59)	40 (61)	
Multiparous, n (%)	27 (41)	26 (39)	
Gestational age, wk (median [interquartile range])	39 [38–40]	39 [38–40]	0.109
Pain score at time of neuraxial analgesia (0–10; median [interquartile range])	8 [6–9]	8 [7–9]	0.112
Cervical dilation at time of neuraxial analgesia in cm (median [interquartile range])	4 [4–5]	4 [3–5]	0.129
Proceduralist, n (%)			0.113
Attending	28 (41)	29 (44)	
Certified registered nurse anesthetist	8 (12)	10 (15)	
Fellow	6 (9)	5 (8)	
Resident	24 (36)	22 (33)	
Induction of labor, n (%)	64 (97)	58 (88)	0.349
Fetal heart rate, beats/min (median [interquartile range])	135 [125–140]	135 [125–145]	0.002
Fetal heart rate decelerations, n (%)			0.442
Variable	6 (9)	1 (2)	
Late	6 (9)	3 (3)	
Fetal heart rate variability, n (%)			0.212
Moderate	58 (88)	62 (94)	
Minimal	2 (3)	1 (2)	
Marked	2 (3)	1 (2)	
Missing or not assessed	4 (6)	2 (3)	
National Institute of Child Health and Human Development fetal heart rate classification, n (%)			0.389
Category 1	48 (73)	58 (79)	
Category 2	14 (21)	6 (9)	
Missing or not assessed	4 (6)	2 (3)	

of resistance resulting from adipose tissue. Furthermore, in the case of emergency cesarean delivery, a well-positioned epidural catheter may be used to achieve surgical anesthesia and potentially avoid severe morbidity from failed intubation or pulmonary aspiration that may occur during general anesthesia. However, our results suggest that the dural puncture epidural technique was not associated with significant improvement in our primary and secondary outcomes compared to the standard epidural technique.

In addition to indirect confirmation of midline epidural placement, dural puncture is hypothesized to increase the transfer of epidural medications into the intrathecal space, thereby hastening block onset while improving analgesia quality and sacral blockade.[3] However, the mechanisms governing flux through the meninges are dependent on multiple factors including total epidural drug mass, size of the dural puncture, and inherent rate of drug transfer through the intact meninges.[4,18–20] The effects of epidural drug mass could have contributed to the lack of analgesic benefit of the dural puncture epidural compared to standard epidural technique in our study. Layera *et al.*[4] postulated that the diffusion gradient generated by dilute epidural solutions and smaller drug masses may be insufficient to drive drug transfer across the meninges or dural

Table 2. Secondary Outcomes Associated with Dural Puncture Epidural *versus* Standard Epidural Techniques

Outcome	Dural Puncture Epidural (n = 66)	Standard Epidural (n = 66)	Difference Measure [95% CI]	*P* Value	Adjusted Q Value
Time to pain score ≤ 1, min (median [interquartile range])	12 [9 to 18]	15 [9 to 21]	3 [–3 to 6]	0.367	> 0.999
Upper sensory block height at 30 min*					
Left (median [interquartile range])	T8 [T7 to T10]	T10 [T8 to T10]	1 [0 to 2]	0.016	0.253
Right (median [interquartile range])	T8 [T7 to T10]	T9 [T7 to T10]	0 [0 to 1]	0.301	> 0.999
Lower sensory block height at 30 min*					
Left (median [interquartile range])	S2 [S1 to S2]	S2 [S1 to S2]	0 [0 to 0]	0.509	> 0.999
Right (median [interquartile range])	S2 [S1 to S2]	S2 [S1 to S2]	0 [0 to 0]	0.766	> 0.999
Bromage score at 30 min†					
Left (median [interquartile range])	5 [5 to 5]	5 [5 to 5]	0 [0 to 0]	0.793	> 0.999
Right (median [interquartile range])	5 [5 to 5]	5 [5 to 5]	0 [0 to 0]	0.398	> 0.999
Lowest Bromage score during labor†					
Left (median [interquartile range])	5 [5 to 5]	5 [5 to 5]	0 [0 to 0]	0.484	> 0.999
Right (median [interquartile range])	5 [5 to 5]	5 [5 to 5]	0 [0 to 0]	0.348	> 0.999
Maximum pain score during labor (median [interquartile range])	0 [0 to 4]	1 [0 to 5]	0 [0 to 1]	0.224	> 0.999
Number of patient-controlled epidural analgesia demands per hour (median [interquartile range])	0.8 [0.3 to 1.3]	0.8 [0.4 to 1.4]	0.1 [–0.1 to 0.2]	0.674	> 0.999
Number of patient-controlled epidural analgesia successful boluses per hour (median [interquartile range])	0.5 [0.2 to 0.9]	0.5 [0.3 to 1.0]	0.1 [–0.2 to 0.3]	0.543	> 0.999
Patient-controlled epidural analgesia successful/demand ratio (median [interquartile range])	0.7 [0.5 to 1.0]	0.7 [0.5 to 1.0]	0.0 [–0.1 to 0.1]	0.916	> 0.999
Time to first patient-controlled epidural analgesia dose, h (median [interquartile range])	1.0 [0.5 to 3.5]	1.9 [0.8 to 4.0]	0.2 [–0.4 to 1.0]	0.597	> 0.999
Duration of neuraxial analgesia, h (median [interquartile range])	8.9 [3.0 to 16.5]	8.9 [5.5 to 14.7]	0.5 [–2.4 to 3.1]	0.728	> 0.999
Total epidural medication consumption, ml · h^{-1} (median [interquartile range])	10.8 [8.5 to 14.8]	10.8 [8.2 to 16.3]	0.3 [–1.3 to 2.1]	0.961	> 0.999
Duration of second stage of labor, h (median [interquartile range])	0.6 [0.2 to 1.2]	0.3 [0.2 to 1.5]	0.0 [–0.3 to 0.2]	0.900	> 0.999
Mode of delivery, n (%)				0.925	> 0.999
Spontaneous vaginal	39 (59)	40 (61)	Reference		
Operative vaginal	4 (6)	3 (5)	1.4 [0.3 to 7.3]		
Cesarean	23 (35)	23 (35)	1.0 [0.5 to 2.2]		
Apgar scores					
1 min (median [interquartile range])	8 [7 to 8]	8 [8 to 8]	0 [0 to 0]	0.735	> 0.999
5 min (median [interquartile range])	9 [9 to 9]	9 [9 to 9]	0 [0 to 0]	0.657	> 0.999
Hypotension, n (%)	2 (3)	6 (9)	0.3 [0.1 to 1.4]	0.274	> 0.999
Nausea, n (%)	11 (17)	11 (17)	1.0 [0.4 to 2.5]	> 0.999	> 0.999
Pruritus, n (%)	27 (41)	25 (38)	1.1 [0.6 to 2.3]	0.859	> 0.999
Postdural puncture headache, n (%)	0	0			
Maternal satisfaction (median [interquartile range])	10 [8 to 10]	9 [8 to 10]	0 [–1 to 0]	0.022	0.253
Fetal heart rate, beats/min (median [interquartile range])	135 [125 to 140]	135 [125 to 140]	0 [–5 to 5]	0.790	> 0.999
Fetal heart rate decelerations, n (%)				0.785	> 0.999
Variable	4 (6)	2 (3)	0.5 [0.1 to 2.6]		
Late	7 (11)	9 (14)	0.4 [0.1 to 2.6]		
Fetal heart rate variability, n (%)				0.435	> 0.999
Moderate	61 (92)	61 (92)	Reference		
Minimal	1 (2)	3 (5)	0.3 [0.2 to 2.7]		
Missing or not assessed	4 (6)	2 (3)	2.0 [0.4 to 14.8]		
National Institute of Child Health and Human Development fetal heart rate classification, n (%)				0.596	> 0.999
Category 1	51 (77)	50 (76)	Reference		
Category 2	11 (17)	14 (21)	0.8 [0.3 to 1.9]		
Missing or not assessed	4 (6)	2 (3)	2.0 [0.4 to 14.6]		

Difference measures correspond to the Hodges–Lehman shift for continuous variables and the risk difference for categorical variables.

*Sensory block height assessed with temperature discrimination using ice. Sensory level was tested to the S2 dermatome in the caudad direction, but no limit was imposed on sensory block height assessment in the cephalad direction.

†Modified Bromage score, where 1 indicates unable to flex feet or knees, 2 indicates able to flex feet only, 3 indicates able to flex knees, 4 indicates detectable weakness in hip flexion, and 5 indicates no weakness with hip flexion.

puncture, which may explain why the use of dilute ropivacaine 0.1% in our study produced similar results to those of Thomas *et al.*,[14] who reported no improvement in analgesia quality or reduction in catheter manipulation or replacement with dural puncture epidural compared to the standard epidural technique using 0.11% bupivacaine. Interestingly, a recent study comparing dural puncture epidural plus continuous infusion, dural puncture epidural

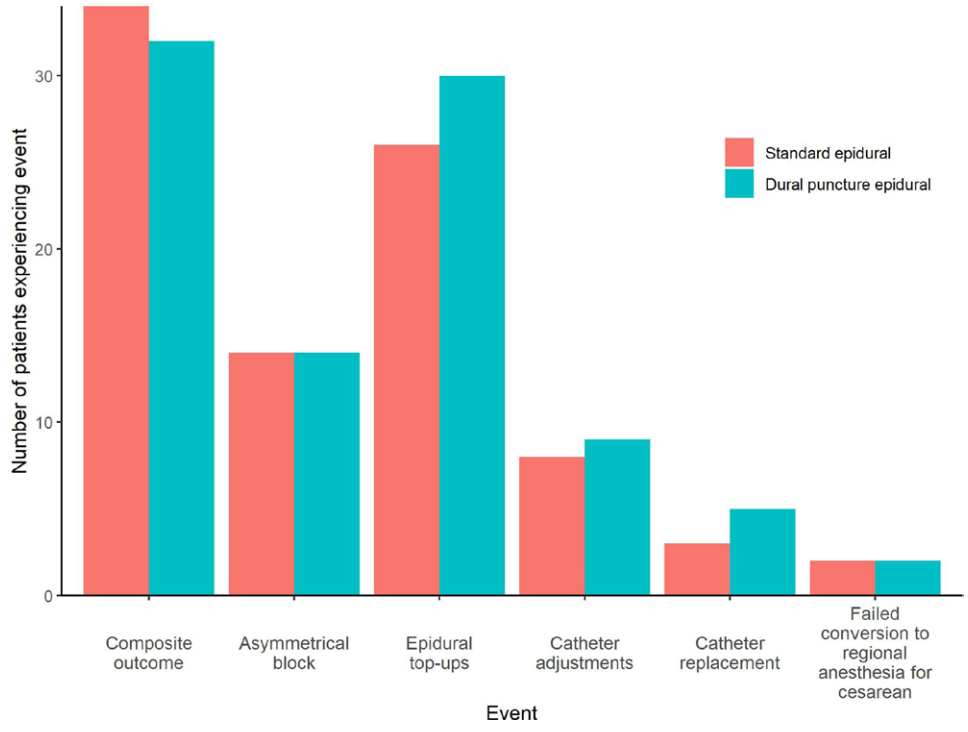

Fig. 2. Primary composite outcome and its individual components. The primary outcome was the quality of labor analgesia defined as a composite of (1) asymmetrical block (difference in sensory level of greater than 2 dermatomes using temperature discrimination to ice), (2) epidural top-ups, (3) catheter adjustments, (4) catheter replacement, and (5) failed conversion to regional anesthesia requiring general anesthesia or replacement neuraxial anesthesia in the event of cesarean delivery. There were no statistically significant differences between the groups in the composite outcome or its individual components. Further details are provided in the Supplemental Digital Content (http://links.lww.com/ALN/C788).

plus intermittent boluses, and standard epidural plus continuous infusion reported that treatment with dural puncture epidural plus intermittent boluses was associated with the greatest analgesia quality and drug-sparing effect compared to the other two techniques.[21] It is possible that the higher injectate pressures used in the intermittent bolus technique may increase drug transfer through the dural puncture, although this technique did not significantly increase analgesia efficacy with dural puncture epidural compared to standard epidural in our study. Another possibility is that the increased epidural drug spread associated with the intermittent bolus technique[1] may obscure any analgesic improvement resulting from increased drug transfer through the dural conduit with the dural puncture epidural technique.

Dural punctures were performed with 25-gauge spinal needles, similar to previous studies that reported reduced sacral block sparing and asymmetrical block with dural puncture epidural compared to standard epidural technique.[5,17] Hence, the size of the dural puncture is unlikely to explain the lack of analgesic benefit of dural puncture epidural compared to standard epidural technique in our study. Finally, the presence of a dural puncture will have greater effect on the rate of transmeningeal drug transfer in medications with inherently slow diffusion rates through intact meninges such as lidocaine or morphine compared to medications that easily diffuse across the intact meninges such as bupivacaine or ropivacaine[20] and may have contributed to the absence of significant analgesic improvement with the dural puncture epidural technique when ropivacaine was used.

In our study, dural puncture with 25-gauge spinal needles did not significantly increase the incidence of adverse effects compared to the standard epidural technique, consistent with the findings of Cappiello *et al.*[17] and Chau *et al.*[5] It is likely that the rate of transmeningeal transfer of epidural medications is slow enough to avoid complications such as hypotension, uterine tachysystole, and fetal bradycardia that are associated with the combined spinal epidural technique.[22] Also, no difference in the incidence of postdural puncture headache was detected. However, it is possible that our study was not sufficiently powered to detect small changes in these rare outcomes.

The main strength of our study is the randomized, double-blind design that minimizes bias and influence of known and unknown confounders. In addition, the composite primary outcome increases study power to detect clinically

relevant differences in overall quality of analgesia. However, we acknowledge several potential limitations. While we found no statistically significant differences between the groups in our primary outcome, it should be noted that the 95% CI ranges were wide and contained potentially clinically relevant differences. Given our observed difference and variability of outcome rate, future large studies would be required to rule out a smaller but clinically relevant difference. The onset of adequate analgesia is challenging to measure given the cyclical nature of labor pain. We attempted to control for this by assessing pain with the preceding contraction and enrolling parturients with moderate to severe labor pain. However, as the frequency of uterine contractions vary during labor, it is possible that adequate analgesia was obtained earlier than what was documented. We included a wide range of cervical dilatation in our study, although cervical dilatation and pain scores at request of analgesia were comparable between the two groups. In addition, maintenance of labor analgesia was achieved *via* intermittent boluses of epidural medications, which may have influenced our findings and reduced the generalizability of our results compared to other studies utilizing continuous infusion of epidural medications. We note that the incidence of our composite outcome was higher than anticipated. This discrepancy may be attributed to the prospective collection of data in this study, which might have captured more interventions compared to the retrospective study that was used for the power analysis, which also used a more concentrated solution compared to the one used in this current study. Furthermore, the long duration of labor in parturients with obesity might lead to increased need for interventions. Finally, the need for epidural top-ups was included in our composite outcome, but it might not indicate definitive catheter failure such as need for catheter replacement during labor or for cesarean delivery. However, it reflects the presence of breakthrough pain and therefore is a measure of inadequate labor analgesia. This has a clinically significant impact on parturient satisfaction and anesthesia provider workload. While epidural top-ups were the predominant component of our composite outcome, our *post hoc* sensitivity analysis indicated that our findings were consistent with or without the inclusion of epidural top-ups in our composite outcome.

In conclusion, we did not find significant differences in quality of analgesia or the incidence of adverse effects between dural puncture epidural and standard epidural techniques for labor analgesia in obese parturients. Those findings do not support routine use of the dural puncture epidural technique for labor analgesia in obese parturients.

Acknowledgments

The authors acknowledge the contribution of the members of the Division of Women's Anesthesiology and Duke Birthing Center (Durham, North Carolina) for their assistance with this study. The authors also thank Mary Cooter-Wright, M.S. (Department of Anesthesiology, Duke University Medical Center, Durham, North Carolina), for statistical advice.

Research Support

Support was provided solely from institutional and/or departmental sources.

Competing Interests

Dr. Habib has received grant support from Pacira Biosciences (Parsippany, New Jersey), Haisco USA (San Diego, California), and Heron Therapeutics (San Diego, California). He has also served on the Advisory Board for Trevena Inc. (Chesterbrook, Pennsylvania), Heron Therapeutics, Takeda (Lexington, Massachusetts), Mdoloris (Loos, France), and Vertex Pharmaceuticals (Boston, Massachusetts). The other authors declare no competing interests.

Reproducible Science

Full protocol available at: ashraf.habib@duke.edu. Raw data available at: ashraf.habib@duke.edu.

Correspondence

Address correspondence to Dr. Habib: Duke University Medical Center, Box 3094, Durham, North Carolina 27710. ashraf.habib@duke.edu. This article may be accessed for personal use at no charge through the Journal Web site, www.anesthesiology.org.

References

1. Sng BL, Zeng Y, de Souza NNA, Leong WL, Oh TT, Siddiqui FJ, Assam PN, Han NR, Chan ES, Sia AT: Automated mandatory bolus *versus* basal infusion for maintenance of epidural analgesia in labour. Cochrane Database Syst Rev 2018; 5:CD011344
2. Suzuki N, Koganemaru M, Onizuka S, Takasaki M: Dural puncture with a 26-gauge spinal needle affects spread of epidural anesthesia. Anesth Analg 1996; 82:1040–2
3. Heesen M, Rijs K, Rossaint R, Klimek M: Dural puncture epidural *versus* conventional epidural block for labor analgesia: A systematic review of randomized controlled trials. Int J Obstet Anesth 2019; 40:24–31
4. Layera S, Bravo D, Aliste J, Tran DQ: A systematic review of dural puncture epidural analgesia for labor. J Clin Anesth 2019; 53:5–10
5. Chau A, Bibbo C, Huang CC, Elterman KG, Cappiello EC, Robinson JN, Tsen LC: Dural puncture epidural technique improves labor analgesia quality with fewer side effects compared with epidural and combined spinal epidural techniques: A randomized clinical trial. Anesth Analg 2017; 124:560–9

6. Patel SD, Habib AS: Anaesthesia for the parturient with obesity. BJA Educ 2021; 21:180–6
7. Petersen S, Khangura R, Fitzgerald M, Sousa D, Goyert G: Risk of cesarean with obesity and advancing maternal age. Obstet Gynecol 2017; 129:31S
8. Draycott T, Lewis G, Stephens I: Executive summary: Executive report of the confidential enquiries into maternal deaths in the UK. BJOG 2011; 118:e12–e21
9. Hawkins JL, Chang J, Palmer SK, Gibbs CP, Callaghan WM: Anesthesia-related maternal mortality in the United States: 1979–2002. Obstet Gynecol 2011; 117:69–74
10. Breen TW, Shapiro T, Glass B, Foster-Payne D, Oriol NE: Epidural anesthesia for labor in an ambulatory patient. Anesth Analg 1993; 77:919–24
11. Electronic fetal heart rate monitoring: Research guidelines for interpretation. National Institute of Child Health and Human Development Research Planning Workshop. Am J Obstet Gynecol 1997; 177:1385–90
12. Tien M, Allen TK, Mauritz A, Habib AS: A retrospective comparison of programmed intermittent epidural bolus with continuous epidural infusion for maintenance of labor analgesia. Curr Med Res Opin 2016; 32:1435–40
13. Hess PE, Pratt SD, Lucas TP, Miller CG, Corbett T, Oriol N, Sarna MC: Predictors of breakthrough pain during labor epidural analgesia. Anesth Analg 2001; 93:414–8
14. Thomas JA, Pan PH, Harris LC, Owen MD, D'Angelo R: Dural puncture with a 27-gauge Whitacre needle as part of a combined spinal–epidural technique does not improve labor epidural catheter function. Anesthesiology 2005; 103:1046–51
15. Yadav P, Kumari I, Narang A, Baser N, Bedi V, Dindor BK: Comparison of dural puncture epidural technique *versus* conventional epidural technique for labor analgesia in primigravida. J Obstet Anaesth Crit Care 2018; 8:24
16. Wilson SH, Wolf BJ, Bingham K, Scotland QS, Fox JM, Woltz EM, Hebbar L: Labor analgesia onset with dural puncture epidural *versus* traditional epidural using a 26-gauge Whitacre needle and 0.125% bupivacaine bolus: A randomized clinical trial. Anesth Analg 2018; 126:545–51
17. Cappiello E, O'Rourke N, Segal S, Tsen LC: A randomized trial of dural puncture epidural technique compared with the standard epidural technique for labor analgesia. Anesth Analg 2008; 107:1646–51
18. Bernards CM, Kopacz DJ, Michel MZ: Effect of needle puncture on morphine and lidocaine flux through the spinal meninges of the monkey *in vitro*: Implications for combined spinal–epidural anesthesia. Anesthesiology 1994; 80:853–8
19. Swenson JD, Wisniewski M, McJames S, Ashburn MA, Pace NL: The effect of prior dural puncture on cisternal cerebrospinal fluid morphine concentrations in sheep after administration of lumbar epidural morphine. Anesth Analg 1996; 83:523–5
20. Clement R, Malinovsky JM, Le Corre P, Dollo G, Chevanne F, Le Verge R: Cerebrospinal fluid bioavailability and pharmacokinetics of bupivacaine and lidocaine after intrathecal and epidural administrations in rabbits using microdialysis. J Pharmacol Exp Ther 1999; 289:1015–21
21. Song Y, Du W, Zhou S, Zhou Y, Yu Y, Xu Z, Liu Z: Effect of dural puncture epidural technique combined with programmed intermittent epidural bolus on labor analgesia onset and maintenance: A randomized controlled trial. Anesth Analg 2021; 132:971–8
22. Hattler J, Klimek M, Rossaint R, Heesen M: The effect of combined spinal–epidural *versus* epidural analgesia in laboring women on nonreassuring fetal heart rate tracings: Systematic review and meta-analysis. Anesth Analg 2016; 123:955–64

ANESTHESIOLOGY

Self-reported Race/Ethnicity and Intraoperative Occult Hypoxemia: A Retrospective Cohort Study

Garrett W. Burnett, M.D., Blaine Stannard, M.D., David B. Wax, M.D., Hung-Mo Lin, Sc.D., Chantal Pyram-Vincent, M.D., M.P.H., Samuel DeMaria, Jr., M.D., Matthew A. Levin, M.D.

ANESTHESIOLOGY 2022; 136:688–96

EDITOR'S PERSPECTIVE

What We Already Know about This Topic

- Pulse oximetry is part of the American Society of Anesthesiologists' Standards for Basic Anesthetic Monitoring
- Pigmentation in dark skin has been associated with overestimation of pulse oximeter values
- Recent critical care literature has renewed concerns regarding the accuracy of pulse oximetry in detecting hypoxemia in Black *versus* White patients

What This Article Tells Us That Is New

- Among 46,523 patients with 151,070 paired arterial oxygen saturation (Sao_2)–oxygen saturation measured by pulse oximetry (Spo_2) intraoperative readings at a single center, the prevalence of occult hypoxemia (Sao_2 less than 88% despite concurrent Spo_2 greater than 92%) was significantly increased in patients self-reporting Black (2.1%) and Hispanic (1.8%) race/ethnicity compared with patients self-reporting White (1.1%) race/ethnicity
- After adjusting for other clinical factors, Black or Hispanic race/ethnicity was independently associated with occult hypoxemia

ABSTRACT

Background: Pulse oximetry is ubiquitous in anesthesia and is generally a reliable noninvasive measure of arterial oxygen saturation. Concerns regarding the impact of skin pigmentation and race/ethnicity on the accuracy of pulse oximeter accuracy exist. The authors hypothesized a greater prevalence of occult hypoxemia (arterial oxygen saturation [Sao_2] less than 88% despite oxygen saturation measured by pulse oximetry [Spo_2] greater than 92%) in patients undergoing anesthesia who self-reported a race/ethnicity other than White.

Methods: Demographic and physiologic data, including self-reported race/ethnicity, were extracted from a departmental data warehouse for patients receiving an anesthetic that included at least one arterial blood gas between January 2008 and December 2019. Calculated Sao_2 values were paired with concurrent Spo_2 values for each patient. Analysis to determine whether Black, Hispanic, Asian, or Other race/ethnicities were associated with occult hypoxemia relative to White race/ethnicity within the Spo_2 range of 92 to 100% was completed.

Results: In total, 151,070 paired Sao_2–Spo_2 readings (70,722 White; 16,011 Black; 21,223 Hispanic; 8,121 Asian; 34,993 Other) from 46,253 unique patients were analyzed. The prevalence of occult hypoxemia was significantly higher in Black (339 of 16,011 [2.1%]) and Hispanic (383 of 21,223 [1.8%]) *versus* White (791 of 70,722 [1.1%]) paired Sao_2–Spo_2 readings ($P < 0.001$ for both). In the multivariable analysis, Black (odds ratio, 1.44 [95% CI, 1.11 to 1.87]; $P = 0.006$) and Hispanic (odds ratio, 1.31 [95% CI, 1.03 to 1.68]; $P = 0.031$) race/ethnicity were associated with occult hypoxemia. Asian and Other race/ethnicity were not associated with occult hypoxemia.

Conclusions: Self-reported Black and Hispanic race/ethnicity are associated with a greater prevalence of intraoperative occult hypoxemia in the Spo_2 range of 92 to 100% when compared with self-reported White race/ethnicity.

(ANESTHESIOLOGY 2022; 136:688–96)

In 1986, the American Society of Anesthesiologists (ASA; Schaumburg, Illinois) adopted the Standards for Basic Intra-Operative Monitoring, which stated, "During all anesthetics, a quantitative method of assessing oxygenation such as pulse oximetry shall be employed."[1] Since that time, pulse oximetry has become ubiquitous in health care and is an important component of the World Health Organization's (Geneva, Switzerland) Safe Surgery Checklist.[2] The addition of widespread pulse oximetry use, in combination with additional perioperative safety initiatives, has coincided

This article is featured in "This Month in Anesthesiology," page A1. This article is accompanied by an editorial on p. 670. Supplemental Digital Content is available for this article. Direct URL citations appear in the printed text and are available in both the HTML and PDF versions of this article. Links to the digital files are provided in the HTML text of this article on the Journal's Web site (www.anesthesiology.org). This article has an audio podcast. This article has a visual abstract available in the online version.

Submitted for publication March 12, 2021. Accepted for publication January 20, 2022. Published online first on March 1, 2022.

Garrett W. Burnett, M.D.: Department of Anesthesiology, Perioperative and Pain Medicine, Icahn School of Medicine at Mount Sinai, New York, New York.

Blaine Stannard, M.D.: Department of Anesthesiology, Perioperative and Pain Medicine, Icahn School of Medicine at Mount Sinai, New York, New York.

David B. Wax, M.D.: Department of Anesthesiology, Perioperative and Pain Medicine, Icahn School of Medicine at Mount Sinai, New York, New York.

Hung-Mo Lin, Sc.D.: Department of Population Health Science and Policy, Icahn School of Medicine at Mount Sinai, New York, New York.

Chantal Pyram-Vincent, M.D., M.P.H.: Department of Anesthesiology, Perioperative and Pain Medicine, Icahn School of Medicine at Mount Sinai, New York, New York.

Samuel DeMaria, Jr., M.D.: Department of Anesthesiology, Perioperative and Pain Medicine, Icahn School of Medicine at Mount Sinai, New York, New York.

Matthew A. Levin, M.D.: Department of Anesthesiology, Perioperative and Pain Medicine and Department of Genetics and Genomic Sciences, Icahn School of Medicine at Mount Sinai, New York, New York.

 Anesthesiology 2022; 136:688–96. DOI: 10.1097/ALN.0000000000004153

with a 90% reduction in anesthesia-related fatalities[3]; its use in postanesthesia care units has likely contributed to the significant reduction in need for patient rescue or intensive care unit admissions.[3,4]

While the measurement of oxygen saturation by pulse oximetry (Spo_2) is generally a reliable noninvasive measure of a patient's true arterial oxygen saturation (Sao_2), several factors may interfere with the accuracy of pulse oximetry measurement.[5] These include inadequate waveform capture from hypotension; motion artifact or hypoperfusion; falsely elevated values due to ambient light or carboxyhemoglobin; or falsely low values from severe anemia, nail polish, or vital dyes.[5–7] Skin pigmentation is another potential source of inaccuracy, and studies have demonstrated conflicting data regarding the impact of skin pigmentation on the difference between Sao_2 concentrations and Spo_2 values (*i.e.*, Spo_2 device bias). Overestimation of Spo_2 (positive device bias) in patients with dark skin pigmentation has been shown to be as high as 5%, although some studies have demonstrated no evidence of Spo_2 device bias.[8–13] More recent studies evaluating modern pulse oximeters have evaluated Spo_2 device bias in hypoxic patients with and without dark skin pigmentation.[14,15] Positive Spo_2 device bias was noted in patients with deeply pigmented skin at Sao_2 concentrations less than 80%, but this discrepancy did not persist at Sao_2 concentrations greater than 80%.

Most recently, Sjoding *et al.* compared pulse oximetry use in Black and White patients in the critical care setting, demonstrating approximately three times the frequency of clinically significant occult hypoxemia (*i.e.*, Sao_2 less than 88% despite Spo_2 greater than 92 to 96%) in Black (11.4%) *versus* White (3.6%) patients.[16] These findings demonstrated Sao_2 and Spo_2 discrepancies in Black patients at much higher Spo_2 values than previously described.[14,15] These are important and concerning findings, but may not be applicable to a population of patients undergoing anesthetic care.

The aim of this retrospective study was to determine if self-reported race/ethnicity, as a surrogate for skin pigmentation, was associated with greater prevalence of occult hypoxemia in a cohort of patients undergoing general anesthesia, regional anesthesia, or monitored anesthesia care. We hypothesized a greater prevalence of occult hypoxemia in those who self-reported a race/ethnicity other than White.

Materials and Methods

After receiving Institutional Review Board approval from the Icahn School of Medicine at Mount Sinai (New York, New York), data were extracted from our departmental data warehouse for all adult patients (older than 18 yr) who received an anesthetic that included at least one arterial blood gas (ABG) sample between January 2008 and December 2019. Our departmental data warehouse is a unified data source that contains data from both our historical anesthesia information management system (CompuRecord; Philips Medical Systems, USA) as well as our electronic health record (Epic; Epic Systems, USA). Matching of historical intraoperative anesthesia information management system data to additional demographics from the electronic health record, and import of these additional data into our departmental data warehouse, is done *via* an automated process and was not specifically undertaken for this project. Informed consent was waived by the institutional review board because of the retrospective nature of the study.

For each Sao_2 concentration calculated by ABG (GEMStat Premier 3000; Instrumentation Laboratory, USA), the corresponding Spo_2 was found by calculating the mean Spo_2 during a 5-min interval starting 10 min before the ABG time (interval ended at 5 min before the ABG time). This interval was chosen to represent the prevailing Spo_2 values at the time the laboratory specimen was likely drawn, as well as to account for specimen transport time before logging/processing of the specimen using point-of-care ABG analyzers. ABG data were excluded if there were no comparative Spo_2 values available during this interval, or if Sao_2 or Spo_2 values were greater than 100% and deemed to be device error. Spo_2 values were captured every 15 s for all cases. The calculated Sao_2 value and calculated Spo_2 value were then linked to one another as a "paired Sao_2–Spo_2 reading" for the purpose of data analyses.

Pulse oximeter device bias was calculated as the difference between the averaged Spo_2 and Sao_2 values. Occult hypoxemia was defined as Sao_2 less than 88% despite a Spo_2 of greater than 92%, based on previously published parameters.[16] Our analysis included the full range of Spo_2 values between 92 to 100%.

Patient- and case-level data extracted included basic patient demographics (age, sex, body mass index, self-identified race, self-identified ethnicity); smoking status at time of surgery (current, previous, or never smoker); year of procedure as a categorical variable; ASA Physical Status; history of relevant comorbidities (hypertension, chronic pulmonary disease, congestive heart failure, coronary artery disease, valvular heart disease, diabetes, peripheral vascular disease, renal failure); anesthesia type (general, monitored anesthesia care, regional anesthesia); use of volatile anesthetic agent (yes/no); use of vasoactive infusion (yes/no [for use of a phenylephrine, norepinephrine, epinephrine, or vasopressin infusion at any time during the portion of the anesthetic]); mean arterial pressure (MAP); hematocrit value as reported at the time of the associated ABG; and set ventilator parameters (fraction of inspired oxygen [Fio_2], tidal volume, positive end-expiratory pressure [PEEP]). Measured ventilatory parameters were not recorded or saved to the departmental data warehouse. For each case, we calculated the mean Fio_2, tidal volume, and PEEP for the same interval that was used to calculate mean Spo_2. The year of procedure was included to account for changes in pulse oximeters used at our institution (primarily Nellcor [Medtronic, USA] before 2011 and Masimo [Masimo, USA] thereafter). Comorbidities were calculated from

International Classification of Diseases, Ninth Revision and Tenth Revision codes using the icd package[17] in R (R Foundation for Statistical Computing, Vienna, Austria). This is an open-source, validated package that assigns comorbidities using the methods of Elixhauser *et al.*[18] and Quan *et al.*[19]

Self-reported race and ethnicity data collected at time of admission were used for our analyses. Options for self-reported race and ethnicity varied during the time of the study period but were cross-referenced for agreement. Race and ethnicity data were classified into a synthetic race/ethnicity variable according to a previously described method.[20] Specifically, we modified the U.S. Census Bureau/Office of Management and Budget (Washington, D.C.) standards for classification of race/ethnicity to assign each patient to one of the following groups: White (European, North African, Middle Eastern, non-Hispanic), Black (African American, sub-Saharan African, non-Hispanic), Hispanic/Latinx, Asian, or Other race/ethnicity.[21,22] Race/ethnicity was synthesized into a single variable in order to include Hispanic/Latinx patients who may be difficult to categorize using standard U.S. Census guidelines, as a growing percentage of these patients identify race as "Other"[23]; thus, all patients who self-identified as Hispanic ethnicity were categorized into the Hispanic race/ethnicity group. Patients self-identifying as Native American/Alaskan Native, Indian/South Asian, and Pacific Islander were grouped into the Other race/ethnicity group due to an extremely low number of these patients in our dataset, which caused instability of the multivariable model during preliminary analysis. The full process used to assign self-reported race/ethnicity responses to the single synthetic race/ethnicity variable is outlined in Supplemental Digital Content 1 (http://links.lww.com/ALN/C797).

Statistical Analysis

No statistical power calculation was conducted before the study since the sample size was based on available data in our data warehouse. The statistical and data analysis plans were defined before accessing the data and were finalized after the data were accessed, with additional statistical analysis completed after peer review. Patient and case characteristics were compared across self-reported race/ethnicity using one-way ANOVA for continuous variables that met parametric assumptions. Continuous variables that did not meet parametric assumptions, including nonnormal distributions as assessed by histograms, were analyzed using Kruskal–Wallis tests. The chi-square test was utilized for categorical variables. Two-tailed testing was used for all statistical tests. The reference group for race/ethnicity was White; the reference group for sex was female. For ASA Physical Status, ASA Physical Status I and II were grouped together because of the small number of ASA Physical Status I patients (less than 1.5%); this combined ASA Physical Status I and II group was used as the reference.

Generalized estimating equations modeling was utilized to determine if any race/ethnicity was an independent predictor of occult hypoxemia relative to White race/ethnicity within the study Spo_2 range of 92 to 100%. A Poisson regression model with logarithmic link was used because of the low prevalence of occult hypoxemia. Multiple paired Sao_2–Spo_2 readings for each patient were accounted for by clustering within patients using independent working correlation structure; however, sandwich estimators were utilized for standard errors. The model was first run without controlling for confounders in order to assess for significant differences in unadjusted prevalence of occult hypoxemia across race/ethnicity groups. A multivariable model was then created to control for all of the collected demographic, comorbidity, and operative variables. A continuous Spo_2 variable was included as a fixed effect, and an interaction term between Spo_2 and race/ethnicity was also assessed for inclusion. Continuous variables (*e.g.*, Fio_2, tidal volume) were entered directly into the model as covariates, without transformation. The year of procedure was assessed as a categorical variable; 2011 was used as the reference level (since this was the approximate year that the pulse oximeter device type changed). All covariates included were assessed as confounding variables rather than effect modifiers. An additional model focusing on 92 to 96% Spo_2 was created as a supplemental analysis, as this was the range focused on in the analysis of occult hypoxemia from Sjoding *et al.*[16]

As an exploratory analysis, the optimal threshold for predicting occult hypoxemia based on Spo_2 was assessed using the F_1 score. The F_1 score is the harmonic mean of the precision (positive predictive value) and recall (sensitivity), and is a measure of a test's accuracy.[24] It can be used to determine the threshold at which a test has the best performance, particularly in cases where the outcome (in this case, occult hypoxemia) is rare. F_1 scores were calculated using univariate analysis for the range of Spo_2 between 92 to 100%, stratified by race/ethnicity, and then plotted. This allowed for visual identification of the best Spo_2 cutoff to identify occult hypoxemia.

The overall design of the analysis and threshold for statistical significance ($P < 0.05$) were established *a priori*. After reviewing our findings, several *post hoc* sensitivity analyses were performed to further elucidate the relationship between race/ethnicity, occult hypoxemia, and comorbid risk factors.

All statistical analysis was performed in R version 3.5.0 (R Foundation for Statistical Computing).

Results

Readings from 47,067 unique patients were collected, totaling 157,482 Sao_2–Spo_2 pairs. Before data analysis, 17 paired Sao_2–Spo_2 readings were excluded because of missing Sao_2 data, and an additional 28 paired Sao_2–Spo_2 readings were excluded for Sao_2 values greater than 100, deemed to be device error. There were 11,232 paired Sao_2–Spo_2 readings

Table 1. Patient Demographics

	Overall	White	Black	Asian	Hispanic	Other	*P* Value
Paired Sa_{O_2}–Sp_{O_2} readings, No.	151,070	70,722	16,011	8,121	21,223	34,993	
Patients, No.	46,253	22,089	5,177	2,612	6,304	10,071	
Age, yr (mean ± SD)	57 ± 21	61 ± 19	54 ± 19	55 ± 21	52 ± 23	54 ± 22	< 0.001
Male sex	25,226 (54.5%)	12,530 (56.7%)	2,381 (46.0%)	1,526 (58.4%)	3,220 (51.1%)	5,569 (55.3%)	< 0.001
Body mass index, kg/m^2, median [interquartile range]	26 [23–30]	27 [23–30]	27 [23–32]	24 [21–27]	27 [23–31]	26 [22–30]	< 0.001
ASA Physical Status							< 0.001
I	688 (1.5%)	329 (1.5%)	75 (1.4%)	49 (1.9%)	102 (1.6%)	133 (1.3%)	
II	6,603 (14.3%)	3,250 (14.7%)	671 (13.0%)	527 (20.2%)	880 (14.0%)	1,275 (12.7%)	
III	19,892 (43.0%)	10,080 (45.6%)	2,198 (42.5%)	1,219 (46.7%)	2,518 (40.0%)	3,877 (38.5%)	
IV	18,232 (39.4%)	8,168 (37.0%)	2,117 (40.9%)	780 (29.9%)	2,664 (42.3%)	4,503 (44.8%)	
V	818 (1.8%)	258 (1.2%)	115 (2.2%)	37 (1.4%)	136 (2.2%)	272 (2.7%)	
Hypertension	12,469 (27.0%)	5,342 (24.2%)	1,254 (24.2%)	581 (22.2%)	1,784 (28.3%)	3,508 (34.8%)	< 0.001
Congestive heart failure	2,805 (6.1%)	1,280 (5.8%)	312 (6.0%)	89 (3.4%)	362 (5.7%)	762 (7.6%)	< 0.001
Valvular heart disease	4,103 (8.9%)	2,428 (11.0%)	233 (4.5%)	127 (4.9%)	396 (6.3%)	919 (9.1%)	< 0.001
Chronic pulmonary disease	3,134 (6.8%)	1,414 (6.4%)	344 (6.6%)	84 (3.2%)	451 (7.2%)	841 (8.4%)	< 0.001
Diabetes	5,409 (11.7%)	1,762 (8.0%)	583 (11.3%)	296 (11.3%)	975 (15.5%)	1,793 (17.8%)	< 0.001
Renal failure	2,246 (4.9%)	729 (3.3%)	315 (6.1%)	85 (3.3%)	395 (6.3%)	722 (7.2%)	< 0.001
Peripheral vascular disease	2,344 (5.1%)	1,067 (4.8%)	243 (4.7%)	103 (3.9%)	336 (5.3%)	595 (5.9%)	< 0.001
Coronary artery disease	5,353 (11.6%)	2,415 (10.9%)	460 (8.9%)	215 (8.2%)	746 (11.8%)	1,517 (15.1%)	< 0.001
Smoking status							< 0.001
Never	31,756 (77.9%)	14,567 (76.3%)	3,465 (74.6%)	1,957 (86.9%)	4,542 (80.2%)	7,225 (79.4%)	
Current	2,913 (7.1%)	1,189 (6.2%)	511 (11.0%)	106 (4.7%)	406 (7.2%)	701 (7.7%)	
Prior	6,082 (14.9%)	3,331 (17.5%)	666 (14.3%)	190 (8.4%)	716 (12.6%)	1,179 (12.9%)	
Anesthesia type							< 0.001
General	43,061 (93.2%)	20,503 (92.9%)	4,802 (92.8%)	2,473 (94.8%)	5,825 (92.5%)	9,458 (94.0%)	
Monitored anesthesia care	1,506 (3.3%)	781 (3.5%)	119 (2.3%)	34 (1.3%)	196 (3.1%)	376 (3.7%)	
Regional	1,643 (3.6%)	785 (3.6%)	252 (4.9%)	103 (3.9%)	273 (4.3%)	230 (2.3%)	
Volatile anesthetic	32,214 (69.6%)	15,126 (68.5%)	3,737 (72.2%)	1,882 (72.1%)	4,460 (70.7%)	7,009 (69.6%)	< 0.001
Vasoactive infusion used	21,158 (45.7%)	10,415 (47.2%)	1,878 (36.3%)	945 (36.2%)	2,746 (43.6%)	5,174 (51.4%)	< 0.001
Tidal volume, ml (mean ± SD)	460 ± 153	477 ± 146	472 ± 151	440 ± 142	438 ± 163	437 ± 159	< 0.001
F_{IO_2}, %, median [interquartile range]	85 [72–97]	85 [73–97]	84 [73–97]	81 [72–97]	86 [72–97]	85 [71–97]	< 0.001
PEEP, cm H_2O, median [interquartile range]	5 [3–5]	5 [3–5]	5 [3–5]	5 [3–5]	5 [3–5]	5 [3–5]	< 0.001
MAP (mean ± SD)	83 ± 17	83 ± 16	85 ± 18	83 ± 16	82 ± 17	82 ± 17	< 0.001
Hematocrit (mean ± SD)	33 ± 6	33 ± 6	33 ± 6	34 ± 6	33 ± 7	33 ± 7	< 0.001
Year of procedure							< 0.001
2008	2,905 (6.3%)	1,574 (7.1%)	372 (7.2%)	157 (6.0%)	468 (7.4%)	334 (3.3%)	
2009	3,692 (8.0%)	1,930 (8.7%)	528 (10.2%)	230 (8.8%)	547 (8.7%)	457 (4.5%)	
2010	3,889 (8.4%)	1,967 (8.9%)	578 (11.2%)	267 (10.2%)	587 (9.3%)	490 (4.9%)	
2011	4,184 (9.0%)	2,137 (9.7%)	548 (10.6%)	284 (10.9%)	635 (10.1%)	580 (5.8%)	
2012	4,673 (10.1%)	2,313 (10.5%)	641 (12.4%)	272 (10.4%)	627 (9.9%)	820 (8.1%)	
2013	4,875 (10.5%)	2,381 (10.8%)	689 (13.3%)	329 (12.6%)	626 (9.9%)	850 (8.4%)	
2014	4,481 (9.7%)	2,036 (9.2%)	544 (10.5%)	288 (11.0%)	540 (8.6%)	1,073 (10.7%)	
2015	5,256 (11.4%)	2,169 (9.8%)	676 (13.1%)	308 (11.8%)	609 (9.7%)	1,494 (14.8%)	
2016	3,071 (6.6%)	1,333 (6.0%)	188 (3.6%)	53 (2.0%)	346 (5.5%)	1,151 (11.4%)	
2017	3,553 (7.7%)	1,690 (7.7%)	265 (5.1%)	152 (5.8%)	466 (7.4%)	980 (9.7%)	
2018	3,099 (6.7%)	1,354 (6.1%)	88 (1.7%)	135 (5.2%)	513 (8.1%)	1,009 (10.0%)	
2019	2,575 (5.6%)	1,205 (5.5%)	60 (1.2%)	137 (5.2%)	340 (5.4%)	833 (8.3%)	

Data are n (%) unless otherwise noted.

ASA, American Society of Anesthesiologists; F_{IO_2}, fraction of inspired oxygen; PEEP, positive end-expiratory pressure; Sa_{O_2}, arterial oxygen saturation; Sp_{O_2}, oxygen saturation measured by pulse oximetry.

for patients whose race was recorded as "Unknown," who were grouped into the Other race/ethnicity group. We then isolated paired Sa_{O_2}–Sp_{O_2} readings to the Sp_{O_2} 92 to 100% range, which left a total of 151,070 paired Sa_{O_2}–Sp_{O_2} readings for 46,253 unique patients. Demographics for the cohort for data analysis are listed in table 1. The most represented race/ethnicity groups by number of unique patients were White (22,089 of 46,253 [47.8%]), Other (10,071 of 46,253 [21.8%]), Hispanic (6,304 of 46,253 [13.6%]), and Black (5,177/46,253 [11.2%]). The White cohort was older (61 *vs.* 52 to 54 yr) than the non-White groups on average, and had a greater proportion of male sex (12,530 of 22,089 [56.7%]) compared to the Black (2,381 of 5,177 [46%]) and Hispanic (3,220 of 6,304 [51.1%]) cohorts. The proportions

of male sex in the Asian (1,526 of 2,612 [58.4%]) and Other (5,569 of 10,071 [55.3%]) cohorts were similar to the White cohort. The Black, Hispanic, and Other cohorts had greater proportions of ASA Physical Status IV and V, diabetes, and renal failure compared with the White and Asian cohorts. Rates of congestive heart failure, hypertension, and chronic pulmonary disease were similar between the White, Black, and Hispanic cohorts, greater in the Other cohort, and lesser in the Asian cohort. Rates of general anesthesia were high across all groups, with few study patients having received monitored anesthesia care or regional anesthesia. The median Spo_2 was 100% (interquartile range, 99 to 100) and median calculated Sao_2 was 100% (interquartile range, 100 to 100) for the overall cohort as well as for each race/ethnicity group.

Prevalence of Occult Hypoxemia and Spo_2 Device Bias by Self-reported Race/Ethnicity (Univariate Analysis)

The prevalence of occult hypoxemia in the Spo_2 study range for each self-reported race/ethnicity group is listed in table 2 and illustrated in figure 1. Overall, occult hypoxemia was present in 1.3% (2,016 of 151,070) of paired Sao_2–Spo_2 readings. The prevalence of occult hypoxemia in Black patients was 2.1% (339 of 16,011 paired Sao_2–Spo_2 readings) *versus* 1.1% (791 of 70,722 paired Sao_2–Spo_2 readings) in White patients ($P < 0.001$). Hispanic patients also had a significantly greater prevalence of 1.8% (383 of 21,223 paired Sao_2–Spo_2 readings; $P < 0.001$). Asian and Other race/ethnicity had a similar prevalence to White race.

The overall Spo_2 device bias was $0.0 \pm 6.8\%$ (mean ± SD). White race/ethnicity was the only group that demonstrated a negative Spo_2 device bias ($-0.2 \pm 6.3\%$). Positive Spo_2 device bias was observed for Black ($0.6 \pm 9.1\%$), Hispanic ($0.5 \pm 7.9\%$), Asian ($0.2 \pm 6.5\%$), and Other ($0.1 \pm 5.9\%$) patients.

Multivariable Analysis Results

Factors associated with occult hypoxemia in the multivariable analysis for the Spo_2 study range are shown in table 3. Black (odds ratio, 1.44 [95% CI, 1.11 to 1.87]; $P = 0.006$) and Hispanic (odds ratio, 1.31 [95% CI, 1.03 to 1.68]; $P = 0.031$) race/ethnicity were associated with significantly greater odds of occult hypoxemia relative to White race/ethnicity. Higher Spo_2 was associated with decreased risk of occult hypoxemia (odds ratio, 0.71 [95% CI, 0.69 to 0.73]; $P < 0.001$). The overall interaction term between race/ethnicity and Spo_2 was not significant ($P = 0.948$) and was thus not included in the final model. ASA Physical Status V was an independent risk factor for occult hypoxemia (odds ratio, 1.83 [95% CI, 1.16 to 2.88]; $P = 0.009$). Higher PEEP (odds ratio, 1.10 [95% CI, 1.06 to 1.13]; $P < 0.001$) and higher hematocrit (odds ratio, 1.05 [95% CI, 1.03 to 1.06]; $P < 0.001$) were also associated with a significantly greater risk of occult hypoxemia. In contrast, higher tidal volume (odds ratio, 0.80, [95% CI, 0.75 to 0.84]; $P < 0.001$) and higher MAP (odds ratio, 0.89 [95% CI, 0.84 to 0.95]; $P < 0.001$) were associated with significantly lower risk of occult hypoxemia. Older age was associated with lower odds of occult hypoxemia (odds ratio, 0.94 [95% CI, 0.89 to 0.99]; $P = 0.012$). A more recent year of procedure (2015 to 2019) was also associated with decreased odds of occult hypoxemia compared with the reference year (2011; table 3).

Several *post hoc* sensitivity analyses were performed based on the results of the multivariable analysis. Specifically, because of the strong association between ASA Physical Status V and occult hypoxemia, as well as the greater proportion of ASA Physical Status V patients in the Black, Hispanic, and Other groups, multivariable analyses were repeated while excluding ASA Physical Status V patients. The association between Black (odds ratio, 1.40 [95% CI, 1.08 to 1.82]; $P = 0.011$) and Hispanic (odds ratio, 1.29 [95% CI 1.01 to 1.64]; $P = 0.039$) race/ethnicity and occult hypoxemia was still significant with comparable odds ratios. Full results of this sensitivity analysis are shown in Supplemental Digital Content 2 (http://links.lww.com/ALN/C797). We also performed a sensitivity analysis limited to the 92 to 96% Spo_2 range, as per Sjoding *et al.*[16] Results were consistent with our primary analysis. Black race/ethnicity was significantly associated with occult hypoxemia (odds ratio, 1.80 [95% CI, 1.10 to 2.94]; $P = 0.020$) *versus* White race/ethnicity, with a greater odds ratio than in the full 92 to 100% Spo_2 model. The association

Table 2. Prevalence of Occult Hypoxemia* Stratified by Self-reported Race/Ethnicity (Univariate Analysis)

Race/Ethnicity	Number of Paired Sao_2–Spo_2 Readings	Prevalence of Occult Hypoxemia (Paired Readings)	Patients, No.	Prevalence of Occult Hypoxemia (Number of Patients)	*P* Value†
Overall	151,070	2,016 (1.3%)	46,253	1,855 (4.0%)	—
White‡	70,722	791 (1.1%)	22,089	731 (3.3%)	—
Black	16,011	339 (2.1%)	5,177	319 (6.2%)	< 0.001
Asian	8,121	92 (1.1%)	2,612	85 (3.3%)	0.865
Hispanic	21,223	383 (1.8%)	6,304	348 (5.5%)	< 0.001
Other	34,993	411 (1.2%)	10,071	372 (3.7%)	0.594

*Occult hypoxemia is defined as Sao_2 at less than 88% despite Spo_2 being greater than 92%. †*P* value calculated for paired readings using generalized estimating equations modeling (with clustering within patients) without controlling for confounders. ‡Reference group.

Sao_2, arterial oxygen saturation; Spo_2, oxygen saturation measured by pulse oximetry.

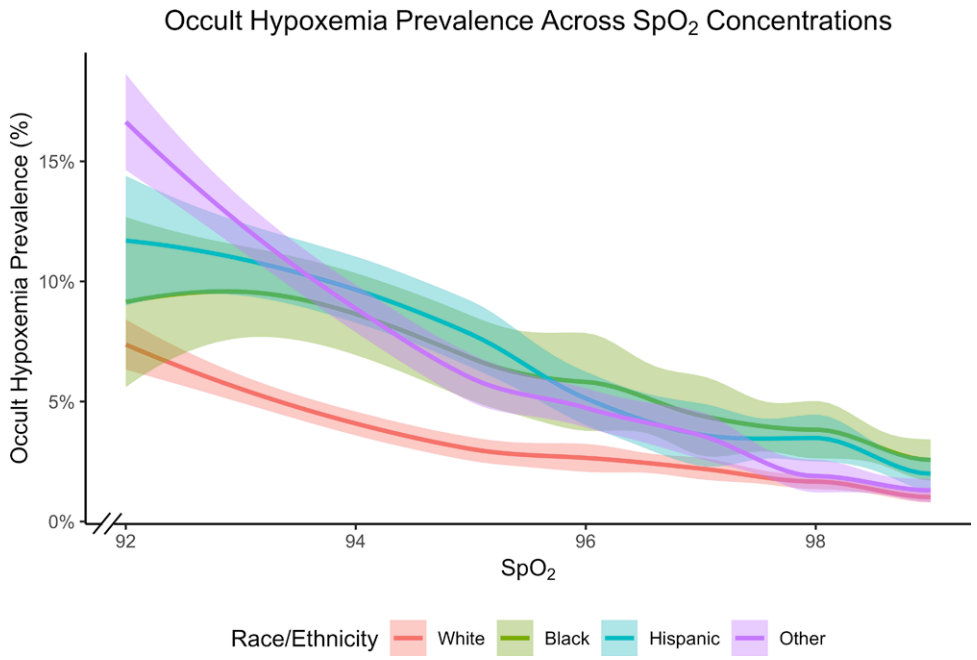

Fig. 1. Prevalence of occult hypoxemia (arterial oxygen saturation at less than 88% despite oxygen saturation measured by pulse oximetry [Spo_2] being greater than 92%) by self-reported race/ethnicity between mean Spo_2 values of 92 to 100%. The curve was generated using the locally weighted scatterplot smoothing method with 50% smoothing to predict the hypoxemia prevalence at a given Spo_2 value. Each prediction is derived from fitting a locally linear regression from the neighboring 50% data points. The shading represents the 95% CI of the locally weighted scatterplot smoothing curve.

of occult hypoxemia in Hispanic patients no longer reached significance using the Spo_2 range of 92 to 96% (odds ratio, 1.46 [95% CI, 0.95 to 2.25]; $P = 0.082$). The full results of this analysis can be found in Supplemental Digital Content 3 (http://links.lww.com/ALN/C797).

Identification of Optimal Spo_2 Threshold for Predicting Occult Hypoxemia (Univariate Analysis)

The F_1 score was calculated for White, Black, and Hispanic patients. F_1 scores for Asian and Other race/ethnicity were not calculated given the lack of significant difference in occult hypoxemia prevalence relative to the White reference group. Supplemental Digital Content 4 (http://links.lww.com/ALN/C797) includes a figure with graphic representation of the calculated F_1 scores. The peak F_1 score for White patients was at Spo_2 94% (F_1 score, 0.08), meaning that Spo_2 values less than 94% were most associated with occult hypoxemia. The F_1 score for Black race/ethnicity peaked at 96% (F_1 score, 0.11). The peak F_1 score was at 95% for Hispanic race/ethnicity (F_1 score, 0.13).

Discussion

In this large, retrospective, single-center analysis, we found that self-reported Black race/ethnicity (339 of 16,011 paired Sao_2–Spo_2 readings [2.1%]; odds ratio, 1.44 [95% CI, 1.11 to 1.87]) and Hispanic race/ethnicity (383 of 21,223 paired Sao_2–Spo_2 readings [1.8%]; odds ratio, 1.31 [95% CI, 1.03 to 1.68]) were significantly associated with occult hypoxemia in the 92 to 100% Spo_2 range compared with White race/ethnicity (791 of 70,222 paired Sao_2–Spo_2 readings [1.1%]). The interaction between Spo_2 and race/ethnicity was not significant, supporting our finding that race/ethnicity is associated with occult hypoxemia independent of Spo_2. These findings are consistent with recent descriptions of occult hypoxemia in the critical care population,[16] but contrary to previous studies suggesting racial discrepancies exist at Spo_2 values less than 80% and are minimal at more commonly encountered Spo_2 values.[14,15] The sensitivity analysis of the 92 to 96% Spo_2 range ([Black race/ethnicity] odds ratio, 1.80 [95% CI, 1.10 to 2.94]) is consistent with the findings of Sjoding *et al.* The lack of statistical significance of Hispanic race/ethnicity *versus* White race/ethnicity in the 92 to 96% analysis is likely attributed to underpowered analyses.

Patients with ASA Physical Status V also demonstrated a significant association with occult hypoxemia (odds ratio, 1.83 [95% CI, 1.16 to 2.88]) across all race/ethnicity groups, potentially because of derangements in physiology or therapeutic interventions associated with patients of ASA Physical Status V. Although a larger percentage of ASA

Table 3. Factors Associated with Occult Hypoxemia*

Perioperative Variable	Odds Ratio	95% CI	*P* Value
Race/ethnicity			
White†	—	—	—
Black	1.44	1.11–1.87	0.006
Asian	0.77	0.51–1.17	0.223
Hispanic	1.31	1.03–1.68	0.031
Other	1.24	1.00–1.53	0.052
Spo_2	0.71	0.69–0.73	< 0.001
ASA Physical Status			
I–II†	—	—	—
III	0.74	0.55–1.01	0.056
IV	1.00	0.74–1.35	0.996
V	1.83	1.16–2.88	0.009
Age, yr‡	0.94	0.89–0.99	0.012
Body mass index, kg/m²‡	0.97	0.91–01.03	0.332
Sex			
Female†	—	—	—
Male	0.89	0.75–1.06	0.189
Fio_2, %‡	0.99	0.95–1.03	0.644
Tidal volume, ml‡	0.80	0.75–0.84	< 0.001
PEEP, cm H_2O‡	1.10	1.06–1.13	< 0.001
MAP, mmHg‡	0.89	0.84–0.95	< 0.001
Hematocrit‡	1.05	1.03–1.06	< 0.001
Volatile anesthetic use	0.87	0.69–1.10	0.248
Vasoactive infusion use	1.08	0.89–1.30	0.445
Diabetes	0.99	0.72–1.35	0.931
Peripheral vascular disease	0.89	0.56–1.41	0.624
Hypertension	0.78	0.59–1.04	0.090
Congestive heart failure	1.29	0.94–1.78	0.118
Chronic pulmonary disease	1.01	0.68–1.51	0.960
Smoking status			
Never†	—	—	—
Current	1.06	0.75–1.50	0.742
Prior	0.88	0.68–1.15	0.343
$ETco_2$‡	0.99	0.98–1.01	0.352
Renal failure	1.14	0.69–1.88	0.611
Year of procedure			
2008	0.97	0.62–1.50	0.877
2009	0.80	0.53–1.21	0.290
2010	0.48	0.31–0.75	0.001
2011†	—	—	—
2012	1.01	0.74–1.36	0.960
2013	0.85	0.62–1.16	0.306
2014	0.76	0.54–1.06	0.106
2015	0.55	0.39–0.78	0.001
2016	0.57	0.38–0.86	0.007
2017	0.58	0.40–0.86	0.006
2018	0.54	0.35–0.86	0.009
2019	0.50	0.30–0.83	0.008

*Occult hypoxemia is defined as Sao_2% at less than 88% despite Spo_2 being greater than 92%. †Reference group. ‡For continuous variables, the odds ratio is calculated per 1-unit increase. Scaled continuous variables were used as follows: age, per 10 yr; body mass index, per 5 kg/m²; Fio_2, per 10%; tidal volume, per 100 ml; and MAP, per 10 mmHg.

ASA, American Society of Anesthesiologists; $ETco_2$, end-tidal carbon dioxide; Fio_2, fraction of inspired oxygen; MAP, mean arterial pressure; PEEP, positive end-expiratory pressure; Sao_2, arterial oxygen saturation; Spo_2, oxygen saturation measured by pulse oximetry.

Physical Status V patients were in the Black and Hispanic groups, sensitivity analyses demonstrated this relationship remained significant with the exclusion of ASA Physical Status V patients in both Black (odds ratio, 1.40 [95% CI, 1.08 to 1.82]) and Hispanic (odds ratio, 1.29 [95% CI, 1.01 to 1.64]) groups.

Surprisingly, neither the use of vasoactive infusions nor the diagnoses of peripheral vascular disease or diabetes were associated with occult hypoxemia despite previous literature indicating an association.[25–27] Sjoding *et al.* excluded diabetic patients from their analysis, so there is no recent and direct comparison to our study available.[16] The associations between age, ventilatory parameters, MAP, and hematocrit with occult hypoxemia were all statistically significant; however, associations were hard to interpret clinically since the magnitude of the effect size was generally very small and often in a contradictory direction (*e.g.*, higher PEEP appeared to be associated with more occult hypoxemia; table 3). Further evaluation of the impact of these covariates is required across all populations and is beyond the scope of this work. There is no clear explanation as to why year was significantly associated with occult hypoxemia, as it does not correspond to the change in pulse oximeter manufacturers in 2011.

Despite our primary findings, the overall Spo_2 device bias in White patients compared to non-White patients was not as striking on univariate analysis, with a difference of less than 1.0% across all groups. The pulse oximeter slightly underestimated Sao_2 in White patients and slightly overestimated Sao_2 in non-White patients. It is likely that Spo_2 device bias does not occur in all non-White patients, which may explain the discrepancy between the increased prevalence of occult hypoxemia in the Black and Hispanic self-reported populations, but more similar prevalence of overall Spo_2 device bias. This discrepancy may be attributed to the wide range of skin pigmentations in patients who self-identify as Black and Hispanic, including multiracial individuals who self-identify as Black or Hispanic because of historical racial integrity laws.[28,29]

As shown in our primary analysis, lower Spo_2 (evaluated as a continuous variable) is significantly associated with a increased risk of occult hypoxemia. The univariate F_1 scores presented in Supplemental Digital Content 4 (http://links.lww.com/ALN/C797) were calculated to explore if there are optimal Spo_2 thresholds for predicting occult hypoxemia. Based on our findings, it may be prudent to have a greater index of suspicion for occult hypoxemia if Spo_2 is less than 96% for Black patients and 95% for Hispanic patients (compared with 94% for White patients). The magnitude of the F_1 scores was not high regardless of race/ethnicity (range, 0.08 to 0.16), indicating the ability of Spo_2 in the 92 to 100% range to reflect hypoxemia is low. This is not surprising since the overall prevalence of hypoxemia in that range is very low and occult hypoxemia is an unexpected event. Thus, the difference in peak F_1 scores between each race/ethnicity should not be overinterpreted.

Limitations of this study are important to consider, given the potential clinical impact of our findings. The retrospective nature of the study contributes to several

limitations including lack of specific self-reported race/ethnicity (hence, the Other race/ethnicity group) for a large portion of our sample and the use of two different manufacturers' pulse oximeters during the study period, as well as other unknown patient-specific confounding factors such as jaundice, presence of nail polish, skin thickness, probe placement, and probe location. The large sample size of this study likely limits the impact of most individual patient factors, but the overall small number of patients found to have occult hypoxemia should be considered a limitation. Additionally, the contribution of each race/ethnicity to the overall number of paired Sao_2–Spo_2 readings compared with the number of patients is slightly different, which potentially indicates selection bias due to repeated values for the same individual. However, this risk for selection bias is limited because of the very small differences in these populations (table 1). To help account for differences in the number of paired Sao_2–Spo_2 readings per patient, we utilized a generalized estimating equations model with clustering within patients. Additionally, we must recognize our use of "race/ethnicity" is a surrogate measurement for skin pigmentation. There is likely wide variation in skin pigmentation among the races/ethnicities represented in our data that cannot be addressed given the retrospective nature of the study.

The variety of pulse oximeters used at our institution during the study period (primarily Nellcor before 2011; Masimo thereafter) was controlled for using the year of procedure as a covariate in the multivariable analysis—although this is an imperfect proxy. It is possible that pulse oximeters from other manufacturers have better or worse performance with differing skin pigmentations, thus limiting the generalizability of our study. Additionally, unknown concentrations of carboxyhemoglobin may exist in this population, but we believe this risk is mitigated by demonstrating a lack of association between smoking status and occult hypoxemia in the multivariable model, as well as the fact that patients suffering from thermal injury are not cared for at our institution. The risk of carboxyhemoglobinemia is also likely mitigated given our institution's adherence to Anesthesia Patient Safety Foundation (Rochester, Minnesota) guidelines on the use of modern carbon dioxide absorbents.[30] Calculated—rather than measured—Sao_2 presents a potential limitation and may limit comparisons to the Sjoding *et al.* study in which cooximetry was used to directly measure Sao_2.

Despite this, previous studies evaluating the ABG analyzer used during the duration of the study demonstrate accuracy of the Sao_2 calculation.[31,32] Body temperature could potentially affect pulse oximetry data and has not been included as a covariate, which must be recognized as a limitation of this study. The clinical indication for ABG sampling is also unknown given the retrospective nature of this study. Finally, anesthesia type may affect our findings: because of the low sample size of the regional anesthesia and monitored anesthesia care cases compared with general anesthesia cases, our model was unable to adjust for anesthesia type as a covariate.

In conclusion, we have found evidence that Black and Hispanic race/ethnicity are significantly associated with occult hypoxemia in the 92 to 100% Spo_2 range in anesthetized patients. Although the lack of objective skin pigmentation information and the retrospective nature of this study may limit the strength of our findings, we believe it is important to recognize the limitations of monitoring devices and maintain vigilance to avoid unrecognized hypoxemia.

Research Support

Support was provided solely from institutional and/or departmental sources.

Competing Interests

The authors declare no competing interests.

Correspondence

Address correspondence to Dr. Burnett: 1 Gustave Levy Place, Klingenstein Clinical Center 8th Floor, Box 411, New York, New York 10029. garrett.burnett@mountsinai.org. This article may be accessed for personal use at no charge through the Journal Web site, www.anesthesiology.org.

References

1. American Society of Anesthesiologists Committee on Standards and Practice Parameters: Standards for basic anesthetic monitoring. Available at: https://www.asahq.org/standards-and-guidelines/standards-for-basic-anesthetic-monitoring. Accessed February 20, 2021.
2. World Health Organization: Surgical safety checklist. Available at: https://www.who.int/patientsafety/topics/safe-surgery/checklist/en/. Accessed February 21, 2021.
3. Severinghaus JW: Takuo Aoyagi: Discovery of pulse oximetry. Anesth Analg 2007; 105(suppl 6):1–4
4. Taenzer AH, Pyke JB, McGrath SP, Blike GT: Impact of pulse oximetry surveillance on rescue events and intensive care unit transfers: A before-and-after concurrence study. Anesthesiology 2010; 112:282–7
5. Kaczka D, Chitilian H, Vidal Melo M: Respiratory monitoring, Miller's Anesthesia, 9th edition. Edited by Gropper M, Eriksson L, Fleisher L, Wiener-Kronish J, Cohen N, Leslie K. Philadelphia, Elsevier, 2020, pp 1298–339
6. Reich DL, Timcenko A, Bodian CA, Kraidin J, Hofman J, DePerio M, Konstadt SN, Kurki T,

Eisenkraft JB: Predictors of pulse oximetry data failure. Anesthesiology 1996; 84:859–64
7. Petterson MT, Begnoche VL, Graybeal JM: The effect of motion on pulse oximetry and its clinical significance. Anesth Analg 2007; 105(suppl 6):78–84
8. Ries AL, Prewitt LM, Johnson JJ: Skin color and ear oximetry. Chest 1989; 96:287–90
9. Cahan C, Decker MJ, Hoekje PL, Strohl KP: Agreement between noninvasive oximetric values for oxygen saturation. Chest 1990; 97:814–9
10. Jubran A, Tobin MJ: Reliability of pulse oximetry in titrating supplemental oxygen therapy in ventilator-dependent patients. Chest 1990; 97:1420–5
11. Lee KH, Hui KP, Tan WC, Lim TK: Factors influencing pulse oximetry as compared to functional arterial saturation in multi-ethnic Singapore. Singapore Med J 1993; 34:385–7
12. Bothma PA, Joynt GM, Lipman J, Hon H, Mathala B, Scribante J, Kromberg J: Accuracy of pulse oximetry in pigmented patients. S Afr Med J 1996; 86(suppl 5):594–6
13. Adler JN, Hughes LA, Vivilecchia R, Camargo CA Jr: Effect of skin pigmentation on pulse oximetry accuracy in the emergency department. Acad Emerg Med 1998; 5:965–70
14. Bickler PE, Feiner JR, Severinghaus JW: Effects of skin pigmentation on pulse oximeter accuracy at low saturation. Anesthesiology 2005; 102:715–9
15. Feiner JR, Severinghaus JW, Bickler PE: Dark skin decreases the accuracy of pulse oximeters at low oxygen saturation: The effects of oximeter probe type and gender. Anesth Analg 2007; 105(suppl 6):18–23
16. Sjoding MW, Dickson RP, Iwashyna TJ, Gay SE, Valley TS: Racial bias in pulse oximetry measurement. N Engl J Med 2020; 383:2477–8
17. Wasey JO, Lang M; R Core Team: icd: Fast comorbidities from ICD-9 and ICD-10 codes, decoding, manipulation and validation. icd: Comorbidities and tools for ICD codes V.4.0.9.9000. Available at https://jackwasey.github.io/icd/. Accessed November 20, 2021.
18. Elixhauser A, Steiner C, Harris DR, Coffey RM: Comorbidity measures for use with administrative data. Med Care 1998; 36:8–27
19. Quan H, Sundararajan V, Halfon P, Fong A, Burnand B, Luthi JC, Saunders LD, Beck CA, Feasby TE, Ghali WA: Coding algorithms for defining comorbidities in ICD-9-CM and ICD-10 administrative data. Med Care 2005; 43:1130–9
20. Stannard B, Levin MA, Lin HM, Weiner MM: Regional cerebral oximetry is consistent across self-reported racial groups and predicts 30-day mortality in cardiac surgery: A retrospective analysis. J Clin Monit Comput 2021; 35:413–21
21. United States Census Bureau: About the topic of race. Available at: https://www.census.gov/topics/population/race/about.html. Accessed March 1, 2021.
22. Office of Management and Budget: Revisions to the standards for the classification of federal data on race and ethnicity. Federal Register 1997; 97-28653:58782–90
23. Parker K, Horowitz JM, Morin R, Lopez MH: Multiracial in America: Proud, diverse and growing in numbers. Washington, D.C., Pew Research Center, 2015 Available at: https://www.pewresearch.org/social-trends/2015/06/11/multiracial-in-america/. Accessed February 16, 2022.
24. Grandini M, Bagli E, Visani G: Metrics for multi-class classification: An overview. arXiv 2020:1–17. Available at: http://arxiv.org/abs/2008.05756. Accessed February 21, 2021.
25. Ibáñez J, Velasco J, Raurich JM: The accuracy of the Biox 3700 pulse oximeter in patients receiving vasoactive therapy. Intensive Care Med 1991; 17:484–6
26. Mardirossian G, Schneider RE: Limitations of pulse oximetry. Anesth Prog 1992; 39:194–6
27. Pu LJ, Shen Y, Lu L, Zhang RY, Zhang Q, Shen WF: Increased blood glycohemoglobin A1c levels lead to overestimation of arterial oxygen saturation by pulse oximetry in patients with type 2 diabetes. Cardiovasc Diabetol 2012; 11:110
28. Wolfe B: Racial integrity laws (1924–1930). Encyclopedia Virginia. February 25, 2021. Available at: https://encyclopediavirginia.org/entries/racial-integrity-laws-1924-1930. Accessed March 10, 2021.
29. Ho AK, Sidanius J, Levin DT, Banaji MR: Evidence for hypodescent and racial hierarchy in the categorization and perception of biracial individuals. J Pers Soc Psychol 2011; 100:492–506
30. Olympio MA: Carbon dioxide absorbent desiccation safety conference convened by APSF. ASPF Newsletter 2005; 20:25–9. Available at: https://www.apsf.org/wp-content/uploads/newsletters/2005/summer/pdf/APSF200506.pdf. Accessed March 1, 2021.
31. Jacobs E, Ancy JJ, Smith M: Multi-site performance evaluation of pH, blood gas, electrolyte, glucose, and lactate determinations with the GEM Premier 3000 critical care analyzer. Point Care 2002; 1:135–44
32. Vukelic N, Papic Futac D, Topic E: Analytical properties of the GEM premier 3000 analyzer evaluated. Biochem Medica 2007; 17:231–41

ANESTHESIOLOGY

Frequency and Risk Factors for Difficult Intubation in Women Undergoing General Anesthesia for Cesarean Delivery: A Multicenter Retrospective Cohort Analysis

Sharon C. Reale, M.D., Melissa E. Bauer, D.O., Thomas T. Klumpner, M.D., Michael F. Aziz, M.D., Kara G. Fields, M.S., Rachel Hurwitz, B.S., Manal Saad, B.S., Sachin Kheterpal, M.D., M.B.A., Brian T. Bateman, M.D., M.Sc.; Multicenter Perioperative Outcomes Group Collaborators*

ANESTHESIOLOGY 2022; 136:697–708

EDITOR'S PERSPECTIVE

What We Already Know about This Topic

- Previous estimates for the frequency of difficult and failed intubation in the obstetric population vary widely, ranging from 0.3 to 3.3% and from 0 to 0.4%, respectively
- These data are largely based on older studies and may be less relevant now, given the increasing use of regional anesthesia, as well as more advanced management of the airway, including video laryngoscopy

What This Article Tells Us That Is New

- In a cohort of more than 14,000 women receiving general anesthetics for cesarean delivery, the risk of difficult intubation was 1 in 49, and the risk of failed intubation was 1 in 808
- Risk factors for difficult intubation included increased body mass index, Mallampati score III or IV, small hyoid-to-mentum distance, limited jaw protrusion, limited mouth opening, and cervical spine limitations

ABSTRACT

Background: Estimates for the incidence of difficult intubation in the obstetric population vary widely, although previous studies reporting rates of difficult intubation in obstetrics are older and limited by smaller samples. The goals of this study were to provide a contemporary estimate of the frequency of difficult and failed intubation in women undergoing general anesthesia for cesarean delivery and to elucidate risk factors for difficult intubation in women undergoing general anesthesia for cesarean delivery.

Methods: This is a multicenter, retrospective cohort study utilizing the Multicenter Perioperative Outcomes Group database. The study population included women aged 15 to 44 yr undergoing general anesthesia for cesarean delivery between 2004 and 2019 at 1 of 45 medical centers. Coprimary outcomes included the frequencies of difficult and failed intubation. Difficult intubation was defined as Cormack–Lehane view of 3 or greater, three or more intubation attempts, rescue fiberoptic intubation, rescue supraglottic airway, or surgical airway. Failed intubation was defined as any attempt at intubation without successful endotracheal tube placement. The rates of difficult and failed intubation were assessed. Several patient demographic, anatomical, and obstetric factors were evaluated for potential associations with difficult intubation.

Results: This study identified 14,748 cases of cesarean delivery performed under general anesthesia. There were 295 cases of difficult intubation, with a frequency of 1:49 (95% CI, 1:55 to 1:44; n = 14,531). There were 18 cases of failed intubation, with a frequency of 1:808 (95% CI, 1:1,276 to 1:511; n = 14,537). Factors with the highest point estimates for the odds of difficult intubation included increased body mass index, Mallampati score III or IV, small hyoid-to-mentum distance, limited jaw protrusion, limited mouth opening, and cervical spine limitations.

Conclusions: In this large, multicenter, contemporary study of more than 14,000 general anesthetics for cesarean delivery, an overall risk of difficult intubation of 1:49 and a risk of failed intubation of 1:808 were observed. Most risk factors for difficult intubation were nonobstetric in nature. These data demonstrate that difficult intubation in obstetrics remains an ongoing concern.

(ANESTHESIOLOGY 2022; 136:697–708)

Estimates for the frequency of difficult and failed intubation in the obstetric population vary widely, ranging from 0.3 to 3.3% and from 0 to 0.4%, respectively. These frequencies are several times higher than those reported for the general surgical population.[1–13] However, the studies that have examined the rates of difficult and failed intubation in obstetrics are from countries other than the United States or in smaller centers. Furthermore, increased rates of neuraxial anesthesia use may have affected observed

This article is featured in "This Month in Anesthesiology," page A1. This article has a visual abstract available in the online version. Part of the work presented in this article has been presented at the Society for Obstetric Anesthesia and Perinatology Virtual Meeting Series as a Best Clinical Papers Presentation on September 17, 2020, and at the American Society of Anesthesiologists Virtual Annual Meeting, as a Young Investigators Outcomes and Database Research Oral Presentation on October 3, 2020.

Submitted for publication August 24, 2021. Accepted for publication January 27, 2022. Published online first on February 21, 2022.

Sharon C. Reale, M.D.: Department of Anesthesiology, Perioperative and Pain Medicine, Brigham and Women's Hospital and Harvard Medical School, Boston, Massachusetts.

Melissa E. Bauer, D.O.: Department of Anesthesiology, Duke University Medical Center, Durham, North Carolina.

 Anesthesiology 2022; 136:697–708. DOI: 10.1097/ALN.0000000000004173

<zdoi; 10.1097/ALN.0000000000004173>

frequencies of difficult intubation in this population.[14] Video laryngoscope availability and use have also proliferated in recent years, which may have affected frequencies of difficult intubation.[15–17]

Given the potential maternal and neonatal morbidity and mortality associated with difficult or failed intubation, it is important to identify patients in whom intubation will be challenging to allow for preparations for difficult intubation to be made and, ideally, to encourage early neuraxial anesthesia in this patient group. Furthermore, studies have variably shown Mallampati score, obesity, age, and emergency surgery status to be potential risk factors for difficult intubation in obstetrics.[2,3,5,11,18,19] However, limitations in the literature regarding risk factors in obstetric patients include studies that are generally older, have limited power, include limited clinically granular data, or represent single-center studies.

This study aimed to provide an updated estimate of the frequency of difficult and failed intubation in women undergoing general anesthesia for cesarean delivery in the United States, leveraging the large number of cesarean delivery records contained in the Multicenter Perioperative Outcomes Group database. We also aimed to elucidate risk factors for difficult intubation to inform risk stratification based on factors that may be unique to women undergoing general anesthesia for cesarean delivery.

Materials and Methods

This is a multicenter, retrospective, observational cohort study utilizing the Multicenter Perioperative Outcomes Group database. The Multicenter Perioperative Outcomes Group is a consortium of institutions founded in 2008 with a shared data set to facilitate the investigation of perioperative outcomes. The comprehensive methodology of the Multicenter Perioperative Outcomes Group research database has been described in detail.[18,20] Each institution that is a part of the Multicenter Perioperative Outcomes Group uses an electronic health record to extract and export data into a shared database. Data and case validation are performed on the institutional level to ensure quality and consistency of data. The number of Multicenter Perioperative Outcomes Group institutions contributing obstetric cases per year is seen in appendix 2. Institutional review board approval has been obtained from each Multicenter Perioperative Outcomes Group center, and informed consent has been waived. The research protocol, including the data analysis and statistical plan, was written, filed, and approved by the Multicenter Perioperative Outcomes Group perioperative clinical research committee before accessing the data, although several elements of the plan were altered in response to peer review.

Our study population included all women aged 15 to 44 yr undergoing general anesthesia for cesarean delivery between February 6, 2004, and January 11, 2019, at 45 Multicenter Perioperative Outcomes Group sites. Applicable procedure codes and a previously described list of search terms for cesarean delivery[21] were used to define the study population.

Outcomes

Coprimary outcomes included the frequencies of difficult and failed intubation in obstetrics. Potential difficult intubation cases were identified in an automated fashion *via* electronic search of the database for any of the following: observed or labeled difficult tracheal intubation, direct or video laryngoscopy Cormack–Lehane view of 3 or higher, three or more intubation attempts, fiberoptic intubation, laryngeal mask airway placement, surgical airway, documentation of neuromuscular blockade administration without concurrent documentation of endotracheal tube placement, or any documented attempt at direct or video laryngoscopy without concurrent documentation of endotracheal tube placement. This initial definition of difficult intubation used to perform the electronic search of the database for difficult intubations was intentionally expansive to allow for maximal sensitivity of results. All cases electronically identified as potentially difficult were reviewed by two independent investigators (S.C.R. and R.H. or M.S.), who manually classified cases as difficult or failed. All discrepancies between reviewers were resolved by discussion among coauthors (S.C.R., R.H., M.S., and T.T.K.). In the final manual review of cases, difficult intubation was identified using previously defined designations: difficult laryngoscopy (defined as direct or video laryngoscopy Cormack–Lehane view of 3 or greater), three or more intubation attempts, flexible scope intubation after failed laryngoscopy, rescue supraglottic airway, or surgical airway. Failed intubation was a subset of difficult intubation and was defined as any attempt at intubation without successful endotracheal tube placement, including mask ventilation or supraglottic airway placement, after an attempt at intubation was made.[16,22,23] We calculated frequencies of difficult and failed intubation and

Thomas T. Klumpner, M.D.: Department of Anesthesiology, University of Michigan Medical School, Ann Arbor, Michigan.

Michael F. Aziz, M.D.: Department of Anesthesiology and Perioperative Medicine, Oregon Health and Science University, Portland, Oregon.

Kara G. Fields, M.S.: Department of Anesthesiology, Perioperative and Pain Medicine, Brigham and Women's Hospital and Harvard Medical School, Boston, Massachusetts.

Rachel Hurwitz, B.S.: Department of Anesthesiology, University of Michigan Medical School, Ann Arbor, Michigan.

Manal Saad, B.S.: Department of Anesthesiology, University of Michigan Medical School, Ann Arbor, Michigan.

Sachin Kheterpal, M.D., M.B.A.: Department of Anesthesiology, University of Michigan Medical School, Ann Arbor, Michigan.

Brian T. Bateman, M.D., M.Sc.: Department of Anesthesiology, Perioperative and Pain Medicine, Stanford University School of Medicine, Stanford, California.

*The Multicenter Perioperative Outcomes Group Collaborators are listed in appendix 1.

associated 95% CI values for women undergoing general anesthesia for cesarean delivery.

Risk Factors

We assessed the following potential risk factors for difficult intubation in women undergoing general anesthesia for cesarean delivery based on biologic plausibility and risk factors previously studied in the literature[2,5,11,18,19,24]: age (35 to 39 yr or more than 40 yr *vs.* less than 35 yr), body mass index (25 to 39.9 kg/m^2 or more than 40 kg/m^2 *vs.* less than 25 kg/m^2), race/ethnicity (Asian or Pacific Islander, Black, Hispanic, or other/unknown *vs.* White), American Society of Anesthesiologists (Schaumburg, Illinois) Physical Status (III or IV *vs.* I or II), year of delivery 2004 to 2011, Mallampati score (III or IV *vs.* I or II), small hyoid-to-mentum distance (less than three fingerbreadths), subjectively limited jaw protrusion, limited mouth opening (less than 3 cm), altered neck anatomy, cervical spine limitations, labor to cesarean status, induction of labor, presence of preterm delivery, presence of multiple gestation, and presence of preeclampsia or eclampsia.

Statistical Analysis

All cases of general anesthesia for cesarean delivery were pooled across 45 institutions to estimate the incidence of difficult intubation, both overall and stratified by individual patient characteristics and number of risk factors, as well as the incidence of failed intubation. The incidences are presented as point estimates with 95% Wilson score CI. The interrater reliabilities between pairs of investigators for manually classifying cases as difficult and failed intubations were quantified as interrater reliability (κ) statistics with 95% CI.

A set of multilevel logistic regression models was used to estimate the association of 16 potential risk factors, both unadjusted and adjusted for other potential risk factors, with the odds of difficult intubation. The correlation between surgeries at the same hospital was accounted for by including a random intercept for hospital identification in each model. Cases with unknown hospital identification (n = 114) were excluded from risk factor analyses. The data set consisted of variables collected for clinical, not research, purposes at 45 hospital sites with varied local documentation practices, electronic health records, and data submission processes during a 15-yr period, so the vast majority (81%) of potential risk factors had missing data. Potential risk factors with less than 40% missing data were deemed appropriate for analysis using multiple imputation and inclusion in the risk factor–adjusted model; these variables had more observed than missing data, allowing for a meaningful comparison between the distributions of the observed and imputed data in the assessment of imputation model fit. In contrast, potential risk factors with 40% or more missing data were determined to be suboptimal candidates for multiple imputation analysis and were only assessed using complete case analysis. Specifically, potential risk factors with 40% or more missing data were each assessed in individual models for their site-adjusted association with the odds of difficult intubation using complete case analysis and not assessed in combination with other potential risk factors. Potential risk factors with less than 40% missing data were each assessed in both individual models for their site-adjusted association with the odds of difficult intubation, as well as in a combined model for their site and other potential risk factor–adjusted association with the odds of difficult intubation using multiple imputation analysis. Specifically, the fully conditional specification approach[25] was used to create 65 imputed data sets based on observed potential risk factors (those with less than 40% missing data) and difficult intubation values. A total of 65 imputations were performed because 63% of deliveries had at least one missing value for the variables included in the imputation model, and it has been recommended that the number of imputations should be at least as large as the number of observations with incomplete data.[26] Imputation model fit was assessed by comparing the distributions of observed *versus* imputed values in each of the first five imputed data sets for each imputed variable. The odds ratios and corresponding standard errors were estimated using multilevel logistic regression for each of the 65 imputed data sets. Point estimates and standard errors were then combined using Rubin's rules[27] to produce pooled odds ratios with corresponding 95% CI values. As a descriptive analysis, the risk of difficult intubation was calculated as stratified by the number of potential risk factors with site-adjusted odds ratios for difficult intubation of 1.5 or higher.

Logistic regression was used to model the association between delivery date and the odds of difficult intubation utilizing a restricted cubic spline with four knots to allow for a nonlinear relationship between the exposure and log odds of the outcome.[28] The logistic regression model was used to estimate the odds ratio for difficult intubation for January 11, 2019 (representing the last day of data), *versus* July 25, 2011 (halfway between the start and end of data), with corresponding 95% CI values.

All statistical hypothesis tests were two-sided. Statistical analyses were performed with SAS software version 9.4 (SAS Institute, USA) and the rms package implemented in R software version 3.6.1 (R Foundation for Statistical Computing, Austria).

Before analysis, we expected to identify approximately 13,000 patients receiving general anesthesia for cesarean delivery in the Multicenter Perioperative Outcomes Group database. The incidence of difficult intubation for patients receiving general anesthesia for cesarean delivery has been reported as 0.2 to 3.0%.[1–5] Assuming a 1.0% incidence of difficult tracheal intubation, we determined that analysis of 13,000 patients would allow for a 99% probability of

obtaining a 95% Wilson CI half-width for the incidence of ±0.2%.

Results

We identified 14,537 cases of cesarean delivery performed under general anesthesia in the Multicenter Perioperative Outcomes Group database in which difficult and/or failed intubation status was reported. Of these, 1,236 cases were identified as potentially difficult (fig. 1). Upon manual review, there were 295 cases of difficult intubation; the frequency of difficult intubation was 2.03% (95% CI, 1.81 to 2.27). There were 18 cases of failed intubation; the frequency of failed intubation was 0.12% (95% CI, 0.08 to 0.20). There were 45 unique institutions in which cesarean deliveries were identified: 31 academic, medical school–affiliated hospitals and 14 community hospitals. The interrater reliability (κ) between independent reviewers for the outcome of difficult intubation was 0.88 (95% CI, 0.85 to 0.90); κ for the outcome of failed intubation was 0.82 (95% CI, 0.78 to 0.86).

Methods for managing difficult and failed intubations are seen in table 1. Of difficult intubations, 87.8% involved difficult laryngoscopy, defined as a direct or video laryngoscopy Cormack–Lehane grade 3 or 4 view (68.5% of cases were classified as difficult intubations solely due to difficult laryngoscopy); 16.3% required three or more attempts at intubation; 11.5% of cases required a supraglottic airway and were followed by a successful intubation; and 2.4% of cases required flexible scope intubation and were followed by a successful intubation. Of the 18 failed intubations, all were rescued by supraglottic airway placement. One case additionally had a failed flexible scope intubation attempt and a subsequent successful rescue surgical airway. There was one maternal cardiac arrest in the difficult intubation cohort, with ensuing cardiopulmonary resuscitation and eventual return of spontaneous circulation; the etiology of arrest was unknown, but hysterectomy was required for ongoing bleeding. There were no maternal deaths in either the difficult or failed intubation cohorts. Of the difficult intubation cases, there was one noted aspiration event, one noted instance of dental injury, and four instances of pharyngeal injury; however, these outcomes were not routinely commented upon in each case and were only noted if specifically found to be mentioned in the intraoperative anesthetic record.

We evaluated 16 different patient characteristics for a potential association with difficult intubation (tables 2 and 3). Potential risk factors with 40% or more missing data were assessed using complete case analysis, whereas factors with less than 40% missing data were assessed using multiple imputation analysis. Appendix 3 shows similar distributions of observed *versus* imputed values in each of the first five imputed data sets for each imputed variable, suggesting acceptable imputation model fit. Elevated body mass index was strongly associated with increased odds of difficult intubation. Compared to women with a body mass index less than 25 kg/m^2, women with a body mass index of 25 to 39.9 kg/m^2 had an odds ratio of 1.55 for difficult intubation (95% CI, 0.88 to 2.73), and women with a body mass index 40 kg/m^2 or higher had an odds ratio of 2.71 (95% CI, 1.53 to 4.8). Of 28 women with a body mass index of 40 kg/m^2 or more, 1 experienced a difficult intubation. Several airway factors were also strongly associated with the

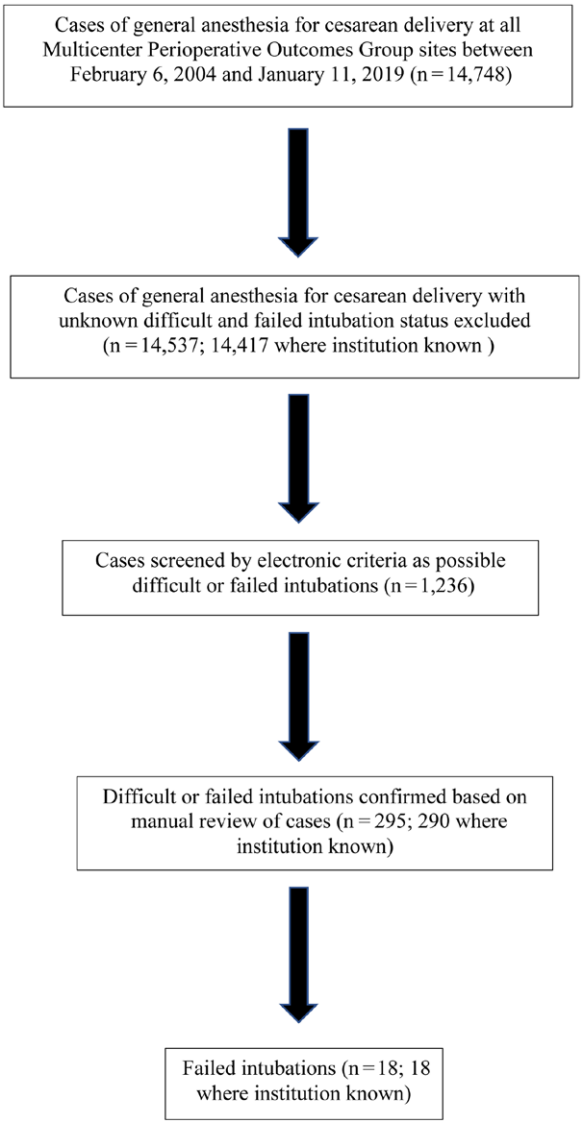

Fig. 1. Cohort selection of obstetric patients. Automated electronic screening criteria were documentation of any of the following: observed or labeled difficult tracheal intubation, direct or video laryngoscopy Cormack–Lehane view of 3 or higher, three or more intubation attempts, fiberoptic intubation, laryngeal mask airway placement, surgical airway, documentation of neuromuscular blockade administration without concurrent documentation of endotracheal tube placement, or any documented attempt at direct or video laryngoscopy without concurrent documentation of endotracheal tube placement.

Table 1. Characteristics of Difficult and Failed Intubations in Obstetric Patients Undergoing General Anesthesia for Cesarean Delivery, 2004 to 2019

Characteristics	Difficult Intubations, No. (%)	Failed Intubations, No. (%)
Total	295 (2.0)	18 (0.1)
Criteria for difficult intubation		
Cormack–Lehane view grade III or IV*	259 (87.8)	8 (44.4)
Requiring three or more attempts at intubation†	48 (16.3)	3 (16.7)
Flexible bronchoscopy attempted after previous failed laryngoscopy	7 (2.4)	1 (5.6)
Supraglottic airway attempted	34 (11.5)	18 (100)
Surgical airway attempted	1 (0.3)	1 (5.6)
Approach to management		
Failed direct laryngoscopy (if attempted)‡	49 (19.2)	14 (100)
Failed video laryngoscopy (if attempted)§	26 (32.1)	10 (100)
Facemask ventilation Han scale 3 or 4	7 (2.4)	2 (11.1)
Complications		
Aspiration noted	1 (0.3)	1 (5.6)
Dental injury noted	1 (0.3)	0
Pharyngeal injury noted	4 (1.4)	0
Cardiac arrest	1 (0.3)	0
Intraoperative death	0	0

*Cormack–Lehane View recorded in 68.3% of patients undergoing general anesthesia for cesarean delivery. †Number of intubation attempts recorded in 63.5% of patients undergoing general anesthesia for cesarean delivery. ‡Direct laryngoscopy attempted in 255 difficult intubations and 14 failed intubations. §Video laryngoscopy attempted in 81 difficult intubations and 10 failed intubations.

risk of difficult intubation. Compared to a Mallampati score of I or II, a Mallampati score of III had an odds ratio of 2.37 (95% CI, 1.72 to, 3.27) for difficult intubation, and a Mallampati score of IV had an odds ratio of 4.6 (95% CI, 2.61 to 8.2) for difficult intubation, such that 1 in 28 women with a Mallampati score of III and 1 in 12 women with a Mallampati score of IV experienced a difficult intubation. Small hyoid-to-mentum distance, limited jaw protrusion, limited mouth opening, and cervical spine limitations were all associated with an increased risk of difficult intubation. Notably, one in nine women with a limited mouth opening experienced a difficult intubation. Of obstetric factors, 1 in 33 women with preeclampsia or eclampsia experienced a difficult intubation.

Factors that retained the strongest associations with the risk of difficult intubation with odds ratios for difficult intubation greater than 1.5 after adjustment for all other potential risk factors (with the exception of small hyoid-to-mentum distance, limited jaw protrusion, limited mouth opening, altered neck anatomy, and cervical spine limitations due to large amounts of missing data) included age 35 yr or more (odds ratio, 1.65; 95% CI, 1.23 to 2.21), age 40 yr or more (odds ratio, 2.17; 95% CI, 1.34 to 3.51); body mass index 40 kg/m^2 or higher (odds ratio, 2.02; 95% CI, 1.12 to 3.63), American Society of Anesthesiologists Physical Status IV (odds ratio, 1.65; 95% CI, 0.93 to 2.92), Mallampati score of III (odds ratio, 2.05; 95% CI, 1.46 to 2.86), and Mallampati score of IV (odds ratio, 3.79; 95% CI, 2.10 to 6.9; table 3).

Figure 2 shows the frequency of difficult intubation stratified by the number of risk factors present, with 1,066 patients having complete documentation of all the factors associated with difficult intubation. Factors included in this analysis were those with odds ratios for difficult intubation of 1.5 or higher without adjustment for other potential risk factors. With increasing numbers of risk factors present, an increasing frequency of difficult intubation was observed. With one risk factor for difficult intubation, the frequency of difficult intubation was 0.8% (95% CI, 0.3 to 2.2); with two risk factors, the frequency was 1.0% (95% CI, 0.3 to 2.8); with three risk factors, the frequency was 3.7% (95% CI, 1.8 to 7.4); with four risk factors, the frequency was 3.8% (95% CI, 1.3 to 10.6); and with five or more risk factors, the frequency was 8.8% (95% CI, 3.0 to 23.0). Figure 3 shows the frequency of difficult intubation over time from 2004 to 2019 as modeled with a restricted cubic spline with four knots. The estimated odds ratio and 95% CI for difficult intubation on January 11, 2019 (representing the last day of data), *versus* July 25, 2011 (halfway between the start and end of data), were 0.41 (95% CI, 0.254 to 0.66).

Discussion

In this large, multicenter study, we examined the frequency of difficult intubation in more than 14,000 general anesthetics for cesarean delivery; we observed a risk of difficult intubation of 1:49 and a risk of failed intubation of 1:808. Most cases of difficult intubation were classified as such due to difficult laryngoscopy, as defined by a grade III or IV Cormack–Lehane view. A total of 18% of difficult intubation cases required three or more attempts at laryngoscopy, and 12% of cases were rescued by a supraglottic airway. We identified several risk factors for difficult intubation in obstetrics, and for some patient characteristics,

Table 2. Obstetric Patient Characteristics

Characteristics	Total, No.	Difficult Intubation, No.	Frequency of Difficult Intubations per 1,000 (95% CI)	Data Complete, %
Age				100
Less than 35 yr	11,526	209	18.1 (15.9–20.7)	
35–39 yr	2,368	66	27.9 (22.0–35.3)	
40 yr or older	637	20	31.4 (20.4–48.0)	
Body mass index				69.6
Less than 25 kg/m^2	1,252	8	6.4 (3.2–12.6)	
25–39.9 kg/m^2	7,089	124	17.5 (14.7–20.8)	
40 kg/m^2 or higher	1,768	63	35.6 (28.0–45.3)	
Race/ethnicity				100
Asian or Pacific Islander	522	6	11.5 (5.3–24.8)	
Black	2,921	72	24.6 (19.6–30.9)	
Hispanic	383	12	31.3 (18.0–54.0)	
White	7,160	126	17.6 (14.8–20.9)	
Other/unknown	3,545	79	22.3 (17.9–27.7)	
ASA Physical Status				96.9
I	519	16	30.8 (19.1–49.5)	
II	8,289	138	16.6 (14.1–19.6)	
III	4,703	119	25.3 (21.2–30.2)	
IV	536	15	28.0 (17.0–45.7)	
V	35	0	0 (0–98.9)	
VI	1	0	0 (0–793.5)	
Year of delivery				100
2004 to 2005	125	2	16.0 (4.4–56.5)	
2006 to 2007	253	1	4.0 (0.7–22.0)	
2008 to 2009	579	15	25.9 (15.8–42.3)	
2010 to 2011	1,346	38	28.2 (20.6–38.5)	
2012 to 2013	2,249	59	26.2 (20.4–33.7)	
2014 to 2015	3,141	70	22.3 (17.7–28.1)	
2016 to 2017	4,722	89	18.8 (15.3–23.1)	
2018 to 2019	2,116	21	9.9 (6.5–15.1)	
Mallampati score				63.9
I or II	7,450	118	15.8 (13.2–18.9)	
III	1,673	59	35.3 (27.4–45.2)	
IV	163	14	85.9 (51.9–139.0)	
Small hyoid-to-mentum distance, n				26.0
No	3,683	78	21.2 (17.0–26.4)	
Yes	88	6	68.2 (31.6–140.9)	
Limited jaw protrusion, n				29.8
No	4,227	74	17.5 (14.0–21.9)	
Yes	107	5	46.7 (20.1–104.8)	
Limited mouth opening, n				29.3
No	4,183	67	16.0 (12.6–20.3)	
Yes	71	8	112.7 (58.2–206.9)	
Altered neck anatomy, n				33.9
No	4,555	68	14.9 (11.8–18.9)	
Yes	376	9	23.9 (12.6–44.9)	
Cervical spine limitations, n				26.3
No	3,771	77	20.4 (16.4–25.4)	
Yes	54	4	74.1 (29.2–175.5)	
Labor to cesarean status, n				72.1
No	8,482	180	21.2 (18.4–24.5)	
Yes	1,990	49	24.6 (18.7–32.4)	
Induction of labor, n				83.9
No	11,701	241	20.6 (18.2–23.3)	
Yes	492	15	30.5 (18.6–49.7)	
Presence of preterm delivery, n				72.4
No	9,098	195	21.4 (18.7–24.6)	
Yes	1,423	27	19.0 (13.1–27.5)	
Presence of multiple gestation, n				72.4
No	9,986	211	21.1 (18.5–24.1)	
Yes	535	11	20.6 (11.5–36.4)	
Presence of preeclampsia or eclampsia, n				72.4
No	9,320	186	20.0 (17.3–23.0)	
Yes	1,201	36	30.0 (21.7–41.2)	

ASA, American Society of Anesthesiologists.

Table 3. Associations between Obstetric Patient Characteristics and Odds of Difficult Intubation

Characteristics	Site-adjusted Odds Ratio (95% CI)	Site- and Factor-adjusted Odds Ratio (95% CI)	Risk of Difficult Intubation
Overall			1:49
Age			
Less than 35 yr	Reference	Reference	1:55
35–39 yr	1.66 (1.24–2.21)	1.65 (1.23–2.21)	1:36
40 yr or more	2.14 (1.33–3.44)	2.17 (1.34–3.51)	1:32
Body mass index			
Less than 25 kg/m^2	Reference	Reference	1:156
25–39.9 kg/m^2	1.55 (0.88–2.73)	1.48 (0.84–2.60)	1:57
40 kg/m^2 or higher	2.71 (1.53–4.8)	2.02 (1.12–3.63)	1:28
Race/ethnicity			
Asian or Pacific Islander	0.89 (0.388–2.06)	0.89 (0.383–2.07)	1:87
Black	1.46 (1.06–2.02)	1.34 (0.96–1.87)	1:41
Hispanic	2.06 (1.07–4.0)	1.91 (0.98–3.75)	1:32
White	Reference	Reference	1:57
Other/unknown	1.17 (0.86–1.59)	1.10 (0.80–1.52)	1:45
ASA status			
I or II	Reference	Reference	1:57
III	1.61 (1.25–2.07)	1.23 (0.93–1.63)	1:40
IV–VI	2.01 (1.17–3.48)	1.65 (0.93–2.92)	1:38
Year of delivery, 2004–2011*	1.21 (0.88–1.67)	1.37 (0.98–1.92)	1:41
Mallampati score			
I or II	Reference	Reference	1:63
III	2.37 (1.72–3.27)	2.05 (1.46–2.86)	1:28
IV	4.6 (2.61–8.2)	3.79 (2.10–6.85)	1:12
Small hyoid-to-mentum distance†	3.03 (1.27–7.3)		1:15
Limited jaw protrusion†	2.67 (1.04–6.9)		1:21
Limited mouth opening†	8.2 (3.72–17.9)		1:9
Altered neck anatomy†	1.85 (0.89–3.86)		1:42
Cervical spine limitation†	4.5 (1.54–13.0)		1:14
Labor to cesarean status	1.11 (0.78–1.59)	1.20 (0.82–1.75)	1:41
Induction of labor	1.13 (0.62–2.06)	1.03 (0.54–1.94)	1:33
Presence of preterm delivery	1.02 (0.67–1.55)	0.98 (0.63–1.51)	1:53
Presence of multiple gestation	1.09 (0.58–2.05)	1.09 (0.57–2.09)	1:49
Presence of preeclampsia or eclampsia	1.67 (1.16–2.40)	1.28 (0.87–1.89)	1:33

All odds ratio and CI values were obtained *via* combination of point estimates and standard errors from 65 imputed data sets using Rubin's rules, except where otherwise specified.

*Reference 2012 to 2019. †Due to missingness of 40% or more, site-adjusted odds ratios and CI values for factors obtained using complete case analysis and factors not included in site- and factor-adjusted model were estimated using multiple imputation.

ASA, American Society of Anesthesiologists.

the risk of difficult intubation was substantial. One in 28 women with a body mass index 40 kg/m^2 or more, 1 in 12 women with a Mallampati score of IV, and 1 in 9 women with a limited mouth opening experienced a difficult intubation. Most factors strongly associated with difficult intubation were nonobstetric in nature and were related to patient or airway characteristics. When examining the rates of difficult intubation over time, we found a decrease in the frequency of difficult intubation in the second half of the study period. The proliferation of video laryngoscopy during the time period may be associated with this observation,[15–17] although additional studies are needed to confirm this finding.

The frequencies of difficult and failed intubation that we observed in our study are in line with those seen in the published literature.[1–13] However, these frequencies are difficult to compare directly among studies, as there is no standard definition for such outcomes, and the patient populations and time frames in which the studies were conducted vary widely. For example, definitions for failed intubation vary from unsuccessful intubations after a single dose of succinylcholine to inability to intubate during general anesthesia, with the latter being closer to the relatively more stringent definition for failed intubation we have adopted.[3,8,9] Nonetheless, our rate of difficult intubation, 1:49, is consistent with results in the published literature, which range widely from 1:30 to 1:400; our rate of failed intubation, 1:808, is also within the range of the published literature, from no cases of failed intubation in one community-based case series to 1:200.[1–5] We also found that all 18 cases of failed intubation were rescued with a supraglottic airway device, which is also consistent with a trend in the literature toward increasing supraglottic airway use in cases of failed intubation.[5,29] However, our large, multicenter,

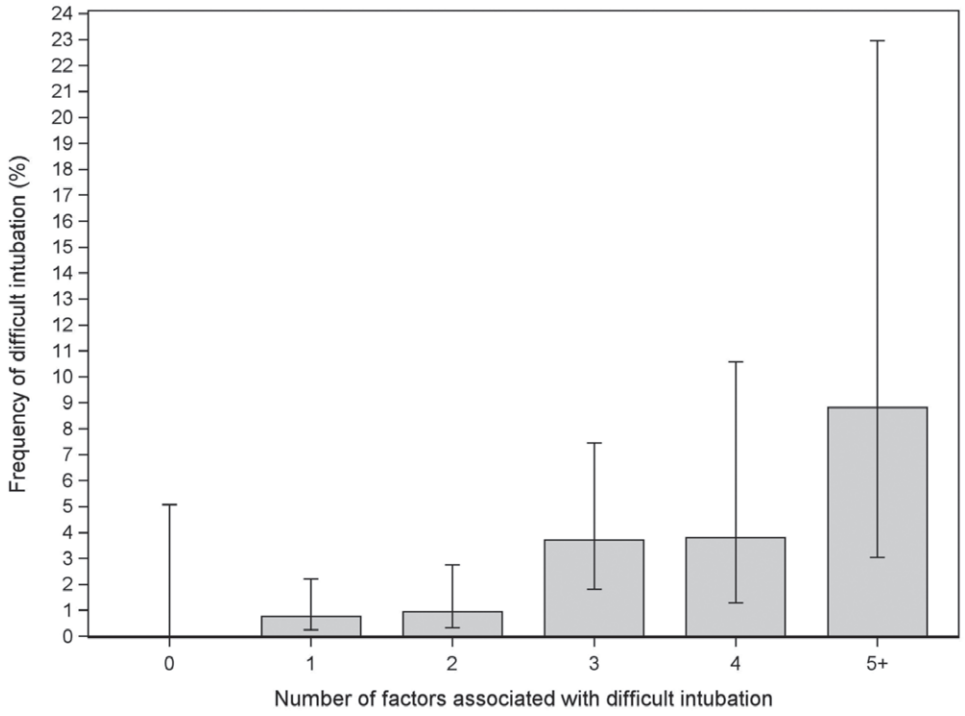

Fig. 2. Frequency of difficult intubation stratified by number of risk factors present. The *x axis* shows the number of factors associated with difficult intubation. The factors included in the analyses are those with univariate odds ratio for difficult intubation greater than 1.50: age 35 yr or more, body mass index of 25 or higher, American Society of Anesthesiologists Physical Status III or IV, Mallampati score III or IV, small hyoid-to-mentum distance, limited jaw protrusion, limited mouth opening, altered neck anatomy, cervical spine limitations, and presence of preeclampsia or eclampsia (race excluded given widely varying estimates). The *y axis* shows the frequency of difficult intubation, with *error bars* representing 95% CI.

United States–based study encompassed multiple hospital types and a variety of patient populations. Further, in contrast to many previous studies in this area, we were also able to examine risk factors for difficult intubation.

Our findings suggest that difficult intubation in women undergoing general anesthesia for cesarean delivery remains a significant concern, particularly among a subset of patients that we have identified with substantial risk factors for difficult intubation, such as elevated body mass index and abnormal airway anatomy. These patients are the ones in whom early anesthetic planning may be preferable to reduce the likelihood that their airway will need to be instrumented. Despite the proliferation of video laryngoscopy and the shift toward neuraxial anesthesia, airway concerns in women undergoing general anesthesia for cesarean delivery remain, and providers should be cognizant of the possibility of difficult intubation, as well as the increased risk of difficult intubation with an increasing number of risk factors.

Strengths of this study include the expansion of our current understanding of difficult intubation in women undergoing general anesthesia for cesarean delivery, based on the largest multicenter sample evaluated to date. Our large sample size provides us with adequate power to more precisely estimate the risk of difficult intubation associated with a variety of patient characteristics and to examine obstetrical risk factors for difficult intubation. Limitations of this study include those inherent to an observational study based on electronic health record data. Risk factors for difficult tracheal intubation may be incompletely identified if documentation is not comprehensive for each case. In particular, many airway factors of interest (small hyoid-to-mentum distance, limited jaw protrusion, limited mouth opening, altered neck anatomy, and cervical spine limitations) had more than 65% missing data, precluding multiple imputation analysis and estimation of their association with difficult intubation while adjusting for other potential risk factors. We attempted to account for missing data in potential risk factors without significant missingness (*i.e.*, less than 40%) using multiple imputation analysis and appeared to obtain a well-fit imputation model. However, all estimates and CI values from both complete case and multiple imputation analyses must be interpreted in the context of this missingness. In addition, there were multiple cases that were labeled as difficult intubations by the provider in the anesthetic record but either did not have a documented reason for this designation or did not meet our criteria for

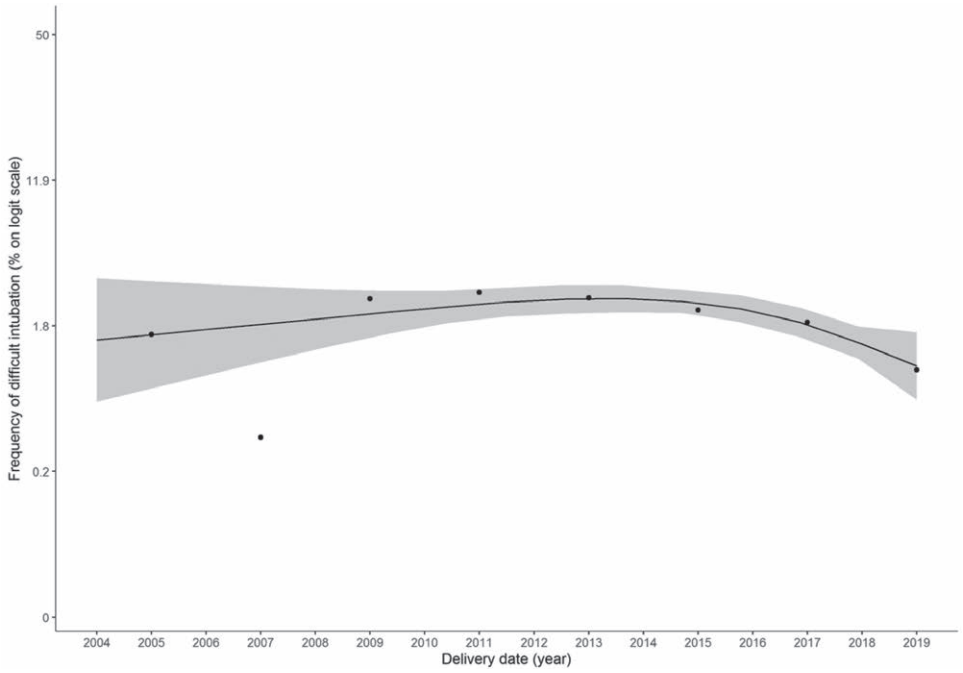

Fig. 3. Frequency of difficult intubation over time. The *x axis* shows the delivery date (yr). On the *y axis*, the *lines* and *band* represent the predicted frequency and 95% CI, respectively, for difficult intubation over time as estimated using a logistic regression model with restricted cubic spline. The axis is on the logit scale to correspond to the logistic regression model. *Scatterplot dots* are shown representing observed percentages of difficult intubations for every 2-yr period.

difficult intubation. Therefore, these cases were not counted as difficult intubations in our final manual review, and this discrepancy could potentially mean that our calculated frequency of difficult intubation is lower than the actual frequency of difficult intubation. Further, although worsening of Mallampati scores throughout labor is a known phenomenon,[30] the Multicenter Perioperative Outcomes Group database contained only one airway examination per patient. It is also not possible to determine provider experience level with each given device or attempt; some attempts at intubation may be performed by relatively inexperienced providers at teaching hospitals. Institutional factors may also differ in determining whether direct *versus* video laryngoscopy is attempted initially, potentially altering the ability to compare rescue device success rates. We were also not able to determine whether cesarean delivery cases were performed on an emergent basis, which might have an impact on a provider's ability to secure an airway. While the Multicenter Perioperative Outcomes Group database consists of a large database of multiple institutions, academic institutions are overrepresented. As a result, the patient population may skew toward a higher acuity and may not be representative of community practices. Furthermore, our results may not be generalizable to all obstetric patients as a whole, given that women with a known or suspected difficult airway may be more likely to have had a planned regional anesthetic.

These data from a large, multicenter sample from the United States demonstrate that we need to continue to be vigilant for the possibility of difficult intubation in women undergoing general anesthesia for cesarean delivery. A thorough evaluation and early epidural analgesia for patients in whom it is appropriate may help minimize the need for intubation in the highest-risk patients.

Research Support

Supported by departmental and institutional resources at each contributing site. In addition, partial funding to support underlying electronic health record data collection into the Multicenter Perioperative Outcomes Group registry was provided by Blue Cross Blue Shield of Michigan/Blue Care Network (Detroit, Michigan) as part of the Blue Cross Blue Shield of Michigan/Blue Care Network Value Partnerships program. Although Blue Cross Blue Shield of Michigan/Blue Care Network and the Multicenter Perioperative Outcomes Group work collaboratively, the opinions, beliefs, and viewpoints expressed by the authors do not necessarily reflect the opinions, beliefs, and viewpoints of Blue Cross Blue Shield of Michigan/Blue Care Network or any of its employees.

Competing Interests

The authors declare no competing interests.

Correspondence

Address correspondence to Dr. Reale: 75 Francis Street, CWN L1, Boston, Massachusetts 02115. screale@bwh.harvard.edu. This article may be accessed for personal use at no charge through the Journal Web site, www.anesthesiology.org.

References

1. Djabatey EA, Barclay PM: Difficult and failed intubation in 3430 obstetric general anaesthetics. Anaesthesia 2009; 64:1168–71
2. McDonnell NJ, Paech MJ, Clavisi OM, Scott KL; ANZCA Trials Group: Difficult and failed intubation in obstetric anaesthesia: An observational study of airway management and complications associated with general anaesthesia for caesarean section. Int J Obstet Anesth 2008; 17:292–7
3. Pollard R, Wagner M, Grichnik K, Clyne BC, Habib AS: Prevalence of difficult intubation and failed intubation in a diverse obstetric community-based population. Curr Med Res Opin 2017; 33:2167–71
4. Kinsella SM, Winton AL, Mushambi MC, Ramaswamy K, Swales H, Quinn AC, Popat M: Failed tracheal intubation during obstetric general anaesthesia: A literature review. Int J Obstet Anesth 2015; 24:356–74
5. Quinn AC, Milne D, Columb M, Gorton H, Knight M: Failed tracheal intubation in obstetric anaesthesia: 2 yr national case-control study in the UK. Br J Anaesth 2013; 110:74–80
6. Rajagopalan S, Suresh M, Clark SL, Serratos B, Chandrasekhar S: Airway management for cesarean delivery performed under general anesthesia. Int J Obstet Anesth 2017; 29:64–9
7. McKeen DM, George RB, O'Connell CM, Allen VM, Yazer M, Wilson M, Phu TC: Difficult and failed intubation: Incident rates and maternal, obstetrical, and anesthetic predictors. Can J Anaesth 2011; 58:514–24
8. Hawthorne L, Wilson R, Lyons G, Dresner M: Failed intubation revisited: 17-yr experience in a teaching maternity unit. Br J Anaesth 1996; 76:680–4
9. Barnardo PD, Jenkins JG: Failed tracheal intubation in obstetrics: A 6-year review in a UK region. Anaesthesia 2000; 55:690–4
10. Rahman K, Jenkins JG: Failed tracheal intubation in obstetrics: No more frequent but still managed badly. Anaesthesia 2005; 60:168–71
11. Tao W, Edwards JT, Tu F, Xie Y, Sharma SK. Incidence of unanticipated difficult airway in obstetric patients in a teaching institution. J Anesth 2012; 117:883–97
12. D'Angelo R, Smiley RM, Riley ET, Segal S: Serious complications related to obstetric anesthesia: The serious complication repository project of the Society for Obstetric Anesthesia and Perinatology. Anesthesiology 2014; 120:1505–12
13. Samsoon GL, Young JR: Difficult tracheal intubation: A retrospective study. Anaesthesia 1987; 42:487–90
14. Palanisamy A, Mitani AA, Tsen LC: General anesthesia for cesarean delivery at a tertiary care hospital from 2000 to 2005: A retrospective analysis and 10-year update. Int J Obstet Anesth 2011; 20:10–6
15. Cook TM, Kelly FE: A national survey of videolaryngoscopy in the United Kingdom. Br J Anaesth 2017; 118:593–600
16. Schroeder RA, Pollard R, Dhakal I, Cooter M, Aronson S, Grichnik K, Buhrman W, Kertai MD, Mathew JP, Stafford-Smith M: Temporal trends in difficult and failed tracheal intubation in a regional community anesthetic practice. Anesthesiology 2018; 128:502–10
17. Aziz MF, Kim D, Mako J, Hand K, Brambrink AM: A retrospective study of the performance of video laryngoscopy in an obstetric unit. Anesth Analg 2012; 115:904–6
18. Kheterpal S, Healy D, Aziz MF, Shanks AM, Freundlich RE, Linton F, Martin LD, Linton J, Epps JL, Fernandez-Bustamante A, Jameson LC, Tremper T, Tremper KK; Multicenter Perioperative Outcomes Group (MPOG) Perioperative Clinical Research Committee: Incidence, predictors, and outcome of difficult mask ventilation combined with difficult laryngoscopy: A report from the multicenter perioperative outcomes group. Anesthesiology 2013; 119:1360–9
19. Honarmand A, Safavi MR: Prediction of difficult laryngoscopy in obstetric patients scheduled for caesarean delivery. Eur J Anaesthesiol 2008; 25:714–20
20. Colquhoun DA, Shanks AM, Kapeles SR, Shah N, Saager L, Vaughn MT, Buehler K, Burns ML, Tremper KK, Freundlich RE, Aziz M, Kheterpal S, Mathis MR: Considerations for integration of perioperative electronic health records across institutions for research and quality improvement: The approach taken by the Multicenter Perioperative Outcomes Group. Anesth Analg 2020; 130:1133–46
21. Lee LO, Bateman BT, Kheterpal S, Klumpner TT, Housey M, Aziz MF, Hand KW, MacEachern M, Goodier CG, Bernstein J, Bauer ME; Multicenter Perioperative Outcomes Group Investigators: Risk of epidural hematoma after neuraxial techniques in thrombocytopenic parturients: A report from the Multicenter Perioperative Outcomes Group. Anesthesiology 2017; 126:1053–63
22. Crosby ET, Cooper RM, Douglas MJ, Doyle DJ, Hung OR, Labrecque P, Muir H, Murphy MF, Preston RP, Rose DK, Roy L: The unanticipated difficult airway with recommendations for management. Can J Anaesth 1998; 45:757–76
23. Shibli KU, Russell IF: A survey of anaesthetic techniques used for caesarean section in the UK in 1997. Int J Obstet Anesth 2000; 9:160–7

24. Shiga T, Wajima Z, Inoue T, Sakamoto A: Predicting difficult intubation in apparently normal patients: A meta-analysis of bedside screening test performance. Anesthesiology 2005; 103:429–37
25. van Buuren S: Multiple imputation of discrete and continuous data by fully conditional specification. Stat Methods Med Res 2007; 16:219–42
26. White IR, Royston P, Wood AM: Multiple imputation using chained equations: Issues and guidance for practice. Stat Med 2011; 30:377–99
27. Rubin DB. Multiple Imputation for Nonresponse in Surveys. New York, Wiley, 1987
28. Harrell JFE. Regression Modeling Strategies: With Applications to Linear Models, Logistic and Ordinal Regression, and Survival Analysis, Springer Series in Statistics, 2nd edition. Cham, Switzerland, Springer International Publishing, 2015.
29. Swales H, Mushambi M, Winton A, Ramaswamy K, Quinn A, Kinsella M. Management of failed intubation and difficult airways in UK obstetric units: An OAA survey. Int J Obstet Anesth 2014; 23:S19
30. Kodali BS, Chandrasekhar S, Bulich LN, Topulos GP, Datta S: Airway changes during labor and delivery. Anesthesiology 2008; 108:357–62

Appendix 1. Multicenter Perioperative Outcomes Group Collaborators

The following Multicenter Perioperative Outcomes Group study group members are collaborators: J. David Clark, M.D., Ph.D., Karen B. Domino, M.D., M.P.H., Robert E. Freundlich, M.D., M.S., M.S.C.I., F.A.S.A., Roya Saffary, M.D., Robert B. Schonberger, M.D., M.H.S., Alvin F. Stewart, M.D., Brad M. Taicher, D.O., M.B.A., Sarah Tingle, M.D., Brandon Michael Togioka, M.D., Richard Urman, M.D., M.B.A., Shital Vachhani, M.D.

Appendix 2. Number of Multicenter Perioperative Outcomes Group Institutions Contributing Obstetric Cases per Year

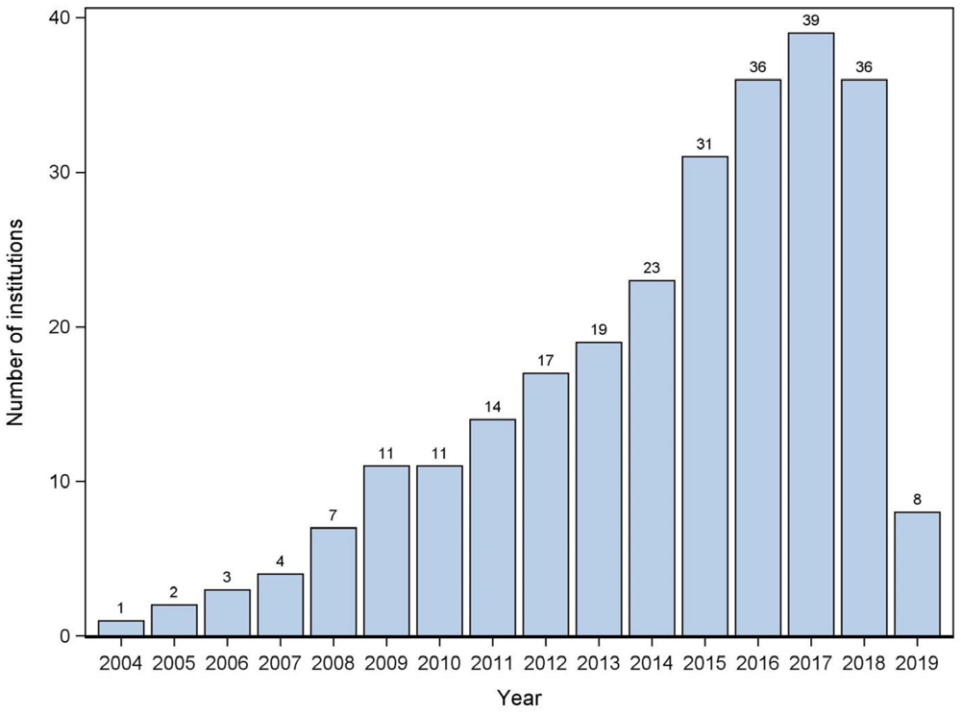

Appendix 3. Distribution of Observed *versus* Imputed Values for Five Imputed Data Sets

Characteristics	Observed Values	Imputed Values 1	Imputed Values 2	Imputed Values 3	Imputed Values 4	Imputed Values 5
Body mass index, No. (%)						
Less than 25 kg/m^2	1,246 (12.5)	550 (12.5)	575 (13.0)	556 (12.6)	553 (12.5)	554 (12.6)
25–39.9 kg/m^2	7,015 (70.1)	3,110 (70.5)	3,078 (69.8)	3,029 (68.7)	3,116 (70.7)	3,004 (68.1)
40 kg/m^2 or more	1,746 (17.5)	750 (17.0)	757 (17.2)	825 (18.7)	741 (16.8)	852 (19.3)
ASA Physical Status						
I or II	8,740 (62.6)	311 (69.9)	298 (67.0)	293 (65.8)	298 (67.0)	311 (69.9)
III	4,664 (33.4)	118 (26.5)	133 (29.9)	141 (31.7)	138 (31.0)	123 (27.6)
IV–VI	568 (4.1)	16 (3.6)	14 (3.2)	11 (2.5)	9 (2.0)	11 (2.5)
Mallampati score, No. (%)						
I or II	7,369 (80.2)	4,263 (81.5)	4,226 (80.8)	4,278 (81.8)	4,213 (80.5)	4,257 (81.4)
III	1,655 (18.0)	884 (16.9)	929 (17.8)	861 (16.5)	915 (17.5)	886 (16.9)
IV	162 (1.8)	84 (1.6)	76 (1.5)	92 (1.8)	103 (2.0)	88 (1.7)
Labor to cesarean status, No. (%)						
No	8,432 (81.3)	3,309 (81.9)	3,291 (81.4)	3,312 (81.9)	3,288 (81.3)	3,321 (82.1)
Yes	1,942 (18.7)	734 (18.2)	752 (18.6)	731 (18.1)	755 (18.7)	722 (17.9)
Induction of labor, No. (%)						
No	11,608 (96.0)	2,224 (95.8)	2,203 (94.9)	2,213 (95.4)	2,203 (94.9)	2,217 (95.5)
Yes	488 (4.0)	97 (4.2)	118 (5.1)	108 (4.7)	118 (5.1)	104 (4.5)
Presence of preterm delivery, No. (%)						
No	9,008 (86.4)	3,415 (85.5)	3,446 (86.3)	3,411 (85.4)	3,374 (84.5)	3,450 (86.4)
Yes	1,414 (13.6)	580 (14.5)	549 (13.7)	584 (14.6)	621 (15.5)	545 (13.6)
Presence of multiple gestations, No. (%)						
No	9,895 (94.9)	3,799 (95.1)	3,793 (94.9)	3,799 (95.1)	3,769 (94.3)	3,797 (95.0)
Yes	527 (5.1)	196 (4.9)	202 (5.1)	196 (4.9)	226 (5.7)	198 (5.0)
Presence of preeclampsia or eclampsia, No. (%)						
No	9,230 (88.6)	3,537 (88.5)	3,548 (88.8)	3,589 (89.8)	3,524 (88.2)	3,557 (89.0)
Yes	1,192 (11.4)	458 (11.5)	447 (11.2)	406 (10.2)	471 (11.8)	438 (11.0)

ASA, American Society of Anesthesiologists.

ANESTHESIOLOGY

A Neural Circuit from the Paraventricular Thalamus to the Bed Nucleus of the Stria Terminalis for the Regulation of States of Consciousness during Sevoflurane Anesthesia in Mice

Jia-Yan Li, M.D., Ph.D., Shao-Jie Gao, M.M., Ran-Ran Li, Ph.D., Wei Wang, Ph.D., Jia Sun, M.M., Long-Qing Zhang, M.M., Jia-Yi Wu, M.M., Dai-Qiang Liu, M.D., Ph.D., Pei Zhang, Ph.D., Bo Tian, M.D., Ph.D., Wei Mei, M.D., Ph.D.

ANESTHESIOLOGY 2022; 136:709–31

EDITOR'S PERSPECTIVE

What We Already Know about This Topic

- The paraventricular thalamus plays a critical role in the maintenance of wakefulness
- The contribution of the paraventricular thalamus to mediating anesthesia mechanisms of actions is incompletely understood

What This Article Tells Us That Is New

- Chemogenetic inhibition of paraventricular glutamatergic neurons in the mouse thalamus projecting to the bed nucleus of the stria terminalis reduced induction time and prolonged emergence from sevoflurane anesthesia, while activation of this pathway had opposite effects
- These observations suggest that glutamatergic neurons of the paraventricular thalamus contribute to the mechanisms of actions of sevoflurane anesthesia *via* their projections to the bed nucleus of the stria terminalis

ABSTRACT

Background: The neural circuitry underlying sevoflurane-induced modulation of consciousness is poorly understood. This study hypothesized that the paraventricular thalamus bed nucleus of the stria terminalis pathway plays an important role in regulating states of consciousness during sevoflurane anesthesia.

Methods: Rabies virus–based transsynaptic tracing techniques were employed to reveal the neural pathway from the paraventricular thalamus to the bed nucleus of the stria terminalis. This study investigated the role of this pathway in sevoflurane anesthesia induction, maintenance, and emergence using chemogenetic and optogenetic methods combined with cortical electroencephalogram recordings. Both male and female mice were used in this study.

Results: Both γ-aminobutyric acid–mediated and glutamatergic neurons in the bed nucleus of the stria terminalis receive paraventricular thalamus glutamatergic projections. Chemogenetic inhibition of paraventricular thalamus glutamatergic neurons prolonged the sevoflurane anesthesia emergence time (mean ± SD, hM4D–clozapine *N*-oxide *vs.* mCherry–clozapine *N*-oxide, 281 ± 88 *vs.* 172 ± 48 s, $P < 0.001$, n = 24) and decreased the induction time (101 ± 32 *vs.* 136 ± 34 s, $P = 0.002$, n = 24), as well as the EC_{50} for the loss or recovery of the righting reflex under sevoflurane anesthesia (mean [95% CI] for the concentration at which 50% of the mice lost their righting reflex, 1.16 [1.12 to 1.20] *vs.* 1.49 [1.46 to 1.53] vol%, $P < 0.001$, n = 20; and for the concentration at which 50% of the mice recovered their righting reflex, 0.95 [0.86 to 1.03] *vs.* 1.34 [1.29 to 1.40] vol%, $P < 0.001$, n = 20). Similar results were observed during suppression of the paraventricular thalamus bed nucleus–stria terminalis pathway. Optogenetic activation of this pathway produced the opposite effects. Additionally, transient stimulation of this pathway efficiently induced behavioral arousal during continuous steady-state general anesthesia with sevoflurane and reduced the depth of anesthesia during sevoflurane-induced burst suppression.

Conclusions: In mice, axonal projections from the paraventricular thalamic neurons to the bed nucleus of the stria terminalis contribute to regulating states of consciousness during sevoflurane anesthesia.

(ANESTHESIOLOGY 2022; 136:709–31)

General anesthetics have been widely used in surgery for nearly two centuries because they can induce reversible unconsciousness and maintain physiologic stability. While great progress has been made in our understanding of how general anesthetics work at the molecular level, little is known about how anesthetics cause a loss

Supplemental Digital Content is available for this article. Direct URL citations appear in the printed text and are available in both the HTML and PDF versions of this article. Links to the digital files are provided in the HTML text of this article on the Journal's Web site (www.anesthesiology.org). This article has a visual abstract available in the online version.

Submitted for publication May 12, 2021. Accepted for publication January 21, 2022. Published online first on March 9, 2022.

Jia-Yan Li, M.D., Ph.D.: Department of Anesthesiology, Tongji Hospital, Tongji Medical College, Huazhong University of Science and Technology, Wuhan, China; and Department of Anesthesiology, First Affiliated Hospital, Sun Yat-sen University, Guangzhou, China.

Shao-Jie Gao, M.M.: Department of Anesthesiology, Tongji Hospital, Tongji Medical College, Huazhong University of Science and Technology, Wuhan, China.

Ran-Ran Li, Ph.D.: Department of Physiology, School of Basic Medicine, Tongji Medical College, Huazhong University of Science and Technology, Wuhan, China.

 Anesthesiology 2022; 136:709–31. DOI: 10.1097/ALN.0000000000004195

<zdoi; 10.1097/ALN.0000000000004195>

of consciousness in neural networks.[1–3] Recent studies have indicated that anesthetic-induced unconsciousness arises via specific interactions with neural circuits that regulate the endogenous sleep–wake systems in the central nervous system,[1,4] such as the parabrachial nucleus,[5] lateral hypothalamus,[6] locus coeruleus,[7,8] tuberomammillary nucleus,[9] ventral tegmental area,[10,11] basal forebrain,[12] ventrolateral preoptic nucleus,[13] and lateral habenula.[14] Multiple sites participate in the maintenance of wakefulness and promote arousal from general anesthesia. However, whether other critical arousal-promoting areas and their neural circuits are implicated in the modulation of consciousness under general anesthesia remains largely unknown.

The paraventricular thalamus, a vital constituent of the midline nucleus of the thalamus, plays a pivotal role in the maintenance of wakefulness.[15] The paraventricular thalamus receives afferent projections from multiple regions involved in the regulation of general anesthesia, including the parabrachial nucleus,[5,16] locus coeruleus,[7,17] dorsal raphe nuclei,[18] hypothalamus,[6,19] and prefrontal cortex,[20] and sends extensive outputs to the limbic system.[21] Recent studies have revealed that the limbic system plays an essential role in anesthetic-induced loss of consciousness.[22] Therefore, we hypothesized that the paraventricular thalamus may be the key hub for the regulation of states of consciousness in general anesthesia. However, the potential mechanism in neural circuits remains unclear.

The bed nucleus of the stria terminalis, located in the limbic forebrain, regulates a variety of endocrine and autonomic nervous responses mainly by projecting to the relay nucleus of the autonomic nervous system, hypothalamus, and central amygdala and plays an important role in stress, fear, and anxiety.[23] The activation of γ-aminobutyric acid–mediated (GABAergic) neurons in the bed nucleus of the stria terminalis promotes the rapid transition from non–rapid eye movement sleep to an awake state in mice.[24] Recent studies have shown that calretinin-positive neurons in the paraventricular thalamus project directly to the bed nucleus of the stria terminalis, and this pathway mediates starvation-induced arousal behavior.[25] Therefore, we speculate that the glutamatergic neurons of the paraventricular thalamus also project to the bed nucleus of the stria terminalis and play a role in modulating the states of consciousness in sevoflurane anesthesia.

To test this hypothesis, we first investigated c-Fos expression in the paraventricular thalamus during sevoflurane anesthesia. We then used anterograde and retrograde tracing strategies to identify the synaptic connections between the paraventricular thalamus and the bed nucleus of the stria terminalis, respectively. Next, we selectively inhibited the paraventricular thalamus bed nucleus of the stria terminalis pathway chemogenetically to explore its role in the time of induction and emergence during sevoflurane anesthesia. Cortical electroencephalogram (EEG) activity was also recorded during the induction and recovery period of sevoflurane anesthesia. We further optogenetically activated paraventricular thalamus glutamatergic neurons or their pathways to observe their effects on the maintenance of light sevoflurane anesthesia under continuous steady-state general anesthesia and deep anesthesia with burst-suppression conditions.

Materials and Methods

Animal Care

In all experiments, male and female C57BL/6J mice and male Vglut2-IRES-Cre and Vgat-IRES-Cre mice weighing 20 to 30 g (8 to 10 weeks old) were used in this study. The male C57BL/6J mice were obtained from Tongji Medical College Experimental Animal Center (Huazhong University of Science and Technology, Wuhan, China; certificate 42009800002519/SCXK(E)2016-0009). The Vglut2-IRES-Cre and Vgat-IRES-Cre mice were obtained from Wuhan National Laboratory for Optoelectronics (Huazhong University of Science and Technology). All mice were housed in a temperature-controlled (22 ± 1°C) and humidity-controlled (50 ± 5%) room with food and water *ad libitum* under an automatically controlled 12 h light/12 h dark cycle (lights on from 7 AM to 7 PM). All procedures involving animals were approved by the Hubei Provincial Animal Care and Use Committee (Wuhan China) and were in accordance with the experimental guidelines of the Animal Experimentation Ethics Committee of Tongji Hospital, Huazhong University of Science and Technology. In this study, we applied online randomization tools (https://www.random.org/lists/) to assign animals to each group, and the animals were tested in sequential order. The experimenters conducting all behavior tests were blinded to group allocation.

Wei Wang, Ph.D.: Department of Physiology, School of Basic Medicine, Tongji Medical College, Huazhong University of Science and Technology, Wuhan, China.

Jia Sun, M.M.: Department of Anesthesiology, Tongji Hospital, Tongji Medical College, Huazhong University of Science and Technology, Wuhan, China.

Long-Qing Zhang, M.M.: Department of Anesthesiology, Tongji Hospital, Tongji Medical College, Huazhong University of Science and Technology, Wuhan, China.

Jia-Yi Wu, M.M.: Department of Anesthesiology, Tongji Hospital, Tongji Medical College, Huazhong University of Science and Technology, Wuhan, China.

Dai-Qiang Liu, M.D., Ph.D.: Department of Anesthesiology, Tongji Hospital, Tongji Medical College, Huazhong University of Science and Technology, Wuhan, China.

Pei Zhang, Ph.D.: Department of Neurobiology, School of Basic Medicine, Tongji Medical College, Huazhong University of Science and Technology, Wuhan, China.

Bo Tian, M.D., Ph.D.: Department of Neurobiology, School of Basic Medicine, Tongji Medical College, Huazhong University of Science and Technology, Wuhan, China.

Wei Mei, M.D., Ph.D.: Department of Anesthesiology, Tongji Hospital, Tongji Medical College, Huazhong University of Science and Technology, Wuhan, China.

Virus Injection

The mice were anesthetized with sodium pentobarbital (50 mg/kg, intraperitoneally) and fixed in a stereotaxic apparatus (RWD Life Science Co. Ltd., China). The eyes were covered with ophthalmic ointment. The body temperature of the anesthetized animals was monitored and maintained at 35 to 37°C by a far-infrared warming pad (RightTemp, Kent Scientific, USA). The heart rate and oxygen saturation were monitored by a MouseSTAT clip sensor (MouseSTAT, Kent Scientific, USA) during surgery. Additional subcutaneous bupivacaine for analgesia was applied to expose the skull, and virus was injected using a glass pipette (opening, 15 to 20 μm) with a stereotaxic injector from Stoelting (USA) as previously described.[26] After injection, the syringe was left in place for 10 min to allow the diffusion of the virus and then slowly retracted. For EEG recordings, 3 weeks after virus injection, the mice were implanted with extradural EEG electrodes for EEG recordings. Briefly, two stainless steel screws were placed in the prefrontal cortex (anterior-posterior, 1.75 mm anterior to bregma; medio-lateral, 0.4 mm lateral to bregma) and cerebellum. Electrodes were then secured to the skull using dental adhesive resin cement (C&B-Superbond; Parkell Inc., USA).

For anterograde tracing, AAV-Ef1α-DIO-ChR2-mCherry (AAV2/9, 4.33E+13 vg/ml, 200 nl; Obio Technology Co. Ltd., China) was injected into the paraventricular thalamus of vglut2-Cre mice. After 4 weeks, the mice were perfused with 4% paraformaldehyde, and the projections from paraventricular thalamus glutamatergic neurons to other brain regions were explored by imaging whole-brain sections using an automatic scanning fluorescence microscope (SV120, Olympus, Japan).

For retrograde monosynaptic tracing, Cre-dependent helper viruses, including AAV-EF1α-DIO-TVA-green fluorescent protein (AAV2/9, 2.0E+12 vg/ml) and AAV-EF1α-DIO-RVG (AAV2/9, 2.0E+12 vg/ml, 1:1, 100 nl), were injected into the bed nucleus of the stria terminalis (anterior-posterior,: +0.26 mm; medio-lateral: −1.0 mm; dorsal-ventral: −4.05 mm) of vglut2-Cre mice or vgat-Cre mice, respectively. After 3 weeks, rabies virus (RV-ENVA-ΔG-dsRed, 2.0E+08 infectious units/ml, 200 nl) was microinjected into the same site of the bed nucleus of the stria terminalis.

Anesthesia Behavioral Experiments

We produced an open-circuit anesthetizing apparatus that ensured identical gaseous anesthetic delivery to each of eight mice in isolated transparent cylindrical chambers while maintaining a constant 37°C environment. The mice were placed in a cylinder with 100% oxygen for habituation for 2 h for 3 consecutive days before testing. The time to the loss of the righting reflex was measured after 1 l/min 100% oxygen with 2.4% sevoflurane was administered, the chambers were rotated 180° every 15 s, and the time to the loss of the righting reflex (induction time) was considered as the time when mice first lost their righting reflex for more than 30 s from the time of sevoflurane initiation. After a 30-min exposure to 2.4% sevoflurane, the sevoflurane was shut off, and the time to the recovery of the righting reflex (emergence time) was defined as the interval from the termination of anesthetic inhalation to the return of the righting reflex. The concentration of sevoflurane was monitored by an anesthetic agent analyzer (G60, Philips, China).

To assess sevoflurane responsiveness with a higher precision, the concentration at which 50% of the mice lost their righting reflex and the concentration at which 50% of the mice recovered their righting reflex were measured as described previously.[27] The EC_{50} was calculated from the dose–response equation. To determine the concentration at which 50% of the mice lost their righting reflex, the initial concentration of sevoflurane was set at 0.7 vol%, and the concentrations were increased by 0.2 vol% every 15 min. The chambers were rotated 180° during the last 2 min of this period to observe whether the righting reflex of the mice had disappeared, and the number of animals that lost their righting reflex at each concentration was recorded. The experiments ended when all animals had lost their righting reflex. To determine the concentration at which 50% of the mice recovered their righting reflex, all of the mice were anesthetized with 2.1% sevoflurane for 30 min, and the concentration was decreased in decrements of 0.2% until all of the mice had recovered their righting reflex. The number of mice that had recovered their righting reflex at each concentration was counted. The concentration of sevoflurane was monitored by an anesthetic agent analyzer (G60, Philips, China). The chamber temperature was maintained at 37°C using a heating pad during the whole experiment.

Arousal Scoring

Arousal behaviors were scored as described previously.[10,28] Briefly, spontaneous actions of the limbs, head, and tail were rated on a scoring sheet with three levels, including absent, mild, or moderate in intensity, and were scored 0, 1, or 2, respectively. In addition, if the loss of the righting reflex remained in the mouse, righting was scored as 0, and if all four paws of the mouse touched the ground, righting was scored as 2. Walking was also scored with three levels as follows: made no further movements (0), crawled without raising the abdomen off the floor (1), and walked with all four paws with the abdomen off the floor (2). The total score for each mouse was determined by the sum of all categories.

Whole-cell Recordings

Whole-cell recordings were conducted as described previously.[29] Briefly, after 4 weeks of viral expression, the mouse brain was rapidly removed from the skull and submerged in ice-cold oxygenated slice-cutting solution containing 125 mM NaCl, 3.5 mM KCl, 25 mM $NaHCO_3$, 1.25 mM

NaH_2PO_4, 0.1 mM $CaCl_2$, 3 mM $MgCl_2$, and 10 mM glucose. Acute coronal brain slices containing the paraventricular thalamus were cut at 200- or 400-μm thickness with a vibratome (VT1000S, Leica, Germany). For neuronal whole-cell recording, the slices were kept at 32°C for 1 h after cutting, kept at subsequently at room temperature before use, and then maintained in ice-cold artificial cerebrospinal fluid containing 125 mM NaCl, 25 mM $NaHCO_3$, 1.25 mM NaH_2PO_4, 3.5 mM KCl, 2 mM $CaCl_2$, 1 mM $MgCl_2$, and 10 mM glucose (saturated with 95% O_2 and 5% CO_2). Neurons in the paraventricular thalamus expressing mCherry were clamped with borosilicate glass micropipettes (4 to 7 MΩ). The pipette intracellular solution contained 140 mM potassium gluconate, 13.4 mM sodium gluconate, 0.5 mM $CaCl_2$, 1.0 mM $MgCl_2$, 5 mM EGTA, 10 mM HEPES, 3 mM Mg^{2+}–adenosine triphosphate, and 0.3 mM Na^+-guanosine triphosphate; 280 to 290 mOsm/l (pH 7.4; osmolarity, 280 to 290 mOsm/kg). The data were obtained using a MultiClamp 700B amplifier and pClamp 10 software (Molecular Devices, USA), digitized at 2 to 10 kHz, and filtered at 2 kHz. The patch-clamp recording data were analyzed by Clampfit 9.0 (Molecular Devices).

To verify the functional validity of AAV-hM4D(Gi), after baseline data were recorded for 5 min, clozapine *N*-oxide was applied to the bath for 2 min, and the cells were inhibited using clozapine *N*-oxide (10 μM). To verify the function of AAV-ChR2, mCherry-expressing neurons were stimulated by blue light (473 nm, 10 Hz, a duration of 10 ms) through an optical fiber placed above the cell.

EEG Recording and Analysis

EEG signals were amplified using a Microelectrode AC amplifier model 1700 (A-M Systems, USA) and digitized at a sampling rate of 500 Hz using a PCIe 6323 data acquisition board (National Instruments, USA), and EEG signals were recorded using Spikehound software (Neurobiological Instrumentation Engineer, USA). The raw EEG signals were analyzed using multitaper methods from the Chronux toolbox (version 2.1.2, http://chronux.org/) in MATLAB 2016a (MathWorks, United Kingdom). EEG power spectra were analyzed as described in previous studies.[30] Briefly, raw EEG data were band-pass filtered (1 to 80 Hz) and band-block filtered (48 to 52 Hz) to remove line noise and were computed for a window size of 4 s (50% overlapping) within the frequency range of 0.5 to 50 Hz using a 5-taper in fast Fourier transform. The average power spectral density and the normalized power spectral density were calculated for the delta (0.5 to 4 Hz), theta (4 to 8 Hz), alpha (8 to 15 Hz), beta (15 to 25 Hz), and gamma (25 to 50 Hz) bands. The normalized power spectral density was performed on the data from the period of induction (5 min after the initiation of anesthesia) and emergence (5 min after the discontinuation of the anesthetic), and the average power spectral density was determined during the optogenetic stimulation period (120 s before and after blue light stimulation during the 2.5% sevoflurane anesthesia-induced burst-suppression period).

The burst-suppression ratio was used to quantify the state of burst suppression and calculated as described previously.[31] Briefly, the original EEG data were first band-pass filtered (10 to 80 Hz) and band-block filtered (48 to 52 Hz) and then detrended and smoothed by convolution with a Gaussian function. Next, EEG bursts were preliminarily assigned a value of 0, and EEG suppressions were assigned a value of 1 to produce a binary time series. Finally, this binary time series was smoothed to calculate the burst-suppression ratio over time with a window function. EEG suppression events were defined based on their voltage (amplitude within −15 to 15 μV) and duration (minimal duration, 200 ms or less), and the events were also regarded as the same suppression when the interevent interval was less than 50 ms. EEG epochs between suppression periods were viewed as EEG burst events.

In Vivo Chemogenetic Manipulation

To inhibit paraventricular thalamus glutamatergic neurons, C57BL/6J mice were injected with AAV-CaMKIIa-hM4D(Gi)-mCherry (AAV2/9, 1.18E + 13 vg/ml, 200 nl; Obio Technology Co. Ltd., China) or AAV-CaMKIIa-mCherry (AAV2/9, 1.08E + 13 vg/ml 200 nl; Obio Technology Co. Ltd.) as a control. To inhibit the paraventricular thalamus bed nucleus of the stria terminalis pathway, AAV_{retro}-hSyn-Cre (AAV2/retro, 2.0E+12 vg/ml; BrainVTA Co. Ltd., China) was bilaterally injected into the bed nucleus of the stria terminalis, and then AAV-EF1α-DIO-hM4D(Gi)-mCherry (AAV2/9, 2.0E+12 vg/ml; BrainVTA Co. Ltd.) or AAV-EF1α-DIO-mCherry (AAV2/9, 2.0E+12 vg/ml; BrainVTA Co. Ltd.) was injected into the paraventricular thalamus of C57BL/6J mice. For chemogenetic experiments, 3 weeks after virus injection, 3 mg/kg clozapine *N*-oxide (Sigma, USA) or saline was administered intraperitoneally 1 h before all behavior testing.

In Vivo Optogenetic Manipulation

For optogenetic activation of paraventricular thalamus glutamatergic neurons, AAV-CaMKIIa-ChR2-mCherry-WPREs (AAV2/9, 2.0E + 12 vg/ml, 200 nl; BrainVTA Co. Ltd., China) or AAV-CaMKIIa-mCherry-WPREs (AAV2/9, 2.0E+12 vg/ml, 200 nl; BrainVTA Co. Ltd.) were delivered into the paraventricular thalamus (anterior-posterior = –1.00 mm; medio-lateral = +0.55 mm; dorsal-ventral = –2.95 mm, with a 10-degree angle to the midline), and an optical fiber was implanted above the paraventricular thalamus (anterior-posterior = –1.00 mm; medio-lateral = +0.55 mm; dorsal-ventral = –2.85 mm, with a 10-degree angle to the midline). To optogenetically activate the paraventricular thalamus bed nucleus of the stria terminalis pathway, AAV-EF1α-DIO-ChR2-mCherry (AAV2/9, 4.33E+12

vg/ml, 200 nl; Obio Technology Co. Ltd., China) or AAV-EF1α-DIO-mCherry (control) was injected into the paraventricular thalamus of vglut2-Cre mice, and the optical fiber cable was implanted into the bed nucleus of the stria terminalis (anterior-posterior = +0.26 mm; medio-lateral = –1.0 mm; dorsal-ventral = –3.95 mm) and then fixed to the skull using dental cement. The mice were connected *via* an optical fiber cannula to a laser diode (Newton Inc., China). To stimulate paraventricular thalamus glutamatergic neurons or the paraventricular thalamus bed nucleus of the stria terminalis pathway, optogenetic manipulation (laser of 473 nm, 10-ms pulses at 10 Hz for 120 s) was conducted during all behavior testing as described previously.[15] Light intensities at the tip of the optical fiber cannula were tested by a power meter (PM100D, Thorlabs, Germany) before the experiment and calibrated to emit 10 to 15 mW/mm^2.

For anesthesia behavior testing, the mice were optically stimulated at the initiation of sevoflurane exposure until they lost their righting reflex during induction. During emergence, optical stimulation was delivered from the time sevoflurane administration stopped until the animals recovered their righting reflex. For optogenetic manipulation during sevoflurane anesthesia maintenance, the animals were initially administered 2.5% sevoflurane for 20 min and then placed in a supine position. Then the sevoflurane concentration was reduced to 1.4%. If the animals showed any signs of the recovery of their righting reflex, the concentration was increased by 0.1% until the loss of the righting reflex was maintained at a constant concentration for at least 20 min. In our experiments, sevoflurane concentrations ranging from 1.4 to 1.5% were used to maintain light sevoflurane anesthesia. Optogenetic manipulation was performed for 2 min during continuous, steady-state general anesthesia with sevoflurane to score arousal behavior. In addition, 2.5% sevoflurane was delivered for 30 min to induce a stable burst-suppression pattern, and optogenetic stimulation was performed for 2 min under burst-suppression conditions.

Histology

For c-Fos immunofluorescence staining, the mice were administered 2.4% (1 minimum alveolar concentration) sevoflurane inhalation for 2 h. After sevoflurane anesthesia, the mice were killed immediately and perfused with 0.01 M phosphate-buffered saline followed by 4% paraformaldehyde. After perfusion, the brains were removed and stored in 4% paraformaldehyde overnight at 4°C for postfixation and dehydrated in 30% sucrose at 4°C until they sank. The brains were then serially sectioned on a freezing microtome (CM1900, Leica, Germany) at –20°C. For c-Fos or vglut2 immunofluorescence staining, briefly, the membrane permeability of sections was strengthened with 0.3% Triton X-100/phosphate-buffered saline for 15 min, and the sections were blocked with 10% goat serum in phosphate-buffered saline for 1 h and incubated overnight at 4°C with rabbit anti-c-Fos antibody (1:250; Abcam, United Kingdom) or anti-vglut2 antibody (1:200; Abcam, United Kingdom). After rinsing with phosphate-buffered saline, the sections were incubated with anti-rabbit secondary antibodies coupled to DyLight-488 (1:300; Alexa Fluor, Molecular Probes Inc., USA) for 2 h at room temperature. After another three 10-min washes with phosphate-buffered saline, the slides were covered with DAPI (AR1177, Boster, China) for 5 min, and the sections were washed, mounted, and coverslipped. Images were captured on a fluorescence microscope (DM2500, Leica Microsystems, Germany). The experimenters involved in microscopy analysis were blinded to group allocation. The mean fluorescence intensity of c-Fos–positive neurons was analyzed on alternate sections in the paraventricular thalamus (approximately from bregma –1.06 to –2.06 mm; n = 6, where n refers to the number of animals, three sections per mouse). In response to peer review, additional experiments for the change in c-Fos expression in the paraventricular thalamus in female mice during sevoflurane anesthesia were added.

Statistical Analysis

In this study, we injected virus into the paraventricular thalamus in 135 male mice. Histological tests were carried out after the behavior tests to identify the position of virus infection. Forty-seven mice with inaccurate injection sites, inaccurate placement of optic fibers, or poor recovery after virus injection were excluded, and the other 88 mice were included in the data analysis. The paraventricular thalamus bed nucleus of the stria terminalis pathway was manipulated in 112 male mice. Eighty-nine mice were used for data analysis, and 23 mice with inaccurate injection sites or poor conditions were excluded. In this study, n refers to the number of animals. In response to peer review, the paraventricular thalamus was manipulated in an additional 60 female mice; 12 mice with inaccurate injection sites were excluded, and the other 48 mice were included in the data analysis. No *a priori* statistical power calculation was performed. Sample sizes were chosen based on similar experiments using chemogenetic and optogenetic methods. Before analysis, all data were tested by the Shapiro–Wilk normality test. Parametric tests or nonparametric tests were used according to the results of the normality tests. Group differences in cell counts were tested with unpaired Student's *t* tests. To determine the EC_{50} at the loss of the righting reflex or the recovery of the righting reflex and the corresponding 95% CI, the population percentage of loss/recovery of the righting *versus* the log scale of inhaled anesthetic concentration curve was generated by nonlinear regression with a variable slope (multiple parameters) using GraphPad Prism 6.0 (GraphPad Software, USA). A Bayesian Monte Carlo method was applied to evaluate the efficacy of optical stimulation for the restoration of righting during continuous, steady-state general anesthesia with sevoflurane, as previously described.[10,28] For this calculation, we assumed a binomial model as the sampling density or likelihood

function for the tendency of mice in a given group to have the righting response. We considered the uniform density in the interval (0,1) as the prior density of each group since it is noninformative. The posterior density of each group is the beta density because the prior density is proportional to the likelihood function of the binomial model, and this uniform density was regarded as the conjugate prior density for the beta density. We calculated the posterior probability that the propensity to right of one group was greater than that of the other group. The posterior probability of the difference in the propensity to right between the two groups (ChR2-on and mCherry-on) was obtained from beta distributions. The Bayesian CIs that did not include 0 and a posterior probability greater than 0.95 were considered statistically significant. The Bayesian estimation was conducted and analyzed by applying appropriate codes in MATLAB 2016a (MathWorks, United Kingdom). Arousal scoring was tested using a Mann–Whitney U test on the total score. Differences in the burst-suppression ratio and the average power spectral density before and during optical stimulation were analyzed using paired Student's *t* tests. Behavior testing, data were analyzed by ordinary one-way ANOVA followed by a *post hoc* Bonferroni test. EEG-normalized power spectral density changes during the induction or emergence period were analyzed by two-way repeated-measures ANOVA followed by a *post hoc* Bonferroni test. The data are expressed as the mean ± SD or median ± interquartile range (25th, 75th). In all cases, a value of $P < 0.05$ was considered statistically significant.

Results

Sevoflurane Inhibits Neuronal Activity in the Paraventricular Thalamus

To determine whether sevoflurane anesthesia is associated with neuron activities in the paraventricular thalamus, we explored the changes in neuronal activities in the paraventricular thalamus under sevoflurane anesthesia. In response to peer review, we examined the expression of c-Fos, a marker of neuronal activity, after treatment with 2.4% (1 minimum alveolar concentration) sevoflurane inhalation for 2 h in both male and female mice. We found that neuronal activities in the paraventricular thalamus were suppressed in both male and female mice under sevoflurane anesthesia, suggesting that neuronal activities in the paraventricular thalamus can be regulated by sevoflurane anesthesia (fig. 1, A and B; Supplemental Digital Content 1, fig. S1, A and B [http://links.lww.com/ALN/C836]).

Effects of Paraventricular Thalamus Glutamatergic Neuron Inhibition on Sevoflurane Induction, Emergence Time, and Anesthesia Sensitivity

To selectively manipulate paraventricular thalamus glutamatergic neurons, an adeno-associated virus expressing engineered hM4D(Gi) receptor (AAV-CaMKIIa-hM4D(Gi)-mCherry) or a control virus (AAV-CaMKIIa-mCherry) was microinjected into the paraventricular thalamus (fig. 2A). Extensive mCherry fluorescence was detected in the paraventricular thalamus at 3 weeks after microinjection (fig. 2B). By obtaining whole-cell recordings from acute brain slices (fig. 2C), we further confirmed that the application of clozapine *N*-oxide (10 μM) could significantly inhibit paraventricular thalamus glutamatergic neurons, suggesting that the activity of hM4D(Gi)-expressing paraventricular thalamus glutamatergic neurons could be suppressed by clozapine *N*-oxide *in vitro*.

The loss of the righting reflex and the recovery of the righting reflex in mice have been considered surrogates of anesthetic-induced loss and recovery of consciousness in humans.[32] To further explore the effects of paraventricular thalamus glutamatergic neuron inhibition on sevoflurane-induced loss and recovery of consciousness, the mice were exposed to 2.4% sevoflurane, and the time to the loss of the righting reflex was investigated in male mice. In response to peer review, female mice were added to this experiment. In addition, we found that the induction time was reduced in the hM4D–clozapine *N*-oxide group compared with that in the hM4D-saline group (male and female: 101 ± 32 *vs.* 132 ± 30 s, $P = 0.009$, n = 24; fig. 2D; male: 116 ± 36 *vs.* 154 ± 23 s, $P = 0.012$, n = 12; Supplemental Digital Content 1, fig. S2A [http://links.lww.com/ALN/C836]; female: 86 ± 20 *vs.* 109 ± 15 s, $P = 0.025$, n = 12; Supplemental Digital Content 1, fig. S3A [http://links.lww.com/ALN/C836]) and the mCherry–clozapine *N*-oxide group (male and female: 101 ± 32 *vs.* 136 ± 34 s, $P = 0.002$, n = 24; fig. 2D; male: 116 ± 36 *vs.* 163 ± 22 s, $P = 0.001$, n = 12; Supplemental Digital Content 1, fig. S2A [http://links.lww.com/ALN/C836]; female: 86 ± 20 *vs.* 110 ± 18 s, $P = 0.019$, n = 12; Supplemental Digital Content 1, fig. S3A [http://links.lww.com/ALN/C836]). After a 30-min 2.4% sevoflurane exposure, the sevoflurane was shut off, and the hM4D group with the delivery of clozapine *N*-oxide showed a significant increase in the duration to the recovery of the righting reflex compared to that in the hM4D-saline group (male and female: 281 ± 88 *vs.* 156 ± 40 s, $P < 0.001$, n = 24; fig. 2E; male: 267 ± 84 *vs.* 157 ± 41 s, $P < 0.001$, n = 12; Supplemental Digital Content 1, fig. S2B [http://links.lww.com/ALN/C836]; female: 295 ± 92 vs. 154 ± 42 s, $P < 0.001$, n = 12; Supplemental Digital Content 1, fig. S3B [http://links.lww.com/ALN/C836]) and the mCherry–clozapine *N*-oxide group (male and female: 281 ± 88 *vs.* 172 ± 48 s, $P < 0.001$, n = 24; fig. 2E; male: 267 ± 84 *vs.* 169 ± 45 s, $P < 0.001$, n = 12; Supplemental Digital Content 1, fig. S2B [http://links.lww.com/ALN/C836]; female: 295 ± 92 *vs.* 176 ± 53 s, $P < 0.001$, n = 12; Supplemental Digital Content 1, fig. S3B [http://links.lww.com/ALN/C836]), indicating that the inhibition of paraventricular thalamus glutamatergic neurons prolonged the sevoflurane anesthesia emergence time.

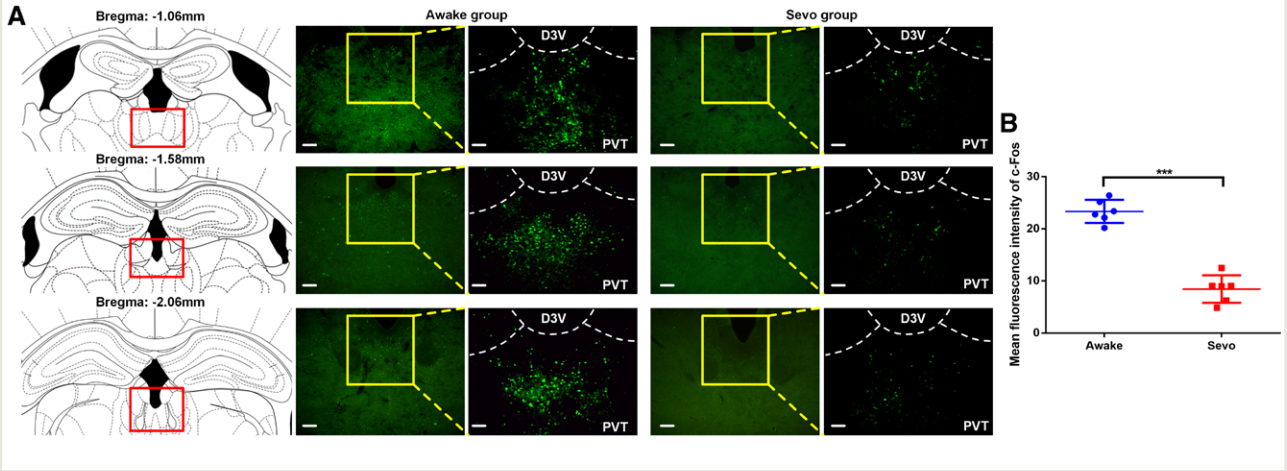

Fig. 1. c-Fos expression in the paraventricular thalamus under sevoflurane anesthesia. (*A*) Representative images of c-Fos immunofluorescence in the paraventricular thalamus between the awake and sevoflurane anesthesia groups in male mice. (*Left*) Representative brain sections stained with c-Fos (*green*). *Scale bars*, 200 μm. (*Right*) Magnified images. *Scale bars*, 100 μm. (*B*) Quantitative analysis of the intensity of c-Fos staining in the paraventricular thalamus. The data are shown as the mean ± SD. ***$P < 0.001$ (n = 6 for each group). D3V, dorsal 3rd ventricle; PVT, paraventricular thalamus; Sevo, sevoflurane.

To further determine the role of paraventricular thalamus glutamatergic neurons in sevoflurane anesthesia sensitivity, the dose–response curve of the percentage of loss of the righting reflex or the recovery of the righting reflex *versus* sevoflurane concentration was plotted. We found that the dose–response curves of both the loss and the recovery of the righting reflex were left-shifted for the hM4D–clozapine *N*-oxide group compared with those in the hM4D-saline group and the mCherry–clozapine *N*-oxide group in male mice. In response to peer review, additional experiments in female mice were added in this experiment. The concentration at which 50% of the mice lost their righting reflex of sevoflurane was significantly decreased in the hM4D–clozapine *N*-oxide group compared with that in the hM4D-saline group (male and female: mean [95% CI], 1.16 [1.12 to 1.20] *vs.* 1.43 [1.40 to 1.46] vol%, $P < 0.001$, n = 20; fig. 2F; Supplemental Digital Content 1, table S1 [http://links.lww.com/ALN/C836]; male: 1.20 [1.18 to 1.21] *vs.* 1.45 [1.44 to 1.46] vol%, $P < 0.001$, n = 10; Supplemental Digital Content 1, fig. S2C, table S2 [http://links.lww.com/ALN/C836]; female: 1.11 [1.04 to 1.18] *vs.* 1.40 [1.35 to 1.46] vol%, $P < 0.001$, n = 10; Supplemental Digital Content 1, fig. S3C, table S3 [http://links.lww.com/ALN/C836]) and the mCherry–clozapine *N*-oxide group (male and female: 1.16 [1.12 to 1.20] *vs.* 1.49 [1.46 to 1.53] vol%, $P < 0.001$, n = 20; fig. 2F; Supplemental Digital Content 1, table S1 [http://links.lww.com/ALN/C836]; male: 1.20 [1.18 to 1.21] *vs.* 1.50 [1.44 to 1.57] vol%, $P < 0.001$, n = 10; Supplemental Digital Content 1, fig. S2C, table S2 [http://links.lww.com/ALN/C836]; female: 1.11 [1.04 to 1.18] *vs.* 1.48 [1.43 to 1.53] vol%, $P < 0.001$, n = 10; Supplemental Digital Content 1, fig. S3C, table S3 [http://links.lww.com/ALN/C836]), and the concentration at which 50% of the mice recovered their righting reflex (EC_{50}) of sevoflurane was lowered in the hM4D–clozapine *N*-oxide group compared with that in the hM4D-saline group (male and female: mean [95% CI], 0.95 [0.86 to 1.03] *vs.* 1.32 [1.29 to 1.34] vol%, $P < 0.001$, n = 20; fig. 2G; Supplemental Digital Content 1, table S1 [http://links.lww.com/ALN/C836]; male: 1.07 [0.94 to 1.22] *vs.* 1.32 [1.29 to 1.36] vol%, $P = 0.009$, n = 10; Supplemental Digital Content 1, fig. S2D, table S2 [http://links.lww.com/ALN/C836]; female: 0.86 [0.81 to 0.91] *vs.* 1.32 [1.27 to 1.36] vol%, $P < 0.001$, n = 10; Supplemental Digital Content 1, fig. S3D, table S3 [http://links.lww.com/ALN/C836]) and the mCherry–clozapine *N*-oxide group (male and female: mean [95% CI], 0.95 [0.86 to 1.03] *vs.* 1.34 [1.29 to 1.40] vol%, $P < 0.001$, n = 20; fig. 2G; Supplemental Digital Content 1, table S1 [http://links.lww.com/ALN/C836]; male: 1.07 [0.94 to 1.22] *vs.* 1.38 [1.34 to 1.42] vol%, $P = 0.003$, n = 10; Supplemental Digital Content 1, fig. S2D, table S2 [http://links.lww.com/ALN/C836]; female: 0.86 [0.81 to 0.91] *vs.* 1.30 [1.23 to 1.36] vol%, $P < 0.001$, n = 10; Supplemental Digital Content 1, fig. S3D, table S3 [http://links.lww.com/ALN/C836]). Taken together, our results indicate that the blockade of the activities of paraventricular thalamus glutamatergic neurons facilitated induction, delayed emergence, and increased sevoflurane anesthesia sensitivity.

Chemogenetic Inhibition of Paraventricular Thalamus Glutamatergic Neurons Accelerates Cortical Sedation and Suppresses Cortical Arousal from Sevoflurane Anesthesia

To further determine how the inhibition of paraventricular thalamus glutamatergic neurons could affect induction

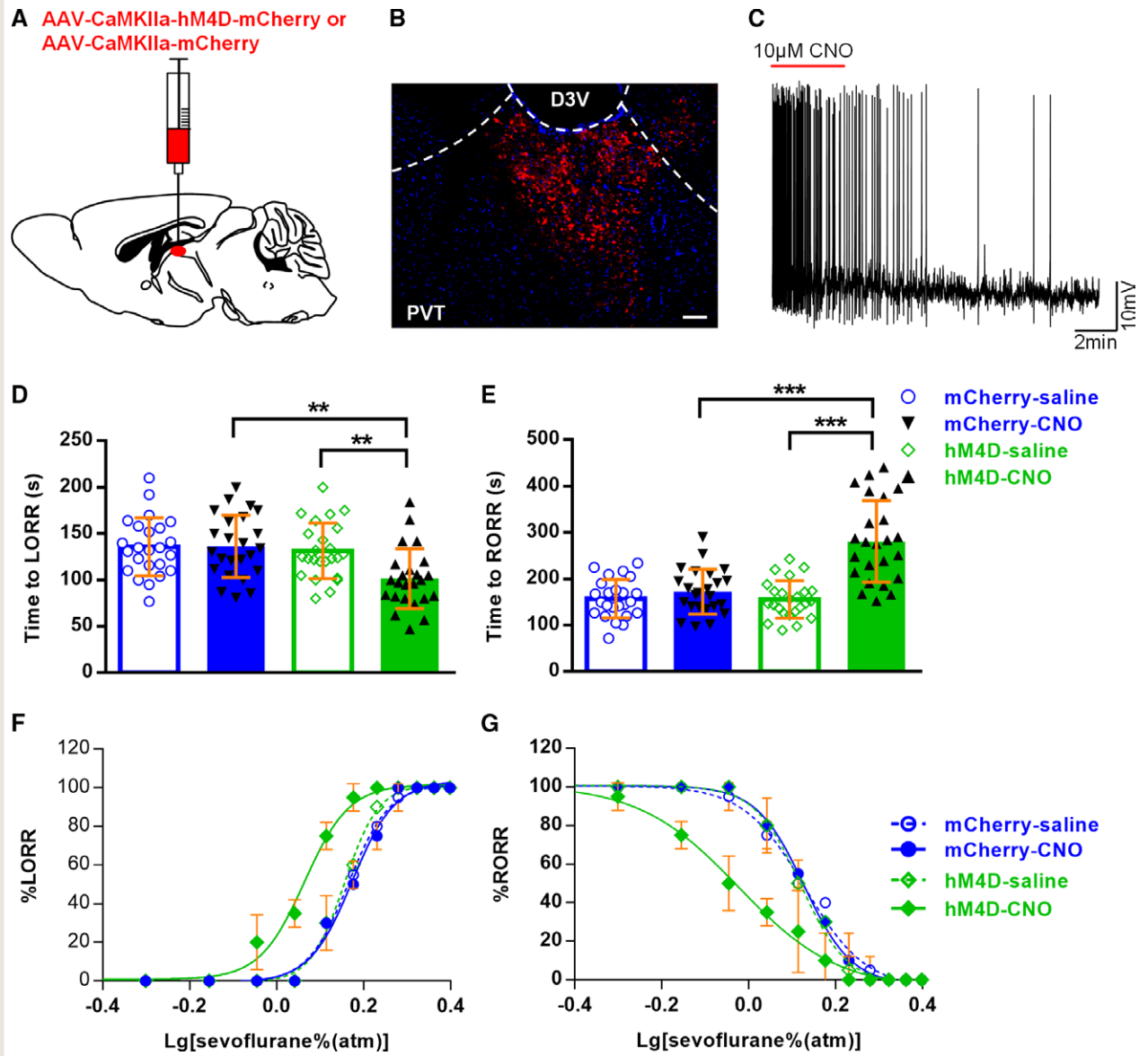

Fig. 2. Effects of chemogenetic inhibition of paraventricular thalamus glutamatergic neurons on sevoflurane induction, emergence time, and anesthesia sensitivity. (*A*) Schematic of virus injection. (*B*) Representative images showing the expression of hM4D(Gi) receptors (*red*) in the paraventricular thalamus. *Scale bar*, 100 μm. (*C*) Whole-cell patch clamping of paraventricular thalamus glutamatergic neurons expressing hM4D showing suppressed action potential responses to the application of clozapine *N*-oxide (10 μM) *in vitro*. (*D* and *E*) Time to induction (*D*) and emergence (*E*) with exposure to 2.4% sevoflurane (1 minimum alveolar concentration) for 30 min after pretreatment with saline or clozapine *N*-oxide in the control group (AAV-CaMKIIa-mCherry) and the hM4D group (AAV-CaMKIIa-hM4D-mCherry), respectively. The data are shown as the mean ± SD (one-way ANOVA). $^{**}P < 0.01$; $^{***}P < 0.001$ (*post hoc* Bonferroni test, hM4D–clozapine *N*-oxide *vs.* hM4D-saline/mCherry–clozapine *N*-oxide, n = 24 for each group). (*F* and *G*) Dose–response curves of the loss of the righting reflex (*F*) and the recovery of the righting reflex (*G*) between paraventricular thalamus inhibition and control mice.

and arousal, we obtained EEG recordings from the somatosensory cortex in male mice. As shown in figure 3, A to C, compared with saline administration, hM4D expression group delivery of clozapine *N*-oxide induced a quick transition from an awake-EEG state to an anesthesia-EEG state because at baseline, the animals were already sedated, with higher delta activity, as described previously.[15] Power spectral density analysis of the EEG signal suggested a prominent interaction between clozapine *N*-oxide and the EEG frequency band during the sevoflurane anesthesia induction and recovery periods. During the anesthesia induction period, the group with the delivery of clozapine *N*-oxide

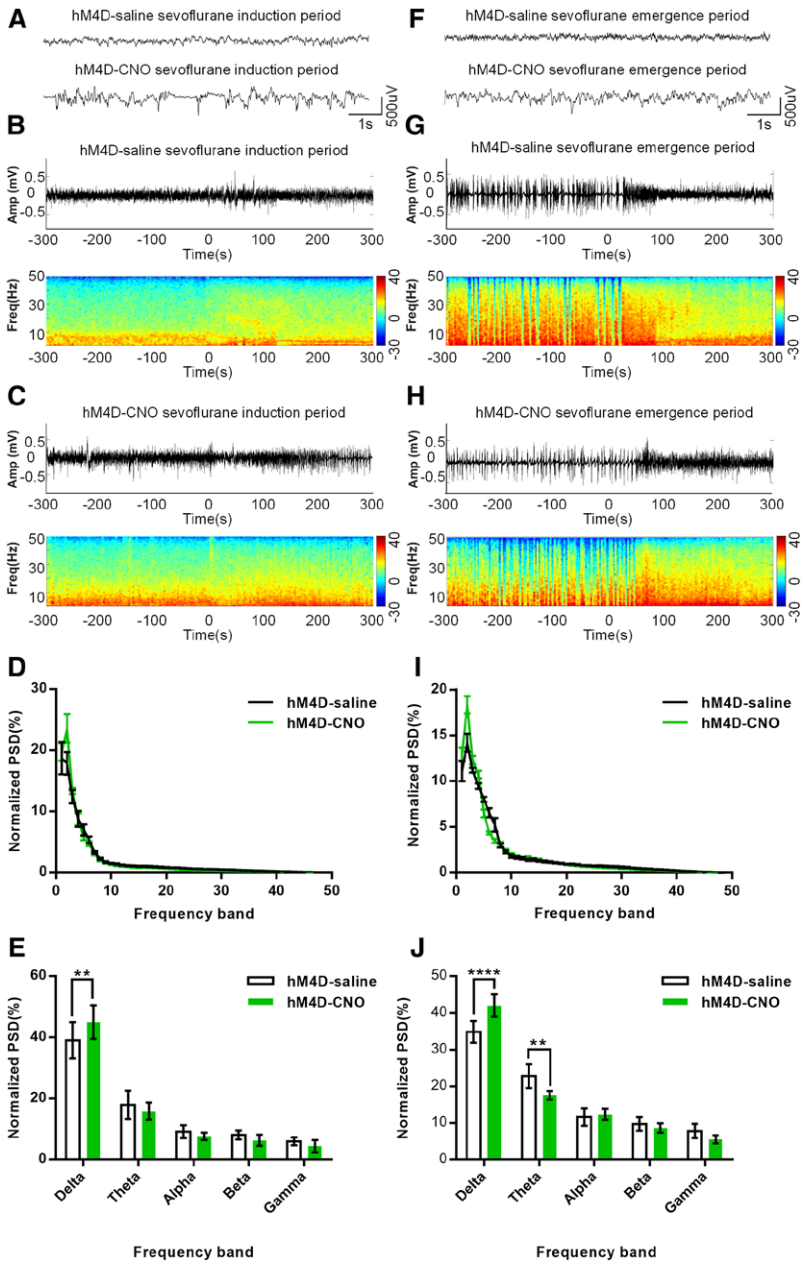

Fig. 3. Chemogenetic inhibition of paraventricular thalamus glutamatergic neurons induced electroencephalogram changes during sevoflurane anesthesia. (*A*) Representative raw electroencephalogram traces during the sevoflurane induction period in hM4D mice after the delivery of clozapine *N*-oxide or saline. (*B* and *C*) Representative electroencephalogram power spectrograms during the induction period after the administration of saline (*B*) or clozapine *N*-oxide (*C*). Time zero on the timeline represents the initiation of sevoflurane anesthesia. (*D*) Electroencephalogram traces 5 min after the initiation of sevoflurane anesthesia were analyzed. Normalized power spectral densities in the hM4D-saline (*black*) and hM4D–clozapine *N*-oxide (*green*) groups during the sevoflurane induction period. (*E*) Quantitative analysis of normalized power spectral density. Compared with the hM4D-saline group, the hM4D–clozapine *N*-oxide group showed a significant increase in electroencephalogram delta power. The data are shown as the mean ± SD (two-way ANOVA). $^{**}P < 0.01$ (*post hoc* Bonferroni test, hM4D–clozapine *N*-oxide *vs.* hM4D-saline, n = 8 for each group). (*F*) Representative raw electroencephalogram traces during the emergence period in hM4D mice after the delivery of clozapine *N*-oxide or saline. (*G* and *H*) Representative electroencephalogram power spectrograms during the sevoflurane anesthesia recovery period in the hM4D-saline (*black*) and hM4D–clozapine *N*-oxide (*green*) groups. Time zero on the timeline indicates the cessation of sevoflurane anesthesia. (*I*) Electroencephalogram traces 5 min after the discontinuation of sevoflurane anesthesia were analyzed. Normalized power spectral density in the hM4D-saline (*black*) and hM4D–clozapine *N*-oxide (*green*) groups during the sevoflurane emergence period. (*J*) In the recovery period, quantitative analysis of normalized power spectral density shows that in the hM4D group, the delivery of clozapine *N*-oxide led to a significant increase in delta power and a decrease in theta power compared with those resulting from the delivery of saline. The data are shown as the mean ± SD (two-way ANOVA). $^{**}P < 0.01$; $^{****}P < 0.0001$ (*post hoc* Bonferroni test, hM4D–clozapine *N*-oxide *vs.* hM4D-saline, n = 8 for each group).

showed a significant increase in the delta band (45.0 ± 5.5%) compared with that in the hM4D-saline group (39.1 ± 6.0%, $P = 0.001$, n = 8), while the other bands (theta, alpha, beta, and gamma bands) showed no significant difference (fig. 3, D and E), indicating that the inhibition of paraventricular thalamus glutamatergic neurons accelerated sevoflurane-induced sedation. During the sevoflurane anesthesia recovery period, the transition from an anesthesia-EEG state to an awake-EEG state was delayed in the hM4D–clozapine *N*-oxide group (fig. 3, F and H). The power in the delta band showed a significant increase in the hM4D–clozapine *N*-oxide group (42.0 ± 3.1%) compared with that in the hM4D-saline group (34.9 ± 3.0%, $P < 0.0001$, n = 8), while the power in the theta band was decreased in the hM4D–clozapine *N*-oxide group (17.6 ± 1.2%) compared with that in the control group (22.8 ± 3.3%, $P = 0.004$, n = 8; fig. 3, I and J). These findings suggest that the inhibition of paraventricular thalamus glutamatergic neurons suppressed cortical arousal from sevoflurane anesthesia.

Optogenetic Activation of Paraventricular Thalamus Glutamatergic Neurons Induces Behavioral Arousal and Reduces the Depth of Anesthesia during the Sevoflurane Anesthesia Maintenance Period

To further test the effects of paraventricular thalamus glutamatergic neurons on sevoflurane anesthesia, we stimulated the neuronal activity of the paraventricular thalamus *in vivo* using optogenetics (fig. 4A). The immunofluorescence results verified that the paraventricular thalamus neurons had been successfully transfected with optogenetic viruses (fig. 4B). Whole-cell recordings showed that neurons expressing the ChR2 virus in the paraventricular thalamus were successfully activated by optical stimulation (fig. 4C). We stimulated the paraventricular thalamus *in vivo* with a 10-ms pulse width of blue light (473 nm) at 10 Hz in male mice according to previous literature.[15] When exposed to 2.4% sevoflurane, constant optogenetic stimulation of the paraventricular thalamus significantly increased the time to the loss of the righting reflex in the ChR2-on group (188 ± 30 s) compared with that in the ChR2-off group (138 ± 33 s, $P = 0.021$, n = 8; fig. 4D) and the mCherry-on group (144 ± 28 s, $P = 0.048$, n = 8; fig. 4D). For sevoflurane anesthesia emergence, the time to recovery of the righting reflex was significantly reduced in the ChR2-on group (102 ± 27 s) compared with that in the ChR2-off group (166 ± 52 s, $P = 0.011$, n = 8; fig. 4E) and the mCherry-on group (159 ± 33 s, $P = 0.029$, n = 8; fig. 4E). These results indicate that the activation of paraventricular thalamus glutamatergic neurons delayed induction and accelerated behavioral arousal from sevoflurane anesthesia.

To further test whether the activation of paraventricular thalamus glutamatergic neurons is capable of restoring states of consciousness during the sevoflurane anesthesia maintenance period, we used optogenetics to instantaneously stimulate neuronal activities in the paraventricular thalamus when mice lost their righting reflex for 20 min during continuous steady-state general anesthesia with 1.4 to 1.5% sevoflurane. We found that optical stimulation of paraventricular thalamus glutamatergic neurons in male mice induced similar evidence of arousal behavior (fig. 4F; Supplemental Digital Content 1, table S5 [http://links.lww.com/ALN/C836]; Supplemental Digital Content 2, video S1 [http://links.lww.com/ALN/C837]), including leg, head, and tail movements (8 of 8), righting (6 of 8), and walking (5 of 8), in mice in the ChR2-on group during the light sevoflurane anesthesia maintenance period (Supplemental Digital Content 1, table S5 [http://links.lww.com/ALN/C836]). To rule out the influence of the light stimulus, we injected AAV-CaMKIIa-mCherry into the paraventricular thalamus as a control experiment, and this evident arousal behavior was scarcely observed in mice in the mCherry-on (Supplemental Digital Content 1, table S5 [http://links.lww.com/ALN/C836]; Supplemental Digital Content 3, video S2 [http://links.lww.com/ALN/C838]) or the ChR2-off group (Supplemental Digital Content 1, table S5 [http://links.lww.com/ALN/C836]). The Bayesian 95% CI for the difference in the propensity of righting derived from the beta distribution between the ChR2-on group and the mCherry-on group was 0.185 to 0.865 under sevoflurane continuous steady-state general anesthesia with optostimulation of paraventricular thalamus glutamatergic neurons at 10 Hz for 120 s (fig. 4, G and H). The posterior probability of the difference in righting between the ChR2-on group and the mCherry-on group greater than 0 was 0.997, which was statistically significant (fig. 4H). These results suggest that the stimulation of paraventricular thalamus glutamatergic neurons was sufficient to evoke behavioral arousal during the light anesthesia maintenance period. In addition, we further explored whether the activation of paraventricular thalamus glutamatergic neurons affects the maintenance period of deep anesthesia under burst suppression. As shown in figure 5, A to E, the photostimulation of the paraventricular thalamus caused a rapid increase in EEG burst duration (fig. 5A) and decreased the burst-suppression ratio from 59.4 ± 19.5 to 11.7 ± 10.4% ($P < 0.001$, n = 7; fig. 5E; Supplemental Digital Content 4, video S3 [http://links.lww.com/ALN/C839]) during the burst-suppression state induced by 2.5% sevoflurane in male mice. Additionally, the average power spectral density analysis of the EEG showed an increase in the delta, alpha, beta, and gamma bands during photostimulation compared with prestimulation (fig. 5, B to D). As shown in figure 5, F to J, there were no significant differences in raw EEG (fig. 5F; Supplemental Digital Content 5, video S4 [http://links.lww.com/ALN/C840]), burst-suppression ratio (fig. 5J), or power spectral densities during optical stimulation compared with prestimulation in mice in the mCherry group (fig. 5, G to I). These results suggest that the stimulation of paraventricular thalamus glutamatergic neurons can drive cortical activation and reduce anesthesia depth during the maintenance period of deep sevoflurane anesthesia.

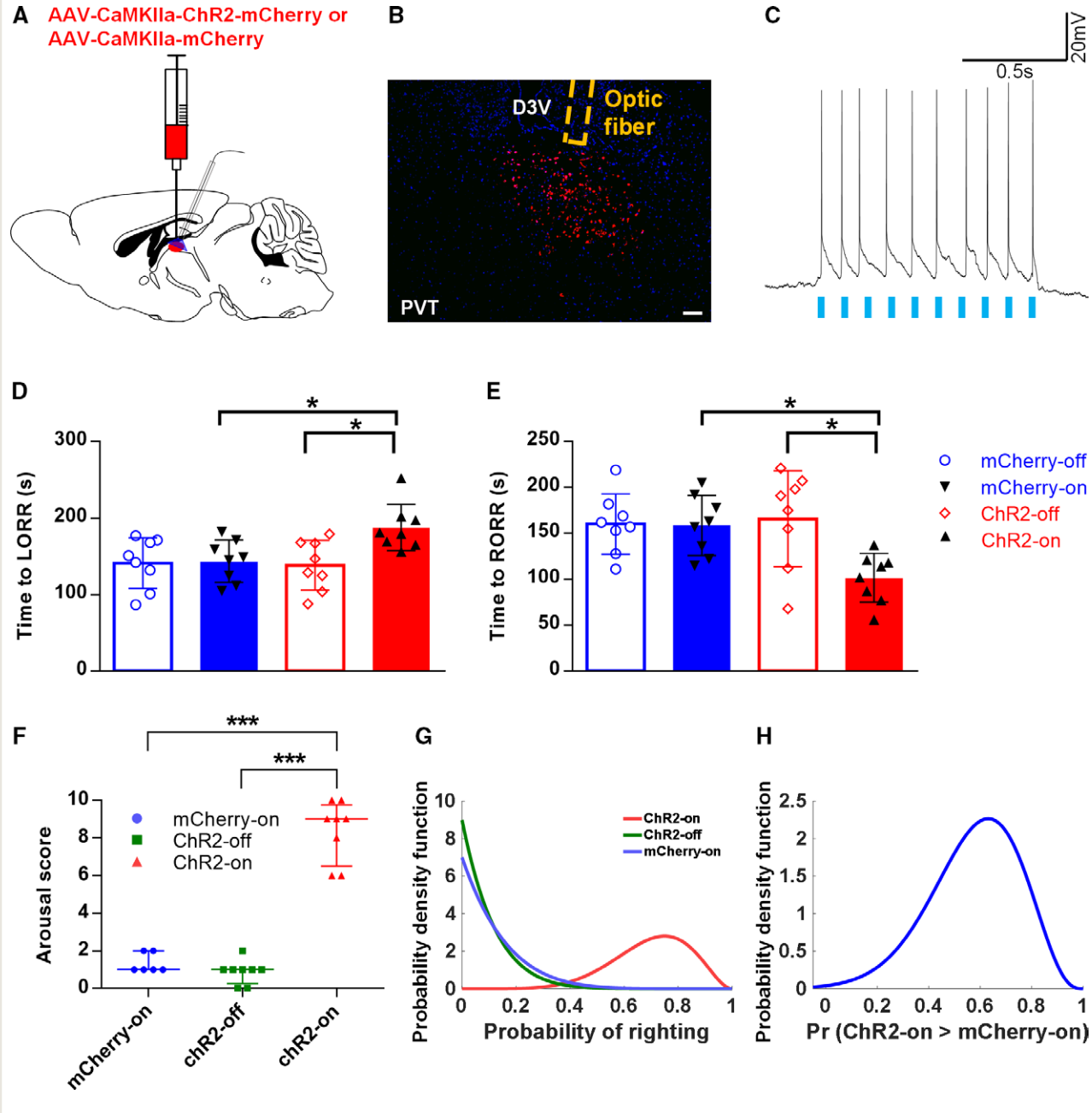

Fig. 4. Optogenetic activation of paraventricular thalamus glutamatergic neurons delayed induction, accelerated emergence, and induced arousal-like responses under continuous steady-state general anesthesia with sevoflurane. (*A*) Schematic representation of virus injection. (*B*) Representative image showing the expression of channelrhodopsin-2 (ChR2) –mCherry (*red*) in the paraventricular thalamus and confirming the location of the optic fiber in the paraventricular thalamus. *Scale bar*, 200 μm. (*C*) Example traces of neuronal firing of ChR2-expressing paraventricular thalamus glutamatergic neurons evoked by 473-nm photostimulation at 10 Hz. (*D* and *E*) Induction time (*D*) and emergence time (*E*) with exposure to 2.4% sevoflurane (1 minimum alveolar concentration) during 10-Hz blue laser stimulation in ChR2-expressing and control mice. The data are shown as the mean ± SD (one-way ANOVA). **P* < 0.05 (*post hoc* Bonferroni test, hM4D–clozapine *N*-oxide *vs.* hM4D-saline/mCherry–clozapine *N*-oxide, n = 8 for each group). (*F*) Total arousal response score for the optical stimulation of paraventricular thalamus glutamatergic neurons (10-ms pulses, 10 Hz, 120 s) during continuous steady-state general anesthesia with 1.4 to 1.5% sevoflurane. The data are shown as the medians and interquartile ranges (25th, 75th). ****P* < 0.001 (n = 8 in the ChR2-on/off group, and n = 6 in the mCherry-on group). (*G*) Posterior densities for the propensity of righting for the ChR2-on (*red*), ChR2-off (*green*), and mCherry-on (*blue*) groups. Posterior densities are obtained from beta distributions. (*H*) Posterior probability of the difference between the ChR2-on group and the mCherry-on group during continuous steady-state general anesthesia with sevoflurane.

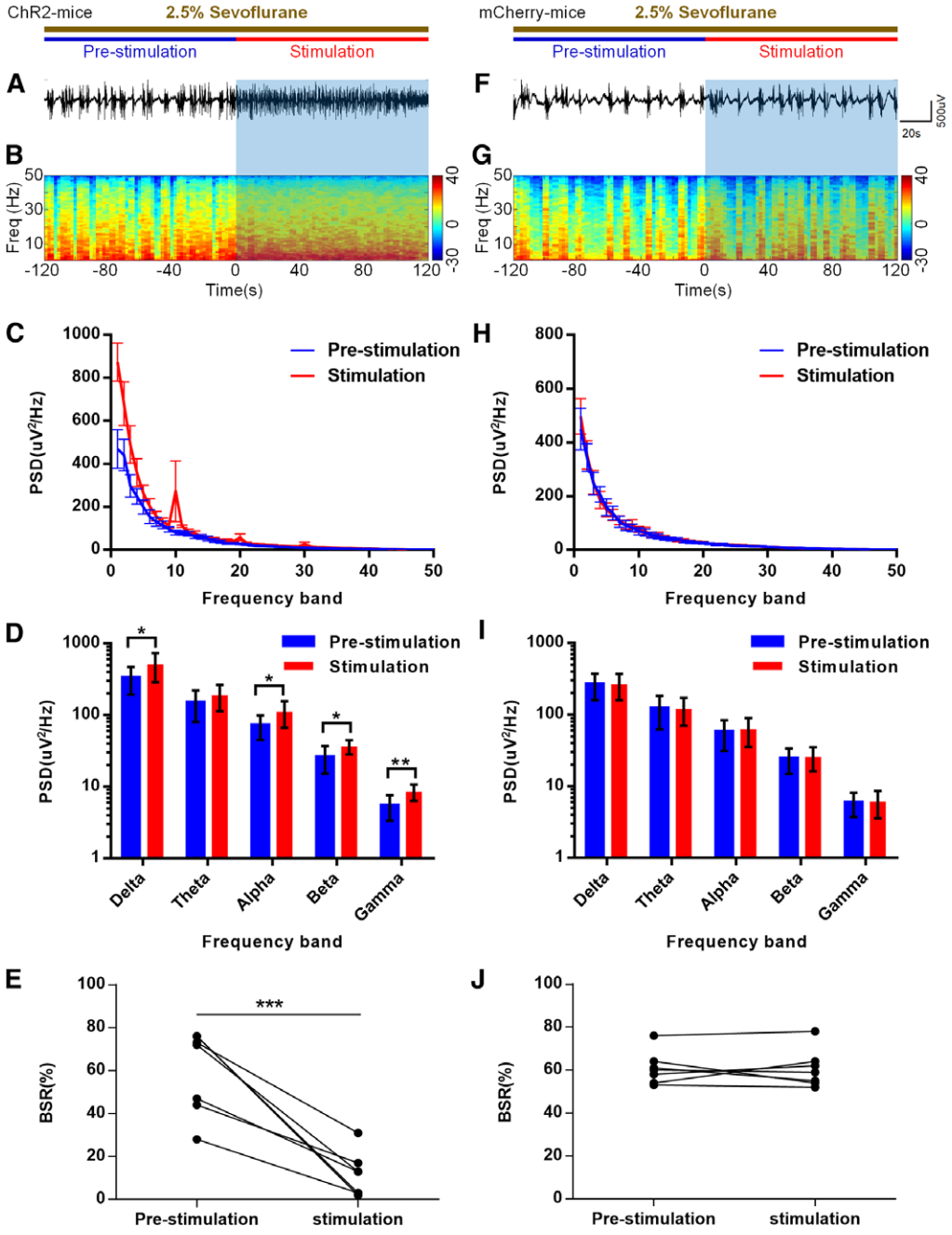

Fig. 5. Optogenetic activation of paraventricular thalamus glutamatergic neurons induced cortical activation under sevoflurane burst-suppression conditions. (*A* and *B*) Representative raw electroencephalogram traces (*A*) and electroencephalogram power spectra (*B*) in a mouse injected with AAV-CaMKIIa-ChR2-mCherry. The *blue shading* represents periods of light stimulation (10-ms pulses; 10 Hz; 120 s). Time zero indicates the beginning of optical stimulation during sevoflurane-induced burst suppression. (*C*) Average power spectral density in the PVT-ChR2 mice computed from 120 s before stimulation (*blue*) to 120 s during optical stimulation (*red*). (*D*) Quantitative analysis of the average power spectral density showed that photostimulation increased the delta, alpha, beta, and gamma power in PVT-ChR2 mice. The data are shown as the mean ± SD). $^{*}P < 0.05$; $^{**}P < 0.01$ (n = 8 in each group). (*E*) The electroencephalogram burst suppression ratio was significantly reduced by optical stimulation during continuous 2.5% sevoflurane anesthesia in PVT-ChR2 mice. $^{***}P < 0.001$ (n = 7 in each group). (*F* and *G*) Typical examples of electroencephalogram traces (*F*) and electroencephalogram power spectra (*G*) in the control group (AAV-CaMKIIa–mCherry). (*H*) Average power spectral density in the control group computed from 120 s before stimulation (*blue*) to 120 s after optical stimulation (*red*). (*I*) Quantitative analysis of the average power spectral density showed no significant difference between the prestimulation and stimulation periods in the control group. (*J*) Effect of optical stimulation on the electroencephalogram burst suppression ratio during continuous sevoflurane anesthesia in the control group ($P = 0.912$, n = 7 for each group).

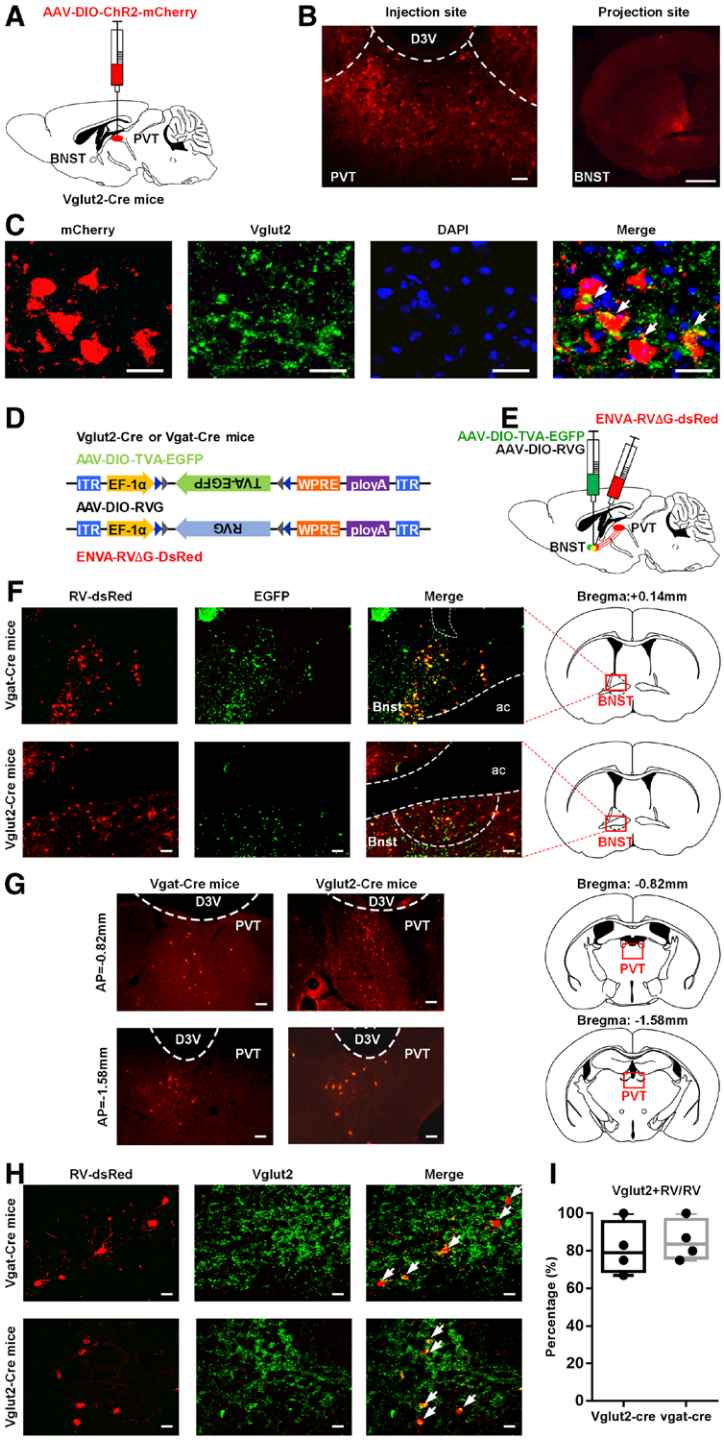

Fig. 6. The paraventricular thalamus glutamatergic neurons project onto the glutamatergic and γ-aminobutyric acid–mediated neurons in the bed nucleus of the stria terminalis. (*A*) Schematic representation of virus injection location and glutamatergic cell type–specific anterograde tracing. (*B*) Representative images showing ChR2-expressing cells in the vglut2$^+$ neurons of the paraventricular thalamus (*left*; *scale bars*, 100 μm) and mCherry-expressing axon terminals in the bed nucleus of the stria terminalis (*right*; *scale bars*, 1 mm) of vglut2-cre mice. (*C*) Coexpression of mCherry$^+$ neurons (*red*) and vglut2$^+$ neurons (*green*) in the paraventricular thalamus. *Scale bars*, 50 μm; *blue*, 4′,6-diamidino-2-phenylindole for nuclear staining. (*D* and *E*) Schematic diagrams of rabies virus–mediated monosynaptic tracing. (*F*) Representative images of the virus injection site and expression within the bed nucleus of the stria terminalis. Starter cells (*yellow*) coexpress avian tumor virus receptor A (TVA)-green fluorescent protein (*green*), rabies virus G, and rabies virus–EnvA-ΔG-DsRed (*red*) in the bed nucleus of the stria terminalis of vgat-Cre mice (*upper*) and vglut2-Cre (*lower*) mice. *Scale bars*, 100 μm. (*G*) Representative images of presynaptic cells in the paraventricular thalamus. Rabies

Chemogenetic Dissection Identification of the Paraventricular Thalamus Bed Nucleus of the Stria Terminalis Pathway

Previous studies have shown that paraventricular thalamus neurons are primarily glutamatergic neurons and are positive for VGLUT2 mRNA but not VGLUT1 mRNA.[33] To characterize contacts between the paraventricular thalamus and the bed nucleus of the stria terminalis, we first microinjected an adeno-associated virus expressing Cre-dependent channelrhodopsin-2 (AAV-DIO-ChR2-mCherry) into the paraventricular thalamus of vglut2-Cre mice (fig. 6, A to C). We observed that mCherry$^+$ glutamatergic cell bodies in the paraventricular thalamus and mCherry$^+$ fibers were mainly detected in the dorsolateral bed nucleus of the stria terminalis, as well as in other brain regions (fig. 6B; Supplemental Digital Content 1, fig. S4 [http://links.lww.com/ALN/C836]).

To further identify the cell type–specific connections between the paraventricular thalamus and the bed nucleus of stria terminalis neurons, we applied a Cre-dependent retrograde transmonosynaptic tracing tactic to ascertain the specific neuronal type of the bed nucleus of the stria terminalis that receives paraventricular thalamus excitatory projections (fig. 6D). Since glutamatergic and GABAergic neurons are typical and dominant cells in the bed nucleus of the stria terminalis, Cre-dependent helper viruses (AAV-EF1α-DIO-TVA-green fluorescent protein and AAV-EF1α-DIO-RVG) were microinjected into the bed nucleus of the stria terminalis of vglut2-Cre mice or vgat-Cre mice (fig. 6E). After 3 weeks, rabies virus (RV-ENVA-ΔG-dsRed) was microinjected into the same site and infected only the helper virus–positive neurons in the bed nucleus of the stria terminalis. Rabies virus could be transmitted retrogradely across monosynapses in the presence of these helper viruses. Glutamatergic or GABAergic neurons in the bed nucleus of the stria terminalis expressing both red and green fluorescent signals simultaneously were considered starter cells (fig. 6F). We observed intensely dsRed-labeled neurons in the paraventricular thalamus of vglut2-Cre mice and vgat-Cre mice (fig. 6G), suggesting that paraventricular thalamus neurons innervate glutamatergic and GABAergic neurons in the bed nucleus of the stria terminalis. Additionally, our immunofluorescence staining showed that the dsRed-labeled signal was largely colocalized with the vglut2 antibody signal (fig. 6, H and I), indicating that both GABAergic and glutamatergic neurons in the bed nucleus of the stria terminalis receive paraventricular thalamus glutamatergic projections directly. Only male mice were used in these experiments.

Fig. 6. (*Continued*) virus–labeled cells within the paraventricular thalamus of vgat-Cre mice (*left*) and vglut2-Cre (*right*) mice. *Scale bars*, 100 μm. (*H*) Identification of rabies virus–labeled neurons in the paraventricular thalamus. *White arrows* represent the colocalization of RV signals (*red*) and vglut2 antibody in vgat-Cre or vglut2-Cre mice. *Scale bars*, 50 μm. (*I*) Quantitation of the percentage of vglut2-expressing rabies virus–positive cells that projected onto the γ-aminobutyric acid–mediated and glutamatergic neurons in the bed nucleus of the stria terminalis (n = 4 for each group).

Chemogenetic Inhibition of the Paraventricular Thalamus Bed Nucleus of the Stria Terminalis Pathway Modulates Sevoflurane Anesthesia

To further verify the necessity of this specific pathway in regulating states of consciousness during sevoflurane anesthesia, retrograde transport Cre recombinase AAV_{retro}-Syn-Cre was bilaterally microinjected into the bed nucleus of the stria terminalis, and Cre-dependent AAV-EF1α-DIO-hM4D-mCherry or AAV-EF1α-DIO-mCherry was injected into the paraventricular thalamus for selective chemogenetic inhibition of paraventricular thalamus neurons that projected to the bed nucleus of the stria terminalis (fig. 7, A to C). We explored the effects on sevoflurane induction and emergence after the delivery of saline or clozapine *N*-oxide into hM4D-mCherry and mCherry (control) mice, respectively. The experiments were performed only in male mice. Our results showed that when exposed to 2.4% sevoflurane, the hM4D–clozapine *N*-oxide group showed a significant decrease in the induction time (87 ± 24 s) compared with that in the hM4D-saline group (136 ± 36 s, $P = 0.002$, n = 12; fig. 7D) and the mCherry–clozapine *N*-oxide group (124 ± 29 s, $P = 0.032$, n = 12; fig. 7D). The time to recovery of the righting reflex of sevoflurane anesthesia was prolonged in the hM4D–clozapine *N*-oxide group (292 ± 108 s) compared with that in the hM4D-saline group (174 ± 59 s, $P = 0.003$, n = 12; fig. 7E) and the mCherry–clozapine *N*-oxide group (160 ± 73 s, $P < 0.001$, n = 12; fig. 7E) after a 30-min exposure to 2.4% sevoflurane. The concentration at which 50% of the mice lost their righting reflex (EC_{50}) of sevoflurane was decreased in the hM4D–clozapine *N*-oxide group compared with that in the hM4D-saline group (1.13 [1.09 to 1.17] *vs.* 1.40 [1.36 to 1.44] vol%, n = 10; fig. 7F; Supplemental Digital Content 1, table S4 [http://links.lww.com/ALN/C836]) and the mCherry–clozapine *N*-oxide group (1.13 [1.09 to 1.17] *vs.* 1.42 [1.38 to 1.47] vol%, n = 10; fig. 7F; Supplemental Digital Content 1, table S4 [http://links.lww.com/ALN/C836]). The concentration at which 50% of the mice recovered their righting reflex (EC_{50}) of sevoflurane was also reduced in the hM4D–clozapine *N*-oxide group compared with that in the hM4D-saline group (1.03 [0.97 to 1.09] *vs.* 1.30 [1.26 to 1.35] vol%, n = 10; fig. 7G; Supplemental Digital Content 1, table S4 [http://links.lww.com/ALN/C836]) and the mCherry–clozapine *N*-oxide group (1.03 [0.97 to 1.09] *vs.* 1.33 [1.28 to 1.39] vol%, n = 10; fig. 7G; Supplemental Digital Content 1, table S4 [http://links.lww.com/ALN/C836]). Taken together, these results suggest that the suppression of the paraventricular

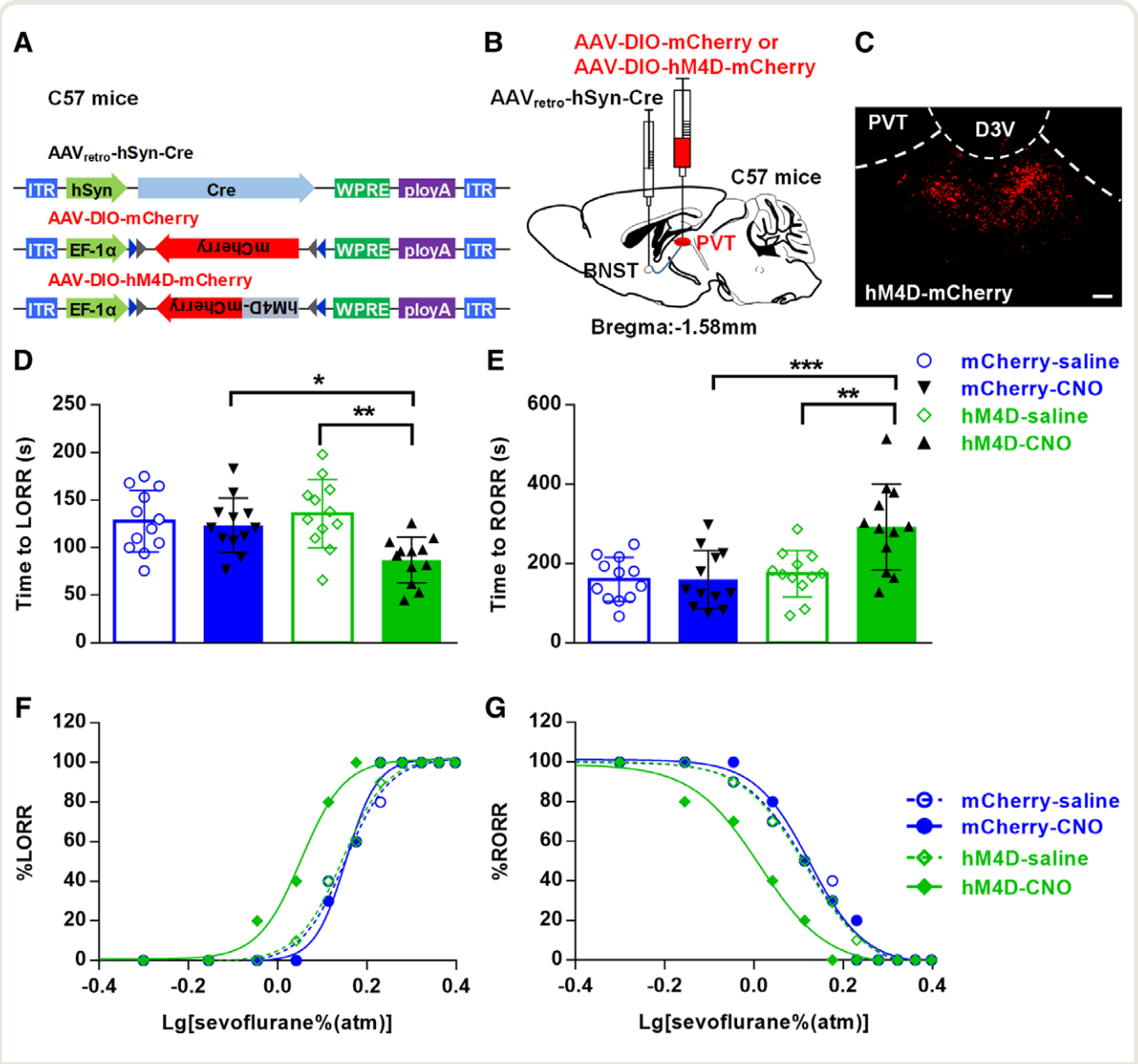

Fig. 7. The inhibition of the pathway from the paraventricular thalamus to the bed nucleus of the stria terminalis promoted induction and prolonged behavioral arousal from sevoflurane anesthesia. (*A* and *B*) Schematic representation of virus injection. AAV-DIO-hM4D-mCherry (or AAV-DIO-mCherry) was injected into the paraventricular thalamus, and AAV$_{retro}$-hSyn-Cre virus was injected into the bed nucleus of the stria terminalis. (*C*) Expression of hM4D-mCherry in neurons of the paraventricular thalamus that project to the bed nucleus of the stria terminalis. *Scale bar*, 100 μm. (*D* and *E*) Induction (*D*) and emergence (*E*) times with exposure to 2.4% sevoflurane (1 minimum alveolar concentration) in the inhibition group and the control group. The data are shown as the mean ± SD (one-way ANOVA). *$P < 0.05$; **$P < 0.01$; ***$P < 0.001$ (*post hoc* Bonferroni test, hM4D–clozapine *N*-oxide *vs.* hM4D-saline/mCherry–clozapine *N*-oxide, n = 12 for each group). (*F* and *G*) Dose–response curves of the loss of the righting reflex (*F*) and the recovery of the righting reflex (*G*) for the inhibition group and the control group.

thalamus bed nucleus of the stria terminalis pathway sped up the induction, delayed the recovery, and increased the sensitivity of sevoflurane anesthesia.

For cortical EEG activity, compared with saline injection, the inhibition of the paraventricular thalamus bed nucleus of the stria terminalis pathway in male mice led to an obvious increase in delta power during sevoflurane anesthesia induction (35.5 ± 3.8% *vs.* 47.2 ± 3.3%, $P < 0.0001$, n = 8; fig. 8, D and E) and emergence periods (39.4 ± 1.5% *vs.* 43.7 ± 2.6%, $P = 0.001$, n = 8; fig. 8, I and J), indicating that the paraventricular thalamus bed nucleus of the stria terminalis pathway could affect cortical sedation and arousal under sevoflurane anesthesia. Taken together, these results suggest that the paraventricular thalamus bed nucleus

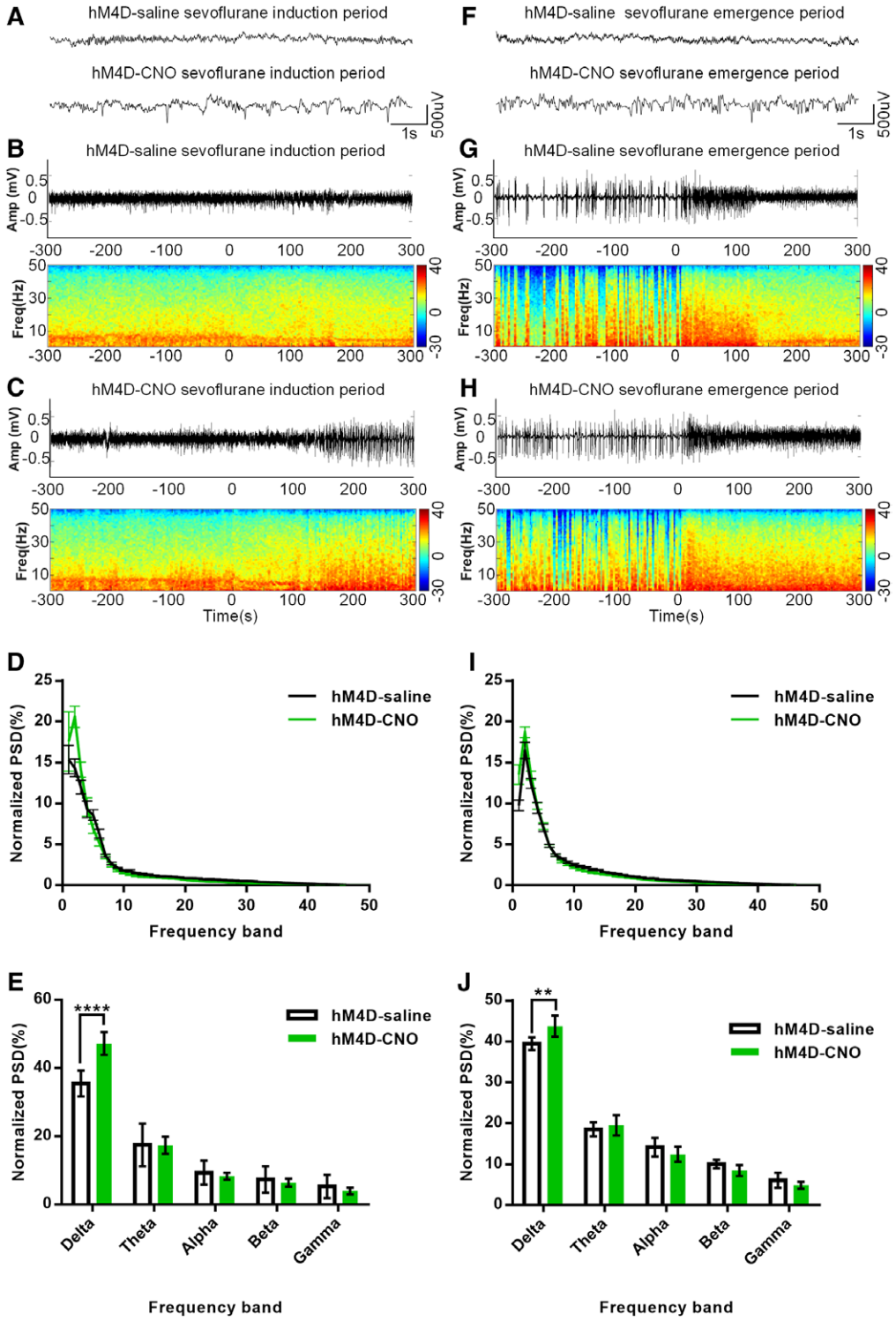

Fig. 8. The inhibition of the pathway from the paraventricular thalamus to the bed nucleus of the stria terminalis suppressed cortical electroencephalogram arousal during sevoflurane anesthesia. (*A*) Example of raw electroencephalogram traces during the induction period in hM4D mice after the delivery of clozapine *N*-oxide or saline. (*B* and *C*) Representative electroencephalogram power spectrograms of the suppression of the pathway from the paraventricular thalamus to the bed nucleus of the stria terminalis during the sevoflurane anesthesia induction period. Time zero on the timeline represents the initiation of sevoflurane anesthesia. (*D*) Normalized power spectral density changes during the sevoflurane induction period after intraperitoneal injection of saline or clozapine *N*-oxide (3 mg/kg). (*E*) Quantitative analysis of normalized power spectral density. Compared with saline, clozapine *N*-oxide induced a significant increase in the electroencephalogram delta power

of the stria terminalis pathway plays a vital role in sevoflurane anesthesia induction and emergence.

Optogenetic Activation of the Paraventricular Thalamus Bed Nucleus of the Stria Terminalis Pathway Modulates States of Consciousness during Sevoflurane Anesthesia

To further examine the role of projections from the paraventricular thalamus to the bed nucleus of the stria terminalis in sevoflurane anesthesia induction, maintenance, and emergence, we injected AAV-DIO-ChR2-mCherry or AAV-DIO-mCherry into the paraventricular thalamus of vglut2-Cre mice and then implanted optical fibers above the bed nucleus of the stria terminalis (fig. 9, A to C). We stimulated $PVT^{vglut2+}$ terminals in the bed nucleus of the stria terminalis with a 10-ms pulse width of blue light (473 nm) at 10 Hz in mice. Only male mice were used in this experiment.

Our results showed that the induction time in the ChR2-on group was significantly prolonged compared with that in the ChR2-off group (154 ± 24 s *vs.* 103 ± 36 s, $P = 0.012$, n = 8; fig. 9D) and the mCherry-on group (154 ± 24 s *vs.* 109 ± 33 s, $P = 0.034$, n = 8; fig. 9D). We also found that the emergence time in the ChR2-on group was significantly reduced compared with that in the ChR2-off group (107 ± 22 s *vs.* 169 ± 41 s, $P = 0.012$, n = 8; fig. 9E) and the mCherry-on group (107 ± 22 s *vs.* 160 ± 34 s, $P = 0.042$, n = 8; fig. 9E). All these results indicate that the paraventricular thalamus bed nucleus of the stria terminalis pathway may be the necessary pathway for the modulation of sevoflurane anesthesia induction and emergence.

Our results also showed that optical stimulation of $PVT^{vglut2+}$ terminals in the bed nucleus of the stria terminalis induced similar evidence of arousal behavior (fig. 9F; Supplemental Digital Content 1, table S6 [http://links.lww.com/ALN/C836]; Supplemental Digital Content 6, video S5 [http://links.lww.com/ALN/C841]), including leg, head, and tail movements (8 of 8), righting (5 of 8), and walking (3 of 8), in mice of the ChR2-on group during continuous steady-state general anesthesia with sevoflurane (Supplemental Digital Content 1, table S6 [http://links.lww.com/ALN/C836]), while this evident arousal behavior was barely seen in mice of the mCherry-on (Supplemental Digital Content 1, table S6 [http://links.lww.com/ALN/C836]; Supplemental Digital Content 7, video S6 [http://links.lww.com/ALN/C842]) or ChR2-off groups (Supplemental Digital Content 1, table S6 [http://links.lww.com/ALN/C836]). The Bayesian 95% CI for the difference in the propensity of righting at 10 Hz between the ChR2-on group and the mCherry-on group was 0.081 to 0.795 under sevoflurane continuous steady-state general anesthesia with the optostimulation of the paraventricular thalamus bed nucleus of the stria terminalis pathway (fig. 9, G and H). The posterior probability of the difference in righting between the two groups greater than 0 was 0.990, which was statistically significant (fig. 9H). In addition, the activation of the paraventricular thalamus bed nucleus of the stria terminalis projections caused a rapid increase in burst duration (fig. 10A; Supplemental Digital Content 8, video S7 [http://links.lww.com/ALN/C843]) and a significant increase in delta power compared with those observed prestimulation (fig. 10, C and D) and a significantly decreased burst-suppression ratio from 43.1 ± 10.4% to 2.8 ± 2.7% ($P < 0.001$, n = 8; fig. 10E) during sevoflurane-induced burst-suppression conditions, which was not seen in mCherry mice (fig. 10, F to J; Supplemental Digital Content 9, video S8 [http://links.lww.com/ALN/C844]). Our results indicate that the activation of the paraventricular thalamus bed nucleus of the stria terminalis pathway is sufficient to induce behavioral emergence during continuous steady-state general anesthesia with sevoflurane and rapidly reduce the depth of anesthesia during deep sevoflurane anesthesia.

Fig. 8. (*Continued*) of hM4D-expressing mice. The data are shown as the mean ± SD (two-way ANOVA). ****$P < 0.0001$ (*post hoc* Bonferroni test, hM4D–clozapine *N*-oxide *vs.* hM4D-saline, n = 8 for each group). (*F*) Representative raw electroencephalogram traces during the emergence period for the inhibition group and the control group. (*G* and *H*) Representative electroencephalogram power spectrograms during the sevoflurane anesthesia recovery period for the inhibition group (*green*) and control group (*black*). Zero on the timeline indicates the discontinuation of sevoflurane anesthesia. (*I*) Normalized power spectral density in the inhibition group (*green*) and control group (*black*) during the sevoflurane emergence period. (*J*) Quantitative analysis of normalized power spectral density shows that the suppression of the paraventricular thalamus bed nucleus of the stria terminalis pathway led to a significant increase in the delta power compared with that in the control mice during the recovery period. The data are shown as the mean ± SD (two-way ANOVA). **$P < 0.01$ (*post hoc* Bonferroni test, hM4D–clozapine *N*-oxide *vs.* hM4D-saline, n = 8 for each group).

Discussion

In the current study, we verified the regulatory effects of paraventricular thalamus glutamatergic neurons and the paraventricular thalamus bed nucleus of the stria terminalis pathway on sevoflurane-induced unconsciousness. Inhibition of paraventricular thalamus glutamatergic neurons or their pathways promoted the loss of consciousness and prolonged the recovery of consciousness, whereas activation induced opposite effects. Moreover, the cortical EEG activity during the induction and recovery periods of sevoflurane anesthesia was remarkably affected by the inhibition of paraventricular thalamus glutamatergic neurons or their pathways. Instantaneous optogenetic stimulation of paraventricular thalamus glutamatergic neurons or their pathways restored awake-like behavior during the maintenance period of light sevoflurane anesthesia and reduced the depth of anesthesia during sevoflurane-induced burst-suppression states.

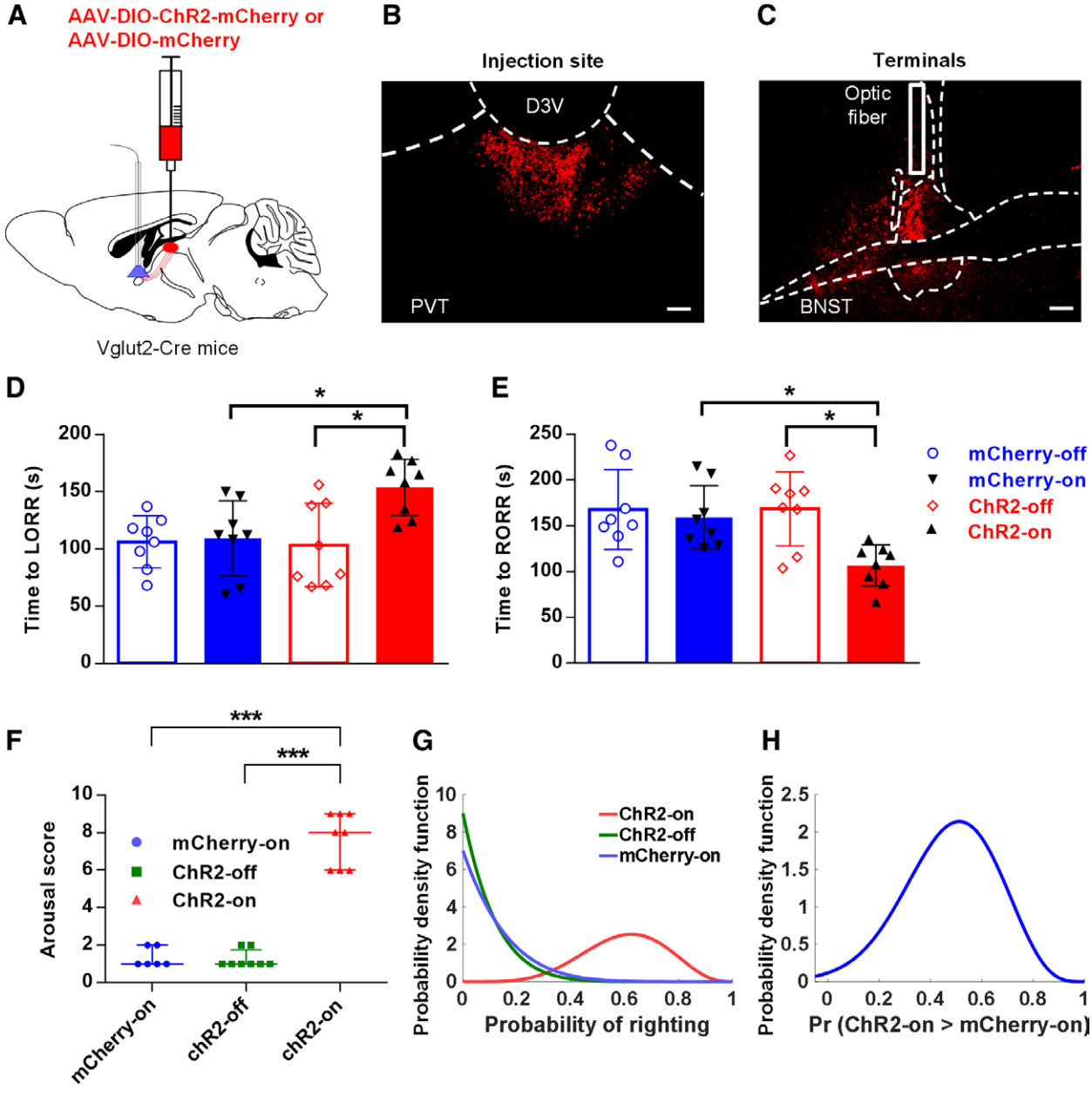

Fig. 9. Optogenetic activation of the paraventricular thalamus bed nucleus of the stria terminalis pathway delayed the induction, accelerated the emergence, and induced behavioral emergence during continuous steady-state general anesthesia with sevoflurane. (*A*) Schematic representation of virus injection and optical implantation. (*B* and *C*) Expression of AAV-DIO-ChR2-mCherry (*red*) in $PVT^{vglut2+}$ neurons (*B*) and mCherry containing $vglut2^{+}$ terminals (*red*) in the bed nucleus of the stria terminalis (*C*). *Solid white lines* show the locations of optical fibers. *Scale bars*, 100 μm. (*D* and *E*) Results of the induction time (*D*) and emergence time (*E*) with exposure to 2.4% sevoflurane during the activation of the paraventricular thalamus bed nucleus of the stria terminalis pathway projections. The data are shown as the mean ± SD (one-way ANOVA). $*P < 0.05$ (*post hoc* Bonferroni test, hM4D–clozapine *N*-oxide *vs.* hM4D-saline/mCherry–clozapine *N*-oxide, n = 8 for each group). (*F*) Total arousal response score for the optical stimulation of the paraventricular thalamus bed nucleus of the stria terminalis pathway (10-ms pulses, 10 Hz, 120 s) during continuous steady-state general anesthesia with 1.4 to 1.5% sevoflurane. The data are reported as the median and interquartile range (25th, 75th). $***P < 0.001$ (n = 8 in the ChR2-on/off group, and n = 6 in the mCherry-on group). (*G*) Posterior densities for the propensity of righting for the ChR2-on (*red*), ChR2-off (*green*), and mCherry-on (*blue*) groups during optical stimulation of the paraventricular thalamus bed nucleus of the stria terminalis pathway. Posterior densities are obtained from beta distributions. (*H*) Posterior probability of the difference between the ChR2-on group and the mCherry-on group during optical stimulation of the paraventricular thalamus bed nucleus of the stria terminalis pathway under continuous steady-state general anesthesia with sevoflurane.

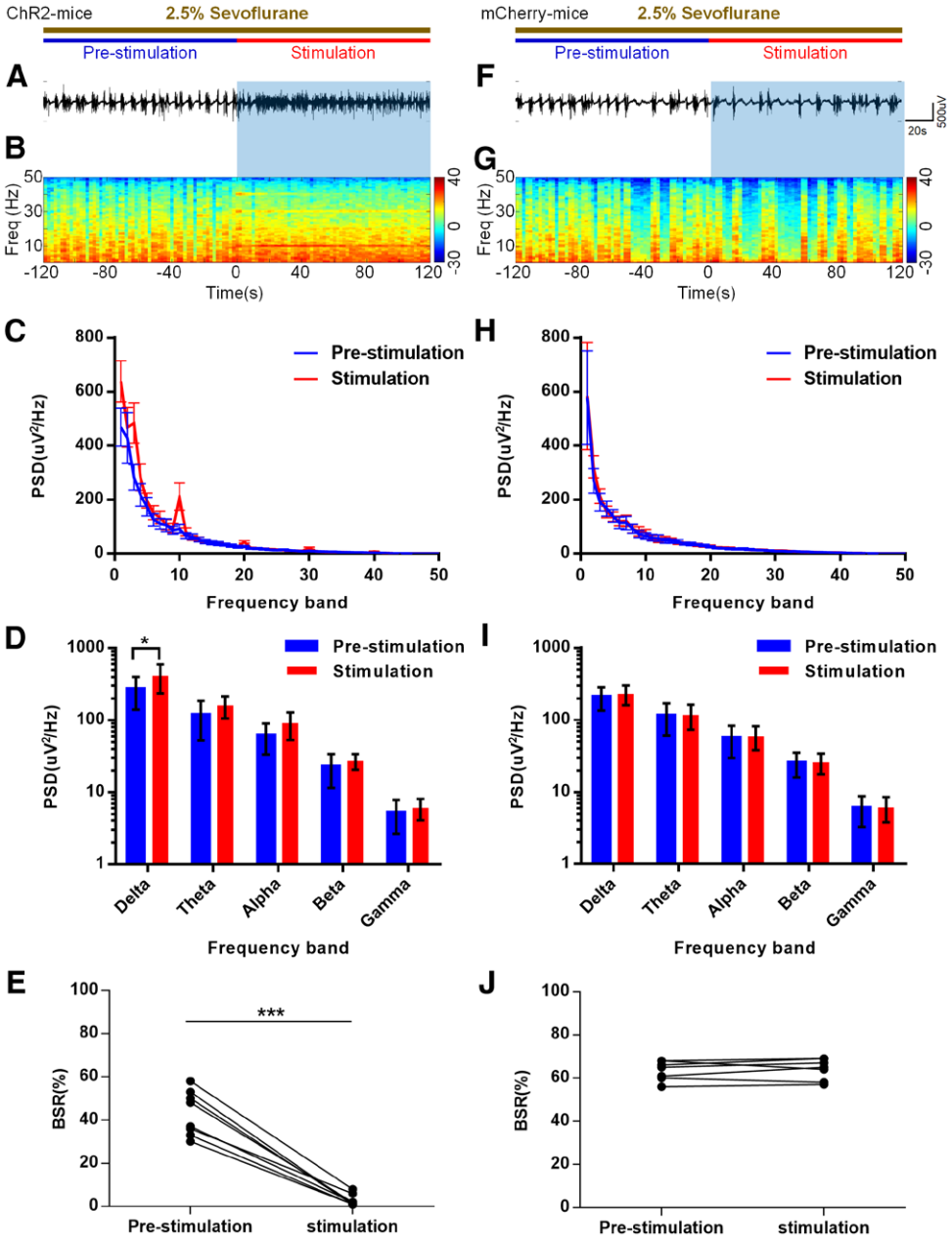

Fig. 10. Optogenetic activation of the paraventricular thalamus bed nucleus of the stria terminalis pathway reduced the depth of anesthesia during sevoflurane-induced burst-suppression conditions. (*A*) Example raw electroencephalogram traces and electroencephalogram power spectra (*B*) in vglut2-cre mice injected with AAV-DIO-ChR2-mCherry. *Blue shading* represents the light stimulation period (10-ms pulses; 10 Hz; 120 s). Time zero indicates the beginning of light stimulation during burst suppression conditions induced by 2.5% sevoflurane. (*C*) Average power spectral density in the stimulation of the paraventricular thalamus bed nucleus of the stria terminalis pathway computed from 120 s before stimulation (*blue*) to 120 s during optical stimulation (*red*). (*D*) Quantitative analysis of the average power spectral density between the prestimulation and stimulation periods in the stimulation of the paraventricular thalamus bed nucleus of the stria terminalis pathway in mice. $^{*}P < 0.05$ (n = 8 for each group). (*E*) Effect of the activation of the paraventricular thalamus bed nucleus of the stria terminalis pathway on the electroencephalogram burst-suppression ratio during continuous sevoflurane anesthesia. $^{***}P < 0.001$ (n = 8 for each group). (*F* and *G*) Typical examples of electroencephalogram traces (*F*) and electroencephalogram power spectra (*G*) in the control group (vglut2-cre mice injected with AAV-DIO-mCherry). (*H*) Average power spectral density in the control group computed from 120 s before stimulation (*blue*) to 120 s after optical stimulation (*red*). (*I*) Quantitative analysis of the average power spectral density between the prestimulation and stimulation periods in the control group. (*J*) Effect of optical stimulation on the electroencephalogram burst-suppression ratio during continuous sevoflurane anesthesia in the control group ($P = 0.527$, n = 7 for each group).

Recent studies have demonstrated that the central medial thalamus is the key hub for initiating sleep or anesthetic-induced unconsciousness.[34] Patients with local lesions in the paramedian region of the thalamus showed disturbances of consciousness.[35] Alkire *et al.*[36] found that local injection of nicotine, a cholinergic nicotinic receptor agonist, into the central medial thalamus could reverse sevoflurane-induced loss of the righting reflex. Ren *et al.*[15] found that optogenetic activation of the paraventricular thalamus promoted emergence from isoflurane anesthesia. In concordance with previous studies, we verified that paraventricular thalamus glutamatergic neurons can greatly affect the general anesthesia emergence time. It is generally believed that emergence from general anesthesia is the reverse of the process of induction, caused by the passive elimination of anesthetic drugs at the site of action in the central nervous system. However, recent studies have shown that the neural substrates mediating induction and emergence are not consistent.[4] Emerging evidence suggests that anesthetic-induced loss of consciousness is related to the disruption of corticocortical or thalamocortical functional connections, while recovery from anesthesia is mostly controlled by ascending arousal pathways involved in sleep–wakefulness.[37,38] In contrast to a previous study, inhibition of the dopaminergic pathway of the paraventricular thalamus prolonged the isoflurane anesthesia recovery time but had no significant effect on the induction time.[39] We found that the sevoflurane anesthesia induction time and recovery time were both significantly affected by the paraventricular thalamus. Our results suggest that there are shared neural circuits involved in the process of regulating the sevoflurane-induced loss and recovery of consciousness.

There is robust evidence of an association between EEG oscillations in the frontal cortex and anesthetic-induced loss of consciousness.[3,40] Recent evidence suggests that the delta power is a reliable predictor of transitions between consciousness and unconsciousness under anesthesia. Delta activity is a typical signature of unconsciousness.[40,41] Our results showed that the delta power was affected by the paraventricular thalamus bed nucleus of the stria terminalis pathway during the period of sevoflurane induction. Delta oscillations during anesthesia resulted from a pronounced hyperpolarization of thalamocortical relay neurons caused by complete withdrawal of excitatory aminergic inputs.[42] Therefore, our results suggested that the inhibition of the paraventricular thalamus or its pathways during sevoflurane anesthesia could exacerbate hyperpolarization and accelerate the synchronized activity of the cerebral cortex, thereby promoting the loss of consciousness. Furthermore, during the sevoflurane emergence period, we found that the inhibition of the paraventricular thalamus increased the delta power and decreased the theta power. Theta waves are associated with attention as an element of some forms of exploratory behavior and of the process of dream formation and expression, both of which are characterized by consciousness.[43] Our results suggested that a reduction in theta power, combined with an increase in sleep-related delta oscillatory activity, might contribute to the delay in the recovery of consciousness. The difference in EEG results between the induction and recovery periods also indicates that the regulatory mechanism of paraventricular thalamus glutamatergic neurons during sevoflurane-induced loss and recovery of consciousness may be different.

Furthermore, inhibition of the paraventricular thalamus bed nucleus of the stria terminalis pathway significantly increased only the delta power, without affecting the theta power, during the sevoflurane emergence period, suggesting that this pathway may be one of the nerve loops mediating the arousal-promoting effect of the paraventricular thalamus. Recent studies have found that neurons expressing dopamine D1 receptor in the nucleus accumbens played a significant role in wakefulness, and the stimulation of these neurons at 20 or 30 Hz regulated the state of consciousness in sevoflurane anesthesia.[28,44] Ren *et al.*[15] reported that the activation of paraventricular thalamus-nucleus accumbens projections promoted the sleep–wake transition. However, Hua *et al.*[25] found that photogenetic activation of the paraventricular thalamus-nucleus accumbens pathway at 5 Hz had no obvious arousal effect. The differences in these findings may be due to differences in the frequency of the stimulation, and it was also reasoned that high-frequency stimulation may cause retrograde activation.[25] Thus, whether the paraventricular thalamus-nucleus accumbens is involved in the regulation of sevoflurane-induced unconsciousness remains unclear.

Burst suppression is observed in various pathologic conditions, including deep general anesthesia, hypoxia-induced deep coma, hypothermia, and childhood encephalopathies, and is often accompanied by a profound obliteration of consciousness.[45] Recent studies have demonstrated that sevoflurane-induced unconsciousness during burst-suppression conditions results from the disruption of functional connectivity between frontal and thalamic networks.[46] It was also reported that anesthetic-induced burst suppression calls for glutamate-mediated excitatory synaptic transmission and that EEG burst activities can be evoked by barrages of glutamate-mediated excitatory events in intrinsic neocortical circuitry.[47] Similar to previous studies,[15] we found that optical stimulation of the paraventricular thalamus bed nucleus of the stria terminalis pathway increased burst duration and burst frequency and decreased the burst-suppression ratio during anesthetic-induced burst-suppression states, suggesting that EEG bursts could be triggered by excitatory events in the paraventricular thalamus glutamatergic neurons and its network. Most EEG arousal represents the transition from mixed high-amplitude slow activity to higher-frequency low-amplitude activity. However, there is a paradoxical delta arousal; that is, the power in the delta band (0.5 to 4 Hz) is increased. Our results showed that optical stimulation of the paraventricular thalamus bed

nucleus of the stria terminalis pathway induced an increase in the delta band during sevoflurane-induced burst suppression. This paradoxical phenomenon has also been observed in the activation of histaminergic transmission in the basal forebrain, and the administration of histamine in the basal forebrain could shift neocortical electroencephalography from a burst-suppression pattern to delta activity, suggesting that EEG delta arousal was induced by histaminergic transmission during deep isoflurane anesthesia.[12] Delta arousal has also been shown to occur when a patient is exposed to noxious stimulation with inadequate analgesia under deep anesthesia.[48] It has also been suggested that the increase in delta power could be induced by high-frequency midbrain reticular stimulation in anesthetized cats.[49] While termed delta arousal, these delta responses may not necessarily imply the progression toward the restoration of consciousness.[48] In our experiments, the delta power and burst duration were increased after optical stimulation, suggesting cortical activation and a decrease in anesthesia depth, but we did not conclude that consciousness was restored after stimulation of the paraventricular thalamus during deep anesthesia with burst suppression. Another unexpected finding was that the activation of the paraventricular thalamus bed nucleus of the stria terminalis pathway was sufficient to induce behavioral arousal during light sevoflurane anesthesia maintenance, which was not seen in isoflurane anesthesia.[15] This difference may be attributed to the different affinities of isoflurane and sevoflurane for the same molecule or receptor in the paraventricular thalamus[1,50] and suggests that the potential neural circuit mechanism of the two anesthetics may not be exactly the same.

However, there are still some limitations of our study. First, whether there are sex differences in the effect of the paraventricular thalamus bed nucleus of the stria terminalis pathway on anesthetic arousal still needs to be further explored. Second, we identified only the cell types of neurons in the bed nucleus of the stria terminalis innervated by paraventricular thalamus glutamatergic neurons, and the functional connections of the paraventricular thalamus bed nucleus of the stria terminalis pathway need to be further characterized. We speculate that the arousal-promoting effect of paraventricular thalamus glutamatergic neurons may be directly mediated by GABAergic neurons in the bed nucleus of the stria terminalis. However, it is not known whether there is a local loop between glutamatergic and GABAergic neurons in the bed nucleus of the stria terminalis, and whether paraventricular thalamus glutamatergic neurons can indirectly activate the GABAergic neurons in the bed nucleus of the stria terminalis through this local loop and then play a role in promoting the arousal effect of sevoflurane anesthesia still needs to be further investigated. Finally, experiments on off-target injections would further enhance the study.

In summary, our findings support the hypothesis that paraventricular thalamus glutamatergic neurons play a significant role in modulating states of consciousness during sevoflurane anesthesia by directly projecting to the bed nucleus of the stria terminalis. Improved general anesthetic drugs should satisfy the desirable outcomes, such as surgery without pain, awareness, or memory, and minimize undesirable results, such as anesthesia-associated delirium, cardiovascular depression, and death. Understanding the neural basis of general anesthesia will facilitate the development of new anesthetics.

Acknowledgments

The authors thank Haohong Li, Ph.D. (Wuhan National Laboratory for Optoelectronics, Huazhong University of Science and Technology, Hubei, China), for providing vglut2-Cre and vgat-Cre mice, and Pengcheng Huang, Ph.D. (Wuhan National Laboratory for Optoelectronics, Huazhong University of Science and Technology), for technical support, and Xinfeng Chen, Ph.D. (Chinese Institute for Brain Research, Beijing, China), for technical support.

Research Support

Supported by grant Nos. 82071556 and 81873793 from the National Natural Science Foundation of China (Beijing, China).

Competing Interests

The authors declare no competing interests.

Correspondence

Address correspondence to Dr. Mei: Tongji Hospital, Tongji Medical College, Huazhong University of Science and Technology, Jiefang Avenue 1095, Wuhan 430030, China. wmei@hust.edu.cn.

References

1. Franks NP: General anaesthesia: From molecular targets to neuronal pathways of sleep and arousal. Nat Rev Neurosci 2008; 9:370–86
2. Kelz MB, Mashour GA: The biology of general anesthesia from paramecium to primate. Curr Biol 2019; 29:R1199–210
3. Hemmings HC Jr, Riegelhaupt PM, Kelz MB, Solt K, Eckenhoff RG, Orser BA, Goldstein PA: Towards a comprehensive understanding of anesthetic mechanisms of action: A decade of discovery. Trends Pharmacol Sci 2019; 40:464–81
4. Kelz MB, Sun Y, Chen J, Cheng Meng Q, Moore JT, Veasey SC, Dixon S, Thornton M, Funato H, Yanagisawa M: An essential role for orexins in emergence from

general anesthesia. Proc Natl Acad Sci U S A 2008; 105:1309–14
5. Wang TX, Xiong B, Xu W, Wei HH, Qu WM, Hong ZY, Huang ZL: Activation of parabrachial nucleus glutamatergic neurons accelerates reanimation from sevoflurane anesthesia in mice. Anesthesiology 2019; 130:106–18
6. Yin L, Li L, Deng J, Wang D, Guo Y, Zhang X, Li H, Zhao S, Zhong H, Dong H: Optogenetic/chemogenetic activation of GABAergic neurons in the ventral tegmental area facilitates general anesthesia via projections to the lateral hypothalamus in mice. Front Neural Circuits 2019; 13:73
7. Vazey EM, Aston-Jones G: Designer receptor manipulations reveal a role of the locus coeruleus noradrenergic system in isoflurane general anesthesia. Proc Natl Acad Sci U S A 2014; 111:3859–64
8. Hu FY, Hanna GM, Han W, Mardini F, Thomas SA, Wyner AJ, Kelz MB: Hypnotic hypersensitivity to volatile anesthetics and dexmedetomidine in dopamine β-hydroxylase knockout mice. Anesthesiology 2012; 117:1006–17
9. Luo T, Leung LS: Involvement of tuberomamillary histaminergic neurons in isoflurane anesthesia. Anesthesiology 2011; 115:36–43
10. Taylor NE, Van Dort CJ, Kenny JD, Pei J, Guidera JA, Vlasov KY, Lee JT, Boyden ES, Brown EN, Solt K: Optogenetic activation of dopamine neurons in the ventral tegmental area induces reanimation from general anesthesia. Proc Natl Acad Sci U S A 2016; 113:12826–31
11. Solt K, Van Dort CJ, Chemali JJ, Taylor NE, Kenny JD, Brown EN: Electrical stimulation of the ventral tegmental area induces reanimation from general anesthesia. Anesthesiology 2014; 121:311–9
12. Luo T, Leung LS: Basal forebrain histaminergic transmission modulates electroencephalographic activity and emergence from isoflurane anesthesia. Anesthesiology 2009; 111:725–33
13. Moore JT, Chen J, Han B, Meng QC, Veasey SC, Beck SG, Kelz MB: Direct activation of sleep-promoting VLPO neurons by volatile anesthetics contributes to anesthetic hypnosis. Curr Biol 2012; 22:2008–16
14. Gelegen C, Miracca G, Ran MZ, Harding EC, Ye Z, Yu X, Tossell K, Houston CM, Yustos R, Hawkins ED, Vyssotski AL, Dong HL, Wisden W, Franks NP: Excitatory pathways from the lateral habenula enable propofol-induced sedation. Curr Biol 2018; 28:580–7.e5
15. Ren S, Wang Y, Yue F, Cheng X, Dang R, Qiao Q, Sun X, Li X, Jiang Q, Yao J, Qin H, Wang G, Liao X, Gao D, Xia J, Zhang J, Hu B, Yan J, Wang Y, Xu M, Han Y, Tang X, Chen X, He C, Hu Z: The paraventricular thalamus is a critical thalamic area for wakefulness. Science 2018; 362:429–34
16. Liang SH, Yin JB, Sun Y, Bai Y, Zhou KX, Zhao WJ, Wang W, Dong YL, Li YQ: Collateral projections from the lateral parabrachial nucleus to the paraventricular thalamic nucleus and the central amygdaloid nucleus in the rat. Neurosci Lett 2016; 629:245–50
17. Otake K, Ruggiero DA, Nakamura Y: Adrenergic innervation of forebrain neurons that project to the paraventricular thalamic nucleus in the rat. Brain Res 1995; 697:17–26
18. Hsu DT, Price JL: Paraventricular thalamic nucleus: Subcortical connections and innervation by serotonin, orexin, and corticotropin-releasing hormone in macaque monkeys. J Comp Neurol 2009; 512:825–48
19. Lee JS, Lee EY, Lee HS: Hypothalamic, feeding/arousal-related peptidergic projections to the paraventricular thalamic nucleus in the rat. Brain Res 2015; 1598:97–113
20. Otis JM, Namboodiri VM, Matan AM, Voets ES, Mohorn EP, Kosyk O, McHenry JA, Robinson JE, Resendez SL, Rossi MA, Stuber GD: Prefrontal cortex output circuits guide reward seeking through divergent cue encoding. Nature 2017; 543:103–7
21. Li S, Kirouac GJ: Projections from the paraventricular nucleus of the thalamus to the forebrain, with special emphasis on the extended amygdala. J Comp Neurol 2008; 506:263–87
22. Crone JS, Lutkenhoff ES, Bio BJ, Laureys S, Monti MM: Testing proposed neuronal models of effective connectivity within the cortico-basal ganglia-thalamo-cortical loop during loss of consciousness. Cereb Cortex 2017; 27:2727–38
23. Lebow MA, Chen A: Overshadowed by the amygdala: The bed nucleus of the stria terminalis emerges as key to psychiatric disorders. Mol Psychiatry 2016; 21:450–63
24. Kodani S, Soya S, Sakurai T: Excitation of GABAergic neurons in the bed nucleus of the stria terminalis triggers immediate transition from non-rapid eye movement sleep to wakefulness in mice. J Neurosci 2017; 37:7164–76
25. Hua R, Wang X, Chen X, Wang X, Huang P, Li P, Mei W, Li H: Calretinin neurons in the midline thalamus modulate starvation-induced arousal. Curr Biol 2018; 28:3948–59.e4
26. Yang Y, Liu DQ, Huang W, Deng J, Sun Y, Zuo Y, Poo MM: Selective synaptic remodeling of amygdalocortical connections associated with fear memory. Nat Neurosci 2016; 19:1348–55
27. Sun Y, Chen J, Pruckmayr G, Baumgardner JE, Eckmann DM, Eckenhoff RG, Kelz MB: High throughput modular chambers for rapid evaluation of anesthetic sensitivity. BMC Anesthesiol 2006; 6:13
28. Bao WW, Xu W, Pan GJ, Wang TX, Han Y, Qu WM, Li WX, Huang ZL: Nucleus accumbens neurons expressing dopamine D1 receptors modulate states

of consciousness in sevoflurane anesthesia. Curr Biol 2021; 31:1893–902.e5
29. Du H, Deng W, Aimone JB, Ge M, Parylak S, Walch K, Zhang W, Cook J, Song H, Wang L, Gage FH, Mu Y: Dopaminergic inputs in the dentate gyrus direct the choice of memory encoding. Proc Natl Acad Sci U S A 2016; 113:E5501–10
30. Arena A, Lamanna J, Gemma M, Ripamonti M, Ravasio G, Zimarino V, De Vitis A, Beretta L, Malgaroli A: Linear transformation of the encoding mechanism for light intensity underlies the paradoxical enhancement of cortical visual responses by sevoflurane. J Physiol 2017; 595:321–39
31. Chemali JJ, Wong KF, Solt K, Brown EN: A state-space model of the burst suppression ratio. Annu Int Conf IEEE Eng Med Biol Soc 2011; 2011:1431–4
32. McCarren HS, Moore JT, Kelz MB: Assessing changes in volatile general anesthetic sensitivity of mice after local or systemic pharmacological intervention. J Vis Exp 2013; 80: e51079
33. Liang SH, Zhao WJ, Yin JB, Chen YB, Li JN, Feng B, Lu YC, Wang J, Dong YL, Li YQ: A neural circuit from thalamic paraventricular nucleus to central amygdala for the facilitation of neuropathic pain. J Neurosci 2020; 40:7837–54
34. Baker R, Gent TC, Yang Q, Parker S, Vyssotski AL, Wisden W, Brickley SG, Franks NP: Altered activity in the central medial thalamus precedes changes in the neocortex during transitions into both sleep and propofol anesthesia. J Neurosci 2014; 34:13326–35
35. Kundu B, Brock AA, Englot DJ, Butson CR, Rolston JD: Deep brain stimulation for the treatment of disorders of consciousness and cognition in traumatic brain injury patients: A review. Neurosurg Focus 2018; 45:E14
36. Alkire MT, McReynolds JR, Hahn EL, Trivedi AN: Thalamic microinjection of nicotine reverses sevoflurane-induced loss of righting reflex in the rat. Anesthesiology 2007; 107:264–72
37. Voss LJ, García PS, Hentschke H, Banks MI: Understanding the effects of general anesthetics on cortical network activity using *ex vivo* preparations. Anesthesiology 2019; 130:1049–63
38. Akeju O, Loggia ML, Catana C, Pavone KJ, Vazquez R, Rhee J, Contreras Ramirez V, Chonde DB, Izquierdo-Garcia D, Arabasz G, Hsu S, Habeeb K, Hooker JM, Napadow V, Brown EN, Purdon PL: Disruption of thalamic functional connectivity is a neural correlate of dexmedetomidine-induced unconsciousness. Elife 2014; 3:e04499
39. Ao Y, Yang B, Zhang C, Li S, Xu H: Application of quinpirole in the paraventricular thalamus facilitates emergence from isoflurane anesthesia in mice. Brain Behav 2021; 11:e01903
40. Mashour GA, Avidan MS: Black swans: Challenging the relationship of anaesthetic-induced unconsciousness and electroencephalographic oscillations in the frontal cortex. Br J Anaesth 2017; 119:563–5
41. Lee M, Sanders RD, Yeom SK, Won DO, Seo KS, Kim HJ, Tononi G, Lee SW: Network properties in transitions of consciousness during propofol-induced sedation. Sci Rep 2017; 7:16791
42. Brown RE, Basheer R, McKenna JT, Strecker RE, McCarley RW: Control of sleep and wakefulness. Physiol Rev 2012; 92:1087–187
43. Valle AC, Timo-Iaria C, Fraga JL, Sameshima K, Yamashita R: Theta waves and behavioral manifestations of alertness and dreaming activity in the rat. Braz J Med Biol Res 1992; 25:745–9
44. Luo YJ, Li YD, Wang L, Yang SR, Yuan XS, Wang J, Cherasse Y, Lazarus M, Chen JF, Qu WM, Huang ZL: Nucleus accumbens controls wakefulness by a subpopulation of neurons expressing dopamine D1 receptors. Nat Commun 2018; 9:1576
45. Amzica F: What does burst suppression really mean? Epilepsy Behav 2015; 49:234–7
46. Ranft A, Golkowski D, Kiel T, Riedl V, Kohl P, Rohrer G, Pientka J, Berger S, Thul A, Maurer M, Preibisch C, Zimmer C, Mashour GA, Kochs EF, Jordan D, Ilg R: Neural correlates of sevoflurane-induced unconsciousness identified by simultaneous functional magnetic resonance imaging and electroencephalography. Anesthesiology 2016; 125:861–72
47. Lukatch HS, Kiddoo CE, Maciver MB: Anesthetic-induced burst suppression EEG activity requires glutamate-mediated excitatory synaptic transmission. Cereb Cortex 2005; 15:1322–31
48. García PS, Kreuzer M, Hight D, Sleigh JW: Effects of noxious stimulation on the electroencephalogram during general anaesthesia: A narrative review and approach to analgesic titration. Br J Anaesth 2021; 126:445–57
49. Kaada BR, Thomas F, Alnaes E, Wester K: EEG synchronization induced by high frequency midbrain reticular stimulation in anesthetized cats. Electroencephalogr Clin Neurophysiol 1967; 22:220–30
50. Kim D, Kim HJ, Ahn S: Anesthetics mechanisms: A review of putative target proteins at the cellular and molecular level. Curr Drug Targets 2018; 19:1333–43

ANESTHESIOLOGY

Extracorporeal Membrane Oxygenation for Respiratory Failure Related to COVID-19: A Nationwide Cohort Study

Nicolas Nesseler, M.D., Ph.D., Guillaume Fadel, M.D., Alexandre Mansour, M.D., Marylou Para, M.D., Pierre-Emmanuel Falcoz, M.D., Ph.D., Nicolas Mongardon, M.D., Ph.D., Alizée Porto, M.D., Astrid Bertier, M.D., Bruno Levy, M.D., Ph.D., Cyril Cadoz, M.D., Pierre-Grégoire Guinot, M.D., Ph.D., Olivier Fouquet, M.D., Ph.D., Jean-Luc Fellahi, M.D., Ph.D., Alexandre Ouattara, M.D., Ph.D., Julien Guihaire, M.D., Ph.D., Vito-Giovanni Ruggieri, M.D., Ph.D., Philippe Gaudard, M.D., Ph.D., François Labaste, M.D., Ph.D., Thomas Clavier, M.D., Kais Brini, M.D., Nicolas Allou, M.D., Corentin Lacroix, M.D., Juliette Chommeloux, M.D., Guillaume Lebreton, M.D., Ph.D., Michael A. Matthay, M.D., Ph.D., Sophie Provenchere, M.D., Ph.D., Erwan Flécher, M.D., Ph.D., André Vincentelli, M.D., Ph.D.; for the ECMOSARS Investigators*

ANESTHESIOLOGY 2022; 136:732–48

EDITOR'S PERSPECTIVE

What We Already Know about This Topic

- Venovenous extracorporeal membrane oxygenation is increasingly used for managing severe respiratory failure; however, the characteristics, management, and patient outcomes continue to be determined
- Determining factors associated with in-hospital mortality for both COVID-19 and non–COVID-19 patients are important factors to consider in patient management

What This Article Tells Us That Is New

- In this investigation, most patients were cannulated by a mobile extracorporeal membrane oxygenation unit without a negative impact on mortality
- Based on this report, venovenous extracorporeal membrane oxygenation support should be considered within the first week of mechanical ventilation initiation for optimal outcomes

ABSTRACT

Background: Despite expanding use, knowledge on extracorporeal membrane oxygenation support during the COVID-19 pandemic remains limited. The objective was to report characteristics, management, and outcomes of patients receiving extracorporeal membrane oxygenation with a diagnosis of COVID-19 in France and to identify pre-extracorporeal membrane oxygenation factors associated with in-hospital mortality. A hypothesis of similar mortality rates and risk factors for COVID-19 and non–COVID-19 patients on venovenous extracorporeal membrane oxygenation was made.

Methods: The Extracorporeal Membrane Oxygenation for Respiratory Failure and/or Heart failure related to Severe Acute Respiratory Syndrome-Coronavirus 2 (ECMOSARS) registry included COVID-19 patients supported by extracorporeal membrane oxygenation in France. This study analyzed patients included in this registry up to October 25, 2020, and supported by venovenous extracorporeal membrane oxygenation for respiratory failure with a minimum follow-up of 28 days after cannulation. The primary outcome was in-hospital mortality. Risk factors for in-hospital mortality were analyzed.

Results: Among 494 extracorporeal membrane oxygenation patients included in the registry, 429 were initially supported by venovenous extracorporeal membrane oxygenation and followed for at least 28 days. The median (interquartile range) age was 54 yr (46 to 60 yr), and 338 of 429 (79%) were men. Management before extracorporeal membrane oxygenation cannulation included prone positioning for 411 of 429 (96%), neuromuscular blockage for 419 of 427 (98%), and NO for 161 of 401 (40%). A total of 192 of 429 (45%) patients were cannulated by a mobile extracorporeal membrane oxygenation unit. In-hospital mortality was 219 of 429 (51%), with a median follow-up of 49 days (33 to 70 days). Among pre-extracorporeal membrane oxygenation modifiable exposure variables, neuromuscular blockage use (hazard ratio, 0.286; 95% CI, 0.101 to 0.81) and duration of ventilation (more than 7 days compared to less than 2 days; hazard ratio, 1.74; 95% CI, 1.07 to 2.83) were independently associated with in-hospital mortality. Both age (per 10-yr increase; hazard ratio, 1.27; 95% CI, 1.07 to 1.50) and total bilirubin at cannulation (6.0 mg/dl or more compared to less than 1.2 mg/dl; hazard ratio, 2.65; 95% CI, 1.09 to 6.5) were confounders significantly associated with in-hospital mortality.

Conclusions: In-hospital mortality was higher than recently reported, but nearly half of the patients survived. A high proportion of patients were cannulated by a mobile extracorporeal membrane oxygenation unit. Several factors associated with mortality were identified. Venovenous extracorporeal membrane oxygenation support should be considered early within the first week of mechanical ventilation initiation.

(ANESTHESIOLOGY 2022; 136:732–48)

Early reports of severe manifestations of COVID-19 such as acute respiratory distress syndrome (ARDS) and acute myocardial injury have suggested a possible role for extracorporeal membrane oxygenation (ECMO) support.[1] Recent experience during the influenza A (H1N1)

This article has been selected for the Anesthesiology CME Program. Learning objectives and disclosure and ordering information can be found in the CME section at the front of this issue. This article is featured in "This Month in Anesthesiology," page A1. Supplemental Digital Content is available for this article. Direct URL citations appear in the printed text and are available in both the HTML and PDF versions of this article. Links to the digital files are provided in the HTML text of this article on the Journal's Web site (www.anesthesiology.org). This article has a visual abstract available in the online version.

Submitted for publication May 26, 2021. Accepted for publication February 4, 2022. Published online first on March 29, 2022.

pandemic demonstrated the value of ECMO support for patients with severe ARDS related to influenza.[2–6] Additionally, a recent meta-analysis of patients from two major randomized controlled trials on ECMO support in severe ARDS patients showed a significant benefit of the technique for improving both morbidity and mortality.[7–9]

Several early retrospective case series showed encouraging results of ECMO support in COVID-19–related respiratory failure.[10–13] However, these case series were limited in sample size (fewer than 90 patients) and restricted to few centers. Consequently, the international report from the Extracorporeal Life Support Organization (Ann Arbor, Michigan) registry, gathering 1,035 ECMO patients from 213 centers in 36 countries, was an important landmark. The study showed an estimated in-hospital mortality of less than 40% for critically ill adults with COVID-19 treated with ECMO in a collection of self-selected and experienced centers worldwide.[14] Recently, a similar mortality rate was reported in a multicenter cohort study of 190 critically ill adults with

Nicolas Nesseler, M.D., Ph.D.: Department of Anesthesia and Critical Care, Pontchaillou, University Hospital of Rennes, France; University of Rennes, University Hospital of Rennes, National Institute of Health and Medical Research, Center of Clinical Investigation of Rennes 1414, Rennes, France; University of Rennes, University Hospital of Rennes, National Research Institute for Agriculture, National Institute of Health and Medical Research, Institute of Nutrition, Metabolism, and Cancer, Mixed Research Unit_1341, Mixed Research Unit_1241, Rennes, France.

Guillaume Fadel, M.D.: Sorbonne University, National Institute of Health and Medical Research, Mixed Research Unit_1166-ICAN, Institute of Cardiometabolism and Nutrition, Paris, France; Department of Thoracic and Cardiovascular, Cardiology Institute, Public Assistance-Hospitals of Paris, Sorbonne University, Pitié-Salpétrière Hospital, Paris, France.

Alexandre Mansour, M.D.: Department of Anesthesia and Critical Care, Pontchaillou, University Hospital of Rennes, Rennes, France; University of Rennes, University Hospital of Rennes, National Institute of Health and Medical Research, Center of Clinical Investigation of Rennes 1414, Rennes, France.

Marylou Para, M.D.: Department of Cardiovascular Surgery and Transplantation, Bichat Hospital, Public Assistance-Hospitals of Paris, Paris, France; University of Paris, Mixed Research Unit_1148, Laboratory of Vascular Translational Science, Paris, France.

Pierre-Emmanuel Falcoz, M.D., Ph.D.: National Institute of Health and Medical Research, Mixed Research Unit_1260, Regenerative Nanomedicine, Translational Medicine Federation, Strasbourg, France; University of Strasbourg, Pharmacy and Medical School, Strasbourg, France; University Hospital of Strasbourg, Thoracic Surgery Department, New Hospital Civil, Strasbourg, France.

Nicolas Mongardon, M.D., Ph.D.: Department of Anesthesia and Critical Care, Medical-University Department, Surgery, Anesthesiology, Surgical Intensive Care Units, University Hospital Department Ageing Thorax-Vessels-Blood, Public Assistance-Hospitals of Paris, Henri Mondor University Hospitals, Créteil, France; University of East Paris Créteil, School of Medicine, Créteil, France; U955-Mondor Institute of Biomedical Research, Equipe 03, Pharmacology and Technologies for Cardiovascular Diseases, National Institute of Health and Medical Research, University of East Paris Créteil, National Veterinary School of Alfort, Maisons-Alfort, France.

Alizée Porto, M.D.: Department of Cardiac Surgery, Timone Hospital, Marseille Public University Hospital System, 13005, Marseille, France.

Astrid Bertier, M.D.: Intensive Care Unit, Bicêtre Hospital, Public Assistance-Hospitals of Paris, Paris, France.

Bruno Levy, M.D., Ph.D.: Intensive Care Unit, CHRU Nancy, Pôle Cardio-Médico-Chirurgical, Vandœuvre-lès-Nancy, France; National Institute of Health and Medical Research U1116, Faculty of Medicine, Vandoeuvre-lès-Nancy, France; University of Lorraine, Nancy, France.

Cyril Cadoz, M.D.: Polyvalent Intensive Care Unit, Mercy Hospital, Regional Hospital, Metz-Thionville, France.

Pierre-Grégoire Guinot, M.D., Ph.D.: Department of Anesthesiology and Critical Care Medicine, Dijon University Hospital, Dijon, France.

Olivier Fouquet, M.D., Ph.D.: Department of Thoracic and Cardiovascular Surgery, University Hospital, Angers, France; Mitochondrial and Cardiovascular Pathophysiology Institute, French National Centre for Scientific Research, Mixed Research Unit_6214, National Institute of Health and Medical Research U1083, University of Angers, Angers, France.

Jean-Luc Fellahi, M.D., Ph.D.: Department of Anesthesia and Critical Care, Louis Pradel Hospital, University Hospital of Lyon, Lyon, France; CarMeN Laboratory, National Institute of Health and Medical Research, Mixed Research Unit_1060, Claude Bernard Lyon University, Lyon, France.

Alexandre Ouattara, M.D., Ph.D.: University Hospital of Bordeaux, Department of Anesthesia and Critical Care, Magellan Medico-Surgical Center, Bordeaux, France; National Institute of Health and Medical Research, Mixed Research Unit 1034, Biology of Cardiovascular Diseases, Pessac, France.

Julien Guihaire, M.D., Ph.D.: Department of Cardiac Surgery, National Institute of Health and Medical Research, Mixed Research Unit_999, Pulmonary Hypertension: Pathophysiology and Novel Therapies, Marie Lannelongue Hospital, Paris Saint-Joseph Hospital Group, University of Paris-Saclay School of Medicine, Le Plessis Robinson, France.

Vito-Giovanni Ruggieri, M.D., Ph.D.: Division of Cardiothoracic and Vascular Surgery, Robert Debré University Hospital, University of Reims Champagne-Ardenne, Reims, France.

Philippe Gaudard, M.D., Ph.D.: Department of Anesthesia and Critical Care, PhyMedExp, Montpellier University, National Institute of Health and Medical Research, French National Centre for Scientific Research, University Hospital of Montpellier, Montpellier, France.

François Labaste, M.D., Ph.D.: Anesthesiology and Intensive Care Department, University Hospital of Toulouse, Toulouse, France; Metabolic and Cardiovascular Diseases Institute, National Institute of Health and Medical Research U1048, University of Toulouse, Paul Sabatier University, Toulouse, France.

Thomas Clavier, M.D.: Department of Anesthesiology, Critical Care and Perioperative Medicine, University Hospital of Rouen, Rouen, France.

Kais Brini, M.D.: Polyvalent and Cardiac Intensive Care Unit, Montsouris Mutualist Institute, Paris, France.

Nicolas Allou, M.D.: Polyvalent Intensive Care Unit, Félix Guyon-Saint-Denis University Hospital, La Réunion, Saint Denis, France.

Corentin Lacroix, M.D.: Department of Cardiothoracic Surgery, University Hospital of Poitiers, Poitiers, France.

Juliette Chommeloux, M.D.: Sorbonne University, National Institute of Health and Medical Research, Mixed Research Unit_1166-ICAN, Institute of Cardiometabolism and Nutrition, Paris, France; Intensive Care Unit, Cardiology Unit, Public Assistance-Hospitals of Paris, Sorbonne University, La Pitié-Salpêtrière Hospital, Paris, France.

Guillaume Lebreton, M.D., Ph.D.: Sorbonne Université, University, National Institute of Health and Medical Research, Mixed Research Unit_1166-ICAN, Institute of Cardiometabolism and Nutrition, Paris, France; Department of Thoracic and Cardiovascular Surgery, Cardiology Institute, Public Assistance-Hospitals of Paris, Sorbonne University, La Pitié-Salpêtrière Hospital, Paris, France.

Michael A. Matthay, M.D., Ph.D.: Departments of Medicine and Anesthesia, Cardiovascular Research Institute, University of California San Francisco, San Francisco, California.

Sophie Provenchere, M.D., Ph.D.: University of Paris, Department of Anesthesiology and Intensive Care, Public Assistance-Hospitals of Paris, Bichat-Claude Bernard Hospital, Paris, France; Clinical Investigation Center 1425, Public Assistance-Hospitals of Paris, National Institute of Health and Medical Research, Paris, France.

Erwan Flécher, M.D., Ph.D.: Department of Thoracic and Cardiovascular Surgery, Pontchaillou University Hospital, University of Rennes 1, Signal and Image Treatment Laboratory, National Institute of Health and Medical Research U1099, Rennes, France.

André Vincentelli, M.D., Ph.D.: Department of Cardiac Surgery, University Hospital of Lille, Lille, France.

*Members of the ECMOSARS Investigators are listed in the appendix.

COVID-19 who received ECMO at 35 sites across the United States.[15]

In France, 485 ECMO consoles are available in 103 academic or nonacademic, public, or private centers due to the wide interest in the technique in the country. During the first wave of the pandemic, a central system was established to coordinate national ECMO resources in France. Regional coordinators met weekly to check the national availability of consoles and circuits. Specific recommendations and algorithms were issued on ECMO indications and organization in the context of the outbreak (https://www.iledefrance.ars.sante.fr/system/files/2020-12/038_ARSIdF-CRAPS_2020-12-02_Doctrine_ECMO.pdf).[16] Collecting data on this initiative is essential to evaluate the results of our organization, to inform clinicians, and to adapt our response to the future developments of the outbreak. Therefore, the goals of our study were (1) to report characteristics, management, and outcomes of patients receiving ECMO with a diagnosis of COVID-19 in France and (2) to identify potentially modifiable variables associated with in-hospital mortality. We hypothesized that the mortality rate and risk factors would be similar for COVID-19 and non–COVID-19 patients on venovenous ECMO.

Materials and Methods

The ECMOSARS registry was launched in April 2020 (ClinicalTrials.gov Identifier: NCT04397588, Extracorporeal Membrane Oxygenation for Respiratory Failure and/or Heart failure related to Severe Acute Respiratory Syndrome-Coronavirus 2 [ECMOSARS] registry, principal investigators: Nicolas Nesseler and André Vincentelli, date of registration: May 21, 2020) and is currently still recruiting. The registry includes 47 centers, academic or nonacademic, which represent 77% of the ECMO consoles available in France. The registry has been endorsed by the French Society of Thoracic and Cardiovascular (Société Française de Chirurgie Thoracique et Cardio-Vasculaire [SFCTCV], Paris, France), the French Society of Thoracic and Cardiovascular Critical Care and Anesthesia (Anesthésie-Réanimation Coeur-Thorax-Vaisseaux [ARCOTHOVA], Paris, France), and the French Society of Anesthesiology and Critical Care Medicine (Société Française d'Anesthésie-Réanimation [SFAR], Paris, France) research network.

The data were collected by research assistants using an electronic case report form from each patient's medical record. Automatic checks were generated for missing or incoherent data, and additional consistency tests were performed by data managers. The nationwide objective of our registry implied the collection of all available data of ECMO patients in France, including data for some patients already published in retrospective studies or case series.[12,14,17] Two studies focused on a specific French area (*e.g.*, the city of Strasbourg or the Greater Paris area), and one study included only a fraction of French patients in an international cohort, which involved only self-selected and experienced centers.

The registry has been approved by the University Hospital of Rennes ethics committee (approval No. 20.43). According to French legislation, written consent is waived because of the study's observational design that does not imply any modification of existing diagnostic or therapeutic strategies. After the information was provided, only non-opposition of patients or their legal representative was obtained for use of the data.

ECMOSARS Registry Inclusion Criteria

All patients, adults or children, tested positive by reverse transcription–polymerase chain reaction for SARS-CoV2 (nasopharyngeal swabs, sputum, endotracheal aspiration, bronchoalveolar lavage, or stool sample) and/or with a diagnosis of COVID-19 made on chest computed tomography findings and supported by venovenous, venoarterial, or venoarterio-venous ECMO can be included in the registry. Patients or proxies who refused consent were excluded from the study, as were legally protected adults.

Data Collection

The data were collected prospectively in the ECMOSARS registry, except for patients whose ECMO was implanted before April 21, 2020. Those data were collected retrospectively. Collected data included patient characteristics and comorbidities, management of COVID-related ARDS before ECMO cannulation, patient characteristics at ECMO cannulation and the day after, management, complications, and patient outcomes on ECMO (see Supplemental Digital Content 1, table S1, http://links.lww.com/ALN/C809, for the definition of the main variables).

Study Population

For the current study, we analyzed all patients included in the registry up to October 25, 2020, initially supported by venovenous ECMO for respiratory failure and with a minimum follow-up of 28 days after ECMO cannulation for alive patients.

Outcomes

Our primary outcome was in-hospital mortality. Secondary outcomes were mortality at day 28, mortality at day 90, ECMO-free days, and intensive care unit (ICU)–free days to day 28. ECMO-free days or ICU-free days are composite outcomes that combine survival and ECMO support duration or survival and ICU length of stay. The numbers of ECMO-free days or ICU-free days were calculated as 28 minus the number of days on ECMO or in the ICU during the first 28 days after ECMO cannulation. Patients who died were assigned the worst possible outcome of 0 ECMO-free days or ICU-free days.

Statistical Analysis

Patient characteristics are expressed as number and percentage for categorical variables and median with interquartile

range for continuous variables. For bivariate comparison between deceased and alive patients, a chi-square test or a Fisher exact test was used for categorical variables, and an independent *t* test or a Wilcoxon rank sum test was used for continuous variables. Blood gases values and ventilator settings before and after ECMO cannulation were compared using a repeated measures ANOVA model. The ventilatory ratio was defined as [minute ventilation (ml/min) × $Paco_2$ (mmHg)]/(predicted body weight × 100 × 37.5).[18]

A statistical analysis plan was made before accessing the data. No *a priori* statistical power calculation was conducted. Regarding the primary outcome, no minimum clinically meaningful hazard ratio was defined before data access. In accordance with reviewers' recommendations, modeling and variable selection strategies were modified and are thus considered *post hoc* analyses. Only pre-ECMO variables were included in these analyses to prevent competing risk bias.

A directed acyclic graph was used to describe the associations between pre-ECMO modifiable exposure variables, patient-related confounders, pre-ECMO hospitalization-related confounders, and in-hospital mortality using DAGitty software (Supplemental Digital Content 1, fig. S1, http://links.lww.com/ALN/C809).[19] No variables were analyzed as effect modifiers. Pre-ECMO modifiable exposure variables comprised anticoagulation, antibiotic therapy, antiviral therapy, noninvasive ventilation, selective digestive decontamination, neuromuscular blocking agents, prone position, high-flow oxygen therapy, cannulation mode, inotropes use, vasopressors use, renal replacement therapy, ECMO cannulation, inhaled NO, positive end-expiratory pressure, tidal volume at cannulation, and ventilation duration before ECMO. The set of pre-ECMO confounders sufficient for adjustment comprised patient-related confounders (sex, age, body mass index, diabetes, chronic obstructive pulmonary disease, chronic respiratory failure, congestive heart failure, chronic kidney disease, malignancy, and previous corticotherapy) and pre-ECMO hospitalization-related confounders (septic shock, total bilirubin at cannulation, pH at cannulation, $Paco_2$ at cannulation, Pao_2/fractional inspired oxygen tension (Fio_2) ratio at cannulation, driving pressure, left ventricular ejection fraction, ventilator-associated pneumonia, and delay from hospitalization to ICU admission).

To estimate hazard ratios between exposure variables and in-hospital mortality, we fitted a univariate and multivariable Cox proportional hazards model including exposure variables and confounders identified using the directed acyclic graph. Four different models were built, for sensitivity analysis (see Supplemental Digital Content 1, table S2, http://links.lww.com/ALN/C809). Model 1 was a univariable Cox model; model 2 was a multivariable Cox model of modifiable exposure variables, adjusted for patient-related confounders; model 3 was a multivariable Cox model of modifiable exposure variables, adjusted for pre-ECMO hospitalization-related confounders; and model 4 was a multivariable Cox model of modifiable exposure variables, fully adjusted for all confounders. Centers were included as a random effect using a γ frailty model. Patients who were still hospitalized were censored at the time of the database lock, and those who were discharged alive were censored at the time of their discharge date. Proportional hazard assumption was assessed using simultaneous time-dependent covariates. To comply with log-linearity assumptions, several continuous variables (body mass index, pH, left ventricular ejection fraction, delay from hospitalization to ICU admission, driving pressure, positive end-expiratory pressure, tidal volume, and ventilation duration before ECMO) were split into categorical variables in accordance with previously published works and guidelines.[8,20–26]

Multiple imputation was used to account for missing values in variables (Supplemental Digital Content 1, table S3, http://links.lww.com/ALN/C809). We used fully specified chained equations in the SAS multiple imputation procedure (SAS Institute, USA). For continuous variables, the regression method was used to impute missing values, and discriminant function methods were used for binary and categorical variables. Passive imputation was used for the derived variables (body mass index, tidal volume, Pao_2/Fio_2 ratio, anticoagulation before ECMO, and malignancy), meaning that each variable needed for the calculation was imputed before the calculation of the derived variable. A total of 50 imputed data sets were created and combined using standard between/within-variance techniques. All tests used a two-tailed hypothesis. Statistical significance was achieved for $P < 0.05$. Statistical analyses were computed with SAS version 9.4 software (SAS Institute, USA).

Results

At the time of the database lock, 38 centers had included 494 patients in the ECMOSARS registry, of whom 462 patients were followed for at least 28 days after ECMO cannulation; 429 patients were initially supported by venovenous ECMO, and 33 were supported by venoarterial ECMO (fig. 1). No patients were initially supported by venoarterio-venous ECMO.

The first venovenous ECMO included in the analysis was implanted on February 25, 2020, and the last venovenous ECMO included in the analysis was implanted on September 17, 2020. Most of the patients (257 [59.9%]) were admitted from another hospital. Venovenous ECMO was cannulated in-hospital by mobile ECMO units in 192 (45%) patients, of whom 79% were transferred subsequently to a referral ECMO center. In total, 13 centers included fewer than 5 patients, 12 centers included between 5 and 10 patients, 5 centers included between 10 and 20 patients, 2 centers included between 20 and 30 patients, 3 centers included between 30 and 40 patients, and 1 center included 124 (26.8%) patients (see Supplemental Digital Content 1, figs. S2 and S3, http://links.lww.com/ALN/C809).

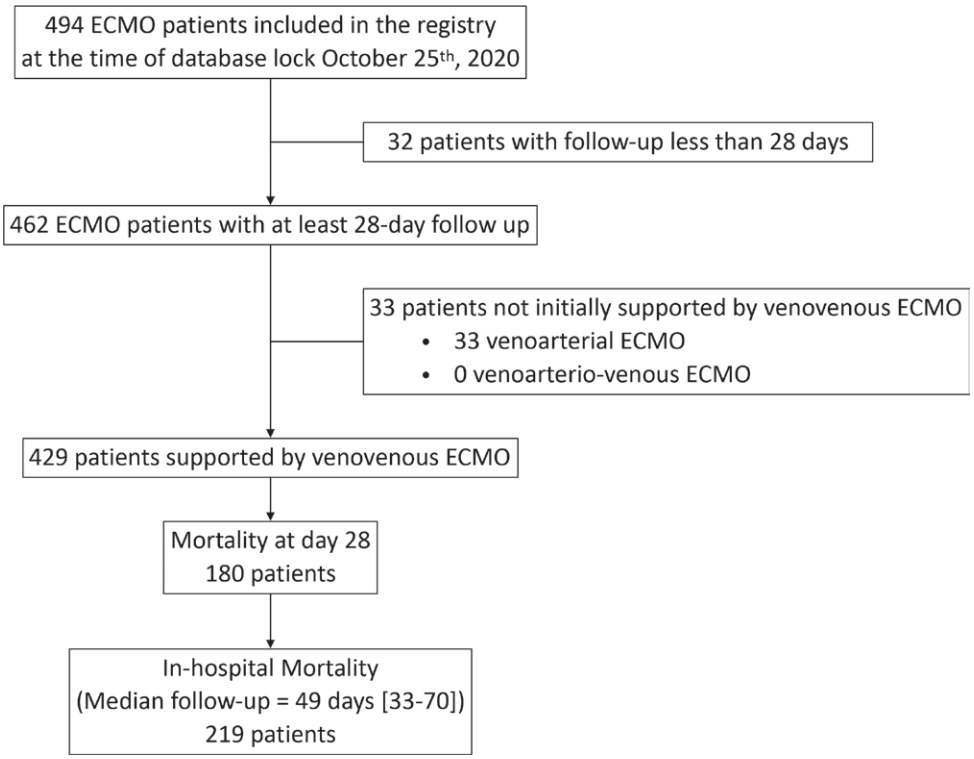

Fig. 1. Flow chart of extracorporeal membrane oxygenation (ECMO) patients included in the study.

Study Population

The median age was 54 (46 to 60) years, 79% of the patients were men, and the median body mass index was 30 (27 to 34). Management before ECMO cannulation included prone positioning (96% [411 of 429]), neuromuscular blocking agent (98% [419 of 427]), and NO (40% [161 of 401]; table 1). Median ventilation duration before ECMO was 5.0 (3.0 to 8.0) days. The median total Sequential Organ Failure Assessment (SOFA) score at cannulation (n = 395) was 9 (8 to 12), and 51% (216 of 422) of the patients had a cardiovascular SOFA score of 3 or higher. The blood lactate level was 1.7 (1.2 to 2.3) mmol/l (n = 366), and 12% (51 of 423) of the patients were on renal replacement therapy. Finally, 99% of the patients met the Berlin ARDS criteria at ECMO cannulation (table 2).

The ventilation settings at the time of the cannulation and the day after the cannulation are shown in table 3. ECMO cannulation was associated with reduced tidal volume, respiratory rate, and F_{IO_2}, as well as lower plateau and driving pressures. A tracheostomy was performed in 21% (90 of 424) of the patients.

Complications on ECMO

Hemorrhagic complications on ECMO were observed in 40% (169 of 426) of the patients, while thrombosis occurred in 37% (159 of 427), and neurologic complications occurred in 11% (47 of 425), including 38 hemorrhagic strokes (table 4). Renal replacement therapy was required in 35%. Bacteremia and cannula site infection were observed in 41% (176 of 428) and 8% (36 of 428) of the patients, respectively. According to cannulation by mobile ECMO units (see Supplemental Digital Content 1, table S4, http://links.lww.com/ALN/C809), cannula site infections were observed significantly more frequently after cannulation by mobile ECMO units, but less cannula site bleeding, although nonsignificant, was observed.

Outcomes

In-hospital mortality was 219 of 429 (51%) with a median follow-up of 49 (33 to 70) days (see Supplemental Digital Content 1, fig. S4, http://links.lww.com/ALN/C809). The extent of missing data across all variables included in the statistical models is described in Supplemental Digital Content 1 (table S3, http://links.lww.com/ALN/C809). Mortality at days 28 and 90 was 42% (180 of 429) and 60% (215 of 357), respectively. At day 28, ventilator-free days (n = 425), ECMO-free days (n = 414), and ICU-free days (n = 412) were 0 (0 to 0), 0 (0 to 14), and 0 (0 to 0) days, respectively. More male patients died, and they were significantly older (table 1). At cannulation, pH was significantly lower, and the $Paco_2$, the ventilatory ratio, and the serum lactate levels were significantly higher in the patients who ultimately died (table 2). Patients who died also had a significantly higher

Table 1. Patient Characteristics before Hospitalization

Characteristics	No.	Full Cohort (n = 429)	Vital Status		*P* Value
			Nonsurvivors (n = 219)	Survivors (n = 210)	
Age	428	54 (46–60)	56 (49–62)	51 (43–58)	< 0.001
< 40 yr		56 (13)	19 of 218 (9)	37 of 210 (18)	
40–49 yr		96 (22)	38 of 218 (17)	58 of 210 (28)	
50–59 yr		160 (37)	85 of 218 (39)	75 of 210 (36)	
60–69 yr		103 (24)	66 of 218 (30)	37 of 210 (18)	
> 70 yr		13 (3)	10 of 218 (5)	3 of 210 (1)	
Sex	429				0.046
Female		91 (21)	38 of 219 (17)	53 of 210 (25)	
Male		338 (79)	181 of 219 (83)	157 of 210 (75)	
Body mass index	413	30 (27–34)	29 (27–34)	31 (28–35)	0.132
< 25 kg of m^2		53 (13)	28 of 206 (14)	25 of 207 (12)	
25–30 kg of m^2		147 (36)	79 of 206 (38)	68 of 207 (33)	
30–35 kg of m^2		121 (29)	61 of 206 (30)	60 of 207 (29)	
35–40 kg of m^2		56 (14)	20 of 206 (10)	36 of 207 (17)	
> 40 kg of m^2		36 (9)	18 of 206 (9)	18 of 207 (9)	
Comorbidities					
Hypertension	429	165 (38)	83 of 219 (38)	82 of 210 (39)	0.807
Diabetes	425	127 (30)	70 of 218 (32)	57 of 207 (28)	0.303
Chronic obstructive pulmonary disease	429	14 (3)	8 of 219 (4)	6 of 210 (3)	0.643
Chronic respiratory failure	429	13 (3)	7 of 219 (3)	6 of 210 (3)	0.838
Congestive heart failure	308	3 (1)	1 of 169 (1)	2 of 169 (1)	0.591
Coronary artery disease	429	21 (5)	10 of 219 (5)	11 of 139 (8)	0.747
Chronic kidney disease	309	11 (4)	7 of 171 (4)	4 of 138 (3)	0.760
Malignancy					
Cancer	306	6 (2)	6 of 168 (4)	0 of 138 (0)	0.034
Hematological malignancy	306	3 (1)	1 of 168 (1)	2 of 138 (1)	0.591
Active smoker	423	17 (4)	10 of 216 (5)	7 of 207 (3)	0.514
Alcohol abuse	301	8 (3)	3 of 166 (2)	5 of 135 (4)	0.474
History of venous thromboembolism	306	11 (4)	7 of 168 (4)	4 of 138 (3)	0.760
Pre-ECMO medications					
Steroids (corticotherapy)	307	17 (6)	10 of 169 (6)	7 of 138 (5)	0.748
Nonsteroidal anti-inflammatory drugs	307	7 (2)	4 of 167 (2)	3 of 140 (2)	> 0.999
Angiotensin-converting enzyme inhibitors	305	29 (10)	14 of 167 (8)	15 of 138 (11)	0.461
Angiotensin receptor blockers	306	44 (14)	23 of 168 (14)	21 of 138 (15)	0.705

The results are presented as n (%) or median (interquartile range).
ECMO, extracorporeal membrane oxygenation.

SOFA score at cannulation, with significantly more patients with a liver (6.0 mg/dl bilirubin or more) and cardiovascular scores of 3 or higher and significantly more patients with renal replacement therapy than patients who survived. While on ECMO, patients who ultimately died experienced significantly more hemorrhagic complications, membrane lung failure, acute kidney injury, and neurologic complications than patients who survived (table 4).

Effect of Pre-ECMO Modifiable Exposure Variables on In-hospital Mortality

Among pre-ECMO modifiable exposure variables, neuromuscular blockage use (hazard ratio, 0.286; 95% CI, 0.101 to 0.81) and duration of ventilation (more than 7 days compared to less than 2 days; hazard ratio, 1.74; 95% CI, 1.07 to 2.83) were independently associated with in-hospital mortality (table 5). Among patient-related and pre-ECMO hospitalization-related confounders, age (per 10-yr increase; hazard ratio, 1.27; 95% CI, 1.07 to 1.50) and total bilirubin at cannulation (6.0 mg/dl or more compared to less than 1.2 mg/dl; hazard ratio, 2.65; 95% CI, 1.09 to 6.5) were both significantly associated with in-hospital mortality. These results remained consistent after sensitivity analysis in two distinct models: (1) modifiable exposure variables and patient-related baseline characteristics and (2) modifiable exposure variables and pre-ECMO hospitalization-related variables (see Supplemental Digital Content 1, table S2, http://links.lww.com/ALN/C809). In the latter model, septic shock (hazard ratio, 1.69; 95% CI, 1.03 to 2.77) at cannulation and pH lower than 7.25 at cannulation (hazard ratio, 1.56; 95% CI, 1.05 to 2.31) were also associated with in-hospital mortality.

Discussion

Our study reports, at a nationwide level, the characteristics, management, and outcomes of COVID-19 patients treated with venovenous ECMO for respiratory failure. We found an in-hospital mortality of 51%, numerically higher

Table 2. Clinical Condition and Management before ECMO

Condition/Management	No.	Full Cohort (n = 429)	Vital Status		*P* Value
			Nonsurvivors (n = 219)	Survivors (n = 210)	
Delay from hospitalization to ICU admission	428	0 (0–0)	0 (0–0)	0 (0–0)	0.622
< 24 h		329 (77)	169 of 218 (78)	160 of 210 (76)	
24–48 h		52 (12)	30 of 218 (14)	22 of 210 (10)	
> 72 h		47 (11)	19 of 218 (9)	28 of 210 (13)	
ECMO cannulation	426				0.141
Referral center		234 (55)	128 of 216 (59)	106 of 210 (50)	
Mobile ECMO unit, no transfer		41 (10)	21 of 216 (10)	20 of 210 (10)	
Mobile ECMO unit, transfer to referral center		151 (35)	67 of 216 (31)	84 of 210 (40)	
ARDS (Berlin criteria) at cannulation	421	417 (99)	210 of 213 (99)	207 of 208 (100)	0.623
Noninvasive ventilation	426	104 (24)	64 of 217 (29)	40 of 209 (19)	0.013
High-flow oxygen therapy	307	125 (41)	74 of 168 (44)	51 of 139 (37)	0.192
Ventilation duration before ECMO	428	5 (3–8)	6 (3–8)	5 (3–7)	0.057
< 2 days		94 (22)	43 of 218 (20)	51 of 210 (24)	
2–7 days		221 (52)	105 of 218 (48)	116 of 210 (55)	
> 7 days		113 (26)	70 of 218 (32)	43 of 210 (20)	
pH at cannulation	408	7.33 (7.25–7.39)	7.31 (7.22–7.37)	7.35 (7.29–7.41)	< 0.001
$Paco_2$ at cannulation, mmHg	406	55 (46–65)	57 (48–68)	54 (45–62)	0.005
Pao_2 of Fio_2 ratio at cannulation, mmHg	404	67 (57–82)	67 (58–84)	67 (57–81)	0.625
PEEP at cannulation, cm H_2O	385	12 (10–14)	12 (10–14)	12 (10–14)	0.747
V_T at cannulation	353	5.9 (5.2–6.3)	5.8 (5.1–6.2)	5.9 (5.3–6.3)	0.244
< 6 ml/kg ideal body weight		216 (61)	113 of 178 (63)	103 of 175 (59)	
6–8 ml/kg ideal body weight		132 (37)	63 of 178 (35)	69 of 175 (39)	
> 8 ml/kg ideal body weight		5 (1)	2 of 178 (1)	3 of 175 (2)	
Respiratory rate at cannulation, breaths/min	348	28 (20–30)	28 (22–30)	28 (20–30)	0.321
Ventilatory ratio*	315	2.2 (1.5–3.0)	2.4 (1.7–3.1)	2.1 (1.5–2.9)	< 0.001
Plateau pressure at cannulation, cm H_2O	331	30 (27–32)	30 (26–33)	30 (27–32)	0.414
Driving pressure at cannulation, cm H_2O	327	17 (14–20)	17 (13–21)	17 (14–20)	0.297
Neuromuscular blocking agents	427	419 (98)	213 of 218 (98)	206 of 209 (99)	0.725
Prone position	429	411 (96)	207 of 219 (95)	204 of 210 (97)	0.176
Inhaled NO	401	161 (40)	90 of 206 (44)	71 of 195 (36)	0.137
Renal replacement therapy	423	51 (12)	34 of 213 (16)	17 of 210 (8)	0.013
Antiviral therapy	305	179 (59)	96 of 168 (57)	83 of 137 (61)	0.544
Remdesivir		7 (2)	4 of 168 (2)	4 of 137 (3)	> 0.999
Lopinavir/ritonavir		58 (19)	36 of 168 (21)	36 of 137 (26)	0.130
Hydroxychloroquine		102 (33)	52 of 168 (31)	52 of 137 (38)	0.360
Interferon-β		4 (1)	4 of 168 (2)	4 of 137 (3)	0.125
Others		59 (19)	34 of 168 (20)	34 of 137 (25)	0.486
Antibiotic therapy	305	296 (97)	162 of 168 (96)	134 of 137 (98)	0.522
Anticoagulation	294				0.033
No		19 (6)	5 of 161 (3)	14 of 133 (11)	
Curative		139 (47)	77 of 161 (48)	62 of 133 (47)	
Prophylactic		136 (46)	79 of 161 (49)	57 of 133 (43)	
Selective digestive decontamination	304	13 (4)	10 of 166 (6)	3 of 138 (2)	0.099
SOFA score at cannulation	395	9 (8–12)	11 (8–13)	9 (8–12)	0.004
Septic shock	312	35 (11)	25 of 172 (15)	10 of 140 (7)	0.040
Cardiovascular SOFA ≥ 3 at cannulation	422	216 (51)	126 of 215 (59)	90 of 207 (43)	0.002
Left ventricular ejection fraction, %	191	60 (60–65)	60 (55–60)	60 (60–65)	0.722
Vasoactive/inotropic drugs					
Norepinephrine	306	176 (58)	103 of 168 (61)	73 of 138 (53)	0.139
Epinephrine	304	10 (3)	8 of 166 (5)	2 of 138 (1)	0.119
Dobutamine	304	8 (3)	5 of 166 (3)	3 of 137 (2)	0.732
Lactatemia at cannulation, mmol/l	366	1.7 (1.2–2.3)	1.7 (1.3–2.4)	1.6 (1.2–2.1)	0.012
Total bilirubin at cannulation	409				0.023
< 1.2 mg/dl		291 (71)	147 of 207 (71)	144 of 202 (71)	
1.2–1.9 mg/dl		50 (12)	20 of 207 (10)	30 of 202 (15)	
2.0–5.9 mg/dl		57 (14)	30 of 207 (14)	27 of 202 (13)	
≥ 6.0 mg/dl		11 (3)	10 of 207 (5)	1 of 202 (0)	

The results are presented as n (%) or median (interquartile range).

*The ventilatory ratio is defined as [minute ventilation (ml/min) × $Paco_2$ (mmHg)]/(predicted body weight × 100 × 37.5).

ARDS, acute respiratory distress syndrome; ECMO, extracorporeal membrane oxygenation; Fio_2, fractional inspired oxygen tension; ICU, intensive care unit; PEEP, positive end-expiratory pressure; SOFA, Sequential Organ Failure Assessment; V_T, tidal volume.

Table 3. Blood Gases and Ventilator Settings Pre-ECMO the Day of Implantation and the Day after Cannulation

	Nonsurvivors (n = 219)					Survivors (n = 210)				
	Pre-ECMO Day of Cannulation		Post-ECMO Day 1			Pre-ECMO Day of Cannulation		Post-ECMO Day 1		
Blood Gases/Settings	No.	Median (Interquartile Range)	No.	Median (Interquartile Range)	*P* Value	No.	Median (Interquartile Range)	No.	Median (Interquartile Range)	*P* Value
pH	207	7.31 (7.22–7.37)	209	7.40 (7.34–7.45)	0.010	201	7.35 (7.29–7.41)	206	7.42 (7.37–7.47)	< 0.001
Pao_2, mmHg	208	64 (57–77)	209	79 (65–101)	0.001	199	65 (54–73)	206	83 (70–106)	< 0.001
$Paco_2$, mmHg	206	57 (48–68)	206	44 (40–50)	< 0.001	200	54 (45–62)	206	45 (39–50)	< 0.001
Fio_2, %	210	100 (100–100)	210	70 (50–100)	< 0.001	201	100 (100–100)	206	60 (50–80)	< 0.001
Pao_2/Fio_2 ratio, mmHg	208	67 (58–84)	209	116 (90–160)	< 0.001	196	67 (57–81)	204	134 (104–208)	< 0.001
PEEP, cm H_2O	201	12 (10–14)	199	12 (10–14)	0.134	184	12 (10–14)	182	12 (10–14)	0.176
V_T, ml/kg ideal body weight	178	5.8 (5.1–6.2)	178	3.2 (2.2–4.5)	< 0.001	175	5.9 (5.3–6.3)	185	3.5 (2.6–4.5)	< 0.001
Respiratory Rate, breaths/min	183	28 (22–30)	190	16 (12–20)	< 0.001	165	28 (20–30)	184	18 (12–20)	< 0.001
Plateau pressure, cm H_2O	173	30 (26–33)	171	26 (24–28)	< 0.001	158	30 (27–32)	166	25 (23–28)	< 0.001
Driving pressure, cm H_2O	171	17 (13–21)	168	14 (11–16)	< 0.001	156	17 (14–20)	159	12 (11–15)	< 0.001

The results are presented as median (interquartile range). The *P* values are for bivariate analysis between pre- and post-ECMO.

ECMO, extracorporeal membrane oxygenation; Fio_2, fractional inspired oxygen tension; PEEP, positive end-expiratory pressure; V_T, tidal volume.

than that reported in two recent studies of venovenous ECMO use in COVID-19 patients.[14,15] The international Extracorporeal Life Support Organization study reported an estimated cumulative incidence of in-hospital mortality 90 days after ECMO initiation of 37%.[13] The Study of the Treatment and Outcomes in Critically Ill Patients with COVID-19 study reported a 60-day mortality rate of 33% in the United States.[15] Similarly, the ECMO to Rescue Lung Injury in Severe ARDS trial reported a mortality of 35% at 60 days in non–COVID-19 ARDS patients supported by venovenous ECMO.[8]

Several factors may explain the higher mortality rate observed in this study. First, this population was older than the populations in the Extracorporeal Life Support Organization or the Study of the Treatment and Outcomes in Critically Ill Patients with COVID-19 studies (median age, 54 [interquartile range, 46 to 60] yr *vs.* 49 [41 to 57] yr in the Extracorporeal Life Support Organization or 49 [41 to 57] years in the Study of the Treatment and Outcomes in Critically Ill Patients with COVID-19 cohort). Second, this population had more severe ARDS at the time of cannulation. In addition, 99% of the patients in this study met the Berlin criteria for ARDS, compared with only 79% in the Extracorporeal Life Support Organization study.[14] Patients in this study tended to have been mechanically ventilated for longer before ECMO cannulation (median 6 days *vs.* 4 days in the Extracorporeal Life Support Organization and 2 days in the Study of the Treatment and Outcomes in Critically Ill Patients with COVID-19), which is known to be associated with worse outcomes.[24] Our patients were also more likely to have been proned (96% *vs.* 60% in the Extracorporeal Life Support Organization or 71% in the Study of the Treatment and Outcomes in Critically Ill Patients with COVID-19 cohort) and/or paralyzed before ECMO cannulation (98% *vs.* 72% or 78%), both suggesting the use of ECMO later in the disease process. Finally, this study included patients from a wide range of both high- and low-volume centers, reflecting the broad use of ECMO in France during the COVID-19 pandemic.[9]

We found several factors independently associated with in-hospital mortality in our cohort, including older age, liver failure (6 mg/dl bilirubin or more) at ECMO cannulation, and a duration of ventilation before ECMO cannulation of more than 7 days; in contrast, only neuromuscular blocking agent use before ECMO was found as a protective factor. These findings were consistent with previous studies[14,24,27,28] and could be useful to the bedside clinician. First, they emphasize the value of early consideration of ECMO when indicated. This finding is particularly important as it can be easily modifiable at the bedside. In our cohort, 26% of the patients were canulated after 7 days of mechanical ventilation. Thus, the clinicians should be strongly encouraged to consider ECMO within 7 days after mechanical ventilation initiation. Second, these findings emphasize that ECMO support seems less beneficial in the sickest patients, as previously described for non–COVID-19 ARDS patients.[24,27,28] In our cohort, liver failure at cannulation appears to be an especially strong marker of severity, which should alert the clinicians before considering ECMO support. Of course, only a limited number of patients presented liver failure, which underlined that the majority of clinicians are already fully aware of the poor results of ECMO support in the sickest patients. Third, the data from this study again emphasize the comparatively poorer outcomes in older patients who received ECMO for COVID-19. Notably, patients of more than 70 yr of age were excluded from the U.S. Study of

Table 4. Outcomes and Complications on ECMO

Outcomes and Complications	No.	Full Cohort (n = 429)	Vital Status		*P* Value
			Nonsurvivors (n = 219)	Survivors (n = 210)	
Total ECMO duration, days		12 (8–21)	11 (6–21)	13 (8–21)	0.751
ECMO-free days at day 28, days	414	0 (0–14)	0 (0–0)	14 (6–19)	< 0.001
Conversion to venoarterial-venous ECMO	429	9 (2)	8 of 219 (4)	1 of 210 (0)	0.038
Cannulation mode	425				0.823
Femoro-jugular		388 (91)	196 of 217 (90)	192 of 208 (92)	
Femoro-femoral		27 (6)	16 of 217 (7)	11 of 208 (5)	
Bicaval dual lumen		6 (1)	2 of 217 (1)	4 of 208 (2)	
Not specified		4 (1)	3 of 217 (1)	1 of 208 (0)	
Total ventilation duration, days	390	27 (16–41)	18 (12–34)	31 (24–46)	< 0.001
Ventilator-free days at day 28, days	425	0 (0–0)	0 (0–0)	0 (0–4)	< 0.001
Tracheostomy	424	90 (21)	11 of 217 (5)	79 of 207 (38)	< 0.001
Prone position	425	301 (71)	145 of 216 (67)	156 of 209 (75)	0.089
Respiratory ECMO Survival Prediction score	240	1 (0–3)	1 (0–3)	2 (0–4)	< 0.001
Vasoactive/inotropic drugs					
Norepinephrine	304	255 (84)	154 of 167 (92)	101 of 137 (74)	< 0.001
Epinephrine	305	15 (5)	13 of 168 (8)	2 of 137 (1)	0.012
Dobutamine	304	16 (5)	11 of 167 (7)	5 of 137 (4)	0.254
Hemorrhagic complications	426	169 (40)	107 of 217 (49)	62 of 209 (30)	< 0.001
Cannula site bleeding		77 (18)	54 of 107 (50)	23 of 62 (37)	
Gastrointestinal bleeding		26 (6)	20 of 107 (19)	6 of 62 (10)	
Pulmonary hemorrhage		37 (9)	27 of 107 (25)	10 of 62 (16)	
Retroperitoneal bleeding		4 (1)	3 of 107 (3)	1 of 62 (2)	
Massive hemorrhage		20 (5)	15 of 107 (14)	5 of 62 (8)	
Number of packed red blood cells transfused	300	4 (2–8)	6 (3–10)	3 (0–6)	< 0.001
Thrombotic complications	427	159 (37)	84 of 217 (39)	75 of 210 (36)	0.522
Deep vein thrombosis		33 (8)	9 of 84 (11)	24 of 75 (32)	
Pulmonary embolism		48 (11)	28 of 84 (33)	20 of 75 (27)	
Circuit clot		66 (15)	32 of 84 (38)	34 of 75 (45)	
Circuit change		56 (13)	32 of 84 (38)	24 of 75 (32)	
Membrane lung failure		35 (8)	25 of 84 (30)	10 of 75 (13)	
Neurologic complications	425	47 (11)	41 of 216 (19)	6 of 209 (3)	< 0.001
Seizures		2 (0)	2 of 41 (5)	0 of 6 (0)	
Ischemic stroke		5 (1)	3 of 41 (7)	2 of 6 (33)	
Hemorrhagic stroke		38 (9)	35 of 41 (85)	3 of 6 (50)	
Acute limb ischemia	424	4	4 (100)	0 (0)	0.124
Acute mesenteric ischemia	427	4	4 (100)	0 (0)	0.123
Acute kidney injury on ECMO	424	192 (45)	134 of 216 (62)	58 of 208 (28)	< 0.001
Renal replacement therapy		149 (35)	104 of 134 (78)	45 of 58 (78)	
Extracorporeal blood purification device	326	50 (15)	34 of 178 (19)	16 of 148 (11)	0.039
Ventilator-associated pneumonia	426	277 (65)	137 of 219 (63)	140 of 210 (67)	0.405
Timing of ventilator-associated pneumonia	169				0.235
Before ECMO		83 (49)	50 of 94 (53)	33 of 75 (44)	
After ECMO		86 (51)	44 of 94 (47)	42 of 75 (56)	
Infectious complications	428	235 (55)	112 of 218 (51)	123 of 210 (59)	0.135
Bacteremia		176 (41)	87 of 112 (78)	89 of 123 (72)	
Cannula site infection		36 (8)	16 of 112 (14)	20 of 123 (16)	
Infection under ECMO-free days, days*	323	9 (3–21)	7 (2–12)	13 (5–28)	< 0.001
ICU duration, days	411	35 (17–54)	18 (10–34)	34 (26–54)	< 0.001
ICU-free days at day 28, days	412	0 (0–0)	0 (0–0)	0 (0–2)	< 0.001
Hospitalization duration, days	395	35 (17–54)	21 (12–36)	52 (37–71)	< 0.001

The results are presented as n (%) or median (interquartile range).

*Infection under ECMO includes ventilator-associated pneumonia, bacteremia, and cannula site infection.

ECMO, extracorporeal membrane oxygenation; ICU, intensive care unit.

the Treatment and Outcomes in Critically Ill Patients with COVID-19.[15] Finally, the favorable results in patients in this cohort who received neuromuscular blocking agent before ECMO cannulation are in line with previous work[24] but should be interpreted with caution here as the vast majority of patients in our cohort received neuromuscular blocking agent before ECMO. Indeed, the very few patients who did not receive neuromuscular blocking agent before cannulation must be considered outliers whose management may have been out of the standard of care.

Table 5. Pre-ECMO Variables Associated with In-hospital Mortality in Multivariable Analysis

Variables	Hazard Ratio (95% CI)*
Neuromuscular blocking agents†	0.286 (0.101–0.81)
Ventilation duration before ECMO†	
< 2 days	1
2–7 days	1.37 (0.89–2.10)
> 7 days	1.74 (1.07–2.83)
Age (10-yr increase)‡	1.27 (1.07–1.50)
Total bilirubin at implantation‡	
< 1.2 mg/dl	1
1.2–1.9 mg/dl	0.88 (0.51–1.50)
2.0–5.9 mg/dl	1.16 (0.72–1.86)
≥ 6.0 mg/dl	2.65 (1.09–6.4)

*Hazard ratio with 95% CI, based on multivariable Cox model of exposure variables fully adjusted for all confounders, after multiple imputation (see model 4, Supplemental Digital Content 1, table S2, http://links.lww.com/ALN/C809). †Defined as pre-ECMO modifiable exposure variables in the model (see Supplemental Digital Content 1, fig. S1, http://links.lww.com/ALN/C809). ‡Defined as patient-related confounders and pre-ECMO hospitalization-related confounders in the model (see Supplemental Digital Content 1, fig. S1, http://links.lww.com/ALN/C809).

ECMO, extracorporeal membrane oxygenation.

While on ECMO, patients who ultimately died experienced significantly more hemorrhagic complications, neurologic complications (mainly hemorrhagic stroke), membrane lung failure, and acute kidney injury than patients who survived. We report more frequent bleeding complications than in the U.S. Study of the Treatment and Outcomes in Critically Ill Patients with COVID-19 study (28% *vs*. 40%) or in the Extracorporeal Life Support Organization study, including cannula site bleeding (18% *vs*. 7%, respectively), gastrointestinal hemorrhage (6% *vs*. 3%, respectively), and pulmonary hemorrhage (8% *vs*. 4%, respectively). Although our definitions of bleeding events were less restrictive, this might be also related to the contemporaneous publication of French guidelines on anticoagulation in COVID-19 patients, which recommended elevated unfractionated heparin targets in ECMO patients after early reports of prothrombotic state in COVID-19 patients.[29] Of note, the ECMO to Rescue Lung Injury in Severe ARDS trial reported 46% of bleeding leading to transfusion. Similarly, we observed a higher proportion of hemorrhagic stroke (9%) than previously reported (2, 4, and 6% in the ECMO to Rescue Lung Injury in Severe ARDS trial, the U.S. Study of the Treatment and Outcomes in Critically Ill Patients with COVID-19, and the Extracorporeal Life Support Organization studies, respectively).

Membrane lung failures were higher than in the Extracorporeal Life Support Organization study (12% vs. 8%), and the higher proportion in the nonsurvivors might reflect the hypercoagulopathy pattern described in the more severe patients.[30] Interestingly, the proportion of acute kidney injury (AKI) requiring renal replacement therapy (35%) was higher than in the Study of the Treatment and Outcomes in Critically Ill Patients with COVID-19 study (22%) but lower than in the Extracorporeal Life Support Organization study (44%) or the ECMO to Rescue Lung Injury in Severe ARDS trial (52%). Nevertheless, as in in the Study of the Treatment and Outcomes in Critically Ill Patients with COVID-19 study, the proportion of AKI was significantly higher in the nonsurvivors, highlighting how the development of AKI might be a turning point in the trajectories of COVID-19 patients on ECMO.

Critically ill patients with COVID-19 have been found at high risk for hospital-acquired infections.[31] In non-ECMO critically ill patients with COVID-19, ventilator-associated pneumonia was found in 25 to 50%, and bacteremia was found in 15 to 34%.[31,32] However, few data are available in COVID-19 patients on ECMO. We found a high proportion of ventilator-associated pneumonia (51%) and bacteremia while on ECMO (41%). The Study of the Treatment and Outcomes in Critically Ill Patients with COVID-19 study reported 35% of ventilator-associated pneumonia and 18% of other documented infections. A similar proportion of 39% of ventilator-associated pneumonia on ECMO was reported in the ECMO to Rescue Lung Injury in Severe ARDS trial. The discrepancy between our study and other reports remains to be elucidated. One hypothesis might be the difficulty of applying infection control procedures in a context of increased workload and a shortage in healthcare workers related to the pandemic surge. Variations in ventilator-associated pneumonia definition applications and microbiologic sampling methods across ICUs and countries might also explain these differences, and further studies are mandated to explore these questions. In contrast, in our cohort, the cannula site infection proportion (8%) was lower than previously described in non–COVID-19 patients.[8,33]

A high proportion of patients were cannulated by mobile ECMO units in our cohort (45%), similar to the percentage previously reported in the Extracorporeal Life Support Organization study (47%). Cannulation by mobile ECMO unit was not found associated with higher mortality, highlighting the importance of mobile ECMO program to rescue patients hospitalized outside of the referral centers as previously suggested.[34] Of note, cannulation by a mobile ECMO unit was not associated with more cannula site bleeding, but more cannula site infections were observed.

Our study has several strengths. This cohort is one of the largest samples of patients supported by venovenous ECMO for COVID-19–related ARDS published to date. Second, the participating centers represented most of the ECMO sites available in France, giving this study a good representation of the ECMO activity between the end of February and September 2020. Additionally, a central system was established to coordinate national ECMO resources, allowing relocation of consoles and circuits, when needed, in the areas the most affected by the virus. Third, the wide adherence during the pre-ECMO period

to known medical interventions in ARDS patient management, such as protective ventilation, prone positioning, or neuromuscular blocking agent infusions, must be emphasized. These data strengthen the fact that in our cohort, ECMO support was proposed to highly severe patients as a rescue therapy after adequate management. Fourth, the multicenter design enables generalization of the data. Finally, the database quality was regularly assessed by dedicated data managers.

However, there are some limitations. Despite broad representation among French ECMO centers, the cohort did not include all ECMO centers, creating potential selection bias. Within our cohort, a significant proportion (26%) of patients came from a single center in Paris, which is a high-volume ECMO center and is also located in an area that was severely affected by the pandemic. In addition, at the time of the database lock, 34 patients (8%) were still hospitalized, leading to a possible underestimation of the in-hospital mortality. Further, as an observational study relying on patients' medical records, this study might be subject to information bias. There were no specific recommendations on cannulation or management of ECMO, introducing variability in management across the study population. However, because we anticipated regional differences in the burden of the pandemic, as well as expertise disparities between participating centers, centers were included as a random effect using a γ frailty model in the Cox model. Additionally, considering that the vast majority of patients in our cohort received neuromuscular blocking agent before ECMO, we underline that the association found between neuromuscular blocking agent use and survival must be interpreted with caution. Finally, it is worth remembering that our study analyzed only patients already receiving ECMO, and thus the results obtained might not be fully relevant in a general population of severe COVID-19 patients.

In conclusion, this analysis of the ECMOSARS registry provides results and outcomes of COVID-19–related respiratory failure patients supported by venovenous ECMO between February and September 2020 in France. In-hospital mortality was higher than recently reported in a multicenter international cohort, but nearly half of the patients survived. A high proportion of patients were cannulated by mobile ECMO unit without negative impact on mortality. Several factors associated with mortality were identified, which may help to guide future clinical decision-making. In particular, venovenous ECMO support should be considered early, within the first week of mechanical ventilation initiation.

Research Support

Supported by a grant from the University Hospital of Rennes (Appel à Projets CFTR2; Rennes, France) and by a grant from the Société Française de Chirurgie Thoracique et Cardiovasculaire (Paris, France), Bourse Marc Laskar.

Competing Interests

Dr. Mongardon received consultant fees from Amomed (Vienna, Austria). Dr. Gaudard received payment from Abiomed (Aachen, Germany), Air Liquide Santé (Gentilly, France), and Abbot (Chicago, Illinois) and consultancy fees from Amomed. Dr. Matthay received payment for his institution from Roche-Genentech (San Francisco, California), from Citius Pharmaceuticals (Cranford, New Jersey) for consulting for ARDS trial design, from Novartis (Bâle, Switzerland) for consulting for ARDS trial design, and from Johnson & Johnson (New Brunswick, New Jersey) and Pliant Therapeutics (San Francisco, California) for ARDS consultation. The other authors declare no competing interests.

Correspondence

Address correspondence to Dr. Nesseler: Hôpital Pontchaillou, Pôle Anesthésie, SAMU, Urgences, Réanimations, Médecine Interne et Gériatrie, Rue Henri Le Guilloux, 35033 Rennes Cedex 9, France. nicolas.nesseler@chu-rennes.fr.

References

1. Wiersinga WJ, Prescott HC: What is COVID-19? JAMA 2020; 324:816
2. Patroniti N, Zangrillo A, Pappalardo F, Peris A, Cianchi G, Braschi A, Iotti GA, Arcadipane A, Panarello G, Ranieri VM, Terragni P, Antonelli M, Gattinoni L, Oleari F, Pesenti A: The Italian ECMO network experience during the 2009 influenza A(H1N1) pandemic: Preparation for severe respiratory emergency outbreaks. Intensive Care Med 2011; 37:1447–57
3. Australia and New Zealand Extracorporeal Membrane Oxygenation (ANZ ECMO) Influenza Investigators; Davies A, Jones D, Bailey M, Beca J, Bellomo R, Blackwell N, Forrest P, Gattas D, Granger E, Herkes R, Jackson A, McGuinness S, Nair P, Pellegrino V, Pettilä V, Plunkett B, Pye R, Torzillo P, Webb S, Wilson M, Ziegenfuss M. Extracorporeal membrane oxygenation for 2009 influenza A(H1N1) acute respiratory distress syndrome. JAMA 2009; 302:1888–95
4. Noah MA, Peek GJ, Finney SJ, Griffiths MJ, Harrison DA, Grieve R, Sadique MZ, Sekhon JS, McAuley DF, Firmin RK, Harvey C, Cordingley JJ, Price S, Vuylsteke A, Jenkins DP, Noble DW, Bloomfield R, Walsh TS, Perkins GD, Menon D, Taylor BL, Rowan KM: Referral to an extracorporeal membrane oxygenation center and mortality among patients with severe 2009 influenza A(H1N1). JAMA 2011; 306:1659–68

5. Pham T, Combes A, Rozé H, Chevret S, Mercat A, Roch A, Mourvillier B, Ara-Somohano C, Bastien O, Zogheib E, Clavel M, Constan A, Richard J-CM, Brun-Buisson C, Brochard L; REVA Research Network: Extracorporeal membrane oxygenation for pandemic influenza A(H1N1)–induced acute respiratory distress syndrome. Am J Resp Crit Care 2013; 187:276–85
6. Quintel M, Bartlett RH, Grocott MPW, Combes A, Ranieri MV, Baiocchi M, Nava S, Brodie D, Camporota L, Vasques F, Busana M, Marini JJ, Gattinoni L: Extracorporeal membrane oxygenation for respiratory failure. Anesthesiology 2020; 132:1257–76
7. Combes A, Schmidt M, Hodgson CL, Fan E, Ferguson ND, Fraser JF, Jaber S, Pesenti A, Ranieri M, Rowan K, Shekar K, Slutsky AS, Brodie D: Extracorporeal life support for adults with acute respiratory distress syndrome. Intensive Care Med 2020; 46:2464–76
8. Combes A, Hajage D, Capellier G, Demoule A, Lavoué S, Guervilly C, Silva DD, Zafrani L, Tirot P, Veber B, Maury E, Levy B, Cohen Y, Richard C, Kalfon P, Bouadma L, Mehdaoui H, Beduneau G, Lebreton G, Brochard L, Ferguson ND, Fan E, Slutsky AS, Brodie D, Mercat A: Extracorporeal membrane oxygenation for severe acute respiratory distress syndrome. New Engl J Med 2018; 378:1965–75
9. Peek GJ, Mugford M, Tiruvoipati R, Wilson A, Allen E, Thalanany MM, Hibbert CL, Truesdale A, Clemens F, Cooper N, Firmin RK, Elbourne D; CESAR Trial Collaboration: Efficacy and economic assessment of conventional ventilatory support *versus* extracorporeal membrane oxygenation for severe adult respiratory failure (CESAR): A multicentre randomised controlled trial. Lancet 2009; 374:1351–63
10. Schmidt M, Hajage D, Lebreton G, Monsel A, Voiriot G, Levy D, Baron E, Beurton A, Chommeloux J, Meng P, Nemlaghi S, Bay P, Leprince P, Demoule A, Guidet B, Constantin JM, Fartoukh M, Dres M, Combes A; Groupe de Recherche Clinique en REanimation et Soins Intensifs du Patient en Insuffisance Respiratoire aiguE (GRC-RESPIRE) Sorbonne Université; Paris-Sorbonne ECMO-COVID Investigators: Extracorporeal membrane oxygenation for severe acute respiratory distress syndrome associated with COVID-19: A retrospective cohort study. Lancet Respir Med 2020; 8:1121–31
11. Yang X, Cai S, Luo Y, Zhu F, Hu M, Zhao Y, Zheng R, Li X, Hu B, Peng Z: Extracorporeal membrane oxygenation for coronavirus disease 2019–induced acute respiratory distress syndrome: A multicenter descriptive study. Crit Care Med 2020; 48:1289–95
12. Falcoz P-E, Monnier A, Puyraveau M, Perrier S, Ludes P-O, Olland A, Mertes P-M, Schneider F, Helms J, Meziani F: Extracorporeal membrane oxygenation for critically ill patients with COVID-19–related acute respiratory distress syndrome: Worth the effort? Am J Resp Crit Care 2020; 202:460–3
13. Mustafa AK, Alexander PJ, Joshi DJ, Tabachnick DR, Cross CA, Pappas PS, Tatooles AJ: Extracorporeal membrane oxygenation for patients with COVID-19 in severe respiratory failure. JAMA Surg 2020; 155:990–2
14. Barbaro RP, MacLaren G, Boonstra PS, Iwashyna TJ, Slutsky AS, Fan E, Bartlett RH, Tonna JE, Hyslop R, Fanning JJ, Rycus PT, Hyer SJ, Anders MM, Agerstrand CL, Hryniewicz K, Diaz R, Lorusso R, Combes A, Brodie D; Extracorporeal Life Support Organization: Extracorporeal membrane oxygenation support in COVID-19: An international cohort study of the Extracorporeal Life Support Organization registry. Lancet 2020; 396:1071–8
15. Shaefi S, Brenner SK, Gupta S, O'Gara BP, Krajewski ML, Charytan DM, Chaudhry S, Mirza SH, Peev V, Anderson M, Bansal A, Hayek SS, Srivastava A, Mathews KS, Johns TS, Leonberg-Yoo A, Green A, Arunthamakun J, Wille KM, Shaukat T, Singh H, Admon AJ, Semler MW, Hernán MA, Mueller AL, Wang W, Leaf DE; STOP-COVID Investigators: Extracorporeal membrane oxygenation in patients with severe respiratory failure from COVID-19. Intensive Care Med 2021; 47:208–21
16. Agence Régionale de Santé: Utilisation de l'ECMO Lors de la Prise en Charge des Patients COVID-19. Available at: https://www.iledefrance.ars.sante.fr/system/files/2020-12/038_ARSIdF-CRAPS_2020-12-02_Doctrine_ECMO.pdf. Accessed May 11, 2021.
17. Lebreton G, Schmidt M, Ponnaiah M, Folliguet T, Para M, Guihaire J, Lansac E, Sage E, Cholley B, Mégarbane B, Cronier P, Zarka J, Da Silva D, Besset S, Morichau-Beauchant T, Lacombat I, Mongardon N, Richard C, Duranteau J, Cerf C, Saiydoun G, Sonneville R, Chiche JD, Nataf P, Longrois D, Combes A, Leprince P; Paris ECMO-COVID-19 investigators: Extracorporeal membrane oxygenation network organisation and clinical outcomes during the COVID-19 pandemic in Greater Paris, France: A multicentre cohort study. Lancet Respir Med 2021; 9:851–62
18. Sinha P, Calfee CS, Beitler JR, Soni N, Ho K, Matthay MA, Kallet RH: Physiologic analysis and clinical performance of the ventilatory ratio in acute respiratory distress syndrome. Am J Respir Crit Care Med 2019; 199:333–41
19. Textor J, Zander B van der, Gilthorpe MS, Liśkiewicz M, Ellison GTH: Robust causal inference using directed acyclic graphs: The R package "DAGitty." Int J Epidemiol 2016; 45:1887–94
20. Lerman BJ, Popat RA, Assimes TL, Heidenreich PA, Wren SM: Association of left ventricular ejection fraction and symptoms with mortality after elective noncardiac surgery among patients with heart failure. JAMA 2019; 321:572–9

21. Williams EC, Motta-Ribeiro GC, Vidal Melo MF: Driving pressure and transpulmonary pressure: How do we guide safe mechanical ventilation? Anesthesiology 2019; 131:155–63
22. Tremblay A, Bandi V: Impact of body mass index on outcomes following critical care. Chest 2003; 123:1202–7
23. Faridi KF, Hennessey KC, Shah N, Soufer A, Wang Y, Sugeng L, Agarwal V, Sharma R, Sewanan LR, Hur DJ, Velazquez EJ, McNamara RL: Left ventricular systolic function and inpatient mortality in patients hospitalized with coronavirus disease 2019 (COVID-19). J Am Soc Echocardiogr 2020; 33:1414–5
24. Schmidt M, Bailey M, Sheldrake J, Hodgson C, Aubron C, Rycus PT, Scheinkestel C, Cooper DJ, Brodie D, Pellegrino V, Combes A, Pilcher D: Predicting survival after extracorporeal membrane oxygenation for severe acute respiratory failure: The Respiratory Extracorporeal Membrane Oxygenation Survival Prediction (RESP) score. Am J Respir Crit Care Med 2014; 189:1374–82
25. Meta-analysis Global Group in Chronic Heart Failure (MAGGIC): The survival of patients with heart failure with preserved or reduced left ventricular ejection fraction: An individual patient data meta-analysis. Eur Heart J 2012; 33:1750–7
26. Boëlle PY, Delory T, Maynadier X, Janssen C, Piarroux R, Pichenot M, Lemaire X, Baclet N, Weyrich P, Melliez H, Meybeck A, Lanoix JP, Robineau O: Trajectories of hospitalization in COVID-19 patients: An observational study in France. J Clin Med 2020; 9:E3148
27. Schmidt M, Zogheib E, Rozé H, Repesse X, Lebreton G, Luyt CE, Trouillet JL, Bréchot N, Nieszkowska A, Dupont H, Ouattara A, Leprince P, Chastre J, Combes A: The PRESERVE mortality risk score and analysis of long-term outcomes after extracorporeal membrane oxygenation for severe acute respiratory distress syndrome. Intensive Care Med 2013; 39:1704–13
28. Roch A, Hraiech S, Masson E, Grisoli D, Forel JM, Boucekine M, Morera P, Guervilly C, Adda M, Dizier S, Toesca R, Collart F, Papazian L: Outcome of acute respiratory distress syndrome patients treated with extracorporeal membrane oxygenation and brought to a referral center. Intensive Care Med 2014; 40:74–83
29. Susen S, Tacquard CA, Godon A, Mansour A, Garrigue D, Nguyen P, Godier A, Testa S, Levy JH, Albaladejo P, Gruel Y; GIHP and GFHT: Prevention of thrombotic risk in hospitalized patients with COVID-19 and hemostasis monitoring. Crit Care 2020; 24:364
30. Tacquard C, Mansour A, Godon A, Godet J, Poissy J, Garrigue D, Kipnis E, Hamada SR, Mertes PM, Steib A, Ulliel-Roche M, Bouhemad B, Nguyen M, Reizine F, Gouin-Thibault I, Besse MC, Collercandy N, Mankikian S, Levy JH, Gruel Y, Albaladejo P, Susen S, Godier A: Impact of high dose prophylactic anticoagulation in critically ill patients with COVID-19 pneumonia. Chest 2021; 159:2417–27
31. Grasselli G, Scaravilli V, Mangioni D, Scudeller L, Alagna L, Bartoletti M, Bellani G, Biagioni E, Bonfanti P, Bottino N, Coloretti I, Cutuli SL, De Pascale G, Ferlicca D, Fior G, Forastieri A, Franzetti M, Greco M, Guzzardella A, Linguadoca S, Meschiari M, Messina A, Monti G, Morelli P, Muscatello A, Redaelli S, Stefanini F, Tonetti T, Antonelli M, Cecconi M, Foti G, Fumagalli R, Girardis M, Ranieri M, Viale P, Raviglione M, Pesenti A, Gori A, Bandera A: Hospital-acquired infections in critically ill patients with COVID-19. Chest 2021; 160:454–65
32. Santis VD, Corona A, Vitale D, Nencini C, Potalivo A, Prete A, Zani G, Malfatto A, Tritapepe L, Taddei S, Locatelli A, Sambri V, Fusari M, Singer M: Bacterial infections in critically ill patients with SARS-2-COVID-19 infection: Results of a prospective observational multicenter study. Infection 2022: 50:139–48
33. Thomas G, Hraiech S, Cassir N, Lehingue S, Rambaud R, Wiramus S, Guervilly C, Klasen F, Adda M, Dizier S, Roch A, Papazian L, Forel JM: Venovenous extracorporeal membrane oxygenation devices-related colonisations and infections. Ann Intensive Care 2017; 7:111
34. Bréchot N, Mastroianni C, Schmidt M, Santi F, Lebreton G, Hoareau AM, Luyt CE, Chommeloux J, Rigolet M, Lebbah S, Hekimian G, Leprince P, Combes A: Retrieval of severe acute respiratory failure patients on extracorporeal membrane oxygenation: Any impact on their outcomes? J Thorac Cardiovasc Surg 2018; 155:1621–1629.e2

Appendix: ECMOSARS Investigators

Marc Pierrot, M.D., University Hospital of Angers, Angers, France, collected data, provided and cared for study patients
Sidney Chocron, M.D., Ph.D., University Hospital of Besançon, Besançon, France, collected data, provided and cared for study patients
Guillaume Flicoteaux, M.D., University Hospital of Besançon, Besançon, France, collected data, provided and cared for study patients
Philippe Mauriat, M.D., University Hospital of Bordeaux, Bordeaux, France, critically reviewed the study proposal
Hadrien Roze, M.D., University Hospital of Bordeaux, Bordeaux, France, collected data, provided and cared for study patients
Olivier Huet, M.D., Ph.D., University Hospital of Brest, Brest, France, collected data, provided and cared for study patients
Marc-Olivier Fischer, M.D., Ph.D., University Hospital of Caen, Caen, France, collected data, provided and cared for study patients
Claire Alessandri, M.D., Public Public Assistance-Hospitals of Paris, University Hospital Henri Mondor, Créteil, France, provided and cared for study patients
Raphel Bellaïche, M.D., Public Assistance-Hospitals of Paris, University Hospital Henri Mondor, Créteil, France, provided and cared for study patients

Ophélie Constant, M.D., Public Assistance-Hospitals of Paris, University Hospital Henri Mondor, Créteil, France, provided and cared for study patients
Quentin de Roux, M.D., Public Assistance-Hospitals of Paris, University Hospital Henri Mondor, Créteil, France, provided and cared for study patients
André Ly, M.D., Public Assistance-Hospitals of Paris, University Hospital Henri Mondor, Créteil, France, provided and cared for study patients
Arnaud Meffert, M.D., Public Assistance-Hospitals of Paris, University Hospital Henri Mondor, Créteil, France, provided and cared for study patients
Jean-Claude Merle, M.D., Public Assistance-Hospitals of Paris, University Hospital Henri Mondor, Créteil, France, provided and cared for study patients
Lucile Picard, M.D., Public Assistance-Hospitals of Paris, University Hospital Henri Mondor, Créteil, France, provided and cared for study patients
Elena Skripkina, M.D, Public Assistance-Hospitals of Paris, University Hospital Henri Mondor, Créteil, France, provided and cared for study patients
Thierry Folliguet, M.D., Ph.D., Public Assistance-Hospitals of Paris, University Hospital Henri Mondor, Créteil, France, provided and cared for study patients
Antonio Fiore, M.D., Public Assistance-Hospitals of Paris, University Hospital Henri Mondor, Créteil, France, provided and cared for study patients
Nicolas d'Ostrevy, M.D., University Hospital of Clermont-Ferrand, collected data, provided and cared for study patients
Marie-Catherine Morgan, M.D., University Hospital of Dijon, Dijon, France, collected data, provided and cared for study patients
Maxime Nguyen, M.D., University Hospital of Dijon, Dijon, France, collected data, provided and cared for study patients
Lucie Gaide-Chevronnay, M.D., University Hospital of Grenoble, Grenoble, France, collected data, provided and cared for study patients
Nicolas Terzi, M.D., Ph.D., University Hospital of Grenoble, Grenoble, France,
collected data, provided and cared for study patients
Gwenhaël Colin, M.D.,Vendée Hospital, La Roche-sur-Yon, France, collected data, provided and cared for study patients
Olivier Fabre, M.D., Hospital of Lens, Lens, France, collected data, provided and cared for study patients
Arash Astaneh, M.D., Marie-Lannelongue Hospital, Le Plessis-Robinson, France, collected data, provided and cared for study patients
Justin Issard, M.D., Marie-Lannelongue Hospital, Le Plessis-Robinson, France, collected data, provided and cared for study patients
Elie Fadel, M.D., Ph.D., Marie-Lannelongue Hospital, Le Plessis-Robinson, France, collected data, provided and cared for study patients
Dominique Fabre, M.D., Marie-Lannelongue Hospital, Le Plessis-Robinson, France, collected data, provided and cared for study patients
Antoine Girault, M.D., Marie-Lannelongue Hospital, Le Plessis-Robinson, France, collected data, provided and cared for study patients
Iolande Ion, M.D., Marie-Lannelongue Hospital, Le Plessis-Robinson, France, collected data, provided and cared for study patients
Jean Baptiste Menager, M.D., Marie-Lannelongue Hospital, Le Plessis-Robinson, France, collected data, provided and cared for study patients
Delphine Mitilian, M.D., Marie-Lannelongue Hospital, Le Plessis-Robinson, France, collected data, provided and cared for study patients
Olaf Mercier, M.D., Ph.D., Marie-Lannelongue Hospital, Le Plessis-Robinson, France, collected data, provided and cared for study patients
François Stephan, M.D., Marie-Lannelongue Hospital, Le Plessis-Robinson, France, collected data, provided and cared for study patients
Jacques Thes, M.D., Marie-Lannelongue Hospital, Le Plessis-Robinson, France, collected data, provided and cared for study patients
Jerôme Jouan, M.D., University Hospital of Limoges, Limoges, France, collected data, provided and cared for study patients
Thibault Duburcq, M.D., University Hospital of Lille, Lille, France, collected data, provided and cared for study patients
Valentin Loobuyck, M.D., University Hospital of Lille, Lille, France, collected data, provided and cared for study patients
Sabrina Manganiello, M.D., University Hospital of Lille, Lille, France, collected data, provided and cared for study patients
Mouhammed Moussa, M.D., University Hospital of Lille, Lille, France, collected data, provided and cared for study patients
Agnes Mugnier, M.D., University Hospital of Lille, Lille, France, collected data, provided and cared for study patients
Natacha Rousse, M.D., University Hospital of Lille, Lille, France, collected data, provided and cared for study patients
Olivier Desebbe, M.D., Clinique de la Sauvegarde, Lyon, France, collected data, provided and cared for study patients
Roland Henaine, M.D., Ph.D., Hospices Civils de Lyon, Lyon, France, critically reviewed the study proposal, provided and cared for study patients
Matteo Pozzi, M.D, Hospices Civils de Lyon, Lyon, France, collected data, provided and cared for study patients
Jean-Christophe Richard, M.D., Ph.D., Hospices Civils de Lyon, Lyon, France, collected data, provided and cared for study patients
Zakaria Riad, M.D., Hospices Civils de Lyon, Lyon, France, collected data, provided and cared for study patients
Christophe Guervilly, M.D., North Hospital, Marseille Public University Hospital System, Marseille, France, collected data, provided and cared for study patients
Sami Hraiech, M.D., North Hospital, Marseille Public University Hospital System, Marseille, France, collected data, provided and cared for study patients

Laurent Papazian, M.D., Ph.D., North Hospital, Marseille Public University Hospital System, Marseille, France, collected data, provided and cared for study patients
Matthias Castanier, M.D., European Hospital, Marseille, France, collected data, provided and cared for study patients
Charles Chanavaz, M.D., Clairval Hospital, Marseille, France, collected data, provided and cared for study patients
Sebastien Gette, M.D., Regional Hospital of Metz-Thionville, Metz-Thionville, France, provided and cared for study patients
Guillaume Louis, M.D., Regional Hospital of Metz-Thionville, Metz-Thionville, France, provided and cared for study patients
Erick Portocarrero, M.D., Regional Hospital of Metz-Thionville, Metz-Thionville, France, provided and cared for study patients
Nicolas Bischoff, M.D., Emile Muller Hospital, Mulhouse, France, collected data, provided and cared for study patients
Antoine Kimmoun, M.D., Ph.D., University Hospital of Nancy, Nancy, France, collected data, provided and cared for study patients
Mathieu Mattei, M.D., University Hospital of Nancy, Nancy, France, collected data, provided and cared for study patients
Pierre Perez, M.D., University Hospital of Nancy, Nancy, France, collected data, provided and cared for study patients
Alexandre Bourdiol, M.D., University Hospital of Nantes, Nantes, France, collected data, provided and cared for study patients
Yannick Hourmant, M.D., University Hospital of Nantes, Nantes, France, collected data, provided and cared for study patients
Pierre-Joachim Mahé, M.D., University Hospital of Nantes, Nantes, France, collected data, provided and cared for study patients
Bertrand Rozec, M.D., Ph.D., University Hospital of Nantes, Nantes, France, collected data, provided and cared for study patients
Mickaël Vourc'h, M.D., University Hospital of Nantes, Nantes, France, collected data, provided and cared for study patients
Stéphane Aubert, M.D., Ambroise Paré Hospital, Neuilly-sur-Seine, France, collected data, provided and cared for study patients
Florian Bazalgette, M.D., University Hospital of Nîmes, Nîmes, France, collected data, provided and cared for study patients
Claire Roger, M.D., University Hospital of Nîmes, Nîmes, France, collected data, provided and cared for study patients
Pierre Jaquet, M.D., Public Assistance-Hospitals of Paris, Bichat-Claude Bernard Hospital, Paris University Hospital, Paris, France, provided and cared for study patients
Brice Lortat-Jacob, M.D., Public Assistance-Hospitals of Paris, Bichat-Claude Bernard Hospital, Paris University Hospital, Paris, France, provided and cared for study patients
Pierre Mordant, M.D., Ph.D., Public Assistance-Hospitals of Paris, Bichat-Claude Bernard Hospital, Paris University Hospital, Paris, France, provided and cared for study patients
Patrick Nataf, M.D., Ph.D., Public Assistance-Hospitals of Paris, Bichat-Claude Bernard Hospital, Paris University Hospital, Paris, France, provided and cared for study patients
Juliette Patrier, M.D., Bichat-Claude Bernard Hospital, Paris University Hospital, Paris, France, provided and cared for study patients
Morgan Roué, M.D., Public Assistance-Hospitals of Paris, Bichat-Claude Bernard Hospital, Paris University Hospital, Paris, France, provided and cared for study patients
Romain Sonneville, M.D., Ph.D., Public Assistance-Hospitals of Paris, Bichat-Claude Bernard Hospital, Paris University Hospital, Paris, France, provided and cared for study patients
Alexy Tran-Dinh, M.D., Bichat-Claude Bernard Hospital, Paris University Hospital, Paris, France, provided and cared for study patients
Paul-Henri Wicky, M.D., Public Assistance-Hospitals of Paris, Bichat-Claude Bernard Hospital, Paris University Hospital, Paris, France, provided and cared for study patients
Charles Al Zreibi, M.D., Public Assistance-Hospitals of Paris, European Hospital Georges Pompidou–Paris University Hospital, Paris, France, collected data, provided and cared for study patients
Bernard Cholley, M.D., Ph.D., Public Assistance-Hospitals of Paris, European Hospital Georges Pompidou–Paris University Hospital, Paris, France, collected data, provided and cared for study patients
Yannis Guyonvarch, M.D., Public Assistance-Hospitals of Paris, European Hospital Georges Pompidou–Paris University Hospital, Paris, France, collected data, provided and cared for study patients
Sophie Hamada, M.D., Public Assistance-Hospitals of Paris, European Hospital Georges Pompidou–Paris University Hospital, Paris, France, collected data, provided and cared for study patients
Claudio Barbanti, M.D., Public Assistance-Hospitals of Paris University Hospital, Paris, France, collected data, provided and cared for study patients
Anatole Harrois, M.D., Public Assistance-Hospitals of Paris Le Kremlin-Bicêtre, Paris University Hospital, Paris, France, collected data, provided and cared for study patients
Jordi Matiello, M.D., Public Assistance-Hospitals of Paris Le Kremlin-Bicêtre, Paris University Hospital, Paris, France, collected data, provided and cared for study patients
Thomas Kerforne, M.D., University Hospital of Poitiers, Poitiers, France, collected data, provided and cared for study patients
Nicolas Brechot, M.D., Public Assistance-Hospitals of Paris, Sorbonne University, La Pitié-Salpêtrière Hospital, Paris, France, collected data, provided and cared for study patients
Alain Combes, M.D., Ph.D., Public Assistance-Hospitals of Paris, Sorbonne University, La Pitié-Salpêtrière Hospital, Paris, France, collected data, provided and cared for study patients

Jean Michel Constantin, M.D., Ph.D., Public Assistance-Hospitals of Paris, Sorbonne University, La Pitié-Salpêtrière Hospital, Paris, France, collected data, provided and cared for study patients

Cosimo D'Alessandro, M.D., Public Assistance-Hospitals of Paris, Sorbonne University, La Pitié-Salpêtrière Hospital, Paris, France, collected data, provided and cared for study patients

Pierre Demondion, M.D., Public Assistance-Hospitals of Paris, Sorbonne University, La Pitié-Salpêtrière Hospital, Paris, France, collected data, provided and cared for study patients

Alexandre Demoule, M.D., Public Assistance-Hospitals of Paris, Sorbonne University, La Pitié-Salpêtrière Hospital, Paris, France, collected data, provided and cared for study patients

Martin Dres, M.D., Public Assistance-Hospitals of Paris, Sorbonne University, La Pitié-Salpêtrière Hospital, Paris, France, collected data, provided and cared for study patients

Muriel Fartoukh, M.D., Public Assistance-Hospitals of Paris, Sorbonne University, La Pitié-Salpêtrière Hospital, Paris, France, collected data, provided and cared for study patients

Guillaume Hekimian, M.D., Public Assistance-Hospitals of Paris, Sorbonne University, La Pitié-Salpêtrière Hospital, Paris, France, collected data, provided and cared for study patients

Charles Juvin, M.D., Public Assistance-Hospitals of Paris, Sorbonne University, La Pitié-Salpêtrière Hospital, Paris, France, collected data, provided and cared for study patients

Pascal Leprince, M.D., Ph.D., Public Assistance-Hospitals of Paris, Sorbonne University, La Pitié-Salpêtrière Hospital, Paris, France, collected data, provided and cared for study patients

David Levy, M.D., Public Assistance-Hospitals of Paris, Sorbonne University, La Pitié-Salpêtrière Hospital, Paris, France, collected data, provided and cared for study patients

Charles Edouard Luyt, M.D., Ph.D., Public Assistance-Hospitals of Paris, Sorbonne University, La Pitié-Salpêtrière Hospital, Paris, France, collected data, provided and cared for study patients

Marc Pineton de Chambrun, M.D., Public Assistance-Hospitals of Paris, Sorbonne University, La Pitié-Salpêtrière Hospital, Paris, France, collected data, provided and cared for study patients

Matthieu Schmidt, M.D., Ph.D., Public Assistance-Hospitals of Paris, Sorbonne University, La Pitié-Salpêtrière Hospital, Paris, France, collected data, provided and cared for study patients

Thibaut Schoell, M.D., Public Assistance-Hospitals of Paris, Sorbonne University, La Pitié-Salpêtrière Hospital, Paris, France, collected data, provided and cared for study patients

Pierre Fillâtre, M.D., Ph.D., Hospital of Saint-Brieuc, Saint-Brieuc, France, collected data, provided and cared for study patients

Nicolas Massart, M.D., Hospital of Saint-Brieuc, Saint-Brieuc, France, collected data, provided and cared for study patients

Roxane Nicolas, M.D., University Hospital of Saint-Etienne, Saint-Etienne, France, collected data, provided and cared for study patients

Maud Jonas, M.D., Saint-Nazaire Hospital, Saint-Nazaire, France, collected data, provided and cared for study patients

Charles Vidal, M.D., University Hospital of Saint-Denis, La Réunion, Saint-Denis, France, collected data, provided and cared for study patients

Salvatore Muccio, M.D., University Hospital of Reims, Reims, France, collected data, provided and cared for study patients

Dario Di Perna, M.D., University Hospital of Reims, Reims, France, collected data, provided and cared for study patients

Bruno Mourvillier, M.D., Ph.D., University Hospital of Reims, Reims, France, collected data, provided and cared for study patients

Amedeo Anselmi, M.D., Ph.D., University Hospital of Rennes, Rennes, France, provided and cared for study patients

Karl Bounader, M.D., University Hospital of Rennes, Rennes, France, provided and cared for study patients

Maxime Esvan, M.Sc., University Hospital of Rennes, Rennes, France, performed statistical analysis

Claire Fougerou-Leurent, Pharm.D., University Hospital of Rennes, Rennes, France, critically reviewed the study proposal

Yoann Launey, M.D., Ph.D., University Hospital of Rennes, Rennes, France, provided and cared for study patients

Thomas Lebouvier, M.D., University Hospital of Rennes, Rennes, France, provided and cared for study patients

Alessandro Parasido, University Hospital of Rennes, Rennes, France, provided and cared for study patients

Florian Reizine, M.D., University Hospital of Rennes, Rennes, France, provided and cared for study patients

Philippe Seguin, M.D., Ph.D., University Hospital of Rennes, Rennes, France, provided and cared for study patients

Emmanuel Besnier, M.D., University Hospital of Rouen, Rouen, France, collected data, provided and cared for study patients

Dorothée Carpentier, M.D., University Hospital of Rouen, Rouen, France, collected data, provided and cared for study patients

Anne Olland, M.D., Ph.D., University Hospital of Strasbourg, Strasbourg, France, collected data, provided and cared for study patients

Marion Villard, M.D., University Hospital of Strasbourg, Strasbourg, France, collected data, provided and cared for study patients

Fanny Bounes, M.D., University Hospital of Toulouse, Toulouse, France, collected data, provided and cared for study patients

Vincent Minville, M.D., Ph.D., University Hospital of Toulouse, Toulouse, France, collected data, provided and cared for study patients
Antoine Guillon, M.D., University Hospital of Tours, Tours, France, collected data, provided and cared for study patients
Yannick Fedun, M.D., Bretagne Atlantique Hospital, Vannes, France, collected data, provided and cared for study patients
James T. Ross, M.D., University of California Davis, Sacramento, California, provided critical revisions of the manuscript

ANESTHESIOLOGY REFLECTIONS FROM THE WOOD LIBRARY-MUSEUM

The Stars Align in Support of Morton's "Anaesthesia"

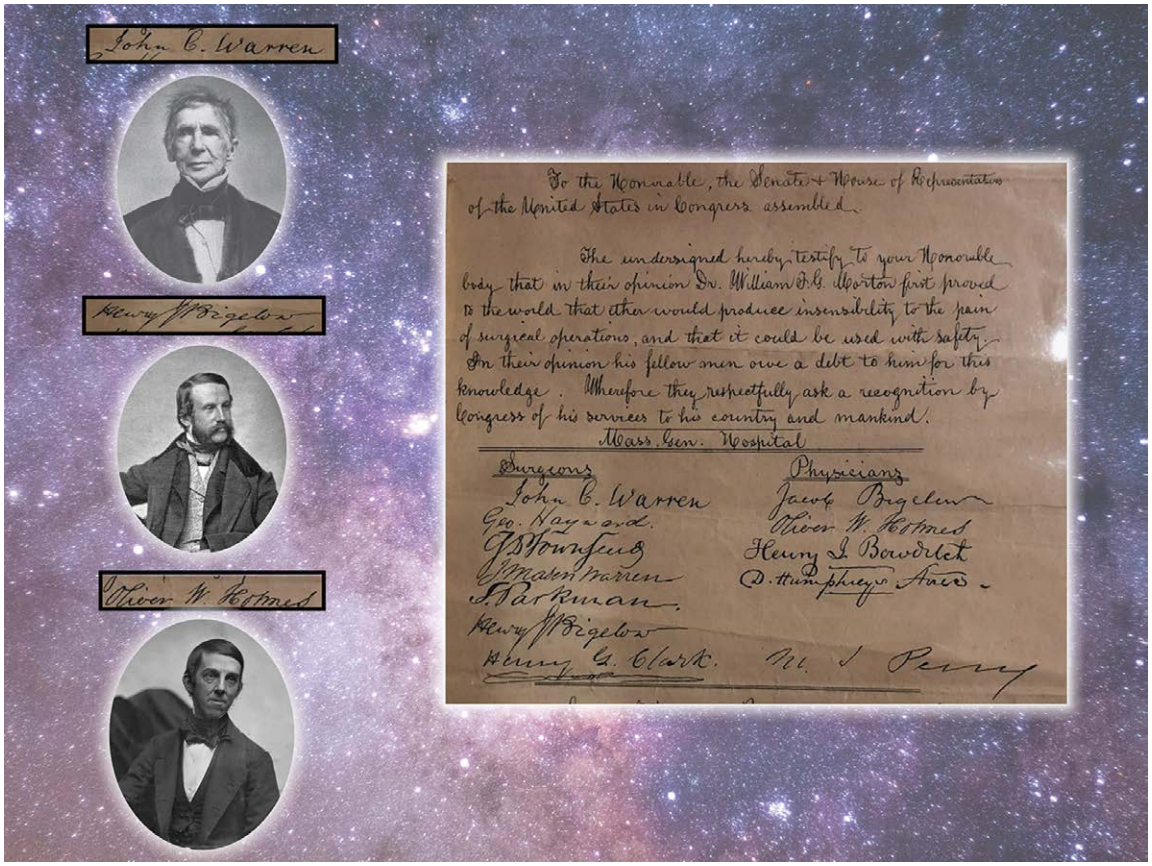

"Never before…did such a brilliant galaxy of medical and surgical talent unite on any one measure." Penned by the brightest stars of Massachusetts General Hospital in 1852, a petition to the United States Congress (*right*) shined a favorable light on Morton, who in a quest for recognition had ignited a national controversy over primacy for the discovery of surgical anesthesia. These medical luminaries declared "that, in their opinion, Dr. William T.G. Morton first proved to the world that ether would produce insensibility to the pain of surgical operations… [and asked for] recognition by [U.S.] Congress of his services to his country and mankind." Among these leading lights were John C. Warren, M.D. (*upper left*), founding father of Massachusetts General Hospital and senior surgeon on Ether Day; Henry J. Bigelow, M.D. (*middle left*), surgeon and organizer of that celebrated day; and Oliver W. Holmes, M.D. (*lower left*), physician-poet who bestowed the name "anaesthesia" onto this new discovery. Whether this was a true endorsement of Morton or the medical discovery that elevated surgical practice may be lost among the stars. (Copyright © the American Society of Anesthesiologists' Wood Library-Museum of Anesthesiology. www.woodlibrarymuseum.org)

Melissa L. Coleman, M.D., Assistant Professor, Department of Anesthesiology and Perioperative Medicine, Penn State College of Medicine, Hershey, Pennsylvania.

ANESTHESIOLOGY

Extracorporeal Membrane Oxygenation for Respiratory Failure Related to COVID-19: A Nationwide Cohort Study

Nicolas Nesseler, M.D., Ph.D., Guillaume Fadel, M.D., Alexandre Mansour, M.D., Marylou Para, M.D., Pierre-Emmanuel Falcoz, M.D., Ph.D., Nicolas Mongardon, M.D., Ph.D., Alizée Porto, M.D., Astrid Bertier, M.D., Bruno Levy, M.D., Ph.D., Cyril Cadoz, M.D., Pierre-Grégoire Guinot, M.D., Ph.D., Olivier Fouquet, M.D., Ph.D., Jean-Luc Fellahi, M.D., Ph.D., Alexandre Ouattara, M.D., Ph.D., Julien Guihaire, M.D., Ph.D., Vito-Giovanni Ruggieri, M.D., Ph.D., Philippe Gaudard, M.D., Ph.D., François Labaste, M.D., Ph.D., Thomas Clavier, M.D., Kais Brini, M.D., Nicolas Allou, M.D., Corentin Lacroix, M.D., Juliette Chommeloux, M.D., Guillaume Lebreton, M.D., Ph.D., Michael A. Matthay, M.D., Ph.D., Sophie Provenchere, M.D., Ph.D., Erwan Flécher, M.D., Ph.D., André Vincentelli, M.D., Ph.D.; for the ECMOSARS Investigators*

ANESTHESIOLOGY 2022; 136:732–48

EDITOR'S PERSPECTIVE

What We Already Know about This Topic

- Venovenous extracorporeal membrane oxygenation is increasingly used for managing severe respiratory failure; however, the characteristics, management, and patient outcomes continue to be determined
- Determining factors associated with in-hospital mortality for both COVID-19 and non–COVID-19 patients are important factors to consider in patient management

What This Article Tells Us That Is New

- In this investigation, most patients were cannulated by a mobile extracorporeal membrane oxygenation unit without a negative impact on mortality
- Based on this report, venovenous extracorporeal membrane oxygenation support should be considered within the first week of mechanical ventilation initiation for optimal outcomes

ABSTRACT

Background: Despite expanding use, knowledge on extracorporeal membrane oxygenation support during the COVID-19 pandemic remains limited. The objective was to report characteristics, management, and outcomes of patients receiving extracorporeal membrane oxygenation with a diagnosis of COVID-19 in France and to identify pre-extracorporeal membrane oxygenation factors associated with in-hospital mortality. A hypothesis of similar mortality rates and risk factors for COVID-19 and non–COVID-19 patients on venovenous extracorporeal membrane oxygenation was made.

Methods: The Extracorporeal Membrane Oxygenation for Respiratory Failure and/or Heart failure related to Severe Acute Respiratory Syndrome-Coronavirus 2 (ECMOSARS) registry included COVID-19 patients supported by extracorporeal membrane oxygenation in France. This study analyzed patients included in this registry up to October 25, 2020, and supported by venovenous extracorporeal membrane oxygenation for respiratory failure with a minimum follow-up of 28 days after cannulation. The primary outcome was in-hospital mortality. Risk factors for in-hospital mortality were analyzed.

Results: Among 494 extracorporeal membrane oxygenation patients included in the registry, 429 were initially supported by venovenous extracorporeal membrane oxygenation and followed for at least 28 days. The median (interquartile range) age was 54 yr (46 to 60 yr), and 338 of 429 (79%) were men. Management before extracorporeal membrane oxygenation cannulation included prone positioning for 411 of 429 (96%), neuromuscular blockage for 419 of 427 (98%), and NO for 161 of 401 (40%). A total of 192 of 429 (45%) patients were cannulated by a mobile extracorporeal membrane oxygenation unit. In-hospital mortality was 219 of 429 (51%), with a median follow-up of 49 days (33 to 70 days). Among pre-extracorporeal membrane oxygenation modifiable exposure variables, neuromuscular blockage use (hazard ratio, 0.286; 95% CI, 0.101 to 0.81) and duration of ventilation (more than 7 days compared to less than 2 days; hazard ratio, 1.74; 95% CI, 1.07 to 2.83) were independently associated with in-hospital mortality. Both age (per 10-yr increase; hazard ratio, 1.27; 95% CI, 1.07 to 1.50) and total bilirubin at cannulation (6.0 mg/dl or more compared to less than 1.2 mg/dl; hazard ratio, 2.65; 95% CI, 1.09 to 6.5) were confounders significantly associated with in-hospital mortality.

Conclusions: In-hospital mortality was higher than recently reported, but nearly half of the patients survived. A high proportion of patients were cannulated by a mobile extracorporeal membrane oxygenation unit. Several factors associated with mortality were identified. Venovenous extracorporeal membrane oxygenation support should be considered early within the first week of mechanical ventilation initiation.

(ANESTHESIOLOGY 2022; 136:732–48)

Early reports of severe manifestations of COVID-19 such as acute respiratory distress syndrome (ARDS) and acute myocardial injury have suggested a possible role for extracorporeal membrane oxygenation (ECMO) support.[1] Recent experience during the influenza A (H1N1)

This article has been selected for the Anesthesiology CME Program. Learning objectives and disclosure and ordering information can be found in the CME section at the front of this issue. This article is featured in "This Month in Anesthesiology," page A1. Supplemental Digital Content is available for this article. Direct URL citations appear in the printed text and are available in both the HTML and PDF versions of this article. Links to the digital files are provided in the HTML text of this article on the Journal's Web site (www.anesthesiology.org). This article has a visual abstract available in the online version.

Submitted for publication May 26, 2021. Accepted for publication February 4, 2022. Published online first on March 29, 2022.

pandemic demonstrated the value of ECMO support for patients with severe ARDS related to influenza.[2–6] Additionally, a recent meta-analysis of patients from two major randomized controlled trials on ECMO support in severe ARDS patients showed a significant benefit of the technique for improving both morbidity and mortality.[7–9]

Several early retrospective case series showed encouraging results of ECMO support in COVID-19–related respiratory failure.[10–13] However, these case series were limited in sample size (fewer than 90 patients) and restricted to few centers. Consequently, the international report from the Extracorporeal Life Support Organization (Ann Arbor, Michigan) registry, gathering 1,035 ECMO patients from 213 centers in 36 countries, was an important landmark. The study showed an estimated in-hospital mortality of less than 40% for critically ill adults with COVID-19 treated with ECMO in a collection of self-selected and experienced centers worldwide.[14] Recently, a similar mortality rate was reported in a multicenter cohort study of 190 critically ill adults with

Nicolas Nesseler, M.D., Ph.D.: Department of Anesthesia and Critical Care, Pontchaillou, University Hospital of Rennes, France; University of Rennes, University Hospital of Rennes, National Institute of Health and Medical Research, Center of Clinical Investigation of Rennes 1414, Rennes, France; University of Rennes, University Hospital of Rennes, National Research Institute for Agriculture, National Institute of Health and Medical Research, Institute of Nutrition, Metabolism, and Cancer, Mixed Research Unit_1341, Mixed Research Unit_1241, Rennes, France.

Guillaume Fadel, M.D.: Sorbonne University, National Institute of Health and Medical Research, Mixed Research Unit_1166-ICAN, Institute of Cardiometabolism and Nutrition, Paris, France; Department of Thoracic and Cardiovascular, Cardiology Institute, Public Assistance-Hospitals of Paris, Sorbonne University, Pitié-Salpétrière Hospital, Paris, France.

Alexandre Mansour, M.D.: Department of Anesthesia and Critical Care, Pontchaillou, University Hospital of Rennes, Rennes, France; University of Rennes, University Hospital of Rennes, National Institute of Health and Medical Research, Center of Clinical Investigation of Rennes 1414, Rennes, France.

Marylou Para, M.D.: Department of Cardiovascular Surgery and Transplantation, Bichat Hospital, Public Assistance-Hospitals of Paris, Paris, France; University of Paris, Mixed Research Unit_1148, Laboratory of Vascular Translational Science, Paris, France.

Pierre-Emmanuel Falcoz, M.D., Ph.D.: National Institute of Health and Medical Research, Mixed Research Unit_1260, Regenerative Nanomedicine, Translational Medicine Federation, Strasbourg, France; University of Strasbourg, Pharmacy and Medical School, Strasbourg, France; University Hospital of Strasbourg, Thoracic Surgery Department, New Hospital Civil, Strasbourg, France.

Nicolas Mongardon, M.D., Ph.D.: Department of Anesthesia and Critical Care, Medical-University Department, Surgery, Anesthesiology, Surgical Intensive Care Units, University Hospital Department Ageing Thorax-Vessels-Blood, Public Assistance-Hospitals of Paris, Henri Mondor University Hospitals, Créteil, France; University of East Paris Créteil, School of Medicine, Créteil, France; U955-Mondor Institute of Biomedical Research, Equipe 03, Pharmacology and Technologies for Cardiovascular Diseases, National Institute of Health and Medical Research, University of East Paris Créteil, National Veterinary School of Alfort, Maisons-Alfort, France.

Alizée Porto, M.D.: Department of Cardiac Surgery, Timone Hospital, Marseille Public University Hospital System, 13005, Marseille, France.

Astrid Bertier, M.D.: Intensive Care Unit, Bicêtre Hospital, Public Assistance-Hospitals of Paris, Paris, France.

Bruno Levy, M.D., Ph.D.: Intensive Care Unit, CHRU Nancy, Pôle Cardio-Médico-Chirurgical, Vandœuvre-lès-Nancy, France; National Institute of Health and Medical Research U1116, Faculty of Medicine, Vandoeuvre-lès-Nancy, France; University of Lorraine, Nancy, France.

Cyril Cadoz, M.D.: Polyvalent Intensive Care Unit, Mercy Hospital, Regional Hospital, Metz-Thionville, France.

Pierre-Grégoire Guinot, M.D., Ph.D.: Department of Anesthesiology and Critical Care Medicine, Dijon University Hospital, Dijon, France.

Olivier Fouquet, M.D., Ph.D.: Department of Thoracic and Cardiovascular Surgery, University Hospital, Angers, France; Mitochondrial and Cardiovascular Pathophysiology Institute, French National Centre for Scientific Research, Mixed Research Unit_6214, National Institute of Health and Medical Research U1083, University of Angers, Angers, France.

Jean-Luc Fellahi, M.D., Ph.D.: Department of Anesthesia and Critical Care, Louis Pradel Hospital, University Hospital of Lyon, Lyon, France; CarMeN Laboratory, National Institute of Health and Medical Research, Mixed Research Unit_1060, Claude Bernard Lyon University, Lyon, France.

Alexandre Ouattara, M.D., Ph.D.: University Hospital of Bordeaux, Department of Anesthesia and Critical Care, Magellan Medico-Surgical Center, Bordeaux, France; National Institute of Health and Medical Research, Mixed Research Unit 1034, Biology of Cardiovascular Diseases, Pessac, France.

Julien Guihaire, M.D., Ph.D.: Department of Cardiac Surgery, National Institute of Health and Medical Research, Mixed Research Unit_999, Pulmonary Hypertension: Pathophysiology and Novel Therapies, Marie Lannelongue Hospital, Paris Saint-Joseph Hospital Group, University of Paris-Saclay School of Medicine, Le Plessis Robinson, France.

Vito-Giovanni Ruggieri, M.D., Ph.D.: Division of Cardiothoracic and Vascular Surgery, Robert Debré University Hospital, University of Reims Champagne-Ardenne, Reims, France.

Philippe Gaudard, M.D., Ph.D.: Department of Anesthesia and Critical Care, PhyMedExp, Montpellier University, National Institute of Health and Medical Research, French National Centre for Scientific Research, University Hospital of Montpellier, Montpellier, France.

François Labaste, M.D., Ph.D.: Anesthesiology and Intensive Care Department, University Hospital of Toulouse, Toulouse, France; Metabolic and Cardiovascular Diseases Institute, National Institute of Health and Medical Research U1048, University of Toulouse, Paul Sabatier University, Toulouse, France.

Thomas Clavier, M.D.: Department of Anesthesiology, Critical Care and Perioperative Medicine, University Hospital of Rouen, Rouen, France.

Kais Brini, M.D.: Polyvalent and Cardiac Intensive Care Unit, Montsouris Mutualist Institute, Paris, France.

Nicolas Allou, M.D.: Polyvalent Intensive Care Unit, Félix Guyon-Saint-Denis University Hospital, La Réunion, Saint Denis, France.

Corentin Lacroix, M.D.: Department of Cardiothoracic Surgery, University Hospital of Poitiers, Poitiers, France.

Juliette Chommeloux, M.D.: Sorbonne University, National Institute of Health and Medical Research, Mixed Research Unit_1166-ICAN, Institute of Cardiometabolism and Nutrition, Paris, France; Intensive Care Unit, Cardiology Unit, Public Assistance-Hospitals of Paris, Sorbonne University, La Pitié-Salpêtrière Hospital, Paris, France.

Guillaume Lebreton, M.D., Ph.D.: Sorbonne Université, University, National Institute of Health and Medical Research, Mixed Research Unit_1166-ICAN, Institute of Cardiometabolism and Nutrition, Paris, France; Department of Thoracic and Cardiovascular Surgery, Cardiology Institute, Public Assistance-Hospitals of Paris, Sorbonne University, La Pitié-Salpêtrière Hospital, Paris, France.

Michael A. Matthay, M.D., Ph.D.: Departments of Medicine and Anesthesia, Cardiovascular Research Institute, University of California San Francisco, San Francisco, California.

Sophie Provenchere, M.D., Ph.D.: University of Paris, Department of Anesthesiology and Intensive Care, Public Assistance-Hospitals of Paris, Bichat-Claude Bernard Hospital, Paris, France; Clinical Investigation Center 1425, Public Assistance-Hospitals of Paris, National Institute of Health and Medical Research, Paris, France.

Erwan Flécher, M.D., Ph.D.: Department of Thoracic and Cardiovascular Surgery, Pontchaillou University Hospital, University of Rennes 1, Signal and Image Treatment Laboratory, National Institute of Health and Medical Research U1099, Rennes, France.

André Vincentelli, M.D., Ph.D.: Department of Cardiac Surgery, University Hospital of Lille, Lille, France.

*Members of the ECMOSARS Investigators are listed in the appendix.

COVID-19 who received ECMO at 35 sites across the United States.[15]

In France, 485 ECMO consoles are available in 103 academic or nonacademic, public, or private centers due to the wide interest in the technique in the country. During the first wave of the pandemic, a central system was established to coordinate national ECMO resources in France. Regional coordinators met weekly to check the national availability of consoles and circuits. Specific recommendations and algorithms were issued on ECMO indications and organization in the context of the outbreak (https://www.iledefrance.ars.sante.fr/system/files/2020-12/038_ARSIdF-CRAPS_2020-12-02_Doctrine_ECMO.pdf).[16] Collecting data on this initiative is essential to evaluate the results of our organization, to inform clinicians, and to adapt our response to the future developments of the outbreak. Therefore, the goals of our study were (1) to report characteristics, management, and outcomes of patients receiving ECMO with a diagnosis of COVID-19 in France and (2) to identify potentially modifiable variables associated with in-hospital mortality. We hypothesized that the mortality rate and risk factors would be similar for COVID-19 and non–COVID-19 patients on venovenous ECMO.

Materials and Methods

The ECMOSARS registry was launched in April 2020 (ClinicalTrials.gov Identifier: NCT04397588, Extracorporeal Membrane Oxygenation for Respiratory Failure and/or Heart failure related to Severe Acute Respiratory Syndrome-Coronavirus 2 [ECMOSARS] registry, principal investigators: Nicolas Nesseler and André Vincentelli, date of registration: May 21, 2020) and is currently still recruiting. The registry includes 47 centers, academic or nonacademic, which represent 77% of the ECMO consoles available in France. The registry has been endorsed by the French Society of Thoracic and Cardiovascular (Société Française de Chirurgie Thoracique et Cardio-Vasculaire [SFCTCV], Paris, France), the French Society of Thoracic and Cardiovascular Critical Care and Anesthesia (Anesthésie-Réanimation Coeur-Thorax-Vaisseaux [ARCOTHOVA], Paris, France), and the French Society of Anesthesiology and Critical Care Medicine (Société Française d'Anesthésie-Réanimation [SFAR], Paris, France) research network.

The data were collected by research assistants using an electronic case report form from each patient's medical record. Automatic checks were generated for missing or incoherent data, and additional consistency tests were performed by data managers. The nationwide objective of our registry implied the collection of all available data of ECMO patients in France, including data for some patients already published in retrospective studies or case series.[12,14,17] Two studies focused on a specific French area (*e.g.*, the city of Strasbourg or the Greater Paris area), and one study included only a fraction of French patients in an international cohort, which involved only self-selected and experienced centers.

The registry has been approved by the University Hospital of Rennes ethics committee (approval No. 20.43). According to French legislation, written consent is waived because of the study's observational design that does not imply any modification of existing diagnostic or therapeutic strategies. After the information was provided, only non-opposition of patients or their legal representative was obtained for use of the data.

ECMOSARS Registry Inclusion Criteria

All patients, adults or children, tested positive by reverse transcription–polymerase chain reaction for SARS-CoV2 (nasopharyngeal swabs, sputum, endotracheal aspiration, bronchoalveolar lavage, or stool sample) and/or with a diagnosis of COVID-19 made on chest computed tomography findings and supported by venovenous, venoarterial, or venoarterio-venous ECMO can be included in the registry. Patients or proxies who refused consent were excluded from the study, as were legally protected adults.

Data Collection

The data were collected prospectively in the ECMOSARS registry, except for patients whose ECMO was implanted before April 21, 2020. Those data were collected retrospectively. Collected data included patient characteristics and comorbidities, management of COVID-related ARDS before ECMO cannulation, patient characteristics at ECMO cannulation and the day after, management, complications, and patient outcomes on ECMO (see Supplemental Digital Content 1, table S1, http://links.lww.com/ALN/C809, for the definition of the main variables).

Study Population

For the current study, we analyzed all patients included in the registry up to October 25, 2020, initially supported by venovenous ECMO for respiratory failure and with a minimum follow-up of 28 days after ECMO cannulation for alive patients.

Outcomes

Our primary outcome was in-hospital mortality. Secondary outcomes were mortality at day 28, mortality at day 90, ECMO-free days, and intensive care unit (ICU)–free days to day 28. ECMO-free days or ICU-free days are composite outcomes that combine survival and ECMO support duration or survival and ICU length of stay. The numbers of ECMO-free days or ICU-free days were calculated as 28 minus the number of days on ECMO or in the ICU during the first 28 days after ECMO cannulation. Patients who died were assigned the worst possible outcome of 0 ECMO-free days or ICU-free days.

Statistical Analysis

Patient characteristics are expressed as number and percentage for categorical variables and median with interquartile

range for continuous variables. For bivariate comparison between deceased and alive patients, a chi-square test or a Fisher exact test was used for categorical variables, and an independent *t* test or a Wilcoxon rank sum test was used for continuous variables. Blood gases values and ventilator settings before and after ECMO cannulation were compared using a repeated measures ANOVA model. The ventilatory ratio was defined as [minute ventilation (ml/min) × $Paco_2$ (mmHg)]/(predicted body weight × 100 × 37.5).[18]

A statistical analysis plan was made before accessing the data. No *a priori* statistical power calculation was conducted. Regarding the primary outcome, no minimum clinically meaningful hazard ratio was defined before data access. In accordance with reviewers' recommendations, modeling and variable selection strategies were modified and are thus considered *post hoc* analyses. Only pre-ECMO variables were included in these analyses to prevent competing risk bias.

A directed acyclic graph was used to describe the associations between pre-ECMO modifiable exposure variables, patient-related confounders, pre-ECMO hospitalization-related confounders, and in-hospital mortality using DAGitty software (Supplemental Digital Content 1, fig. S1, http://links.lww.com/ALN/C809).[19] No variables were analyzed as effect modifiers. Pre-ECMO modifiable exposure variables comprised anticoagulation, antibiotic therapy, antiviral therapy, noninvasive ventilation, selective digestive decontamination, neuromuscular blocking agents, prone position, high-flow oxygen therapy, cannulation mode, inotropes use, vasopressors use, renal replacement therapy, ECMO cannulation, inhaled NO, positive end-expiratory pressure, tidal volume at cannulation, and ventilation duration before ECMO. The set of pre-ECMO confounders sufficient for adjustment comprised patient-related confounders (sex, age, body mass index, diabetes, chronic obstructive pulmonary disease, chronic respiratory failure, congestive heart failure, chronic kidney disease, malignancy, and previous corticotherapy) and pre-ECMO hospitalization-related confounders (septic shock, total bilirubin at cannulation, pH at cannulation, $Paco_2$ at cannulation, Pao_2/fractional inspired oxygen tension (Fio_2) ratio at cannulation, driving pressure, left ventricular ejection fraction, ventilator-associated pneumonia, and delay from hospitalization to ICU admission).

To estimate hazard ratios between exposure variables and in-hospital mortality, we fitted a univariate and multivariable Cox proportional hazards model including exposure variables and confounders identified using the directed acyclic graph. Four different models were built, for sensitivity analysis (see Supplemental Digital Content 1, table S2, http://links.lww.com/ALN/C809). Model 1 was a univariable Cox model; model 2 was a multivariable Cox model of modifiable exposure variables, adjusted for patient-related confounders; model 3 was a multivariable Cox model of modifiable exposure variables, adjusted for pre-ECMO hospitalization-related confounders; and model 4 was a multivariable Cox model of modifiable exposure variables, fully adjusted for all confounders. Centers were included as a random effect using a γ frailty model. Patients who were still hospitalized were censored at the time of the database lock, and those who were discharged alive were censored at the time of their discharge date. Proportional hazard assumption was assessed using simultaneous time-dependent covariates. To comply with log-linearity assumptions, several continuous variables (body mass index, pH, left ventricular ejection fraction, delay from hospitalization to ICU admission, driving pressure, positive end-expiratory pressure, tidal volume, and ventilation duration before ECMO) were split into categorical variables in accordance with previously published works and guidelines.[8,20–26]

Multiple imputation was used to account for missing values in variables (Supplemental Digital Content 1, table S3, http://links.lww.com/ALN/C809). We used fully specified chained equations in the SAS multiple imputation procedure (SAS Institute, USA). For continuous variables, the regression method was used to impute missing values, and discriminant function methods were used for binary and categorical variables. Passive imputation was used for the derived variables (body mass index, tidal volume, Pao_2/Fio_2 ratio, anticoagulation before ECMO, and malignancy), meaning that each variable needed for the calculation was imputed before the calculation of the derived variable. A total of 50 imputed data sets were created and combined using standard between/within-variance techniques. All tests used a two-tailed hypothesis. Statistical significance was achieved for $P < 0.05$. Statistical analyses were computed with SAS version 9.4 software (SAS Institute, USA).

Results

At the time of the database lock, 38 centers had included 494 patients in the ECMOSARS registry, of whom 462 patients were followed for at least 28 days after ECMO cannulation; 429 patients were initially supported by venovenous ECMO, and 33 were supported by venoarterial ECMO (fig. 1). No patients were initially supported by venoarterio-venous ECMO.

The first venovenous ECMO included in the analysis was implanted on February 25, 2020, and the last venovenous ECMO included in the analysis was implanted on September 17, 2020. Most of the patients (257 [59.9%]) were admitted from another hospital. Venovenous ECMO was cannulated in-hospital by mobile ECMO units in 192 (45%) patients, of whom 79% were transferred subsequently to a referral ECMO center. In total, 13 centers included fewer than 5 patients, 12 centers included between 5 and 10 patients, 5 centers included between 10 and 20 patients, 2 centers included between 20 and 30 patients, 3 centers included between 30 and 40 patients, and 1 center included 124 (26.8%) patients (see Supplemental Digital Content 1, figs. S2 and S3, http://links.lww.com/ALN/C809).

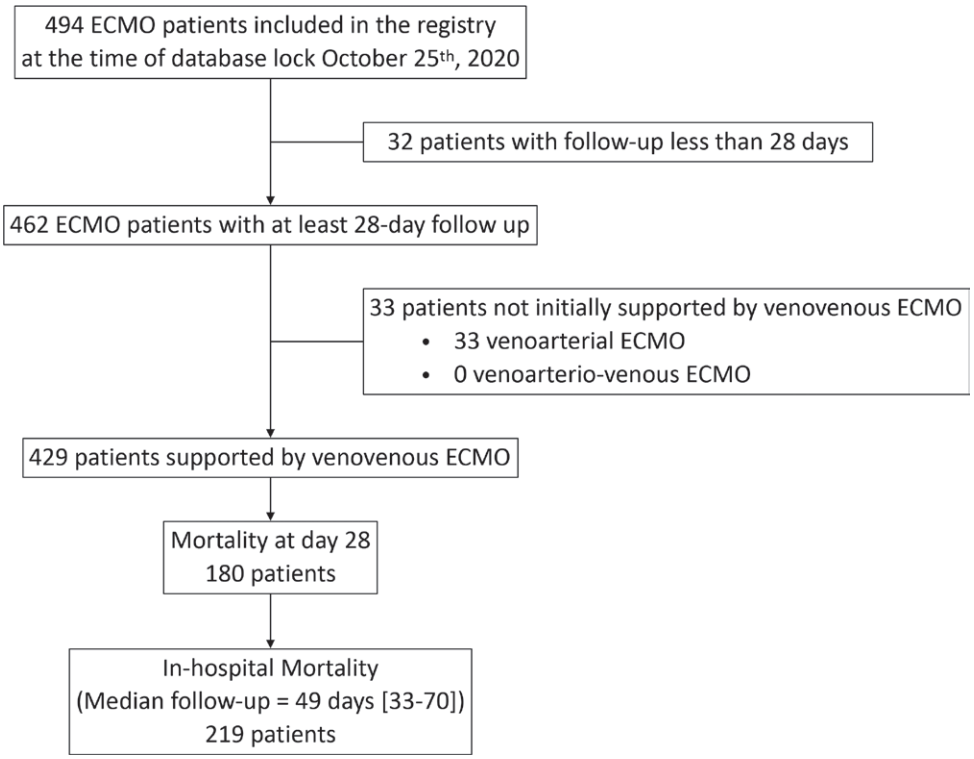

Fig. 1. Flow chart of extracorporeal membrane oxygenation (ECMO) patients included in the study.

Study Population

The median age was 54 (46 to 60) years, 79% of the patients were men, and the median body mass index was 30 (27 to 34). Management before ECMO cannulation included prone positioning (96% [411 of 429]), neuromuscular blocking agent (98% [419 of 427]), and NO (40% [161 of 401]; table 1). Median ventilation duration before ECMO was 5.0 (3.0 to 8.0) days. The median total Sequential Organ Failure Assessment (SOFA) score at cannulation (n = 395) was 9 (8 to 12), and 51% (216 of 422) of the patients had a cardiovascular SOFA score of 3 or higher. The blood lactate level was 1.7 (1.2 to 2.3) mmol/l (n = 366), and 12% (51 of 423) of the patients were on renal replacement therapy. Finally, 99% of the patients met the Berlin ARDS criteria at ECMO cannulation (table 2).

The ventilation settings at the time of the cannulation and the day after the cannulation are shown in table 3. ECMO cannulation was associated with reduced tidal volume, respiratory rate, and F_{IO_2}, as well as lower plateau and driving pressures. A tracheostomy was performed in 21% (90 of 424) of the patients.

Complications on ECMO

Hemorrhagic complications on ECMO were observed in 40% (169 of 426) of the patients, while thrombosis occurred in 37% (159 of 427), and neurologic complications occurred in 11% (47 of 425), including 38 hemorrhagic strokes (table 4). Renal replacement therapy was required in 35%. Bacteremia and cannula site infection were observed in 41% (176 of 428) and 8% (36 of 428) of the patients, respectively. According to cannulation by mobile ECMO units (see Supplemental Digital Content 1, table S4, http://links.lww.com/ALN/C809), cannula site infections were observed significantly more frequently after cannulation by mobile ECMO units, but less cannula site bleeding, although nonsignificant, was observed.

Outcomes

In-hospital mortality was 219 of 429 (51%) with a median follow-up of 49 (33 to 70) days (see Supplemental Digital Content 1, fig. S4, http://links.lww.com/ALN/C809). The extent of missing data across all variables included in the statistical models is described in Supplemental Digital Content 1 (table S3, http://links.lww.com/ALN/C809). Mortality at days 28 and 90 was 42% (180 of 429) and 60% (215 of 357), respectively. At day 28, ventilator-free days (n = 425), ECMO-free days (n = 414), and ICU-free days (n = 412) were 0 (0 to 0), 0 (0 to 14), and 0 (0 to 0) days, respectively. More male patients died, and they were significantly older (table 1). At cannulation, pH was significantly lower, and the $Paco_2$, the ventilatory ratio, and the serum lactate levels were significantly higher in the patients who ultimately died (table 2). Patients who died also had a significantly higher

Table 1. Patient Characteristics before Hospitalization

Characteristics	No.	Full Cohort (n = 429)	Vital Status		*P* Value
			Nonsurvivors (n = 219)	Survivors (n = 210)	
Age	428	54 (46–60)	56 (49–62)	51 (43–58)	< 0.001
< 40 yr		56 (13)	19 of 218 (9)	37 of 210 (18)	
40–49 yr		96 (22)	38 of 218 (17)	58 of 210 (28)	
50–59 yr		160 (37)	85 of 218 (39)	75 of 210 (36)	
60–69 yr		103 (24)	66 of 218 (30)	37 of 210 (18)	
> 70 yr		13 (3)	10 of 218 (5)	3 of 210 (1)	
Sex	429				0.046
Female		91 (21)	38 of 219 (17)	53 of 210 (25)	
Male		338 (79)	181 of 219 (83)	157 of 210 (75)	
Body mass index	413	30 (27–34)	29 (27–34)	31 (28–35)	0.132
< 25 kg of m^2		53 (13)	28 of 206 (14)	25 of 207 (12)	
25–30 kg of m^2		147 (36)	79 of 206 (38)	68 of 207 (33)	
30–35 kg of m^2		121 (29)	61 of 206 (30)	60 of 207 (29)	
35–40 kg of m^2		56 (14)	20 of 206 (10)	36 of 207 (17)	
> 40 kg of m^2		36 (9)	18 of 206 (9)	18 of 207 (9)	
Comorbidities					
Hypertension	429	165 (38)	83 of 219 (38)	82 of 210 (39)	0.807
Diabetes	425	127 (30)	70 of 218 (32)	57 of 207 (28)	0.303
Chronic obstructive pulmonary disease	429	14 (3)	8 of 219 (4)	6 of 210 (3)	0.643
Chronic respiratory failure	429	13 (3)	7 of 219 (3)	6 of 210 (3)	0.838
Congestive heart failure	308	3 (1)	1 of 169 (1)	2 of 169 (1)	0.591
Coronary artery disease	429	21 (5)	10 of 219 (5)	11 of 139 (8)	0.747
Chronic kidney disease	309	11 (4)	7 of 171 (4)	4 of 138 (3)	0.760
Malignancy					
Cancer	306	6 (2)	6 of 168 (4)	0 of 138 (0)	0.034
Hematological malignancy	306	3 (1)	1 of 168 (1)	2 of 138 (1)	0.591
Active smoker	423	17 (4)	10 of 216 (5)	7 of 207 (3)	0.514
Alcohol abuse	301	8 (3)	3 of 166 (2)	5 of 135 (4)	0.474
History of venous thromboembolism	306	11 (4)	7 of 168 (4)	4 of 138 (3)	0.760
Pre-ECMO medications					
Steroids (corticotherapy)	307	17 (6)	10 of 169 (6)	7 of 138 (5)	0.748
Nonsteroidal anti-inflammatory drugs	307	7 (2)	4 of 167 (2)	3 of 140 (2)	> 0.999
Angiotensin-converting enzyme inhibitors	305	29 (10)	14 of 167 (8)	15 of 138 (11)	0.461
Angiotensin receptor blockers	306	44 (14)	23 of 168 (14)	21 of 138 (15)	0.705

The results are presented as n (%) or median (interquartile range).
ECMO, extracorporeal membrane oxygenation.

SOFA score at cannulation, with significantly more patients with a liver (6.0 mg/dl bilirubin or more) and cardiovascular scores of 3 or higher and significantly more patients with renal replacement therapy than patients who survived. While on ECMO, patients who ultimately died experienced significantly more hemorrhagic complications, membrane lung failure, acute kidney injury, and neurologic complications than patients who survived (table 4).

Effect of Pre-ECMO Modifiable Exposure Variables on In-hospital Mortality

Among pre-ECMO modifiable exposure variables, neuromuscular blockage use (hazard ratio, 0.286; 95% CI, 0.101 to 0.81) and duration of ventilation (more than 7 days compared to less than 2 days; hazard ratio, 1.74; 95% CI, 1.07 to 2.83) were independently associated with in-hospital mortality (table 5). Among patient-related and pre-ECMO hospitalization-related confounders, age (per 10-yr increase; hazard ratio, 1.27; 95% CI, 1.07 to 1.50) and total bilirubin at cannulation (6.0 mg/dl or more compared to less than 1.2 mg/dl; hazard ratio, 2.65; 95% CI, 1.09 to 6.5) were both significantly associated with in-hospital mortality. These results remained consistent after sensitivity analysis in two distinct models: (1) modifiable exposure variables and patient-related baseline characteristics and (2) modifiable exposure variables and pre-ECMO hospitalization-related variables (see Supplemental Digital Content 1, table S2, http://links.lww.com/ALN/C809). In the latter model, septic shock (hazard ratio, 1.69; 95% CI, 1.03 to 2.77) at cannulation and pH lower than 7.25 at cannulation (hazard ratio, 1.56; 95% CI, 1.05 to 2.31) were also associated with in-hospital mortality.

Discussion

Our study reports, at a nationwide level, the characteristics, management, and outcomes of COVID-19 patients treated with venovenous ECMO for respiratory failure. We found an in-hospital mortality of 51%, numerically higher

Table 2. Clinical Condition and Management before ECMO

Condition/Management	No.	Full Cohort (n = 429)	Vital Status		*P* Value
			Nonsurvivors (n = 219)	Survivors (n = 210)	
Delay from hospitalization to ICU admission	428	0 (0–0)	0 (0–0)	0 (0–0)	0.622
< 24 h		329 (77)	169 of 218 (78)	160 of 210 (76)	
24–48 h		52 (12)	30 of 218 (14)	22 of 210 (10)	
> 72 h		47 (11)	19 of 218 (9)	28 of 210 (13)	
ECMO cannulation	426				0.141
Referral center		234 (55)	128 of 216 (59)	106 of 210 (50)	
Mobile ECMO unit, no transfer		41 (10)	21 of 216 (10)	20 of 210 (10)	
Mobile ECMO unit, transfer to referral center		151 (35)	67 of 216 (31)	84 of 210 (40)	
ARDS (Berlin criteria) at cannulation	421	417 (99)	210 of 213 (99)	207 of 208 (100)	0.623
Noninvasive ventilation	426	104 (24)	64 of 217 (29)	40 of 209 (19)	0.013
High-flow oxygen therapy	307	125 (41)	74 of 168 (44)	51 of 139 (37)	0.192
Ventilation duration before ECMO	428	5 (3–8)	6 (3–8)	5 (3–7)	0.057
< 2 days		94 (22)	43 of 218 (20)	51 of 210 (24)	
2–7 days		221 (52)	105 of 218 (48)	116 of 210 (55)	
> 7 days		113 (26)	70 of 218 (32)	43 of 210 (20)	
pH at cannulation	408	7.33 (7.25–7.39)	7.31 (7.22–7.37)	7.35 (7.29–7.41)	< 0.001
$Paco_2$ at cannulation, mmHg	406	55 (46–65)	57 (48–68)	54 (45–62)	0.005
Pao_2 of Fio_2 ratio at cannulation, mmHg	404	67 (57–82)	67 (58–84)	67 (57–81)	0.625
PEEP at cannulation, cm H_2O	385	12 (10–14)	12 (10–14)	12 (10–14)	0.747
V_T at cannulation	353	5.9 (5.2–6.3)	5.8 (5.1–6.2)	5.9 (5.3–6.3)	0.244
< 6 ml/kg ideal body weight		216 (61)	113 of 178 (63)	103 of 175 (59)	
6–8 ml/kg ideal body weight		132 (37)	63 of 178 (35)	69 of 175 (39)	
> 8 ml/kg ideal body weight		5 (1)	2 of 178 (1)	3 of 175 (2)	
Respiratory rate at cannulation, breaths/min	348	28 (20–30)	28 (22–30)	28 (20–30)	0.321
Ventilatory ratio*	315	2.2 (1.5–3.0)	2.4 (1.7–3.1)	2.1 (1.5–2.9)	< 0.001
Plateau pressure at cannulation, cm H_2O	331	30 (27–32)	30 (26–33)	30 (27–32)	0.414
Driving pressure at cannulation, cm H_2O	327	17 (14–20)	17 (13–21)	17 (14–20)	0.297
Neuromuscular blocking agents	427	419 (98)	213 of 218 (98)	206 of 209 (99)	0.725
Prone position	429	411 (96)	207 of 219 (95)	204 of 210 (97)	0.176
Inhaled NO	401	161 (40)	90 of 206 (44)	71 of 195 (36)	0.137
Renal replacement therapy	423	51 (12)	34 of 213 (16)	17 of 210 (8)	0.013
Antiviral therapy	305	179 (59)	96 of 168 (57)	83 of 137 (61)	0.544
Remdesivir		7 (2)	4 of 168 (2)	4 of 137 (3)	> 0.999
Lopinavir/ritonavir		58 (19)	36 of 168 (21)	36 of 137 (26)	0.130
Hydroxychloroquine		102 (33)	52 of 168 (31)	52 of 137 (38)	0.360
Interferon-β		4 (1)	4 of 168 (2)	4 of 137 (3)	0.125
Others		59 (19)	34 of 168 (20)	34 of 137 (25)	0.486
Antibiotic therapy	305	296 (97)	162 of 168 (96)	134 of 137 (98)	0.522
Anticoagulation	294				0.033
No		19 (6)	5 of 161 (3)	14 of 133 (11)	
Curative		139 (47)	77 of 161 (48)	62 of 133 (47)	
Prophylactic		136 (46)	79 of 161 (49)	57 of 133 (43)	
Selective digestive decontamination	304	13 (4)	10 of 166 (6)	3 of 138 (2)	0.099
SOFA score at cannulation	395	9 (8–12)	11 (8–13)	9 (8–12)	0.004
Septic shock	312	35 (11)	25 of 172 (15)	10 of 140 (7)	0.040
Cardiovascular SOFA ≥ 3 at cannulation	422	216 (51)	126 of 215 (59)	90 of 207 (43)	0.002
Left ventricular ejection fraction, %	191	60 (60–65)	60 (55–60)	60 (60–65)	0.722
Vasoactive/inotropic drugs					
Norepinephrine	306	176 (58)	103 of 168 (61)	73 of 138 (53)	0.139
Epinephrine	304	10 (3)	8 of 166 (5)	2 of 138 (1)	0.119
Dobutamine	304	8 (3)	5 of 166 (3)	3 of 137 (2)	0.732
Lactatemia at cannulation, mmol/l	366	1.7 (1.2–2.3)	1.7 (1.3–2.4)	1.6 (1.2–2.1)	0.012
Total bilirubin at cannulation	409				0.023
< 1.2 mg/dl		291 (71)	147 of 207 (71)	144 of 202 (71)	
1.2–1.9 mg/dl		50 (12)	20 of 207 (10)	30 of 202 (15)	
2.0–5.9 mg/dl		57 (14)	30 of 207 (14)	27 of 202 (13)	
≥ 6.0 mg/dl		11 (3)	10 of 207 (5)	1 of 202 (0)	

The results are presented as n (%) or median (interquartile range).

*The ventilatory ratio is defined as [minute ventilation (ml/min) × $Paco_2$ (mmHg)]/(predicted body weight × 100 × 37.5).

ARDS, acute respiratory distress syndrome; ECMO, extracorporeal membrane oxygenation; Fio_2, fractional inspired oxygen tension; ICU, intensive care unit; PEEP, positive end-expiratory pressure; SOFA, Sequential Organ Failure Assessment; V_T, tidal volume.

Table 3. Blood Gases and Ventilator Settings Pre-ECMO the Day of Implantation and the Day after Cannulation

	Nonsurvivors (n = 219)					Survivors (n = 210)				
	Pre-ECMO Day of Cannulation		Post-ECMO Day 1			Pre-ECMO Day of Cannulation		Post-ECMO Day 1		
Blood Gases/Settings	No.	Median (Interquartile Range)	No.	Median (Interquartile Range)	*P* Value	No.	Median (Interquartile Range)	No.	Median (Interquartile Range)	*P* Value
pH	207	7.31 (7.22–7.37)	209	7.40 (7.34–7.45)	0.010	201	7.35 (7.29–7.41)	206	7.42 (7.37–7.47)	< 0.001
Pa_{O_2}, mmHg	208	64 (57–77)	209	79 (65–101)	0.001	199	65 (54–73)	206	83 (70–106)	< 0.001
$Paco_2$, mmHg	206	57 (48–68)	206	44 (40–50)	< 0.001	200	54 (45–62)	206	45 (39–50)	< 0.001
Fio_2, %	210	100 (100–100)	210	70 (50–100)	< 0.001	201	100 (100–100)	206	60 (50–80)	< 0.001
Pa_{O_2}/Fio_2 ratio, mmHg	208	67 (58–84)	209	116 (90–160)	< 0.001	196	67 (57–81)	204	134 (104–208)	< 0.001
PEEP, cm H_2O	201	12 (10–14)	199	12 (10–14)	0.134	184	12 (10–14)	182	12 (10–14)	0.176
V_T, ml/kg ideal body weight	178	5.8 (5.1–6.2)	178	3.2 (2.2–4.5)	< 0.001	175	5.9 (5.3–6.3)	185	3.5 (2.6–4.5)	< 0.001
Respiratory Rate, breaths/min	183	28 (22–30)	190	16 (12–20)	< 0.001	165	28 (20–30)	184	18 (12–20)	< 0.001
Plateau pressure, cm H_2O	173	30 (26–33)	171	26 (24–28)	< 0.001	158	30 (27–32)	166	25 (23–28)	< 0.001
Driving pressure, cm H_2O	171	17 (13–21)	168	14 (11–16)	< 0.001	156	17 (14–20)	159	12 (11–15)	< 0.001

The results are presented as median (interquartile range). The *P* values are for bivariate analysis between pre- and post-ECMO.

ECMO, extracorporeal membrane oxygenation; Fio_2, fractional inspired oxygen tension; PEEP, positive end-expiratory pressure; V_T, tidal volume.

than that reported in two recent studies of venovenous ECMO use in COVID-19 patients.[14,15] The international Extracorporeal Life Support Organization study reported an estimated cumulative incidence of in-hospital mortality 90 days after ECMO initiation of 37%.[13] The Study of the Treatment and Outcomes in Critically Ill Patients with COVID-19 study reported a 60-day mortality rate of 33% in the United States.[15] Similarly, the ECMO to Rescue Lung Injury in Severe ARDS trial reported a mortality of 35% at 60 days in non–COVID-19 ARDS patients supported by venovenous ECMO.[8]

Several factors may explain the higher mortality rate observed in this study. First, this population was older than the populations in the Extracorporeal Life Support Organization or the Study of the Treatment and Outcomes in Critically Ill Patients with COVID-19 studies (median age, 54 [interquartile range, 46 to 60] yr *vs.* 49 [41 to 57] yr in the Extracorporeal Life Support Organization or 49 [41 to 57] years in the Study of the Treatment and Outcomes in Critically Ill Patients with COVID-19 cohort). Second, this population had more severe ARDS at the time of cannulation. In addition, 99% of the patients in this study met the Berlin criteria for ARDS, compared with only 79% in the Extracorporeal Life Support Organization study.[14] Patients in this study tended to have been mechanically ventilated for longer before ECMO cannulation (median 6 days *vs.* 4 days in the Extracorporeal Life Support Organization and 2 days in the Study of the Treatment and Outcomes in Critically Ill Patients with COVID-19), which is known to be associated with worse outcomes.[24] Our patients were also more likely to have been proned (96% *vs.* 60% in the Extracorporeal Life Support Organization or 71% in the Study of the Treatment and Outcomes in Critically Ill Patients with COVID-19 cohort) and/or paralyzed before ECMO cannulation (98% *vs.* 72% or 78%), both suggesting the use of ECMO later in the disease process. Finally, this study included patients from a wide range of both high- and low-volume centers, reflecting the broad use of ECMO in France during the COVID-19 pandemic.[9]

We found several factors independently associated with in-hospital mortality in our cohort, including older age, liver failure (6 mg/dl bilirubin or more) at ECMO cannulation, and a duration of ventilation before ECMO cannulation of more than 7 days; in contrast, only neuromuscular blocking agent use before ECMO was found as a protective factor. These findings were consistent with previous studies[14,24,27,28] and could be useful to the bedside clinician. First, they emphasize the value of early consideration of ECMO when indicated. This finding is particularly important as it can be easily modifiable at the bedside. In our cohort, 26% of the patients were canulated after 7 days of mechanical ventilation. Thus, the clinicians should be strongly encouraged to consider ECMO within 7 days after mechanical ventilation initiation. Second, these findings emphasize that ECMO support seems less beneficial in the sickest patients, as previously described for non–COVID-19 ARDS patients.[24,27,28] In our cohort, liver failure at cannulation appears to be an especially strong marker of severity, which should alert the clinicians before considering ECMO support. Of course, only a limited number of patients presented liver failure, which underlined that the majority of clinicians are already fully aware of the poor results of ECMO support in the sickest patients. Third, the data from this study again emphasize the comparatively poorer outcomes in older patients who received ECMO for COVID-19. Notably, patients of more than 70 yr of age were excluded from the U.S. Study of

Table 4. Outcomes and Complications on ECMO

Outcomes and Complications	No.	Full Cohort (n = 429)	Vital Status		*P* Value
			Nonsurvivors (n = 219)	Survivors (n = 210)	
Total ECMO duration, days		12 (8–21)	11 (6–21)	13 (8–21)	0.751
ECMO-free days at day 28, days	414	0 (0–14)	0 (0–0)	14 (6–19)	< 0.001
Conversion to venoarterial-venous ECMO	429	9 (2)	8 of 219 (4)	1 of 210 (0)	0.038
Cannulation mode	425				0.823
Femoro-jugular		388 (91)	196 of 217 (90)	192 of 208 (92)	
Femoro-femoral		27 (6)	16 of 217 (7)	11 of 208 (5)	
Bicaval dual lumen		6 (1)	2 of 217 (1)	4 of 208 (2)	
Not specified		4 (1)	3 of 217 (1)	1 of 208 (0)	
Total ventilation duration, days	390	27 (16–41)	18 (12–34)	31 (24–46)	< 0.001
Ventilator-free days at day 28, days	425	0 (0–0)	0 (0–0)	0 (0–4)	< 0.001
Tracheostomy	424	90 (21)	11 of 217 (5)	79 of 207 (38)	< 0.001
Prone position	425	301 (71)	145 of 216 (67)	156 of 209 (75)	0.089
Respiratory ECMO Survival Prediction score	240	1 (0–3)	1 (0–3)	2 (0–4)	< 0.001
Vasoactive/inotropic drugs					
Norepinephrine	304	255 (84)	154 of 167 (92)	101 of 137 (74)	< 0.001
Epinephrine	305	15 (5)	13 of 168 (8)	2 of 137 (1)	0.012
Dobutamine	304	16 (5)	11 of 167 (7)	5 of 137 (4)	0.254
Hemorrhagic complications	426	169 (40)	107 of 217 (49)	62 of 209 (30)	< 0.001
Cannula site bleeding		77 (18)	54 of 107 (50)	23 of 62 (37)	
Gastrointestinal bleeding		26 (6)	20 of 107 (19)	6 of 62 (10)	
Pulmonary hemorrhage		37 (9)	27 of 107 (25)	10 of 62 (16)	
Retroperitoneal bleeding		4 (1)	3 of 107 (3)	1 of 62 (2)	
Massive hemorrhage		20 (5)	15 of 107 (14)	5 of 62 (8)	
Number of packed red blood cells transfused	300	4 (2–8)	6 (3–10)	3 (0–6)	< 0.001
Thrombotic complications	427	159 (37)	84 of 217 (39)	75 of 210 (36)	0.522
Deep vein thrombosis		33 (8)	9 of 84 (11)	24 of 75 (32)	
Pulmonary embolism		48 (11)	28 of 84 (33)	20 of 75 (27)	
Circuit clot		66 (15)	32 of 84 (38)	34 of 75 (45)	
Circuit change		56 (13)	32 of 84 (38)	24 of 75 (32)	
Membrane lung failure		35 (8)	25 of 84 (30)	10 of 75 (13)	
Neurologic complications	425	47 (11)	41 of 216 (19)	6 of 209 (3)	< 0.001
Seizures		2 (0)	2 of 41 (5)	0 of 6 (0)	
Ischemic stroke		5 (1)	3 of 41 (7)	2 of 6 (33)	
Hemorrhagic stroke		38 (9)	35 of 41 (85)	3 of 6 (50)	
Acute limb ischemia	424	4	4 (100)	0 (0)	0.124
Acute mesenteric ischemia	427	4	4 (100)	0 (0)	0.123
Acute kidney injury on ECMO	424	192 (45)	134 of 216 (62)	58 of 208 (28)	< 0.001
Renal replacement therapy		149 (35)	104 of 134 (78)	45 of 58 (78)	
Extracorporeal blood purification device	326	50 (15)	34 of 178 (19)	16 of 148 (11)	0.039
Ventilator-associated pneumonia	426	277 (65)	137 of 219 (63)	140 of 210 (67)	0.405
Timing of ventilator-associated pneumonia	169				0.235
Before ECMO		83 (49)	50 of 94 (53)	33 of 75 (44)	
After ECMO		86 (51)	44 of 94 (47)	42 of 75 (56)	
Infectious complications	428	235 (55)	112 of 218 (51)	123 of 210 (59)	0.135
Bacteremia		176 (41)	87 of 112 (78)	89 of 123 (72)	
Cannula site infection		36 (8)	16 of 112 (14)	20 of 123 (16)	
Infection under ECMO-free days, days*	323	9 (3–21)	7 (2–12)	13 (5–28)	< 0.001
ICU duration, days	411	35 (17–54)	18 (10–34)	34 (26–54)	< 0.001
ICU-free days at day 28, days	412	0 (0–0)	0 (0–0)	0 (0–2)	< 0.001
Hospitalization duration, days	395	35 (17–54)	21 (12–36)	52 (37–71)	< 0.001

The results are presented as n (%) or median (interquartile range).

*Infection under ECMO includes ventilator-associated pneumonia, bacteremia, and cannula site infection.

ECMO, extracorporeal membrane oxygenation; ICU, intensive care unit.

the Treatment and Outcomes in Critically Ill Patients with COVID-19.[15] Finally, the favorable results in patients in this cohort who received neuromuscular blocking agent before ECMO cannulation are in line with previous work[24] but should be interpreted with caution here as the vast majority of patients in our cohort received neuromuscular blocking agent before ECMO. Indeed, the very few patients who did not receive neuromuscular blocking agent before cannulation must be considered outliers whose management may have been out of the standard of care.

Table 5. Pre-ECMO Variables Associated with In-hospital Mortality in Multivariable Analysis

Variables	Hazard Ratio (95% CI)*
Neuromuscular blocking agents†	0.286 (0.101–0.81)
Ventilation duration before ECMO†	
< 2 days	1
2–7 days	1.37 (0.89–2.10)
> 7 days	1.74 (1.07–2.83)
Age (10-yr increase)‡	1.27 (1.07–1.50)
Total bilirubin at implantation‡	
< 1.2 mg/dl	1
1.2–1.9 mg/dl	0.88 (0.51–1.50)
2.0–5.9 mg/dl	1.16 (0.72–1.86)
≥ 6.0 mg/dl	2.65 (1.09–6.4)

*Hazard ratio with 95% CI, based on multivariable Cox model of exposure variables fully adjusted for all confounders, after multiple imputation (see model 4, Supplemental Digital Content 1, table S2, http://links.lww.com/ALN/C809). †Defined as pre-ECMO modifiable exposure variables in the model (see Supplemental Digital Content 1, fig. S1, http://links.lww.com/ALN/C809). ‡Defined as patient-related confounders and pre-ECMO hospitalization-related confounders in the model (see Supplemental Digital Content 1, fig. S1, http://links.lww.com/ALN/C809).

ECMO, extracorporeal membrane oxygenation.

While on ECMO, patients who ultimately died experienced significantly more hemorrhagic complications, neurologic complications (mainly hemorrhagic stroke), membrane lung failure, and acute kidney injury than patients who survived. We report more frequent bleeding complications than in the U.S. Study of the Treatment and Outcomes in Critically Ill Patients with COVID-19 study (28% *vs*. 40%) or in the Extracorporeal Life Support Organization study, including cannula site bleeding (18% *vs*. 7%, respectively), gastrointestinal hemorrhage (6% *vs*. 3%, respectively), and pulmonary hemorrhage (8% *vs*. 4%, respectively). Although our definitions of bleeding events were less restrictive, this might be also related to the contemporaneous publication of French guidelines on anticoagulation in COVID-19 patients, which recommended elevated unfractionated heparin targets in ECMO patients after early reports of prothrombotic state in COVID-19 patients.[29] Of note, the ECMO to Rescue Lung Injury in Severe ARDS trial reported 46% of bleeding leading to transfusion. Similarly, we observed a higher proportion of hemorrhagic stroke (9%) than previously reported (2, 4, and 6% in the ECMO to Rescue Lung Injury in Severe ARDS trial, the U.S. Study of the Treatment and Outcomes in Critically Ill Patients with COVID-19, and the Extracorporeal Life Support Organization studies, respectively).

Membrane lung failures were higher than in the Extracorporeal Life Support Organization study (12% vs. 8%), and the higher proportion in the nonsurvivors might reflect the hypercoagulopathy pattern described in the more severe patients.[30] Interestingly, the proportion of acute kidney injury (AKI) requiring renal replacement therapy (35%) was higher than in the Study of the Treatment and Outcomes in Critically Ill Patients with COVID-19 study (22%) but lower than in the Extracorporeal Life Support Organization study (44%) or the ECMO to Rescue Lung Injury in Severe ARDS trial (52%). Nevertheless, as in in the Study of the Treatment and Outcomes in Critically Ill Patients with COVID-19 study, the proportion of AKI was significantly higher in the nonsurvivors, highlighting how the development of AKI might be a turning point in the trajectories of COVID-19 patients on ECMO.

Critically ill patients with COVID-19 have been found at high risk for hospital-acquired infections.[31] In non-ECMO critically ill patients with COVID-19, ventilator-associated pneumonia was found in 25 to 50%, and bacteremia was found in 15 to 34%.[31,32] However, few data are available in COVID-19 patients on ECMO. We found a high proportion of ventilator-associated pneumonia (51%) and bacteremia while on ECMO (41%). The Study of the Treatment and Outcomes in Critically Ill Patients with COVID-19 study reported 35% of ventilator-associated pneumonia and 18% of other documented infections. A similar proportion of 39% of ventilator-associated pneumonia on ECMO was reported in the ECMO to Rescue Lung Injury in Severe ARDS trial. The discrepancy between our study and other reports remains to be elucidated. One hypothesis might be the difficulty of applying infection control procedures in a context of increased workload and a shortage in healthcare workers related to the pandemic surge. Variations in ventilator-associated pneumonia definition applications and microbiologic sampling methods across ICUs and countries might also explain these differences, and further studies are mandated to explore these questions. In contrast, in our cohort, the cannula site infection proportion (8%) was lower than previously described in non–COVID-19 patients.[8,33]

A high proportion of patients were cannulated by mobile ECMO units in our cohort (45%), similar to the percentage previously reported in the Extracorporeal Life Support Organization study (47%). Cannulation by mobile ECMO unit was not found associated with higher mortality, highlighting the importance of mobile ECMO program to rescue patients hospitalized outside of the referral centers as previously suggested.[34] Of note, cannulation by a mobile ECMO unit was not associated with more cannula site bleeding, but more cannula site infections were observed.

Our study has several strengths. This cohort is one of the largest samples of patients supported by venovenous ECMO for COVID-19–related ARDS published to date. Second, the participating centers represented most of the ECMO sites available in France, giving this study a good representation of the ECMO activity between the end of February and September 2020. Additionally, a central system was established to coordinate national ECMO resources, allowing relocation of consoles and circuits, when needed, in the areas the most affected by the virus. Third, the wide adherence during the pre-ECMO period

to known medical interventions in ARDS patient management, such as protective ventilation, prone positioning, or neuromuscular blocking agent infusions, must be emphasized. These data strengthen the fact that in our cohort, ECMO support was proposed to highly severe patients as a rescue therapy after adequate management. Fourth, the multicenter design enables generalization of the data. Finally, the database quality was regularly assessed by dedicated data managers.

However, there are some limitations. Despite broad representation among French ECMO centers, the cohort did not include all ECMO centers, creating potential selection bias. Within our cohort, a significant proportion (26%) of patients came from a single center in Paris, which is a high-volume ECMO center and is also located in an area that was severely affected by the pandemic. In addition, at the time of the database lock, 34 patients (8%) were still hospitalized, leading to a possible underestimation of the in-hospital mortality. Further, as an observational study relying on patients' medical records, this study might be subject to information bias. There were no specific recommendations on cannulation or management of ECMO, introducing variability in management across the study population. However, because we anticipated regional differences in the burden of the pandemic, as well as expertise disparities between participating centers, centers were included as a random effect using a γ frailty model in the Cox model. Additionally, considering that the vast majority of patients in our cohort received neuromuscular blocking agent before ECMO, we underline that the association found between neuromuscular blocking agent use and survival must be interpreted with caution. Finally, it is worth remembering that our study analyzed only patients already receiving ECMO, and thus the results obtained might not be fully relevant in a general population of severe COVID-19 patients.

In conclusion, this analysis of the ECMOSARS registry provides results and outcomes of COVID-19–related respiratory failure patients supported by venovenous ECMO between February and September 2020 in France. In-hospital mortality was higher than recently reported in a multicenter international cohort, but nearly half of the patients survived. A high proportion of patients were cannulated by mobile ECMO unit without negative impact on mortality. Several factors associated with mortality were identified, which may help to guide future clinical decision-making. In particular, venovenous ECMO support should be considered early, within the first week of mechanical ventilation initiation.

Research Support

Supported by a grant from the University Hospital of Rennes (Appel à Projets CFTR2; Rennes, France) and by a grant from the Société Française de Chirurgie Thoracique et Cardiovasculaire (Paris, France), Bourse Marc Laskar.

Competing Interests

Dr. Mongardon received consultant fees from Amomed (Vienna, Austria). Dr. Gaudard received payment from Abiomed (Aachen, Germany), Air Liquide Santé (Gentilly, France), and Abbot (Chicago, Illinois) and consultancy fees from Amomed. Dr. Matthay received payment for his institution from Roche-Genentech (San Francisco, California), from Citius Pharmaceuticals (Cranford, New Jersey) for consulting for ARDS trial design, from Novartis (Bâle, Switzerland) for consulting for ARDS trial design, and from Johnson & Johnson (New Brunswick, New Jersey) and Pliant Therapeutics (San Francisco, California) for ARDS consultation. The other authors declare no competing interests.

Correspondence

Address correspondence to Dr. Nesseler: Hôpital Pontchaillou, Pôle Anesthésie, SAMU, Urgences, Réanimations, Médecine Interne et Gériatrie, Rue Henri Le Guilloux, 35033 Rennes Cedex 9, France. nicolas.nesseler@chu-rennes.fr.

References

1. Wiersinga WJ, Prescott HC: What is COVID-19? JAMA 2020; 324:816
2. Patroniti N, Zangrillo A, Pappalardo F, Peris A, Cianchi G, Braschi A, Iotti GA, Arcadipane A, Panarello G, Ranieri VM, Terragni P, Antonelli M, Gattinoni L, Oleari F, Pesenti A: The Italian ECMO network experience during the 2009 influenza A(H1N1) pandemic: Preparation for severe respiratory emergency outbreaks. Intensive Care Med 2011; 37:1447–57
3. Australia and New Zealand Extracorporeal Membrane Oxygenation (ANZ ECMO) Influenza Investigators; Davies A, Jones D, Bailey M, Beca J, Bellomo R, Blackwell N, Forrest P, Gattas D, Granger E, Herkes R, Jackson A, McGuinness S, Nair P, Pellegrino V, Pettilä V, Plunkett B, Pye R, Torzillo P, Webb S, Wilson M, Ziegenfuss M. Extracorporeal membrane oxygenation for 2009 influenza A(H1N1) acute respiratory distress syndrome. JAMA 2009; 302:1888–95
4. Noah MA, Peek GJ, Finney SJ, Griffiths MJ, Harrison DA, Grieve R, Sadique MZ, Sekhon JS, McAuley DF, Firmin RK, Harvey C, Cordingley JJ, Price S, Vuylsteke A, Jenkins DP, Noble DW, Bloomfield R, Walsh TS, Perkins GD, Menon D, Taylor BL, Rowan KM: Referral to an extracorporeal membrane oxygenation center and mortality among patients with severe 2009 influenza A(H1N1). JAMA 2011; 306:1659–68

5. Pham T, Combes A, Rozé H, Chevret S, Mercat A, Roch A, Mourvillier B, Ara-Somohano C, Bastien O, Zogheib E, Clavel M, Constan A, Richard J-CM, Brun-Buisson C, Brochard L; REVA Research Network: Extracorporeal membrane oxygenation for pandemic influenza A(H1N1)–induced acute respiratory distress syndrome. Am J Resp Crit Care 2013; 187:276–85
6. Quintel M, Bartlett RH, Grocott MPW, Combes A, Ranieri MV, Baiocchi M, Nava S, Brodie D, Camporota L, Vasques F, Busana M, Marini JJ, Gattinoni L: Extracorporeal membrane oxygenation for respiratory failure. Anesthesiology 2020; 132:1257–76
7. Combes A, Schmidt M, Hodgson CL, Fan E, Ferguson ND, Fraser JF, Jaber S, Pesenti A, Ranieri M, Rowan K, Shekar K, Slutsky AS, Brodie D: Extracorporeal life support for adults with acute respiratory distress syndrome. Intensive Care Med 2020; 46:2464–76
8. Combes A, Hajage D, Capellier G, Demoule A, Lavoué S, Guervilly C, Silva DD, Zafrani L, Tirot P, Veber B, Maury E, Levy B, Cohen Y, Richard C, Kalfon P, Bouadma L, Mehdaoui H, Beduneau G, Lebreton G, Brochard L, Ferguson ND, Fan E, Slutsky AS, Brodie D, Mercat A: Extracorporeal membrane oxygenation for severe acute respiratory distress syndrome. New Engl J Med 2018; 378:1965–75
9. Peek GJ, Mugford M, Tiruvoipati R, Wilson A, Allen E, Thalanany MM, Hibbert CL, Truesdale A, Clemens F, Cooper N, Firmin RK, Elbourne D; CESAR Trial Collaboration: Efficacy and economic assessment of conventional ventilatory support *versus* extracorporeal membrane oxygenation for severe adult respiratory failure (CESAR): A multicentre randomised controlled trial. Lancet 2009; 374:1351–63
10. Schmidt M, Hajage D, Lebreton G, Monsel A, Voiriot G, Levy D, Baron E, Beurton A, Chommeloux J, Meng P, Nemlaghi S, Bay P, Leprince P, Demoule A, Guidet B, Constantin JM, Fartoukh M, Dres M, Combes A; Groupe de Recherche Clinique en REanimation et Soins Intensifs du Patient en Insuffisance Respiratoire aiguE (GRC-RESPIRE) Sorbonne Université; Paris-Sorbonne ECMO-COVID Investigators: Extracorporeal membrane oxygenation for severe acute respiratory distress syndrome associated with COVID-19: A retrospective cohort study. Lancet Respir Med 2020; 8:1121–31
11. Yang X, Cai S, Luo Y, Zhu F, Hu M, Zhao Y, Zheng R, Li X, Hu B, Peng Z: Extracorporeal membrane oxygenation for coronavirus disease 2019–induced acute respiratory distress syndrome: A multicenter descriptive study. Crit Care Med 2020; 48:1289–95
12. Falcoz P-E, Monnier A, Puyraveau M, Perrier S, Ludes P-O, Olland A, Mertes P-M, Schneider F, Helms J, Meziani F: Extracorporeal membrane oxygenation for critically ill patients with COVID-19–related acute respiratory distress syndrome: Worth the effort? Am J Resp Crit Care 2020; 202:460–3
13. Mustafa AK, Alexander PJ, Joshi DJ, Tabachnick DR, Cross CA, Pappas PS, Tatooles AJ: Extracorporeal membrane oxygenation for patients with COVID-19 in severe respiratory failure. JAMA Surg 2020; 155:990–2
14. Barbaro RP, MacLaren G, Boonstra PS, Iwashyna TJ, Slutsky AS, Fan E, Bartlett RH, Tonna JE, Hyslop R, Fanning JJ, Rycus PT, Hyer SJ, Anders MM, Agerstrand CL, Hryniewicz K, Diaz R, Lorusso R, Combes A, Brodie D; Extracorporeal Life Support Organization: Extracorporeal membrane oxygenation support in COVID-19: An international cohort study of the Extracorporeal Life Support Organization registry. Lancet 2020; 396:1071–8
15. Shaefi S, Brenner SK, Gupta S, O'Gara BP, Krajewski ML, Charytan DM, Chaudhry S, Mirza SH, Peev V, Anderson M, Bansal A, Hayek SS, Srivastava A, Mathews KS, Johns TS, Leonberg-Yoo A, Green A, Arunthamakun J, Wille KM, Shaukat T, Singh H, Admon AJ, Semler MW, Hernán MA, Mueller AL, Wang W, Leaf DE; STOP-COVID Investigators: Extracorporeal membrane oxygenation in patients with severe respiratory failure from COVID-19. Intensive Care Med 2021; 47:208–21
16. Agence Régionale de Santé: Utilisation de l'ECMO Lors de la Prise en Charge des Patients COVID-19. Available at: https://www.iledefrance.ars.sante.fr/system/files/2020-12/038_ARSIdF-CRAPS_2020-12-02_Doctrine_ECMO.pdf. Accessed May 11, 2021.
17. Lebreton G, Schmidt M, Ponnaiah M, Folliguet T, Para M, Guihaire J, Lansac E, Sage E, Cholley B, Mégarbane B, Cronier P, Zarka J, Da Silva D, Besset S, Morichau-Beauchant T, Lacombat I, Mongardon N, Richard C, Duranteau J, Cerf C, Saiydoun G, Sonneville R, Chiche JD, Nataf P, Longrois D, Combes A, Leprince P; Paris ECMO-COVID-19 investigators: Extracorporeal membrane oxygenation network organisation and clinical outcomes during the COVID-19 pandemic in Greater Paris, France: A multicentre cohort study. Lancet Respir Med 2021; 9:851–62
18. Sinha P, Calfee CS, Beitler JR, Soni N, Ho K, Matthay MA, Kallet RH: Physiologic analysis and clinical performance of the ventilatory ratio in acute respiratory distress syndrome. Am J Respir Crit Care Med 2019; 199:333–41
19. Textor J, Zander B van der, Gilthorpe MS, Liśkiewicz M, Ellison GTH: Robust causal inference using directed acyclic graphs: The R package "DAGitty." Int J Epidemiol 2016; 45:1887–94
20. Lerman BJ, Popat RA, Assimes TL, Heidenreich PA, Wren SM: Association of left ventricular ejection fraction and symptoms with mortality after elective noncardiac surgery among patients with heart failure. JAMA 2019; 321:572–9

21. Williams EC, Motta-Ribeiro GC, Vidal Melo MF: Driving pressure and transpulmonary pressure: How do we guide safe mechanical ventilation? Anesthesiology 2019; 131:155–63
22. Tremblay A, Bandi V: Impact of body mass index on outcomes following critical care. Chest 2003; 123:1202–7
23. Faridi KF, Hennessey KC, Shah N, Soufer A, Wang Y, Sugeng L, Agarwal V, Sharma R, Sewanan LR, Hur DJ, Velazquez EJ, McNamara RL: Left ventricular systolic function and inpatient mortality in patients hospitalized with coronavirus disease 2019 (COVID-19). J Am Soc Echocardiogr 2020; 33:1414–5
24. Schmidt M, Bailey M, Sheldrake J, Hodgson C, Aubron C, Rycus PT, Scheinkestel C, Cooper DJ, Brodie D, Pellegrino V, Combes A, Pilcher D: Predicting survival after extracorporeal membrane oxygenation for severe acute respiratory failure: The Respiratory Extracorporeal Membrane Oxygenation Survival Prediction (RESP) score. Am J Respir Crit Care Med 2014; 189:1374–82
25. Meta-analysis Global Group in Chronic Heart Failure (MAGGIC): The survival of patients with heart failure with preserved or reduced left ventricular ejection fraction: An individual patient data meta-analysis. Eur Heart J 2012; 33:1750–7
26. Boëlle PY, Delory T, Maynadier X, Janssen C, Piarroux R, Pichenot M, Lemaire X, Baclet N, Weyrich P, Melliez H, Meybeck A, Lanoix JP, Robineau O: Trajectories of hospitalization in COVID-19 patients: An observational study in France. J Clin Med 2020; 9:E3148
27. Schmidt M, Zogheib E, Rozé H, Repesse X, Lebreton G, Luyt CE, Trouillet JL, Bréchot N, Nieszkowska A, Dupont H, Ouattara A, Leprince P, Chastre J, Combes A: The PRESERVE mortality risk score and analysis of long-term outcomes after extracorporeal membrane oxygenation for severe acute respiratory distress syndrome. Intensive Care Med 2013; 39:1704–13
28. Roch A, Hraiech S, Masson E, Grisoli D, Forel JM, Boucekine M, Morera P, Guervilly C, Adda M, Dizier S, Toesca R, Collart F, Papazian L: Outcome of acute respiratory distress syndrome patients treated with extracorporeal membrane oxygenation and brought to a referral center. Intensive Care Med 2014; 40:74–83
29. Susen S, Tacquard CA, Godon A, Mansour A, Garrigue D, Nguyen P, Godier A, Testa S, Levy JH, Albaladejo P, Gruel Y; GIHP and GFHT: Prevention of thrombotic risk in hospitalized patients with COVID-19 and hemostasis monitoring. Crit Care 2020; 24:364
30. Tacquard C, Mansour A, Godon A, Godet J, Poissy J, Garrigue D, Kipnis E, Hamada SR, Mertes PM, Steib A, Ulliel-Roche M, Bouhemad B, Nguyen M, Reizine F, Gouin-Thibault I, Besse MC, Collercandy N, Mankikian S, Levy JH, Gruel Y, Albaladejo P, Susen S, Godier A: Impact of high dose prophylactic anticoagulation in critically ill patients with COVID-19 pneumonia. Chest 2021; 159:2417–27
31. Grasselli G, Scaravilli V, Mangioni D, Scudeller L, Alagna L, Bartoletti M, Bellani G, Biagioni E, Bonfanti P, Bottino N, Coloretti I, Cutuli SL, De Pascale G, Ferlicca D, Fior G, Forastieri A, Franzetti M, Greco M, Guzzardella A, Linguadoca S, Meschiari M, Messina A, Monti G, Morelli P, Muscatello A, Redaelli S, Stefanini F, Tonetti T, Antonelli M, Cecconi M, Foti G, Fumagalli R, Girardis M, Ranieri M, Viale P, Raviglione M, Pesenti A, Gori A, Bandera A: Hospital-acquired infections in critically ill patients with COVID-19. Chest 2021; 160:454–65
32. Santis VD, Corona A, Vitale D, Nencini C, Potalivo A, Prete A, Zani G, Malfatto A, Tritapepe L, Taddei S, Locatelli A, Sambri V, Fusari M, Singer M: Bacterial infections in critically ill patients with SARS-2-COVID-19 infection: Results of a prospective observational multicenter study. Infection 2022: 50:139–48
33. Thomas G, Hraiech S, Cassir N, Lehingue S, Rambaud R, Wiramus S, Guervilly C, Klasen F, Adda M, Dizier S, Roch A, Papazian L, Forel JM: Venovenous extracorporeal membrane oxygenation devices-related colonisations and infections. Ann Intensive Care 2017; 7:111
34. Bréchot N, Mastroianni C, Schmidt M, Santi F, Lebreton G, Hoareau AM, Luyt CE, Chommeloux J, Rigolet M, Lebbah S, Hekimian G, Leprince P, Combes A: Retrieval of severe acute respiratory failure patients on extracorporeal membrane oxygenation: Any impact on their outcomes? J Thorac Cardiovasc Surg 2018; 155:1621–1629.e2

Appendix: ECMOSARS Investigators

Marc Pierrot, M.D., University Hospital of Angers, Angers, France, collected data, provided and cared for study patients
Sidney Chocron, M.D., Ph.D., University Hospital of Besançon, Besançon, France, collected data, provided and cared for study patients
Guillaume Flicoteaux, M.D., University Hospital of Besançon, Besançon, France, collected data, provided and cared for study patients
Philippe Mauriat, M.D., University Hospital of Bordeaux, Bordeaux, France, critically reviewed the study proposal
Hadrien Roze, M.D., University Hospital of Bordeaux, Bordeaux, France, collected data, provided and cared for study patients
Olivier Huet, M.D., Ph.D., University Hospital of Brest, Brest, France, collected data, provided and cared for study patients
Marc-Olivier Fischer, M.D., Ph.D., University Hospital of Caen, Caen, France, collected data, provided and cared for study patients
Claire Alessandri, M.D., Public Public Assistance-Hospitals of Paris, University Hospital Henri Mondor, Créteil, France, provided and cared for study patients
Raphel Bellaïche, M.D., Public Assistance-Hospitals of Paris, University Hospital Henri Mondor, Créteil, France, provided and cared for study patients

Ophélie Constant, M.D., Public Assistance-Hospitals of Paris, University Hospital Henri Mondor, Créteil, France, provided and cared for study patients
Quentin de Roux, M.D., Public Assistance-Hospitals of Paris, University Hospital Henri Mondor, Créteil, France, provided and cared for study patients
André Ly, M.D., Public Assistance-Hospitals of Paris, University Hospital Henri Mondor, Créteil, France, provided and cared for study patients
Arnaud Meffert, M.D., Public Assistance-Hospitals of Paris, University Hospital Henri Mondor, Créteil, France, provided and cared for study patients
Jean-Claude Merle, M.D., Public Assistance-Hospitals of Paris, University Hospital Henri Mondor, Créteil, France, provided and cared for study patients
Lucile Picard, M.D., Public Assistance-Hospitals of Paris, University Hospital Henri Mondor, Créteil, France, provided and cared for study patients
Elena Skripkina, M.D, Public Assistance-Hospitals of Paris, University Hospital Henri Mondor, Créteil, France, provided and cared for study patients
Thierry Folliguet, M.D., Ph.D., Public Assistance-Hospitals of Paris, University Hospital Henri Mondor, Créteil, France, provided and cared for study patients
Antonio Fiore, M.D., Public Assistance-Hospitals of Paris, University Hospital Henri Mondor, Créteil, France, provided and cared for study patients
Nicolas d'Ostrevy, M.D., University Hospital of Clermont-Ferrand, collected data, provided and cared for study patients
Marie-Catherine Morgan, M.D., University Hospital of Dijon, Dijon, France, collected data, provided and cared for study patients
Maxime Nguyen, M.D., University Hospital of Dijon, Dijon, France, collected data, provided and cared for study patients
Lucie Gaide-Chevronnay, M.D., University Hospital of Grenoble, Grenoble, France, collected data, provided and cared for study patients
Nicolas Terzi, M.D., Ph.D., University Hospital of Grenoble, Grenoble, France,
collected data, provided and cared for study patients
Gwenhaël Colin, M.D.,Vendée Hospital, La Roche-sur-Yon, France, collected data, provided and cared for study patients
Olivier Fabre, M.D., Hospital of Lens, Lens, France, collected data, provided and cared for study patients
Arash Astaneh, M.D., Marie-Lannelongue Hospital, Le Plessis-Robinson, France, collected data, provided and cared for study patients
Justin Issard, M.D., Marie-Lannelongue Hospital, Le Plessis-Robinson, France, collected data, provided and cared for study patients
Elie Fadel, M.D., Ph.D., Marie-Lannelongue Hospital, Le Plessis-Robinson, France, collected data, provided and cared for study patients
Dominique Fabre, M.D., Marie-Lannelongue Hospital, Le Plessis-Robinson, France, collected data, provided and cared for study patients
Antoine Girault, M.D., Marie-Lannelongue Hospital, Le Plessis-Robinson, France, collected data, provided and cared for study patients
Iolande Ion, M.D., Marie-Lannelongue Hospital, Le Plessis-Robinson, France, collected data, provided and cared for study patients
Jean Baptiste Menager, M.D., Marie-Lannelongue Hospital, Le Plessis-Robinson, France, collected data, provided and cared for study patients
Delphine Mitilian, M.D., Marie-Lannelongue Hospital, Le Plessis-Robinson, France, collected data, provided and cared for study patients
Olaf Mercier, M.D., Ph.D., Marie-Lannelongue Hospital, Le Plessis-Robinson, France, collected data, provided and cared for study patients
François Stephan, M.D., Marie-Lannelongue Hospital, Le Plessis-Robinson, France, collected data, provided and cared for study patients
Jacques Thes, M.D., Marie-Lannelongue Hospital, Le Plessis-Robinson, France, collected data, provided and cared for study patients
Jerôme Jouan, M.D., University Hospital of Limoges, Limoges, France, collected data, provided and cared for study patients
Thibault Duburcq, M.D., University Hospital of Lille, Lille, France, collected data, provided and cared for study patients
Valentin Loobuyck, M.D., University Hospital of Lille, Lille, France, collected data, provided and cared for study patients
Sabrina Manganiello, M.D., University Hospital of Lille, Lille, France, collected data, provided and cared for study patients
Mouhammed Moussa, M.D., University Hospital of Lille, Lille, France, collected data, provided and cared for study patients
Agnes Mugnier, M.D., University Hospital of Lille, Lille, France, collected data, provided and cared for study patients
Natacha Rousse, M.D., University Hospital of Lille, Lille, France, collected data, provided and cared for study patients
Olivier Desebbe, M.D., Clinique de la Sauvegarde, Lyon, France, collected data, provided and cared for study patients
Roland Henaine, M.D., Ph.D., Hospices Civils de Lyon, Lyon, France, critically reviewed the study proposal, provided and cared for study patients
Matteo Pozzi, M.D, Hospices Civils de Lyon, Lyon, France, collected data, provided and cared for study patients
Jean-Christophe Richard, M.D., Ph.D., Hospices Civils de Lyon, Lyon, France, collected data, provided and cared for study patients
Zakaria Riad, M.D., Hospices Civils de Lyon, Lyon, France, collected data, provided and cared for study patients
Christophe Guervilly, M.D., North Hospital, Marseille Public University Hospital System, Marseille, France, collected data, provided and cared for study patients
Sami Hraiech, M.D., North Hospital, Marseille Public University Hospital System, Marseille, France, collected data, provided and cared for study patients

Laurent Papazian, M.D., Ph.D., North Hospital, Marseille Public University Hospital System, Marseille, France, collected data, provided and cared for study patients
Matthias Castanier, M.D., European Hospital, Marseille, France, collected data, provided and cared for study patients
Charles Chanavaz, M.D., Clairval Hospital, Marseille, France, collected data, provided and cared for study patients
Sebastien Gette, M.D., Regional Hospital of Metz-Thionville, Metz-Thionville, France, provided and cared for study patients
Guillaume Louis, M.D., Regional Hospital of Metz-Thionville, Metz-Thionville, France, provided and cared for study patients
Erick Portocarrero, M.D., Regional Hospital of Metz-Thionville, Metz-Thionville, France, provided and cared for study patients
Nicolas Bischoff, M.D., Emile Muller Hospital, Mulhouse, France, collected data, provided and cared for study patients
Antoine Kimmoun, M.D., Ph.D., University Hospital of Nancy, Nancy, France, collected data, provided and cared for study patients
Mathieu Mattei, M.D., University Hospital of Nancy, Nancy, France, collected data, provided and cared for study patients
Pierre Perez, M.D., University Hospital of Nancy, Nancy, France, collected data, provided and cared for study patients
Alexandre Bourdiol, M.D., University Hospital of Nantes, Nantes, France, collected data, provided and cared for study patients
Yannick Hourmant, M.D., University Hospital of Nantes, Nantes, France, collected data, provided and cared for study patients
Pierre-Joachim Mahé, M.D., University Hospital of Nantes, Nantes, France, collected data, provided and cared for study patients
Bertrand Rozec, M.D., Ph.D., University Hospital of Nantes, Nantes, France, collected data, provided and cared for study patients
Mickaël Vourc'h, M.D., University Hospital of Nantes, Nantes, France, collected data, provided and cared for study patients
Stéphane Aubert, M.D., Ambroise Paré Hospital, Neuilly-sur-Seine, France, collected data, provided and cared for study patients
Florian Bazalgette, M.D., University Hospital of Nîmes, Nîmes, France, collected data, provided and cared for study patients
Claire Roger, M.D., University Hospital of Nîmes, Nîmes, France, collected data, provided and cared for study patients
Pierre Jaquet, M.D., Public Assistance-Hospitals of Paris, Bichat-Claude Bernard Hospital, Paris University Hospital, Paris, France, provided and cared for study patients
Brice Lortat-Jacob, M.D., Public Assistance-Hospitals of Paris, Bichat-Claude Bernard Hospital, Paris University Hospital, Paris, France, provided and cared for study patients
Pierre Mordant, M.D., Ph.D., Public Assistance-Hospitals of Paris, Bichat-Claude Bernard Hospital, Paris University Hospital, Paris, France, provided and cared for study patients
Patrick Nataf, M.D., Ph.D., Public Assistance-Hospitals of Paris, Bichat-Claude Bernard Hospital, Paris University Hospital, Paris, France, provided and cared for study patients
Juliette Patrier, M.D., Bichat-Claude Bernard Hospital, Paris University Hospital, Paris, France, provided and cared for study patients
Morgan Roué, M.D., Public Assistance-Hospitals of Paris, Bichat-Claude Bernard Hospital, Paris University Hospital, Paris, France, provided and cared for study patients
Romain Sonneville, M.D., Ph.D., Public Assistance-Hospitals of Paris, Bichat-Claude Bernard Hospital, Paris University Hospital, Paris, France, provided and cared for study patients
Alexy Tran-Dinh, M.D., Bichat-Claude Bernard Hospital, Paris University Hospital, Paris, France, provided and cared for study patients
Paul-Henri Wicky, M.D., Public Assistance-Hospitals of Paris, Bichat-Claude Bernard Hospital, Paris University Hospital, Paris, France, provided and cared for study patients
Charles Al Zreibi, M.D., Public Assistance-Hospitals of Paris, European Hospital Georges Pompidou–Paris University Hospital, Paris, France, collected data, provided and cared for study patients
Bernard Cholley, M.D., Ph.D., Public Assistance-Hospitals of Paris, European Hospital Georges Pompidou–Paris University Hospital, Paris, France, collected data, provided and cared for study patients
Yannis Guyonvarch, M.D., Public Assistance-Hospitals of Paris, European Hospital Georges Pompidou–Paris University Hospital, Paris, France, collected data, provided and cared for study patients
Sophie Hamada, M.D., Public Assistance-Hospitals of Paris, European Hospital Georges Pompidou–Paris University Hospital, Paris, France, collected data, provided and cared for study patients
Claudio Barbanti, M.D., Public Assistance-Hospitals of Paris University Hospital, Paris, France, collected data, provided and cared for study patients
Anatole Harrois, M.D., Public Assistance-Hospitals of Paris Le Kremlin-Bicêtre, Paris University Hospital, Paris, France, collected data, provided and cared for study patients
Jordi Matiello, M.D., Public Assistance-Hospitals of Paris Le Kremlin-Bicêtre, Paris University Hospital, Paris, France, collected data, provided and cared for study patients
Thomas Kerforne, M.D., University Hospital of Poitiers, Poitiers, France, collected data, provided and cared for study patients
Nicolas Brechot, M.D., Public Assistance-Hospitals of Paris, Sorbonne University, La Pitié-Salpêtrière Hospital, Paris, France, collected data, provided and cared for study patients
Alain Combes, M.D., Ph.D., Public Assistance-Hospitals of Paris, Sorbonne University, La Pitié-Salpêtrière Hospital, Paris, France, collected data, provided and cared for study patients

Jean Michel Constantin, M.D., Ph.D., Public Assistance-Hospitals of Paris, Sorbonne University, La Pitié-Salpêtrière Hospital, Paris, France, collected data, provided and cared for study patients

Cosimo D'Alessandro, M.D., Public Assistance-Hospitals of Paris, Sorbonne University, La Pitié-Salpêtrière Hospital, Paris, France, collected data, provided and cared for study patients

Pierre Demondion, M.D., Public Assistance-Hospitals of Paris, Sorbonne University, La Pitié-Salpêtrière Hospital, Paris, France, collected data, provided and cared for study patients

Alexandre Demoule, M.D., Public Assistance-Hospitals of Paris, Sorbonne University, La Pitié-Salpêtrière Hospital, Paris, France, collected data, provided and cared for study patients

Martin Dres, M.D., Public Assistance-Hospitals of Paris, Sorbonne University, La Pitié-Salpêtrière Hospital, Paris, France, collected data, provided and cared for study patients

Muriel Fartoukh, M.D., Public Assistance-Hospitals of Paris, Sorbonne University, La Pitié-Salpêtrière Hospital, Paris, France, collected data, provided and cared for study patients

Guillaume Hekimian, M.D., Public Assistance-Hospitals of Paris, Sorbonne University, La Pitié-Salpêtrière Hospital, Paris, France, collected data, provided and cared for study patients

Charles Juvin, M.D., Public Assistance-Hospitals of Paris, Sorbonne University, La Pitié-Salpêtrière Hospital, Paris, France, collected data, provided and cared for study patients

Pascal Leprince, M.D., Ph.D., Public Assistance-Hospitals of Paris, Sorbonne University, La Pitié-Salpêtrière Hospital, Paris, France, collected data, provided and cared for study patients

David Levy, M.D., Public Assistance-Hospitals of Paris, Sorbonne University, La Pitié-Salpêtrière Hospital, Paris, France, collected data, provided and cared for study patients

Charles Edouard Luyt, M.D., Ph.D., Public Assistance-Hospitals of Paris, Sorbonne University, La Pitié-Salpêtrière Hospital, Paris, France, collected data, provided and cared for study patients

Marc Pineton de Chambrun, M.D., Public Assistance-Hospitals of Paris, Sorbonne University, La Pitié-Salpêtrière Hospital, Paris, France, collected data, provided and cared for study patients

Matthieu Schmidt, M.D., Ph.D., Public Assistance-Hospitals of Paris, Sorbonne University, La Pitié-Salpêtrière Hospital, Paris, France, collected data, provided and cared for study patients

Thibaut Schoell, M.D., Public Assistance-Hospitals of Paris, Sorbonne University, La Pitié-Salpêtrière Hospital, Paris, France, collected data, provided and cared for study patients

Pierre Fillâtre, M.D., Ph.D., Hospital of Saint-Brieuc, Saint-Brieuc, France, collected data, provided and cared for study patients

Nicolas Massart, M.D., Hospital of Saint-Brieuc, Saint-Brieuc, France, collected data, provided and cared for study patients

Roxane Nicolas, M.D., University Hospital of Saint-Etienne, Saint-Etienne, France, collected data, provided and cared for study patients

Maud Jonas, M.D., Saint-Nazaire Hospital, Saint-Nazaire, France, collected data, provided and cared for study patients

Charles Vidal, M.D., University Hospital of Saint-Denis, La Réunion, Saint-Denis, France, collected data, provided and cared for study patients

Salvatore Muccio, M.D., University Hospital of Reims, Reims, France, collected data, provided and cared for study patients

Dario Di Perna, M.D., University Hospital of Reims, Reims, France, collected data, provided and cared for study patients

Bruno Mourvillier, M.D., Ph.D., University Hospital of Reims, Reims, France, collected data, provided and cared for study patients

Amedeo Anselmi, M.D., Ph.D., University Hospital of Rennes, Rennes, France, provided and cared for study patients

Karl Bounader, M.D., University Hospital of Rennes, Rennes, France, provided and cared for study patients

Maxime Esvan, M.Sc., University Hospital of Rennes, Rennes, France, performed statistical analysis

Claire Fougerou-Leurent, Pharm.D., University Hospital of Rennes, Rennes, France, critically reviewed the study proposal

Yoann Launey, M.D., Ph.D., University Hospital of Rennes, Rennes, France, provided and cared for study patients

Thomas Lebouvier, M.D., University Hospital of Rennes, Rennes, France, provided and cared for study patients

Alessandro Parasido, University Hospital of Rennes, Rennes, France, provided and cared for study patients

Florian Reizine, M.D., University Hospital of Rennes, Rennes, France, provided and cared for study patients

Philippe Seguin, M.D., Ph.D., University Hospital of Rennes, Rennes, France, provided and cared for study patients

Emmanuel Besnier, M.D., University Hospital of Rouen, Rouen, France, collected data, provided and cared for study patients

Dorothée Carpentier, M.D., University Hospital of Rouen, Rouen, France, collected data, provided and cared for study patients

Anne Olland, M.D., Ph.D., University Hospital of Strasbourg, Strasbourg, France, collected data, provided and cared for study patients

Marion Villard, M.D., University Hospital of Strasbourg, Strasbourg, France, collected data, provided and cared for study patients

Fanny Bounes, M.D., University Hospital of Toulouse, Toulouse, France, collected data, provided and cared for study patients

Vincent Minville, M.D., Ph.D., University Hospital of Toulouse, Toulouse, France, collected data, provided and cared for study patients
Antoine Guillon, M.D., University Hospital of Tours, Tours, France, collected data, provided and cared for study patients
Yannick Fedun, M.D., Bretagne Atlantique Hospital, Vannes, France, collected data, provided and cared for study patients
James T. Ross, M.D., University of California Davis, Sacramento, California, provided critical revisions of the manuscript

ANESTHESIOLOGY REFLECTIONS FROM THE WOOD LIBRARY-MUSEUM

The Stars Align in Support of Morton's "Anaesthesia"

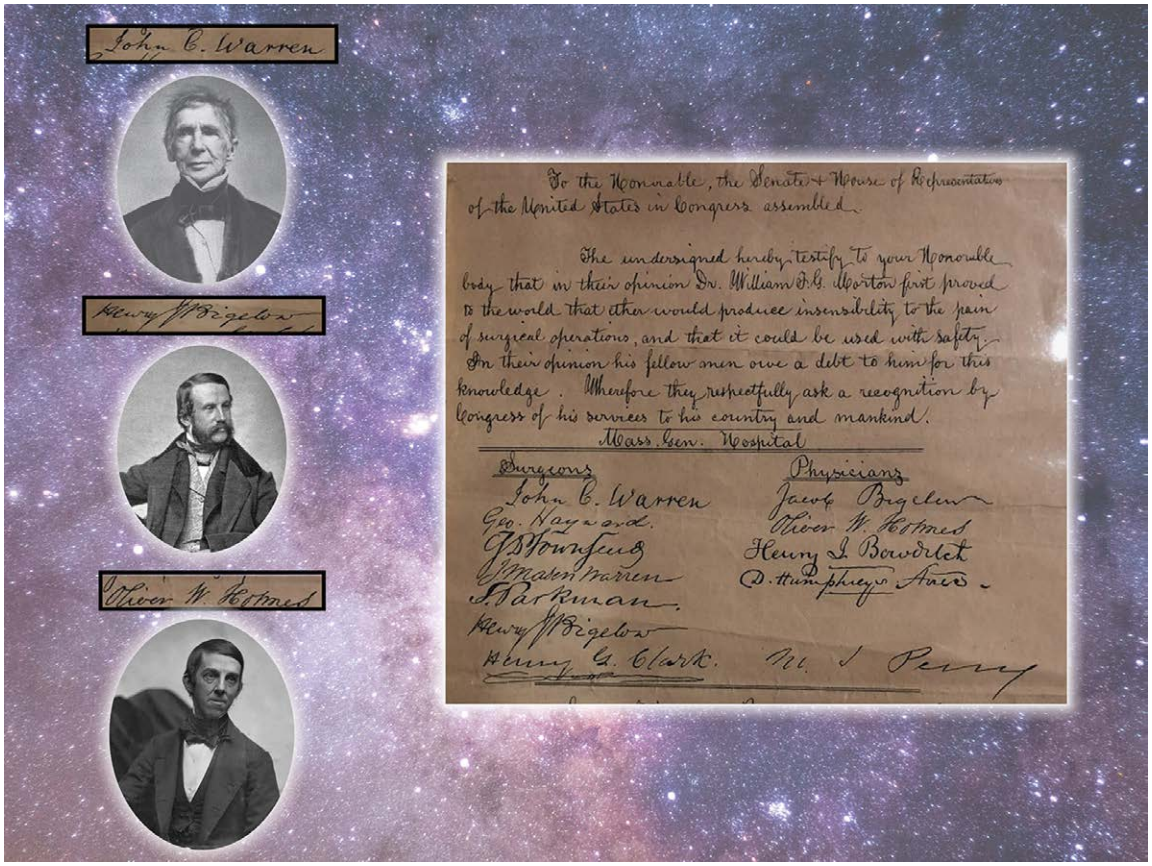

"Never before…did such a brilliant galaxy of medical and surgical talent unite on any one measure." Penned by the brightest stars of Massachusetts General Hospital in 1852, a petition to the United States Congress (*right*) shined a favorable light on Morton, who in a quest for recognition had ignited a national controversy over primacy for the discovery of surgical anesthesia. These medical luminaries declared "that, in their opinion, Dr. William T.G. Morton first proved to the world that ether would produce insensibility to the pain of surgical operations… [and asked for] recognition by [U.S.] Congress of his services to his country and mankind." Among these leading lights were John C. Warren, M.D. (*upper left*), founding father of Massachusetts General Hospital and senior surgeon on Ether Day; Henry J. Bigelow, M.D. (*middle left*), surgeon and organizer of that celebrated day; and Oliver W. Holmes, M.D. (*lower left*), physician-poet who bestowed the name "anaesthesia" onto this new discovery. Whether this was a true endorsement of Morton or the medical discovery that elevated surgical practice may be lost among the stars. (Copyright © the American Society of Anesthesiologists' Wood Library-Museum of Anesthesiology. www.woodlibrarymuseum.org)

Melissa L. Coleman, M.D., Assistant Professor, Department of Anesthesiology and Perioperative Medicine, Penn State College of Medicine, Hershey, Pennsylvania.

Vincent Minville, M.D., Ph.D., University Hospital of Toulouse, Toulouse, France, collected data, provided and cared for study patients
Antoine Guillon, M.D., University Hospital of Tours, Tours, France, collected data, provided and cared for study patients
Yannick Fedun, M.D., Bretagne Atlantique Hospital, Vannes, France, collected data, provided and cared for study patients
James T. Ross, M.D., University of California Davis, Sacramento, California, provided critical revisions of the manuscript

ANESTHESIOLOGY REFLECTIONS FROM THE WOOD LIBRARY-MUSEUM

The Stars Align in Support of Morton's "Anaesthesia"

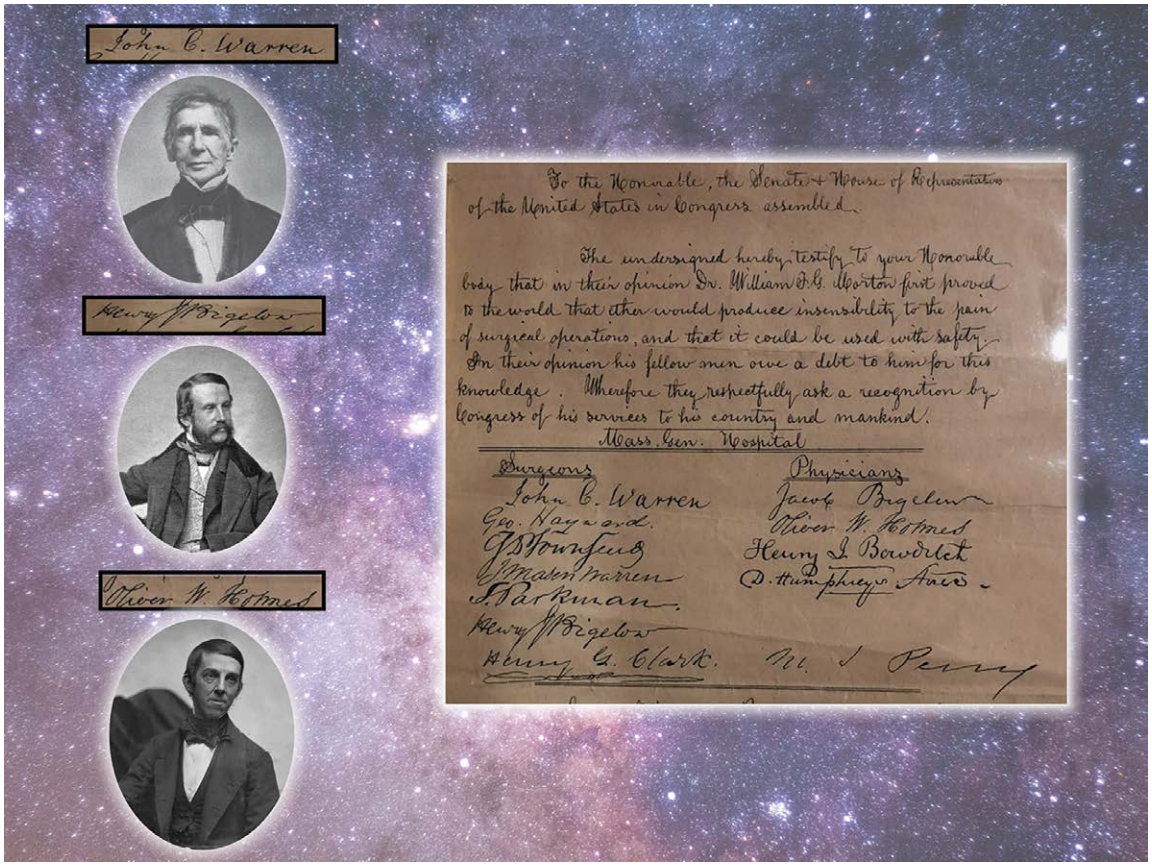

"Never before…did such a brilliant galaxy of medical and surgical talent unite on any one measure." Penned by the brightest stars of Massachusetts General Hospital in 1852, a petition to the United States Congress (*right*) shined a favorable light on Morton, who in a quest for recognition had ignited a national controversy over primacy for the discovery of surgical anesthesia. These medical luminaries declared "that, in their opinion, Dr. William T.G. Morton first proved to the world that ether would produce insensibility to the pain of surgical operations… [and asked for] recognition by [U.S.] Congress of his services to his country and mankind." Among these leading lights were John C. Warren, M.D. (*upper left*), founding father of Massachusetts General Hospital and senior surgeon on Ether Day; Henry J. Bigelow, M.D. (*middle left*), surgeon and organizer of that celebrated day; and Oliver W. Holmes, M.D. (*lower left*), physician-poet who bestowed the name "anaesthesia" onto this new discovery. Whether this was a true endorsement of Morton or the medical discovery that elevated surgical practice may be lost among the stars. (Copyright © the American Society of Anesthesiologists' Wood Library-Museum of Anesthesiology. www.woodlibrarymuseum.org)

Melissa L. Coleman, M.D., Assistant Professor, Department of Anesthesiology and Perioperative Medicine, Penn State College of Medicine, Hershey, Pennsylvania.

ANESTHESIOLOGY

Early Restrictive Fluid Strategy Impairs the Diaphragm Force in Lambs with Acute Respiratory Distress Syndrome

Marloes M. Ijland, M.D., Saranke A. Ingelse, M.D., Ph.D., Lex M. van Loon, M.Sc., Ph.D., Merijn van Erp, M.Sc., Benno Kusters, M.D., Ph.D., Coen A. C. Ottenheijm, Ph.D., Matthijs Kox, Ph.D., Johannes G. van der Hoeven, M.D., Ph.D., Leo M. A. Heunks, M.D., Ph.D., Joris Lemson, M.D., Ph.D.

ANESTHESIOLOGY 2022; 136:749–62

EDITOR'S PERSPECTIVE

What We Already Know about This Topic

- Clinical data suggest improved outcome with a restrictive fluid protocol in adults suffering from acute respiratory distress syndrome; due to very limited data, it is unclear whether this also applies to pediatric acute respiratory distress syndrome
- The effects of fluid management on diaphragmatic function in pediatric acute respiratory distress syndrome, a key factor in successful ventilator weaning, are unknown

What This Article Tells Us That Is New

- Using an ovine model of pediatric acute respiratory distress syndrome with lung-protective ventilation, the authors compared a strict restrictive fluid strategy with norepinephrine to a liberal fluid strategy over a 6-h period evaluating transdiaphragmatic pressure over a wide range of positive end-expiratory pressure levels along with evaluation of diaphragm microcirculation, histology, and biomarkers reflective of inflammation and oxidative stress
- Baseline measurements of transdiaphragmatic pressures before lung injury showed an inverse relationship with increasing positive end-expiratory pressure
- Fluid restriction significantly reduced transdiaphragmatic pressures at positive end-expiratory pressure levels of 5 and 10 cm H_2O but not at 15 or 20 cm H_2O
- Microvessel density was significantly reduced, although the histology and markers of inflammation and oxidative stress were not affected

ABSTRACT

Background: The effect of fluid management strategies in critical illness–associated diaphragm weakness are unknown. This study hypothesized that a liberal fluid strategy induces diaphragm muscle fiber edema, leading to reduction in diaphragmatic force generation in the early phase of experimental pediatric acute respiratory distress syndrome in lambs.

Methods: Nineteen mechanically ventilated female lambs (2 to 6 weeks old) with experimental pediatric acute respiratory distress syndrome were randomized to either a strict restrictive fluid strategy with norepinephrine or a liberal fluid strategy. The fluid strategies were maintained throughout a 6-h period of mechanical ventilation. Transdiaphragmatic pressure was measured under different levels of positive end-expiratory pressure (between 5 and 20 cm H_2O). Furthermore, diaphragmatic microcirculation, histology, inflammation, and oxidative stress were studied.

Results: Transdiaphragmatic pressures decreased more in the restrictive group (–9.6 cm H_2O [95% CI, –14.4 to –4.8]) compared to the liberal group (–0.8 cm H_2O [95% CI, –5.8 to 4.3]) during the application of 5 cm H_2O positive end-expiratory pressure ($P = 0.016$) and during the application of 10 cm H_2O positive end-expiratory pressure (–10.3 cm H_2O [95% CI, –15.2 to –5.4] *vs.* –2.8 cm H_2O [95% CI, –8.0 to 2.3]; $P = 0.041$). In addition, diaphragmatic microvessel density was decreased in the restrictive group compared to the liberal group (34.0 crossings [25th to 75th percentile, 22.0 to 42.0] *vs.* 46.0 [25th to 75th percentile, 43.5 to 54.0]; $P = 0.015$). The application of positive end-expiratory pressure itself decreased the diaphragmatic force generation in a dose-related way; increasing positive end-expiratory pressure from 5 to 20 cm H_2O reduced transdiaphragmatic pressures with 27.3% (17.3 cm H_2O [95% CI, 14.0 to 20.5] at positive end-expiratory pressure 5 cm H_2O *vs.* 12.6 cm H_2O [95% CI, 9.2 to 15.9] at positive end-expiratory pressure 20 cm H_2O; $P < 0.0001$). The diaphragmatic histology, markers for inflammation, and oxidative stress were similar between the groups.

Conclusions: Early fluid restriction decreases the force-generating capacity of the diaphragm and diaphragmatic microcirculation in the acute phase of pediatric acute respiratory distress syndrome. In addition, the application of positive end-expiratory pressure decreases the force-generating capacity of the diaphragm in a dose-related way. These observations provide new insights into the mechanisms of critical illness–associated diaphragm weakness.

(ANESTHESIOLOGY 2022; 136:749–62)

Critical illness–associated diaphragm weakness develops in the majority of mechanically ventilated critically ill patients and may be associated with difficult weaning, prolonged duration of mechanical ventilation, and even an increase in mortality.[1–5] In addition to mechanical ventilation, other risk factors for this phenomenon have been identified.[6] However, the effects of fluids have not been described in the literature so far. This seems remarkable as fluid resuscitation remains the cornerstone in hemodynamic resuscitation in critically ill children. Therefore, to clarify the mechanism involved in critical illness–associated diaphragm dysfunction, the role of fluids in diaphragm function needs to be investigated.

In mechanically ventilated children with pediatric acute respiratory distress syndrome (ARDS), hemodynamic

<zdoi;. DOI: 10.1097/ALN.0000000000004162>

instability may develop due to an increased pulmonary vascular resistance and the application of high positive end-expiratory pressure (PEEP) with subsequent negative effects on the venous return. This is often counteracted by fluid loading using intravenous fluids.[7] However, an association between fluid overload in the first few days of pediatric ARDS and deterioration of oxygenation due to alveolar edema and adverse outcomes, such as fewer ventilator-free days, have been reported.[8–11] In adults with ARDS, early fluid restriction seems beneficial with regard to lung function, ventilator-free days, and organ failure–free days.[12] Recently, a delay in weaning from the ventilator and an inability to ambulate at hospital discharge have been described in survivors of septic shock with volume overload.[13] The question of by what mechanism fluid overload might influence this outcome remains unanswered. It has been hypothesized that changes at the cellular level, such as edema of skeletal myocytes, swelling of mitochondria in skeletal muscle fibers, and endomysial edema, may contribute to muscle fiber damage, indirectly influencing muscle force.[14,15] In addition, as fluids might also exert their effects on the microcirculation,[16] their effect on the diaphragm microcirculation is of interest but unknown so far.

We developed an experimental animal model of pediatric ARDS in which we assessed the early effects of a restrictive *versus* a liberal fluid strategy on diaphragmatic function. We hypothesized that a liberal fluid strategy induces edema formation of diaphragm muscle fibers, leading to a reduction in diaphragmatic force–generating capacity.

Materials and Methods

This study was part of an extensive experiment with the same research design but with different research questions all focused on the cardiopulmonary effects of fluid strategy during experimental pediatric ARDS.[17] The current study focused on the effects of a restrictive fluid strategy *versus* a liberal fluid strategy on diaphragm structure and function. The effect of a contraction stimulus on the transdiaphragmatic pressures and the formation of diaphragmatic muscle fiber edema were the primary outcomes. Secondary outcomes were changes in diaphragmatic microcirculation, inflammation, and oxidative stress and the direct effect of the application of PEEP on the transdiaphragmatic pressures.

Procedures involving animal data, anesthetics, mechanical ventilation, and surgical techniques were performed in accordance with previously described methods.[17] See appendix in the Supplemental Digital Content 1 (http://links.lww.com/ALN/C802) for further details. Experimental details concerning the current study are mentioned separately in this article.

Ethical Statement

This study was approved by the local ethics committee on animal research of the Radboud University Medical Center (Nijmegen, The Netherlands; license No. RU-DEC 2016-0089) and was performed in accordance with the Dutch and European legal requirements on the use and protection of laboratory animals. The experimental procedures were designed to minimize the number of animals used, as well as to minimize animal suffering. The Animal Research: Reporting of *In Vivo* Experiments (ARRIVE) guidelines for animal research were followed.[18]

Animals

Twenty-one female lambs with a mean weight of 12.7 kg (95% CI, 10.6 to 14.8) and approximately 2 to 6 weeks of age were studied. The lambs were of the Texelaar–Flevolander breed, except one that was a Romanov lamb due to unavailability of a Texelaar–Flevolander lamb. Only female lambs were used as precise urine production monitoring (in the context of fluid balance) was important for this study, and urethral catheterization is more difficult in male lambs.

Instrumentation and Data Acquisition

Force-generating Capacity of the Diaphragm. For the estimation of pleural pressure,[19] an air-filled balloon catheter (5-French, Cooper Surgical, USA) was positioned in the esophagus. Catheter positioning and validation were performed according to a recent consensus statement.[20] Briefly,

This article is featured in "This Month in Anesthesiology," page A1. This article is accompanied by an editorial on p. 672. Supplemental Digital Content is available for this article. Direct URL citations appear in the printed text and are available in both the HTML and PDF versions of this article. Links to the digital files are provided in the HTML text of this article on the Journal's Web site (www.anesthesiology.org). This article has a video abstract. This article has a visual abstract available in the online version.

Submitted for publication July 8, 2021. Accepted for publication January 31, 2022. Published online first on March 23, 2022.

Marloes M. Ijland, M.D.: Department of Intensive Care Medicine, Radboud Institute for Health Sciences, Radboud University Medical Center, Nijmegen, The Netherlands.

Saranke A. Ingelse, M.D., Ph.D.: Department of Pediatric Intensive Care, Emma Children's Hospital, Amsterdam University Medical Center, University of Amsterdam, Amsterdam, The Netherlands.

Lex. M. van Loon, M.Sc., Ph.D.: Cardiovascular and Respiratory Physiology Group, Faculty of Science and Technology, Technical Medical Centre, University of Twente, Enschede, The Netherlands.

Merijn van Erp, M.Sc.: Technology Center of Microscopy, Radboud University Medical Center, Nijmegen, The Netherlands.

Benno Kusters, M.D., Ph.D.: Department of Pathology, Radboud University Medical Center, Nijmegen, The Netherlands.

Coen A. C. Ottenheijm, Ph.D.: Department of Physiology, Amsterdam University Medical Center, Amsterdam, The Netherlands.

Matthijs Kox, Ph.D.: Department of Intensive Care Medicine, Radboud Institute for Health Sciences; and Radboud Center for Infectious Diseases, Radboud University Medical Center, Nijmegen, The Netherlands.

Johannes G. van der Hoeven, M.D., Ph.D.: Department of Intensive Care Medicine, Radboud Institute for Health Sciences, Radboud University Medical Center, Nijmegen, The Netherlands.

Leo M. A. Heunks, M.D., Ph.D.: Department of Intensive Care Medicine, Erasmus Medical Center, Rotterdam, The Netherlands.

Joris Lemson, M.D., Ph.D.: Department of Intensive Care Medicine, Radboud Institute for Health Sciences, Radboud University Medical Center, Nijmegen, The Netherlands.

after positioning, the balloon was inflated with 1 ml of air.[21–23] The intragastric position of the balloon was confirmed by the visualization of positive deflections of balloon pressure during external compression of the left upper abdominal quadrant. Subsequently, the catheter was withdrawn until cardiac artefacts appeared on the pressure tracings, indicating that the balloon was placed in the lower third of the esophagus.

Equilibration of the system with ambient pressure was performed before each measurement (at baseline and after 6 h). To validate the correct position of the balloon, a dynamic occlusion test was performed. This was performed by measuring the ratio of change in esophageal pressure (ΔP_{eso}) to the change in airway opening pressure (ΔP_{aw}) during three spontaneous inspiratory efforts against a closed airway at end expiration. Catheter inflation was acceptable if $\Delta P_{es}/\Delta P_{aw}$ ratio was between 0.8 and 1.2.[19,24]

Via a small laparotomy of 1 to 2 cm, a second pressure balloon catheter (5-French, Cooper Surgical, USA) was placed in the right upper abdominal cavity for measuring intraabdominal pressure, after which the abdominal wall was closed. Transdiaphragmatic pressures were used to estimate the force-generating capacity of the diaphragm and were calculated as transdiaphragmatic pressure (cm H_2O) = intraabdominal pressure (cm H_2O) – P_{eso} (cm H_2O).

The phrenic nerves were stimulated at baseline and after 6 h of mechanical ventilation by bilateral transvenous stimulation with a fixed frequency of 40 Hz, a fixed pulse width of 210 μs, an intermittent stimulation of 1 to 2 s on and 2 to 3 s off,[25] and a fixed supramaximal stimulation (70 V). For this reason, an electric stimulation catheter (IBI-81102, decapolar 6 French, electrode spacing: 2-5-2 mm, St. Jude Medical, USA) was placed in the brachiocephalic vein *via* the left internal jugular vein for bilateral transvenous phrenic nerve pacing. In feasibility experiments before the current study, the optimal position of the catheter was determined with the pacing electrodes at the transition of the brachiocephalic and superior caval vein as, in lambs, the left and right phrenic nerves are positioned close to each other at that point. At this point, maximal bilateral stimulation of the diaphragm was obtained, leading to maximal negative esophageal pressures and clinically visual bilateral diaphragm contraction. The stimulation catheter was connected *via* an 8-pin extension cable (model 990066, Medtronic Inc., The Netherlands) and electrode switch box (model 19038, Medtronic Inc.) to an external neurostimulator (model 37022, Medtronic Inc.) and programmed *via* an N'Vision clinician programmer (model 8840, Medtronic Inc.).

Microcirculation of the Diaphragm

For quantification of the microcirculation of the diaphragm, a video microscope based on incident dark-field (IDF) imaging (Cytocam, Breadius Medical, The Netherlands) was placed at the left side of the diaphragm *via* the abdominal cavity by reopening the closed laparotomy at the end of the experiment before euthanasia. For optimal imaging of the diaphragm, transparent silicone oil (Oxane 5700, Bausch and Lomb, USA) was placed on the surface of the video microscope. Five sequences of steady 10-s clips were obtained from the diaphragm microcirculation while avoiding pressure artefacts with the video microscope.

A blinded investigator (L.M.v.L.) scored the captured IDF clips according to the Microcirculation Image Quality Score defined by Massey and Shapiro[26] and Massey *et al.*[27] In short, the images were scored on six categories: illumination, duration, focus, content, stability, and pressure. The videos were assigned a score of 0 = good, 1 = acceptable, or 10 = unacceptable for each category. Any video with a composed score of 10 or higher was discarded from future analysis.

Image acquisition was performed according to published consensus criteria.[28] The videos were assessed on microvascular flow index and microvascular density. Quantification of flow (microvascular flow index) was based on determination of the predominant type of flow in four quadrants, categorized as 0 = no flow, 1 = intermittent flow, 2 = sluggish flow, and 3 = continuous flow. The values of the four quadrants were averaged. Microvascular density was calculated as the number of vessels crossing arbitrary lines divided by the total length of these lines (*i.e.*, number of crossings).

Ventilatory and Hemodynamic Parameters

Ventilation parameters were acquired using Servo Tracker (version 4.1, Maquet, Sweden), a software tool for the collection and presentation of performance data from Servo-i (Maquet). These recorded signals were analyzed using custom-written MATLAB scripts (Matlab R2017b, MathWorks Inc., USA).

Plateau pressure (P_{plat}) was determined as the airway pressure when the flow became 0 during an inspiratory occlusion. Total PEEP ($PEEP_{tot}$) was determined as the airway pressure when flow became 0 during an expiratory occlusion. Driving pressure was defined as $P_{plat} - PEEP_{tot}$. Static lung mechanics were collected and defined as follows: lung compliance (ml/cm H_2O), tidal volume (V_T)/($P_{plat} - P_{eso}$, end-inspiratory) – ($PEEP_{tot} - P_{eso}$, end-expiratory); chest compliance (ml/cm H_2O), V_T/(P_{eso}, end-inspiratory – P_{eso}, end-expiratory); airway resistance (cmH_2O/L/s), Peak airway pressure (P_{MAX}) – P_{plat}/flow; transpulmonary pressure at end exhalation (cm H_2O), PEEP – P_{eso}, end-expiratory. The hemodynamic parameters were collected using a PiCCO device (Pulsion Medical Systems, Germany) for measuring intraarterial blood pressure and cardiac output *via* a transpulmonary thermodilution method according to previously described methods.[29]

Experimental Protocol

The experimental protocol was previously described in detail.[17] In summary, the animals (n = 19) were randomized into two groups receiving either a restrictive (n =10) or a liberal (n = 9) fluid regimen (fig. 1). Randomization was

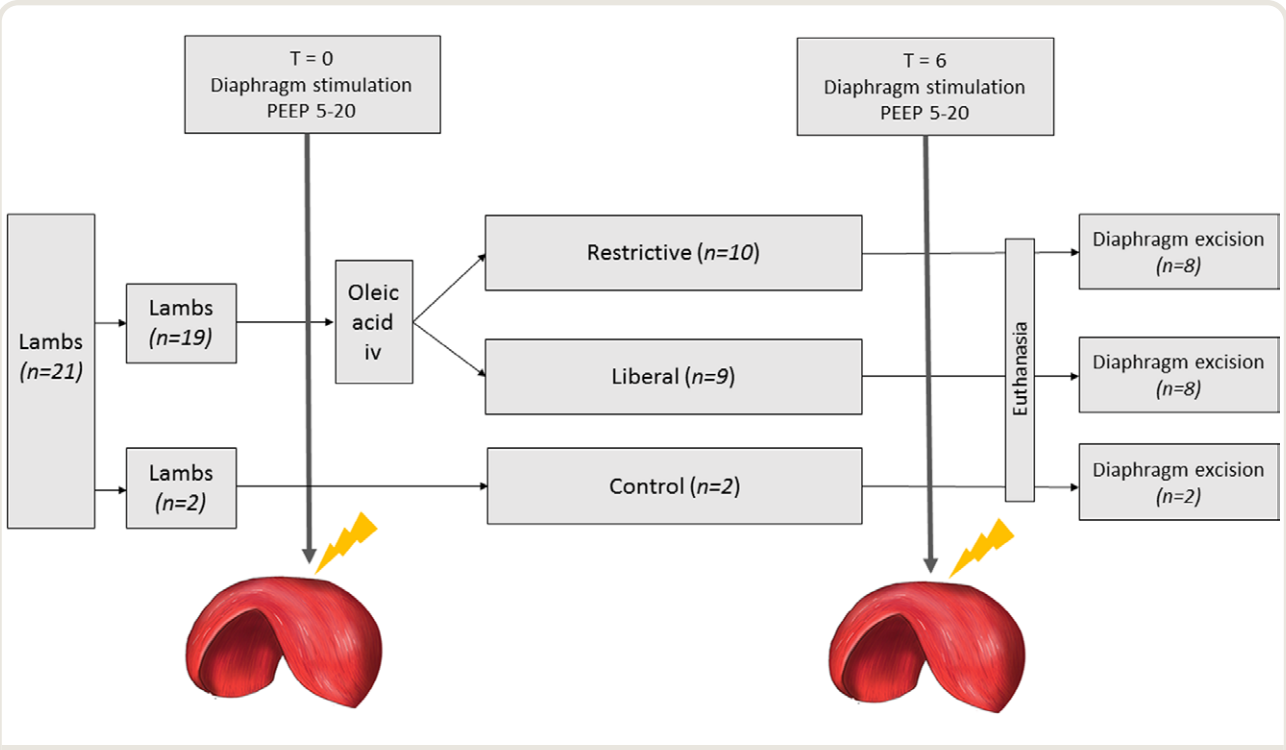

Fig. 1. Flow chart showing the experimental protocol with the number of animals used (n) and included in the study. Two animals in the restrictive group and one animal in the restrictive group died. At baseline (T = 0) and after 6 h (T= 6) of mechanical ventilation, the diaphragm was stimulated under different levels of positive end-expiratory pressure (PEEP; 5, 10, 15, and 20 cm H_2O). iv, intravenous.

conducted by drawing from randomly generated treatment allocations within sealed opaque envelopes. Subsequently, these animals received intravenous oleic acid into the right jugular vein catheter to induce acute lung injury as a model for pediatric ARDS.[30,31] Also, two randomly chosen animals were taken as controls. These animals did not receive oleic acid to induce ARDS but only received anesthesia and mechanical ventilation to observe the effects of the anesthetics and mechanical ventilation on the studied outcome parameters.

During the 6-h study period of mechanical ventilation, the animals in the liberal group received fluids at a maintenance of 120 ml · kg^{-1} · day^{-1}, and the animals in the restrictive group received 60 ml · kg^{-1} · day^{-1}. In case of hemodynamic instability, defined as blood pressure and cardiac output at less than 80% of baseline values, the liberal group was resuscitated mainly with Ringer's lactate and whole blood, and the restrictive group was resuscitated mainly with norepinephrine. During the experiment, the aim was to keep the hematocrit within the same range compared to baseline values in all animals. If the hematocrit declined 10% or more, a whole-blood transfusion was administered.

The animals were ventilated in a volume-controlled mode according to the principles of protective lung ventilation aiming V_T between 6 and 8 ml/kg and limiting inspiratory plateau pressures of less than 30 cm H_2O.[32] The $PaCO_2$ target was set between 4.5 and 6.0 kPa by adjusting the ventilatory parameters with respect to a maximum V_T of 8 ml/kg. Permissive hypercapnia was accepted if the pH remained acceptable (greater than 7.20) to keep the V_T at or less than 8 ml/kg. PEEP was set according to the lower PEEP titration model according to the ARDS network ventilatory protocol.[33]

It was expected that, in contrast to the restrictive group, the animals in the liberal fluid group would need higher levels of PEEP due to the development of pulmonary edema with subsequent compression atelectasis resulting in changes in the end-expiratory lung volume. Changes in the end-expiratory lung volume will influence the position of the diaphragm, subsequently affecting the force-generating capacity of the diaphragm.[34] Since we aimed to study the diaphragm function under equal circumstances, the transdiaphragmatic stimulation was performed at various levels of PEEP in both groups. In doing so, at baseline and after 6 h of mechanical ventilation, diaphragmatic stimulations were performed, during an occlusion test (expiratory hold) at PEEP levels of 5, 10, 15, and 20 cm H_2O. During these measurements, PEEP was applied in increasing order (PEEP 5-10-15-20 cm H_2O) and immediately afterward in reverse order (PEEP 20-15-10-5 cm H_2O) to evaluate consistency in the force-generating capacity of the diaphragm. The average of three measurements was calculated.

Before the end of the experiment (after 6 h of mechanical ventilation, just before euthanasia), diaphragmatic microcirculation was obtained. At the end of the experiment, the lambs were euthanized with intravenous pentobarbital (150 mg/kg). After euthanasia, the whole diaphragm was immediately dissected, and biopsies were obtained for histological measurements.

Biopsy Handling

Full-thickness biopsies were obtained from the same region of the right anterior costal diaphragm lateral to the insertion of the phrenic nerve in all animals (Supplemental Digital Content 2, http://links.lww.com/ALN/C803). Muscle biopsies were frozen immediately in liquid isopentane for histochemistry and collected in 4% buffered formalin for paraffin embedding. Paraffin sections stained with hematoxylin and eosin were prepared from longitudinal sectioned muscle fibers. For histochemistry, transverse sections of the muscle fibers were used as these sections yield much more information than longitudinal sections for light microscopy.[35] Frozen cryostat sections (5 mm thick) were used for staining with hematoxylin and eosin and for immunohistochemistry using antibodies clones BAD-5 and Sc-71, directed against the slow (type 1) and fast (type 2) isoforms of myosin heavy chain, respectively. These cryosections were rehydrated for 10 min in phosphate buffer and subsequently blocked with phosphate buffer containing 0.3% (w/v) bovine serum albumin. Endogenous peroxidase activity was blocked by treatment in 3% hydrogen peroxide in phosphate-buffered saline for 20 min. After preincubation with phosphate buffer containing 0.3% (w/v) bovine serum albumin 1%, the cryosections were incubated with the primary antibody for 1 h at room temperature, rinsed in phosphate-buffered saline, and incubated with a biotin-conjugated rabbit antimouse antibody for 1 h at room temperature. Subsequently the sections were incubated with Avidin-Biotin Complex kits (VECTASTAIN PK6100, Brunschwig Chemistry, The Netherlands) for 1 h. The peroxidase activity was visualized by staining with diaminobenzidine as substrate.

To objectively quantify slow and fast twitch fibers, the Fiji image-processing package (Jug and Tomancak, Max Planck Institute of Molecular Cell Biology and Genetics, Germany) was used.[36] A Fiji macro was created and automatically applied to all images. The Fiji macro first uses median filtering and thresholding to separate the marked parts of the image from the background. This foreground mask is next processed by reducing the number of small holes that result from uneven marking in cells. Finally, a distance transform watershed is used to segment the foreground mask into individual cell segments, which are counted and measured. Manually annotated images were used to verify the macro output and to optimize the parameters used in the macro.

Inflammatory Mediators and Oxidative Stress

To determine inflammatory mediators and oxidative stress, 50- to 100-mg frozen cryostat diaphragm biopsies were dissolved in a tissue protein extraction buffer and protease inhibitor cocktail. After obtaining homogenate, the proinflammatory cytokines (interleukins 1β, 6, and 8 and tumor necrosis factor α) and anti-inflammatory cytokines (interleukin 10) were determined using a multiplex cytokine panel (Luminex kit; SCYT1-91K, MILLIPLEX ovine cytokine/chemokine panel 1, Merck Chemicals B.V., The Netherlands). The lower limits of quantification for the cytokines were 25.6 pg/ml (interleukin 1β), 15.4 pg/ml (interleukin 6), 1.54 pg/ml (interleukin 8), 96 pg/ml (tumor necrosis factor α), and 3.2 pg/ml (interleukin 10). Oxidative stress was determined by measuring malondialdehyde, which is produced due to the oxidation of fatty acids, using the thiobarbituric acid reactive substances assay kit (ZeptoMetrics, Bio-connect B.V., The Netherlands). The cytokine and malondialdehyde data were normalized to total protein content (measured using a bicinchoninic acid protein assay kit; Thermo Scientific, USA) and expressed as picogram per milligram protein (cytokines) or nanomoles per milligram protein (malondialdehyde).

Statistical Analysis

Statistical analysis was performed with SPSS (version 25.0; IBM, USA) and GraphPad Prism (version 5.03; GraphPad, USA). Continuous variables were presented as medians (25th to 75th percentile) unless otherwise specified, and comparison between groups was performed by Mann–Whitney U tests.

Mixed model analysis was conducted for hypothesis testing in which we included a random intercept for sheep and accounted for repeated measurements and multiple inferences for PEEP. We adjusted for baseline values of PEEP and accounted for multiple testing (Bonferroni). The data are presented as the estimated marginal means with 95% CI.

The minimal sample size was taken to detect a difference in transdiaphragmatic pressure of 4 cm H_2O, with an SD of 2.6.[37] Considering an α error 0.05 and a power of 80%, a sample size of seven lambs was required in each randomization arm of the study. To compensate for possible dropouts, the sample size was increased with two to three lambs in each arm of the study. A two-sided *P* value of less than 0.05 was considered statistically significant. In the study, n refers to number of animals.

Availability of Data and Materials

The data sets analyzed during the current study are available from the corresponding author on reasonable request.

Results

Characteristics

Three of nineteen lambs died prematurely due to refractory circulatory deterioration after oleic acid induction. Because measurement of the transdiaphragmatic pressures at 6 h could not be performed in these animals, they were excluded from the final analysis. At baseline, mechanical ventilation settings were similar between the two groups,

and both groups developed a clinical comparable moderate pediatric ARDS (table 1). As expected, the control animals (n = 2) did not develop clinical signs of ARDS, and the characteristics of these animals are portrayed in Supplemental Digital Content 3 (http://links.lww.com/ALN/C804). At the end of the experiment, the cumulative fluid balance in the liberal group (liberal *vs.* restrictive: 86.0 ml/kg *vs.* 23.3 ml/kg; $P < 0.001$) and the cumulative dose of norepinephrine in the restrictive group (restrictive *vs.* liberal group: 130.7 μg/kg *vs.* 64.9 μg/kg; $P = 0.001$) were significantly higher.[17]

Effect of Fluids on Transdiaphragmatic Pressures

The baseline transdiaphragmatic pressures for the individual lambs are shown in Supplemental Digital Content 4 (http://links.lww.com/ALN/C846). Overall, there was a significant difference for intervention ($P < 0.05$). The pressure-generating capacity of the diaphragm after 6 h of mechanical ventilation decreased more in the restrictive group (–9.6 cm H_2O [95% CI, –14.4 to –4.8]) compared to the liberal group (–0.8 cm H_2O [95% CI, –5.8 to 4.3]) during the application of 5 cm H_2O PEEP ($P = 0.016$) and during the application of 10 cm H_2O PEEP (–10.3 cm H_2O [95% CI, –15.2 to –5.4] *vs.* –2.8 cm H_2O [95% CI, –8.0 to 2.3]; $P = 0.041$; fig. 2A). No significant difference in absolute transdiaphragmatic pressure after 6 h of mechanical ventilation between the two groups was observed for the higher levels of PEEP (15 and 20 cm H_2O PEEP; fig. 2A).

The mean estimated transdiaphragmatic pressure decreased for each applied PEEP level in the restrictive group contrary to the liberal group, although the change was not statistically significant for PEEP 20 cm H_2O (fig. 2B). No differences in the transdiaphragmatic pressures were observed with the application of the same level of PEEP when applied in an increasing (PEEP 5-10-15-20 cm H_2O) or decreasing order (PEEP 20-15-10-5 cm H_2O; data not shown).

Effects of Fluids on Diaphragmatic Microcirculation

In two animals (restrictive group: n = 1; liberal group: n = 1), no microcirculation could be assessed due to technical problems with the video microscope. There was a significant decrease in the density of the present microvessels, expressed as the number of crossings, in animals receiving a restrictive fluid regimen (34.0 [25th to 75th percentile, 22.0 to 42.0]) compared to animals receiving liberal fluids (46.0 [25th to 75th percentile, 43.5 to 54.0]; $P = 0.015$). The difference in microvascular flow between the two groups was not significant ($P = 0.176$; fig. 3, A and B). Representative still images of microvascular flow are shown in fig. 3, C and D.

Table 1. Characteristics of the Intervention Groups

	Liberal Group (n = 8)	Restrictive Group (n = 8)	*P* Value
Sex, female	8 (100)	8 (100)	
Body weight, kg	10.0 (7.6 to 17.6)	14.0 (10.8 to 17.9)	0.382
Ventilator settings (time, baseline)			
V_T, ml/kg	7.9 (6.7 to 8.3)	6.8 (6.3 to 7.6)	0.234
Total PEEP, cm H_2O	3.6 (3.3 to 4.2)	3.6 (2.8 to 4.3)	0.645
Fio_2	0.45 (0.4 to 0.5)	0.50 (0.5 to 0.5)	0.161
Driving pressure, cm H_2O	7.8 (5.8 to 9.4)	8.0 (7.4 to 9.9)	0.442
Plateau pressure, cm H_2O	11.3 (9.5 to 13.0)	11.6 (10.7 to 13.4)	0.505
Lung compliance, ml/cm H_2O*	32.6 (16.8 to 82.4)	26.3 (16.7 to 32.5)	0.383
Chest wall compliance, ml/cm H_2O*	21.3 (14.5 to 30.5)	26.2 (16.8 to 31.5)	0.383
Airway resistance, cm $H_2O \cdot ml^{-1} \cdot s^{-1}$	39.9 (26.8 to 47.3)	33.1 (29.5 to 56.7)	0.574
Transpulmonary pressure end exhalation, cm H_2O*	1.51 (0.45 to 2.26)	0.43 (–0.43 to 2.63)	0.318
Ventilator settings (time, 6 h after baseline)			
V_T, ml/kg	7.6 (7.2 to 8.6)	7.7 (6.9 to 8.5)	0.878
Total PEEP, cm H_2O	10.4 (9.0 to 11.5)	11.8 (8.1 to 12.8)	0.878
Fio_2	0.7 (0.5 to 0.7)	0.8 (0.6 to 1.0)	0.189
Driving pressure, cm H_2O	13.5 (12.3 to 6.4)	15.1 (13.1 to 20.7)	0.382
Plateau pressure, cm H_2O	24.6 (21.3 to 28.7)	26.0 (21.8 to 33.4)	0.505
Lung compliance, ml/cm H_2O*	7.5 (6.0 to 18.8)	9.7 (7.8 to 14.1)	0.620
Chest wall compliance, ml/cm H_2O*	27.3 (15.7 to 30.8)	27.6 (18.8 to 35.6)	0.620
Airway resistance, cm $H_2O \cdot ml^{-1} \cdot s^{-1}$	72.4 (48.5 to 86.4)	58.1 (38.1 to 65.8)	0.279
Transpulmonary pressure end exhalation, cm H_2O*	0.44 (0.03 to 2.57)	2.68 (1.13 to 3.61)	0.073
Pao_2/Fio_2 ratio, mmHg			
Time, baseline	416 (220 to 540)	269 (228 to 432)	0.328
Time, 6 h after baseline	185 (129 to 232)	187 (102 to 261)	0.955

The results are presented as medians (25th to 75th percentile) or number (%). The transpulmonary pressure at end exhalation is equal to $PEEP_{tot}$ minus the end-expiratory esophageal pressure.

*n = 7 in both groups due to missing value of esophageal pressure measurement.

Fio_2, fractional inspired oxygen tension; PEEP, positive end-expiratory pressure; V_T, tidal volume.

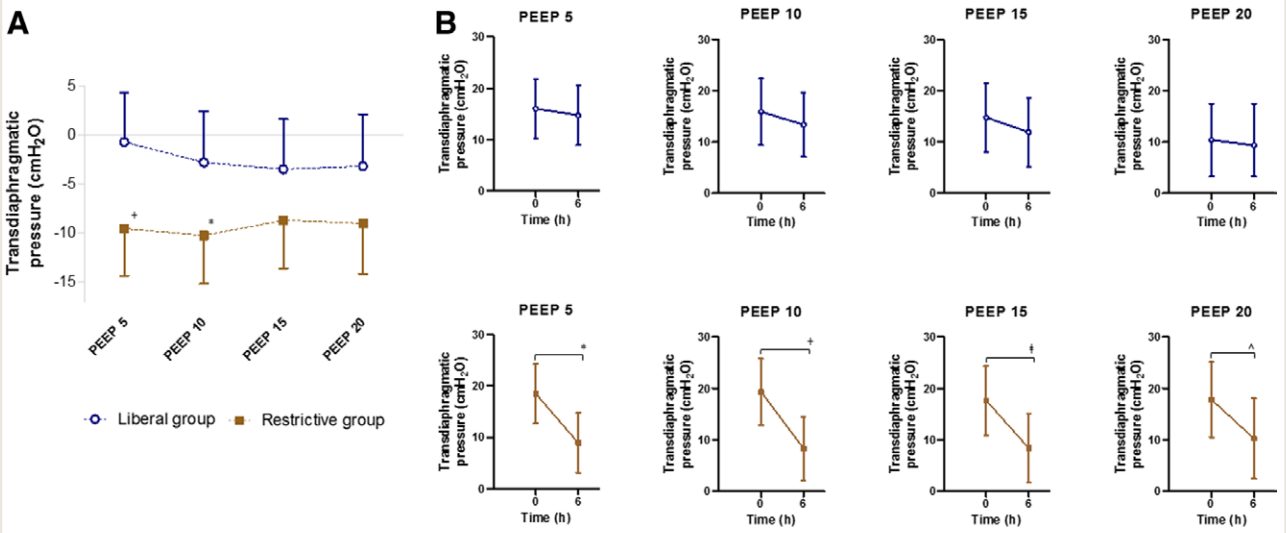

Fig. 2. Between-group difference in transdiaphragmatic pressures changes (*A*) and within-group differences in transdiaphragmatic pressures (*B*) during 6 h of mechanical ventilation for different levels of positive end-expiratory pressure (PEEP; in cm H_2O). (*A*) +$P = 0.016$; *$P = 0.042$ compared to same level of PEEP in the liberal group. Bonferroni was applied for multiple testing. PEEP, intervention, and the interaction between PEEP and intervention were defined as fixed factors. Adjustment for the baseline value of PEEP was performed. (*B*) *$P = 0.001$; +$P < 0.001$; ǂ$P = 0.007$; ^$P = 0.113$. Bonferroni was applied for multiple testing. A full factorial design for PEEP, intervention, and time was applied. The results are displayed as estimated marginal means with 95% CI.

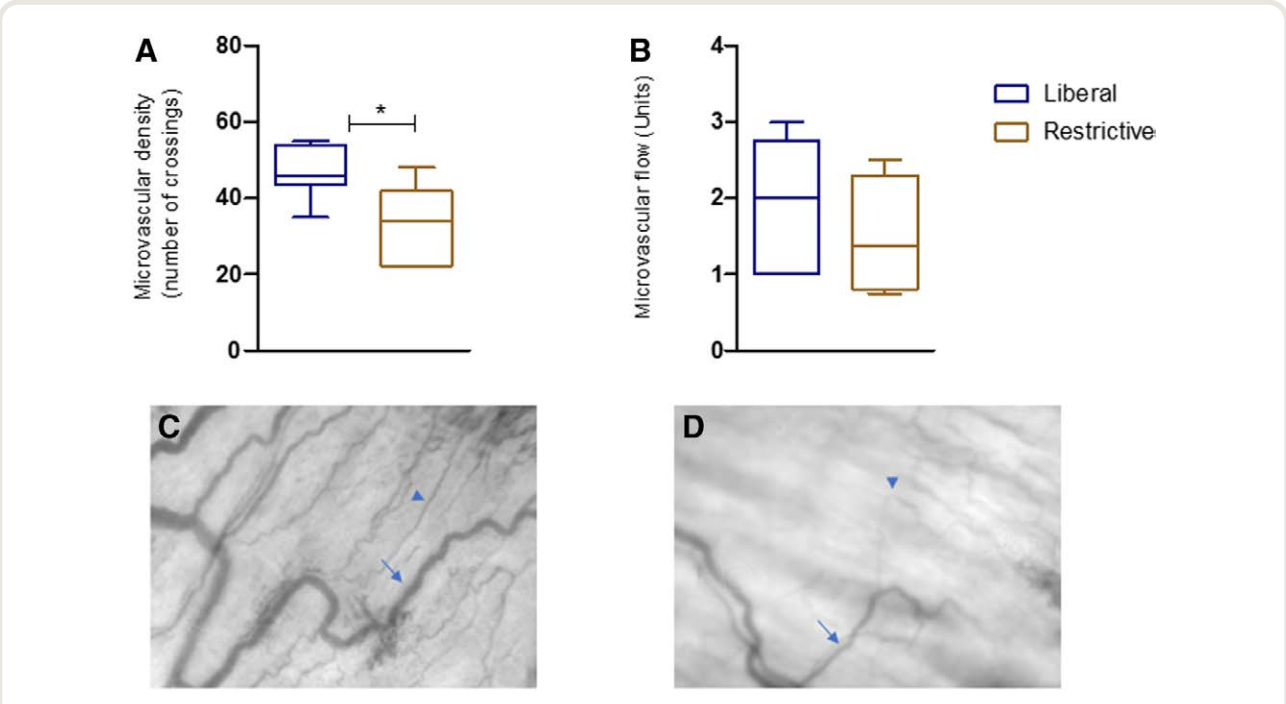

Fig. 3. Microcirculation diaphragm. (*A*) Median density of microvascular vessels. *$P = 0.015$. (*B*) Median flow index of the diaphragm at the end of the experiment (6 h after baseline). The data are expressed as the median with whiskers representing the minimum and maximum. Shown are representative still images of the diaphragmatic microcirculation in the liberal (n = 7; *C*) and restrictive (n = 7; *D*) fluid strategy. (*D*) shows fewer small vessels (mostly capillaries) than (*C*). *Arrows*, venule; *triangles*, capillary.

Effect of PEEP on Transdiaphragmatic Pressures

When studying the effect of diaphragm stimulation at various levels of PEEP, it was observed that increasing the PEEP level caused a decline in the generated transdiaphragmatic pressure. To establish the effect of the level of PEEP on the transdiaphragmatic pressures without the effect of induced pediatric ARDS or fluids, we used the baseline measurements of the entire group (restrictive and liberal group together) because in both groups, no difference in treatment existed at that time. High levels of PEEP caused a significant reduction in transdiaphragmatic pressures (fig. 4). For example, an acute increase in PEEP from 5 to 20 cm H_2O PEEP reduced transdiaphragmatic pressures by 27.3% (17.3 cm H_2O [95% CI, 14.0 to 20.5] *vs.* 12.6 cm H_2O [95% CI, 9.2 to 15.9]; $P < 0.0001$).

Histopathologic Findings

Standard hematoxylin and eosin staining did not show considerable endomysial edema or vacuolization of muscle fibers, especially not in the liberal group (fig. 5). As expected in this time window, no modification in the myosin heavy chain isoform expression profile occurred between the groups as the percentages of type 1 and type 2 muscle fibers were not different.

Quantification of fiber size in type 1 and type 2 fiber populations did not reveal significant differences between the groups. The median cross-sectional areas of slow-twitch (type 1) and fast-twitch fibers (type 2) in the liberal group were 470 μm^2 (interquartile range, 342 to 522) and 458 μm^2 (interquartile range, 309 to 500), respectively, and for the restrictive group, 498 μm^2 (interquartile range, 379 to 687) and 467 μm^2 (interquartile range, 368 to 574), respectively (fig. 6). The groups did not differ with respect to fiber proportion (%) and the numerical proportions or area fractions of slow-twitch (I) and fast-twitch fibers (fig. 6).

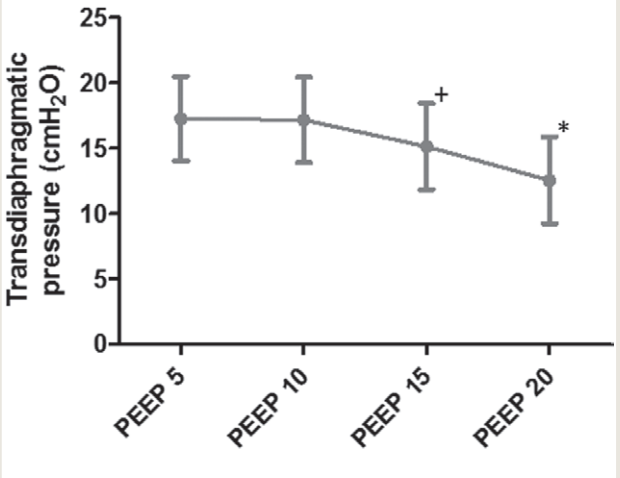

Fig. 4. Transdiaphragmatic pressures during increasing levels of positive end-expiratory pressure (PEEP; cm H_2O). The data are shown for the entire intervention group (restrictive and liberal group together) at baseline. The results are displayed as estimated marginal means with 95% CI. Bonferroni adjustment was applied to account for multiple testing. In the mixed model, PEEP was applied as a fixed factor. *$P = 0.003$; $P < 0.001$; $P < 0.001$ compared to PEEP 15, PEEP 10, and PEEP 5, respectively. +$P = 0.017$; $P = 0.011$ compared to PEEP 10 and PEEP 5, respectively.

Inflammatory Mediators and Oxidative Stress

The diaphragmatic levels of proinflammatory cytokines interleukins 1β, 6, and 8 and tumor necrosis factor α, as well as the anti-inflammatory cytokine interleukin 10, were similar between the groups (fig. 7). Furthermore, no between-group differences in the concentration of malondialdehyde in diaphragm tissue were observed (fig. 7).

Discussion

A restrictive fluid regimen causes a decline in diaphragmatic muscle force compared to a liberal fluid regimen. Contrary to our hypothesis, we observed that the use of a liberal fluid strategy did not lead to the formation of edema in or around the diaphragm muscle fibers in the early phase of experimental pediatric ARDS. Furthermore, we demonstrated that the acute application of PEEP decreases the force-generating capacity of the diaphragm in a dose-related way. These findings are novel and provide new insight into the mechanism of critical illness–associated diaphragm dysfunction and may have implications for the treatment of patients with pediatric ARDS in future.

Effect of a Restrictive Fluid Strategy

After 6 h of mechanical ventilation, the force-generating capacity of the diaphragm was lower in the restrictive fluid group compared to the liberal fluid group, especially at lower PEEP. No histological explanation can be provided, as we found no differences, in particular those pertaining to necrosis in muscle fibers, between the two groups.

Furthermore, although previous studies have shown that proinflammatory cytokines and oxidative stress may impair the diaphragmatic contractility,[38,39] we observed similar concentrations of these mediators between the groups. Our results are comparable to previous studies comparing proinflammatory cytokines in the lung between a liberal fluid resuscitation strategy *versus* a restrictive fluid resuscitation strategy in animals, also showing similar levels of proinflammatory cytokines in both groups.[17,40,41]

The restrictive fluid group can be characterized as having a lower intravascular volume while being treated with relatively high dosage of vasopressors. A possible explanation for the reduced diaphragm force–generating capacity in the restrictive group may be the result of disturbances in the perfusion of the (capillary) blood vessel network as the capillary density of the diaphragm microcirculation

was significantly lower in the restrictive group compared to the liberal group. The vasoconstrictive effect of norepinephrine in high dosages in a situation of relative hypovolemia might have led to a decrease in microvascular density, which ultimately may have resulted in decreased diaphragmatic tissue oxygenation and force-generating capacity of the diaphragm.

Another explanation for the reduced diaphragm force–generating capacity in the restrictive group could also be the (additional) result of disturbances at the level of the neuromuscular junction. In experimental studies on isolated phrenic-diaphragm preparation of mice, it was demonstrated that norepinephrine may decrease the frequency of spontaneous quantal release of acetylcholine and increase the degree of asynchrony of acetylcholine secretion.[42,43] This might negatively affect the force-generating capacity of the diaphragm and is in line with our findings. However, research on this topic was beyond the scope of the current study.

Effect of a Liberal Fluid Strategy

Contrary to our hypothesis, liberal fluids in the early phase of pediatric ARDS did not lead to the formation of endomysial edema or swelling of the diaphragm muscle fibers as the endomysial space and the mean cross-sectional areas between the two groups were comparable. Myofibrillar and endomysial edema have been demonstrated in animal septic shock and ischemic models.[14,15] However, the causal mechanism, such as septic shock and ischemia, responsible for the formation of edema was different in the previously mentioned studies. Therefore, it is possible that the formation of edema in and around the diaphragm muscle fibers during fluid overload may not occur or develop later during the course of the disease.

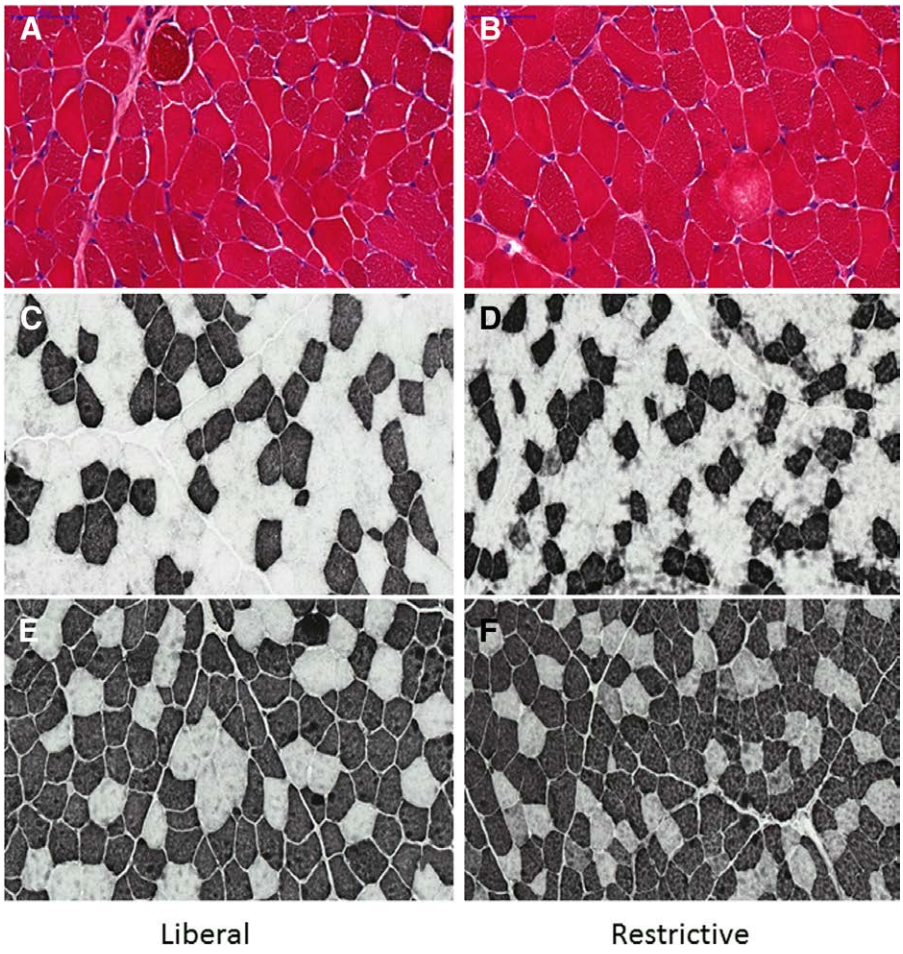

Fig. 5. (*A* and *B*) Representative examples of hematoxylin and eosin staining in the liberal (*A*) and restrictive groups (*B*). (*C* to *F*) The diaphragm fibers preincubated with BAD-5 antibody (*C* and *D*) and with Sc-71 antibody (*E* and *F*) were specific for the slow (type 1) and fast (type 2) isoforms of myosin heavy chain, respectively. In each of the sections, fibers reacting with the antibody appear black, whereas fibers not reacting with the antibody appear white.

Effect of PEEP

In the early stage of pediatric ARDS, the acute application of PEEP decreases the *in vivo* force-generating capacity of the diaphragm in a dose-related effect; the higher the PEEP, the greater the decrease in transdiaphragmatic pressure. To our knowledge, no studies have explored this dose-related effect of PEEP on the transdiaphragmatic pressures *in vivo* in an animal model of pediatric ARDS.

A possible explanation for the decrease in transdiaphragmatic pressure as a result of the application of PEEP is that the acute application of PEEP causes a caudal movement of the diaphragm dome, causing fiber and sarcomere reduction in the zone of apposition, as has been shown *in vitro* in rat studies.[34] In this way, the diaphragm muscle fibers are forced to contract at a shorter length, leading to a reduction in the force-generating capacity of the diaphragm.[34] As an explanation for the dose-related effect, we postulate that the reduction in sarcomere length becomes more pronounced with the higher levels of PEEP. Second, as recently shown, mechanical ventilation increases vascular resistance and impairs diaphragm perfusion, an effect more pronounced with higher PEEP levels.[44] Whether the decrease in diaphragm perfusion indeed causes lower transdiaphragmatic pressures in our model warrants further investigation.

No differences in the diaphragm function were found between the two groups with the application of 20 cm H_2O PEEP. A possible explanation might be that with this high level of PEEP, the diaphragm behaves as a widening piston,[45] forcing the muscle fibers to act at a suboptimal

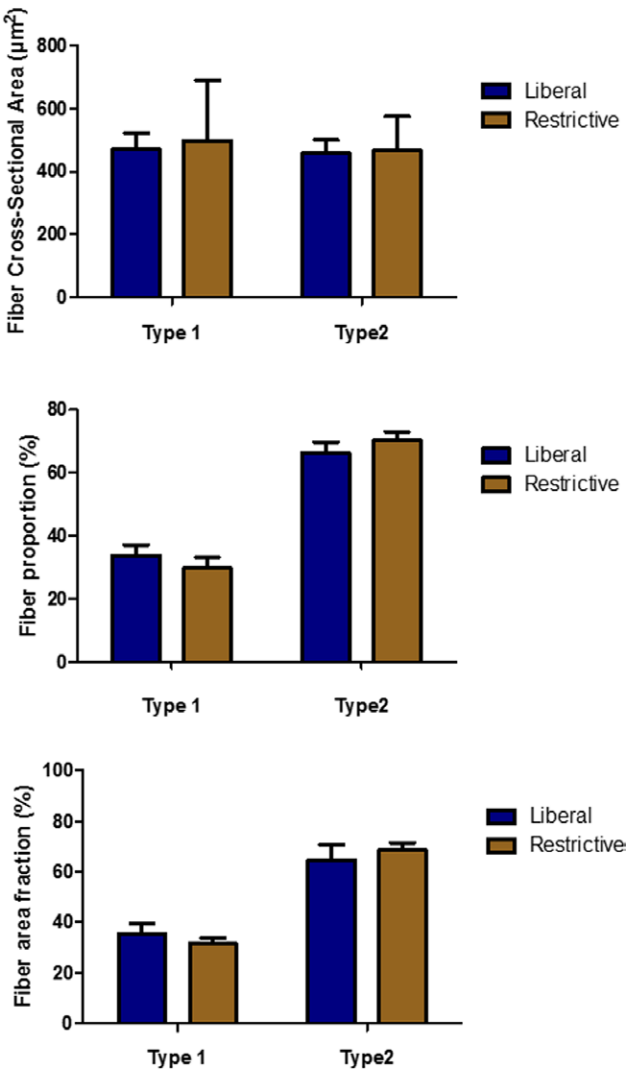

Fig. 6. Diaphragm-biopsy specimen with respect to fiber size of phenotype. The results are presented as the medians (25th to 75th percentile). There were no significant differences between the fiber cross-sectional area, fiber proportion, or fiber area fraction between the liberal and restrictive groups.

length, generating low force. The impact of such a high level of PEEP is tremendous on the diaphragm force–generating capacity, leaving no additional effect for other negative factors.

Strength and Limitations

Some limitations of our study should be acknowledged. First, complete blinding after allocation of the groups was not possible for the research group as they were responsible for the assigned treatment. However, biopsy handling and scoring of the microvascular images was blinded for the researcher. Second, we observed that the use of a liberal fluid strategy did not lead to the formation of edema in the diaphragm in the early phase of experimental pediatric ARDS. Whether edema of the diaphragm develops beyond the time frame of the study remains to be investigated.

Third, as no functional measurements (force generations and microvasculature) were performed on nonrespiratory skeletal muscles, it is unclear whether our findings are specific to the diaphragm muscle.

Fourth, we expected that animals in the liberal group would need higher levels of PEEP due to the development of compression atelectasis, subsequently leading to a change in the end-expiratory lung volume. These changes may influence the position of the diaphragm at the zone of apposition, subsequently affecting the force-generating capacity of the diaphragm.[34] However, at the end of the experiment, no significant difference in transpulmonary pressure at end exhalation, lung compliance, chest wall compliance, and driving pressure between the two groups existed, suggesting that no change in the end-expiratory lung volume occurred. This means we may not have had to perform diaphragm stimulations under different levels of PEEP. However, by performing the diaphragm stimulations under different levels of PEEP, we have now gained additional insight into the acute effects of PEEP *in vivo* on the diaphragm function. However, further studies are needed to gain insight in the long-term effects of different levels of PEEP on diaphragm function.

Fifth, due to technical reasons, it was not possible to measure the transdiaphragmatic pressure during all different levels of PEEP in all animals.

Sixth, our experiment was performed in female lambs only. Studies have shown that testosterone might increase diaphragm contractility in rats.[46,47] Given the young age of the lambs, we consider changes in the level of testosterone to be small between the two sexes, and it is unlikely that the

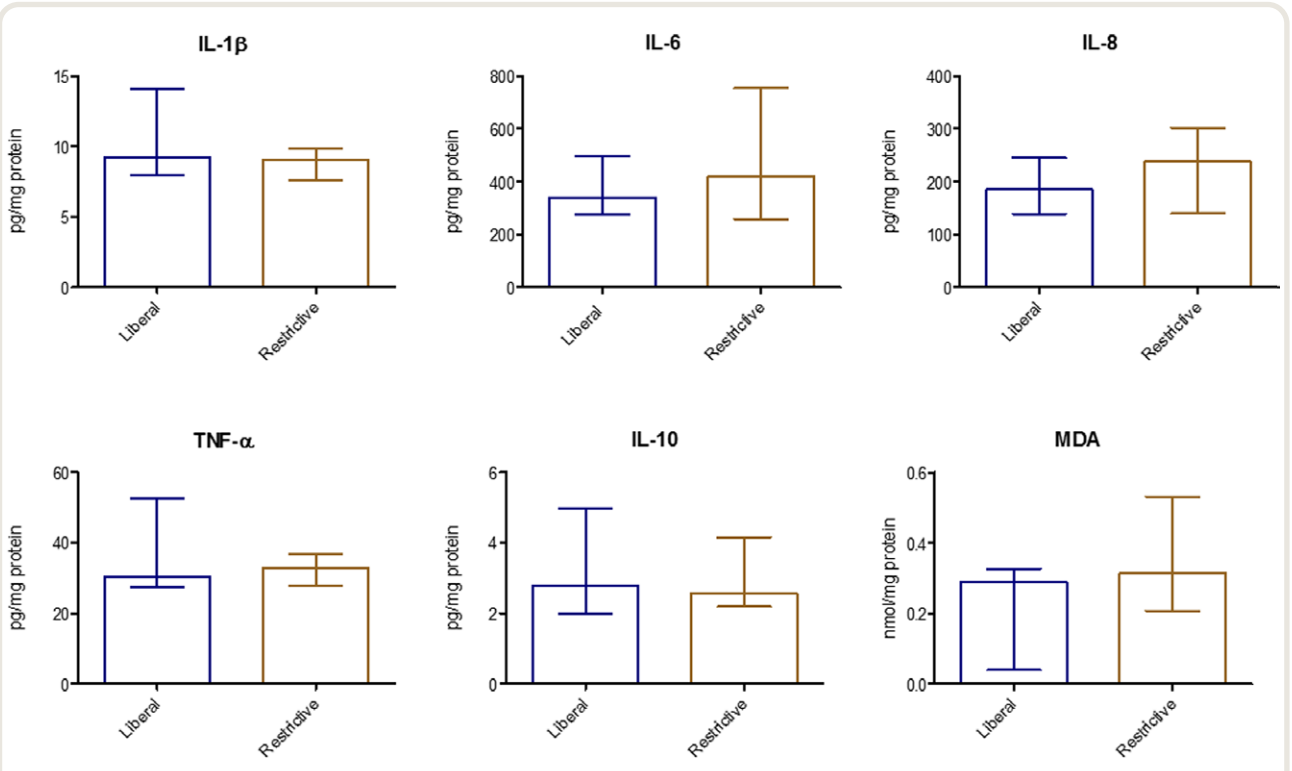

Fig. 7. Diaphragm muscle concentrations of proinflammatory cytokines (interleukins 1β, 6, and 8 and tumor necrosis factor α) and anti-inflammatory cytokine (interleukin 10). The cytokines are expressed as pg/mg protein. Free radical activity was measured with malondialdehyde and expressed as nmol/mg protein. No differences were found between groups ($P = 0.645$ for interleukin 1β; $P = 0.442$ for interleukin 6; $P = 0.382$ for interleukin 8; $P = 0.798$ for interleukin 10; $P = 0.234$ for malondialdehyde). n = 8 for the restrictive and liberal groups. The data are expressed as medians (25th to 75th percentile).

female predominance has influenced our results. In addition, there are no data to support the possibility that the effects of the oleic acid or resuscitation strategy are sex-dependent.

Finally, as this is an experimental animal model, the results cannot directly be translated to clinical strategies but emphasize the importance of future studies in humans.

The strength of our study was that we performed this experiment under controlled and uniform conditions with standardized, validated, and direct measurements in which we included *in vivo* function, perfusion, and histology of the diaphragm. Furthermore, as our study was part of a more extensive experiment with the same research design but with different research questions (focused on the cardiopulmonary effects of fluid strategy during pediatric ARDS),[17] we were able to minimize the number of animals used.

Clinical Implications and Future Perspectives

Critical illness–associated diaphragm weakness develops in the majority of mechanically ventilated critically ill patients, may be associated with prolonged duration of mechanical ventilation, and may be associated with mortality.[1–5] The current study shows that in the early phase of severe experimental pediatric ARDS, a restrictive fluid strategy may adversely affect diaphragm force–generating capacity. Although the exact mechanism has yet to be elucidated, our findings are novel and hypothesis-generating for future clinical studies. In addition, our study underscores that the optimal modalities of fluid management and PEEP titration in patients with ARDS are challenging and that the effects appear to be organ-specific. In other words, a lung-protective strategy characterized by high PEEP and early fluid restriction may have detrimental effects on other organs, including the respiratory muscles.

These new mechanisms may help identify patients at risk for diaphragm dysfunction. The ultimate goal is an individualized integrated lung and diaphragm-protective approach for the management of pediatric ARDS.

Conclusions

Early fluid restriction decreases the force-generating capacity of the diaphragm in the acute phase of experimental pediatric ARDS. In addition, the application of PEEP itself decreases the force-generating capacity of the diaphragm in a dose-related way, which was more pronounced in a restrictive regimen compared to a liberal fluid regimen. These observations provide new insights into the mechanism of critical illness–associated diaphragm dysfunction.

Acknowledgments

The authors thank Alex Hanssen, Ing. (Animal Research Facility, Radboud University Nijmegen, The Netherlands), for his excellent technical assistance during the experiment. They also express their gratitude to Theo G. M. Hafmans, BsC., Paul H. K. Jap, M.D., Ph.D. (Department of Biochemistry, Radboud University Medical Centre, Nijmegen, The Netherlands), and Jelle Gerretsen, BsC., (Department of Intensive Care Medicine, Radboud University Medical Centre, Nijmegen, The Netherlands) for their extensive effort in the histological preparations and biochemical analysis. Medtronic Inc. (Maastricht, The Netherlands) and Maquet (Hilversum, The Netherlands) provided the equipment for the external stimulator (models 990066, 19038, 37022, and 8840) and the mechanical ventilator (Servo-i), respectively.

Research Support

Support was provided solely from institutional and/or departmental sources.

Competing Interests

Dr. Heunks has received funding from Getinge (Gothenburg, Sweden), Fisher and Paykel (Tilburg, The Netherlands), and Liberate Medical (Crestwood, Kentucky). The other authors declare no competing interests.

Correspondence

Address correspondence to Dr. Ijland: Radboud University Medical Center, P.O. Box 9000, 6500 HB Nijmegen, The Netherlands. marloes.ijland@radboudumc.nl.

References

1. Goligher EC, Dres M, Fan E, Rubenfeld GD, Scales DC, Herridge MS, Vorona S, Sklar MC, Rittayamai N, Lanys A, Murray A, Brace D, Urrea C, Reid WD, Tomlinson G, Slutsky AS, Kavanagh BP, Brochard LJ, Ferguson ND: Mechanical ventilation-induced diaphragm atrophy strongly impacts clinical outcomes. Am J Respir Crit Care Med 2018; 197:204–13
2. Demoule A, Jung B, Prodanovic H, Molinari N, Chanques G, Coirault C, Matecki S, Duguet A, Similowski T, Jaber S: Diaphragm dysfunction on admission to the intensive care unit: Prevalence, risk factors, and prognostic impact-a prospective study. Am J Respir Crit Care Med 2013; 188:213–9
3. Xue Y, Yang CF, Ao Y, Qi J, Jia FY: A prospective observational study on critically ill children with diaphragmatic dysfunction: Clinical outcomes and risk factors. BMC Pediatr 2020; 20:422
4. Glau CL, Conlon TW, Himebauch AS, Yehya N, Weiss SL, Berg RA, Nishisaki A: Diaphragm atrophy during pediatric acute respiratory failure is associated with prolonged noninvasive ventilation requirement following extubation. Pediatr Crit Care Med 2020; 21:e672–8
5. Hooijman PE, Beishuizen A, Witt CC, de Waard MC, Girbes AR, Spoelstra-de Man AM, Niessen HW,

Manders E, van Hees HW, van den Brom CE, Silderhuis V, Lawlor MW, Labeit S, Stienen GJ, Hartemink KJ, Paul MA, Heunks LM, Ottenheijm CA: Diaphragm muscle fiber weakness and ubiquitin-proteasome activation in critically ill patients. Am J Respir Crit Care Med 2015; 191:1126–38
6. Dres M, Goligher EC, Heunks LMA, Brochard LJ: Critical illness–associated diaphragm weakness. Intensive Care Med 2017; 43:1441–52
7. Vieillard-Baron A, Matthay M, Teboul JL, Bein T, Schultz M, Magder S, Marini JJ: Experts' opinion on management of hemodynamics in ARDS patients: Focus on the effects of mechanical ventilation. Intensive Care Med 2016; 42:739–49
8. Flori HR, Church G, Liu KD, Gildengorin G, Matthay MA: Positive fluid balance is associated with higher mortality and prolonged mechanical ventilation in pediatric patients with acute lung injury. Crit Care Res Pract 2011; 2011:854142
9. Valentine SL, Sapru A, Higgerson RA, Spinella PC, Flori HR, Graham DA, Brett M, Convery M, Christie LM, Karamessinis L, Randolph AG; Pediatric Acute Lung Injury and Sepsis Investigator's (PALISI) Network; Acute Respiratory Distress Syndrome Clinical Research Network (ARDSNet): Fluid balance in critically ill children with acute lung injury. Crit Care Med 2012; 40:2883–9
10. Arikan AA, Zappitelli M, Goldstein SL, Naipaul A, Jefferson LS, Loftis LL: Fluid overload is associated with impaired oxygenation and morbidity in critically ill children. Pediatr Crit Care Med 2012; 13:253–8
11. Alobaidi R, Morgan C, Basu RK, Stenson E, Featherstone R, Majumdar SR, Bagshaw SM: Association between fluid balance and outcomes in critically ill children: A systematic review and meta-analysis. JAMA Pediatr 2018; 172:257–68
12. National Heart, Lung, and Blood Institute Acute Respiratory Distress Syndrome Clinical Trials Network, Wiedemann HP, Wheeler AP, Bernard GR, Thompson BT, Hayden D, deBoisblanc B, Connors AF, Jr, Hite RD, Harabin AL: Comparison of two fluid-management strategies in acute lung injury. N Engl J Med 2006; 354: 2564–75
13. Mitchell KH, Carlbom D, Caldwell E, Leary PJ, Himmelfarb J, Hough CL: Volume overload: Prevalence, risk factors, and functional outcome in survivors of septic shock. Ann Am Thorac Soc 2015; 12:1837–44
14. Hauptmann S, Klosterhalfen B, Weis J, Mittermayer C, Kirkpatrick CJ: Skeletal muscle oedema and muscle fibre necrosis during septic shock: Observations with a porcine septic shock model. Virchows Arch 1994; 424:653–9
15. Bragadeesh T, Jayaweera AR, Pascotto M, Micari A, Le DE, Kramer CM, Epstein FH, Kaul S: Post-ischaemic myocardial dysfunction (stunning) results from myofibrillar oedema. Heart 2008; 94:166–71
16. Bennett VA, Vidouris A, Cecconi M: Effects of fluids on the macro- and microcirculations. Crit Care 2018; 22:74
17. Ingelse SA, IJland MM, van Loon LM, Bem RA, van Woensel JB, Lemson J: Early restrictive fluid resuscitation has no clinical advantage in experimental severe pediatric acute respiratory distress syndrome. Am J Physiol Lung Cell Mol Physiol 2021; 320:L1126–36
18. Percie du Sert N, Ahluwalia A, Alam S, Avey MT, Baker M, Browne WJ, Clark A, Cuthill IC, Dirnagl U, Emerson M, Garner P, Holgate ST, Howells DW, Hurst V, Karp NA, Lazic SE, Lidster K, MacCallum CJ, Macleod M, Pearl EJ, Petersen OH, Rawle F, Reynolds P, Rooney K, Sena ES, Silberberg SD, Steckler T, Wurbel H: Reporting animal research: Explanation and elaboration for the ARRIVE guidelines 2.0. PLoS Biol 2020; 18:e3000411
19. Akoumianaki E, Maggiore SM, Valenza F, Bellani G, Jubran A, Loring SH, Pelosi P, Talmor D, Grasso S, Chiumello D, Guérin C, Patroniti N, Ranieri VM, Gattinoni L, Nava S, Terragni PP, Pesenti A, Tobin M, Mancebo J, Brochard L; PLUG Working Group (Acute Respiratory Failure Section of the European Society of Intensive Care Medicine): The application of esophageal pressure measurement in patients with respiratory failure. Am J Respir Crit Care Med 2014; 189:520–31
20. Mauri T, Yoshida T, Bellani G, Goligher EC, Carteaux G, Rittayamai N, Mojoli F, Chiumello D, Piquilloud L, Grasso S, Jubran A, Laghi F, Magder S, Pesenti A, Loring S, Gattinoni L, Talmor D, Blanch L, Amato M, Chen L, Brochard L, Mancebo J; PLeUral Pressure Working Group (PLUG–Acute Respiratory Failure Section of the European Society of Intensive Care Medicine): Esophageal and transpulmonary pressure in the clinical setting: Meaning, usefulness and perspectives. Intensive Care Med 2016; 42:1360–73
21. Mojoli F, Chiumello D, Pozzi M, Algieri I, Bianzina S, Luoni S, Volta CA, Braschi A, Brochard L: Esophageal pressure measurements under different conditions of intrathoracic pressure: An *in vitro* study of second generation balloon catheters. Minerva Anestesiol 2015; 81:855–64
22. Yang YL, He X, Sun XM, Chen H, Shi ZH, Xu M, Chen GQ, Zhou JX: Optimal esophageal balloon volume for accurate estimation of pleural pressure at end-expiration and end-inspiration: An *in vitro* bench experiment. Intensive Care Med Exp 2017; 5:35
23. Hotz JC, Sodetani CT, Van Steenbergen J, Khemani RG, Deakers TW, Newth CJ: Measurements obtained from esophageal balloon catheters are affected by the esophageal balloon filling volume in children with ARDS. Respir Care 2018; 63:177–86
24. Baydur A, Behrakis PK, Zin WA, Jaeger M, Milic-Emili J: A simple method for assessing the validity of the esophageal balloon technique. Am Rev Respir Dis 1982; 126:788–91

25. Dekker LR, Gerritse B, Scheiner A, Kornet L: Mapping for acute transvenous phrenic nerve stimulation study (MAPS study). Pacing Clin Electrophysiol 2017; 40:294–300
26. Massey MJ, Shapiro NI: A guide to human *in vivo* microcirculatory flow image analysis. Crit Care 2016; 20:35
27. Massey MJ, Larochelle E, Najarro G, Karmacharla A, Arnold R, Trzeciak S, Angus DC, Shapiro NI: The microcirculation image quality score: Development and preliminary evaluation of a proposed approach to grading quality of image acquisition for bedside videomicroscopy. J Crit Care 2013; 28:913–7
28. De Backer D, Hollenberg S, Boerma C, Goedhart P, Büchele G, Ospina-Tascon G, Dobbe I, Ince C: How to evaluate the microcirculation: Report of a round table conference. Crit Care 2007; 11:R101
29. Proulx F, Lemson J, Choker G, Tibby SM: Hemodynamic monitoring by transpulmonary thermodilution and pulse contour analysis in critically ill children. Pediatr Crit Care Med 2011; 12:459–66
30. Ballard-Croft C, Wang D, Sumpter LR, Zhou X, Zwischenberger JB: Large-animal models of acute respiratory distress syndrome. Ann Thorac Surg 2012; 93:1331–9
31. Wang HM, Bodenstein M, Markstaller K: Overview of the pathology of three widely used animal models of acute lung injury. Eur Surg Res 2008; 40:305–16
32. Rimensberger PC, Cheifetz IM; Pediatric Acute Lung Injury Consensus Conference Group: Ventilatory support in children with pediatric acute respiratory distress syndrome: Proceedings from the Pediatric Acute Lung Injury Consensus Conference. Pediatr Crit Care Med 2015; 16:S51–60
33. Brower RG, Lanken PN, MacIntyre N, Matthay MA, Morris A, Ancukiewicz M, Schoenfeld D, Thompson BT; National Heart, Lung, and Blood Institute ARDS Clinical Trials Network: Higher *versus* lower positive end-expiratory pressures in patients with the acute respiratory distress syndrome. N Engl J Med 2004; 351:327–36
34. Lindqvist J, van den Berg M, van der Pijl R, Hooijman PE, Beishuizen A, Elshof J, de Waard M, Girbes A, Spoelstra-de Man A, Shi ZH, van den Brom C, Bogaards S, Shen S, Strom J, Granzier H, Kole J, Musters RJP, Paul MA, Heunks LMA, Ottenheijm CAC: Positive end-expiratory pressure ventilation induces longitudinal atrophy in diaphragm fibers. Am J Respir Crit Care Med 2018; 198:42–85
35. Dubowitz V SC, Oldfors A.: Muscle Biopsy: A Practical Approach, 4th edition. Philadelphia, Saunders Ltd., Elsevier, 2013
36. Schindelin J, Arganda-Carreras I, Frise E, Kaynig V, Longair M, Pietzsch T, Preibisch S, Rueden C, Saalfeld S, Schmid B, Tinevez JY, White DJ, Hartenstein V, Eliceiri K, Tomancak P, Cardona A: Fiji: An open-source platform for biological-image analysis. Nat Methods 2012; 9:676–82
37. Jung B, Constantin JM, Rossel N, Le Goff C, Sebbane M, Coisel Y, Chanques G, Futier E, Hugon G, Capdevila X, Petrof B, Matecki S, Jaber S: Adaptive support ventilation prevents ventilator-induced diaphragmatic dysfunction in piglet: An *in vivo* and *in vitro* study. Anesthesiology 2010; 112:1435–43
38. Heunks LM, Machiels HA, de Abreu R, Zhu XP, van der Heijden HF, Dekhuijzen PN: Free radicals in hypoxic rat diaphragm contractility: No role for xanthine oxidase. Am J Physiol Lung Cell Mol Physiol 2001; 281:L1402–12
39. Reid MB, Lännergren J, Westerblad H: Respiratory and limb muscle weakness induced by tumor necrosis factor-alpha: Involvement of muscle myofilaments. Am J Respir Crit Care Med 2002; 166:479–84
40. Ye S, Li Q, Yuan S, Shu H, Yuan Y: Restrictive fluid resuscitation leads to better oxygenation than non-restrictive fluid resuscitation in piglets with pulmonary or extrapulmonary acute respiratory distress syndrome. Med Sci Monit 2015; 21:2008–20
41. Byrne L, Obonyo NG, Diab SD, Dunster KR, Passmore MR, Boon AC, Hoe LS, Pedersen S, Fauzi MH, Pimenta LP, Van Haren F, Anstey CM, Cullen L, Tung JP, Shekar K, Maitland K, Fraser JF: Unintended consequences: Fluid resuscitation worsens shock in an ovine model of endotoxemia. Am J Respir Crit Care Med 2018; 198:1043–54
42. Tsentsevitsky AN KI, Bukharaeva EA, Nikolsky EE.: Effect of noradrenaline on the kinetics of evoked acetylcholine secretion in mouse neuromuscular junction. Biochemistry (Moscow) 2018; 12:327–332
43. Tsentsevitsky AN, Kovyazina IV, Bukharaeva EA: Diverse effects of noradrenaline and adrenaline on the quantal secretion of acetylcholine at the mouse neuromuscular junction. Neuroscience 2019; 423:162–71
44. Horn AG, Baumfalk DR, Schulze KM, Kunkel ON, Colburn TD, Weber RE, Bruells CS, Musch TI, Poole DC, Behnke BJ: Effects of elevated positive end-expiratory pressure on diaphragmatic blood flow and vascular resistance during mechanical ventilation. J Appl Physiol (1985) 2020; 129:626–35
45. Gauthier AP, Verbanck S, Estenne M, Segebarth C, Macklem PT, Paiva M: Three-dimensional reconstruction of the *in vivo* human diaphragm shape at different lung volumes. J Appl Physiol (1985) 1994; 76:495–506
46. Prezant DJ, Karwa ML, Kim HH, Maggiore D, Chung V, Valentine DE: Short- and long-term effects of testosterone on diaphragm in castrated and normal male rats. J Appl Physiol (1985) 1997; 82:134–43
47. Prezant DJ, Valentine DE, Gentry EI, Richner B, Cahill J, Freeman K: Effects of short-term and long-term androgen treatment on the diaphragm in male and female rats. J Appl Physiol (1985) 1993; 75:1140–9

25. Dekker LR, Gerritse B, Scheiner A, Kornet L: Mapping for acute transvenous phrenic nerve stimulation study (MAPS study). Pacing Clin Electrophysiol 2017; 40:294–300
26. Massey MJ, Shapiro NI: A guide to human *in vivo* microcirculatory flow image analysis. Crit Care 2016; 20:35
27. Massey MJ, Larochelle E, Najarro G, Karmacharla A, Arnold R, Trzeciak S, Angus DC, Shapiro NI: The microcirculation image quality score: Development and preliminary evaluation of a proposed approach to grading quality of image acquisition for bedside videomicroscopy. J Crit Care 2013; 28:913–7
28. De Backer D, Hollenberg S, Boerma C, Goedhart P, Büchele G, Ospina-Tascon G, Dobbe I, Ince C: How to evaluate the microcirculation: Report of a round table conference. Crit Care 2007; 11:R101
29. Proulx F, Lemson J, Choker G, Tibby SM: Hemodynamic monitoring by transpulmonary thermodilution and pulse contour analysis in critically ill children. Pediatr Crit Care Med 2011; 12:459–66
30. Ballard-Croft C, Wang D, Sumpter LR, Zhou X, Zwischenberger JB: Large-animal models of acute respiratory distress syndrome. Ann Thorac Surg 2012; 93:1331–9
31. Wang HM, Bodenstein M, Markstaller K: Overview of the pathology of three widely used animal models of acute lung injury. Eur Surg Res 2008; 40:305–16
32. Rimensberger PC, Cheifetz IM; Pediatric Acute Lung Injury Consensus Conference Group: Ventilatory support in children with pediatric acute respiratory distress syndrome: Proceedings from the Pediatric Acute Lung Injury Consensus Conference. Pediatr Crit Care Med 2015; 16:S51–60
33. Brower RG, Lanken PN, MacIntyre N, Matthay MA, Morris A, Ancukiewicz M, Schoenfeld D, Thompson BT; National Heart, Lung, and Blood Institute ARDS Clinical Trials Network: Higher *versus* lower positive end-expiratory pressures in patients with the acute respiratory distress syndrome. N Engl J Med 2004; 351:327–36
34. Lindqvist J, van den Berg M, van der Pijl R, Hooijman PE, Beishuizen A, Elshof J, de Waard M, Girbes A, Spoelstra-de Man A, Shi ZH, van den Brom C, Bogaards S, Shen S, Strom J, Granzier H, Kole J, Musters RJP, Paul MA, Heunks LMA, Ottenheijm CAC: Positive end-expiratory pressure ventilation induces longitudinal atrophy in diaphragm fibers. Am J Respir Crit Care Med 2018; 198:42–85
35. Dubowitz V SC, Oldfors A.: Muscle Biopsy: A Practical Approach, 4th edition. Philadelphia, Saunders Ltd., Elsevier, 2013
36. Schindelin J, Arganda-Carreras I, Frise E, Kaynig V, Longair M, Pietzsch T, Preibisch S, Rueden C, Saalfeld S, Schmid B, Tinevez JY, White DJ, Hartenstein V, Eliceiri K, Tomancak P, Cardona A: Fiji: An open-source platform for biological-image analysis. Nat Methods 2012; 9:676–82
37. Jung B, Constantin JM, Rossel N, Le Goff C, Sebbane M, Coisel Y, Chanques G, Futier E, Hugon G, Capdevila X, Petrof B, Matecki S, Jaber S: Adaptive support ventilation prevents ventilator-induced diaphragmatic dysfunction in piglet: An *in vivo* and *in vitro* study. Anesthesiology 2010; 112:1435–43
38. Heunks LM, Machiels HA, de Abreu R, Zhu XP, van der Heijden HF, Dekhuijzen PN: Free radicals in hypoxic rat diaphragm contractility: No role for xanthine oxidase. Am J Physiol Lung Cell Mol Physiol 2001; 281:L1402–12
39. Reid MB, Lännergren J, Westerblad H: Respiratory and limb muscle weakness induced by tumor necrosis factor-alpha: Involvement of muscle myofilaments. Am J Respir Crit Care Med 2002; 166:479–84
40. Ye S, Li Q, Yuan S, Shu H, Yuan Y: Restrictive fluid resuscitation leads to better oxygenation than non-restrictive fluid resuscitation in piglets with pulmonary or extrapulmonary acute respiratory distress syndrome. Med Sci Monit 2015; 21:2008–20
41. Byrne L, Obonyo NG, Diab SD, Dunster KR, Passmore MR, Boon AC, Hoe LS, Pedersen S, Fauzi MH, Pimenta LP, Van Haren F, Anstey CM, Cullen L, Tung JP, Shekar K, Maitland K, Fraser JF: Unintended consequences: Fluid resuscitation worsens shock in an ovine model of endotoxemia. Am J Respir Crit Care Med 2018; 198:1043–54
42. Tsentsevitsky AN KI, Bukharaeva EA, Nikolsky EE.: Effect of noradrenaline on the kinetics of evoked acetylcholine secretion in mouse neuromuscular junction. Biochemistry (Moscow) 2018; 12:327–332
43. Tsentsevitsky AN, Kovyazina IV, Bukharaeva EA: Diverse effects of noradrenaline and adrenaline on the quantal secretion of acetylcholine at the mouse neuromuscular junction. Neuroscience 2019; 423:162–71
44. Horn AG, Baumfalk DR, Schulze KM, Kunkel ON, Colburn TD, Weber RE, Bruells CS, Musch TI, Poole DC, Behnke BJ: Effects of elevated positive end-expiratory pressure on diaphragmatic blood flow and vascular resistance during mechanical ventilation. J Appl Physiol (1985) 2020; 129:626–35
45. Gauthier AP, Verbanck S, Estenne M, Segebarth C, Macklem PT, Paiva M: Three-dimensional reconstruction of the *in vivo* human diaphragm shape at different lung volumes. J Appl Physiol (1985) 1994; 76:495–506
46. Prezant DJ, Karwa ML, Kim HH, Maggiore D, Chung V, Valentine DE: Short- and long-term effects of testosterone on diaphragm in castrated and normal male rats. J Appl Physiol (1985) 1997; 82:134–43
47. Prezant DJ, Valentine DE, Gentry EI, Richner B, Cahill J, Freeman K: Effects of short-term and long-term androgen treatment on the diaphragm in male and female rats. J Appl Physiol (1985) 1993; 75:1140–9

ANESTHESIOLOGY

Phrenic Nerve Block and Respiratory Effort in Pigs and Critically Ill Patients with Acute Lung Injury

Sérgio M. Pereira, M.D., Ph.D., Bruno E. Sinedino, M.D., Eduardo L. V. Costa, M.D., Ph.D., Caio C. A. Morais, P.T., Ph.D., Michael C. Sklar, M.D., Cristhiano Adkson Sales Lima, P.T., Maria A. M. Nakamura, P.T., Ph.D., Otavio T. Ranzani, M.D., Ph.D., Ewan C. Goligher, M.D., Mauro R. Tucci, M.D., Ph.D., Yeh-Li Ho, M.D., Leandro U. Taniguchi, M.D., Ph.D., Joaquim E. Vieira, M.D., Ph.D., Laurent Brochard, M.D., Marcelo B. P. Amato, M.D., Ph.D.

ANESTHESIOLOGY 2022; 136:763–78

EDITOR'S PERSPECTIVE

What We Already Know about This Topic

- Excessive spontaneous inspiratory efforts potentially resulting in high tidal volumes in patients on mechanical ventilation for acute respiratory distress syndrome may exacerbate lung injury
- Strategies to control such efforts without involving overly deep sedation or neuromuscular blockade may be beneficial
- Phrenic nerve blockade with local anesthetics has seen limited use for select medical indications but has not been evaluated in the setting of acute lung injury

What This Article Tells Us That Is New

- The authors evaluated the effects of phrenic nerve block in a porcine model of acute respiratory distress syndrome and in nine patients with excessive inspiratory effort with acute respiratory distress syndrome on mechanical ventilation by evaluating transdiaphragmatic pressures and electrical activity, as well as distribution of ventilation by electrical impedance tomography
- In both groups, tidal volume, driving pressure, peak transpulmonary pressure, and electrical activity of the diaphragm decreased significantly with phrenic nerve block, with a slight decrease in dependent ventilation, while the respiratory rate was unchanged
- Duration of the block was approximately 12 h

ABSTRACT

Background: Strong spontaneous inspiratory efforts can be difficult to control and prohibit protective mechanical ventilation. Instead of using deep sedation and neuromuscular blockade, the authors hypothesized that perineural administration of lidocaine around the phrenic nerve would reduce tidal volume (V_T) and peak transpulmonary pressure in spontaneously breathing patients with acute respiratory distress syndrome.

Methods: An established animal model of acute respiratory distress syndrome with six female pigs was used in a proof-of-concept study. The authors then evaluated this technique in nine mechanically ventilated patients under pressure support exhibiting driving pressure greater than 15 cm H_2O or V_T greater than 10 ml/kg of predicted body weight. Esophageal and transpulmonary pressures, electrical activity of the diaphragm, and electrical impedance tomography were measured in pigs and patients. Ultrasound imaging and a nerve stimulator were used to identify the phrenic nerve, and perineural lidocaine was administered sequentially around the left and right phrenic nerves.

Results: Results are presented as median [interquartile range, 25th to 75th percentiles]. In pigs, V_T decreased from 7.4 ml/kg [7.2 to 8.4] to 5.9 ml/kg [5.5 to 6.6] ($P < 0.001$), as did peak transpulmonary pressure (25.8 cm H_2O [20.2 to 27.2] to 17.7 cm H_2O [13.8 to 18.8]; $P < 0.001$) and driving pressure (28.7 cm H_2O [20.4 to 30.8] to 19.4 cm H_2O [15.2 to 22.9]; $P < 0.001$). Ventilation in the most dependent part decreased from 29.3% [26.4 to 29.5] to 20.1% [15.3 to 20.8] ($P < 0.001$). In patients, V_T decreased (8.2 ml/ kg [7.9 to 11.1] to 6.0 ml/ kg [5.7 to 6.7]; $P < 0.001$), as did driving pressure (24.7 cm H_2O [20.4 to 34.5] to 18.4 cm H_2O [16.8 to 20.7]; $P < 0.001$). Esophageal pressure, peak transpulmonary pressure, and electrical activity of the diaphragm also decreased. Dependent ventilation only slightly decreased from 11.5% [8.5 to 12.6] to 7.9% [5.3 to 8.6] ($P = 0.005$). Respiratory rate did not vary. Variables recovered 1 to 12.7 h [6.7 to 13.7] after phrenic nerve block.

Conclusions: Phrenic nerve block is feasible, lasts around 12 h, and reduces V_T and driving pressure without changing respiratory rate in patients under assisted ventilation.

(ANESTHESIOLOGY 2022; 136:763–78)

Protective mechanical ventilation is a cornerstone treatment for patients with acute respiratory distress syndrome (ARDS).[1] High levels of sedatives and neuromuscular blocking agents are often required to maintain protective ventilation and avoid asynchronies.[2,3] Yet this practice is controversial because deep sedation is associated with unfavorable patient-centered outcomes such as delirium, prolonged mechanical ventilation, intensive care unit–acquired weakness, higher in-hospital, and 180-day mortality.[4]

The progression from controlled to assisted mechanical ventilation may obviate the need for deep sedation and has

Supplemental Digital Content is available for this article. Direct URL citations appear in the printed text and are available in both the HTML and PDF versions of this article. Links to the digital files are provided in the HTML text of this article on the Journal's Web site (www.anesthesiology.org). This article has a visual abstract available in the online version. The results of this study were presented at the Pleural Pressure Working Group online meeting on April 16, 2021. S.M.P. and B.E.S. contributed equally to this article.

Submitted for publication May 18, 2021. Accepted for publication January 26, 2022. Published online first on March 29, 2022.

<zdoi; 10.1097/ALN.0000000000004161>

additional benefits such as lung recruitment, better oxygenation, and hemodynamic improvement.[5] Conversely, these benefits might be outweighed by vigorous inspiratory efforts, resulting in loss of lung protection,[6] load-induced diaphragmatic injury, as observed in patients with chronic obstructive pulmonary disease, as well as in animal studies,[7] and possibly patient self-inflicted lung injury.[8–10]

Both pharmacologic and nonpharmacologic strategies have been proposed to reduce inspiratory effort and keep patients under protective mechanical ventilation settings.[11] Doorduin *et al.* tested partial neuromuscular blockade in patients with ARDS[12]; however, their approach still utilized neuromuscular blocking agents and did not entirely avert their side effects, such as global muscle atrophy.[13]

Phrenic nerve block has been used for the treatment of chronic and perioperative hiccups[14] and it is also frequently observed in patients undergoing interscalene block for upper limb surgery.[15] These patients may have transient hemidiaphragmatic palsy depending on local anesthetic concentration,[16] volume administered,[17] and injection site,[15] but experience few symptoms that do not require specific treatment.[18] The use of ultrasound is proposed to decrease the risk of complications related to brachial plexus blocks (*e.g.,* accidental vascular puncture[19] or intraneural administration of local anesthetics[20]).

This proof-of-concept study proposes a novel approach to maintain lung-protective ventilation in spontaneously breathing patients. We hypothesized that perineural administration of lidocaine to the phrenic nerve reduces diaphragm electrical activity without the need for systemic paralysis and deeper sedation. First we tested our hypothesis in a proof-of-concept experiment in a porcine model of ARDS. Then we assessed the safety, feasibility, and efficacy of this approach in patients breathing spontaneously with invasive mechanical ventilation. We reasoned that a lidocaine-associated decrease in electrical activity of the diaphragm could decrease esophageal pressure swings (ΔP_{eso}) and tidal volume (V_T) and ultimately maintain lung-protective ventilation while keeping pigs and patients under moderate to light sedation.

Materials and Methods

These studies were approved by two different ethics committees: one for animal experiments and one for clinical studies. Both protocols were funded by the University of São Paulo Medical School (São Paulo, Brazil). For further information and complete methods, please refer to Supplemental Digital Content 1 (http://links.lww.com/ALN/C800).

Animal Protocol

After the approval by the Ethics Committee for Animal Studies (No. 967/2017, Faculdade de Medicina da Universidade de São Paulo), six female Landrace pigs with average weights of 36.9 kg were chosen (bladder catheterization in females was easier). The experimental protocol has been described previously.[6] Briefly, pigs monitored with electrocardiogram and pulse oximetry were anesthetized with intramuscular ketamine and midazolam, followed by intravenous midazolam, fentanyl, and pancuronium (a neuromuscular blocking agent). An internal jugular vein catheter and femoral artery line were placed to sample blood gases, administer vasoactive drugs, and monitor blood pressure. An esophageal balloon (Nutrivent; Sidam, Italy) was inserted to allow measurement of P_{eso}; correct placement was verified using the occlusion technique.[21] We measured electrical activity of the

Sérgio M. Pereira, M.D., Ph.D.: Division of Pneumology (Laboratory of Medical Investigation 09), Faculty of Medicine, University of São Paulo, São Paulo, Brazil; Department of Anesthesia and Pain Medicine, Unity Health Toronto; Interdepartmental Division of Critical Care; and Keenan Center for Biomedical Research, Li Ka Shing Knowledge Institute, St. Michael's Hospital, Toronto, Ontario, Canada.

Bruno E. Sinedino, M.D.: Anesthesiology Discipline, Department of Surgery, Faculty of Medicine, University of São Paulo, São Paulo, Brazil.

Eduardo L. V. Costa, M.D., Ph.D.: Division of Pneumology (Laboratory of Medical Investigation 09) Faculty of Medicine, University of São Paulo, São Paulo, Brazil; Syrian-Lebanese Institute of Teaching and Research, Hospital Sírio-Libanês, São Paulo, Brazil.

Caio C. A. Morais, P.T., Ph.D.: Division of Pneumology (Laboratory of Medical Investigation 09) Faculty of Medicine, University of São Paulo, São Paulo, Brazil; and Department of Physiotherapy, Federal University of Pernambuco, Recife, Brazil.

Michael C. Sklar, M.D.: Department of Anesthesia and Pain Medicine, Unity Health Toronto; Interdepartmental Division of Critical Care; and Keenan Center for Biomedical Research, Li Ka Shing Knowledge Institute, St. Michael's Hospital, Toronto, Ontario, Canada.

Cristhiano Adkson Sales Lima, P.T.: Division of Pneumology (Laboratory of Medical Investigation 09) Faculty of Medicine, University of São Paulo, São Paulo, Brazil.

Maria A. M. Nakamura, P.T., Ph.D.: Division of Pneumology (Laboratory of Medical Investigation 09) Faculty of Medicine, University of São Paulo, São Paulo, Brazil.

Otavio T. Ranzani, M.D., Ph.D.: Division of Pneumology (Laboratory of Medical Investigation 09) Faculty of Medicine, University of São Paulo, São Paulo, Brazil; Barcelona Institute for Global Health, ISGlobal, Barcelona, Spain.

Ewan C. Goligher, M.D.: Interdepartmental Division of Critical Care Medicine, University of Toronto, Toronto, Ontario, Canada; Department of Medicine, Division of Respirology, University Health Network, Toronto, Ontario, Canada; Toronto General Hospital Research Institute, Toronto, Ontario, Canada.

Mauro R. Tucci, M.D., Ph.D.: Division of Pneumology (Laboratory of Medical Investigation 09) Faculty of Medicine, University of São Paulo, São Paulo, Brazil.

Yeh-Li Ho, M.D.: Intensive Care Unit, Division of Clinical Infectious and Parasitic Diseases, Clinical Hospital, Faculty of Medicine, University of São Paulo, São Paulo, Brazil.

Leandro U. Taniguchi, M.D., Ph.D.: Syrian-Lebanese Institute of Teaching and Research, São Paulo, Brazil; Emergency Medicine Discipline, Clinical Hospital, University of São Paulo, São Paulo, Brazil.

Joaquim E. Vieira, M.D., Ph.D.: Anesthesiology Discipline, Department of Surgery, Faculty of Medicine, University of São Paulo, São Paulo, Brazil.

Laurent Brochard, M.D.: Interdepartmental Division of Critical Care, and Keenan Center for Biomedical Research, Li Ka Shing Knowledge Institute, St. Michael's Hospital, Toronto, Ontario, Canada; Interdepartmental Division of Critical Care Medicine, University of Toronto, Toronto, Ontario, Canada.

Marcelo B. P. Amato, M.D., Ph.D.: Respiratory Intensive Care Unit and Laboratory of Medical Investigation 09, INCOR, Heart Institute, Faculty of Medicine, University of São Paulo, São Paulo, Brazil.

diaphragm using a dedicated Neurally Adjusted Ventilatory Assist catheter (Maquet Critical Care, Sweden). Electrical impedance tomography was recorded using an Enlight monitor (Timpel, Brazil) with 32 electrodes embedded in a customized silicon belt placed on the perimeter, defining a cross-sectional plane of the thorax at the level of the sixth intercostal space (*i.e.,* parasternal line).

The experimental protocol consisted of two phases: (phase 1) lung injury and pressure support titration, and (phase 2) phrenic nerve blockade (fig. 1). In phase 1, we induced severe ARDS by lung lavage with Tween (an astringent solution) followed by injurious mechanical ventilation until a Pao_2/inspiratory oxygen fraction ratio less than or equal to 150 mmHg with a positive end-expiratory pressure (PEEP) of 10 cm H_2O (during the whole procedure) was reached under deep sedation (propofol, ketamine, and remifentanil). Then anesthesia was titrated down until spontaneous inspiratory effort reached a ΔP_{eso} greater than or equal to 10 cm H_2O during an airway occlusion procedure.[6] After lung injury and sedation titration, 1 mg/kg succinylcholine and 1 to 2 mg/kg propofol were administered, and pigs were briefly ventilated on pressure-controlled ventilation. We calculated respiratory system compliance (C_{dyn}), and titrated inspiratory pressure to guarantee a V_T greater than 4 ml/kg. After succinylcholine and propofol had weaned and the pig was back to assisted ventilation, and regardless of the pig's inspiratory effort, this guaranteed V_T greater than 4 ml/kg after bilateral phrenic nerve block. The inspiratory pressure was kept unchanged during the entire protocol.

In phase 2, we performed bilateral phrenic nerve block using ultrasound imaging and a neurostimulator to identify the cervical plexus by the motor response on the ipsilateral arm (Plexygon, Vygon, Italy). The identification was followed by the injection of 20 ml lidocaine, 2%. Please refer to Supplemental Digital Content 2 (http://links.lww.com/ALN/C828) for further information.

Electrical activity of the diaphragm, ΔP_{eso}, V_T, peak transpulmonary pressure, driving pressure, and dorsal and left lung ventilation were monitored. Peak transpulmonary pressure was calculated as pressure support − ΔP_{eso} during spontaneous breathing. Driving pressure was calculated as V_T/C_{dyn} because no inspiratory pauses were performed. Please refer to Supplemental Digital Content 3 (http://links.lww.com/ALN/C829) for further information. For ventilation distribution analysis, the electrical impedance tomography image was divided into the right and left lung, and into four regions of interest, each covering 25% of the ventrodorsal diameter. The percentage of ventilation in the most dependent region of the lung was calculated as reflecting the inspiratory activity of the diaphragm and being the most gravity-dependent zone. Please refer to Supplemental Digital Content 4 (http://links.lww.com/ALN/C830) for further information. The percentage of left lung ventilation was analyzed to estimate any changes in ventilation distribution that could have been induced by the sequential phrenic nerve blockade. During assisted ventilation, *pendelluft* was quantified, a phenomenon that occurs when a strong diaphragmatic contraction leads to deflation

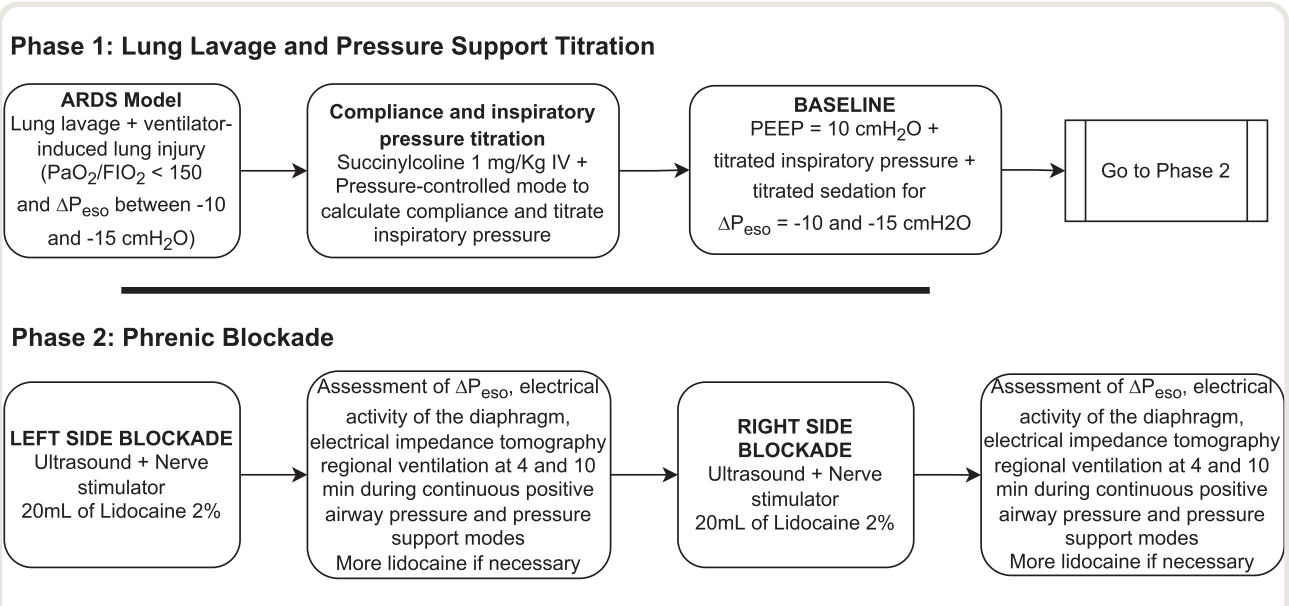

Fig. 1. Animal study protocol. In phase 1, acute respiratory distress syndrome (ARDS) was induced by lung lavage and injurious invasive mechanical ventilation. Deep sedation was halted when Pao_2/inspiratory oxygen fraction (FIO_2) ratio was lower than 150 mmHg with positive end-expiratory pressure (PEEP) of 10 cm H_2O. Sedation was then titrated to maintain pigs with high inspiratory effort, defined as change in esophageal pressure (ΔP_{eso}) greater than or equal to 10 cm H_2O during an inspiratory pause. A bolus of propofol and succinil was administered to calculate respiratory system compliance, and to titrate inspiratory pressure. In phase 2, the authors performed bilateral phrenic nerve block using ultrasound and a neurostimulator. In all pigs, the left phrenic nerve was blocked first, and the right phrenic nerve was blocked last. IV, intravenous.

of the ventral portion of the lung and overdistention of the dorsal portion of the lung during early inflation[22] and that can cause regional lung injury.[6] Data acquisition in pigs occurred at five time points: before phrenic nerve blockade during assisted ventilation (*i.e.,* baseline); 4 min after left phrenic block; 10 min after the left phrenic block; 4 min after the right phrenic block; and 10 min after right phrenic block.

Our primary goal was to evaluate whether this technique was feasible and efficient at reducing V_T or peak transpulmonary pressure. Secondary objectives were to quantify the decrease in electrical activity of the diaphragm, ΔP_{eso}, and driving pressure, as well as changes in the distribution of ventilation.

Human Protocol

After obtaining Institutional Review Board approval (Certificate for Ethics Presentation and Appreciation number: 02029118.2.0000.0068), patients admitted for ARDS and under assisted spontaneous breathing were screened for inclusion in the study between May 2019 and September 2020. Informed consent was obtained from legal guardians. Of note, written informed consent was obtained for the first three patients, but during the COVID-19 outbreak, strict visiting policies were implemented, and oral consent was authorized and taken from the substitute decision-maker *via* telephone. Data collection was carried out in the respiratory intensive care unit at Heart Institute (Instituto do Coração) of the Hospital das Clínicas (University of São Paulo Medical School). This study was registered at clinicaltrials.gov (NCT03978845).

Patients eligible for the study protocol had to be older than 18 yr; on invasive pressure support ventilation with a Pao_2/inspiratory oxygen fraction ratio less than 300 mmHg triggering the ventilator; and a driving pressure greater than 15 cm H_2O or a V_T greater than 10 ml/kg of predicted body weight. We evaluated if a reliable plateau pressure could be obtained and calculated the driving pressure by subtracting PEEP from plateau pressure during an inspiratory pause.[23] If driving pressure was greater than 15 cm H_2O and/or V_T was greater than 10 ml/kg, the patient fulfilled inclusion criteria. Exclusion criteria included use of long-acting neuromuscular blocking agents in the previous 3 h; pain or Richmond Agitation–Sedation Scale score greater than 0; arterial pH less than 7.25; hemodynamic instability or a need for increased doses of vasopressor drugs in the previous 2 h; intracranial hypertension; presence of chest or abdominal fistula; neuromuscular disease; spinal cord trauma; massive ascites; burns in the thoracic region; tetanus; and pregnancy.

The Richmond Agitation–Sedation Scale was used for measurement of their level of sedation; in addition, two patients were monitored *via* Bispectral Index to assess sedation depth. An electrode belt (Timpel Enlight 1800 Model; Timpel) was installed in the thoracic region between the fourth and fifth intercostal spaces. Two esophageal catheters (Nutrivent and Neurally Adjusted Ventilatory Assist catheter) were positioned and calibrated to measure esophageal pressure and electrical activity of the diaphragm, respectively. Flow, pressures (peak, plateau, PEEP), and V_T were continuously recorded from the electrical impedance tomography device and from the SERVO-i ventilator (Maquet Critical Care) connected to a laptop using the Servo Tracker application (Maquet Critical Care). ΔP_{eso} was monitored using either the Optivent (Optivent Sidam, Italy) or the Pneumodrive device (Bionica, Brazil). Correct placement of the esophageal catheter was verified using the occlusion technique.[21] Heart rate, blood pressure, and peripheral oxygenation were continuously monitored. After inclusion of the patient in the protocol, sedation was not changed, and vasoactive drugs were titrated at the discretion of the attending physician.

The clinical protocol consisted of three phases: (phase 1) inspiratory pressure titration, (phase 2) bilateral phrenic nerve block, and (phase 3) recovery phase (fig. 2). During phase 1, succinylcholine (1 mg/kg) and propofol (1.5 to 2.5 mg/kg) were administered, and patients were briefly ventilated on pressure-controlled ventilation. We calculated respiratory system compliance, and titrated inspiratory pressure that was kept unchanged after the effect of succinylcholine and propofol had weaned. This way, regardless of the patient's inspiratory effort, we would guarantee V_T greater than 4 ml/kg of after bilateral phrenic nerve block.

During phase 2, a trained anesthesiologist performed phrenic nerve block using an ultrasound (Mindray M6 Ultrasound System; China) and a peripheral nerve stimulator (Stimuplex HNS 12B Braun; Germany). Of note, an anesthesiologist who has performed 15 peripheral blocks is able to distinguish anatomical landmarks and has a success rate close to 90%.[24] Please refer to Supplemental Digital Content 5 (http://links.lww.com/ALN/C831) for further information. The combination of ultrasound and neurostimulator minimizes the risk of intravascular or intraneural injection, neural damage, and vascular bruising.[25] Use of ultrasound minimizes the risk of complications and allows observation of local anesthetic dispersion; the neurostimulator avoids intraneural administration of local anesthetic, thus minimizing risk of a potential association with neural damage.[25] When the patient has motor response at low current output (*e.g.*, less than 0.2 mA), one cannot ensure that the needle is not intraneural. We did not administer lidocaine if the phrenic nerve could not be visualized or if the patient had a motor response at a current output that was lower than 0.50 mA, greatly minimizing risk of intraneural injection.[26] Finally, we used lidocaine due to its pharmacokinetic and pharmacodynamic properties: shorter half-life, better cardiovascular stability, low latency, and faster onset than other local anesthetics.[27]

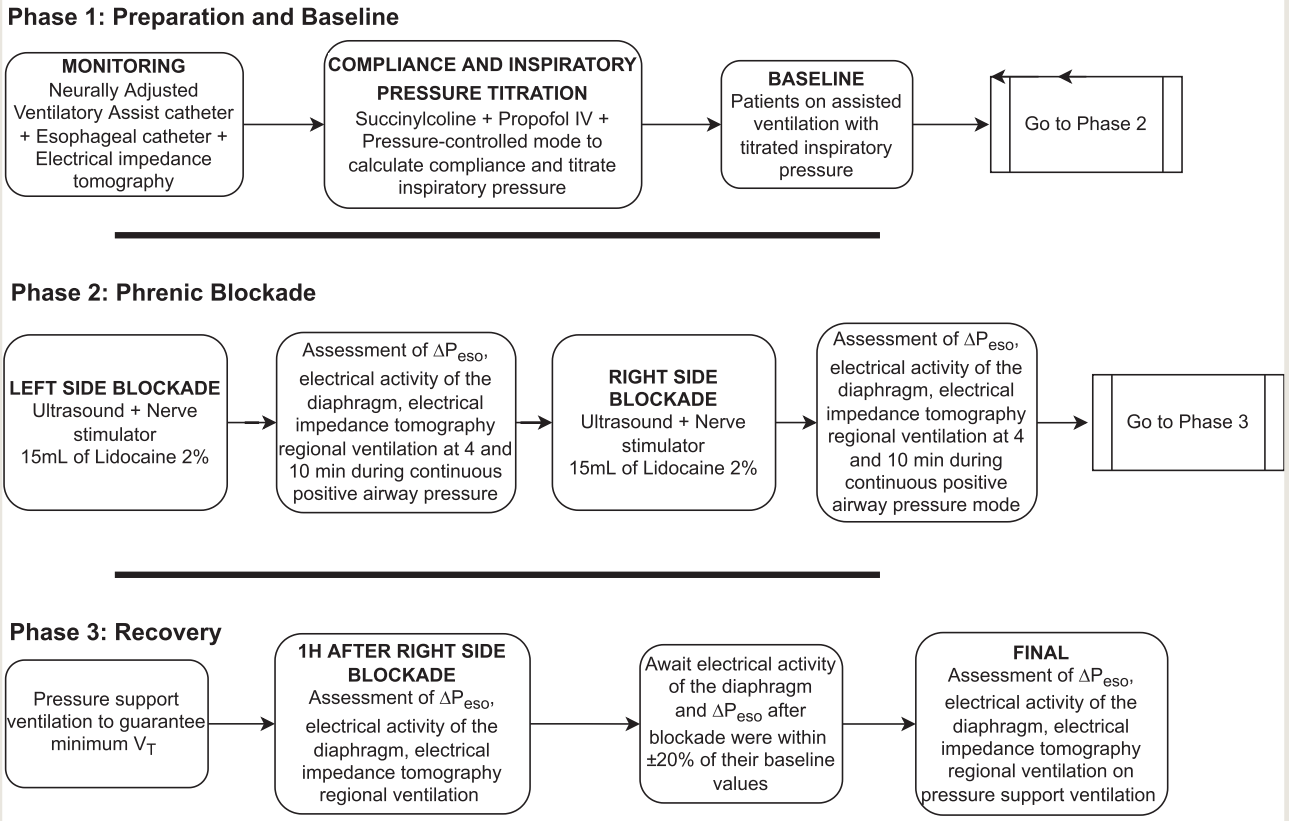

Fig. 2. Clinical study protocol. In phase 1, patients were monitored with Neurally Adjusted Ventilatory Assist catheter (Maquet Critical Care, Sweden), esophageal balloon, and electrical impedance tomography. A bolus of succinylcholine and propofol was administered to titrate inspiratory pressure and calculate respiratory system compliance. The final time point was recorded when electrical activity of the diaphragm, change in esophageal pressure (ΔP_{eso}), and tidal volume (V_T) were within ±20% of baseline values. In phase 2, left phrenic nerve and right phrenic nerve were blocked using ultrasound and a neurostimulator. The authors assessed respiratory variables at 4 and 10 min after each block. In phase 3, the recovery phase started after bilateral phrenic nerve block and ended when patients had fully recovered (*i.e.*, the final time point). IV, intravenous.

The study protocol was conducted under a predefined sequence: the protocol was initiated on the left nerve, then followed by blockade of the right phrenic nerve 10 min later. We assessed the phrenic nerve block with three tools: electrical activity of the diaphragm signal, ΔP_{eso}, and regional ventilation distribution on continuous positive airway pressure. We evaluated the (1) percentage of patients blocked, (2) amount of time spent from scanning to administration of lidocaine, and (3) duration until recovery. Full recovery from bilateral phrenic nerve blockade was defined as the time after bilateral nerve block when the electrical activity of the diaphragm, ΔP_{eso}, and V_T were within ±20% of baseline values.

Electrical activity of the diaphragm, ΔP_{eso}, V_T per predicted body weight, peak transpulmonary pressure, driving pressure, respiratory rate in breaths per minutes, and ventilation distribution were analyzed. Peak transpulmonary pressure was calculated as pressure support − ΔP_{eso}. Driving pressure was calculated as V_T/C_{dyn} because no inspiratory pauses were performed. Please refer to Supplemental Digital Content 3 (http://links.lww.com/ALN/C829) for further information. Ventilation distribution was also assessed. Finally, the percentage of left lung ventilation was analyzed. Please refer to Supplemental Digital Content 4 (http://links.lww.com/ALN/C830) for further information. Data acquisition occurred at seven time points: before phrenic nerve blockade during assisted ventilation (*i.e.,* baseline), 4 min after left phrenic block, 10 min after the left phrenic block, 4 min after the right phrenic block, 10 min after right phrenic block, 1 h after right phrenic block, and on the following day (*i.e.,* final).

The primary goal was to evaluate the reduction in V_T or peak transpulmonary pressure. Secondary objectives included changes in electrical activity of the diaphragm, ΔP_{eso}, driving pressure, and respiratory rate. We also analyzed ventilation distribution using electrical impedance tomography and assessed whether a bilateral phrenic nerve block could either reduce or abolish pendelluft. Finally, we

aimed to evaluate the time to wean from the block, as well as feasibility, safety, and efficacy of this technique.

Statistical Analysis

No statistical power calculation was used to guide sample size. An initial sample size of 10 patients was planned, but only 9 were included because a Neurally Adjusted Ventilatory Assist catheter malfunctioned. The unadjusted results are reported as median and interquartile range. We fitted linear mixed models for each outcome, accounting for the repeated measurements on each subject with a random intercept. Models were adjusted for time (baseline, 4 min after left phrenic block, 10 min after the left phrenic block, 4 min after the right phrenic block, 10 min after right phrenic block, 1 h after right phrenic block, and final), PEEP (continuous variable), and pressure support (continuous variable) at each time point for humans; and for time (baseline, 4 min after left phrenic block, 10 min after the left phrenic block, 4 min after the right phrenic block, 10 min after right phrenic block) and pressure support (continuous variable) at each time point for pigs. Data from pigs and humans were analyzed separately. No imputation was performed for missing data. All outcome variables, except for ventilation in the most dependent region of the lungs in humans and V_T during continuous airway pressure in pigs, were log-transformed to obtain a normal distribution of residuals. *P* values were corrected for multiple comparisons using the Bonferroni method; a two-sided corrected *P* value less than 0.05 was considered statistically significant. In humans, we performed 21 comparisons (pairwise combination of seven levels). Therefore, the target *P* value was 0.002 (*i.e.,* 0.05/21). We presented instead the "corrected *P* value," *i.e.*, the unadjusted *P* value × 21. The same method was applied for pigs, where we performed 10 comparisons (pairwise combination of five levels). For the analysis of heart rate and blood pressure, which were collected in two time points, we performed a Wilcoxon signed-rank test.

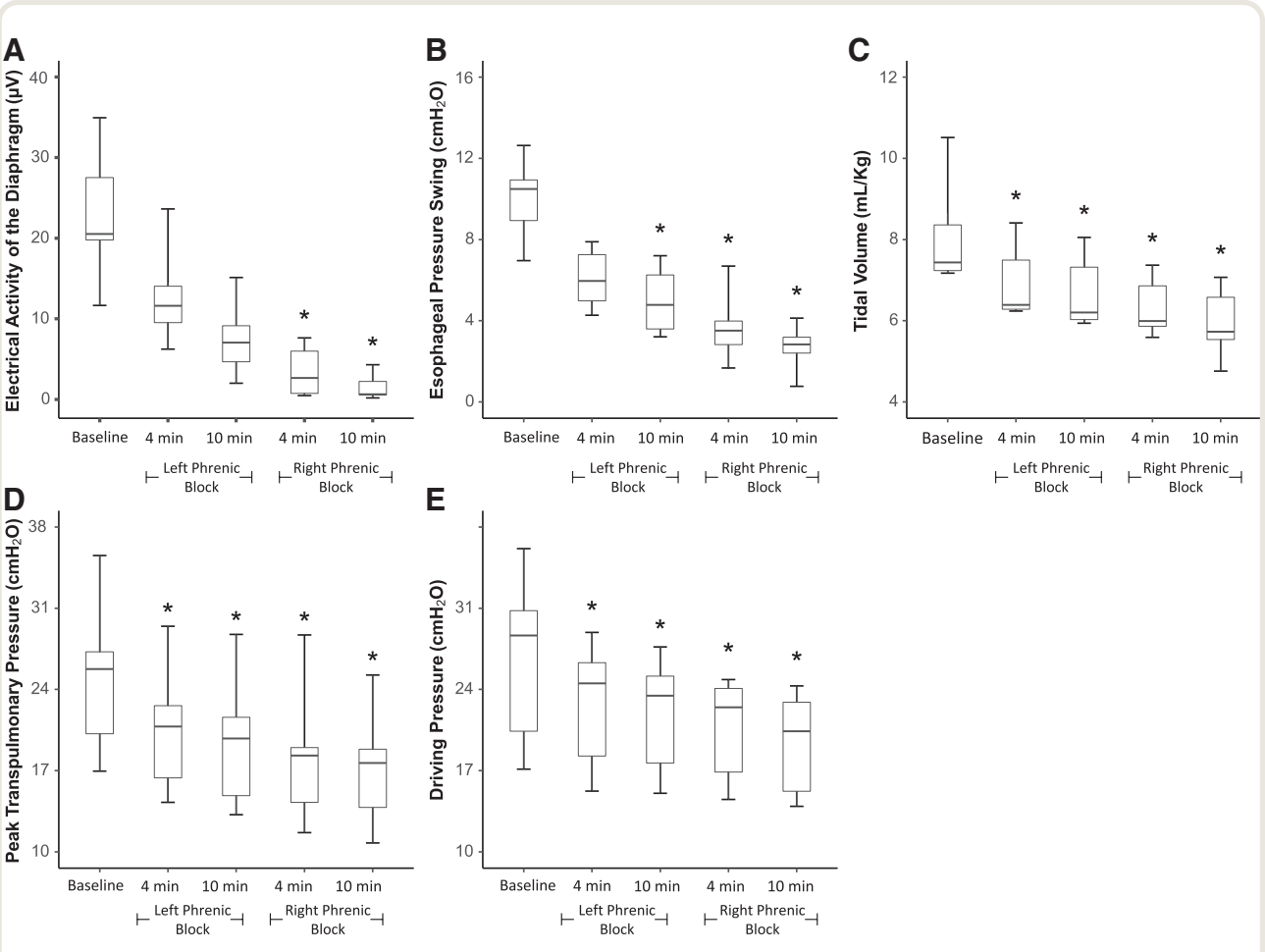

Fig. 3. Progress of respiratory variables in pigs. Unadjusted data presented as median [interquartile range]. (*A*) Electrical activity of the diaphragm in microvolts. (*B*) Esophageal pressure swing in cm H_2O. (*C*) Tidal volume in ml/kg of predicted body weight. (*D*) Peak transpulmonary pressure in cm H_2O. (*E*) Driving pressure in cm H_2O. After lidocaine administration, all variables progressively decreased over time. *Corrected $P < 0.05$ when compared to baseline.

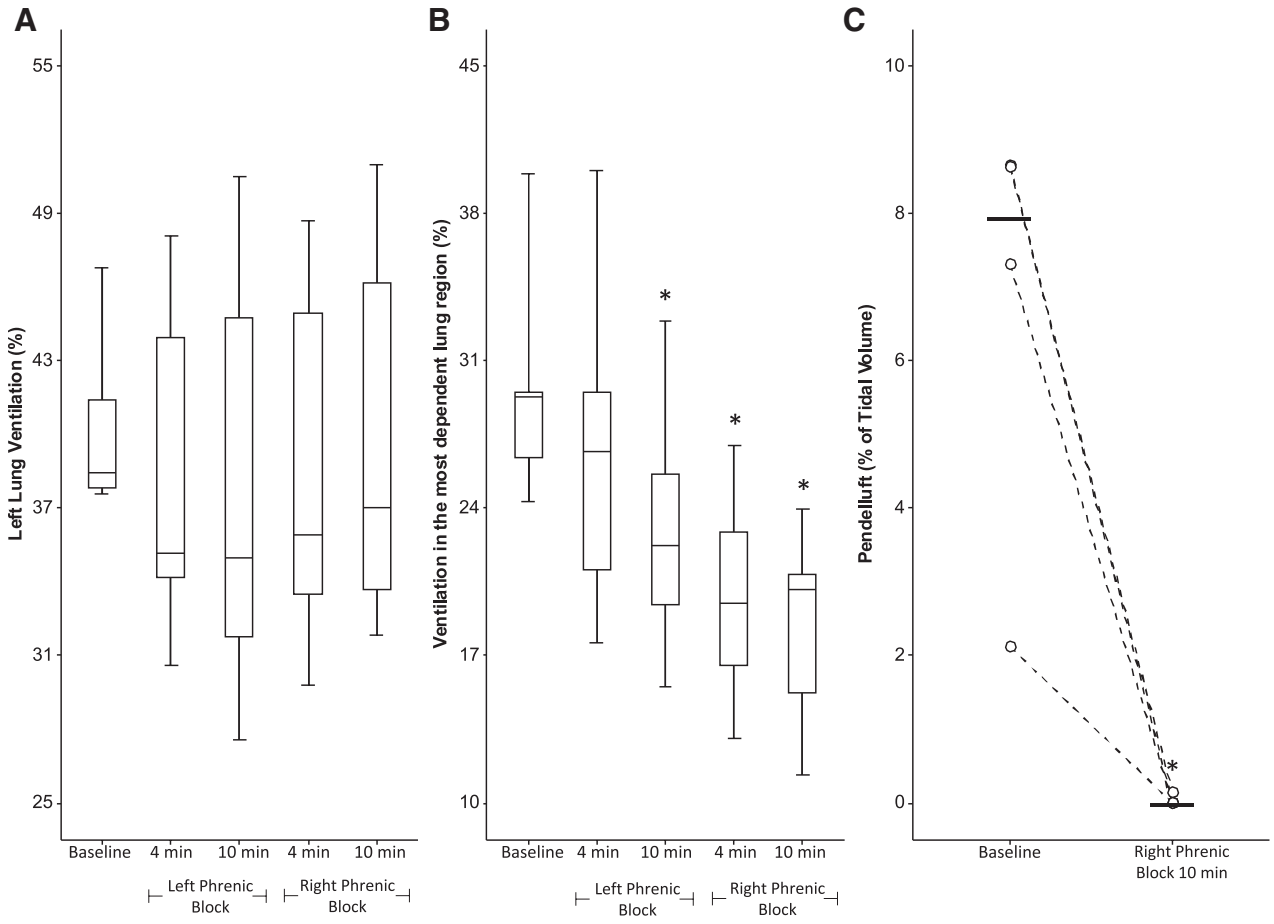

Fig. 4. Ventilation distribution and pendelluft in pigs. Unadjusted data presented as median [interquartile range]. (*A*) Left lung ventilation (%). (*B*) Ventilation in the most dependent lung region (%). (*C*) Amount of pendelluft at baseline and 10 min after bilateral phrenic nerve block in four pigs. *Corrected $P < 0.05$ when compared to baseline.

All figures were plotted, and statistical analyses were performed in software R 3.5.1 (R Foundation for Statistical Computing, Austria) and Rstudio (Rstudio Team, USA).

Results

Six pigs and nine patients were successfully included in this study. All values are presented as median [interquartile range, 25th to 75th percentile]. Please refer to Supplemental Digital Content 1 (http://links.lww.com/ALN/C800) and Supplemental Digital Content 6 (http://links.lww.com/ALN/C832) for further information.

Pig Study

We successfully blocked the phrenic nerve bilaterally in six pigs (100%). All variables but left lung ventilation decreased significantly when compared from baseline to 10 min after left phrenic block (figs. 3 and 4; table 1): electrical activity of the diaphragm from 20.5 μV [19.8 to 27.5] to 0.7 μV [0.6 to 2.2] (corrected $P < 0.001$); ΔP_{eso} from 10.5 cm H_2O [8.9 to 10.9] to 2.7 cm H_2O [2.4 to 3.2] (corrected $P < 0.001$); V_T from 7.4 ml/kg [7.2 to 8.4] to 5.9 ml/kg [5.5 to 6.7] of predicted body weight (corrected $P < 0.001$); peak transpulmonary pressure from 25.8 cm H_2O [20.2 to 27.2] to 17.7 cm H_2O [13.8 to 18.8] (corrected $P < 0.001$); and driving pressure from 28.7 cm H_2O [20.4 to 30.8] to 19.4 cm H_2O [15.2 to 22.9] (corrected $P < 0.001$). The percentage of ventilation in the most dependent region of the lung decreased from 29.3% [26.4 to 29.5] to 20.1% [15.3 to 20.8] (corrected $P < 0.001$), and the percentage of ventilation distribution to the left lung ventilation did not change from 38.5 [37.8 to 41.4] to 37.0 [33.7 to 46.2] (corrected $P > 0.999$).

In four pigs ventilated on continuous positive airway pressure (fig. 5), there was a decrease in V_T from 5.9 ml/kg [4.9 to 7.2] to 3.1 ml/kg [2.0 to 4.0] of predicted body weight (corrected $P = 0.009$) when baseline was compared to 10 min after right phrenic block. At baseline, four pigs had pendelluft. After bilateral phrenic nerve block, pendelluft was reduced from 8% [6.0 to 8.6] to 0% [0 to 0.0] ($P < 0.001$) of V_T before the ventilator was triggered (fig. 4C).

Table 1. Progress of Respiratory Variables in Pigs

Parameter	Baseline	Four Minutes after Left Phrenic Block × Baseline	Ten Minutes after Left Phrenic Block × Baseline	Four Minutes after Right Phrenic Block × Baseline	Ten Minutes after Right Phrenic Block × Baseline
Electrical activity of the diaphragm, μV	3.0 (2.3 to 3.8)	−0.6 (−2.0 to 0.8)	−1.2 (−2.6 to 0.2)	−2.3 (−3.7 to −0.9)*	−3.1 (−4.5 to −1.7)*
Esophageal pressure swing, cm H_2O	2.3 (2.0 to 2.5)	−0.5 (−1.0 to 0.0)	−0.7 (−1.2 to −0.2)*	−1.0 (−1.5 to −0.6)*	−1.4 (−1.9 to −0.9)*
Tidal volume, ml/kg of predicted body weight	2.1 (1.9 to 2.2)	−0.2 (−0.2 to −0.1)*	−0.2 (−0.3 to −0.1)*	−0.2 (−0.3 to −0.2)*	−0.3 (−0.4 to −0.2)*
Peak transpulmonary pressure, cm H_2O	3.2 (3.1 to 3.3)	−0.2 (−0.3 to −0.1)*	−0.2 (−0.3 to −0.1)*	−0.3 (−0.4 to −0.2)*	−0.4 (−0.5 to −0.2)*
Driving Pressure, cm H_2O	3.2 (3.0 to 3.5)	−0.1 (−0.1 to −0.2)*	−0.2 (−0.1 to −0.3)*	−0.2 (−0.1 to −0.3)*	−0.3 (−0.2 to −0.4)
Left lung ventilation, %	3.7 (3.5 to 3.9)	−0.1 (−0.2 to 0.1)	−0.1 (−0.2 to 0.1)	−0.1 (−0.2 to 0.1)	0.0 (−0.2 to 0.1)
Ventilation in the most dependent portion of the lung, %	3.4 (3.1 to 3.7)	−0.1 (−0.3 to 0.1)	−0.3 (−0.5 to −0.1)*	−0.4 (−0.6 to −0.2)*	−0.5 (−0.7 to −0.3)*

Estimates from the mixed-model analyses with outcomes log transformed and adjusted to time and pressure support. Data presented as the contrast between time point and baseline. 99.5% CI; *P* values corrected by Bonferroni method.

*$P < 0.05$ when compared to baseline.

Human Study

Nine patients (three women and six men) with ARDS were included in this study. Table 2 shows patient characteristics and respiratory variables after pressure support titration at baseline.

Primary Outcomes

Feasibility and Efficacy. The phrenic nerves could be visualized bilaterally in all patients. Bilateral phrenic nerve block was then successfully performed in all patients with the administration of 15 ml lidocaine, 2%, around each phrenic

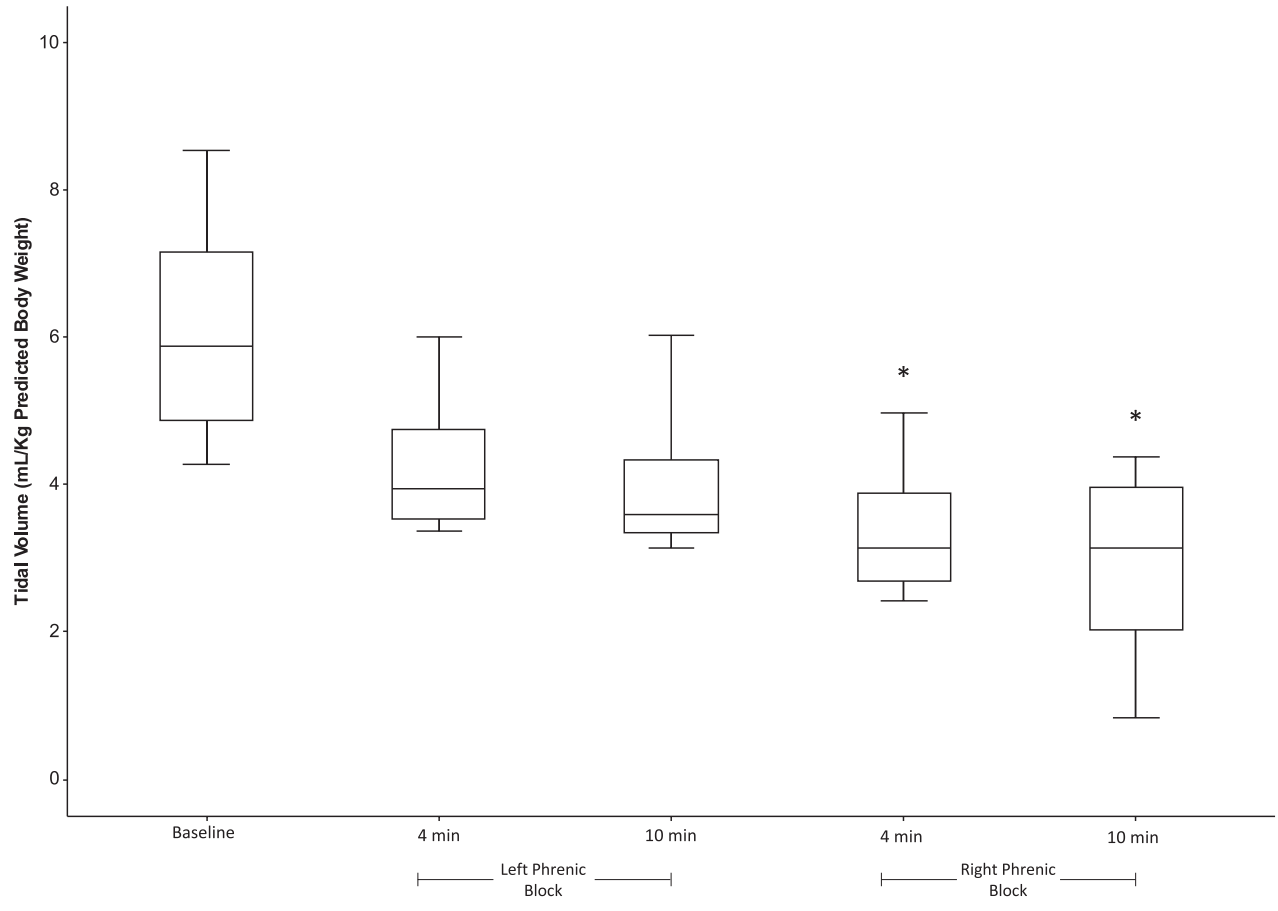

Fig. 5. Progress of tidal volume in pigs on continuous positive airway pressure. Unadjusted data presented as median [interquartile range]. *Corrected $P < 0.05$ when compared to baseline.

Table 2. Diagnosis, Time to Full Recovery, and Ventilatory Settings before Phrenic Nerve Blockade

No.	FIO_2, %	Sex	PEEP, cm H_2O	Support Level, cm H_2O	V_T, ml/kg	Driving Pressure, cm H_2O	Electrical Activity of the Diaphragm, μV	ΔP_{eso}, cm H_2O	Peak Transpulmonary Pressure, cm H_2O	Richmond Agitation–Sedation Scale	Sedation	Pao_2/FIO_2, mmHg	Admission Diagnosis	Final, min
1	50	Female	8	8	11.1	20.3	24.16	12.4	20.4	–3	Propofol + fentanyl	210	Tuberculosis	195
2	100	Male	8	12	15.1	61.4	42.86	35	55	–4	Propofol + fentanyl + midazolam	138	Giant cell pneumonia	1421
3	60	Male	8	27	7.4	34.8	26.89	5.9	32.9	–5	Propofol + fentanyl + midazolam	160	Pneumocystosis + cytomegalovirus	390
4	30	Male	6	18	10.3	30.8	—	8.33	26.3	–2	Midazolam + fentanyl	215	COVID-19	399
5	30	Male	5	12	8.2	19.2	39	7.21	19.2	–1	Ketamine	271	COVID-19	699
6	50	Female	5	15	12.5	41.7	12.4	3.92	20.9	–1	—	146	COVID-19	769
7	40	Male	5	14	6.8	16.6	15.9	8.9	21.9	–5	Propofol + ketamine	110	COVID-19	927
8	40	Male	8	25	7.0	26.8	3.15	4.5	29.5	–5	Propofol	184	COVID-19	821
9	50	Female	10	17	7.9	22.0	11.4	—	22	–3	Fentanyl	147	COVID-19	763

Baseline data were recorded after patients had been included in the study and the titration of inspiratory pressure had been done. All patients were breathing spontaneously. "Baseline" refers to this period in all tables and figures. Driving pressure, calculated as tidal volume over respiratory system compliance, was assessed while patients were making inspiratory efforts during pressure support ventilation.

ΔP_{eso}, esophageal pressure swing; FIO_2, inspiratory oxygen fraction; PEEP, positive end-expiratory pressure; V_T, tidal volume.

nerve. The left phrenic nerve block required 6.5 min [4.5 to 12.2] (between baseline and 4 min after left phrenic block), and the right phrenic block required 7.4 min [5.8 to 11.1] (between the 10 min after left phrenic block and 4 min after right phrenic block time points). From baseline to bilateral phrenic nerve block, the time was 14.6 [11.3 to 23.4] min.

Safety. No complications such as severe tachycardia or prolonged phrenic nerve palsy were observed in any participant. In addition, none of our patients presented elevation of diaphragm the day after the phrenic nerve block.

Reduction and Recovery of V_T and Peak Transpulmonary Pressure. After bilateral phrenic nerve block and compared to baseline (figs. 6 and 7; table 3), there was a decrease (10 min after right phrenic block) in V_T from 8.2 ml/kg [7.9 to 11.1] to 6.0 ml/kg [5.7 to 6.7] of predicted body weight (corrected $P < 0.001$) and peak transpulmonary pressure from 24.1 cm H_2O [20.1 to 30.4] to 18.3 cm H_2O [14.4 to 26.5] (corrected $P = 0.025$).

One hour after right phrenic block, when compared to baseline (figs. 6 and 7; table 3), V_T decreased from 8.2 [7.9 to 11.1] to 6.5 [6.1 to .9] (corrected $P < 0.001$), but peak transpulmonary pressure did not decrease (24.1 cm H_2O [20.1 to 30.4] to 21.7 cm H_2O [16.3 to 29.3] corrected $P > 0.999$). In the following day (*i.e.*, the final time point), V_T of 7.7 ml/kg [7.2 to 9.6] of predicted body weight and peak transpulmonary pressure of 31.9 cm H_2O [22.1 to 43.7] were not different from baseline (corrected $P > 0.999$ for both).

Secondary Outcomes

Electrical Activity of the Diaphragm, Driving Pressure, Respiratory Rate, ΔP_{eso}, and Ventilation Distribution. Bilateral phrenic nerve block (10 min after right phrenic block) compared to baseline (figs. 6 and 7) decreased electrical activity of the diaphragm from 20 [12.2 to 29.9] to 0.3 [0.2 to 1.0] μV (corrected $P < 0.001$), driving pressure from 24.7 cm H_2O [20.4 to 34.5] to 18.4 cm H_2O [16.8 to 20.7] (corrected $P < 0.001$), ΔP_{eso} from 7.8 cm H_2O [5.6 to 9.8] to 1.9 cm H_2O [1.6 to 3.3] (corrected $P < 0.001$), and percentage of ventilation in the most dependent region from 11.5% [8.5 to 12.6] to 7.9% [5.3 to 8.6] (corrected $P = 0.005$). There was no difference in respiratory rate (27 breaths/min [24 to 30] to 25 breaths/min [22 to 30]; corrected $P > 0.999$) and percentage of left lung ventilation (45.7% [37.3 to 47.1] to 47.4% [39.0 to 47.8]; corrected $P > 0.999$).

One hour after bilateral phrenic nerve block, electrical activity of the diaphragm (20 μV [12.2 to 29.9] to 8.4 μV [1.5 to 17.4]; corrected $P = 0.062$) and ΔP_{eso} (7.8 cm H_2O [5.6 to 9.8] to 4.9 cm H_2O [3.9 to 5.6]; corrected $P = 0.230$) were not different from baseline, while driving pressure decreased from 24.7 cm H_2O [20.4 to 34.5] to 19.4 cm H_2O [18.4 to 24.8] (corrected $P < 0.001$). The respiratory rate did not change (27 breaths/min [24 to 30] to 24 breaths/min [23 to 25]; corrected $P > 0.999$), as well as the percentage of ventilation in the most dependent region of the lung (11.5% [8.5 to 12.6] to 7.5% [3.6 to 13.4];

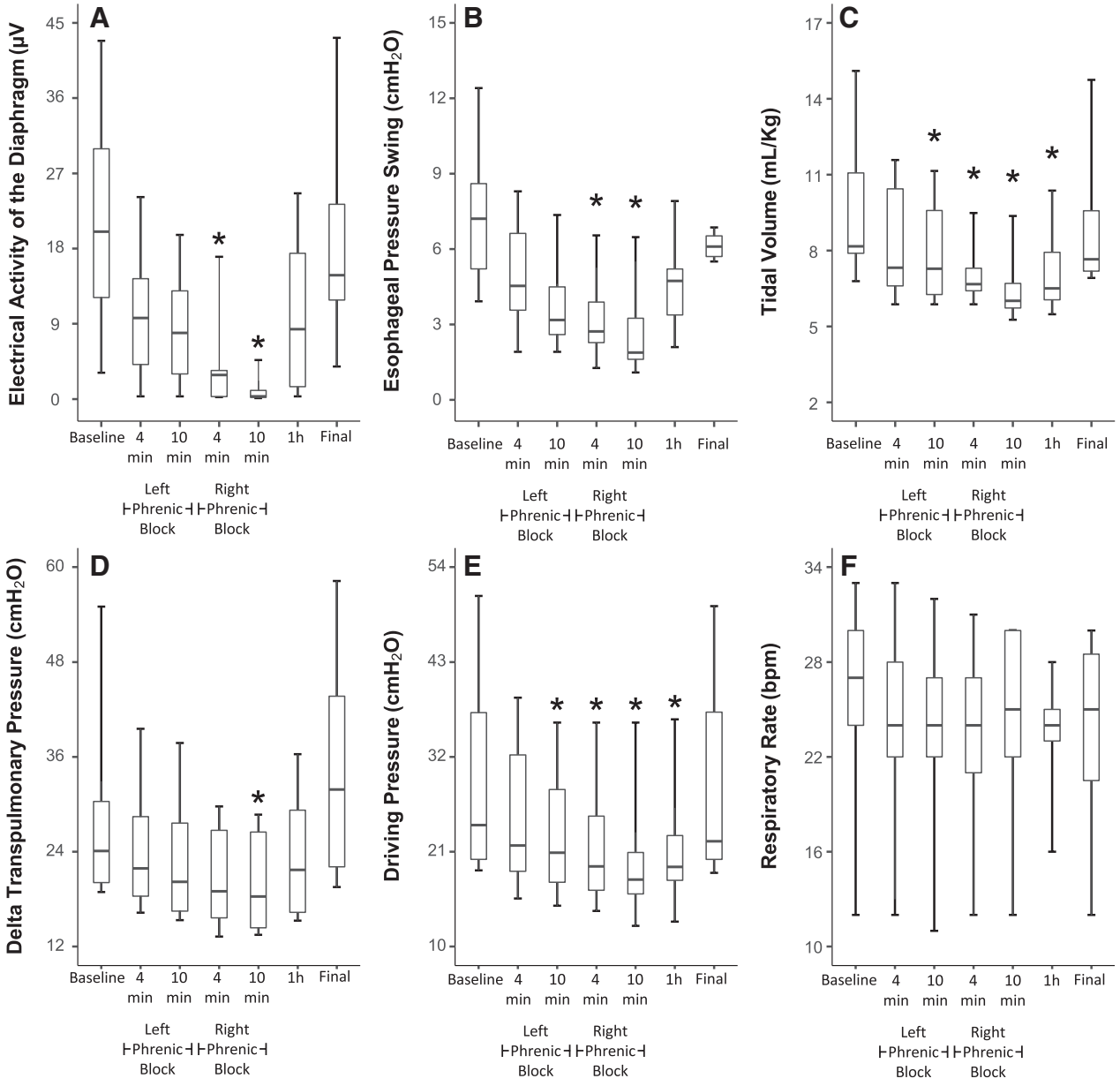

Fig. 6. Progress of respiratory variables in patients. Unadjusted data presented as median [interquartile range]. (*A*) Electrical activity of the diaphragm in microvolts. (*B*) Esophageal pressure swing in cm H_2O. (*C*) Tidal volume in ml/kg of predicted body weight. (*D*) Peak transpulmonary pressure in cm H_2O. (*E*). Driving pressure in cm H_2O. (*F*) Respiratory rate (breaths/min). After lidocaine administration, all variables progressively decreased over time. One outlier was excluded from *B*. *Corrected $P < 0.05$ when compared to baseline.

corrected $P > 0.999$) and left lung ventilation (45.7% [37.3 to 47.1] to 45.7% [37.8 to 47.0]; corrected $P > 0.999$). On the following day (*i.e.,* the final time point), electrical activity of the diaphragm of 14.8 μV [11.9 to 23.3], driving pressure of 23.8 cm H_2O [20.1 to 33.4], ΔP_{eso} of 6.5 cm H_2O [5.9 to 20.5], respiratory rate of 25 breaths/min [20 to 28], percentage of ventilation in the most dependent region of the lung of 10.2% [5.2 to 13.72], and left lung ventilation of 39.3% [36.9 to 43.6] were not different from baseline (corrected $P > 0.999$ for all variables).

Cardiovascular Response and Recovery Time

There was no change from baseline to bilateral phrenic nerve block in heart rate (89 beats/min [79 to 92] *vs.* 95 beats/min [89 to 101]; [95% CI, –3.1 to 16.6]; $P = 0.164$; fig. 8A) and mean blood pressure (87 mmHg [83 to 90] *vs.*

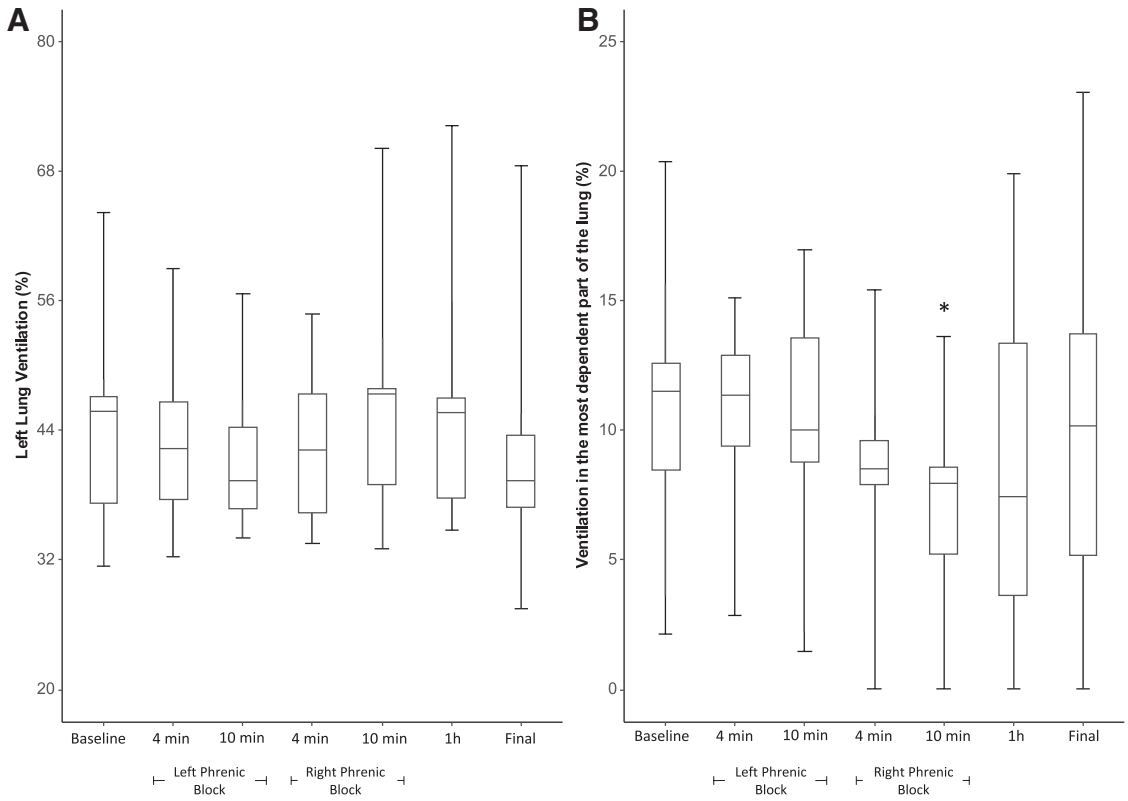

Fig. 7. Ventilation distribution in patients: left lung ventilation and ventilation in the most dependent portion of the lung. Unadjusted data presented as median [interquartile range]. (*A*) Left lung ventilation (%). (*B*) Ventilation in the most dependent part of the lung (%). *Corrected $P < 0.05$ when compared to baseline.

99 mmHg [87 to 103]; [95% CI, −4.6 to 19.0]; $P = 0.213$; fig. 8B).

For one patient, we did not acquire data during the following day. For another patient, deep sedation and neuromuscular blocking agents were reinstated due to strong inspiratory effort before full recovery. A third patient had sedation raised due to agitation during the night, and thus, ΔP_{eso} did not recover. Finally, another patient presented activation of expiratory abdominal muscle in the final time point, a condition that was not present at the beginning of the protocol; therefore, his peak transpulmonary pressure and ΔP_{eso} at the final time point were higher than at baseline. All these patients were included in the final analysis. Of note, all these patients were eventually weaned from the ventilator. Finally, none of our patients presented elevation of diaphragm the day after the phrenic nerve block.

Electrical activity of the diaphragm, peak transpulmonary pressure, and ΔP_{eso} fully recovered from bilateral phrenic nerve block within 1 h. V_T and driving pressure recovered from bilateral phrenic nerve block in 12.7 h [6.7 to 13.7].

Discussion

In this proof-of-concept study, we evaluated a novel strategy to deliver lung-protective ventilation in six pigs and in nine ARDS patients without the use of deep sedation and systemic neuromuscular blocking agents. We found that (1) bilateral phrenic nerve block was feasible, safe, and effective in the short term; (2) it reduced electrical activity of the diaphragm, V_T, ΔP_{eso}, peak transpulmonary pressure, and driving pressure without modifying respiratory rate; and (3) all parameters fully recovered after an average of 13 h.

Respiratory Variables

V_T, Driving Pressure, Peak Transpulmonary Pressure, ΔP_{eso}, Electrical Activity of the Diaphragm, and Ventilation Distribution. Excessively strong respiratory efforts have the potential to be injurious for the lung and the diaphragm.[28] There is no consensus, however, on managing patients with vigorous spontaneous inspiratory efforts. Animal studies have demonstrated the existence of self-inflicted lung injury,[9,10,29] but no human data yet have shown if and when it occurs.[6,29–31] Case reports or small series have associated

Table 3. Progress of Respiratory Variables in Patients

Parameter	Baseline	Four Minutes after Left Phrenic Block × Baseline	Ten Minutes after Left Phrenic Block × Baseline	Four Minutes after Right Phrenic Block × Baseline	Ten Minutes after Right Phrenic Block × Baseline	1 h after Block × Baseline	Final × Baseline
Electrical activity of the diaphragm, μV	2.9 (2.1 to 3.7)	−1.1 (−2.6 to 0.5)	−1.3 (−2.8 to −0.2)	−2.4 (−4.0 to −0.9)*	−3.6 (−5.1 to −2.1)*	−1.7 (−3.4 to 0.0)	−0.1 (−1.7 to 0.1)
Esophageal pressure swing, cm H_2O	2.1 (1.6 to 2.6)	−0.4 (−1.1 to 0.2)	−0.7 (−1.3 to 0.0)*	−1.0 (−1.7 to −0.4)*	−1.3 (−1.9 to −0.7)*	−0.5 (−1.2 to 0.1)	−0.3 (−0.4 to 1.0)
Tidal volume, ml/kg of predicted body weight	2.2 (2.1 to 2.4)	−0.1 (−0.3 to 0.0)	−0.2 (−0.4 to 0.0)*	−0.3 (−0.5 to −0.1)*	−0.4 (−0.5 to −0.2)*	−0.3 (−0.5 to −0.1)*	0.0 (−0.2 to 0.2)
Peak transpulmonary pressure, cm H_2O	3.3 (3.1 to 3.5)	−0.1 (−0.4 to 0.2)	−0.2 (−0.5 to 0.1)	−0.3 (−0.6 to 0.0)	−0.3 (−0.6 to 0.0)*	−0.2 (−0.5 to 0.1)	−0.1 (−0.2 to 0.4)
Driving pressure, cm H_2O	3.3 (3.1 to 3.5)	−0.1 (−0.3 to 0.0)	−0.2 (−0.4 to 0.0)*	−0.3 (−0.5 to −0.1)*	−0.4 (−0.5 to −0.2)*	−0.3 (−0.5 to −0.1)*	0.0 (−0.2 to 0.1)
Respiratory rate, breaths/min	3.2 (2.9 to 3.4)	0.0 (−0.2 to 0.2)	−0.1 (−0.3 to 0.1)	0.0 (−0.2 to 0.1)	0.0 (−0.2 to 0.2)	0.0 (−0.2 to 0.2)	0.0 (−0.2 to 0.2)
Left lung ventilation, %	3.8 (3.6 to 3.9)	0.0 (−0.2 to 0.1)	−0.1 (−0.2 to 0.1)	0.0 (−0.2 to 0.1)	0.1 (−0.1 to 0.2)	0.1 (−0.1 to 0.2)	−0.1 (−0.2 to 0.1)
Ventilation in the most dependent part of the lung, %†	10.6 (6.0 to 15.2)	−0.6 (−4.0 to 2.7)	−0.7 (−4.0 to 2.7)	−2.8 (−6.2 to 0.5)	−4.2 (−7.5 to −0.8)*	−2.1 (−5.7 to 1.4)	−0.1 (−3.7 to 3.6)

Estimates from the mixed-model analyses with outcomes log-transformed and adjusted to time, positive end-expiratory pressure, and pressure support. Data presented as the contrast between time point and baseline. 99.9% CI and *P* values corrected by Bonferroni method.

*$P < 0.05$ when compared to baseline. †Ventilation in the most dependent part of the lung was not log transformed.

strong inspiratory efforts with worse clinical outcomes in patients but do not demonstrate causality.[8,32,33] Before phrenic nerve blockade, pigs and patients had V_T, driving pressure, or both above the limits of lung protection recently proposed.[28] Moreover, pigs had electrical activity of the diaphragm and ΔP_{eso} comparable to other studies that associated vigorous inspiratory efforts and self-inflicted lung injury.[6,29]

After bilateral block, there was a decrease in V_T toward values within purported lung protective thresholds. Moreover, driving pressure and peak transpulmonary pressure, an indication of maximal lung stress, are dependent from the set level of inspiratory pressure support and significantly decreased from baseline to bilateral block. The decrease of peak transpulmonary pressure in our study is lower than that described in patients with partial neuromuscular blockade by Doorduin *et al.*[12] Airway driving pressure is associated to mortality in ARDS[34] and assisted ventilation.[35] Recent studies showed that driving pressure can be reliably measured during pressure support ventilation.[23,36] Airway driving pressure is a surrogate for lung cyclic strain,[37] defined as the ratio between tidal volume and functional residual capacity. Available data suggest that the prognostic values of airway and transpulmonary driving pressures seem similar.[38] Finally, airway driving pressure is easier to measure and offers less technical difficulties than transpulmonary driving pressure. Hence, a strategy that lowers airway driving pressure or tidal volume may benefit patients.

One hour after bilateral phrenic nerve block, electrical activity of the diaphragm, ΔP_{eso}, and peak transpulmonary pressure had fully recovered, while V_T and driving pressure had recovered only partially. It is possible that the decrease in minute ventilation increased $Paco_2$ and stimulated the respiratory drive, which ultimately increased the use of the diaphragm and other respiratory muscles, offsetting the phrenic nerve block. Unfortunately, we did not use a specific clinical scale to measure respiratory distress, or assess accessory muscle activity. In addition to likely $Paco_2$ accumulation, the effect of lidocaine may have partly weaned off 1 h after bilateral block.[39] Taken together, both conditions may have contributed to an early partial recovery.

Ventilation in the most dependent part of the lung decreased after phrenic nerve paralysis in pigs and humans. Phrenic nerve block suppressed diaphragmatic contraction, thus reducing ventilation near the diaphragm area. Bilateral phrenic nerve block could favor lung collapse, a consequence that may be prevented with PEEP. Moreover, the suppression of the diaphragmatic contraction abolished pendelluft (*i.e.*, an internal redistribution of tidal ventilation), a phenomenon related to regional distension and adverse outcomes.[22,40] Finally, sequential phrenic nerve block did not cause left lung to right lung pendelluft.

Unlike partial neuromuscular blockade,[12] our technique does not need sedatives, analgesics, or neuromuscular blocking agents. The two patients monitored with Bispectral

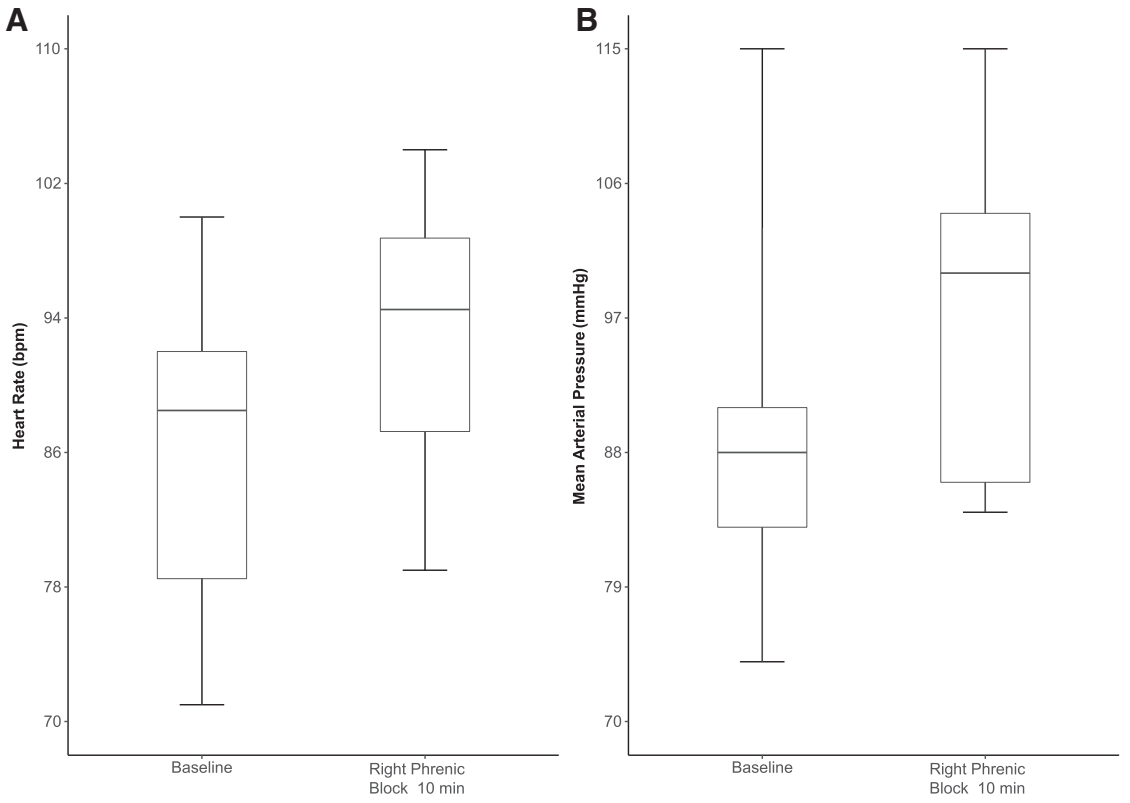

Fig. 8. Heart rate and blood pressure on baseline and after bilateral phrenic nerve block. Compared to baseline, there was no difference in heart rate or mean blood pressure.

Index presented levels between 70 and 85, compatible with light sedation. Half of our patients were under mild to moderate sedation; one was off continuous sedation and had a Richmond Agitation–Sedation Scale score of −1 (table 1).

During resting breathing in healthy subjects, the diaphragm is responsible for 60 to 80% of the inspiratory pressure, while the accessory muscles are responsible for the remaining activity.[41] Lidocaine blocks the propagation of the action potential, hence reducing electrical activity of the diaphragm, but does not interfere with other respiratory muscles due to their different innervation, which explains the residual ΔP_{eso} seen in pigs and in patients. The remaining ΔP_{eso} was able to trigger the ventilator, allowing patients and pigs to continue under assisted ventilation.

Clinical Implications and Considerations

Patients on invasive mechanical ventilation are at high risk for diaphragm myotrauma, a condition that may be a result of overassistance, load-induced injury, eccentric contractile injury, and excessive shortening.[42] Such associations were evidenced through mediation analysis and need further confirmation in prospective studies. Despite controversial results, a common strategy to temporarily reduce diaphragm myotrauma is to use paralyzing agents.[2,43] However, systemic paralyzing agents may contribute to intensive care unit–acquired weakness and general muscle atrophy. Our novel method could maintain patients under protective mechanical ventilation while avoiding deep sedation and paralyzing agents. To abolish electrical activity of the diaphragm and therefore diaphragm contraction with phrenic nerve block, however, may hold the same risks as using systemic paralyzing agents referring to diaphragm atrophy. This risk of diaphragm atrophy may be diminished if it is possible to titrate a continuous infusion of local anesthetics through a perineural catheter to reduce, but not abolish, electrical activity of the diaphragm. Moreover, phrenic nerve block paralyzes the diaphragm, but does not paralyze other muscles, which may prevent accessory muscle atrophy.[44]

Our approach takes less than 15 min to perform with a trained anesthesiologist. It reduces peak transpulmonary pressure, V_T, and driving pressure and can be performed in patients under light to moderate sedation. Altogether, it may be possible to keep a patient under protective assisted ventilation while allowing for participation in physical and occupational therapy, an intervention that is associated with

better functional outcomes.[45] Furthermore, since the intervention is a superficial peripheral ultrasound-guided nerve block done in an area susceptible to compression, anticoagulation is not a contraindication.[46]

Limitations

First, only female pigs were included in this protocol, which could limit the results. However, there are no studies associating sex of animals with clinically significant differences in respiratory physiology and anatomy. Second, the current study was a single-center, proof-of-concept, feasibility study. We did not aim to detect patient-centered outcomes, but rather surrogate physiologic variables associated with ventilator-induced lung injury. Third, the duration of the block was longer than expected. There is a wide variation in the length of lidocaine-induced motor paralysis,[47,48] but no studies have administered the same dose of lidocaine we used in the cervical portion of the phrenic nerve, where there is less room for lidocaine dispersion than in a supraclavicular block, for instance. Finally, the lidocaine dose administered may have been higher than necessary, further extending recovery periods. Fourth, the use of ultrasound imaging and a neurostimulator for phrenic nerve block requires training, which may limit this approach. Fifth, we did not routinely measure $Paco_2$ in pigs or in patients and did not assess the use of extra-diaphragmatic inspiratory muscles or activation of expiratory muscles. Therefore, the effects of bilateral phrenic nerve block on $Paco_2$ and muscle activity need further investigation. Finally, although we cannot comment on the recovery of three of our patients, they were all weaned off the ventilator.

Conclusion

In conclusion, the current proof-of-concept study demonstrates that bilateral phrenic nerve block can be feasible and efficient in the short term, and may reduce strong spontaneous inspiratory efforts. This technique might reduce the need for deep sedation and neuromuscular blocking agents in patients under mechanical ventilation.

Acknowledgments

The authors thank Takeshi Yoshida, M.D., Ph.D. (Department of Anesthesiology and Intensive Care Medicine, Osaka University Graduate School of Medicine, Osaka, Japan), and Susimeire Gomes, Ph.D. (Division of Pulmonology [Laboratory of Medical Investigation 09], Faculty of Medicine, University of São Paulo, São Paulo, Brazil) for their insights in designing the study, as well as data acquisition and analysis.

Research Support

Dr. Costa has received financial support from Timpel S.A. (São Paulo, Brazil). Dr. Brochard has received financial support from Medtronic (Minneapolis, Minnesota), Draeger (Lubeck, Germany), and Fisher Paykel (Auckland, New Zeland), as well as equipment from Sentec (Therwill, Switzerland).

Competing Interests

The authors declare no competing interests.

Correspondence

Address correspondence to Dr. Pereira: Department of Anesthesia, St. Michael's Hospital, 30 Bond St., Toronto Ontario, M5B 1W8, Canada. pereira.sm@gmail.com.

References

1. Fan E, Del Sorbo L, Goligher EC, Hodgson CL, Munshi L, Walkey AJ, Adhikari NKJ, Amato MBP, Branson R, Brower RG, Ferguson ND, Gajic O, Gattinoni L, Hess D, Mancebo J, Meade MO, McAuley DF, Pesenti A, Ranieri VM, Rubenfeld GD, Rubin E, Seckel M, Slutsky AS, Talmor D, Thompson BT, Wunsch H, Uleryk E, Brozek J, Brochard LJ; American Thoracic Society, European Society of Intensive Care Medicine, and Society of Critical Care Medicine: An official American Thoracic Society/European Society of Intensive Care Medicine/Society of Critical Care Medicine Clinical Practice Guideline: Mechanical ventilation in adult patients with acute respiratory distress syndrome. Am J Respir Crit Care Med 2017; 195:1253–63
2. Papazian L, Forel JM, Gacouin A, Penot-Ragon C, Perrin G, Loundou A, Jaber S, Arnal JM, Perez D, Seghboyan JM, Constantin JM, Courant P, Lefrant JY, Guérin C, Prat G, Morange S, Roch A; ACURASYS Study Investigators: Neuromuscular blockers in early acute respiratory distress syndrome. N Engl J Med 2010; 363:1107–16
3. Amato MB, Barbas CS, Medeiros DM, Magaldi RB, Schettino GP, Lorenzi-Filho G, Kairalla RA, Deheinzelin D, Munoz C, Oliveira R, Takagaki TY, Carvalho CR: Effect of a protective-ventilation strategy on mortality in the acute respiratory distress syndrome. N Engl J Med 1998; 338:347–54
4. Shehabi Y, Bellomo R, Reade MC, Bailey M, Bass F, Howe B, McArthur C, Seppelt IM, Webb S, Weisbrodt L; Sedation Practice in Intensive Care Evaluation (SPICE) Study Investigators; ANZICS Clinical Trials Group: Early intensive care sedation predicts long-term mortality in ventilated critically ill patients. Am J Respir Crit Care Med 2012; 186:724–31

5. Putensen C, Zech S, Wrigge H, Zinserling J, Stüber F, Von Spiegel T, Mutz N: Long-term effects of spontaneous breathing during ventilatory support in patients with acute lung injury. Am J Respir Crit Care Med 2001; 164:43–9
6. Morais CCA, Koyama Y, Yoshida T, Plens GM, Gomes S, Lima CAS, Ramos OPS, Pereira SM, Kawaguchi N, Yamamoto H, Uchiyama A, Borges JB, Vidal Melo MF, Tucci MR, Amato MBP, Kavanagh BP, Costa ELV, Fujino Y: High positive end-expiratory pressure renders spontaneous effort noninjurious. Am J Respir Crit Care Med 2018; 197:1285–96
7. Hillas G, Perlikos F, Toumpanakis D, Litsiou E, Nikolakopoulou S, Sagris K, Vassilakopoulos T: Controlled mechanical ventilation attenuates the systemic inflammation of severe chronic obstructive pulmonary disease exacerbations. Am J Respir Crit Care Med 2016; 193:696–8
8. Leray V, Bourdin G, Flandreau G, Bayle F, Wallet F, Richard JC, Guérin C: A case of pneumomediastinum in a patient with acute respiratory distress syndrome on pressure support ventilation. Respir Care 2010; 55:770–3
9. Mascheroni D, Kolobow T, Fumagalli R, Moretti MP, Chen V, Buckhold D: Acute respiratory failure following pharmacologically induced hyperventilation: An experimental animal study. Intensive Care Med 1988; 15:8–14
10. Yoshida T, Grieco DL, Brochard L, Fujino Y: Patient self-inflicted lung injury and positive end-expiratory pressure for safe spontaneous breathing. Curr Opin Crit Care 2020; 26:59–65
11. Goligher EC, Jonkman AH, Dianti J, Vaporidi K, Beitler JR, Patel BK, Yoshida T, Jaber S, Dres M, Mauri T, Bellani G, Demoule A, Brochard L, Heunks L: Clinical strategies for implementing lung and diaphragm-protective ventilation: Avoiding insufficient and excessive effort. Intensive Care Med 2020; 46:2314–26
12. Doorduin J, Nollet JL, Roesthuis LH, van Hees HW, Brochard LJ, Sinderby CA, van der Hoeven JG, Heunks LM: Partial neuromuscular blockade during partial ventilatory support in sedated patients with high tidal volumes. Am J Respir Crit Care Med 2017; 195:1033–42
13. Price DR, Mikkelsen ME, Umscheid CA, Armstrong EJ: Neuromuscular blocking agents and neuromuscular dysfunction acquired in critical illness: A systematic review and meta-analysis. Crit Care Med 2016; 44:2070–8
14. Renes SH, van Geffen GJ, Rettig HC, Gielen MJ, Scheffer GJ: Ultrasound-guided continuous phrenic nerve block for persistent hiccups. Reg Anesth Pain Med 2010; 35:455–7
15. El-Boghdadly K, Chin KJ, Chan VWS: Phrenic nerve palsy and regional anesthesia for shoulder surgery: Anatomical, physiologic, and clinical considerations. Anesthesiology 2017; 127:173–91
16. Wong AK, Keeney LG, Chen L, Williams R, Liu J, Elkassabany NM: Effect of local anesthetic concentration (0.2% vs 0.1% ropivacaine) on pulmonary function, and analgesia after ultrasound-guided interscalene brachial plexus block: A randomized controlled study. Pain Med 2016; 17:2397–403
17. Lee JH, Cho SH, Kim SH, Chae WS, Jin HC, Lee JS, Kim YI: Ropivacaine for ultrasound-guided interscalene block: 5 mL provides similar analgesia but less phrenic nerve paralysis than 10 mL. Can J Anaesth 2011; 58:1001–6
18. Palhais N, Brull R, Kern C, Jacot-Guillarmod A, Charmoy A, Farron A, Albrecht E: Extrafascial injection for interscalene brachial plexus block reduces respiratory complications compared with a conventional intrafascial injection: A randomized, controlled, double-blind trial. Br J Anaesth 2016; 116:531–7
19. Abrahams MS, Aziz MF, Fu RF, Horn JL: Ultrasound guidance compared with electrical neurostimulation for peripheral nerve block: A systematic review and meta-analysis of randomized controlled trials. Br J Anaesth 2009; 102:408–17
20. Bigeleisen PE: Nerve puncture and apparent intraneural injection during ultrasound-guided axillary block does not invariably result in neurologic injury. Anesthesiology 2006; 105:779–83
21. Baydur A, Behrakis PK, Zin WA, Jaeger M, Milic-Emili J: A simple method for assessing the validity of the esophageal balloon technique. Am Rev Respir Dis 1982; 126:788–91
22. Yoshida T, Torsani V, Gomes S, De Santis RR, Beraldo MA, Costa EL, Tucci MR, Zin WA, Kavanagh BP, Amato MB: Spontaneous effort causes occult pendelluft during mechanical ventilation. Am J Respir Crit Care Med 2013; 188:1420–7
23. Bellani G, Grassi A, Sosio S, Foti G: Plateau and driving pressure in the presence of spontaneous breathing. Intensive Care Med 2019; 45:97–8
24. Rosenblatt MA, Fishkind D: Proficiency in interscalene anesthesia-how many blocks are necessary? J Clin Anesth 2003; 15:285–8
25. Bomberg H, Wetjen L, Wagenpfeil S, Schöpe J, Kessler P, Wulf H, Wiesmann T, Standl T, Gottschalk A, Döffert J, Hering W, Birnbaum J, Kutter B, Winckelmann J, Liebl-Biereige S, Meissner W, Vicent O, Koch T, Bürkle H, Sessler DI, Volk T: Risks and benefits of ultrasound, nerve stimulation, and their combination for guiding peripheral nerve blocks: A retrospective registry analysis. Anesth Analg 2018; 127:1035–43
26. Neal JM, Barrington MJ, Brull R, Hadzic A, Hebl JR, Horlocker TT, Huntoon MA, Kopp SL, Rathmell JP, Watson JC: The second ASRA practice advisory on neurologic complications associated with regional

anesthesia and pain medicine: Executive summary 2015. Reg Anesth Pain Med 2015; 40:401–30
27. Gropper MA. Miller's Anesthesia. Philadelphia: Elsevier; 2019.
28. Goligher EC, Dres M, Patel BK, Sahetya SK, Beitler JR, Telias I, Yoshida T, Vaporidi K, Grieco DL, Schepens T, Grasselli G, Spadaro S, Dianti J, Amato M, Bellani G, Demoule A, Fan E, Ferguson ND, Georgopoulos D, Guérin C, Khemani RG, Laghi F, Mercat A, Mojoli F, Ottenheijm CAC, Jaber S, Heunks L, Mancebo J, Mauri T, Pesenti A, Brochard L: Lung- and diaphragm-protective ventilation. Am J Respir Crit Care Med 2020; 202:950–61
29. Yoshida T, Uchiyama A, Matsuura N, Mashimo T, Fujino Y: Spontaneous breathing during lung-protective ventilation in an experimental acute lung injury model: High transpulmonary pressure associated with strong spontaneous breathing effort may worsen lung injury. Crit Care Med 2012; 40:1578–85
30. Yoshida T, Uchiyama A, Matsuura N, Mashimo T, Fujino Y: The comparison of spontaneous breathing and muscle paralysis in two different severities of experimental lung injury. Crit Care Med 2013; 41:536–45
31. Yoshida T, Roldan R, Beraldo MA, Torsani V, Gomes S, De Santis RR, Costa EL, Tucci MR, Lima RG, Kavanagh BP, Amato MB: Spontaneous effort during mechanical ventilation: Maximal injury with less positive end-expiratory pressure. Crit Care Med 2016; 44:e678–88
32. Kallet RH, Alonso JA, Luce JM, Matthay MA: Exacerbation of acute pulmonary edema during assisted mechanical ventilation using a low-tidal volume, lung-protective ventilator strategy. Chest 1999; 116:1826–32
33. Esnault P, Cardinale M, Hraiech S, Goutorbe P, Baumstrack K, Prud'homme E, Bordes J, Forel JM, Meaudre E, Papazian L, Guervilly C: High respiratory drive and excessive respiratory efforts predict relapse of respiratory failure in critically ill patients with COVID-19. Am J Respir Crit Care Med 2020; 202:1173–8
34. Amato MB, Meade MO, Slutsky AS, Brochard L, Costa EL, Schoenfeld DA, Stewart TE, Briel M, Talmor D, Mercat A, Richard JC, Carvalho CR, Brower RG: Driving pressure and survival in the acute respiratory distress syndrome. N Engl J Med 2015; 372:747–55
35. Bellani G, Grassi A, Sosio S, Gatti S, Kavanagh BP, Pesenti A, Foti G: Driving pressure is associated with outcome during assisted ventilation in acute respiratory distress syndrome. Anesthesiology 2019; 131:594–604
36. Sajjad H, Schmidt GA, Brower RG, Eberlein M: Can the plateau be higher than the peak pressure? Ann Am Thorac Soc 2018; 15:754–9
37. Williams EC, Motta-Ribeiro GC, Vidal Melo MF: Driving pressure and transpulmonary pressure: How do we guide safe mechanical ventilation? Anesthesiology 2019; 131:155–63
38. Baedorf Kassis E, Loring SH, Talmor D: Mortality and pulmonary mechanics in relation to respiratory system and transpulmonary driving pressures in ARDS. Intensive Care Med 2016; 42:1206–13
39. Stoelting RK, Shafer SL, Rathmell JP, Flood P. Stoelting's Handbook of Pharmacology and Physiology in Anesthetic Practice. Philadelphia: Wolters Kluwer; 2015.
40. Coppadoro A, Grassi A, Giovannoni C, Rabboni F, Eronia N, Bronco A, Foti G, Fumagalli R, Bellani G: Occurrence of pendelluft under pressure support ventilation in patients who failed a spontaneous breathing trial: An observational study. Ann Intensive Care 2020; 10:39
41. De Troyer A, Boriek AM: Mechanics of the respiratory muscles. Compr Physiol 2011; 1:1273–300
42. Goligher EC, Brochard LJ, Reid WD, Fan E, Saarela O, Slutsky AS, Kavanagh BP, Rubenfeld GD, Ferguson ND: Diaphragmatic myotrauma: A mediator of prolonged ventilation and poor patient outcomes in acute respiratory failure. Lancet Respir Med 2019; 7:90–8
43. National Heart, Lung, and Blood Institute PETAL Clinical Trials Network, Moss M, Huang DT, Brower RG, Ferguson ND, Ginde AA, Gong MN, Grissom CK, Gundel S, Hayden D, Hite RD, Hou PC, Hough CL, Iwashyna TJ, Khan A, Liu KD, Talmor D, Thompson BT, Ulysse CA, Yealy DM, Angus DC. Early neuromuscular blockade in the acute respiratory distress syndrome. N Engl J Med 2019; 380: 1997–2008.
44. Shi ZH, de Vries H, de Grooth HJ, Jonkman AH, Zhang Y, Haaksma M, van de Ven PM, de Man AAME, Girbes A, Tuinman PR, Zhou JX, Ottenheijm C, Heunks L: Changes in respiratory muscle thickness during mechanical ventilation: Focus on expiratory muscles. Anesthesiology 2021; 134:748–59
45. Wang YT, Lang JK, Haines KJ, Skinner EH, Haines TP. Physical rehabilitation in the ICU: A systematic review and meta-analysis. Crit Care Med 2022; 50:375–88.
46. Horlocker TT, Vandermeuelen E, Kopp SL, Gogarten W, Leffert LR, Benzon HT: Regional anesthesia in the patient receiving antithrombotic or thrombolytic therapy: American Society of Regional Anesthesia and Pain Medicine evidence-based guidelines (fourth edition). Reg Anesth Pain Med 2018; 43:263–309
47. Thomson CJ, Lalonde DH: Randomized double-blind comparison of duration of anesthesia among three commonly used agents in digital nerve block. Plast Reconstr Surg 2006; 118:429–32
48. Hull J, Heath J, Bishop W: Supraclavicular brachial plexus block for arteriovenous hemodialysis access procedures. J Vasc Interv Radiol 2016; 27:749–52

ANESTHESIOLOGY

Prone Position Minimizes the Exacerbation of Effort-dependent Lung Injury: Exploring the Mechanism in Pigs and Evaluating Injury in Rabbits

Takeshi Yoshida, M.D., Ph.D., Doreen Engelberts, Han Chen, M.D., Xuehan Li, M.D., Bhushan H. Katira, M.D., Ph.D., Gail Otulakowski, Ph.D., Yuji Fujino, M.D., Ph.D.

ANESTHESIOLOGY 2022; 136:779–91

EDITOR'S PERSPECTIVE

What We Already Know about This Topic

- Prone positioning during mechanical ventilation for patients with acute lung injury has been shown to increase oxygenation and possibly improve outcome
- It is now widely used for patients with COVID-19 failing routine ventilation protocols
- Its use during spontaneous ventilation has increased as result of the pandemic, yet detailed data on its ventilatory effects have not been well established

What This Article Tells Us That Is New

- The authors utilized porcine and rabbit models of lung injury to evaluate pulmonary mechanics, distribution of ventilation, and biochemical and histologic effects on lung injury with varying positive end-expiratory pressure levels
- Independent of positive end-expiratory pressure levels, prone positioning reduced maldistribution of lung stress and reduced effort-dependent evidence of lung injury

ABSTRACT

Background: Vigorous spontaneous effort can potentially worsen lung injury. This study hypothesized that the prone position would diminish a maldistribution of lung stress and inflation after diaphragmatic contraction and reduce spontaneous effort, resulting in less lung injury.

Methods: A severe acute respiratory distress syndrome model was established by depleting surfactant and injurious mechanical ventilation in 6 male pigs ("mechanism" protocol) and 12 male rabbits ("lung injury" protocol). In the mechanism protocol, regional inspiratory negative pleural pressure swing (intrabronchial balloon manometry) and the corresponding lung inflation (electrical impedance tomography) were measured with a combination of position (supine or prone) and positive end-expiratory pressure (high or low) matching the intensity of spontaneous effort. In the lung injury protocol, the intensities of spontaneous effort (esophageal manometry) and regional lung injury were compared in the supine position *versus* prone position.

Results: The mechanism protocol (pigs) found that in the prone position, there was no ventral-to-dorsal gradient in negative pleural pressure swing after diaphragmatic contraction, irrespective of the positive end-expiratory pressure level (–10.3 ± 3.3 cm H_2O *vs.* –11.7 ± 2.4 cm H_2O at low positive end-expiratory pressure, $P = 0.115$; –10.4 ± 3.4 cm H_2O *vs.* –10.8 ± 2.3 cm H_2O at high positive end-expiratory pressure, $P = 0.715$), achieving homogeneous inflation. In the supine position, however, spontaneous effort during low positive end-expiratory pressure had the largest ventral-to-dorsal gradient in negative pleural pressure swing (–9.8 ± 2.9 cm H_2O *vs.* –18.1 ± 4.0 cm H_2O, $P < 0.001$), causing dorsal overdistension. Higher positive end-expiratory pressure in the supine position reduced a ventral-to-dorsal gradient in negative pleural pressure swing, but it remained (–9.9 ± 2.8 cm H_2O *vs.* –13.3 ± 2.3 cm H_2O, $P < 0.001$). The lung injury protocol (rabbits) found that in the prone position, spontaneous effort was milder and lung injury was less without regional difference (lung myeloperoxidase activity in ventral *vs.* dorsal lung, 74.0 ± 30.9 μm · min^{-1} · mg^{-1} protein *vs.* 61.0 ± 23.0 μm · min^{-1} · mg^{-1} protein, $P = 0.951$). In the supine position, stronger spontaneous effort increased dorsal lung injury (lung myeloperoxidase activity in ventral *vs.* dorsal lung, 67.5 ± 38.1 μm · min^{-1} · mg^{-1} protein *vs.* 167.7 ± 65.5 μm · min^{-1} · mg^{-1} protein, $P = 0.003$).

Conclusions: Prone position, independent of positive end-expiratory pressure levels, diminishes a maldistribution of lung stress and inflation imposed by spontaneous effort and mitigates spontaneous effort, resulting in less effort-dependent lung injury.

(ANESTHESIOLOGY 2022; 136:779–91)

Supplemental Digital Content is available for this article. Direct URL citations appear in the printed text and are available in both the HTML and PDF versions of this article. Links to the digital files are provided in the HTML text of this article on the Journal's Web site (www.anesthesiology.org). This article has a visual abstract available in the online version.

Submitted for publication June 12, 2021. Accepted for publication January 27, 2022. Published online first on March 18, 2022.

Takeshi Yoshida, M.D., Ph.D.: Department of Anesthesiology and Intensive Care Medicine, Osaka University Graduate School of Medicine, Suita, Japan.

Doreen Engelberts: Translational Medicine Program, Hospital for Sick Children, University of Toronto, Toronto, Ontario, Canada.

Han Chen, M.D.: Surgical Intensive Care Unit, Fujian Provincial Hospital, Fuzhou, China.

Xuehan Li, M.D.: Department of Anesthesiology and the Laboratory of Anesthesia and Intensive Care Medicine, West China Hospital of Sichuan University, Chengdu, China.

Bhushan H. Katira, M.D., Ph.D.: Department of Pediatrics, Washington University in St. Louis, School of Medicine, St. Louis, Missouri.

Gail Otulakowski, Ph.D.: Translational Medicine Program, Hospital for Sick Children, University of Toronto, Toronto, Ontario, Canada.

Yuji Fujino, M.D., Ph.D.: Department of Anesthesiology and Intensive Care Medicine, Osaka University Graduate School of Medicine, Suita, Japan.

 Anesthesiology 2022; 136:779–91. DOI: 10.1097/ALN.0000000000004165

<zdoi;. DOI: 10.1097/ALN.0000000000004165>

Spontaneous breathing using respiratory muscles is physiologically normal and therefore has been traditionally facilitated during mechanical ventilation.[1] Negative deflection ("swing") in pleural pressure resulting from diaphragmatic contraction is evenly transmitted across the whole lung surface, creating a uniform increase in transpulmonary pressure at any given airway pressure (P_{aw}): this is called "fluid-like" behavior.[2] Thus, spontaneous breathing achieves homogeneous inflation at lower levels of P_{aw} during mechanical ventilation, improving ventilation/perfusion and gas exchange, and preserving diaphragm function.[1,3] Although such benefits of spontaneous breathing have been reported during mechanical ventilation, it may also potentially injure the lungs and diaphragm when spontaneous effort is vigorous and/or when lung injury is severe.[3–6]

In the severely injured lung, negative deflection in pleural pressure resulting from diaphragmatic contraction is partially used on local lung deformation (*i.e.*, dense, atelectatic area resisting dynamic shape changes) and thus is not evenly transmitted to the entire lung; this is called "solid-like" behavior.[2,7] Such a maldistribution of lung stress imposed by spontaneous breathing is known to cause injurious inflation patterns (*e.g.*, pendelluft, local volutrauma[2,7]). In addition, several factors increase the strength and injury potential of spontaneous breathing effort in severe acute respiratory distress syndrome (ARDS), including acidemia, hypercapnia, and hypoxemia,[8] as well as reduced lung volume due to dorsal atelectasis.[9,10]

Turning to the prone position gravitationally translocates atelectasis (dense solid-like lung tissue resisting dynamic shape changes) from the dorsal to ventral lung, as is obvious from previous studies.[11] Because the dorsal lung (facing muscular parts of diaphragm) is now open and less solid-like atelectatic in the prone position, it might diffuse the inspiratory stress after diaphragmatic contraction from being local and injurious to generalized and less injurious (*e.g.*, less pendelluft, less local volutrauma). In several studies, the prone position is also shown to have the similar effect of recruiting lung and increasing lung volume as higher positive end-expiratory pressure (PEEP).[11,12] Lung recruitment may minimize the injurious effect of spontaneous effort (*e.g.*, large tidal volume, high transpulmonary pressure) by increasing lung volume, shortening diaphragm length, and thereby generating less force from the diaphragm.[6,9,10,13–15]

The prone position has been traditionally used under passive conditions (*e.g.*, more than 90% of patients in the prone position received muscle paralysis for more than 5 days),[16] and the interaction of the prone position with spontaneous breathing has not been evaluated well in severe ARDS. Based on this reasoning, we hypothesized that if spontaneous effort is permitted while in the prone position, it would diminish a maldistribution of lung stress and inflation imposed by spontaneous effort and decrease spontaneous effort, resulting in less lung injury.

We tested this hypothesis in established models of severe ARDS. First, in the "mechanism" protocol using pigs, to evaluate regional lung stress and the corresponding inflation pattern caused by spontaneous effort, we measured the impact of PEEP (high and low) and position (supine and prone) on regional lung inflation (electrical impedance tomography in pigs) and regional inspiratory negative pleural pressure swings (intrabronchial balloon manometry[2,17] in pigs). Second, in the "lung injury" protocol using rabbits, we measured the impact of position on the strength of spontaneous effort (negative deflection in esophageal pressure [P_{eso}] in rabbits), and on regional injury associated with spontaneous effort (total protein in bronchoalveolar lavage, lung myeloperoxidase activity in rabbits).

Materials and Methods

Two series of animal experiments (pigs, rabbits) were conducted from 2017 through 2018 (before the COVID-19 pandemic), both approved by the Animal Care Committee of the Hospital for Sick Children in Toronto (Toronto, Ontario, Canada; approval No. 45697). The animals were cared for in accordance with the hospital's standards for the care and use of laboratory animals.

Series 1 Mechanism Protocol: Anesthetized Pig Experiments

The schematic of study protocol is described in figure 1A. Six male Yorkshire pigs (n = 6; 30.9 to 39.3 kg) were anesthetized with 7 mg · kg^{-1} · h^{-1} ketamine and 2 mg · kg^{-1} · h^{-1} propofol and tracheostomized. Negative toe pinch was confirmed throughout the protocol. An esophageal balloon catheter (NutriVent, Sidam, Italy) was inserted to measure P_{eso}, filled with 1.0 ml as a minimal nonstress volume, and calibrated.[18] Neuromuscular blockade rocuronium bromide boluses of 0.5 mg · kg^{-1} were used to prevent spontaneous breathing effort when necessary.

Lung Injury. Experimental lung injury was induced in the supine position by repeated saline lung lavage (30 ml · kg^{-1}, 37°C),[19] and surfactant depletion was considered stable when the Pao_2/fractional inspired oxygen tension (Fio_2) ratio was less than 100 mmHg for 10 min, at a PEEP of 5 cm H_2O. Injurious mechanical ventilation was commenced and continued for 60 min using assisted pressure control: Fio_2, 1.0; rate, 25 breaths/min; and pressure trigger, –2 cm H_2O (Servo 300, Siemens-Elema AB, Sweden). Ventilator-induced lung injury was induced with the following driving pressure/PEEP combinations adjusted every 15 min to maintain Pao_2 of greater than 55 to 65 mmHg: 41/1, 39/3, 37/5, 35/7, 33/9, 31/11, or 29/13 cm H_2O.[13]

Experimental Protocol. The animals were then randomly assigned to four acquisition periods (each period comprised high or low PEEP and supine or prone position):

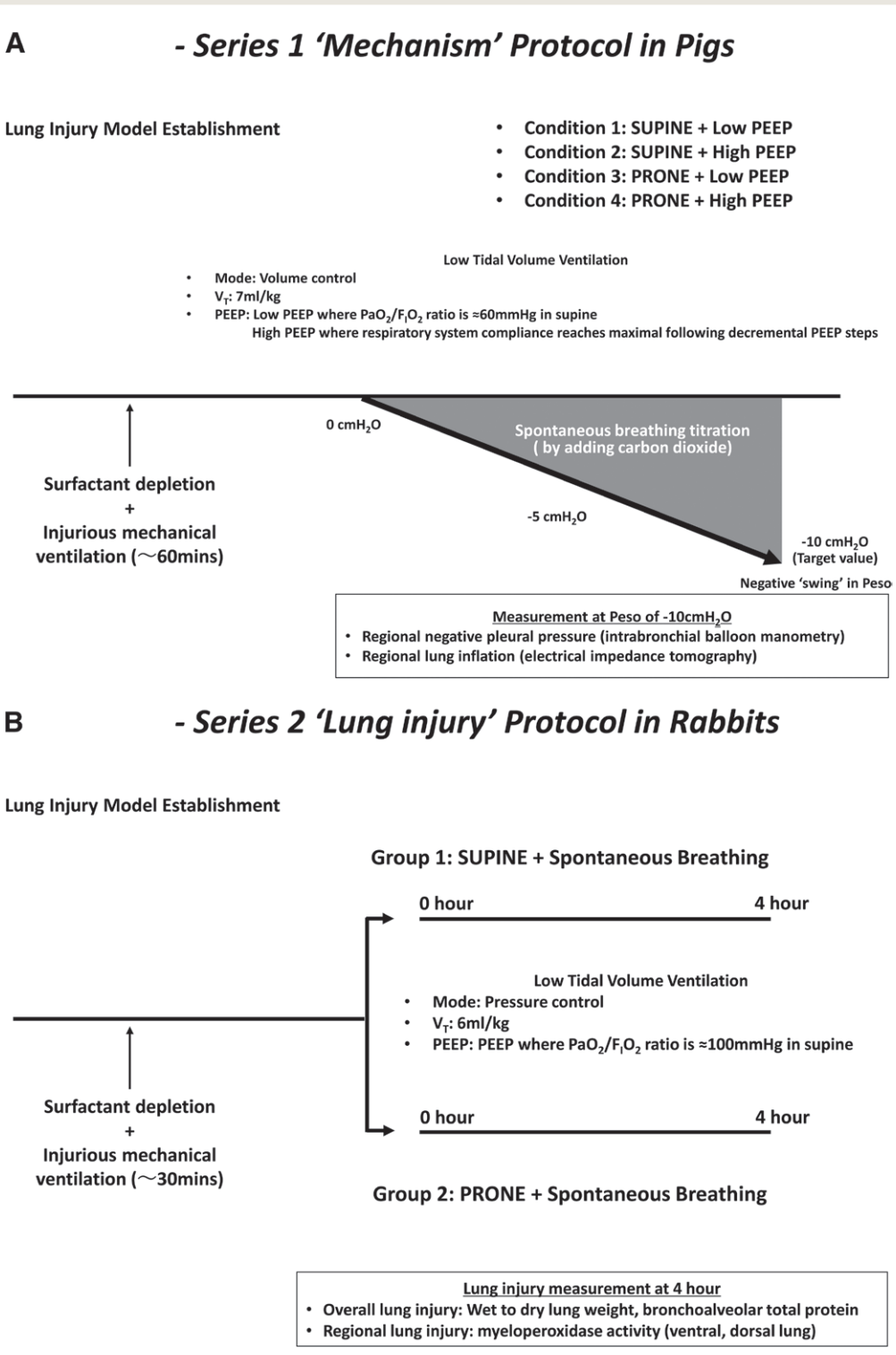

Fig. 1. Schematic of protocol. (*A*) Series 1 mechanism protocol in pigs. Lung-injured pigs (n = 6) were randomly assigned to each of four acquisition periods (conditions 1 to 4), and spontaneous effort was subsequently facilitated by adding carbon dioxide until a negative swing in esophageal pressure (P_{eso}) of –10 cm H_2O was reached. Then, the regional lung stress and lung inflation pattern were analyzed by intrabronchial balloon manometry and electrical impedance tomography, respectively. (*B*) Series 2 lung injury protocol in rabbits. Lung-injured rabbits (n = 12) were randomized to either group 1 (supine and spontaneous breathing) or group 2 (prone and spontaneous breathing). Lung injury was evaluated after 4-h preservation of spontaneous effort under mechanical ventilation. FIO_2, fractional inspired oxygen tension; PEEP, positive end-expiratory pressure; V_T, tidal volume.

- Low PEEP, supine
- High PEEP, supine
- Low PEEP, prone
- High PEEP, prone

Randomization was from a bag of coded letters. Static respiratory system compliance was measured with decremental PEEP steps (modified from Yoshida *et al.*[20]), starting at a PEEP of 20 cm H_2O and reducing by 2 cm H_2O every 30 s until an oxygen saturation measured by pulse oximetry of approximately 90% was reached. Ventilation was set at F_{IO_2} 1.0, inspiratory pressure was set at 15 cm H_2O, and the respiratory rate was 40 breaths/min. At a PEEP of 20 cm H_2O, the P_{aO_2}/F_{IO_2} ratio was approximately 400 mmHg in all animals. High and low PEEP were defined as follows:

- High PEEP is the PEEP at which respiratory system compliance is maximal after decremental PEEP steps
- Low PEEP is the PEEP at which oxygen saturation measured by pulse oximetry is approximately 90% (P_{aO_2} is approximately 60 mmHg)

The lungs were fully recruited in the supine position to homogenize lung volume history before randomization to each acquisition period and ventilated for approximately 15 min for stabilization. In each acquisition period, low tidal volume (V_T) ventilation employed assisted volume-controlled ventilation: V_T, 7 ml · kg^{-1}; rate, 30 breaths/min; inspiratory to expiratory ratio, 1:2 (no inspiratory pause); pressure trigger, –2 cm H_2O; and F_{IO_2}, 1.0.

At the start of each acquisition period, the absence of respiratory effort was confirmed by a lack of negative deflection in P_{eso}. Spontaneous breathing effort was subsequently facilitated by adding carbon dioxide (up to 0.10) until a negative swing in P_{eso} of –10 cm H_2O was reached. It usually took approximately 30 min to reach the target value of P_{eso}. The animals were sacrificed with IV sodium pentobarbital.

Electric Impedance Tomography. In all animals (n = 6), electrical impedance tomography data were recorded (PulmoVista 500, Dräger, Germany) continuously during the spontaneous breathing titration period (from paralysis to P_{eso} of –10 cm H_2O). Local lung inflation was analyzed after division of the image into four equal zones, from zone 1 (most ventral) to zone 4 (most dorsal), where each zone comprised 25% of the ventrodorsal distance and encompassed the complete area of the lung encircled by the band. We considered zone 1 (the most ventral one) and zone 4 (the most dorsal one) as representative of ventral lung and dorsal lung to be analyzed, respectively. The magnitude of local lung inflation imposed by spontaneous effort was estimated by the size of passive V_T during muscle paralysis to achieve the same degree of local lung inflation.[2] This estimation in each sequence was performed when ΔP_{eso} was –10 cm H_2O (*i.e.*, the same intensity of spontaneous effort). After measuring the magnitude of local lung inflation (represented by ΔZ in electrical impedance tomography) when ΔP_{eso} was –10 cm H_2O at a fixed, global V_T of 7 ml/kg during assisted volume-controlled ventilation, we paralyzed the animal and started to increase V_T setting during volume-controlled ventilation, until the same magnitude of local lung inflation (represented by ΔZ in electrical impedance tomography) developed in the dorsal lung.

Pleural Pressure Measurement. The local negative swing in pleural pressure was determined in nondependent and dependent regions (one pig did not survive; n = 5) by balloon catheter occlusion of subsegmental bronchi *via* a fibreoptic bronchoscope, as follows: nondependent region, left B; dependent region: left lower lobe beyond D4. The occluded subsegments were connected to a differential pressure transducer through the intrabronchial balloon catheter without airflow influx, thereby allowing continuous measurement of changes in occluded subsegment pressure. The pressure swings in the occluded subsegments were used as surrogates for negative pleural pressure swings, as described previously.[2,17] The occluded lung regions were filled with air until the alveolar pressure inside each target subsegmental region reached 20 (or 30) cm H_2O in nondependent (and dependent) lung regions, respectively, assuming that this opening pressure was sufficient to recruit the occluded lung regions. Simultaneous pressure recording of negative pleural pressure swings and ΔP_{eso} were performed, while preserving spontaneous effort. All measurements were performed when ΔP_{eso} was –10 cm H_2O.

Series 2 Lung Injury Protocol: Anesthetized Rabbit Experiments

A schematic of study protocol is shown in figure 1B. Twelve New Zealand white rabbits (adult, male, 2.9 to 3.9 kg) were anesthetized with intravenous propofol (10 to 100 mg · kg^{-1} · h^{-1}) and ketamine (1 to 5 mg · kg^{-1} · h^{-1}) and tracheostomized. Negative toe pinch was confirmed throughout the protocol. An esophageal balloon (SmartCath, Bicore, USA) was inserted to measure P_{eso} and filled with air (0.3 ml as minimal nonstress volume), and its position was verified.[18]

Lung Injury. Experimental lung injury was induced in the supine position by repeated lung lavage,[19] and surfactant depletion was considered stable when the P_{aO_2}/F_{IO_2} ratio was less than 150 mmHg for 10 min at a PEEP of 3 cm H_2O. Injurious mechanical ventilation using assisted pressure control consisted of V_T of approximately 15 ml · kg^{-1} (by adjusting inspiratory pressure), and a PEEP of 2 cm H_2O. PEEP was adjusted (increased or decreased) by 2 cm H_2O to maintain a P_{aO_2}/F_{IO_2} of 55 to 65 mmHg after 15 min and continued for 30 min.

Experimental Protocol. The lungs were fully recruited in the supine position, and PEEP was set at where the P_{aO_2}/F_{IO_2} ratio was approximately 100 mmHg in the supine position. Then the animals were randomly assigned to one of two groups (n = 6 for each group):

- Supine plus spontaneous breathing
- Prone plus spontaneous breathing

Randomization was from a bag of coded letters. The animals were then ventilated for 4 h using low V_T ventilation, using pressure-controlled ventilation: V_T, 6 ml · kg^{-1} (by adjusting inspiratory pressure); respiratory rate, 60 to 120 breaths/min (targeted to $Paco_2$ of less than 50 mmHg); inspiratory time, 0.2 s; minimum flow trigger; and Fio_2 adjusted to target Pao_2 of 100 mmHg. All of the animals (n = 12) survived the protocol. After 4 h of mechanical ventilation, the animals were sacrificed with IV sodium pentobarbital, and the lungs were excised.

Wet to Dry Lung Weight. The right upper and middle lobes of the lung were weighed, placed in a warming oven (37°C), and weighed daily until the weight was stable.

Lung Inflammation. Bronchoalveolar fluid was collected from the left whole lung by injecting 10 ml of normal saline three times; then the total protein in the bronchoalveolar fluid was quantified. Lung myeloperoxidase activity was measured[21] from lung biopsies; a lung tissue sample (8 × 8 × 8 mm) was taken from the nondependent and dependent right middle lobes. One investigator (G.O.), who was blind to sampling regions and group allocation, performed the analysis.

Lung Histology. The right lower lobe was fixed with intratracheal insufflation of 10% formalin of 15 ml for at least 24 h. The right lower lobe was sectioned transversely (5-mm slices) and embedded in paraffin. In addition, 3-μm slices were stained with hematoxylin and eosin. Representative histologic images in each group are presented.

Definitions. The definitions of pulmonary pressures are as follows:

- Negative swing in P_{eso}: ΔP_{eso} was determined from the amount of decrease (spontaneous breathing) in P_{eso} from the start of inspiration.
- Negative swing in pleural pressure: Δ pleural pressure was determined from the amount of decrease (spontaneous breathing) in pleural pressure from the start of inspiration.
- Maximal (inspiratory) transpulmonary pressure: Peak transpulmonary pressure equaled the maximal value of [$P_{aw} - P_{eso}$] cm H_2O, usually corresponding to the time of the most negative value of P_{eso} (maximum inspiration).
- Plateau (inspiratory) transpulmonary pressure: Plateau transpulmonary pressure equaled [plateau P_{aw} – end-inspiratory P_{eso}] cm H_2O.
- Plateau pressure: P_{aw} measured during a short inspiratory hold (*i.e.*, zero flow phase).
- Driving pressure equaled [plateau P_{aw} – PEEP] cm H_2O.
- Peak Δ transpulmonary pressure: Peak Δ transpulmonary pressure equaled [P_{aw} – PEEP – (ΔP_{eso})] cm H_2O, corresponding to the time of maximal value of peak Δ transpulmonary pressure.
- Compliance of the respiratory system equaled [V_T/(driving pressure)] mL · cm H_2O^{-1}.

Statistical Analysis

Statistical analyses were performed using SPSS13.0 for Windows (SPSS, USA). The study was exploratory, and the sample size was not formally calculated, but it was based on experience. Normal distribution of data was checked with histography. The results are expressed as mean ± SD. One-way ANOVA was used to compare myeloperoxidase activities among regions. Two-way ANOVA with repeated measures evaluated the effects of time and group on respiratory variables. Two-way ANOVA was applied to evaluate the effects of lung regions (ventral *vs.* dorsal) and condition differences on lung stress and lung inflation imposed by spontaneous effort. In the *post hoc* analysis, a Dunnett's test was used to compare repeated values with the value at the start of the protocol (*i.e.*, 0 h), and Tukey's pairwise multiple comparison test was used to determine condition differences. Unpaired *t* tests were used to compare the wet to dry ratio and bronchoalveolar fluid protein. All tests were two-tailed, and differences were considered significant when $P < 0.05$.

Results

Mechanism Protocol in the Anesthetized Pig

Respiratory Variables. V_T was low and similar (volume-controlled ventilation: 6.7 ± 0.6 to 6.9 ± 0.5 ml/kg) in all four conditions ("condition" $P = 0.772$ by two-way repeated ANOVA) at baseline (paralyzed) and throughout titration of spontaneous effort ("time" $P = 0.081$ by two-way repeated ANOVA; Supplemental Digital Content table S1, http://links.lww.com/ALN/C801). The development of spontaneous breathing did not alter global V_T (as anticipated, given the volume-controlled ventilation). The swing (deflection) in esophageal pressure (ΔP_{eso}) increased until it reached –10 cm H_2O during spontaneous effort titration as per protocol in all groups (Supplemental Digital Content table S1, http://links.lww.com/ALN/C801).

Local Pleural Pressure during Spontaneous Effort. The regional distribution of pleural pressure (fig. 2) was measured and evaluated under the same amount of spontaneous effort in all conditions (*i.e.*, ΔP_{eso} = –10 cm H_2O). The magnitude of negative inspiratory pleural pressure in the dorsal (dependent) lung was almost twofold greater than negative inspiratory pleural pressure in the ventral (nondependent) lung at low PEEP in the supine position (Δ pleural pressure in ventral *vs.* dorsal lung: –9.8 ± 2.9 cm H_2O *vs.* –18.1 ± 4.0 cm H_2O; $P < 0.001$; fig. 2A). High PEEP in the supine position significantly reduced a ventral to dorsal gradient in inspiratory Δ pleural pressure (dorsal Δ pleural pressure in low PEEP *vs.* high PEEP: –18.1 ± 4.0 cm H_2O *vs.* –13.3 ± 2.3 cm H_2O; $P < 0.001$; fig. 2A *vs.* fig. 2B). In the prone position, however, there was no ventral to dorsal gradient in local Δ pleural pressure after diaphragmatic contraction, irrespective

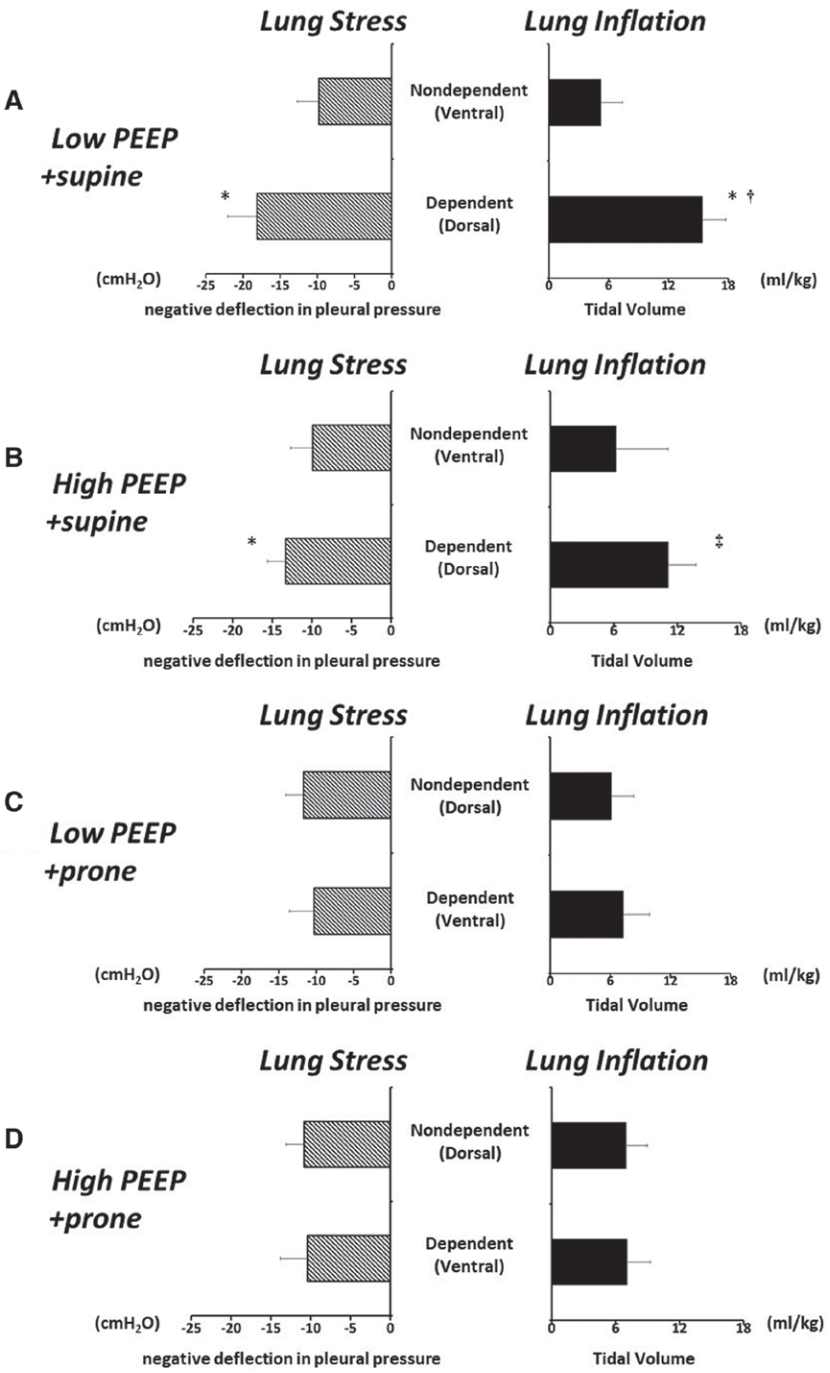

Fig. 2. Local pleural pressure and inflation imposed by spontaneous effort: series 1 mechanism protocol in pigs. The data are expressed as mean ± SD (*error bars*). The magnitudes of inspiratory negative pleural pressure (*left*) and lung inflation (*right*) were estimated at negative swing in esophageal pressure (P_{eso}) of approximately –10 cm H_2O and tidal volume (V_T) of approximately 7 ml/kg during volume-controlled ventilation in all conditions (*A* to *D*). The *x axes* in the *left panels* represent negative swings in pleural pressure measured by balloon catheter occlusion technique. In contrast, the *x axes* in the *right panels* represent the V_T levels required during controlled breaths (muscle paralysis) to obtain the same magnitude of local inflation (ΔZ in electrical impedance tomography) imposed by spontaneous effort (P_{eso} approximately –10 cm H_2O). (*A*) In low positive end-expiratory pressure (PEEP) and supine, a passive V_T of almost 16 ml/kg was required to obtain the same magnitude of local inflation imposed by spontaneous effort in the dependent lung, the same lung region where higher lung stress was concentrated. (*B*) High PEEP in supine decreased the ventral to dorsal gradient of negative pleural pressure swing, leading to decrease the degree of local dependent lung inflation imposed by spontaneous effort. In contrast, in the prone position, the distribution of lung stress and inflation during spontaneous effort was the same as during muscle paralysis, either at low PEEP (*C*) or high PEEP (*D*). *$P < 0.01$ compared with values in nondependent lung regions within groups; †$P < 0.01$ compared with values in dependent lung regions among all other conditions; ‡$P < 0.05$ compared with values in dependent lung regions among all other conditions.

of the PEEP level (Δ pleural pressure in ventral [dependent] *vs.* dorsal [nondependent] lung: −10.3 ± 3.3 cm H_2O *vs.* −11.7 ± 2.4 cm H_2O at low PEEP, $P = 0.115$; −10.4 ± 3.4 cm H_2O *vs.* −10.8 ± 2.3 cm H_2O at high PEEP, $P = 0.715$; fig. 2, C and D).

Local Lung Inflation during Spontaneous Effort versus *Muscle Paralysis.* When comparing the regional distribution of lung inflation, the strength of spontaneous effort was matched among animals (*i.e.*, ΔP_{eso} equaled −10 cm H_2O) under a fixed global V_T (volume-controlled mode: approximately 7 ml/kg, Supplemental Digital Content table S1, http://links.lww.com/ALN/C801). Local distribution of lung inflation imposed by spontaneous effort in electrical impedance tomography reflected the ventral to dorsal gradient in negative Δ pleural pressure during diaphragmatic contraction.

In the supine position during low PEEP, spontaneous effort increased local lung inflation in the dependent (dorsal) lung, in the same region where more negative Δ pleural pressure was localized (fig. 2A). At low PEEP and supine, a significantly larger passive V_T (15.4 ± 2.3 ml/kg, $P = 0.009$ *vs.* high PEEP and supine, $P < 0.001$ *vs.* high PEEP and prone, $P < 0.001$ *vs.* low PEEP and prone) was required to achieve inspiratory inflation of the dependent lung (fig. 2A) comparable to that achieved during spontaneous effort, despite limiting global V_T to approximately 7 ml/kg. The magnitude of local dependent lung inflation imposed by spontaneous effort was significantly less at high PEEP and supine ($P = 0.009$ *vs.* low PEEP and supine), and thus the distribution of lung inflation was similar among lung regions (passive V_T required in ventral [nondependent] *vs.* dorsal [dependent] lung: 6.2 ± 4.9 ml/kg *vs.* 11.2 ± 2.6 ml/kg; $P = 0.062$; fig. 2B). In the prone position, the distribution of lung inflation was not altered by spontaneous effort at low PEEP (passive V_T required in ventral [dependent] *vs.* dorsal [nondependent] lung: 7.3 ± 2.6 ml/kg *vs.* 6.1 ± 2.2 ml/kg; $P = 0.512$; fig. 2C) and at high PEEP (passive V_T required in ventral [dependent] *vs.* dorsal [nondependent] lung: 7.1 ± 2.2 ml/kg *vs.* 7.0 ± 2.0 ml/kg; $P = 0.943$; fig. 2D).

Lung Injury Protocol in the Anesthetized Rabbit

Respiratory Variables. The dose of propofol and ketamine was similar in the supine position *versus* the prone position (propofol: 19 ± 5 mg · kg^{-1} · h^{-1} *vs.* 22 ± 5 mg · kg^{-1} · h^{-1}, $P = 0.394$; ketamine: 3.1 ± 1.9 mg · kg^{-1} · h^{-1} *vs.* 2.1 ± 0.7 mg · kg^{-1} · h^{-1}, $P = 0.273$). The values of V_T (approximately 6 ml/kg) were similar in both groups ("group" $P = 0.853$ by two-way repeated ANOVA) throughout the protocol ("time" $P = 0.837$ by two-way repeated ANOVA). Oxygenation (Pao_2/Fio_2) was greater during spontaneous effort in the prone *versus* supine position (group $P = 0.008$ by two-way repeated ANOVA; table 1). In the supine position, oxygenation increased transiently for approximately the first hour after commencement of spontaneous breathing and decreased thereafter (table 1). Respiratory system compliance decreased over time in the supine position with spontaneous effort but did not decrease in the prone position with spontaneous effort. Respiratory system compliance was higher after 2 h in the prone position *vs.* supine position (respiratory system compliance at 4 h: 2.1 ± 0.9 ml/cm H_2O *vs.* 1.1 ± 0.2 ml/cm H_2O; $P = 0.034$; table 1).

Spontaneous Effort in Supine versus *Prone Position.* The intensity of spontaneous effort in terms of frequency (estimated by respiratory rate) and magnitude (estimated by negative ΔP_{eso}) was significantly less in the prone *versus* supine groups (table 1; fig. 3A) despite the use of the same doses of sedatives, the maintenance of constant Pao_2 (approximately 100 mg by adjusting Fio_2), and the same value of $Paco_2$ (table 1). The deflections in ΔP_{eso} became significantly more negative in the supine position but remained constant in the prone position (ΔP_{eso} at 4 h: −3.9 ± 1.3 cm H_2O *vs.* −1.6 ± 1.1 cm H_2O; $P = 0.008$; fig. 3A). Spontaneous respiratory rate (and thus minute ventilation) was significantly higher in the supine *vs.* prone groups (table 1). At all times during spontaneous breathing after time zero, the peak Δ transpulmonary pressure (at maximum inspiration) was greater in the supine group *versus* the prone group (fig. 3B).

Lung Injury in Supine versus *Prone Position.* Overall lung injury was less in the prone *versus* supine groups in terms of wet/dry lung weight ratio (fig. 4A) and protein concentration in bronchoalveolar fluid (fig. 4B). The regional patterns of injury also differed between the groups. In the supine group, the lung tissue myeloperoxidase expression was higher in the dependent (dorsal) lung, in the same regions where spontaneous effort increased lung stress and inflation (67.5 ± 38.1 μm/min/mg protein *vs.* 167.7 ± 65.5 μm/min/mg protein in the nondependent *vs.* dependent lung; $P = 0.003$; fig. 5A), but there were no regional differences in myeloperoxidase expression in the prone group (61.0 ± 23.0 μm/min/mg protein *vs.* 74.0 ± 30.9 μm/min/mg protein in the nondependent *vs.* dependent lung; $P = 0.951$; fig. 5B). The distribution of "histologic" injury in each group is presented with illustrative sections (Fig. 5).

Discussion

The prone position in severe ARDS has been traditionally used under passive conditions (*i.e.*, under muscle paralysis or deep sedation).[16] The current data suggest that the prone position could be an option to minimize lung injury from spontaneous effort in severe ARDS. This is because the prone position, independent of PEEP levels, diminishes the maldistribution of lung stress and thus the asymmetric, injurious lung inflation associated with spontaneous effort, and also because the prone position mitigates the magnitude of spontaneous efforts.

Ventilator-induced Lung Injury *versus* Effort-dependent Lung Injury

Using histology, computed tomography, and positron emission tomography imaging of [^{18}F]fluoro-2-deoxy-D-glucose,

Table 1. Respiratory Parameters in the Anesthetized Rabbit (n = 6/Each Group)

Parameter	Group	Lung Injury	Measurement				
			0 h after Start of Lung Injury Protocol	1 h after Start of Lung Injury Protocol	2 h after Start of Lung Injury Protocol	3 h after Start of Lung Injury Protocol	4 h after Start of Lung Injury Protocol
Pa_{O_2}/F_{IO_2}, mmHg	Supine	100 ± 15	204 ± 84	298 ± 138	219 ± 71	148 ± 75	106 ± 32
	Prone	113 ± 19	343 ± 159	422 ± 159	432 ± 161*	418 ± 171*	420 ± 179*
Pa_{CO_2}, mmHg	Supine	40 ± 9	65 ± 17	51 ± 6	44 ± 10†	39 ± 9†	39 ± 5†
	Prone	40 ± 10	63 ± 11	56 ± 10†	41 ± 7†	40 ± 8†	38 ± 11†
Peak airway pressure, cm H_2O	Supine	22.7 ± 3.7	25.6 ± 4.8	28.7 ± 6.5†	29.1 ± 3.7†	29.4 ± 4.0†	29.1 ± 4.0†
	Prone	21.3 ± 4.3	23.9 ± 9.1	24.0 ± 8.6	22.2 ± 9.0	20.6 ± 8.1*†	20.6 ± 8.6*†
Plateau airway pressure, cm H_2O	Supine	20.5 ± 2.9	21.7 ± 3.2	26.5 ± 5.5†	26.6 ± 3.4†	26.7 ± 3.9†	26.3 ± 3.6†
	Prone	19.3 ± 3.8	21.1 ± 8.5	20.5 ± 7.8	20.0 ± 7.9	18.3 ± 7.2*†	18.3 ± 7.6*†
Mean airway pressure, cm H_2O	Supine	13.0 ± 2.6	13.6 ± 3.1	14.6 ± 3.6	14.8 ± 2.5	14.3 ± 3.2	14.3 ± 2.5
	Prone	12.0 ± 4.6	12.8 ± 5.5	12.7 ± 5.3	12.2 ± 5.4	11.7 ± 4.8†	11.9 ± 4.9†
Positive end-expiratory pressure, cm H_2O	Supine	8.4 ± 2.6	8.4 ± 3.0	8.3 ± 3.0	8.1 ± 3.1	8.1 ± 3.3	8.0 ± 2.9
	Prone	7.5 ± 4.2	7.5 ± 3.7	7.6 ± 3.8	7.6 ± 3.8	7.1 ± 3.4	7.3 ± 3.6
Tidal volume, ml/kg	Supine	5.5 ± 1.2	6.0 ± 0.4	6.2 ± 0.7	6.1 ± 0.6	6.1 ± 0.4	6.2 ± 0.5
	Prone	5.4 ± 1.7	5.9 ± 0.5	6.2 ± 0.2	6.1 ± 0.5	6.1 ± 0.6	6.1 ± 0.9
Respiratory rate, breaths/min	Supine	40 ± 0	107 ± 23	113 ± 19	113 ± 11	112 ± 10	112 ± 12
	Prone	40 ± 0	84 ± 4	81 ± 5*	82 ± 7*	78 ± 7*	78 ± 8*
Minute volume, l/min	Supine	0.8 ± 0.2	2.2 ± 0.4	2.4 ± 0.6	2.4 ± 0.5	2.4 ± 0.4	2.4 ± 0.5
	Prone	0.8 ± 0.3	1.8 ± 0.2*	1.8 ± 0.2*	1.7 ± 0.1*	1.7 ± 0.1*	1.7 ± 0.3*
Respiratory system compliance, ml/cm H_2O	Supine	1.6 ± 0.3	1.5 ± 0.1	1.1 ± 0.4†	1.0 ± 0.2†	1.0 ± 0.2†	1.1 ± 0.2†
	Prone	1.6 ± 0.5	1.7 ± 0.8	1.8 ± 0.8	1.8 ± 0.8*	2.0 ± 0.7*	2.1 ± 0.9*
Peak transpulmonary pressure, cm H_2O	Supine	18.8 ± 3.6	22.9 ± 2.9	28.0 ± 5.7†	29.1 ± 2.6†	28.2 ± 2.4†	28.5 ± 2.4†
	Prone	16.8 ± 3.3	19.6 ± 8.8	19.0 ± 8.6	18.3 ± 8.4*	16.8 ± 8.5*†	16.4 ± 7.9*†
Plateau transpulmonary pressure, cm H_2O	Supine	16.4 ± 3.0	18.4 ± 1.9	22.2 ± 4.7†	22.4 ± 2.9†	21.5 ± 2.6†	22.3 ± 2.0†
	Prone	14.4 ± 2.9	14.4 ± 8.0	13.6 ± 7.9*	13.8 ± 7.3*	12.6 ± 7.7*	12.2 ± 7.2*

*$P < 0.05$ compared with supine. †$P < 0.05$ compared with 0 (at the start of the protocol) within groups.
F_{IO_2}, fractional inspired oxygen tension.

previous studies revealed that ventilator-induced lung injury occurred in nondependent (ventral) lung regions in animal models of ARDS (rats, rabbits, pigs)[6,22,23] and patients with ARDS.[24,25] During a controlled breath, ventilation is likely to shift to nondependent (ventral) lung regions because of spatial heterogeneity of lung aeration, *i.e.*, more atelectasis in the more dependent (dorsal) lung, and therefore a small percentage of the nondependent lung is more susceptible to higher inspiratory stress and strain in the supine position. On the other hand, the prone position decreases such spatial heterogeneity of lung aeration, leading to more even distribution of tidal strain and [^{18}F]fluoro-2-deoxy-D-glucose uptake.[26] Therefore, the prone position is known to reduce ventilator-induced lung injury[12] and improve mortality in severe ARDS[16]

The current study confirmed that spontaneous effort altered the locus of lung injury: the bulk of effort-dependent lung injury occurred in the dependent (dorsal) lung,[6,27,28] the same region where spontaneous inspiratory effort increased greater inspiratory lung stress and caused overinflation (figs. 2 and 5). Of note, the combination of low levels of PEEP and the supine position appears to pose the greatest risk of effort-dependent lung injury (fig. 2).

The maldistribution of lung stress during spontaneous effort was most manifested in the supine position with low PEEP. While the strength of spontaneous effort (measured as ΔP_{eso} equals −10 cm H_2O) was maintained to be the same among all conditions in the pig experiments, lower PEEP in the supine position was associated with the highest local lung stress in the dependent lung and thus the greatest magnitude of local lung inflation in the dependent lung. Therefore, overall lung injury from spontaneous effort was greater in the supine position (fig. 4), and the lung tissue myeloperoxidase expression and lung histologic injury were higher in dependent (dorsal) lung (fig. 5).

Mechanisms of Protection: Impact of Position

Prone position (*vs.* supine position) was effective to minimize effort-dependent lung injury, as evident from better gas exchange, better respiratory system compliance, lower wet/dry lung weight ratio, lower bronchoalveolar fluid protein concentration, and less lung tissue myeloperoxidase activity. The overall burden of lung injury was less, and there was no difference between degrees of injury in dorsal *versus* ventral lung. Several mechanisms were revealed from this study.

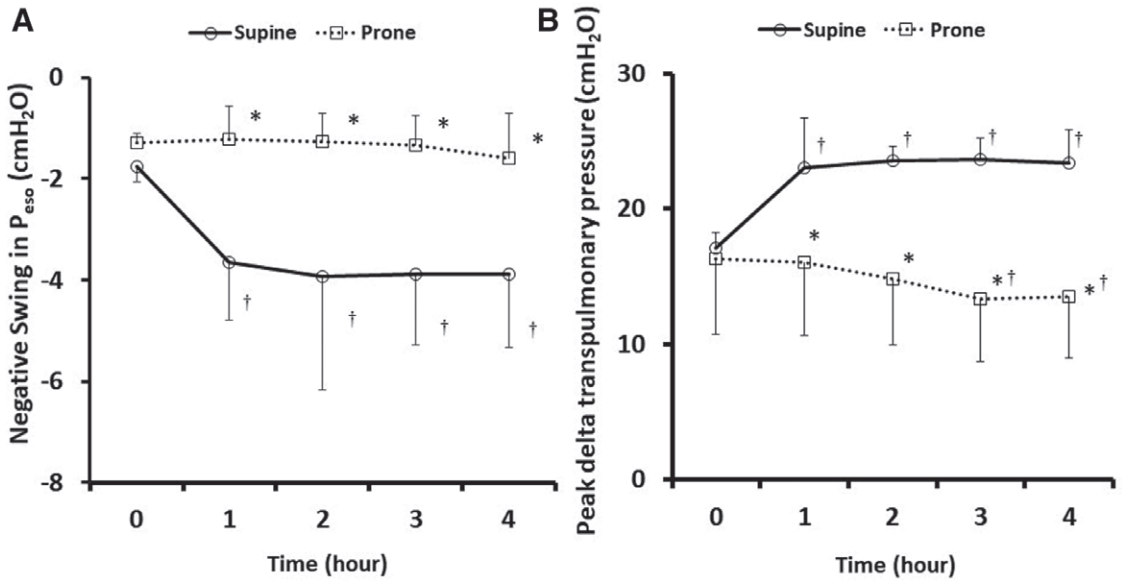

Fig. 3. Intensity of spontaneous effort and dynamic lung stress in supine *versus* prone- series 2 lung injury protocol in rabbits. The data are expressed as mean ± SD (*error bars*). The intensity of inspiratory effort (series 2 rabbit) was evaluated as the magnitude of the negative swing in esophageal pressure (ΔP_{eso}). (*A*) ΔP_{eso} was less in the prone position *versus* the supine position throughout the protocol. (*B*) As a result, peak Δ transpulmonary pressure, a surrogate of dynamic lung stress, was less in the prone position *versus* the supine position throughout the protocol. Peak Δ transpulmonary pressure decreased over time in the prone position. $P < 0.05$ compared with supine; †$P < 0.05$ compared with 0 h (at the start of the protocol) within groups.

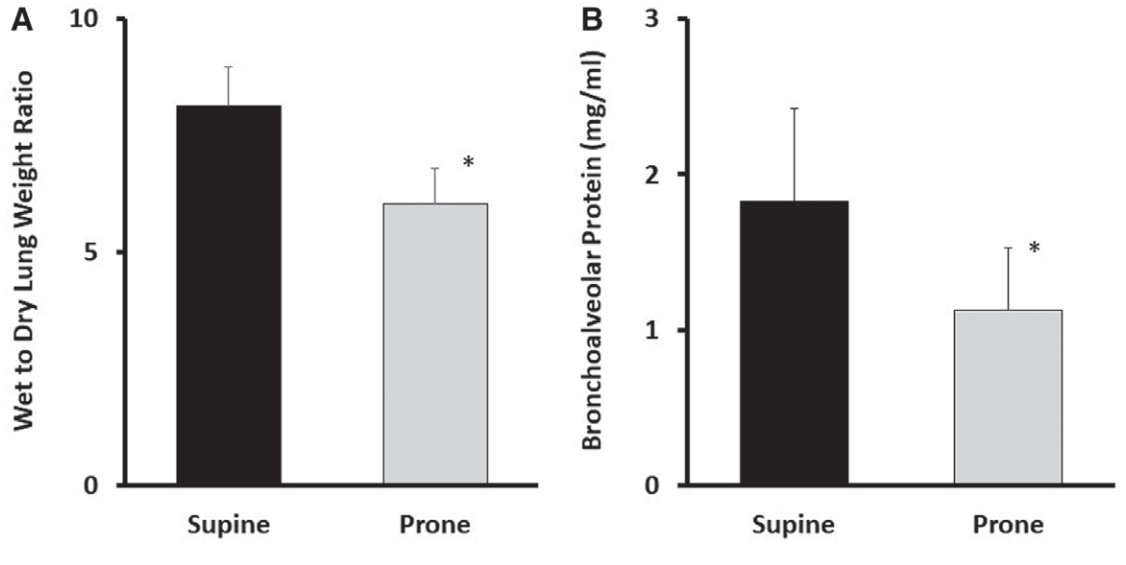

Fig. 4. Overall lung injury in the supine position *versus* prone position: series 2 lung injury protocol in rabbits. The data are expressed as mean ± SD (*error bars*). (*A*) Wet/dry lung weight ratio was less in the prone position. (*B*) Protein in bronchoalveolar fluid was less in the prone position. *$P < 0.01$ compared with supine.

First, the prone position had no ventral to dorsal gradient in local Δ pleural pressure after diaphragmatic contraction, and therefore the magnitude of local lung inflation during spontaneous breathing is the same as under V_T at approximately ≈7 ml/kg during muscle paralysis (fig. 2, C and D). This might be explained partially by the gravitational

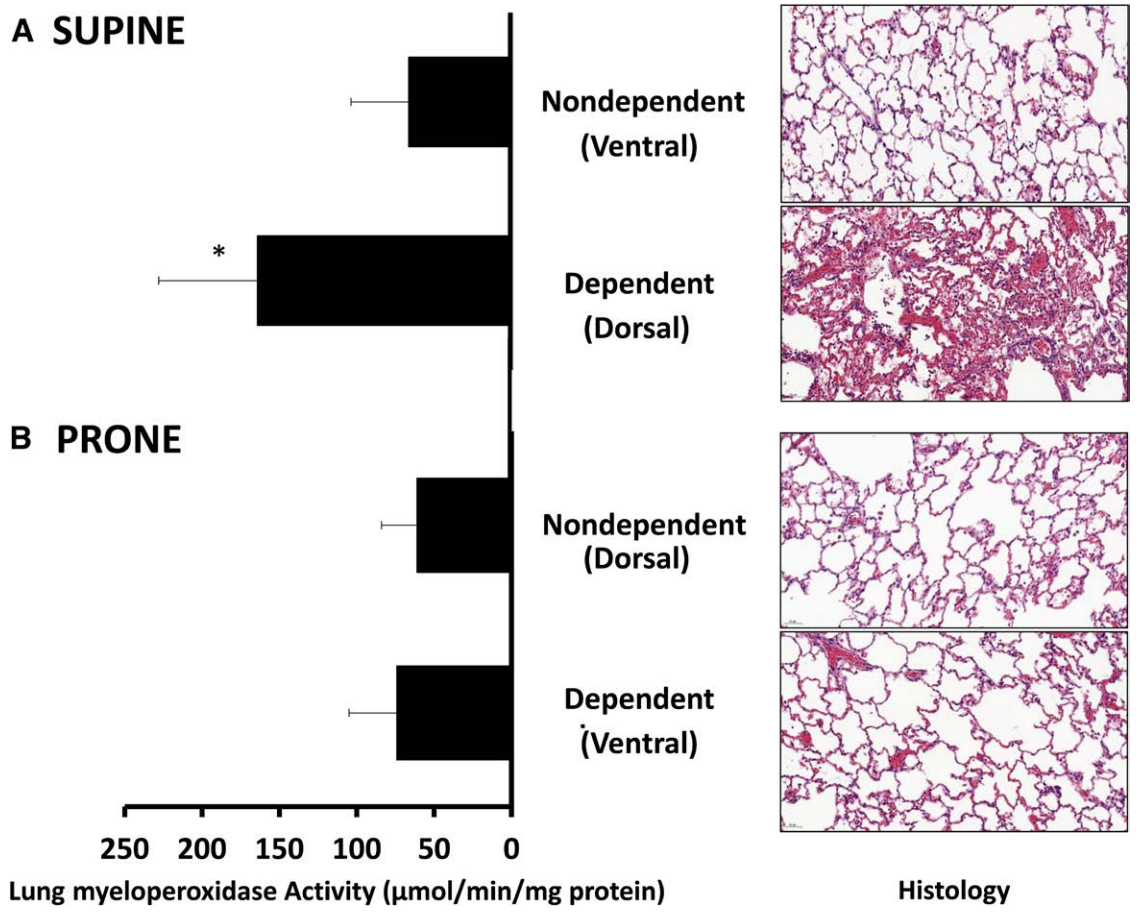

Fig. 5. Regional lung injury in the supine position *versus* prone position: series 2 lung injury protocol in rabbits. The data are expressed as mean ± SD (*error bars*). The regional patterns of injury differed between the groups. (*A*) The lung tissue myeloperoxidase expression was higher in the dependent (dorsal) lung, in the same region where spontaneous effort increased lung inflation, *versus* the nondependent (ventral) lung in the supine position. Representative images (original magnification, ×20; hematoxylin and eosin) are shown. (*Right upper*) Nondependent lung in the supine position. (*Right lower*) Dependent lung in the supine position. In accordance with the regional patterns of lung tissue myeloperoxidase expression, in the supine position, spontaneous effort increased dependent lung injury, *i.e.*, more hyaline membrane formation, severe alveolar hemorrhaging, more neutrophil infiltration into the alveoli and interstitium. (*B*) There were no regional differences in myeloperoxidase expression in the prone position. Representative images (original magnification, ×20; hematoxylin and eosin) are shown. (*Right upper*) Nondependent lung in the prone position. (*Right lower*) Dependent lung in the prone position. In the prone position, the magnitude of lung injury was not different between nondependent lung and dependent lung. *$P < 0.01$ compared with all other regions.

translocation of atelectatic solid-like lung tissue (which impedes pressure transmission) from the dorsal to ventral lung. This explanation is likely because "baby lung" is considered a functional entity (but not an anatomical entity) that can change its location with position and level of PEEP.[11,29] Importantly, previous studies show that dorsal muscular regions of the diaphragm move more than ventral regions of the diaphragm during spontaneous breathing, regardless of the body position.[30,31] Thus, the prone position decreases atelectatic solid-like lung tissue in the dorsal lung facing the well-moved, dorsal muscular regions of the diaphragm, which may facilitate the uniform transmission of Δ pleural pressure to the entire lung surface from where it was generated, after diaphragmatic contraction.

Second, the intensity of spontaneous effort (indicated by ΔP_{eso}, respiratory rate in fig. 3A and table 1) was lower in the prone position (*vs.* supine position), despite matching levels of sedation. Because the prone position mitigates injurious spontaneous effort, it resulted in lower peak Δ transpulmonary pressure (*i.e.*, dynamic lung stress). Of note, the benefit of the prone position in reducing the intensity of spontaneous effort was documented not only in rabbits (fig. 3A) but also in humans (infants,[32,33] patients with ARDS,[34] hypoxic patients with COVID-19[35]). Several plausible explanations are offered. First, the prone position increases end-expiratory lung volume in some patients (probably depending on lung recruitablity, the shape of the chest wall, the presence of abdominal

hypertension, and the presence of support).[11] In this study, the prone position was effective to recruit lung and increase lung volume in rabbits, suggested by higher respiratory system compliance in the prone position (table 1). Higher lung volume shortens diaphragm length, resulting in less force generation from the diaphragm.[9,10] Second, the prone position *per se* is known to shorten diaphragm length even with the same end-expiratory lung volume as in the supine position, probably due to altered chest wall configuration and diaphragm geometry.[36,37] Of course, the force generated by diaphragmatic contraction decreases as its length shortens.[38]

Therefore, the current study adds a promising technique to facilitate safe spontaneous breathing during mechanical ventilation in severe ARDS. It may synergize the benefits of spontaneous breathing (less muscle atrophy, more physiologic) with the benefits of the prone position *per se* (less ventilator-induced lung injury, more opening of well perfused regions). The current data support a larger clinical study as a next step to confirm the benefits of the prone position to render spontaneous effort less injurious in patients with ARDS whose spontaneous effort is vigorous.

Spontaneous Breathing and Prone Position Related to COVID-19

In the era of the COVID-19 pandemic, the indication of the prone position has been expanding: the prone position is now applied to nonintubated, hypoxic patients with COVID-19 (before intubation, not as severe as moderate-to-severe ARDS), hoping that being awake in the prone position might improve gas exchange, decrease the strength of spontaneous effort, minimizing the risk of effort-dependent lung injury, and thereby avoiding tracheal intubation.[35,39,40] A few case reports observed that the prone position was associated with better gas exchange and lower respiratory rate,[41,42] and a recent large randomized clinical trial has confirmed that being awake in the prone position significantly improved oxygenation, decreased the respiratory rate, and decreased the incidence of treatment failure and the need of intubation.[35] Therefore, the beneficial effects of the prone position to mitigate effort-dependent lung injury has been found not only in mechanically ventilated patients with ARDS[34] but also in nonintubated hypoxemic patients with COVID-19.[35] The current physiologic study may reveal potential protective mechanisms of the prone position from spontaneous breathing.

Limitations

There are several limitations to the current work. First, we utilized two different species (pigs and rabbits). Larger animals are closer to human physiology, so they are suitable for exploring the mechanism. The smaller animals are known to have a shorter (and steeper) trajectory of lung injury, so rabbits are more suitable for evaluating injury in a shorter time period; the overall consistent results in rabbits (location of injury) and pigs (location of lung stress and inflation) are reassuring. Second, different ventilatory modes were used (volume-controlled in pigs, pressure-controlled in rabbits). No differences in the patterns and magnitudes of dependent lung inflation imposed by spontaneous effort were observed between the volume-controlled mode and the pressure-controlled mode.[7] Thus, the difference in ventilatory mode does not affect interpretation of the data. Third, the current study lacked paralyzed groups in the lung injury protocol. We chose supine and spontaneous breathing as a control group to compare with prone and spontaneous breathing. We cannot separate completely the benefits of lowering spontaneous effort from those of prone position *per se*. Fourth, our study included a single sex (males), the rationale being minimizing data variability. The potentially confounding effects of this sex bias on the meaning of single-sex experimental data should be considered.[43]

Conclusions

The current animal study found that the prone position, independent of PEEP levels, diminished a maldistribution of lung stress and thus asymmetric, injurious lung inflation associated with spontaneous effort and mitigated spontaneous effort, resulting in less effort-dependent lung injury.

Acknowledgments

Brian P. Kavanagh, M.D., sadly passed away on June 15, 2019. Prof. Kavanagh designed the study, interpreted all of the data, revised the manuscript, and was overall supervisor. The authors sincerely thank Prof. Kavanagh for his outstanding leadership and mentorship in completing this complex study.

Research Support

Supported by Grant-in-Aid for Young Scientists 19K18294, funds from the Ministry of Education, Culture, Sports, Science and Technology of Japan (Tokyo, Japan; to Dr. Yoshida), a Grant for the Promotion of Joint Research, funds from the Fukuda Foundation for Medical Technology of Japan (Tokyo, Japan; to Dr. Yoshida), a Research Training Competition (RESTRACOMP) Award, funds from the Hospital for Sick Children (Toronto, Ontario, Canada; to Dr. Yoshida), and funds from the Canadian Institutes of Health Research (Ottawa, Ontario, Canada; to Dr. Kavanagh).

Competing Interests

The authors declare no competing interests.

Correspondence

Address correspondence to Dr. Yoshida: 2-15 Yamadaoka, Suita, Osaka, 565-0871, Japan. takeshiyoshida@hp-icu.med.osaka-u.ac.jp. Anesthesiology's articles are made

References

1. Putensen C, Muders T, Varelmann D, Wrigge H: The impact of spontaneous breathing during mechanical ventilation. Curr Opin Crit Care 2006; 12:13–8
2. Yoshida T, Torsani V, Gomes S, De Santis RR, Beraldo MA, Costa EL, Tucci MR, Zin WA, Kavanagh BP, Amato MB: Spontaneous effort causes occult pendelluft during mechanical ventilation. Am J Respir Crit Care Med 2013; 188:1420–7
3. Goligher EC, Dres M, Fan E, Rubenfeld GD, Scales DC, Herridge MS, Vorona S, Sklar MC, Rittayamai N, Lanys A, Murray A, Brace D, Urrea C, Reid WD, Tomlinson G, Slutsky AS, Kavanagh BP, Brochard LJ, Ferguson ND: Mechanical ventilation-induced diaphragm atrophy strongly impacts clinical outcomes. Am J Respir Crit Care Med 2018; 197:204–13
4. Yoshida T, Uchiyama A, Matsuura N, Mashimo T, Fujino Y: The comparison of spontaneous breathing and muscle paralysis in two different severities of experimental lung injury. Crit Care Med 2013; 41:536–45
5. Güldner A, Pelosi P, Gama de Abreu M: Spontaneous breathing in mild and moderate *versus* severe acute respiratory distress syndrome. Curr Opin Crit Care 2014; 20:69–76
6. Morais CCA, Koyama Y, Yoshida T, Plens GM, Gomes S, Lima CAS, Ramos OPS, Pereira SM, Kawaguchi N, Yamamoto H, Uchiyama A, Borges JB, Vidal Melo MF, Tucci MR, Amato MBP, Kavanagh BP, Costa ELV, Fujino Y: High positive end-expiratory pressure renders spontaneous effort noninjurious. Am J Respir Crit Care Med 2018; 197:1285–96
7. Yoshida T, Nakahashi S, Nakamura MAM, Koyama Y, Roldan R, Torsani V, De Santis RR, Gomes S, Uchiyama A, Amato MBP, Kavanagh BP, Fujino Y: Volume-controlled ventilation does not prevent injurious inflation during spontaneous effort. Am J Respir Crit Care Med 2017; 196:590–601
8. Spinelli E, Mauri T, Beitler JR, Pesenti A, Brodie D: Respiratory drive in the acute respiratory distress syndrome: Pathophysiology, monitoring, and therapeutic interventions. Intensive Care Med 2020; 46:606–18
9. Pengelly LD, Alderson AM, Milic-Emili J: Mechanics of the diaphragm. J Appl Physiol 1971; 30:797–805
10. Laghi F, Harrison MJ, Tobin MJ: Comparison of magnetic and electrical phrenic nerve stimulation in assessment of diaphragmatic contractility. J Appl Physiol (1985) 1996; 80:1731–42
11. Gattinoni L, Taccone P, Carlesso E, Marini JJ: Prone position in acute respiratory distress syndrome: Rationale, indications, and limits. Am J Respir Crit Care Med 2013; 188:1286–93
12. Broccard A, Shapiro RS, Schmitz LL, Adams AB, Nahum A, Marini JJ: Prone positioning attenuates and redistributes ventilator-induced lung injury in dogs. Crit Care Med 2000; 28:295–303
13. Yoshida T, Roldan R, Beraldo MA, Torsani V, Gomes S, De Santis RR, Costa EL, Tucci MR, Lima RG, Kavanagh BP, Amato MB: Spontaneous effort during mechanical ventilation: Maximal injury with less positive end-expiratory pressure. Crit Care Med 2016; 44:e678–88
14. Teggia Droghi M, De Santis Santiago RR, Pinciroli R, Marrazzo F, Bittner EA, Amato MBP, Kacmarek RM, Berra L: High positive end-expiratory pressure allows extubation of an obese patient. Am J Respir Crit Care Med 2018; 198:524–5
15. Grieco DL, Maggiore SM, Roca O, Spinelli E, Patel BK, Thille AW, Barbas CSV, de Acilu MG, Cutuli SL, Bongiovanni F, Amato M, Frat JP, Mauri T, Kress JP, Mancebo J, Antonelli M: Non-invasive ventilatory support and high-flow nasal oxygen as first-line treatment of acute hypoxemic respiratory failure and ARDS. Intensive Care Med 2021; 47:851–66
16. Guérin C, Reignier J, Richard JC, Beuret P, Gacouin A, Boulain T, Mercier E, Badet M, Mercat A, Baudin O, Clavel M, Chatellier D, Jaber S, Rosselli S, Mancebo J, Sirodot M, Hilbert G, Bengler C, Richecoeur J, Gainnier M, Bayle F, Bourdin G, Leray V, Girard R, Baboi L, Ayzac L; PROSEVA Study Group: Prone positioning in severe acute respiratory distress syndrome. N Engl J Med 2013; 368:2159–68
17. Martin CJ, Young AC, Ishikawa K: Regional lung mechanics in pulmonary disease. J Clin Invest 1965; 44:906–13
18. Baydur A, Behrakis PK, Zin WA, Jaeger M, Milic-Emili J: A simple method for assessing the validity of the esophageal balloon technique. Am Rev Respir Dis 1982; 126:788–91
19. Lachmann B, Robertson B, Vogel J: *In vivo* lung lavage as an experimental model of the respiratory distress syndrome. Acta Anaesthesiol Scand 1980; 24:231–6
20. Yoshida T, Engelberts D, Otulakowski G, Katira B, Post M, Ferguson ND, Brochard L, Amato MBP, Kavanagh BP: Continuous negative abdominal pressure recruits lungs at lower distending pressures. Am J Respir Crit Care Med 2018; 197:534–7
21. Rodriguez-Palacios A, Kodani T, Kaydo L, Pietropaoli D, Corridoni D, Howell S, Katz J, Xin W, Pizarro TT, Cominelli F: Stereomicroscopic 3D-pattern profiling of murine and human intestinal inflammation reveals unique structural phenotypes. Nat Commun 2015; 6:7577
22. Tsuchida S, Engelberts D, Peltekova V, Hopkins N, Frndova H, Babyn P, McKerlie C, Post M, McLoughlin P, Kavanagh BP: Atelectasis causes alveolar injury in

nonatelectatic lung regions. Am J Respir Crit Care Med 2006; 174:279–89
23. Borges JB, Costa EL, Suarez-Sipmann F, Widström C, Larsson A, Amato M, Hedenstierna G: Early inflammation mainly affects normally and poorly aerated lung in experimental ventilator-induced lung injury. Crit Care Med 2014; 42:e279–87
24. Bellani G, Messa C, Guerra L, Spagnolli E, Foti G, Patroniti N, Fumagalli R, Musch G, Fazio F, Pesenti A: Lungs of patients with acute respiratory distress syndrome show diffuse inflammation in normally aerated regions: A [18F]-fluoro-2-deoxy-D-glucose PET/CT study. Crit Care Med 2009; 37:2216–22
25. Bellani G, Guerra L, Musch G, Zanella A, Patroniti N, Mauri T, Messa C, Pesenti A: Lung regional metabolic activity and gas volume changes induced by tidal ventilation in patients with acute lung injury. Am J Respir Crit Care Med 2011; 183:1193–9
26. Motta-Ribeiro GC, Hashimoto S, Winkler T, Baron RM, Grogg K, Paula LFSC, Santos A, Zeng C, Hibbert K, Harris RS, Bajwa E, Vidal Melo MF: Deterioration of regional lung strain and inflammation during early lung injury. Am J Respir Crit Care Med 2018; 198:891–902
27. Kiss T, Bluth T, Braune A, Huhle R, Denz A, Herzog M, Herold J, Vivona L, Millone M, Bergamaschi A, Andreeff M, Scharffenberg M, Wittenstein J, Vidal Melo MF, Koch T, Rocco PRM, Pelosi P, Kotzerke J, Gama de Abreu M: Effects of positive end-expiratory pressure and spontaneous breathing activity on regional lung inflammation in experimental acute respiratory distress syndrome. Crit Care Med 2019; 47:e358–65
28. Hurtado DE, Erranz B, Lillo F, Sarabia-Vallejos M, Iturrieta P, Morales F, Blaha K, Medina T, Diaz F, Cruces P: Progression of regional lung strain and heterogeneity in lung injury: Assessing the evolution under spontaneous breathing and mechanical ventilation. Ann Intensive Care 2020; 10:107
29. Gattinoni L, Pesenti A: The concept of "baby lung." Intensive Care Med 2005; 31:776–84
30. Krayer S, Rehder K, Vettermann J, Didier EP, Ritman EL: Position and motion of the human diaphragm during anesthesia-paralysis. Anesthesiology 1989; 70:891–8
31. Tomita K, Sakai Y, Monma M, Ohse H, Imura S: Analysis of diaphragmatic motion with prone positioning using dynamic MRI. J Phys Ther Sci 2004; 16: 85–89
32. Dimitriou G, Greenough A, Pink L, McGhee A, Hickey A, Rafferty GF: Effect of posture on oxygenation and respiratory muscle strength in convalescent infants. Arch Dis Child Fetal Neonatal Ed 2002; 86:F147–50
33. Baudin F, Emeriaud G, Essouri S, Beck J, Portefaix A, Javouhey E, Guerin C: Physiological effect of prone position in children with severe bronchiolitis: A randomized cross-over study (BRONCHIO-DV). J Pediatr 2019; 205:112–9.e4
34. Yoshida T, Tanaka A, Roldan R, Quispe R, Taenaka H, Uchiyama A, Fujino Y: Prone position reduces spontaneous inspiratory effort in patients with acute respiratory distress syndrome: A bicenter study. Am J Respir Crit Care Med 2021; 203:1437–40
35. Ehrmann S, Li J, Ibarra-Estrada M, Perez Y, Pavlov I, McNicholas B, Roca O, Mirza S, Vines D, Garcia-Salcido R, Aguirre-Avalos G, Trump MW, Nay MA, Dellamonica J, Nseir S, Mogri I, Cosgrave D, Jayaraman D, Masclans JR, Laffey JG, Tavernier E; Awake Prone Positioning Meta-Trial Group: Awake prone positioning for COVID-19 acute hypoxaemic respiratory failure: A randomised, controlled, multinational, open-label meta-trial. Lancet Respir Med 2021; 9:1387–95
36. Rehan VK, Nakashima JM, Gutman A, Rubin LP, McCool FD: Effects of the supine and prone position on diaphragm thickness in healthy term infants. Arch Dis Child 2000; 83:234–8
37. Sprung J, Deschamps C, Margulies SS, Hubmayr RD, Rodarte JR: Effect of body position on regional diaphragm function in dogs. J Appl Physiol (1985) 1990; 69:2296–302
38. Evans CL, Hill AV: The relation of length to tension development and heat production on contraction in muscle. J Physiol 1914; 49:10–6
39. Marini JJ, Gattinoni L: Management of COVID-19 respiratory distress. JAMA 2020; 323:2329–30
40. Coppo A, Bellani G, Winterton D, Di Pierro M, Soria A, Faverio P, Cairo M, Mori S, Messinesi G, Contro E, Bonfanti P, Benini A, Valsecchi MG, Antolini L, Foti G: Feasibility and physiological effects of prone positioning in non-intubated patients with acute respiratory failure due to COVID-19 (PRON-COVID): A prospective cohort study. Lancet Respir Med 2020; 8:765–74
41. Sartini C, Tresoldi M, Scarpellini P, Tettamanti A, Carcò F, Landoni G, Zangrillo A: Respiratory parameters in patients with COVID-19 after using noninvasive ventilation in the prone position outside the intensive care unit. JAMA 2020; 323:2338–40
42. Damarla M, Zaeh S, Niedermeyer S, Merck S, Niranjan-Azadi A, Broderick B, Punjabi N: Prone positioning of nonintubated patients with COVID-19. Am J Respir Crit Care Med 2020; 202:604–6
43. Vutskits L, Clark JD, Kharasch ED: Reporting laboratory and animal research in Anesthesiology: The importance of sex as a biologic variable. Anesthesiology 2019; 131:949–52

ANESTHESIOLOGY

Ketamine Psychedelic and Antinociceptive Effects Are Connected

Erik Olofsen, Ph.D., Jasper Kamp, Ph.D., Thomas K. Henthorn, M.D., Monique van Velzen, Ph.D., Marieke Niesters, M.D., Ph.D., Elise Sarton, M.D., Ph.D., Albert Dahan, M.D., Ph.D.

ANESTHESIOLOGY 2022; 136:792–801

EDITOR'S PERSPECTIVE

What We Already Know about This Topic

- Ketamine produces potent analgesia and psychedelic effects related to its dissociative properties at subanesthetic doses
- It has been suggested that ketamine analgesia may be generated by its dissociative effects, although there is evidence that suggests the two endpoints are independent and not connected

What This Article Tells Us That Is New

- In a planned secondary analysis, a population pharmacokinetic–pharmacodynamic model of ketamine and its metabolite norketamine was developed to describe the relationship between effect site concentrations of *S*- and *R*-ketamine and their metabolites and pressure pain threshold and the change in external perception as a measure of ketamine psychotropic effect
- The pharmacodynamics of *S*-ketamine did not differ for antinociception and external perception, which had the same potency parameter (C_{50}) and plasma-effect site equilibration half-time whether administered as racemic ketamine or *S*-ketamine
- *R*-ketamine did not contribute to either endpoint, while *S*-norketamine had a small antagonistic effect for both endpoints

ABSTRACT

Background: Ketamine produces potent analgesia combined with psychedelic effects. It has been suggested that these two effects are associated and possibly that analgesia is generated by ketamine-induced dissociation. The authors performed a *post hoc* analysis of previously published data to quantify the pharmacodynamic properties of ketamine-induced antinociception and psychedelic symptoms. The hypothesis was that ketamine pharmacodynamics (*i.e.,* concentration–effect relationship as well as effect onset and offset times) are not different for these two endpoints.

Methods: Seventeen healthy male volunteers received escalating doses of *S*- and racemic ketamine on separate occasions. Before, during, and after ketamine infusion, changes in external perception were measured together with pain pressure threshold. A population pharmacokinetic–pharmacodynamic analysis was performed that took *S*- and *R*-ketamine and *S*- and *R*-norketamine plasma concentrations into account.

Results: The pharmacodynamics of *S*-ketamine did not differ for antinociception and external perception with potency parameter (median [95% CI]) C_{50}, 0.51 (0.38 to 0.66) nmol/ml; blood-effect site equilibration half-life, 8.3 [5.1 to 13.0] min), irrespective of administration form (racemic ketamine or *S*-ketamine). *R*-ketamine did not contribute to either endpoint. For both endpoints, *S*-norketamine had a small antagonistic effect.

Conclusions: The authors conclude that their data support an association or connectivity between ketamine analgesia and dissociation. Given the intricacies of the study related to the pain model, measurement of dissociation, and complex modeling of the combination of ketamine and norketamine, it is the opinion of the authors that further studies are needed to detect functional connectivity between brain areas that produce the different ketamine effects.

(ANESTHESIOLOGY 2022; 136:792–801)

Ketamine is a versatile drug that is used by anesthesiologists, pain physicians, and more recently by psychiatrists.[1] At high doses, ketamine produces a dissociative anesthetic state; at low (subanesthetic) doses, it produces potent analgesia. Additionally, ketamine produces psychedelic effects related to its dissociative properties. At low doses, these dissociative effects cause inner feelings and thoughts that can cause misperception of reality, and misperception of external stimuli such as abnormal alterations of the extremities or aberrant experience of time and surroundings.[2] At increasing doses, overt paranoia, hallucinations, severe derealization and depersonalization, and anxiety

This article is featured in "This Month in Anesthesiology," page A1. This article is accompanied by an editorial on p. 675. This article has a visual abstract available in the online version.

Submitted for publication July 1, 2021. Accepted for publication February 15, 2022. Published online first on February 21, 2022.

Erik Olofsen, Ph.D.: Department of Anesthesiology, Leiden University Medical Center, Leiden, The Netherlands.

Jasper Kamp, Ph.D.: Department of Anesthesiology, Leiden University Medical Center, Leiden, The Netherlands.

Thomas K. Henthorn, M.D.: Department of Anesthesiology, University of Colorado School of Medicine, Aurora, Colorado; Department of Pharmaceutical Sciences, Skaggs School of Pharmacy and Pharmaceutical Sciences, University of Colorado, Aurora, Colorado.

Monique van Velzen, Ph.D.: Department of Anesthesiology, Leiden University Medical Center, Leiden, The Netherlands.

Marieke Niesters, M.D., Ph.D.: Department of Anesthesiology, Leiden University Medical Center, Leiden, The Netherlands.

Elise Sarton, M.D., Ph.D.: Department of Anesthesiology, Leiden University Medical Center, Leiden, The Netherlands.

Albert Dahan, M.D., Ph.D.: Department of Anesthesiology, Leiden University Medical Center, Leiden, The Netherlands.; Outcomes Research Consortium, Cleveland, Ohio.

 Anesthesiology 2022; 136:792–801. DOI: 10.1097/ALN.0000000000004176

attacks may occur.[2] Due to these serious adverse effects, pain physicians are often hesitant to consider ketamine for treatment of chronic pain, and patient compliance can be low due to fear of dissociation. It has been suggested that ketamine analgesia and antidepressant properties are highly associated and possibly even generated by its dissociative effects.[3–5] This would suggest that the dissociative and analgesic effects of ketamine and its metabolites have common pharmacodynamic properties with a similar potency and onset/offset time. This then suggests that the two endpoints are connected in the sense that brain areas "wire together if they fire together."[6] This is a key concept applied in the analysis of resting state function magnetic resonance imaging data.[7] However, there is also some evidence that suggests that the two endpoints are independent and not connected. For example, in healthy volunteers, Gitlin *et al.*[8] recently studied the effect of ketamine on cuff pain intensity and psychedelic symptoms with and without coadministration of midazolam. Their statistical analysis revealed that analgesia was not associated with the dissociative effects of ketamine. This indirect evidence agrees with earlier findings from our laboratory that showed that a NO donor, sodium nitroprusside, modestly reduced psychedelic symptoms in volunteers receiving racemic ketamine but not in those receiving *S*-ketamine.[9] Such an effect was not observed for ketamine analgesia (A. Dahan, M.D., Ph.D., unpublished data, digital communication March 4, 2022). To determine whether ketamine-induced dissociation and analgesic behavior are connected, we performed a population pharmacokinetic–pharmacodynamic analysis in healthy volunteers. All subjects received increasing doses of racemic ketamine and *S*-ketamine on different occasions, and were tested concomitantly for pain relief to a pressure pain stimulus and alterations in perception of external stimuli as a measure of psychedelic effect. We chose to analyze the perception of external stimuli as we argued that internal perception could be influenced by the imposed painful stimuli. Our null hypothesis was that ketamine pharmacodynamics (*i.e.,* concentration–effect relationship, as well as times for onset and offset of effect) are not different for these two endpoints, an indication that dissociation and analgesia from ketamine are interconnectedly generated in the brain.

Materials and Methods

Ethics and Subjects

The data used in this analysis are part of a larger data set that was used previously to study the effects of sodium nitroprusside on ketamine-induced adverse effects,[9] and to construct a population pharmacokinetic model of ketamine and its metabolites,[10] as well as a pharmacodynamic model of ketamine-induced changes in cardiac output.[11] In the secondary analysis that is currently planned, we developed a population pharmacokinetic–pharmacodynamic model of ketamine and its metabolite norketamine to describe the relationship between plasma concentrations of *S*- and *R*-ketamine (and their metabolites) and pressure pain threshold and the change in external perception as a measure of ketamine psychotropic effect. The study protocol was approved by the Institutional Review Board (Medical Ethics Review Committee Leiden, Den Haag, Delft, Leiden University Medical Center, Leiden, The Netherlands) and registered at the trial register of the Dutch Cochrane Center (www.trialregister.nl) under registration No. 5359 (principal investigator: A. Dahan; registration date, August 11, 2015). The study was performed in 20 healthy male volunteers (age, 18 to 34 yr; body mass index, 20 to 30 kg/m^2). All subjects gave written informed consent before participation in the study. Specific inclusion and exclusion criteria are found in Jonkman *et al.*[9]

Study Design

The original study was a four-arm, randomized, double-blind crossover study during which *S*-ketamine or racemic ketamine was infused against a background of either sodium nitroprusside or normal saline (placebo). For the current analysis, we used the data obtained on two occasions in which subjects received escalating intravenous doses of *S*-ketamine (Ketanest-S, Eurocept BV, The Netherlands) or racemic ketamine (Ketalar, Pfizer, Germany) during a period of 3 h. *S*-ketamine doses were 0.14 $mg \cdot kg^{-1} \cdot h^{-1}$ for 1 h, then 0.28 $mg \cdot kg^{-1} \cdot h^{-1}$ for 1 h, and finally 0.57 $mg \cdot kg^{-1} \cdot h^{-1}$ for the last 1-h period. The equivalent administered racemic ketamine doses were as follows: first hour, 0.28 mg/kg; second hour, 0.57 mg/kg; and third hour, 1.14 mg/kg. All infusions were against a background of normal saline infusion.

Data Collection

Data were collected before and during racemic ketamine infusion.

Pain Pressure Threshold. The pain pressure threshold was measured by applying an increasing pressure to a 1-cm^2 skin area between the thumb and index finger, using the FP 100 N Algometer (FDN 100, Wagner Instruments Inc., USA). The applied pressure was gradually increased until the subject indicated when the pressure became painful, after which the pressure was released. The FDN 100 has a force capacity (± accuracy) of 100 ± 2 N and graduation of 1 N. Pressure pain thresholds were obtained before the start of the racemic ketamine infusion (baseline), followed by measurements at 15-min intervals during and after racemic ketamine infusion. Measurements continued until 2 h after termination of the racemic ketamine infusion.

Bowdle Questionnaire. External perception was obtained from the Bowdle questionnaire.[12] The Bowdle questionnaire is a validated list of 13 items developed to quantify the psychedelic effects of ketamine in healthy volunteers. The subject is asked to rate each item on a 100-mm visual analog scale that ranges from "not at all" to "extreme." External perception relates to the misapprehension of external stimuli

or surroundings, including body parts, and is derived from the following items: "My body or body parts seemed to change their shape or position"; "My surroundings seemed to change in size, depth, or shape"; "The passing of time was altered"; "The intensity of colors changed"; and "The intensity of sound changed." External perception was measured at time = 0 (baseline) and 20, 40, 55, 80, 100, 115, 140, 160, 175, 200, 220, 240, 260, and 280 min after the start of ketamine infusion.

Plasma Concentrations: R-*and* S-*ketamine,* R-*and* S-*norketamine.* *R*- and *S*-dehydronorketamine and total hydroxynorketamine were not considered in the current analysis. At regular time points (time = 0 [baseline] and time = 2, 6, 30, 59, 62, 66, 100, 119, 122, 126, 150, 179, 182, 186, 195, 210, and 300 min after the start of ketamine infusion), 8 ml blood was drawn from an arterial line placed in the radial artery (opposite to the infusion arm). Plasma concentrations were measured in the laboratory of Evan Kharasch, M.D., Ph.D., at Washington University School of Medicine, St. Louis, Missouri, as described by Rao *et al.*, by enantioselective high-performance liquid chromatography–tandem mass spectrometry after solid-phase extraction.[13]

Data Analysis

The pharmacokinetic data were analyzed separately in NONMEM (ICON Development Solution, USA) and previously reported.[10] The pharmacokinetic data were analyzed with a two-compartment ketamine, two-compartment norketamine, one-compartment dehydronorketamine, and two-compartment hydroxynorketamine model. In between the central ketamine and norketamine compartments, two metabolism or delay compartments were included (see fig. 2 in Kamp *et al.*[10]). In this study, we use the measured *R*- and *S*-ketamine and norketamine plasma concentration data. From the earlier model, empirical Bayesian estimates of the pharmacokinetics parameters were obtained, and their fixed values were used as input to the pharmacodynamic model.

To account for a possible delay between plasma concentrations and effect, effect compartments for *S*- and *R*-ketamine and *S*- and *R*-norketamine were postulated that were assumed to equilibrate with the central compartment with an effect half-time of $t_{½} = \ln(2)/k_{e0}$, where k_{e0} is a rate constant.

For the two endpoints, pressure pain threshold and external perception, and the two compounds, *S*- and racemic ketamine, four initial pharmacodynamic models were built and next combined, by testing if typical parameter values and their interindividual variances could be set to the same value. We focus on the final model, but show how the objective function values and 95% CI of the parameter estimates change with changing assumptions.

Pressure pain was modeled as follows:

$$PTT(t) = BLN \times \left(1 + C_k(t)^{\gamma}\right) \text{and } C_K(t) = \left(\frac{C_R(t)}{C_{50R}}\right) + \left(\frac{C_S(t)}{C_{50S}}\right) \quad (1)$$

where $PPT(t)$ is the amount of pressure in newtons applied at which the subjects first reported pain at time t, BLN is the estimated pressure pain threshold at baseline, $C_R(t)$ and $C_S(t)$ are the effect-site concentration of *S*- and *R*-ketamine in nanomoles per milliliter at time t, C_{50R} and C_{50S} are the estimated *S*- and *R*-ketamine effect-site concentrations needed to increase the pain pressure threshold by 100% (in nanomoles per milliliter),[14] and γ is the Hill coefficient.

External perception was described by a sigmoid E_{max} model:

$$ExP(t) = E_{max} \times \left(\frac{C_k(t)^{\gamma}}{1 + C_k(t)^{\gamma}}\right) \text{and}$$
$$C_K(t) = \left(\frac{C_R(t)}{C_{50R}}\right) + \left(\frac{C_S(t)}{C_{50S}}\right) \quad (2)$$

where $ExP(t)$ is the experienced level of external perception as rated on a 100-mm visual analog scale at time t, E_{max} is the maximum effect on external perception (100), $C_R(t)$ and $C_S(t)$ are the effect-site concentration of *S*- and *R*-ketamine in nanomoles per milliliter at time t, C_{50R} and C_{50S} are the *R*- and *S*-ketamine effect-site concentration in nanomoles per milliliter needed to reach 50% of E_{max} of external perception, and γ is the Hill coefficient. Since external perception was measured on a 100-mm visual analog scale, ratings could not be more than 100 points.

Since we observed a small discrepancy in the individual model fits for external perception and to a lesser extent for pain pressure threshold during the infusion phase, we postulated that a norketamine effect might be present. We therefore added *S*- and *R*-norketamine as input to the models, based on a receptor kinetics approach, in which *S*- and *R*-norketamine could displace *S*- and *R*-ketamine from the receptor. The consequence of this would be a counteracting effect of *S*- or *R*-norketamine on the effects of *S*- and *R*-ketamine.[15] The effects of *S*- and/or *R*-norketamine were defined as follows:

$$EFF_{NK}(t) = \frac{C_{NK}(t)}{C_{100NK}} \quad (3)$$

where $C_{NK}(t)$ is the *S*- or *R*-norketamine plasma concentration in nanomoles per milliliter, and C_{100NK} is the *S*- or *R*-norketamine effect-site concentration causing a 100% increase in C_{50K}. So, in equations 1 and 2, C_{50R} and C_{50S} were replaced by the following:

$$C_{50KN}(t) = C_{50x} \times [1 + EFF_{NK}(t)] \quad (4)$$

where x is either *S*- or *R*-ketamine and C_{50KN} the plasma ketamine concentration needed to increase the pain pressure threshold by 100% for pressure pain and reach 50%

of E_{max} for external perception considering a counteracting effect of *S*- or *R*-norketamine on the effects of *S*- and *R*-ketamine.

Statistical Analysis

Data analysis was performed using NONMEM version 7.5.0 with *P* values less than 0.01 considered significant. To account for interindividual variability, random effects were included in the model in an exponential relation: $\theta_i = \theta \times \exp(\eta_i)$, where θ_i is the parameter for individual i, θ is the population parameter, and η_i is the random difference between the population and individual parameters, where its variance is the sum of interoccasion (ν^2) and interindividual variability (ω^2). In addition to the $COV step in NONMEM to determine the standard error of the (parameter) estimate, Perl-speaks-NONMEM's log likelihood profiling (llp) utility was used to determine the 95% CI for parameters *S*- and/or *R*-ketamine C_{50}, *S*- and/or *R*-norketamine C_{100}, and $t_{½}k_{e0}$. *P* values less than 0.01 were considered significant.

We did not perform an *a priori* sample size analysis as this was a secondary analysis from existing data. We did earlier perform a sample size analysis based on this data set and calculated an effect size of 20% as clinically relevant and concluded that 17 subjects were necessary to detect a difference between single-treatment arms at $P < 0.05$ and $1 - \beta > 0.80$.[9] This would translate into a 20% difference in C_{50} values between endpoints in the current analysis as a clinically relevant endpoint in our population of 17 subjects. The current data set is larger than the set used for sample size analysis (one arm of the study) and consists of a comparison of endpoints using data derived from two study arms (one treated with *S*-ketamine and the other with racemic ketamine). We therefore assume to have sufficient power to detect a difference in C_{50} values between endpoints.

Results

While all 20 subjects completed the experimental session without serious adverse events, data from three subjects were discarded because these subjects were unable to reliably score the external perception outcome. For the remaining 17 subjects, the mean age ± SD (range) was 23 ± 2 (19 to 28) yr; mean weight, 82 ± 10 (60 to 98) kg; height, 190 ± 6 (175 to 193) cm; and body mass index, 24 ± 2 (20 to 28) kg/m^2.

We tested various pharmacodynamic models, with separate analyses of external perception *versus* pressure pain threshold, and separate analyses of *S*-ketamine *versus* racemic ketamine, and tested whether the parameter values and their interindividual variances could be set at equal values. The objective function values of the models and the 95% CI of the parameter estimates are given in fig. 1 and table 1. They show the large overlap of 95% CI of the parameter estimates when analyzed separately, and the improvement in objective function in the final model that combined the two endpoints and the two formulations into one model. An important observation was that adding *R*-ketamine or its metabolite *R*-norketamine did not cause a significant improvement of any of the models, and these were therefore not incorporated (*i.e.,* values for *R*-ketamine and *R*-norketamine C_{50} were disproportionally high, without a significant decrease in NONMEM's objective function value). Our analyses indicate that the final model is one with similar pharmacodynamic parameter estimates for the two endpoints, irrespective of formulation. Moreover, in the analyses, we tested whether a model that included *S*-norketamine would improve the objective function values. It did so for the final model by 373 points. Finally, for the two endpoints and two formulations, no differences in k_{e0} could be detected.

Plots showing the population predicted pharmacodynamic outcomes and the observed data points for each individual *versus* time are given in fig. 2. Goodness-of-fit plots are given in fig. 3 (observed *vs.* individual predicted; observed *vs.* population predicted; individual weighted residual *vs.* time; normalized prediction discrepancy error *vs.* time; and conditioned weighted residuals *vs.* population predicted) for the two endpoints, and the two formulations; visual predictive checks are given in fig. 4. All indicate that the final model adequately describes the data from both endpoints. Estimated pharmacodynamic parameter estimates are given in table 2 (estimate ± standard error of the estimate): C_{50} *S*-ketamine, 0.51 ± 0.12 nmol/ml; C_{100} *S*-norketamine, 0.34 ± 0.13 nmol/ml; and $t_{½}k_{e0}$, 8.3 ± 3.4 min. Log likelihood profiles (fig. 5) for parameters *S*-ketamine C_{50}, *S*-norketamine C_{100}, and $t_{½}k_{e0}$, showed 95% CI of 0.39 to 0.66 nmol/ml, 0.23 to 0.53 nmol/ml, and 5.1 to 12.6 min, respectively.

Interoccasion variance was not estimable for the baseline of the pressure pain threshold, whereas interindividual variability was not estimable for the remaining parameters. The interindividual and interoccasion variances may not both be identifiable from variable pharmacodynamic (and indeed also often with usually less variable pharmacokinetic) data with a limited number of subjects. Therefore, the total variance may be attributed to the component that has the largest estimation precision, which does not imply that the other component has no variability. Apparently, the interindividual variability of the baseline of the pressure pain threshold had larger estimation precision than its interoccasion variability, and the reverse was true for the remaining parameters.

Discussion

We were unable to detect a difference in the *S*-ketamine and *S*-norketamine pharmacodynamic model parameters (*i.e.,* potency and onset/offset times) for endpoints pain pressure threshold and changes in external perception, as

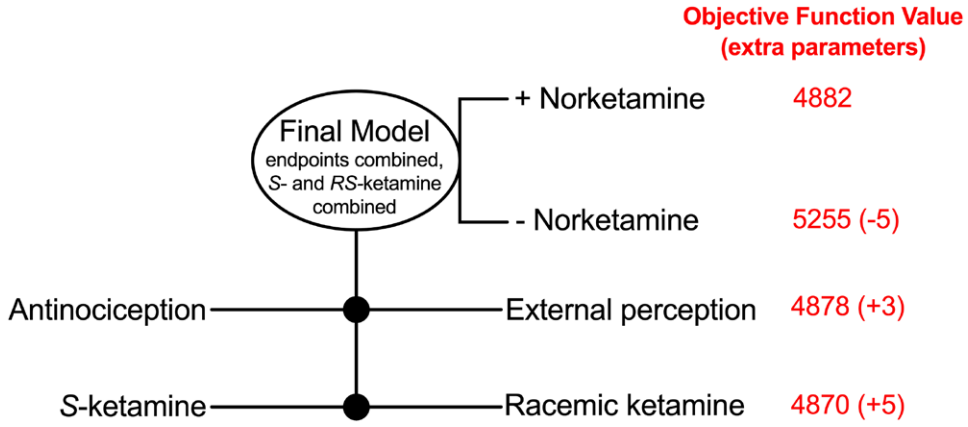

Fig. 1. Objective function values of the different models used to model the effect of *S*-ketamine and/or racemic ketamine on pain pressure threshold and/or external perception. The objective function values are given with the additional model parameters for each step in brackets.

Table 1. 95% Confidence Intervals

		Models with the Two Endpoints Analyzed Separately		Models with the Two Administration Forms Analyzed Separately	
	Final Model	Pain Pressure Threshold	External Perception	*S*-ketamine	Racemic Ketamine
C_{50S} ketamine, nmol/ml	0.38–0.66	0.40–0.81	0.34–0.58	0.35–0.76	0.35–0.60
C_{100S} norketamine, nmol/ml	0.23–0.53	0.21–0.63	0.22–0.49	0.18–0.52	0.22–0.55
$t_{½}k_{e0}$, min	5.1–13.0	5.0–16.0	5.0–13.0	4.0–17.0	4.6–13.0

R-ketamine did not contribute to the pain pressure response or to external perception.

C_{50S} ketamine, *S*-ketamine concentrations causing a 100% increase in pain pressure threshold or causing half-maximum effect in external perception; C_{100S} norketamine, *S*-norketamine concentration causing a 100% increase in C_{50} of *S*-ketamine; $t_{½}k_{e0}$, blood-effect compartment equilibrium half-life for both ketamine and norketamine.

a measure of ketamine dissociation, irrespective of administered formulation (*S*-ketamine or racemic ketamine). Additionally, we observed that *R*-ketamine did not contribute to the measured effects after racemic ketamine administration. Since our results disagree with earlier findings,[8,9] it is important to discuss in detail the different items of our protocol that yielded the current results.

Pain Test

We used a manual pressure pain device to detect the pain pressure threshold. Testing was done by a single experienced researcher who displayed a high reproducibility in obtaining the pain threshold response. Still, it may well be that different pain tests give different results with significant differences in pharmacodynamics. For example, in a previous study, we tested the effect of the opioid alfentanil on noxious electrical and thermal stimuli, and while the potency parameter was similar between tests, the value of the onset/offset parameter, $t½k_{e0}$, differed significantly between tests.[16] We argued at the time that this indicates that the two tests are comparably potent under steady-state conditions but differ in their behavior under dynamic conditions. These differences in dynamic conditions were related to different neuronal circuits activated by the two tests. Hence, the outcome of the study may have been influenced by the choice of pain assay. This not only relates to our study but is equally relevant to other studies. Studying pain relief in chronic (neuropathic) pain patients may overcome this issue. Note further that cold pressor pain and cuff pain require many minutes to complete, which may affect the values of k_{e0} and C_{50}. Pressure pain (and also thermal and electrical pain) require a few seconds to complete.

Dissociation

Dissociation was measured by the external perception questions of the Bowdle questionnaire.[12] This questionnaire was developed in 1998 as a psychologic inventory (a hallucinogen rating scale) to quantify ketamine-induced psychedelic symptoms in volunteers and has been used in multiple studies on the effect of various psychedelics on dissociative

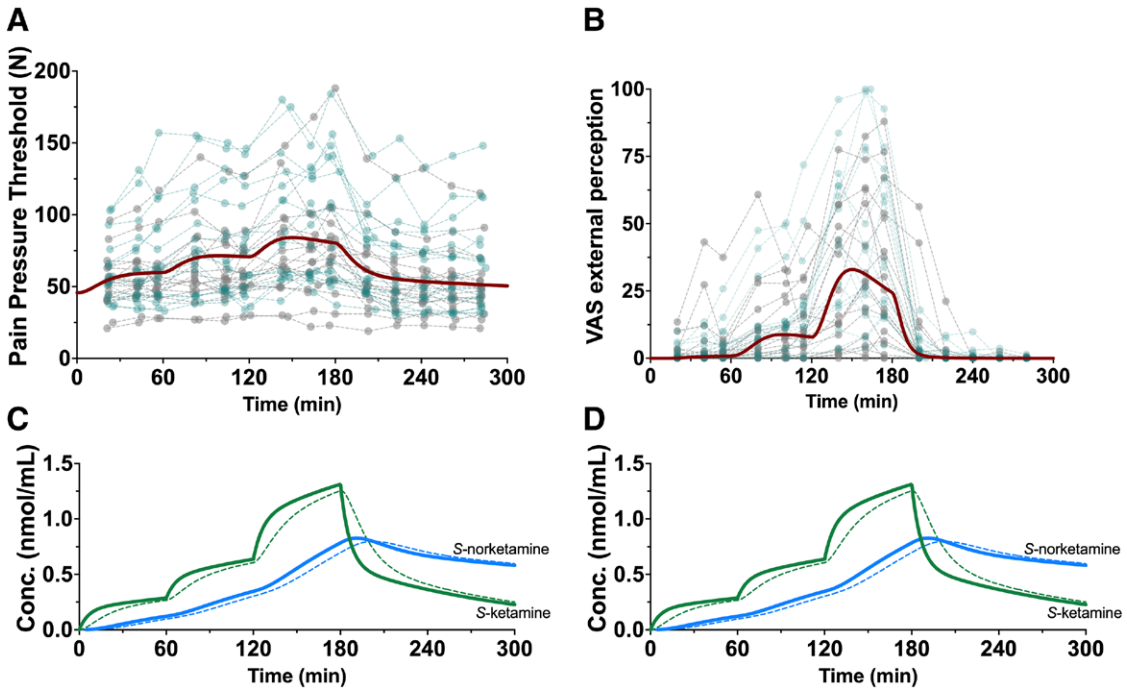

Fig. 2. Plots showing the population predicted pharmacodynamic outcomes (*red lines*) and the observed data points for each individual *versus* time (*gray dots* for *S*-ketamine, *green dots* for racemic ketamine formulations). (*A*) Plot showing pressure pain data and population predicted values and (*B*) plot showing external perception data and population predicted values. *C* and *D* show the *S*-ketamine (*green line*) and *S*-norketamine (*blue line*) plasma concentration–time profiles and corresponding estimated effect-site concentrations (*broken green line* for *S*-ketamine and *broken blue line* for *S*-norketamine). VAS, visual analog scale.

symptoms. Apart from external perception, the questionnaire encompasses internal perception and drug high. To test the internal validity of our results, we additionally tested these other two measures of dissociation with similar results as with external perception (data not shown). This indicates that our approach yielded a reliable effect–response relationship. Still, we cannot exclude that other measures of dissociation or other forms of parametrization might have given different results.

Participants

In our study, healthy male volunteers were included. We restricted ourselves to a single sex to reduce variability from possible sex differences. Sex differences have been observed in ketamine pharmacokinetics and pharmacodynamics.[16,17] For example, Morgan *et al.*[17] showed a greater decrease in cognitive performance in men compared with women after ketamine administration. Further studies are needed to determine the connectivity of ketamine endpoints in mixed populations to determine a possible difference between the sexes. Additionally, it may well be that a model with better applicability than the healthy and young volunteer is the patient (of either sex) with acute or chronic pain. Ketamine behavior as an analgesic (*i.e.*, reducing existing pain) may well be different from its behavior as an antinociceptive agent (*i.e.*, by subduing an experimentally induced pain response) due to differences in activated pain circuits in brain and spinal cord from these two distinct stimuli.

Pharmacodynamic Modeling

We successfully modeled the two endpoints simultaneously in our pharmacodynamic analysis. An interesting observation in our data is that pressure pain threshold and external perception tended to decrease before the ketamine infusion ended (fig. 2). We reasoned that this might be related to the slow but steady increase in concentration of one of ketamine's metabolites. Addition of a norketamine component to the model improved the data fits significantly. This agrees with earlier findings in which norketamine had an antagonistic effect on ketamine-induced pain relief and neurocognitive impairment.[15] Whether this is related to the adaptation of the pain system (which we cannot test as we did not include a placebo arm), due the competition for binding locations on the *N*-methyl-D-aspartate receptor and assuming that norketamine has no inherent efficacy at the receptor, or is related to an effect of norketamine at other receptor

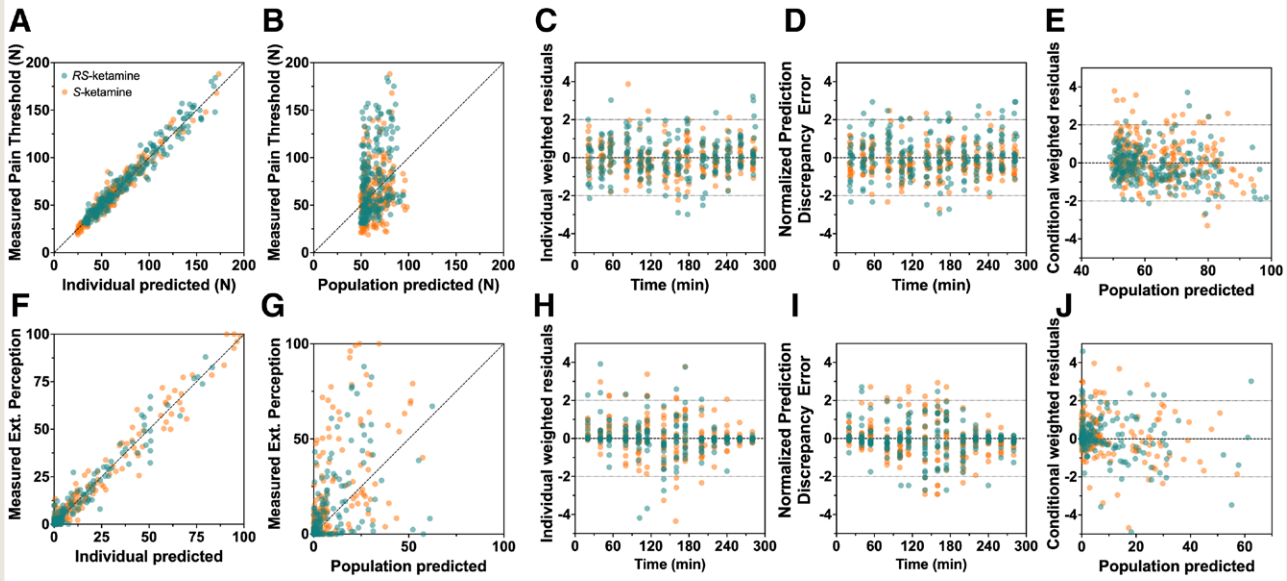

Fig. 3. Goodness-of-fit plots for the population pharmacodynamic model: pain pressure threshold (*A* to *E*) and external perception (*F* to *J*). (*A*) Observed *versus* individual predicted. (*B*) Observed pain pressure threshold *versus* population predicted pain pressure threshold. (*C*) Individual weighted residual *versus* time. (*D*) Normalized prediction discrepancy error *versus* time. (*E*) Conditioned weighted residuals *versus* population predicted. (*F*) Observed *versus* individual predicted. (*G*) Observed *versus* population predicted. (*H*) Individual weighted residual *versus* time. (*I*) Normalized prediction discrepancy error *versus* time. (*J*) Conditioned weighted residuals *versus* population predicted.

systems, remains unknown. The former hypothesis stands in contrast with studies in rodents showing that norketamine has analgesic properties.[18]

We detected no differences between endpoints with respect to potency parameter C_{50}. This indicates that the pain relief and external perception behaved similarly in the steady state. Parameterization of the pharmacodynamic models with distinct C_{50} values for pain pressure threshold and external perception gave similar results (table 1). The values of ketamine C_{50} depend on the parametrization of the pharmacodynamic models. Apparently, the C_{50} for external perception matches the C_{50} for antinociception, considering the fact that the power function of pain pressure threshold is an inverse sigmoid.[14] Additionally, the dynamic properties of the pain pressure threshold and external perception responses were similar with the need for only one

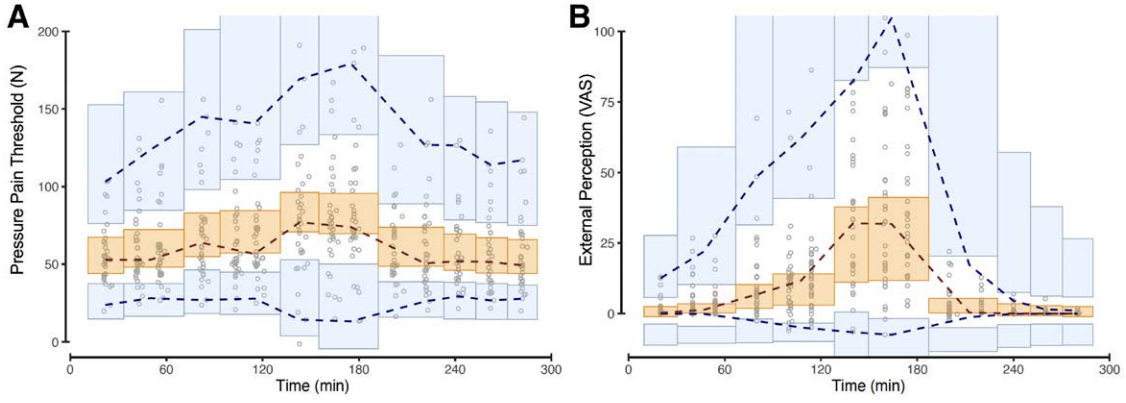

Fig. 4. Visual predictive checks for the pressure pain threshold (*A*) and external perception (*B*) data. The middle *dotted line* represents the 50th percentile of the observed data. The upper and lower *broken lines* show the 5th and 95th percentiles of the observed data, respectively. The 95% CI of the 50th percentile of the simulated data is given by the *orange shaded area*. The upper and lower *gray/blue shaded areas* represent the 95% CI of the 5th and 95th percentile of the simulated data. VAS, visual analog scale.

Table 2. Population Pharmacodynamic Parameter Values of the Final Pharmacokinetic–Pharmacodynamic Model

	Typical Parameter Value ± Standard Error of the Estimate	Interoccasion Variances (v^2) ± Standard Error of the Estimate	Interindividual Variances (ω^2) ± Standard Error of the Estimate
Baseline pressure pain threshold, N	45.7 ± 4.2	—	0.18 ± 0.05
E_{MAX} external perception, mm	100 (FIXED)*	0.44 ± 0.32	—
Shape parameter (GAMMA) pain threshold	1.31 ± 0.41	0.28 ± 0.12	—
Shape parameter (GAMMA) external perception	5.33 ± 1.23	—	—
C_{50S} ketamine, nmol/ml	0.51 ± 0.12	0.16 ± 0.09	—
C_{100S} norketamine, nmol/ml	0.34 ± 0.13	0.37 ± 0.29	—
$t_{½}k_{e0}$, min	8.3 ± 3.4	0.39 ± 0.16	—
Additive error pressure pain threshold (σ^2), N^2	54 ± 10.1		
Additive error external perception (σ^2), mm^2	19.2 ± 5.1		

*Parameter fixed to 100. —Dash indicates parameters not included in the statistical model

C_{50S} ketamine, *S*-ketamine concentrations causing a 100% increase in pain pressure threshold or causing half-maximum effect in external perception; C_{100S} norketamine, *S*-norketamine concentration causing a 100% increase in C_{50S} of ketamine; E_{MAX}, external perception is the maximum possible effect of external perception; $t_{½}k_{e0}$, blood-effect compartment equilibrium half-life for both ketamine and norketamine.

parameter for the equilibration between plasma and postulated effect-site concentration (k_{e0}); a model without effect compartment was inferior to the model with just one k_{e0}. Since ketamine displays rapid receptor kinetics,[19] the hysteresis in response is best explained by the transfer of ketamine from plasma to its sites of action within the central nervous system and neuronal dynamics.

We did not detect a contributing effect of the *R*-ketamine isomer to either pain relief or dissociation. An absence of an *R*-ketamine effect was observed for cardiac output and further agrees with earlier observations.[11] For example, at anesthetic doses, blood pressure effects of *S*-ketamine exceed those of racemic ketamine,[20] and *S*-ketamine produces a greater reduction of the electroencephalogram power spectrum compared to either *R*- or racemic ketamine.[21] At subanesthetic doses, the analgesic *S*-ketamine:racemic ketamine potency is about 2,[9] indicative of a lack of efficacy of *R*-ketamine in producing pain relief. These data contrast with the observation that particularly *R*-ketamine produces potent antidepression, at least in animal models.[22,23]

Comparison with the Literature

We reasoned that similar values for potency (C_{50} and C_{100}) and $t_{1/2}k_{e0}$ indicate a close, possibly even mechanistic, connectivity between endpoints, in agreement with earlier statements that ketamine analgesia is intricately bound to its dissociative effects.[3] Still, this reasoning stands in contrast to earlier observations from Gitlin *et al.*,[8] Hahm *et al.*,[24] and Jonkman *et al.*[9]

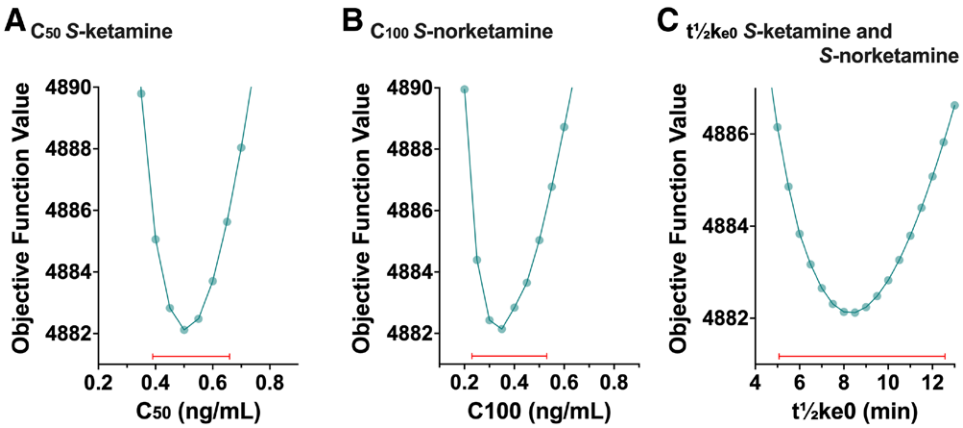

Fig. 5. Log likelihood profiles for C_{50} *S*-ketamine (*A*), C_{100} *S*-norketamine (*B*), and $t_{1/2}k_{e0}$ (*C*) parameters. The *red line* shows the final parameter 95% CI as determined by Perl speaks NONMEM, "llp" utility. C_{50} *S*-ketamine, estimated *S*-ketamine effect-site concentration needed to increase the pain pressure threshold by 100%; C_{100} *S*-norketamine, effect-site *S*-norketamine concentration causing a 100% increase in C_{50} *S*-ketamine; $t_{1/2}k_{e0}$, *S*-ketamine and *S*-norketamine blood-effect site equilibration half-life.

Gitlin *et al.*[8] and Hahm *et al.*[24] used a statistical approach to show that racemic ketamine analgesic and dissociative effects are not correlated. They studied racemic ketamine effect with and without one bolus dose of midazolam and with and without sevoflurane anesthesia, and state that ketamine's analgesic effects are not *exclusively* caused by dissociation. However, in contrast to our study, Gitlin *et al.*[8] and Hahm *et al.*[24] used supra-analgesic doses of intravenous racemic ketamine (140 mg in their average 70-kg subject) far greater than the advocated dose for analgesia. Additionally, they did not measure plasma ketamine or norketamine concentrations and therefore were not aware of the pharmacokinetic–pharmacodynamic relationship under control conditions or conditions in which racemic ketamine was combined with either midazolam or sevoflurane. Both pharmacokinetic and pharmacodynamic interactions may have influenced the outcome of the studies of Gitlin *et al.*[8] and Hahm *et al.*[24] Furthermore, in contrast to our approach with mechanistic and data-rich analyses, Gitlin *et al.*[8] analyzed their data using a time-squared function (parabola), which has no mechanistic meaning. Finally, to attenuate dissociation, they gave 2 mg midazolam, which is insufficient to tame the dissociation from 140 mg ketamine. We argue that a better approach would have been to administer a continuous midazolam infusion rather than one low-dose midazolam bolus.

Jonkman *et al.*[9] studied NO donation during *S*-ketamine and racemic ketamine infusion and concluded that NO depletion after blockade of the *N*-methyl-D-aspartate receptor is associated with the psychedelic effects induced by ketamine. The theory behind this observation is that reduced intraneural levels of NO lead to reduction in neuroprotection, neuroplasticity, and neurotrophic conditions. Adding NO restores these protective effects and ameliorates psychedelic experience. Interestingly, NO donation had an effect on racemic ketamine, but not *S*-ketamine–induced psychedelic effect. This suggests that *S*-ketamine induces its psychedelic effect *via* a NO-independent pathway.

Limitations and Future Perspectives

We have discussed the different components of our study that may have influenced the outcome of our study. One important further limitation is that, while this was a planned secondary analysis, the initial setup of the study was not aimed at finding a difference in the pharmacodynamics between endpoints. Hence, further studies are needed to definitely determine the link between dissociation and pain relief, and possibly also other outcomes such as antidepression induced by ketamine. It is possible that functional magnetic resonance imaging studies may provide more definitive answers.

Conclusions

Intuitively, a dissociation between the thalamus and limbic system, resulting from the dissociative state induced by ketamine, seems mechanistically well able to subdue the perception of pain and increase satisfaction with pain relief. We tested this assumption by performing a secondary preplanned analysis of an information-rich data set and compared the pharmacodynamics of two ketamine endpoints: antinociception and changes in the perception of external stimuli using state-of-the-art modeling analyses in NONMEM. We conclude that our data support an association or connectivity between ketamine analgesia and dissociation. Further studies are needed to definitely detect functional connectivity and possibly even dependency between brain areas that produce the different ketamine effects.

Research Support

Support was provided from institutional and/or departmental sources. This work is part of the TAPTOE (Tackling and Preventing the Opioid Epidemic) research project. This research received funding from the Dutch Research Council (The Hague, The Netherlands) in the framework of the NWA-ORC (Netherlands Science Agenda - Research On Routes by Consortia) Call (NWA.1160.18.300).

Competing Interests

The Anesthesia and Pain Research Unit of the Department of Anesthesiology, Leiden University Medical Center (Leiden, The Netherlands), received/receives funding from AMO Pharma Ltd. (Leeds, United Kingdom), Bedrocan BV (Veendam, The Netherlands), Grünenthal GmbH (Aachen, Germany), Medasense Biometrics Ltd. (Ramat Gan, Israel), Medtronic (Minneapolis, Minnesota), MSD Nederland BV (Haarlem, The Netherlands), LTS Lohmann Therapie Systeme AG (Andernach, Germany), and Trevena Inc. (Chesterbrook, Pennsylvania). Dr. Dahan received consultancy and/or speaker fees from Enalare Therapeutics Inc. (Princeton, New Jersey), Grünenthal BV (Woerden, The Netherlands), Medasense Biometrics Ltd. (Ramat Gan, Israel), Trevena Inc., and MSD Nederland BV and received grants/awards from ZonMW (The Hague, The Netherlands) and the U.S. Food and Drug Administration (Silver Spring, Maryland).

Reproducible Science

Full protocol available at: a.dahan@lumc.nl. Raw data available at: a.dahan@lumc.nl.

Correspondence

Address correspondence to: Dr. Albert Dahan, Department of Anesthesiology, Anesthesia and Pain Research Unit, Leiden University Medical Center, H5-022, 2300 RC Leiden, The Netherlands. a.dahan@lumc.nl.

References

1. Kamp J, Van Velzen M, Olofsen E, Boon M, Dahan A, Niesters M: Pharmacokinetic and pharmacodynamic considerations for NMDA-receptor antagonist ketamine in the treatment of chronic neuropathic pain: An update of the most recent literature. Expert Opin Drug Metab Toxicol 2019; 15:1033–41
2. Niesters M, Dahan A: Pharmacokinetic and pharmacodynamic considerations for NMDA receptor antagonists in the treatment of chronic neuropathic pain. Expert Opin Drug Metab Toxicol 2012; 8:1409–17
3. Schwenk ES, Viscusi ER, Buvanendran A, Hurley RW, Wasan AD, Narouze S, Bhatia A, Davis FN, Hooten WM, Cohen SP: Consensus guidelines on the use of intravenous ketamine infusions for acute pain management from the American Society of Regional Anesthesia and Pain Medicine, the American Academy of Pain Medicine, and the American Society of Anesthesiologists. Reg Anesth Pain Med 2018; 43:456–66
4. Oye I, Paulsen O, Maurset A: Effects of ketamine on sensory perception: Evidence for a role of N-methyl-D-aspartate receptors. J Pharmacol Exp Ther 1992; 260:1209–13
5. Brown EN, Purdon PL, Van Dort CJ: General anesthesia and altered states of arousal: A systems neuroscience analysis. Annu Rev Neurosci 2011; 34:601–28
6. Hebb DO: Organization of Behavior: A Neuropsychological Theory. New York, Wiley and Sons, 1949.
7. Huettel SA, Song AW, McCarthy G: Chapter 11 in Functional Magnetic Resonance Imaging, 3rd edition. Sunderland, Massachusetts, Sinnauer Associates, Inc, 2014, pp 416–7
8. Gitlin J, Chamadia S, Locascio JJ, Ethridge BR, Pedemonte JC, Hahm EY, Ibala R, Mekonnen J, Colon KM, Qu J, Akeju O: Dissociative and analgesic properties of ketamine are independent. Anesthesiology 2020; 133:1021–8
9. Jonkman K, van der Schrier R, van Velzen M, Aarts L, Olofsen E, Sarton E, Niesters M, Dahan A: Differential role of nitric oxide in the psychedelic symptoms induced by racemic ketamine and esketamine in human volunteers. Br J Anaesth 2018; 120:1009–18
10. Kamp J, Jonkman K, van Velzen M, Aarts L, Niesters M, Dahan A, Olofsen E: Pharmacokinetics of ketamine and its major metabolites norketamine, hydroxynorketamine and dehydronorketamine: A model-based analysis. Br J Ananesth 2020; 125: 750–61
11. Kamp J, van Velzen M, Aarts L, Niesters M, Dahan A, Olofsen E: Stereoselective ketamine effect on cardiac output: A population pharmacokinetic/pharmacodynamic modelling study in healthy volunteers. Br J Anaesth 2021; 127:23–31
12. Bowdle TA, Radant AD, Cowley DS, Kharasch ED, Strassman RJ, Roy-Byrne PP: Psychedelic effects of ketamine in healthy volunteers: Relationship to steady-state plasma concentrations. Anesthesiology 1998; 88:82–8
13. Rao LK, Flaker AM, Friedel CC, Kharasch ED: Role of cytochrome P4502B6 polymorphisms in ketamine metabolism and clearance. Anesthesiology 2016; 125:1103–12
14. Sarton E, Olofsen E, Romberg R, den Hartigh J, Kest B, Nieuwenhuijs D, Burm A, Teppema L, Dahan A: Sex differences in morphine analgesia: An experimental study in healthy volunteers. Anesthesiology 2000; 93:1245–54; discussion 6A
15. Olofsen E, Noppers I, Niesters M, Kharasch E, Aarts L, Sarton E, Dahan A: Estimation of the contribution of norketamine to ketamine-induced acute pain relief and neurocognitive impairment in healthy volunteers. Anesthesiology 2012; 117:353–64
16. Sigtermans M, Dahan A, Mooren R, Bauer M, Kest B, Sarton E, Olofsen E: S(+)-ketamine effect on experimental pain and cardiac output: A population pharmacokinetic-pharmacodynamic modeling study in healthy volunteers. Anesthesiology 2009; 111:892–903
17. Morgan CJA, Perry EB, Cho H-S, Krystal JH, D'Souza DC: Greater vulnerability to the amnesic effects of ketamine in males. Pyschopharmacol 2006; 187: 405–14
18. Holtman JR, Crooks PA, Johnson-Hardy JK, Hojomat M, Kleven M, Wala EP: Effect of norketamine enantiomers in rodent models of persistent pain. Pharm Biochem Behav 2008; 90: 676–85
19. Shaffer CL, Osgood SM, Smith DL, Liu J, Trapa PE: Enhancing ketamine translational pharmacology via receptor occupancy normalization. Neuropharmacology 2014; 86:174–80
20. Geisslinger G, Hering W, Thomann P, Knoll R, Kamp HD, Brune K: Pharmacokinetics and pharmacodynamics of ketamine enantiomers in surgical patients using a stereoselective analytical method. Br J Anaesth 1993; 70:666–71
21. Schüttler J, Stanski DR, White PF, Trevor AJ, Horai Y, Verotta D, Sheiner LB: Pharmacodynamic modeling of the EEG effects of ketamine and its enantiomers in man. J Pharmacokinet Biopharm 1987; 15:241–53
22. Hashimoto K: Molecular mechanisms of the rapid-acting and long-lasting antidepressant actions of (R)-ketamine. Biochem Pharmacol 2020; 177:113935
23. Zanos P, Highland JN, Liu X, Troppoli TA, Georgiou P, Lovett J, Morris PJ, Stewart BW, Thomas CJ, Thompson SM, Moaddel R, Gould TD: (R)-Ketamine exerts antidepressant actions partly via conversion to (2R,6R)-hydroxynorketamine, while causing adverse effects at sub-anaesthetic doses. Br J Pharmacol 2019; 176:2573–92
24. Hahm EY, Chamadia S, Locascio JJ, Pedemonte JC, Gitlin J, Mekonnen J, Ibala R, Ethridge BR, Colon KM, Qu J, Akeju O: Dissociative and analgesic properties of ketamine are independent and unaltered by sevoflurane general anesthesia. Pain Rep 2021; 6:e936

ANESTHESIOLOGY

Slick Potassium Channels Control Pain and Itch in Distinct Populations of Sensory and Spinal Neurons in Mice

Cathrin Flauaus, R.Ph., Patrick Engel, R.Ph., Fangyuan Zhou, M.S., Jonas Petersen, Ph.D., Peter Ruth, Ph.D., Robert Lukowski, Ph.D., Achim Schmidtko, M.D., Ph.D., Ruirui Lu, M.D., Ph.D.

Anesthesiology 2022; 136:802–22

EDITOR'S PERSPECTIVE

What We Already Know about This Topic

- The activity of sensory and dorsal horn neurons controls the sensations of pain and itch
- The recently identified potassium ion channel Slick is expressed on sensory and spinal neurons, but its functional roles are poorly understood

What This Article Tells Us That Is New

- Using male and female mouse models, it was observed that Slick reduces responses to noxious thermal and chemical stimulation
- Conversely, Slick expressed on spinal interneurons facilitates somatostatin-induced itch
- Analgesics targeting Slick channels may decrease pain but could increase itching if they reach the central nervous system

ABSTRACT

Background: Slick, a sodium-activated potassium channel, has been recently identified in somatosensory pathways, but its functional role is poorly understood. The authors of this study hypothesized that Slick is involved in processing sensations of pain and itch.

Methods: Immunostaining, *in situ* hybridization, Western blot, and real-time quantitative reverse transcription polymerase chain reaction were used to investigate the expression of Slick in dorsal root ganglia and the spinal cord. Mice lacking Slick globally (Slick$^{-/-}$) or conditionally in neurons of the spinal dorsal horn (Lbx1-Slick$^{-/-}$) were assessed in behavioral models.

Results: The authors found Slick to be enriched in nociceptive Aδ-fibers and in populations of interneurons in the spinal dorsal horn. Slick$^{-/-}$ mice, but not Lbx1-Slick$^{-/-}$ mice, showed enhanced responses to noxious heat in the hot plate and tail-immersion tests. Both Slick$^{-/-}$ and Lbx1-Slick$^{-/-}$ mice demonstrated prolonged paw licking after capsaicin injection (mean ± SD, 45.6 ± 30.1 s [95% CI, 19.8 to 71.4]; and 13.1 ± 16.1 s [95% CI, 1.8 to 28.0]; $P = 0.006$ [Slick$^{-/-}$ {n = 8} and wild-type {n = 7}, respectively]), which was paralleled by increased phosphorylation of the neuronal activity marker extracellular signal–regulated kinase in the spinal cord. In the spinal dorsal horn, Slick is colocalized with somatostatin receptor 2 (SSTR2), and intrathecal preadministration of the SSTR2 antagonist CYN-154806 prevented increased capsaicin-induced licking in Slick$^{-/-}$ and Lbx1-Slick$^{-/-}$ mice. Moreover, scratching after intrathecal delivery of the somatostatin analog octreotide was considerably reduced in Slick$^{-/-}$ and Lbx1-Slick$^{-/-}$ mice (Slick$^{-/-}$ [n = 8]: 6.1 ± 6.7 bouts [95% CI, 0.6 to 11.7]; wild-type [n =8]: 47.4 ± 51.1 bouts [95% CI, 4.8 to 90.2]; $P = 0.039$).

Conclusions: Slick expressed in a subset of sensory neurons modulates heat-induced pain, while Slick expressed in spinal cord interneurons inhibits capsaicin-induced pain but facilitates somatostatin-induced itch.

(ANESTHESIOLOGY 2022; 136:802–22)

Nociceptive pain serves as an important protective mechanism for drawing attention to potentially injured tissue. It results from the stimulation of nociceptors: sensory neurons with thinly myelinated Aδ-fibers and unmyelinated C-fibers that terminate in the skin or deep tissues. When encountering an acute noxious stimulus (*e.g.,* heat, cold, pressure, chemical stimulation), several ion channels in nociceptors are activated, leading to neuronal depolarization. The information is then transmitted through dorsal root ganglia or trigeminal ganglia into the

Supplemental Digital Content is available for this article. Direct URL citations appear in the printed text and are available in both the HTML and PDF versions of this article. Links to the digital files are provided in the HTML text of this article on the Journal's Web site (www.anesthesiology.org). This article has a visual abstract available in the online version.

Submitted for publication August 22, 2021. Accepted for publication January 31, 2022. Published online first on March 18, 2022.

Cathrin Flauaus, R.Ph.: Institute of Pharmacology and Clinical Pharmacy, Goethe University Frankfurt, Frankfurt am Main, Germany.

Patrick Engel, R.Ph.: Institute of Pharmacology and Clinical Pharmacy, Goethe University Frankfurt, Frankfurt am Main, Germany.

Fangyuan Zhou, M.S.: Institute of Pharmacology and Clinical Pharmacy, Goethe University Frankfurt, Frankfurt am Main, Germany.

Jonas Petersen, Ph.D.: Institute of Pharmacology and Clinical Pharmacy, Goethe University Frankfurt, Frankfurt am Main, Germany.

Peter Ruth, Ph.D.: Department of Pharmacology, Toxicology and Clinical Pharmacy, Institute of Pharmacy, University of Tuebingen, Tuebingen, Germany.

Robert Lukowski, Ph.D.: Department of Pharmacology, Toxicology and Clinical Pharmacy, Institute of Pharmacy, University of Tuebingen, Tuebingen, Germany.

Achim Schmidtko, M.D., Ph.D.: Institute of Pharmacology and Clinical Pharmacy, Goethe University Frankfurt, Frankfurt am Main, Germany.

Ruirui Lu, M.D., Ph.D.: Institute of Pharmacology and Clinical Pharmacy, Goethe University Frankfurt, Frankfurt am Main, Germany.

 Anesthesiology 2022; 136:802–22. DOI: 10.1097/ALN.0000000000004163

dorsal horn of the spinal cord and the brainstem, where the central terminals of nociceptors synapse with intrinsic second-order projection neurons and interneurons. Then the information is conveyed to higher centers in the brain, ultimately resulting in the perception of pain.[1] Similar to pain, itch is also encoded by distinct neurons in both the peripheral and central nervous systems, and the interaction between pain and itch is widely distributed along somatosensory pathways.[2]

Research in the past few decades has revealed that different stimuli are decoded by different subsets of sensory neurons with distinct receptors and ion channels.[3] Potassium channels are emerging targets for understanding this process and developing novel treatments. In general, potassium channels are the most populous and diverse class of neuronal ion channels that are governed by nearly 80 genes in humans.[4] Recently, two distinct potassium channels, both regulated by cytosolic sodium, have attracted significant interest as regulators of pain and itch: Slack (sequence like a Ca^{2+}-activated potassium channel, also termed $K_{Na}1.1$, *Kcnt1*, or *Slo2.2*) and Slick (sequence like an intermediate conductance potassium channel, also termed $K_{Na}1.2$, *Kcnt2*, or *Slo2.1*).[5–8] Slack, which is highly expressed in nonpeptidergic nociceptors, plays an important role in the processing of neuropathic pain and itching, but it seems to have a limited contribution to nociceptive pain sensing.[5,6] Slick has been detected in various regions of the nervous system and in nonneuronal tissues such as the heart, smooth muscle, and pancreatic duct epithelial cells.[6–9] In a previous study addressing the role of Slick in processing pain, Slick immunoreactivity was detected in a population of peptidergic sensory neurons, and Slick knockout mice lacking exons 2 to 7 of the *Kcnt2* gene demonstrated increased sensitivity to noxious heat.[7] Interestingly, a subsequent single-cell RNA-sequencing study detected Slick in dorsal horn neurons and suggested that Slick together with other markers defines 4 of the 15 identified populations of inhibitory interneurons in the dorsal horn.[10] Based on this distribution pattern, we hypothesized that Slick might exert additional functions in somatosensory processing.

Here, we aimed to further characterize the role of Slick in pain and itch processing. We thoroughly assessed the cellular distribution of Slick in neuronal subpopulations in dorsal root ganglia and the spinal dorsal horn by immunostaining and *in situ* hybridization, and we analyzed the pain and itch behavior of global and tissue-specific knockout lines lacking exon 22 of the *Kcnt2* gene.

Materials and Methods

In response to peer review, several experiments were added, including the allyl isothiocyanate test, itch behavior induced by intrathecal injection of 300 ng octreotide, and itch behavior induced by intradermal injection of histamine and chloroquine.

Animals

To generate global Slick knockouts (referred to as $Slick^{-/-}$), Slick floxed ($Slick^{fl/fl}$) mice bearing loxP sites flanking exon 22 of the *Kcnt2* gene (B6(129S4)-*Kcnt2*$^{tm1.1Clin}$/J, JAX stock No. 028419; The Jackson Laboratory, USA)[6] were crossed with cytomegalovirus (CMV)-Cre mice (B6.C-Tg(CMV-cre)1Cgn/J, JAX stock No. 006054, The Jackson Laboratory)[11] and backcrossed with C57BL/6N mice to eliminate the Cre recombinase. Wild-type and $Slick^{-/-}$ mice were obtained from heterozygous breeding. To ablate Slick selectively in dorsal horn neurons, $Slick^{fl/fl}$ mice were crossed with Lbx1-Cre mice[12] to obtain homozygous conditional Slick knockouts (referred to as Lbx1-$Slick^{-/-}$) and control ($Slick^{fl/fl}$) mice. Mice were genotyped by polymerase chain reaction using primer pairs for Kcnt2 (forward: 5′-aactttatgagttcctcttccatg-3′; reverse: 5′-gagcatcatactttgctttttggg-3′; Biomers, Germany) with standard thermocycler amplification conditions using polymerase chain reaction RedMastermix (Genaxxon bioscience, Germany) and an annealing temperature of 60°C. Resulting amplicons were 579 bp for wild-type and 269 bp for $Slick^{-/-}$,[6] and predicted amplicons were 694 bp for Slick-floxed alleles. In addition, Sprague-Dawley rats (Charles River, Germany) were used for immunostaining.

All animals were housed on a 12/12 light/dark cycle with free access to food and water *ad libitum*. Experiments were performed in animals of either sex, but sex had no significant effects in any assay. The total numbers used for each experiment are listed in the Materials and Methods and Results sections, as well as in figure legends, and the numbers of male and female mice are listed in the Materials and Methods. All mice weighed 20 ± 4 g and were a mean age of 12 weeks at the begin of the experiments. Animals were numbered, randomly assigned to different experimental groups according to the experimental strategy, and tested in sequential order. All behavioral tests and anatomical studies, including quantification, were performed by investigators who were blinded to the genotype of the animals. All experiments adhered to the guidelines of the International Association for the Study of Pain, Animal Research: Reporting In Vivo Experiments, and the 3Rs Principles, and were approved by our local Ethics Committee for Animal Research (Regierungspräsidium Darmstadt, Germany).

Real-time Reverse Transcription Polymerase Chain Reaction

Lumbar (L1–L6) dorsal root ganglia, lumbar (L3–L5) spinal cord, and prefrontal cortex of mice ($Slick^{-/-}$: n = 3 [2 females and 1 male]; wild-type: n = 3 [2 females and 1 male]; Lbx1-$Slick^{-/-}$: n = 4 [2 females and 2 males]; control: n = 4 [2 females and 2 males]) were rapidly dissected, snap-frozen in liquid nitrogen, and stored at −80°C until use. Total RNA from spinal cord and cortex was extracted using TRIzol reagent (No. 15596026; Thermo Fisher Scientific,

Germany) or QIAzol lysis reagent (No. 79306; Qiagen, The Netherlands) and chloroform in combination with the RNeasy Mini Kit (No. 74104; Qiagen, The Netherlands) according to the manufacturer's recommendations. Total RNA from dorsal root ganglia was isolated using the innuPREP Micro RNA Kit (No. C-6134; Analytik Jena, Germany) following the manufacturer's instructions.

Isolated RNA was quantified with a NanoDrop 2000 (Thermo Fisher Scientific), and cDNA was synthesized from 200 ng using the first strand cDNA synthesis kit (No. 10774691; Thermo Fisher Scientific) with random hexamer primer. Quantitative real-time reverse transcription polymerase chain reaction was performed on a CFX96 Touch Real-Time System (Bio-Rad, Germany) using the iTaq Universal SYBR Green SuperMix (No. 1725120; Bio-Rad) and primer pairs for Kcnt2 (forward: 5′-gaaagcaccatgagtgcaga-3′, reverse: 5′-gttttgaaagcgcgagagag-3′), Kcnt1 (forward: 5′-ctgctgtgcctggtcttca-3′, reverse: 5′-aaggaggtcagcaggttcaa-3′) and glyceraldehyde 3-phosphate dehydrogenase (forward: 5′-caatgtgtccgtcgtggatct-3′, reverse: 5′-gtcctcagtgtagcccaagatg-3′; all from Biomers, Germany). Reactions were performed in duplicate or triplicate by incubating for 2 min at 50°C and 10 min at 95°C, followed by 40 15-s cycles at 95°C and 60 s at 60°C. Water and template controls were included to ensure specificity. Relative expression of target gene levels was determined using the comparative $2^{-\Delta\Delta Ct}$ method and normalized to glyceraldehyde 3-phosphate dehydrogenase.

Western Blots

For Slick detection, lumbar (L1–L5) dorsal root ganglia and lumbar (L1–L5) spinal cord of Slick$^{-/-}$ and wild-type mice (n = 3 males per group) were rapidly dissected, frozen in liquid nitrogen, and stored at −80°C until use. Lysates were prepared with buffer containing 0.32 M sucrose, 0.1 M NaF, 5 mM sodium phosphate buffer (pH, 7.4 [protocol from University of California–Davis/National Institutes of Health NeuroMab Facility, USA]) mixed with a protease inhibitor cocktail (Complete Mini, No. 4693132001; Roche Diagnostics, Germany). For phosphorylated extracellular signal–regulated kinase (pERK) and ERK detection, lumbar (L4–L5) spinal cord of Slick$^{-/-}$ and wild-type mice (n = 4 per group [1 female and 3 males]) was homogenized in Phosphosafe extraction reagent (No. 71296, Novagen, Germany) mixed with the protease inhibitor cocktail. For somatostatin receptor 2 (SSTR2) detection, the lumbar (L4–L5) spinal cord of Slick$^{-/-}$, wild-type, Lbx1-Slick$^{-/-}$, and control mice (n = 3 per group [1 female and 2 males]) were prepared with radioimmunoprecipitation assay buffer containing 150 mM sodium chloride, 1% Triton X-100, 0.5% sodium deoxycholate, 0.1% sodium dodecyl sulfate, and 50 mM Tris (protocol from Abcam, United Kingdom) mixed with the protease inhibitor cocktail. Extracted proteins (40 to 50 μg per lane) were separated by 6 or 10% SDS-PAGE and blotted onto a nitrocellulose membrane. After blocking of nonspecific binding sites with blocking buffer (Intercept Blocking Buffer, No. 927-70001; LI-COR Bioscience, USA), membranes were incubated with mouse anti-KCNT2/Slo2.1/Slick (1:500, clone N11/33, No. 75-055; NeuroMab, USA), rabbit anti-phospho-p44/42 mitogen-activated protein kinase ([MAPK] Thr202/Tyr204, 1:700, No. 9101S; Cell Signaling, USA), rabbit anti-p44/42 MAPK (Erk1/2; 1:600, No.4695S; Cell Signaling), mouse anti-SSTR2 (1:200, No. sc-365502, Santa Cruz, USA) and mouse anti–α-tubulin (1:1,000; clone DM1A, No. 05-829; Sigma-Aldrich, Germany) dissolved in blocking buffer containing Tween 20, 0.1%, overnight at 4°C. After incubation with secondary antibodies for 1 h at room temperature, proteins were detected using an Odyssey Infrared Imaging System (LI-COR Bioscience). Quantification of band densities was done using Image Studio Lite software (LI-COR Bioscience).

Immunostaining and *In Situ* Hybridization

Mice (n = 5 per group [2 females and 3 males]) and rats (n = 2 females) were killed by carbon dioxide and immediately perfused intracardially with 0.9% saline, followed by 1% or 4% paraformaldehyde in phosphate-buffered saline (pH, 7.4). Lumbar (L3–L5) dorsal root ganglia and lumbar (L3–L5) spinal cord were dissected and cryoprotected in 20% sucrose for 4 h, followed by 30% sucrose overnight. Tissues were frozen in tissue freezing medium (Tissue-Tek O.C.T. Compound, No. 4583; Sakura, USA) on dry ice, cryostat-sectioned at a thickness of 14 μm, and stored at −80°C.

For immunostaining, sections were permeabilized for 5 min in Triton X-100, 0.1%, in phosphate-buffered saline, blocked for 1 h using normal goat serum, 10%, (No. 10000C; Thermo Fisher Scientific) and bovine serum albumin, 3%, (No. A6003; Sigma-Aldrich) in phosphate-buffered saline, and incubated with primary antibodies diluted in 3% bovine serum albumin in phosphate-buffered saline overnight at 4°C or for 2 h at room temperature. The following antibodies were used: mouse anti-Slick (1:500, clone N11/33, No. 75-055; NeuroMab); rabbit anti–calcitonin gene-related peptide ([CGRP] 1:800, No. PC205L; Sigma-Aldrich); guinea pig anti-CGRP (1:600, No. 414 004; Synaptic Systems, Germany); mouse anti-neurofilament 200 ([NF200] 1:2,000, No. N0142; Sigma-Aldrich); rabbit anti-NF200 (1:2,000, No. N4142; Sigma-Aldrich); rabbit anti-transient receptor potential vanilloid 1 ([TRPV1] 1:800, No. ACC-030; Alomone, Israel); and rabbit anti–vesicular glutamate transporter type 3 ([VGLUT3] 1:400, No. 135203; Synaptic Systems). Sections were then washed in phosphate-buffered saline and stained with secondary antibodies conjugated with Alexa Fluor 350, 488, or 555, or Cy5 (1:1,200; all from Thermo Fisher Scientific). For staining of class III β-tubulin (TUBB3), Alexa Fluor 488–conjugated anti-TUBB3 (1:1,000; clone TUJ1, No.

801203; BioLegend, USA) diluted in bovine serum albumin, 3%, in phosphate-buffered saline was incubated for 2 h at 4°C. For staining with *Griffonia simplicifolia* isolectin B4, sections were incubated with Alexa Fluor 488–conjugated isolectin B4 (10 μg/ml in buffer containing 1 mM $CaCl_2 \cdot 2H_2O$, 1 mM $MgCl_2$, 1 mM $MnCl_2$, and Triton X-100, 0.2%; pH, 7.4 [No. 121411; Thermo Fisher Scientific]) for 2 h at room temperature. After immunostaining, slices were immersed for 5 min in 0.06% Sudan black B (No. 199664; Sigma-Aldrich) in 70% ethanol to reduce lipofuscin-like autofluorescence, washed in phosphate-buffered saline, and coverslipped. In double-labeling experiments, primary antibodies were consecutively incubated.

For *in situ* hybridization, we used the QuantiGene ViewRNA tissue assay (Thermo Fisher Scientific), in which target mRNA signals appear as puncta in microscopy. Experiments were performed according to the manufacturer's instructions using a type-1 probe set designed by Thermo Fisher Scientific to the coding region of mouse Slick (Kcnt2; No. VB1-17744) and type-6 probe sets for mouse Slack (Kcnt1; No. VB6-21049), vesicular γ-aminobutyric acid (GABA) transporter ([VGAT] No.VB6-17400), vesicular glutamate transporter 2 (VGLUT2; No. VB6-16625), galanin (GAL; No. VB6-3199892), nitric oxide synthase 1 (nNOS; No.VB6-3197829), neuropeptide Y (NPY; No.VB6-16274), parvalbumin (PVALB; No.VB6-13220), SSTR2 (No. VB6-3201802), and gastrin-releasing peptide receptor ([GRPR] No. VB6-3197053). Controls included scramble type-1 (No.VF1-17155) and type-6 (No. VF6-18580) probe sets. Briefly, tissue sections were fixed in 4% paraformaldehyde for 16 to 18 h at 4°C, dehydrated through 50%, 70%, and 100% ethanol, treated with protease QF for 25 min at 40°C, and incubated with probe sets for 2 h at 40°C. In double *in situ* hybridization experiments, type-1 and type-6 labeled probes were simultaneously incubated. After preamplifier and amplifier hybridization, the signal was developed *via* reaction with fast red and blue substrate (for type-1 and -6 probes, respectively). Finally, sections were costained with 4′,6-diamidino-2-phenylindole (No. D1306; Thermo Fisher Scientific) and mounted with Fluoromount G (No. 00-4958-02; Thermo Fisher Scientific).

Images were taken using an Eclipse Ni-U (Nikon, Germany) microscope equipped with a monochrome charge-coupled device, and were pseudocolored and superimposed. Adjustment of brightness and contrast was done using Adobe Photoshop 2020 software (Adobe Systems, USA). Controls were performed by omitting the first and/or the second primary antibodies, incubating type-1 and type-6 scramble probes, and incubating tissues of $Slick^{-/-}$ mice.

Cell Counting

For quantification of the number of cells expressing Slick or marker, at least three nonadjacent sections per dorsal root ganglia or spinal cords per animal (three mice per genotype) were counted. Only cells showing staining clearly above background were included. The specificity of Slick immunoreactivity was confirmed by simultaneous staining of coembedded tissues of wild-type and $Slick^{-/-}$ mice. The percentage of marker-positive dorsal root ganglia neurons in wild-type and $Slick^{-/-}$ mice is expressed as a proportion of marker-positive cells per total number of dorsal root ganglia neurons. The percentage of Slick-positive dorsal root ganglia neurons that expressed marker was calculated by dividing the number of Slick-positive cells colocalized with marker by the total number of Slick-positive cells. For quantification of mRNA-positive dorsal horn neurons, only nuclei-positive cells with hybridization signals clearly above background were counted.

Behavioral Testing

All behavioral studies were performed with littermate mice. Animals were habituated to the experimental room and randomized to different groups. All experiments were conducted between 9:00 AM and 5:00 PM.

Rotarod Test. Motor coordination was assessed with a Rotarod Treadmill for mice (Ugo Basile, Italy) at a constant rotating speed of 13 rpm. All mice had at least two training sessions before the day of the experiment ($Slick^{-/-}$: n = 16 [7 females and 9 males]; wild-type: n = 16 [9 females and 7 males]; $Lbx1\text{-}Slick^{-/-}$: n = 14 [8 females and 6 males]; control: n = 18 [9 female and 9 males]). The latency to fall was recorded during a maximum period of 120 s. The mean from three latencies was used for analysis.

Hot Plate Test. Mice were individually confined in a Plexiglas chamber on a heated metal surface (Hot/Cold Plate; Ugo Basile, Italy). The time between placement and a nocifensive behavior (shaking or licking of a hind paw, jumping) was recorded, and the animal was removed from the plate immediately after a response. To prevent tissue damage, temperatures of 48°C ($Slick^{-/-}$: n = 12 [6 females and 6 males]; wild-type: n = 12 [5 females and 7 males]; $Lbx1\text{-}Slick^{-/-}$: n = 13 [7 females and 6 males]; control: n = 14 [9 females and 5 males]); 50°C ($Slick^{-/-}$: n = 18 [7 females and 11 males]; wild-type: n = 18 [7 females and 11 males]; $Lbx1\text{-}Slick^{-/-}$: n = 13 [7 females and 6 males]; control: n = 14 [9 females and 5 males]); 52°C ($Slick^{-/-}$: n = 18 [7 females and 11 males]; wild-type: n = 18 [7 females and 11 males]; $Lbx1\text{-}Slick^{-/-}$: n = 12 [6 females and 6 males]; control: n = 12 [7 females and 5 males]); and 54°C ($Slick^{-/-}$: n = 18 [7 females and 11 males]; wild-type: n = 18 [7 females and 11 males]; $Lbx1\text{-}Slick^{-/-}$: n = 12 [6 females and 6 males]; control: n = 12 [7 females and 5 males]) were applied with cutoff times of 80, 40, 30, and 20 s, respectively. Only one test per animal per temperature was performed.

Tail-immersion Test. Mice were immobilized in aluminum foil, which allowed free tail movement. For accommodation, the tip of the tail (approximately one third of the tail length) was first immersed in a water bath (Sunlab D-8810;

neoLab, Germany) at 32°C for 20 s. Then the tip of the tail was immersed in another water bath maintained at 46°C (Slick$^{-/-}$: n = 17 [7 females and 10 males]; wild-type: n = 17 [6 females and 11 males]; Lbx1-Slick$^{-/-}$: n = 16 [9 females and 7 males]; control: n = 16 [8 females and 8 males]); 47°C (Slick$^{-/-}$: n = 18 [12 females and 6 males]; wild-type: n = 18 [9 females and 9 males]; Lbx1-Slick$^{-/-}$: n = 16 [9 females and 7 males]; control: n = 16 [8 females and 8 males]); 48°C (Slick$^{-/-}$: n = 18 [9 females and 9 males]; wild-type: n = 18 [6 females and 12 males]; Lbx1-Slick$^{-/-}$: n = 16 [9 females and 7 males]; control: n = 16 [8 females and 8 males]); 49°C (Slick$^{-/-}$: n = 18 [8 females and 10 males]; wild-type: n = 18 [11 females and 7 males]; Lbx1-Slick$^{-/-}$: n = 16 [9 females and 7 males]; control: n = 16 [8 females and 8 males]); or 50°C (Slick$^{-/-}$: n = 19 [6 females and 13 males]; wild-type: n = 19 [8 females and 11 males]; Lbx1-Slick$^{-/-}$: n = 16 [9 females and 7 males]; control: n = 16 [8 females and 8 males]) with cutoff times of 80, 60, 40, 30, and 20 s, respectively. The latency time to a tail withdrawal reflex was recorded, and the tail was removed from the bath immediately after response.[13] Only one test per animal per temperature was used for analysis.

Cold Plate Test. Mice were individually placed in a Plexiglas chamber on a cold metal surface (Hot/Cold Plate; Ugo Basile) maintained at 10°C or 5°C. The total time the mouse spent lifting the forepaw during a 60-s period was measured *via* stopwatch (Slick$^{-/-}$: n = 12 [8 females and 4 males]; wild-type: n = 11 [6 females and 5 males]).[14] Only one test per animal per temperature was performed.

Cold Plantar Test. Mice were acclimated on a borosilicate glass plate (6.5-mm thickness; GVB GmbH, Germany) in transparent plastic enclosures and acclimated for 40 to 60 min. Powdered dry ice was packed into a modified syringe (3 ml; B. Braun, Germany) with a cut top (1-cm diameter). The open end of the syringe was held against a flat surface while pressure was applied to the plunger to compress the dry ice, and then the dense dry ice pellet was applied to the glass surface underneath a hind paw.[15] The latency to move the paw vertically or horizontally away from the glass plate was measured with a stopwatch. An interval of at least 7 min was allowed between testing separate paws of a single mouse, and an interval of at least 15 min was allowed between trials on any single paw. Three to five measurements per paw were performed (Slick$^{-/-}$: n = 15 [7 females and 8 males]; wild-type: n = 13 [5 females and 8 males]).

Dynamic Plantar Test. Paw withdrawal latency after mechanical stimulation was assessed using a dynamic plantar aesthesiometer (Ugo Basile), which pushes a thin probe (0.5-mm diameter) with increasing force through a wire-gated floor against the plantar surface of the hind paw from beneath. The force increased from 0 to 5 g within 10 s and was then held at 5 g for an additional 10 s.[5] The latency was calculated as the average of four to six exposures with at least 20 s in between (Slick$^{-/-}$: n = 10 [5 females and 5 males]; wild-type: n = 9 [4 females and 5 males]).

Tail-clip Test. Mice were individually placed in a Plexiglass chamber and habituated for 5 min. A plastic clip (force, approximately 300 g; Ericotry, China) was applied on the base of the tail, and the latency to the first response (biting, grasping, or jumping) was recorded (Slick$^{-/-}$: n = 14 [6 females and 8 males]; wild-type: n = 13 [4 females and 9 males]).[16]

Tape-response Test. Mice were individually placed in Plexiglas cylinders and habituated for 5 min. A 3-cm piece of a common laboratory tape (marking tape; Diversified Biotech, USA) was put on the back of the mouse. A response was considered when the mouse stopped moving and bit the piece of tape or showed a visible "wet-dog shake" motion in an attempt to remove the tape.[16] Responses occurring within 5 min were counted (Slick$^{-/-}$: n = 18 [9 females and 9 males]; wild-type: n = 15 [9 females and 9 males]).

Capsaicin Test. Mice were individually confined in a Plexiglas cylinder and habituated for 30 min. Capsaicin (5 μg in 20 μl phosphate-buffered saline containing dimethyl sulfoxide, 2% [Sigma-Aldrich]) was injected into the dorsal surface of a hind paw. The time spent licking the injected paw was recorded with a stopwatch in 1-min intervals during a 20-min period (Slick$^{-/-}$: n = 8 [4 females and 4 males]; wild-type: n = 7 [4 females and 3 males]; Lbx1-Slick$^{-/-}$: n = 8 [3 females and 5 males]; control: n = 9 [6 females and 3 males]). In experiments with the SSTR2 antagonist CYN-154806 (500 ng in 5 μl NaCl, 0.9%; No. C2490; Sigma-Aldrich), the compound was intrathecally administered by direct lumbar puncture under short isoflurane anesthesia 30 min before capsaicin injection into a hind paw (Slick$^{-/-}$: n = 5 [1 female and 4 males]; wild-type: n = 6 [1 female and 5 males]; Lbx1-Slick$^{-/-}$: n = 5 [1 female and 4 males]; control: n = 5 [1 female and 4 males]). The time spent licking the injected paw was recorded during the 20 min after capsaicin injection.

Allyl Isothiocyanate Test. Mice were individually habituated in a Plexiglass cylinder for 30 min. Allyl isothiocyanate (10 nmol in 20 μl phosphate-buffered saline containing dimethyl sulfoxide, 0.05% [Sigma-Aldrich]) was injected into the plantar side of a hind paw. The time spent licking the injected paw was recorded in 5-min intervals up to 30 min after allyl isothiocyanate injection.[17] Mechanical sensitivity was evaluated with a series of von Frey hairs stiffness (0.04 to 2.00 g; Ugo Basile) at 1, 3, 5, and 24 h after allyl isothiocyanate injection (Slick$^{-/-}$: n = 8 [4 females and 4 males]; wild-type: n = 6 [2 females and 4 males]; Lbx1-Slick$^{-/-}$: n = 7 [4 females and 3 males]; control: n = 8 [4 females and 4 males]).

Itch Behavior. Mice were habituated in a Plexiglass cylinder for 30 min. The pruritogens octreotide ([100 ng or 300 ng in 5 μl NaCl, 0.9%; No. O1014; Sigma-Aldrich]; 100 ng octreotide: Slick$^{-/-}$: n = 8 [4 females and 4 males]; wild-type: n = 8 [2 females and 6 males]; Lbx1-Slick$^{-/-}$: n = 8 [6 females and 2 males]; control: n = 8 [4 females and 4 males]; 300 ng octreotide: Slick$^{-/-}$: n = 7 [3 females and 4

males]; wild-type: n = 7 [3 females and 4 males]) or gastrin-releasing peptide (1 nmol in 5 μl NaCl, 0.9% [No. 4011670; Bachem, Switzerland]; Slick$^{-/-}$: n = 8 [4 females and 4 males]; wild-type: n = 8 [4 females and 4 males]) were intrathecally administered by direct lumbar puncture under short isoflurane anesthesia. The pruritogens histamine (200 μg in 10 μl NaCl, 0.9% [No. H7125; Sigma-Aldrich]; Lbx1-Slick$^{-/-}$: n = 5 [3 females and 2 males]; control: n = 6 [2 females and 4 males]) and chloroquine (200 μg in 10 μl NaCl, 0.9% [No. C6628; Sigma-Aldrich]; Lbx1-Slick$^{-/-}$: n = 5 [3 females and 2 males]; control: n = 6 [2 females and 4 males]) were injected intradermally into the nape of the neck. The number of scratching bouts that occurred during a 30-min period was recorded using a video tracking system (VideoMot; TSE Systems, Germany) without human presence in the experiment room.[18]

Statistical Analysis

Statistical analysis was performed with GraphPad Prism software version 8.0 (GraphPad, USA). No statistical power calculation was conducted before the study, and the sample sizes were determined based on our previous knowledge and experience with this design. Group sizes and experimental units are indicated in the Materials and Methods and Results sections, as well as figure legends. No outliers were observed, and no data were excluded from statistical analysis. Rotarod fall-off latencies were analyzed with Mann–Whitney U test and are expressed as medians and interquartile ranges. All other data are presented as mean ± SD. For some data, 95% CI are reported in the Results section, and *t* or F values are reported in the figure legends. Differences between two groups (*e.g.,* responses to the hot plate, tail-immersion, cold plate, cold plantar, dynamic plantar, tail-clip, and tape test; sum of licking time after allyl isothiocyanate injection; sum of scratching bouts after injection of histamine and chloroquine) were determined using two-tailed, unpaired *t* tests. Differences in Slack mRNA expression, dorsal root ganglia neurons subpopulations, Slick mRNA expression, sum of licking time after capsaicin, and Western blots of phosphorylated extracellular signal-regulated kinase and extracellular signal-regulated kinase, and sum of scratching bouts after injection of octreotide with two doses were determined using multiple *t* tests. Allyl isothiocyanate–induced mechanical hypersensitivity was determined using two-way repeated-measures ANOVA followed by the *post hoc* Sidak multiple comparison test. For all tests, $P < 0.05$ was considered as statistically significant.

Results

Slick Is Expressed in Aδ-Fiber Nociceptors and Dorsal Horn Interneurons

To study the functions of Slick potassium channels in pain processing, we first produced mice lacking Slick globally by crossing a mouse strain containing exon 22 of the *Kcnt2* gene flanked by two loxP sites[6] with transgenic mice expressing Cre under the transcriptional control of the cytomegalovirus promotor.[11] The resulting knockout mice (referred to as Slick$^{-/-}$) were viable and fertile, and in accordance with previous studies, there were no obvious differences in gross appearance and general behavior among Slick$^{-/-}$ and wild-type littermates.[6] The deletion of Slick was confirmed by Western blotting in tissue extracts from dorsal root ganglia and the spinal cord (n = 3 per group; fig. 1A). The mRNA expression of Slack, a paralogous potassium channel that has been reported to form heteromers with Slick,[19] was unaltered in dorsal root ganglia (Slick$^{-/-}$ [n = 3]: 0.8 ± 0.2 [95% CI, 0.4 to 1.3]; wild-type [n = 3]: 1.0 ± 0.1 [95% CI, 0.8 to 1.2]; $P = 0.163$; fig. 1B) and the spinal cord of Slick$^{-/-}$ mice (Slick$^{-/-}$ [n = 3]: 0.5 ± 0.0 [95% CI, 0.4 to 0.6]; wild-type [n = 3]: 0.5 ± 0.1 [95% CI, 0.2 to 0.8]; $P > 0.999$; fig. 1B). Moreover, the overall frequencies of dorsal root ganglia neuron populations positive for the established markers isolectin B4 (Slick$^{-/-}$ [n = 3]: 29.8 ± 3.6% [95% CI, 20.8 to 38.9%]; wild-type [n = 3]: 31.4 ± 2.4% [95% CI, 25.5 to 37.3%]; $P = 0.920$; fig. 1C); CGRP (Slick$^{-/-}$ [n = 3]: 33.0 ± 8.6% [95% CI, 11.8 to 54.3%]; wild-type [n = 3]: 39.6 ± 1.0% [95% CI, 37.0 to 42.2%]; $P = 0.371$; fig. 1C); and NF200 (Slick$^{-/-}$ [n = 3]: 58.3 ± 0.8% [95% CI, 56.2 to 60.4%]; wild-type [n = 3]: 58.5 ± 8.0% [95% CI, 38.7 to 78.3%]; $P = 0.953$; fig. 1C) were similar between genotypes, suggesting that there are no general defects in Slick$^{-/-}$ mice.

We then analyzed the cellular distribution of Slick in dorsal root ganglia by immunostaining and detected Slick immunoreactivity in a population of sensory neurons of wild-type mice (fig. 1D). Costaining with the pan-neuronal marker TUBB3 revealed that 9.3 ± 4.2% of total dorsal root ganglia neurons in wild-type mice expressed Slick (n = 4 per group; fig. 1D). No Slick immunoreactivity was seen in dorsal root ganglia from Slick$^{-/-}$ mice (fig. 1E), validating the specificity of our Slick antibody–based staining protocol. In further costaining experiments, we found that the vast majority (91.5 ± 12.0%) of Slick-positive (Slick^{+}) cells expressed CGRP, a marker of the peptidergic population of nociceptors (fig. 1, F and H), confirming a previous report.[7] Conversely, 36.3 ± 25.1% of CGRP^{+} cells coexpressed Slick, suggesting that Slick is localized to only a fraction of CGRP^{+} cells. Interestingly, 93.9 ± 8.6% of Slick^{+} cells were immunoreactive for NF200, which labels myelinated dorsal root ganglia neurons, and 90.2 ± 13.8% of Slick^{+} cells expressed both CGRP and NF200 (n = 5 per group; fig. 1, F and H). This finding implicates that Slick is mainly localized to thinly myelinated Aδ-fiber nociceptors, which are CGRP^{+} and NF200^{+}.[20–22] This subclass of dorsal root ganglia neurons has recently been classified as peptidergic 2 (PEP2) neurons in a single-cell RNA-sequencing study.[23]

Slick immunostaining was virtually absent from sensory neurons binding isolectin B4, a marker of nonpeptidergic unmyelinated C-fiber nociceptors (n = 5 per

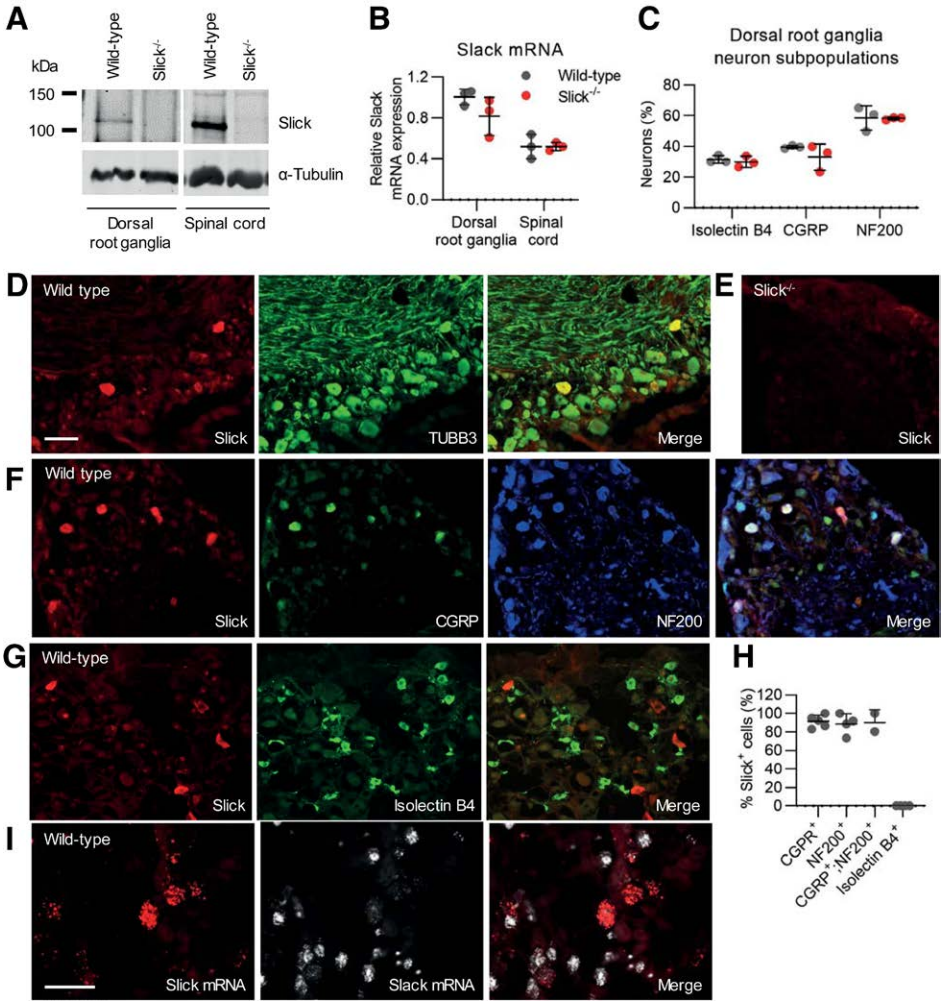

Fig. 1. Distribution of Slick in dorsal root ganglia. (*A*) Western blot analysis of Slick (130 kDa) in dorsal root ganglia and spinal cord from wild-type and Slick$^{-/-}$ mice. Slick was specifically detected in tissues of wild-type, but not Slick$^{-/-}$, mice. α-Tubulin (55 kd) was used as loading control. (*B*) Quantitative reverse transcription polymerase chain reaction in dorsal root ganglia and the spinal cords of wild-type and Slick$^{-/-}$ mice revealed that Slack mRNA expression is not compensatory regulated in the absence of Slick (dorsal root ganglia: $t_8 = 1.96$, $P = 0.163$; spinal cord: $t_8 = 0.00$, $P > 0.999$; n = 3 per group). Values were normalized to wild-type dorsal root ganglia. (*C*) Percentages of dorsal root ganglia neurons that are isolectin B4–binding or immunoreactive for calcitonin gene-related peptide (CGRP) or neurofilament 200 (NF200) are comparable between wild-type and Slick$^{-/-}$ mice (isolectin B4: $t_{12} = 0.37$, $P = 0.920$; CGRP: $t_{12} = 1.57$, $P = 0.371$; NF200: $t_{12} = 0.06$, $P = 0.953$; n = 3 per group). (*D*) Double-immunostaining of Slick with the pan-neuronal marker class III β-tubulin (TUBB3) in dorsal root ganglia of wild-type mice reveals Slick expression in 9.3 ± 2.4% of TUBB3-positive dorsal root ganglia neurons (892 neurons counted; n = 4 per group). (*E*) No Slick immunoreactivity was detected in dorsal root ganglia of Slick$^{-/-}$ mice, confirming the specificity of the anti-Slick antibody. (*F*) Triple-immunostaining of Slick with CGRP and NF200 shows that Slick is mainly localized to dorsal root ganglia neurons that are positive for both CGRP and NF200 (*i.e.,* are in myelinated Aδ nociceptors). (*G*) Double-labeling of Slick and isolectin B4 shows that Slick is absent from isolectin B4–binding dorsal root ganglia neurons. (*H*) Percentage of marker-positive neurons that coexpress Slick (5,959 cells counted; n = 5 per group). (*I*) Double *in situ* hybridization of Slick mRNA with Slack mRNA confirms that Slick and Slack are not coexpressed in dorsal root ganglia neurons. Data are shown as mean ± SD. Scale bars = 50 μm.

group; fig. 1, G and H). Considering that Slack is nearly exclusively expressed in isolectin B4–binding nociceptors,[5] this observation suggests that Slick and Slack do not form heteromers in dorsal root ganglia neurons, unlike in other tissues.[6,24] Indeed, double-labeling fluorescent *in situ* hybridization confirmed that Slick and Slack mRNA do not overlap in dorsal root ganglia neurons (n = 3 per group; fig. 1I). Furthermore, a similar distribution pattern of Slick with enrichment in CGRP$^+$;NF200$^+$ cells and absence from isolectin B4–binding cells was observed in dorsal root ganglia from rats (Supplemental Digital Content 1 fig. 1, http://links.lww.com/ALN/C805). Together, these analyses of dorsal root ganglia tissues indicate that Slick is mainly expressed in Aδ-fiber nociceptors.

We next assessed the distribution of Slick in the spinal cord and observed profound immunoreactivity in the superficial dorsal horn of wild-type mice (fig. 2A, left). Control experiments confirmed that Slick immunoreactivity was absent in the spinal cord of Slick$^{-/-}$ mice (fig. 2A, right). Inconsistent with the expression pattern of Slick in dorsal root ganglia neurons, Slick immunoreactivity in the dorsal horn was not limited to the central terminals of Aδ-fibers that terminate mainly in lamina I and V.[25] Colabeling experiments revealed that Slick immunoreactivity is present in lamina I and outer lamina II (marked by CGRP staining; fig. 2B), in the dorsal region of inner lamina II (marked by isolectin B4 binding; fig. 2C), and in the ventral region of inner lamina II (marked by VGLUT3 staining; fig. 2D).[26] These observations, together with available single-cell RNA-sequencing data,[10] suggest that in addition to dorsal root ganglia neurons, populations of intrinsic neurons in the dorsal horn express Slick.

To further investigate the expression of Slick in the spinal dorsal horn, we performed fluorescent *in situ* hybridization experiments of Slick mRNA. Consistent with the protein expression pattern previously described (fig. 2), multiple hybridization signals were detected in the dorsal horn (fig. 3A, left). As our hybridization probe (which binds to nucleotides 624 to 1568 of Slick mRNA, corresponding to exons 8 through 16) cannot distinguish between tissues from wild-type and Slick$^{-/-}$ mice (in which exon 22 is deleted), we used a scramble probe as a specificity control (fig. 3A, right). To estimate the distribution of Slick in inhibitory and excitatory interneurons of the superficial dorsal horn, we performed double-labeling *in situ* hybridization of Slick mRNA with VGAT mRNA, a marker of inhibitory neurons, and VGLUT2 mRNA, which marks excitatory neurons.[10] We found that 67.3 ± 2.5% of Slick^{+} cells in the superficial dorsal horn expressed VGAT (fig. 3B), whereas 28.7 ± 8.8% of Slick^{+} cells were positive for VGLUT2 (fig. 3C). Conversely, 69.8 ± 4.5% of VGAT^{+} neurons and 21.5 ± 5.6% of VGLUT2^{+} neurons in the superficial dorsal horn express Slick (fig. 3, B and C). These data indicate that Slick is predominantly, but not exclusively, expressed in inhibitory interneurons of the superficial dorsal horn of the spinal cord.

We then further analyzed the cellular distribution of Slick in subpopulations of inhibitory interneurons in the dorsal horn. Previous studies have identified five largely nonoverlapping neurochemical populations that express GAL, nNOS, NPY, PVALB, and calretinin.[25] We found that 38.4 ± 5.7%, 11.9 ± 2.8%, and 10.8 ± 2.7% of Slick^{+} cells coexpressed GAL, nNOS, and NPY, respectively (fig. 3, D to F). Conversely, 80.2 ± 1.1% of GAL^{+}, 49.5 ± 4.8% of nNOS^{+}, and 25.4 ± 8.8% of NPY^{+} neurons coexpressed Slick (fig. 3, D to F). By contrast, there was virtually no colocalization of Slick with PVALB (fig. 3G). We did not analyze the colocalization of Slick and calretinin, because this marker is also significantly expressed by excitatory interneurons.[27] Altogether, the localization in distinct populations of dorsal horn neurons in combination with the enrichment in Aδ-fiber nociceptors supports the idea that Slick is involved in somatosensory processing.

Slick$^{-/-}$ Mice Display Increased Heat Sensitivity but Normal Cold and Mechanical Sensitivity

To assess the functional relevance of Slick for somatosensory processing, we tested the sensitivity of Slick$^{-/-}$ and littermate wild-type mice to various innocuous and noxious sensory stimuli. As a prerequisite for behavioral testing, we first characterized their motor coordination and balance using the rotarod test. Slick$^{-/-}$ and wild-type mice demonstrated intact motor coordination, as analyzed in the rotarod test (median fall-off latencies: Slick$^{-/-}$ [n = 16]: 120 s [interquartile range, 108.0 to 120.0]; wild-type [n = 16]: 120 s [interquartile range, 120.0 to 120.0]; $P = 0.174$), suggesting that Slick$^{-/-}$ mice are suitable for behavioral analyses. We then tested the ability of Slick$^{-/-}$ mice to respond to heat. In the hot plate test, Slick$^{-/-}$ mice exhibited significantly shorter latencies than wild-type mice when the plate was set at 48°C (Slick$^{-/-}$ [n = 12]: 29.3 ± 11.0 s [95% CI, 22.3 to 36.3]; wild-type [n = 12]: 47.3 ± 17.8 s [95% CI, 36.0 to 58.6]; $P = 0.007$) and 50°C (Slick$^{-/-}$ [n = 18]: 22.1 ± 9.0 s [95% CI, 17.6 to 26.6]; wild-type [n = 18]: 28.6 ± 6.0 s [95% CI, 25.6 to 31.5]; $P = 0.015$), but they responded normally at higher temperatures of 52°C (Slick$^{-/-}$ [n = 18]: 15.6 ± 6.3 s [95% CI, 12.5 to 18.8]; wild-type [n = 18]: 18.4 ± 4.8 s [95% CI, 16.0 to 20.7]; $P = 0.149$) and 54°C (Slick$^{-/-}$ [n = 18]: 8.5 ± 2.5 s [95% CI, 7.3 to 9.7]; wild-type [n = 18]: 10.1 ± 3.3 s [95% CI, 8.4 to 11.7]; $P = 0.122$; fig. 4A; results for female and male cohorts are shown in Supplemental Digital Content 2 fig. 2, A and B, http://links.lww.com/ALN/C806). Similarly, in the tail-immersion assay, Slick$^{-/-}$ animals showed significantly shorter tail flick latencies compared with wild-type littermates for bath temperatures of 46°C (Slick$^{-/-}$ [n = 17]: 20.1 ± 13.0 s [95% CI, 13.4 to 26.8]; wild-type [n = 17]: 32.7 ± 19.0 s [95% CI, 22.9 to 42.4]; $P = 0.032$), 47°C (Slick$^{-/-}$ [n = 18]: 7.6 ± 3.5 s [95% CI, 5.9 to 9.3]; wild-type [n = 18]: 11.4 ± 5.3 s [95% CI, 8.7 to 14.0]; $P = 0.016$), and 48°C (Slick$^{-/-}$ [n = 18]: 5.0 ± 2.0 s [95% CI, 4.0 to 6.0]; wild-type [n = 18]: 7.1 ± 2.1 s [95% CI, 6.0 to 8.1]; $P = 0.004$), whereas responses to the higher temperatures 49°C (Slick$^{-/-}$ [n = 18]: 3.1 ± 1.7 s [95% CI, 2.2 to 3.9]; wild-type [n = 18]: 7.1 ± 2.1 s [95% CI, 3.3 to 4.3]; $P = 0.107$) and 50°C (Slick$^{-/-}$ [n = 19]: 2.5 ± 1.0 s [95% CI, 2.1 to 3.0]; wild-type [n = 19]: 3.0 ± 1.6 s [95% CI, 2.2 to 3.7]; $P = 0.323$) were unaltered (fig. 4B; results for female and male cohorts are presented in Supplemental Digital Content 2 fig. 2, C to E, http://links.lww.com/ALN/C806). These data suggest that Slick specifically controls heat sensation at distinct temperatures.

We next analyzed cold sensitivity of Slick$^{-/-}$ and wild-type littermates. In the cold plate test, the duration of forepaw lifting[14] at either 10°C or 5°C was comparable between

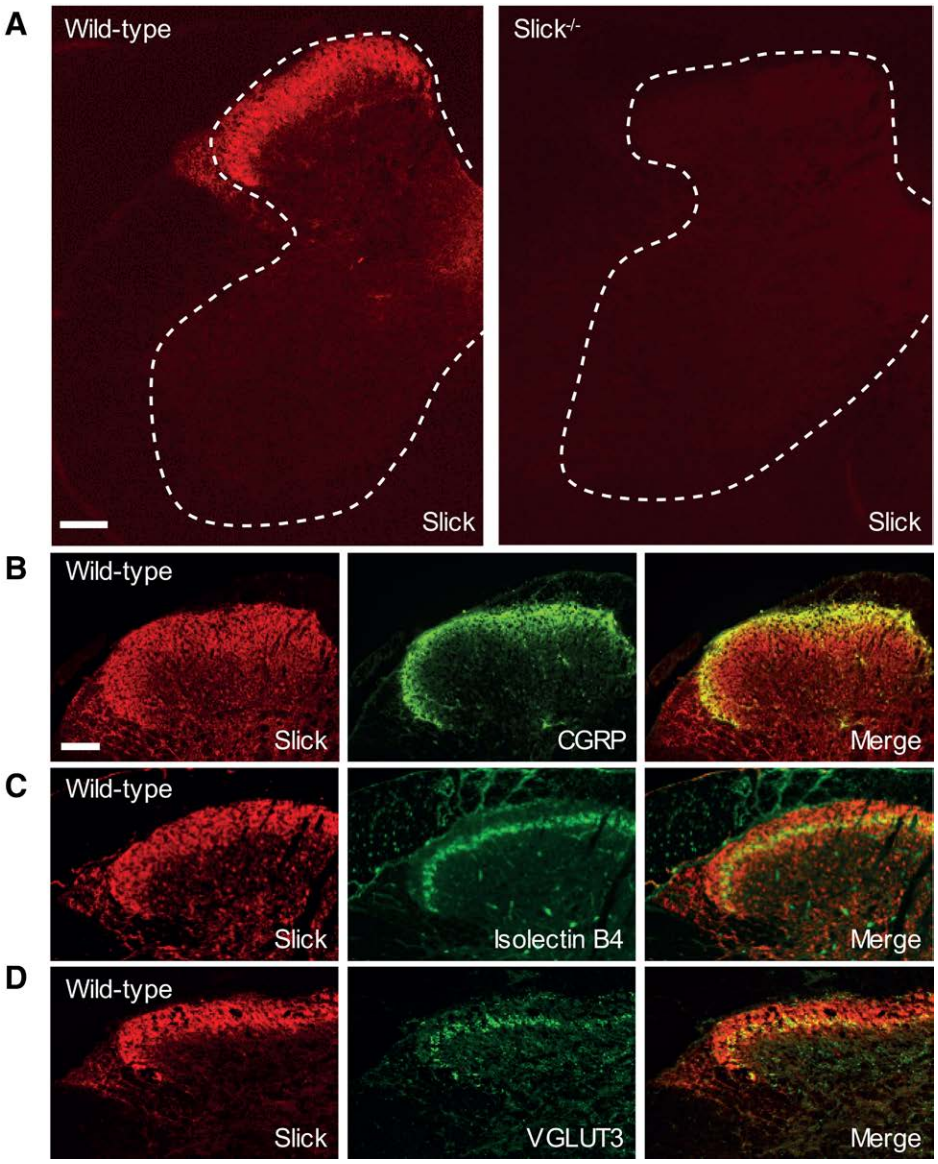

Fig. 2. Distribution of Slick protein in the spinal cord. (*A*) Immunostaining of Slick in the lumbar spinal cord of wild-type (*left*) and Slick$^{-/-}$ (*right*) mice reveals specific Slick expression in the superficial dorsal horn. Dotted lines delineate the gray matter. (*B* through *D*) Double-labeling of Slick with calcitonin gene-related peptide ([CGRP] which labels lamina I and outer lamina II [*B*]), isolectin B4 (inner/dorsal region of lamina II [*C*]), and vesicular glutamate transporter type 3 ([VGLUT3] inner/ventral region of lamina II [*D*]) shows that Slick immunoreactivity expands from lamina I to the ventral part of inner lamina II. Scale bars = 100 μm.

genotypes (10°C: Slick$^{-/-}$ [n = 12]: 16.2 ± 8.7 s [95% CI, 10.6 to 21.7]; wild-type [n = 11]: 16.9 ± 7.5 s [95% CI, 11.9 to 21.9]; P = 0.915; 5°C: Slick$^{-/-}$ [n = 12]: 39.5 ± 13.1 s [95% CI, 31.1 to 47.8]; wild-type [n = 11]: 41.0 ± 8.5 s [95% CI, 35.3 to 46.7]; P = 0.915; fig. 4C). Similar to the cold plate test, Slick$^{-/-}$ mice showed normal latencies in the cold plantar test (Slick$^{-/-}$ [n = 15]: 11.6 ± 2.0 s [95% CI, 10.5 to 12.7]; wild-type [n = 13]: 11.8 ± 2.4 s [95% CI, 10.4 to 13.2]; P = 0.814; fig. 4D), in which a dry ice pellet is pushed to a glass surface beneath the hind paw.[15] These data suggest an unimpaired cold sensitivity in the absence of Slick. In tests of mechanosensitivity, Slick$^{-/-}$ mice showed normal withdrawal latencies to an increasing mechanical force applied to the hind paw with a dynamic plantar aesthesiometer (Slick$^{-/-}$ [n = 10]: 9.1 ± 0.9 s [95% CI, 8.4 to 9.7]; wild-type [n = 9]: 9.1 ± 0.7 s [95% CI, 8.6 to 9.6 s]; P = 0.956; fig. 4E). They also demonstrated unaltered responses to a noxious mechanical stimulus in the tail-clip test (Slick$^{-/-}$ [n = 14]: 6.7 ± 7.0 s [95% CI, 2.7 to 10.7]; wild-type [n =13]: 6.8 ± 6.0 s [95% CI, 3.1 to 10.4];

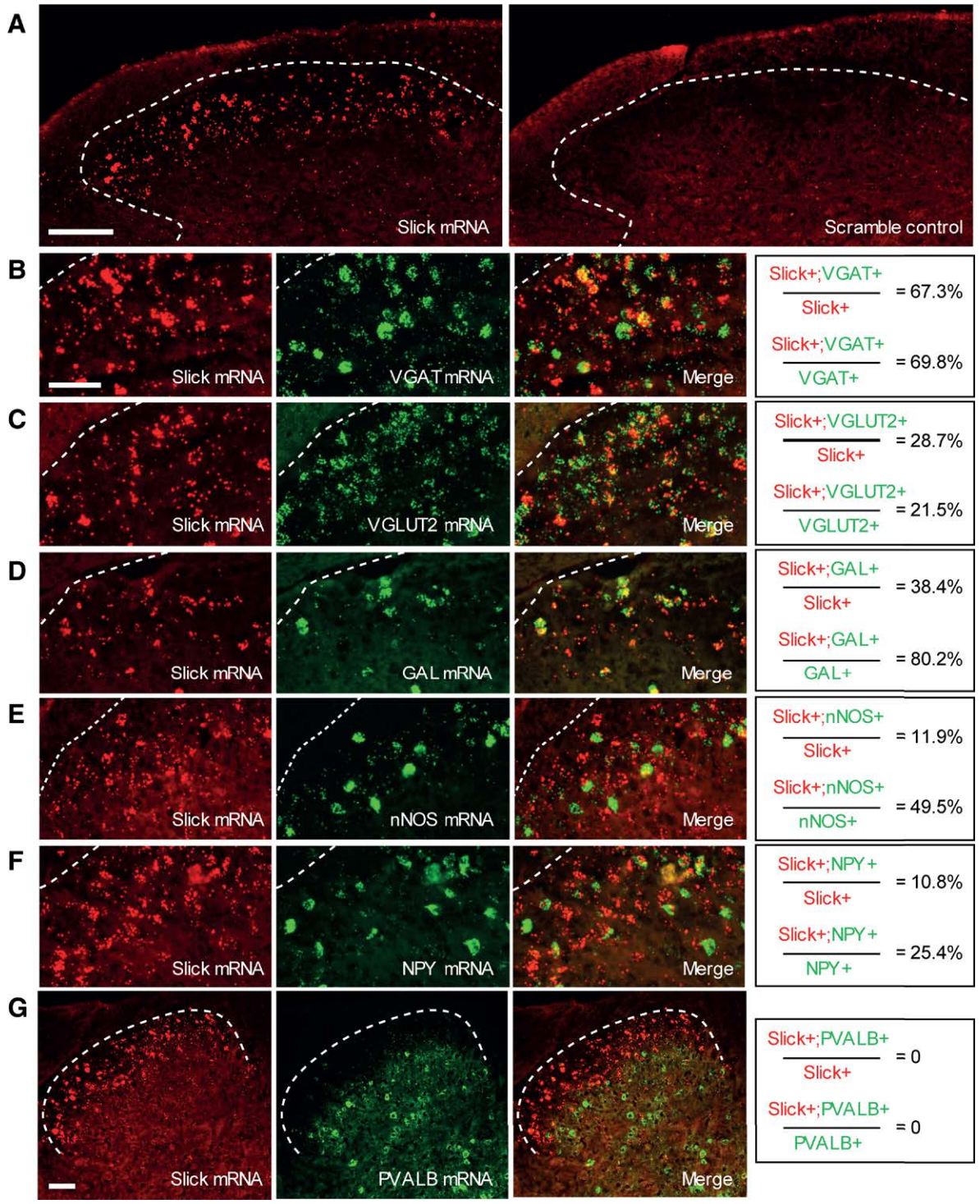

Fig. 3. Expression of Slick mRNA in the spinal dorsal horn. (*A*) Distribution of Slick mRNA (*left*) in the dorsal horn of the spinal cord assessed by fluorescent *in situ* hybridization. No hybridization signal was detected using a scramble control (*right*). (*B* and *C*) Double *in situ* hybridization of Slick mRNA with mRNA of VGAT (*B*), a marker of inhibitory interneurons, and of VGLUT2 (*C*), a marker of excitatory interneurons. (*D* through *G*) Double *in situ* hybridization of Slick mRNA with mRNA of galanin (GAL; *D*), neuronal nitric oxide synthase (nNOS; *E*), neuropeptide Y (NPY; *F*), and parvalbumin (PVALB; *G*), which mark subpopulations of inhibitory interneurons. The percentage of Slick$^+$ neurons that coexpress the selected marker and the percentage of marker-positive neurons that coexpress Slick are presented in the column (*right*). Scale bar = 100 μm (*A*); scale bars = 50 μm (*B* and *G*).

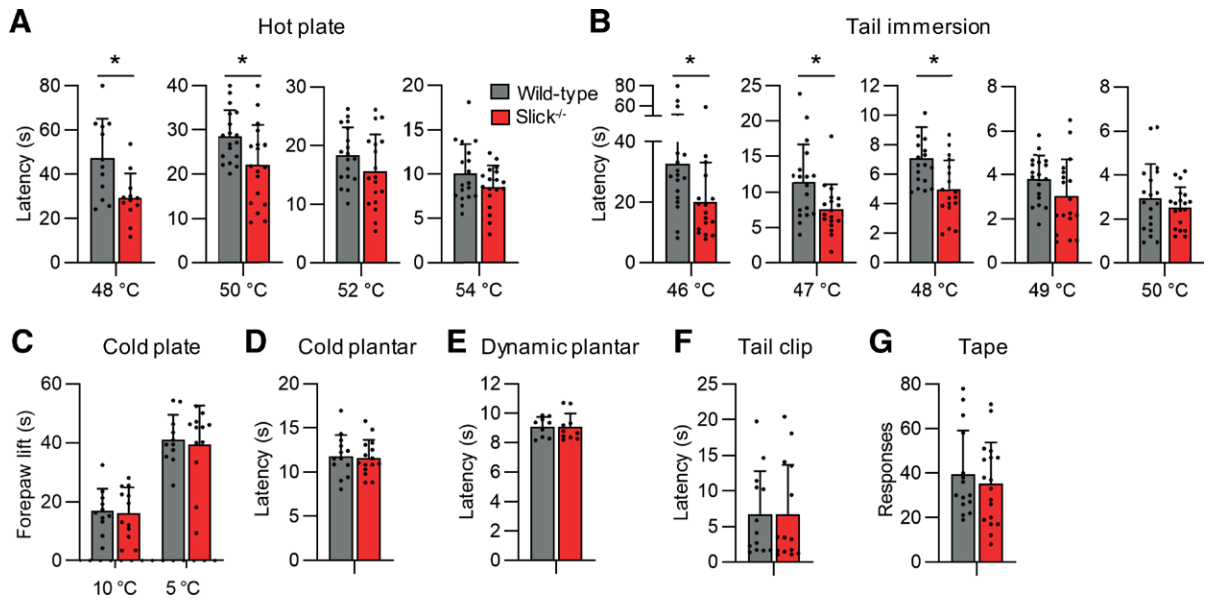

Fig. 4. Behavioral responses of Slick$^{-/-}$ mice to heat, cold, and mechanical stimuli. (*A* and *B*) Responses to heat stimuli. (*A*) In the hot plate test, Slick$^{-/-}$ mice showed significantly reduced latencies compared with wild-type mice at 48° and 50°C, but showed unaltered responses at 52° and 54°C (48°C [n = 12 per group]: $t_{22} = 2.99$, $P = 0.007$; 50°C [n = 18 per group]: $t_{34} = 2.55$, $P = 0.015$; 52°C [n = 18 per group]: $t_{34} = 1.48$, $P = 0.149$; 54°C [n = 18 per group]: $t_{34} = 1.58$, $P = 0.122$). (*B*) In the tail-immersion test, tail withdrawal latencies were significantly reduced in Slick$^{-/-}$ mice compared with wild-type mice at 46°C ($t_{32} = 2.24$, $P = 0.032$; n = 17 per group), 47°C ($t_{34} = 2.53$, $P = 0.016$; n = 18 per group), and 48°C ($t_{34} = 3.05$, $P = 0.004$; n = 18 per group), but were normal at 49°C ($t_{34} = 1.65$, $P = 0.107$; n = 18 per group) and 50°C ($t_{36} = 1.00$, $P = 0.323$; n = 19 per group). (*C* and *D*) Responses to cold stimuli. (*C*) On a cold plate maintained at 10°C or 5°C, the duration of forepaw lifting within 1 min was comparable between groups (10°C: $t_{21} = 0.22$, $P = 0.831$; n = 12 [Slick$^{-/-}$], n = 11 [wild-type]; 5°C: $t_{21} = 0.33$, $P = 0.744$; n = 12 [Slick$^{-/-}$], n = 11 [wild-type]). (*D*) Paw withdrawal latencies in the cold plantar test were similar between groups ($t_{26} = 0.24$, $P = 0.814$; n = 15 [Slick$^{-/-}$], n = 13 [wild-type]). (*E* through *G*) Responses to mechanical stimuli. Slick$^{-/-}$ mice showed normal responses to mechanical stimuli in the dynamic plantar test ([*E*] $t_{17} = 0.06$, $P = 0.956$; n = 10 [Slick$^{-/-}$], n = 9 [wild-type]); tail-clip test ([*F*] $t_{25} = 0.02$, $P = 0.982$; n = 14 [Slick$^{-/-}$], n = 13 [wild-type]) and tape response test ([*G*] $t_{31} = 0.64$, $P = 0.526$; n = 18 [Slick$^{-/-}$], n = 15 [wild-type]). Data are presented as mean ± SD. *$P < 0.05$.

$P = 0.982$; fig. 4F) and to innocuous mechanical stimuli evoked by applying an adhesive tape to the hairy skin of the back (Slick$^{-/-}$ [n = 18]: 35.3 ± 18.5 s [95% CI, 26.1 to 44.5]; wild-type [n = 15]: 39.5 ± 19.6 s [95% CI, 28.7 to 50.4]; $P = 0.526$; fig. 4G). Altogether, these behavioral assays implicate a specific alteration of noxious heat sensation in Slick$^{-/-}$ mice.

Slick in the Spinal Dorsal Horn Is Dispensable for Heat Sensation

Given the significant expression of Slick in dorsal horn neurons, we aimed to assess to what extent Slick in intrinsic spinal cord neurons contributes to pain processing. For that purpose, we crossed Lbx1-Cre mice, in which Cre is mainly restricted to neurons of the dorsal spinal cord and the dorsal hindbrain,[12] with Slick$^{fl/fl}$ mice. In the resulting conditional knockouts (referred to as Lbx1-Slick$^{-/-}$), Slick mRNA expression in the spinal cord was significantly downregulated as compared to control (Slick$^{fl/fl}$) mice (Lbx1-Slick$^{-/-}$ [n = 4]: 0.3 ± 0.0 [95% CI, 0.2 to 0.3]; control [n = 4]: 0.9 ± 0.0 [95% CI, 0.9 to 0.9]; $P < 0.001$; fig. 5A), whereas Slick mRNA expression was unaltered in dorsal root ganglia (Lbx1-Slick$^{-/-}$ [n = 4]: 0.9 ± 0.1 *vs.* 1.0 ± 0.1; $P = 0.420$; fig. 5A) or brain cortex (Lbx1-Slick$^{-/-}$ [n = 4] *vs.* control [n = 4]: 4.0 ± 0.2 *vs.* 3.7 ± 0.3; $P = 0.122$; fig. 5A). Immunostainings confirmed a considerable reduction of Slick immunoreactivity in the spinal dorsal horn of Lbx1-Slick$^{-/-}$ mice (fig. 5B), and the antibody specificity was confirmed by staining of Slick$^{-/-}$ tissues (fig. 5B). The expression of Slack mRNA in dorsal root ganglia, the spinal cord and brain cortex was not compensatory regulated in Lbx1-Slick$^{-/-}$ mice (Lbx1-Slick$^{-/-}$ [n = 4] *vs.* control [n = 4]: dorsal root ganglia: 2.4 ± 0.3 *vs.* 2.1 ± 0.3; $P = 0.218$; spinal cord: 1.1 ± 0.2 *vs.* 1.0 ± 0.1; $P = 0.816$; cortex: 1.1 ± 0.3 *vs.* 1.0 ± 0.3; $P = 0.816$; fig. 5C). Furthermore, in the rotarod test, Lbx1-Slick$^{-/-}$ and control mice demonstrated intact motor coordination, as analyzed in the rotarod test (median fall-off latencies: Lbx1-Slick$^{-/-}$ [n = 14]: 120 s [interquartile range, 120.0 to 120.0]; control [n = 18]: 120 s [interquartile range, 120.0 to 120.0]; $P = 0.806$), indicating intact motor coordination and balance.

We then tested heat, cold, and mechanical sensations in Lbx1-Slick$^{-/-}$ mice. Unlike Slick$^{-/-}$ mice, the responses to acute heat stimuli in the hot plate (Lbx1-Slick$^{-/-}$ [n = 13] *vs.* control [n = 14]: 48°C: 48.5 ± 18.4 s *vs.* 51.3 ± 14.8 s; $P = 0.661$; 50°C: 27.4 ± 7.6 s *vs.* 25.2 ± 4.7 s; $P = 0.383$; and Lbx1-Slick$^{-/-}$ [n = 12] *vs.* control [n = 12]: 52°C: 18.2 ± 4.0 s *vs.* 18.9 ± 3.5 s; $P = 0.665$; 54°C, 12.1 ± 2.6 s *vs.* 11.2 ± 3.1 s; $P = 0.431$) and tail immersion test (Lbx1-Slick$^{-/-}$ [n = 16] *vs.* control [n = 16]: 46°C: 13.8 ± 8.1 s *vs.* 14.8 ± 7.6 s; $P = 0.640$; 47°C: 5.5 ± 2.4 s *vs.* 8.0 ± 4.6 s; $P = 0.496$; 48°C: 3.4 ± 1.5 s *vs.* 3.4 ± 2.0 s; $P = 0.942$; 49°C: 2.0 ± 0.8 s *vs.* 1.7 ± 0.5 s; $P = 0.856$) were unaltered in Lbx1-Slick$^{-/-}$ mice (fig. 5, D and E). Moreover, similar to Slick$^{-/-}$ mice, Lbx1-Slick$^{-/-}$ mice demonstrated normal responses to cold and mechanical stimuli (cold plate, cold plantar, dynamic plantar, tail-clip, and tape-response test: data not shown). These data suggest that Slick in dorsal horn neurons is dispensable for the immediate behavioral responses to acute heat, cold, and mechanical stimuli.

Slick in the Spinal Dorsal Horn Modulates Capsaicin-induced Behavior

We then analyzed the tonic pain behavior of Slick$^{-/-}$ and wild-type mice using the capsaicin test. Intraplantar injection of capsaicin (5 μg) into a hind paw elicits a robust paw licking behavior that typically lasts for a few minutes and is mainly driven by TRPV1 activation.[28] As shown in figure 6A, the paw licking response was similar in Slick$^{-/-}$ and wild-type mice during the first 5 min after the capsaicin injection (Slick$^{-/-}$ [n = 8]: 27.0 ± 11.1 s [95% CI, 17.7 to 36.4]; wild-type [n = 7]: 21.4 ± 7.7 s [95% CI, 14.3 to 28.5]; $P = 0.574$). Interestingly however, Slick$^{-/-}$ mice continued to lick the paw during 6 to 20 min after the capsaicin injection, while this late-stage licking behavior was virtually absent in wild-type mice. The sum of licking time during the 6 to 20 min period was significantly increased in Slick$^{-/-}$ mice compared with wild-type mice (Slick$^{-/-}$ [n = 8]: 45.6 ± 30.1 s [95% CI, 19.8 to 71.4]; wild-type [n = 7]: 13.1 ± 16.1 s [95% CI, –1.8 to 28.0]; $P = 0.006$; fig. 6A; results for female and male cohorts are presented in Supplemental Digital Content 3 fig. 3, A and B, http://links.lww.com/ALN/C807), suggesting that Slick controls the nocifensive behavior at late stages of the capsaicin test.

We then exposed Lbx1-Slick$^{-/-}$ mice to capsaicin injection. Notably, similar to Slick$^{-/-}$ mice, the licking behavior in Lbx1-Slick$^{-/-}$ mice was enhanced in the later phase, *i.e.*, 6 to 20 min after capsaicin injection (Lbx1-Slick$^{-/-}$

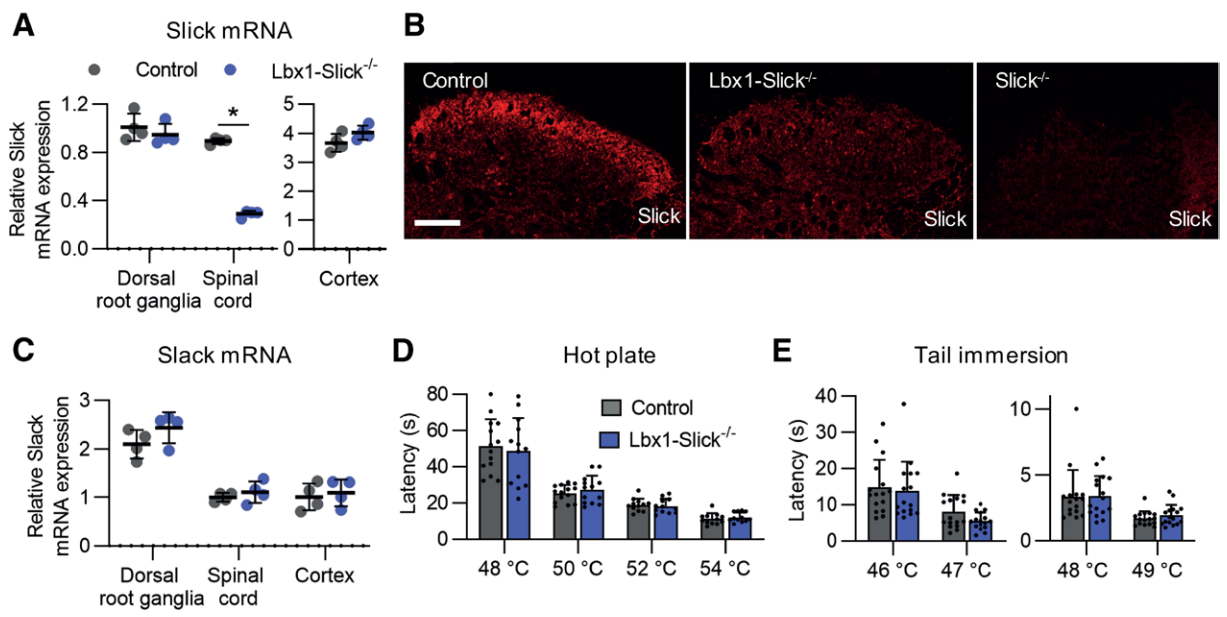

Fig. 5. Lbx1-Slick$^{-/-}$ mice show normal heat responses. (*A* and *B*) Confirmation of tissue-specific deletion of Slick in Lbx1-Slick$^{-/-}$ mice. (*A*) Quantitative reverse transcription polymerase chain reaction revealed that in Lbx1-Slick$^{-/-}$ mice, Slick mRNA is selectively reduced in the spinal cord ($t_6 = 32.7$, $P < 0.001$), but remains unaltered in dorsal root ganglia ($t_6 = 0.87$, $P = 0.420$) and the brain cortex ($t_6 = 1.80$, $P = 0.122$; n = 4 per group). Values were normalized to wild-type dorsal root ganglia. (*B*) Immunostaining revealed that Slick immunoreactivity in the superficial dorsal horn is considerably reduced in spinal cords of Lbx1-Slick$^{-/-}$ mice compared with control mice. Weak Slick immunoreactivity was detected throughout the spinal cords of Lbx1-Slick$^{-/-}$ mice, as revealed by comparison with spinal cords of Slick$^{-/-}$ mice. (*C*) Expression of Slack mRNA in Lbx1-Slick$^{-/-}$ and control mice is comparable in dorsal root ganglia ($t_{18} = 1.86$, $P = 0.218$), the spinal cord ($t_{18} = 0.58$, $P = 0.816$), and the brain cortex ($t_{18} = 0.47$, $P = 0.816$; n = 4 per group). (*D* and *E*) Responses to heat stimuli in Lbx1-Slick$^{-/-}$ mice. The behavior of Lbx1-Slick$^{-/-}$ mice was unaltered as compared to control mice in the hot plate test ([*D*] 48°C: $t_{25} = 0.44$, $P = 0.661$; n = 13 [Lbx1-Slick$^{-/-}$], n = 14 [control]; 50°C: $t_{25} = 0.89$, $P = 0.383$; n = 13 [Lbx1-Slick$^{-/-}$], n = 14 [control]; 52°C: $t_{22} = 0.44$, $P = 0.665$; n = 12 per group; 54°C: $t_{22} = 0.80$, $P = 0.431$; n = 12 per group), and in the tail-immersion test ([*E*] 46°C: $t_{30} = 0.37$, $P = 0.714$; 47°C: $t_{30} = 1.85$, $P = 0.075$; 48°C: $t_{30} = 0.05$, $P = 0.957$; 49°C: $t_{30} = 1.00$, $P = 0.323$; n = 16 per group). Data are presented as mean ± SD. *$P < 0.05$. Scale bar = 100 μm (*B*).

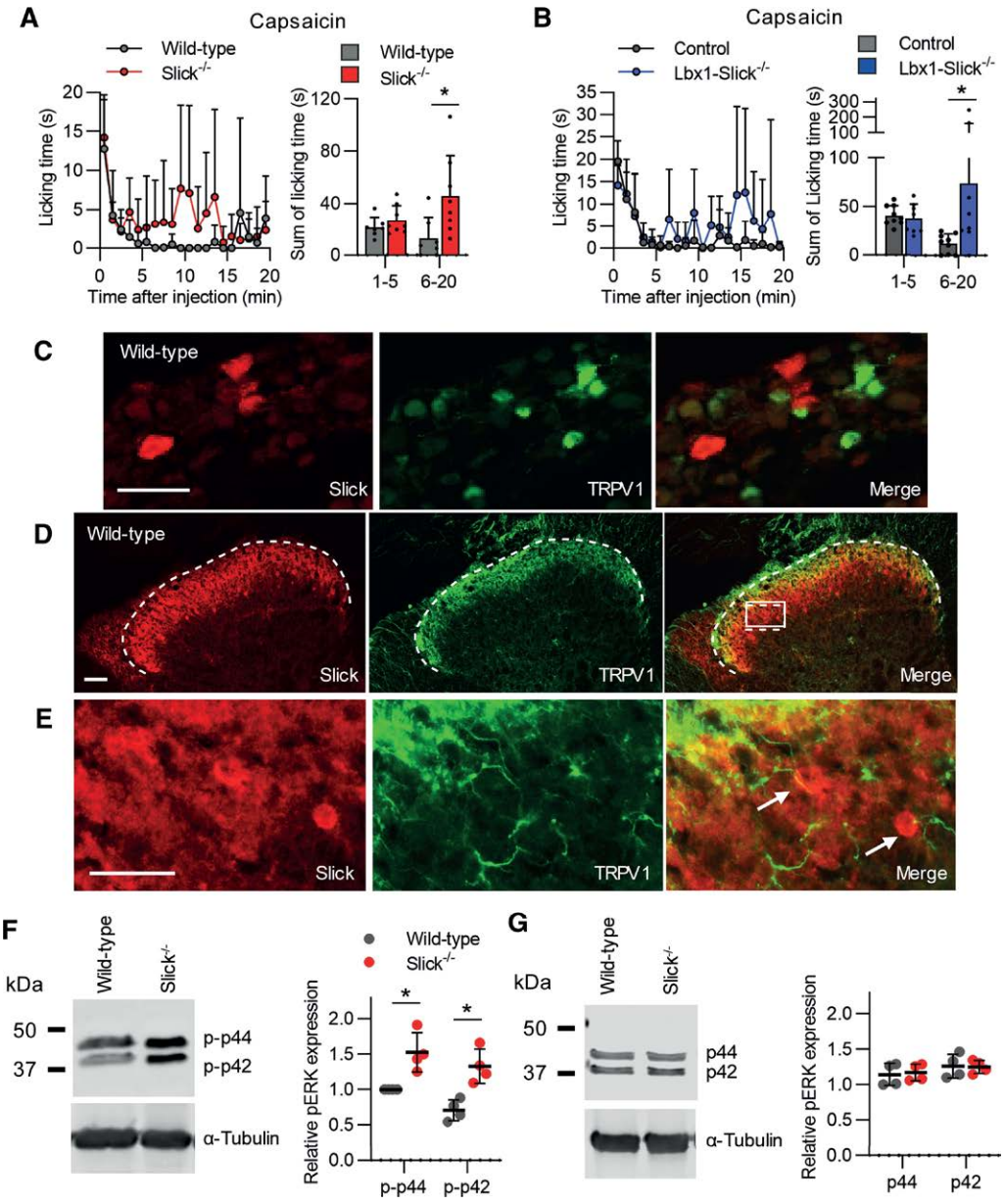

Fig. 6. Increased capsaicin-induced pain behavior in Slick$^{-/-}$ and Lbx1-Slick$^{-/-}$ mice. (*A* and *B*) Capsaicin test in Slick$^{-/-}$ and wild-type mice. *(A)* Capsaicin-induced licking behavior. *(A, left)* Time course of paw licking induced by injection of 5 μg capsaicin into a hind paw. *(A, right)* Sum of paw licking shows that the behavior of Slick$^{-/-}$ mice compared with wild-type mice is normal during the 0- to 5-min period ($t_{26} = 0.57$, $P = 0.574$; n = 8 [Slick$^{-/-}$], n = 7 [wild-type]), but significantly increased during the 6- to 20-min period ($t_{26} = 3.30$, $P = 0.006$; n = 8 [Slick$^{-/-}$], n = 7 [wild-type]) after the capsaicin injection. (*B*) Capsaicin test in Lbx1-Slick$^{-/-}$ and control mice. Similar to Slick$^{-/-}$ mice, Lbx1-Slick$^{-/-}$ mice exhibited an unaltered paw-licking behavior compared with control mice in the first 5 min after capsaicin injection ($t_{30} = 0.16$, $P = 0.871$; n = 8 [Slick$^{-/-}$], n = 9 [wild-type]), whereas the paw licking was significantly increased during the 6- to 20-min period ($t_{30} = 2.97$, $P = 0.012$; n = 8 [Slick$^{-/-}$], n = 9 [wild-type]). (*C*) Double immunostaining of Slick and transient receptor potential vanilloid 1 (TRPV1) in dorsal root ganglia reveals that Slick is virtually absent from TRPV1-positive sensory neurons. (*D*) Double immunostaining of Slick and TRPV1 in the spinal cord shows some overlap of Slick and TRPV1 immunoreactivity. (*E*) Higher magnification of the area marked in the merge picture in *D*. Slick immunoreactivity is in close proximity to the central projections of TRPV1-positive afferent fibers. (*F*) Western blot analysis of phosphorylated extracellular signal–regulated kinase in the spinal cord of wild-type and Slick$^{-/-}$ mice 10 min after capsaicin injection into a hind paw. Data show that phosphorylation of both p44 ($t_{12} = 3.72$, $P = 0.003$; n = 4 per group) and p42 ($t_{12} = 4.39$, $P = 0.002$; n = 4 per group) mitogen-activated protein kinase is significantly increased in Slick$^{-/-}$ mice as compared to wild-type mice. (*G*) Western blot of extracellular signal–regulated kinase in the spinal cord confirmed a similar expression of p44 ($t_{12} = 0.32$, $P = 0.940$; n = 4 per group) and p42 ($t_{12} = 0.10$, $P = 0.940$; n = 4 per group) in Slick$^{-/-}$ and wild-type mice. Values in *F* and *G* were normalized to α-tubulin as loading control and are expressed as relative values compared to phosphorylated p44 expression of wild-type control. Data are presented as mean ± SD. *$P < 0.05$. Scale bars = 50 μm (*C* and *D*); scale bar = 25 μm (*E*).

[n = 8]: 73.6 ± 85.4 s [95% CI, 2.2 to 145.1]; control [n = 9]: 12.3 ± 9.9 s [95% CI, 4.6 to 19.9]; P = 0.012; fig. 6B), but unaltered in the first 5 min as compared with control mice (Lbx1-Slick$^{-/-}$ [n = 8]: 37.5 ± 15.3 s [95% CI, 24.7 to 50.3]; control [n = 9]: 40.9 ± 10.3 s [95% CI, 33.0 to 48.9]; P = 0.871; fig. 6B; results for female and male cohorts are shown in Supplemental Digital Content 3 fig. 3, C and D, http://links.lww.com/ALN/C807). These results indicate that Slick in dorsal horn neurons modulates the pain behavior at a late stage of the capsaicin test.

To further explore this finding, we performed double-labeling immunostaining of Slick and TRPV1 in dorsal root ganglia and the spinal cord. Consistent with the observation that Slick is enriched in Aδ-fibers (fig. 1, F and H) and most TRPV1$^+$ sensory neurons are C-fibers,[28] we found that Slick$^+$ sensory neurons virtually do not coexpress TRPV1 (fig. 6C). In the dorsal horn of the spinal cord, Slick immunoreactivity is partly colocalized with the central projections of TRPV1$^+$ afferent fibers (fig. 6D). Interestingly, at higher magnification, we detected TRPV1$^+$ fibers in close proximity to somata of Slick$^+$ cells (fig. 6E), pointing to a possible interaction of Slick$^+$ dorsal horn neurons and TRPV1$^+$ sensory neurons that respond to capsaicin.

We then performed Western blot analyses of pERK as a marker for neuronal activation in the dorsal horn.[29] Lumbar (L4–L5) spinal cords from wild-type and Slick$^{-/-}$ mice were obtained 10 min after intraplantar capsaicin injection, *i.e.*, at a time point of increased paw licking in Slick$^{-/-}$ mice (compared to fig. 6A). Of note, phosphorylation of ERK1 (p44 MAPK) and ERK2 (p42 MAPK), which both are detected by the anti-pERK antibody, was significantly increased in Slick$^{-/-}$ mice compared with wild-type mice (p-p44, Slick$^{-/-}$: 1.5 ± 0.3 [95% CI, 1.1 to 2.0], wild-type: 1.0 ± 0.0 [95% CI, 1.0 to 1.0], P = 0.003; p-p42, Slick$^{-/-}$: 1.3 ± 0.2 [95% CI, 0.9 to 1.7], wild-type: 0.7 ± 0.1 [95% CI, 0.5 to 0.9]; P = 0.002; n = 4/group; fig. 6F). Control experiments confirmed that ERK1 and ERK2 protein expression is similar between wild-type and Slick$^{-/-}$ mice in the lumbar spinal cord (p44, Slick$^{-/-}$: 1.2 ± 0.1 [95% CI, 1.0 to 1.4], wild-type: 1.1 ± 0.2 [95% CI, 0.9 to 1.4]; P = 0.940; p42, Slick$^{-/-}$: 1.3 ± 0.1 [95% CI, 1.1 to 1.4], wild-type: 1.3 ± 0.2 [95% CI, 1.0 to 1.5]; P = 0.940; n = 4/group; fig. 6G). Together, these data indicate that Slick modulates the activity of dorsal horn neurons in response to TRPV1 activation in sensory neurons.

Slick Is Dispensable for Allyl Isothiocyanate–induced Pain Behavior

In response to peer review, we assessed the behavior after intraplantar injection of the transient receptor potential ankyrin 1 (TRPA1) activator, allyl isothiocyanate, to explore the role of Slick in TRPA1-dependent pain processing. Compared to wild-type mice, Slick$^{-/-}$ mice demonstrated unaltered licking behavior after allyl isothiocyanate injection (Slick$^{-/-}$ [n = 8]: 210.4 ± 127.0 s [95% CI, 104.1 to 316.6]; wild-type [n = 6]: 253.9 ± 166.3 s [95% CI, 79.4 to 428.4]; P = 0.587; fig. 7A). We also tested allyl isothiocyanate–induced mechanical pain sensitivity, but did not observe significant differences between Slick$^{-/-}$ and wild-type mice (baseline: Slick$^{-/-}$ [n = 8]: 0.9 ± 0.1 g [95% CI, 0.8 to 1.0]; wild-type [n = 6]: 0.8 ± 0.1 g [95% CI, 0.7 to 0.9]; P = 0.844; 1 h: Slick$^{-/-}$ [n = 8]: 0.2 ± 0.1 g [95% CI, 0.1 to 0.3]; wild-type [n = 6]: 0.2 ± 0.1 g [95% CI, 0.1 to 0.3]; P > 0.999; 3 h: Slick$^{-/-}$ [n = 8]: 0.2 ± 0.1 g [95% CI, 0.1 to 0.3]; wild-type [n = 6]: 0.2 ± 0.1 g [95% CI, 0.1 to 0.3]; P = 0.935; 5 h: Slick$^{-/-}$ [n = 8]: 0.3 ± 0.2 g [95% CI, 0.2 to 0.4]; wild-type [n = 6]: 0.2 ± 0.1 g [95% CI, 0.1 to 0.2]; P = 0.230; 24 h: Slick$^{-/-}$ [n = 8]: 0.5 ± 0.2 g [95% CI, 0.4 to 0.7]; wild-type: 0.4 ± 0.2 g [95% CI, 0.2 to 0.6]; P = 0.917; fig. 7B). Similar to Slick$^{-/-}$ mice, Lbx1-Slick$^{-/-}$ mice demonstrated intact licking behavior (Lbx1-Slick$^{-/-}$ [n = 7]: 158.3 ± 111.5 s [95% CI, 55.2 to 261.5]; control [n = 8]: 103.0 ± 90.5 s [95% CI, 27.3 to 178.6]; P = 0.308; fig. 7C) and mechanical hypersensitivity (baseline: Lbx1-Slick$^{-/-}$ [n = 5]: 0.9 ± 0.1 g [95% CI, 0.8 to 1.0]; control [n = 6]: 0.9 ± 0.1 g [95% CI, 0.7 to 1.0]; P = 0.995; 1 h: Lbx1-Slick$^{-/-}$ [n = 5]: 0.2 ± 0.1 g [95% CI, 0.1 to 0.3]; control [n = 6]: 0.2 ± 0.1 g [95% CI, 0.1 to 0.3]; P = 0.998; 3 h: Lbx1-Slick$^{-/-}$ [n = 5]: 0.2 ± 0.1 g [95% CI, 0.1 to 0.4]; control [n = 6]: 0.2 ± 0.1 g [95% CI, 0.1 to 0.4]; P > 0.999; 5 h: Lbx1-Slick$^{-/-}$ [n = 5]: 0.3 ± 0.1 g [95% CI, 0.1 to 0.5]; control [n = 6]: 0.2 ± 0.1 g [95% CI, 0.1 to 0.4]; P = 0.986; 24 h: Lbx1-Slick$^{-/-}$ [n = 5]: 0.9 ± 0.2 g [95% CI, 0.6 to 1.2]; control: 0.8 ± 0.2 g [95% CI, 0.6 to 1.0]; P = 0.997; fig. 7D) compared with control mice. Thus, unlike the capsaicin test, Slick seems not to be involved in allyl isothiocyanate–induced pain.

Slick in the Spinal Dorsal Horn Modulates Somatostatin Signaling

To further explore the functional role of Slick in dorsal horn neurons, we focused on the neuropeptide somatostatin, because (1) previous studies reported that somatostatin is released from capsaicin-sensitive sensory nerve terminals in the dorsal horn[30]; (2) immunostaining revealed that SSTR2, the most abundant somatostatin receptor in the spinal cord,[31] is expressed by virtually all GAL$^+$ cells in the dorsal horn[32]—of which approximately 80% are Slick$^+$ (fig. 3D); and (3) single-cell RNA-sequencing data further support a colocalization of SSTR2 and Slick in dorsal horn neuron populations (*i.e.,* both were detected in the Gaba2, 3, 8, and 9 populations of inhibitory interneurons in the dorsal horn).[10] In accordance with these data, we observed a substantial degree of coexpression of Slick mRNA and SSTR2 mRNA in the dorsal horn using double *in situ* hybridization experiments; 50.4 ± 1.6% of Slick$^+$ cells expressed SSTR2, whereas 61.3 ± 7.4% of SSTR2$^+$ cells were positive for Slick (fig. 8A).

We then assessed whether Slick and somatostatin pathways might functionally interact in the dorsal horn. For that purpose, we intrathecally administered the selective SSTR2

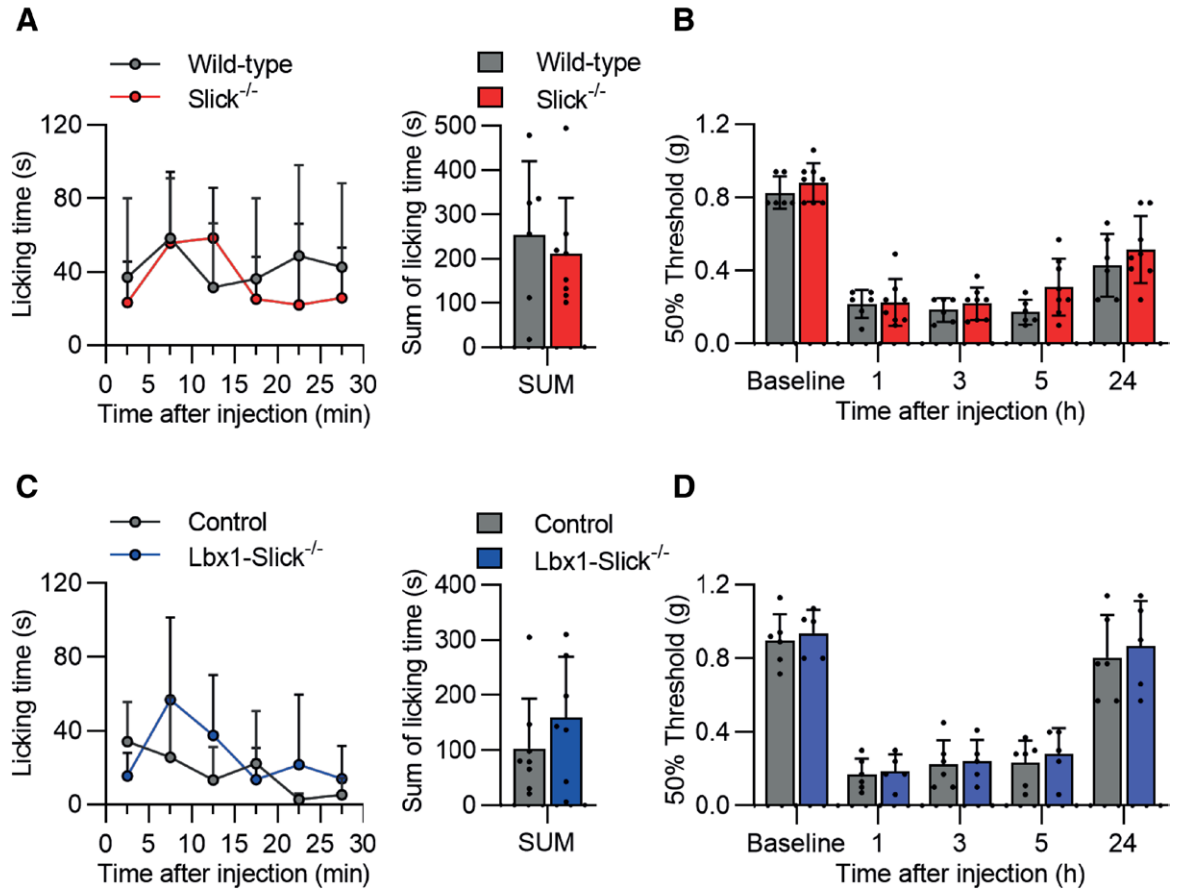

Fig. 7. Allyl isothiocyanate–induced pain behavior in Slick$^{-/-}$ and Lbx1-Slick$^{-/-}$ mice. (*A*) Allyl isothiocyanate test in Slick$^{-/-}$ and wild-type mice. (*A, left*) Time course of paw licking induced by injection of 10 nmol allyl isothiocyanate into a hind paw. (*A, right*) Sum of paw licking shows that the behavior of Slick$^{-/-}$ mice is comparable to wild-type mice during 30 min after the allyl isothiocyanate injection ($t_{12} = 0.56$, $P = 0.587$; n = 8 [Slick$^{-/-}$], n = 6 [wild-type]). (*B*) Intraplantar injection of allyl isothiocyanate elicits similar mechanical hypersensitivity in Slick$^{-/-}$ and wild-type mice ($F[4,48] = 0.91$, $P = 0.464$; n = 8 [Slick$^{-/-}$], n = 6 [wild-type]). (*C*) Allyl isothiocyanate test in Lbx1-Slick$^{-/-}$ and control mice. (*Left*) Time course of paw licking induced by injection of 10 nmol allyl isothiocyanate into a hind paw. (*Right*) Sum of paw licking shows that the behavior of Lbx1-Slick$^{-/-}$ mice is comparable to control mice during 30 min after the allyl isothiocyanate injection ($t_{13} = 1.06$, $P = 0.308$; n = 7 [Lbx1-Slick$^{-/-}$], n = 8 [control]). (*D*) Intraplantar injection of allyl isothiocyanate elicits similar mechanical hypersensitivity in Lbx1-Slick$^{-/-}$ and control mice ($F[4,36] = 0.05$, $P = 0.464$; n = 5 [Lbx1-Slick$^{-/-}$], n = 6 [control]). Data are presented as mean ± SD.

antagonist CYN-154806[18] in Slick$^{-/-}$ and wild-type mice 30 min before intraplantar capsaicin injection and analyzed the pain behavior. Interestingly, the enhanced paw licking in the later phase (6 to 20 min after capsaicin injection; fig. 6A) was absent in Slick$^{-/-}$ mice pretreated with CYN-154806 (Slick$^{-/-}$ [n = 5] *vs.* wild-type [n = 6]: 6.8 ± 4.1 s *vs.* 10.1 ± 12.9 s, respectively; $P = 0.862$; fig. 8B). Similarly, intrathecal CYN-154806 pretreatment prevented the later phase of paw licking in Lbx1-Slick$^{-/-}$ mice (Lbx1-Slick$^{-/-}$ [n = 5] *vs.* control [n = 5]: 16.1 ± 18.9 s *vs.* 19.1 ± 9.9 s, respectively; $P = 0.942$; fig. 8C [compared to fig. 6B]). Together, these data point to a signaling pathway that involves TRPV1^{+} sensory neurons and Slick^{+}/SSTR2^{+} dorsal horn neurons.

Recent studies revealed that somatostatin contributes to the processing of itch in the dorsal horn, and that intrathecal administration of somatostatin or its analog octreotide induces scratching in rodents *via* binding to SSTR2 and subsequent inhibition of inhibitory interneurons.[18,33] We therefore analyzed the scratching behavior of Slick$^{-/-}$ and wild-type mice after intrathecal injection of octreotide. Interestingly, the scratching behavior induced by 100 ng octreotide was observed in wild-type mice but considerably reduced in Slick$^{-/-}$ mice (Slick$^{-/-}$: 6.1 ± 6.7 bouts [95% CI, 0.5 to 11.7]; wild-type: 47.5 ± 51.1 bouts [95% CI, 4.8 to 90.2]; $P = 0.039$, n = 8/group; fig. 8D; results for female and male cohorts are presented in Supplemental Digital Content 4 fig. 4, A and B, http://links.lww.com/ALN/

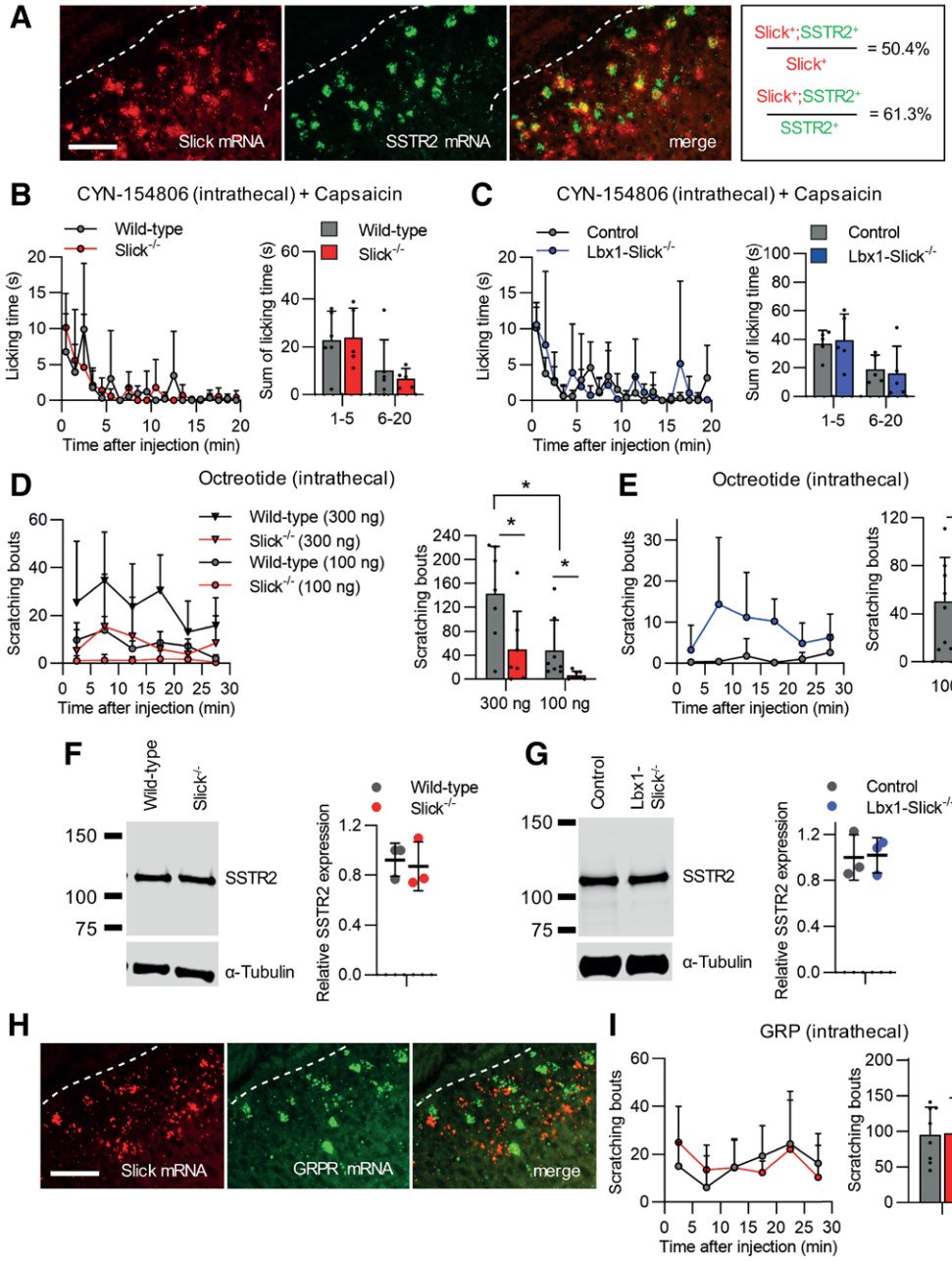

Fig. 8. Slick interacts with somatostatin pathways in pain and itch. (*A*) Double *in situ* hybridization experiments show that Slick and somatostatin receptor 2 (SSTR2) are colocalized in the spinal dorsal horn. (*B* and *C*) Capsaicin test after intrathecal pretreatment with the SSTR2 antagonist CYN-154806 (500 ng in 5 µl NaCl, 0.9%). (*B*) In Slick$^{-/-}$ mice, intrathecal CYN-154806 delivery 30 min before capsaicin injection into a hind paw prevented increased paw licking from 6 to 20 min after capsaicin injection ([compare with fig. 6A] 0 to 5 min: $t_{18} = 0.17$, $P = 0.871$; 5 to 20 min: $t_{18} = 0.50$, $P = 0.862$; n = 5 [Slick$^{-/-}$], n = 6 [wild-type]). (*C*) Similarly, increased paw licking at 6 to 20 min after capsaicin injection (compare with fig. 6B) did not occur in Lbx1-Slick$^{-/-}$ mice pretreated with intrathecal CYN-154806 (0 to 5 min: $t_{16} = 0.26$, $P = 0.942$; 6 to 20 min: $t_{16} = 0.31$, $P = 0.942$; n = 5 per group). (*D* and *E*) Somatostatin-induced itch behavior in Slick$^{-/-}$ and Lbx1-Slick$^{-/-}$ mice. After intrathecal injection of the somatostatin analog octreotide (100 ng and 300 ng in 5 µl NaCl, 0.9%), the scratching behavior during a 30-min period was significantly reduced in Slick$^{-/-}$ mice compared with wild-type mice ([*D*] 100 ng: $t_{14} = 2.27$, $P = 0.039$; n = 8 per group; 300 ng: $t_{12} = 2.43$, $P = 0.032$; n = 7 per group), and in Lbx1-Slick$^{-/-}$ mice compared with control mice ([*E*] $t_{14} = 3.35$, $P = 0.005$; n = 8 per group). (*F* and *G*) Western blot of SSTR2 in the spinal cord from Slick$^{-/-}$ and wild-type mice ([*F*] $t_4 = 0.38$, $P = 0.725$; n = 3 per group) and from Lbx1-Slick$^{-/-}$ and control mice ([*G*] $t_4 = 0.13$, $P = 0.904$; n = 3 per group) demonstrated unaltered SSTR2 expression in the absence of Slick. Values were normalized to α-tubulin as loading control. (*H*) Double *in situ* hybridization of Slick mRNA with gastrin-releasing peptide receptor (GRPR) mRNA in the spinal dorsal horn shows virtually no colocalization. (*I*) After intrathecal injection of gastrin-releasing peptide (GRP), the scratching behavior was unaltered in Slick$^{-/-}$ mice compared to wild-type mice (unpaired two-tailed *t* test: $t_{11} = 0.10$, $P = 0.921$; n = 8 per group). Data are presented as mean ± SD. *$P < 0.05$. Scale bar = 50 µm.

C808). In response to peer review, we also injected 300 ng octreotide to investigate whether the effect is dose-dependent. Indeed, a dose-dependent response to intrathecal octreotide was observed in wild-type mice (100 ng [n = 8]: 47.5 ± 51.1 bouts [95% CI, 4.8 to 90.2]; 300 ng [n = 7]: 142.9 ± 79.1 bouts [95% CI, 69.7 to 216.1]; P = 0.005; fig. 8D), and again, a significant difference in scratching behavior was observed between genotypes (Slick$^{-/-}$ [n = 7]: 49.9 ± 63.4 bouts [95% CI, –8.8 to 108.5]; wild-type [n = 7]: 142.9 ± 79.1 bouts [95% CI, 69.7 to 216.1]; P = 0.032; fig. 8D). Similarly, Lbx1-Slick$^{-/-}$ mice showed a significantly reduced scratching behavior compared with control mice after intrathecal administration of 100 ng octreotide (Lbx1-Slick$^{-/-}$ [n = 8]: 6.1 ± 6.2 bouts [95% CI, 0.9 to 11.3]; control [n = 8]: 50.3 ± 36.8 bouts [95% CI, 19.5 to 81.0]; P = 0.005; fig. 8E; Supplemental Digital Content 4 fig. 4, C and D, http://links.lww.com/ALN/C808). Western blot experiments demonstrated similar SSTR2 levels in the spinal cord and dorsal root ganglia of wild-type and Slick$^{-/-}$ mice (Slick$^{-/-}$ [n = 3] *vs.* wild-type [n =3]: 0.9 ± 0.2 *vs.* 0.9 ± 0.1, respectively; P = 0.725; fig. 7F), and of control and Lbx1-Slick$^{-/-}$ mice (Lbx1-Slick$^{-/-}$ [n = 3] *vs.* control [n = 3]: 1.0 ± 0.2 *vs.* 1.0 ± 0.2, respectively; P = 0.904; fig. 8G), suggesting that there was no compensatory regulation due to the Slick knockout that might have contributed to the observed itch behavior. Together, these data suggest that Slick expressed in dorsal horn neurons is required for the behavioral response to intrathecally administered octreotide.

In control experiments, we intrathecally injected GRP, which evokes scratching *via* activation of its receptor, GRPR, which is almost exclusively expressed in excitatory interneurons.[2,10] Double *in situ* hybridization experiments revealed that GRPR mRNA is virtually absent from Slick^{+} neurons in the dorsal horn (fig. 8H). In line with this observation, the scratching behavior after intrathecal injection of GRP was not significantly altered in Slick$^{-/-}$ mice as compared with wild-type mice (Slick$^{-/-}$ [n = 8] *vs.* wild-type [n = 8]: 97.8 ± 49.5 bouts *vs.* 95.5 ± 38.6 bouts, respectively; P = 0.921; fig. 8I), indicating that the scratching behavior is not generally impaired in Slick knockouts. Altogether, these data suggest that Slick at distinct neuronal populations contributes to pain and itch processing.

Slick Is Not Required for Histamine or Chloroquine-induced Itch

Recent evidence has indicated that Slick$^{-/-}$ mice exhibit normal responses to the pruritic stimuli histamine and chloroquine,[6] but the specific contribution of Slick in the spinal dorsal horn to these pruritic stimuli is unclear. In response to peer review, we analyzed the scratching behavior after intradermal injection of histamine (200 μg) and chloroquine (200 μg) into the nape of the neck. As expected, histamine and chloroquine evoked robust scratching behavior in control mice (fig. 9, A and B). However, similar to Slick$^{-/-}$ and wild-type mice, no differences between Lbx1-Slick$^{-/-}$ mice and control littermates were observed for either histamine (Lbx1-Slick$^{-/-}$ [n = 5] *vs.* control [n = 6]: 59.6 ± 33.6 bouts *vs.* 101 ± 68.7 bouts, respectively; P = 0.249; fig. 9A) or chloroquine (Lbx1-Slick$^{-/-}$ [n = 5] *vs.* control n = 6]): 105.0 ± 28.0 bouts *vs.* 150 ± 88.3 bouts, respectively; P = 0.305; fig. 9B). These results suggest that Slick does not contribute to the processing of histamine- and chloroquine-evoked itch.

Discussion

Using multiple tissue-staining procedures, biochemical assays, and behavioral tests in global and conditional knockout mice, we delineated novel roles of the potassium channel Slick in sensations of both pain and itch. Using immunostaining and *in situ* hybridization, we identified Slick in Aδ-fiber nociceptors and in populations of interneurons in the spinal dorsal horn. Global Slick knockouts demonstrated increased nocifensive responses to noxious heat and intraplantar capsaicin, whereas the scratching behavior induced by intrathecal octreotide was abolished. Our experiments in tissue-specific Lbx1-Slick$^{-/-}$ mice revealed that Slick localized to dorsal horn neurons modulates capsaicin and octreotide behavior, but not noxious heat responses. In combination with previous reports,[6,7] the fact that in our study both Slick$^{-/-}$ and Lbx1-Slick$^{-/-}$ mice displayed normal responses to cold and mechanical stimuli, as well as after intrathecal GRP injection supports the hypothesis that Slick exerts distinct functions in pain and itch pathways.

Slick$^{-/-}$ mice showed enhanced sensitivity to heat stimuli at 48° to 50°C in the hot plate test and at 46° to 48°C in the tail-immersion test, but had normal responses after exposure to higher temperatures. This implies that Slick, which may inhibit pain processing in sensory neurons by potassium efflux across the plasma membrane, modulates heat pain only in a certain temperature range. During the past 2 decades, several ion channels have been identified as potential molecular thermosensors in mammals. These include various temperature-sensitive members of the TRP channel family (*e.g.,* TRPV1, TRPV2, TRPV3, TRPV4, TRPA1, TRPM2, TRPM3, and TRPM8); the Ca^{2+}-activated chloride channel, anoctamin 1; stromal interaction molecule 1 (STIM1); members of the two-pore domain potassium channel family (such as KCNK2, KCNK4, and KCNK10); and Nav1.8 channels.[34] Many studies illustrate that these channels are sensitive to heat or cold at different temperature ranges. This is also reflected by the phenotypic profile of respective knockout mice in pain models. For example, TRPV1$^{-/-}$ mice showed impaired behavioral responses in the hot plate test at temperatures greater than or equal to 52.5°C, as well as in the tail-immersion test at temperatures of 50°C, but showed normal responses at lower temperatures.[28] Furthermore, TRPM3$^{-/-}$ mice exhibited increased hot plate latencies at temperatures 52°C or

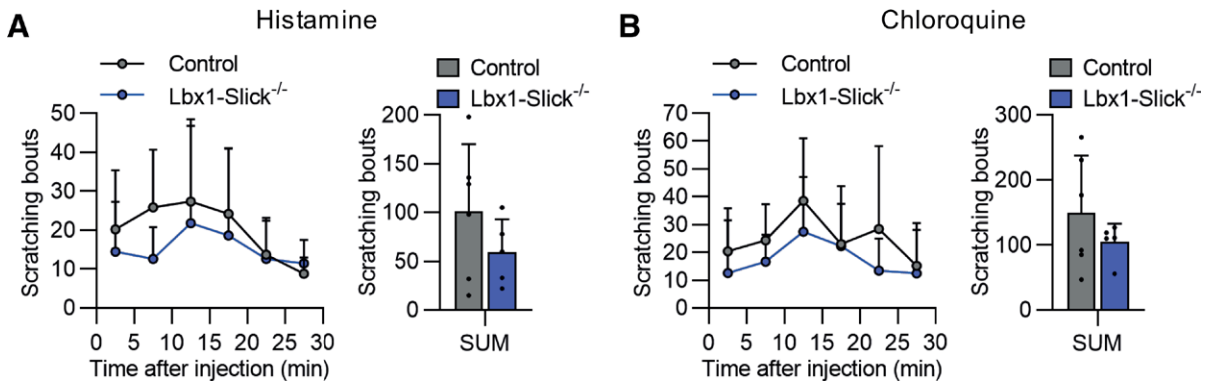

Fig. 9. Lbx1-Slick$^{-/-}$ mice show normal itch behavior after injection of histamine or chloroquine. (*A*) Histamine-induced scratching behavior in Lbx1-Slick$^{-/-}$ and control mice. (*A, left*) Time course of scratching bouts induced by injection of 200 µg histamine into the nape of the neck. (*A, right*) Total scratching bouts within 30 min after histamine injection. Note that histamine-induced itch behavior is comparable between Lbx1-Slick$^{-/-}$ and control mice (unpaired two-tailed *t* test: $t_9 = 1.23$, $P = 0.249$; n = 5 [Lbx1-Slick$^{-/-}$], n = 6 [control]). (*B*) Chloroquine-induced itch behavior in Lbx1-Slick$^{-/-}$ and control mice. (*B, left*) Time course of scratching bouts induced *via* 200 µg chloroquine injection into nape of the neck. (*B, right*) Total scratching bouts within 30 min after chloroquine injection (unpaired two-tailed *t* test: $t_9 = 1.09$, $P = 0.305$; n = 5 [Lbx1-Slick$^{-/-}$], n = 6 [control]). Data are presented as mean ± SD.

higher and unaltered latencies at 50°C, whereas their latencies in the tail immersion test were increased in the range of 45° to 57°C.[35] Conversely, TRPM2$^{-/-}$ mice showed a deficit in their sensation of non-noxious warm temperatures.[36] While TRPA1$^{-/-}$ mice demonstrated a normal behavior on a 50 to 55°C hot plate,[37] a recent study revealed that triple knockouts lacking TRPA1, TRPV1 and TRPM3 show considerably reduced responses to noxious heat at 45° to 52°C in the hot plate test and at 45° to 57°C in the tail-flick test,[13,38] implicating that noxious heat sensing in a wide temperature spectrum essentially relies on these three TRP channels. Future work will be necessary to determine the mechanism underlying the specific modulation of heat sensation by Slick.

In addition to its function in acute heat pain, our study provides several lines of evidence that Slick expressed in the spinal cord contributes to nociceptive signaling between TRPV1$^+$ sensory neurons and SSTR2$^+$ dorsal horn neurons. First, both Slick$^{-/-}$ and Lbx1-Slick$^{-/-}$ mice showed a prolonged paw licking behavior after intraplantar injection of the TRPV1 activator capsaicin. The altered behavior in Lbx1-Slick$^{-/-}$ mice suggests that this phenotype is driven by Slick in dorsal horn neurons. Second, the prolonged capsaicin paw licking was paralleled by increased phosphorylation of the neuronal activity marker ERK in spinal cord extracts of Slick$^{-/-}$ mice. Third, the prolonged capsaicin paw licking in Slick$^{-/-}$ and Lbx1-Slick$^{-/-}$ mice was abolished by intrathecal pretreatment with the SSTR2 antagonist CYN-154806. This finding is in accordance with previous reports that the activation of TRPV1$^+$ sensory neurons—which largely project to lamina I and outer lamina II in the spinal cord[39]—results not only in glutamate release from presynaptic terminals[40] but also in the release of neuropeptides, including somatostatin.[41] In general, somatostatin exerts a wide range of effects that are mediated *via* SSTR1-5 (somatostatin cell-surface receptor subtypes 1 through 5), which belong to the seven transmembrane G protein–coupled receptor superfamily.[42] Among these, SSTR2 is dominantly detected in the dorsal horn of the spinal cord,[10,43] and several studies implicate important functions of SSTR2 in the processing of pain and itch.[18,33] Like all other SST receptors, SSTR2 associates with the pertussis toxin–sensitive Gi protein and is coupled to adenylate cyclase and other signaling pathways,[42] and SSTR2 activation has been shown to result in membrane hyperpolarization and inhibition of exocytosis.[42,44] Our finding that intrathecal CYN-154806 abolished the prolonged capsaicin-induced licking behavior in Slick$^{-/-}$ and Lbx1-Slick$^{-/-}$ mice, but did not affect the behavior in control mice, points to an increased activity of SSTR2$^+$ dorsal horn neurons in the absence of Slick. Considering that SSTR2$^+$ dorsal horn neurons mostly release GABA,[10] one might assume that after capsaicin injection, somatostatin inhibits the GABA release from SSTR2$^+$ dorsal horn neurons in a Slick-dependent manner. Further studies are needed to elucidate the mechanisms by which Slick$^+$/SSTR2$^+$ dorsal horn neurons limit the nocifensive response to intraplantar capsaicin. It must also be considered that the response of an interneuronal population to a given sensory modality is defined not only by its peripheral afferent input but also by the neuronal input it receives from other local circuit interneurons.[45]

A function of Slick in SSTR2$^+$ dorsal horn neurons is further supported by the considerably reduced scratching

behavior of Slick$^{-/-}$ and Lbx1-Slick$^{-/-}$ mice after intrathecal injection of octreotide, which binds preferentially to SSTR2 with only moderate affinity for SSTR5 and SSTR3.[42] Given the prolonged nocifensive behavior of Slick-deficient mice after intraplantar capsaicin, their ameliorated itch behavior was quite surprising. However, these apparently contrasting functions of Slick in pain and itch are in line with the complex interactions between the circuitries for pain and itch within the dorsal horn that were reported in previous studies (for review, see Lay and Dong,[2] Koch *et al.*,[45] and Chen and Sun[46]). The essential function of SSTR2$^+$ interneurons in both pain and itch has been demonstrated in several previous studies. For example, Huang *et al.* demonstrated that intrathecal octreotide potentiates itch through disinhibition of SSTR2$^+$ inhibitory interneurons, which results in disinhibition of GRPR$^+$ neurons that exert a key function in the processing of itch.[18] Moreover, many SSTR2$^+$ dorsal horn neurons contain the transcription factor helix-loop-helix family member B5 (Bhlhb5).[44] The essential function of Bhlhb5$^+$ interneurons in itch processing is reflected by the observation that mice lacking Bhlhb5 develop self-inflicted skin lesions and elevated scratching in response to various pruritogens.[47] As the deletion of Bhlhb5 resulted in a substantial loss of spinal interneurons expressing GAL and nNOS, while other inhibitory neuronal populations expressing NPY or PVALB remained intact, it was concluded that spinal GAL$^+$ and nNOS$^+$ interneurons both can play a key role in gating chemical itch.[47] Therefore, the enrichment of Slick in spinal interneurons expressing GAL, nNOS (fig. 3, D and E), and SSTR2 (fig. 8A) further supports a function of Slick in itch pathways. Furthermore, Bhlhb5$^+$ interneurons are thought to suppress itch *via* cross-activation by nociceptive afferents (including those responding to capsaicin), such that the priming of Bhlhb5$^+$ interneurons by a nociceptive stimulus inhibits itch transmission.[45,48] These findings are in accordance with the contrasting pain and itch behavior of Slick-deficient mice we report in our study. Similar contrasting phenotypes have also been observed in other knockout strains, such as mice lacking somatostatin[18] or VGLUT2.[49] Future studies are needed to further elucidate the circuits of pain and itch, and the mechanisms by which they interact.

In conclusion, we here provide evidence that Slick in distinct populations of sensory neurons and dorsal horn neurons exerts specific functions in the processing of pain and itch.

Acknowledgments

The authors thank Carmen Birchmeier, Ph.D., (Max Delbrueck Center for Molecular Medicine, Berlin, Germany) for providing Lbx1-Cre mice and Sylvia Oßwald, Cyntia Schäfer, R.Ph., and Uli Hermanni (Institute of Pharmacology and Clinical Pharmacy, Goethe University Frankfurt, Frankfurt am Main, Germany) for their excellent technical assistance.

Research Support

This work was supported by the Else Kröner-Fresenius-Stiftung (2015_A98; to Dr. Lu), and the German Research Foundation (LU 2514/1-1; to Dr. Lu, and FOR 2060 project SCHM 2629/3-1; to Dr. Schmidtko).

Competing Interests

Dr. Lukowski received research support from Cyclerion (Cambridge, Massachusetts). Dr. Schmidtko has acted as a consultant in the last 2 yr for Merz Pharma (Frankfurt, Germany) and STADA (Bad Vilbel, Germany). The other authors declare no competing interests.

Correspondence

Address correspondence to Dr. Lu: Institute of Pharmacology and Clinical Pharmacy, Goethe University Frankfurt, Max-von-Laue-Str. 9, 60438 Frankfurt am Main, Germany. lu@em.uni-frankfurt.de.

References

1. Dubin AE, Patapoutian A: Nociceptors: The sensors of the pain pathway. J Clin Invest 2010; 120:3760–72
2. Lay M, Dong X: Neural mechanisms of itch. Annu Rev Neurosci 2020; 43:187–205
3. Waxman SG, Zamponi GW: Regulating excitability of peripheral afferents: Emerging ion channel targets. Nat Neurosci 2014; 17:153–63
4. Tsantoulas C, McMahon SB: Opening paths to novel analgesics: The role of potassium channels in chronic pain. Trends Neurosci 2014; 37:146–58
5. Lu R, Bausch AE, Kallenborn-Gerhardt W, Stoetzer C, Debruin N, Ruth P, Geisslinger G, Leffler A, Lukowski R, Schmidtko A: Slack channels expressed in sensory neurons control neuropathic pain in mice. J Neurosci 2015; 35:1125–35
6. Martinez-Espinosa PL, Wu J, Yang C, Gonzalez-Perez V, Zhou H, Liang H, Xia XM, Lingle CJ: Knockout of Slo2.2 enhances itch, abolishes KNa current, and increases action potential firing frequency in DRG neurons. Elife 2015; 4:e10013
7. Tomasello DL, Hurley E, Wrabetz L, Bhattacharjee A: Slick (Kcnt2) sodium-activated potassium channels limit peptidergic nociceptor excitability and hyperalgesia. J Exp Neurosci 2017; 11:1179069517726996
8. Kaczmarek LK: Slack, slick and sodium-activated potassium channels. ISRN Neurosci 2013; 2013:354262
9. Ferreira JJ, Butler A, Stewart R, Gonzalez-Cota AL, Lybaert P, Amazu C, Reinl EL, Wakle-Prabagaran M,

Salkoff L, England SK, Santi CM: Oxytocin can regulate myometrial smooth muscle excitability by inhibiting the Na+ -activated K+ channel, Slo2.1. J Physiol 2019; 597:137–49
10. Häring M, Zeisel A, Hochgerner H, Rinwa P, Jakobsson JET, Lönnerberg P, La Manno G, Sharma N, Borgius L, Kiehn O, Lagerström MC, Linnarsson S, Ernfors P: Neuronal atlas of the dorsal horn defines its architecture and links sensory input to transcriptional cell types. Nat Neurosci 2018; 21:869–80
11. Schwenk F, Baron U, Rajewsky K: A cre-transgenic mouse strain for the ubiquitous deletion of loxP-flanked gene segments including deletion in germ cells. Nucleic Acids Res 1995; 23:5080–1
12. Sieber MA, Storm R, Martinez-de-la-Torre M, Müller T, Wende H, Reuter K, Vasyutina E, Birchmeier C: Lbx1 acts as a selector gene in the fate determination of somatosensory and viscerosensory relay neurons in the hindbrain. J Neurosci 2007; 27:4902–9
13. Vandewauw I, De Clercq K, Mulier M, Held K, Pinto S, Van Ranst N, Segal A, Voet T, Vennekens R, Zimmermann K, Vriens J, Voets T: A TRP channel trio mediates acute noxious heat sensing. Nature 2018; 555:662–6
14. Luiz AP, MacDonald DI, Santana-Varela S, Millet Q, Sikandar S, Wood JN, Emery EC: Cold sensing by NaV1.8-positive and NaV1.8-negative sensory neurons. Proc Natl Acad Sci U S A 2019; 116:3811–6
15. Brenner DS, Golden JP, Gereau RW IV: A novel behavioral assay for measuring cold sensation in mice. PLoS One 2012; 7:e39765
16. Ranade SS, Woo SH, Dubin AE, Moshourab RA, Wetzel C, Petrus M, Mathur J, Bégay V, Coste B, Mainquist J, Wilson AJ, Francisco AG, Reddy K, Qiu Z, Wood JN, Lewin GR, Patapoutian A: Piezo2 is the major transducer of mechanical forces for touch sensation in mice. Nature 2014; 516:121–5
17. Lu R, Flauaus C, Kennel L, Petersen J, Drees O, Kallenborn-Gerhardt W, Ruth P, Lukowski R, Schmidtko A: KCa3.1 channels modulate the processing of noxious chemical stimuli in mice. Neuropharmacology 2017; 125:386–95
18. Huang J, Polgár E, Solinski HJ, Mishra SK, Tseng PY, Iwagaki N, Boyle KA, Dickie AC, Kriegbaum MC, Wildner H, Zeilhofer HU, Watanabe M, Riddell JS, Todd AJ, Hoon MA: Circuit dissection of the role of somatostatin in itch and pain. Nat Neurosci 2018; 21:707–16
19. Chen H, Kronengold J, Yan Y, Gazula VR, Brown MR, Ma L, Ferreira G, Yang Y, Bhattacharjee A, Sigworth FJ, Salkoff L, Kaczmarek LK: The N-terminal domain of Slack determines the formation and trafficking of Slick/Slack heteromeric sodium-activated potassium channels. J Neurosci 2009; 29:5654–65
20. Castañeda-Corral G, Jimenez-Andrade JM, Bloom AP, Taylor RN, Mantyh WG, Kaczmarska MJ, Ghilardi JR, Mantyh PW: The majority of myelinated and unmyelinated sensory nerve fibers that innervate bone express the tropomyosin receptor kinase A. Neuroscience 2011; 178:196–207
21. Albisetti GW, Ghanem A, Foster E, Conzelmann KK, Zeilhofer HU, Wildner H: Identification of two classes of somatosensory neurons that display resistance to retrograde infection by rabies virus. J Neurosci 2017; 37:10358–71
22. The Oxford Handbook of the Neurobiology of Pain. Edited by Wood JN. New York, Oxford University Press, 2020
23. Usoskin D, Furlan A, Islam S, Abdo H, Lönnerberg P, Lou D, Hjerling-Leffler J, Haeggström J, Kharchenko O, Kharchenko PV, Linnarsson S, Ernfors P: Unbiased classification of sensory neuron types by large-scale single-cell RNA sequencing. Nat Neurosci 2015; 18:145–53
24. Tejada MA, Hashem N, Calloe K, Klaerke DA: Heteromeric Slick/Slack K+ channels show graded sensitivity to cell volume changes. PLoS One 2017; 12:e0169914
25. Hughes DI, Todd AJ: Central nervous system targets: Inhibitory interneurons in the spinal cord. Neurotherapeutics 2020; 17:874–85
26. Peirs C, Williams SP, Zhao X, Walsh CE, Gedeon JY, Cagle NE, Goldring AC, Hioki H, Liu Z, Marell PS, Seal RP: Dorsal horn circuits for persistent mechanical pain. Neuron 2015; 87:797–812
27. Smith KM, Browne TJ, Davis OC, Coyle A, Boyle KA, Watanabe M, Dickinson SA, Iredale JA, Gradwell MA, Jobling P, Callister RJ, Dayas CV, Hughes DI, Graham BA: Calretinin positive neurons form an excitatory amplifier network in the spinal cord dorsal horn. Elife 2019; 8:e49190
28. Caterina MJ, Leffler A, Malmberg AB, Martin WJ, Trafton J, Petersen-Zeitz KR, Koltzenburg M, Basbaum AI, Julius D: Impaired nociception and pain sensation in mice lacking the capsaicin receptor. Science 2000; 288:306–13
29. Gao YJ, Ji RR: c-Fos and pERK, which is a better marker for neuronal activation and central sensitization after noxious stimulation and tissue injury? Open Pain J 2009; 2:11–7
30. Helyes Z, Szabó A, Németh J, Jakab B, Pintér E, Bánvölgyi A, Kereskai L, Kéri G, Szolcsányi J: Antiinflammatory and analgesic effects of somatostatin released from capsaicin-sensitive sensory nerve terminals in a Freund's adjuvant-induced chronic arthritis model in the rat. Arthritis Rheum 2004; 50:1677–85
31. Günther T, Tulipano G, Dournaud P, Bousquet C, Csaba Z, Kreienkamp HJ, Lupp A, Korbonits M, Castaño JP, Wester HJ, Culler M, Melmed S, Schulz S: International Union of Basic and Clinical Pharmacology. CV.

Somatostatin receptors: Structure, function, ligands, and new nomenclature. Pharmacol Rev 2018; 70:763–835
32. Polgár E, Durrieux C, Hughes DI, Todd AJ: A quantitative study of inhibitory interneurons in laminae I-III of the mouse spinal dorsal horn. PLoS One 2013; 8:e78309
33. Fatima M, Ren X, Pan H, Slade HFE, Asmar AJ, Xiong CM, Shi A, Xiong AE, Wang L, Duan B: Spinal somatostatin-positive interneurons transmit chemical itch. Pain 2019; 160:1166–74
34. Vriens J, Nilius B, Voets T: Peripheral thermosensation in mammals. Nat Rev Neurosci 2014; 15:573–89
35. Vriens J, Owsianik G, Hofmann T, Philipp SE, Stab J, Chen X, Benoit M, Xue F, Janssens A, Kerselaers S, Oberwinkler J, Vennekens R, Gudermann T, Nilius B, Voets T: TRPM3 is a nociceptor channel involved in the detection of noxious heat. Neuron 2011; 70:482–94
36. Tan CH, McNaughton PA: The TRPM2 ion channel is required for sensitivity to warmth. Nature 2016; 536:460–3
37. Kwan KY, Allchorne AJ, Vollrath MA, Christensen AP, Zhang DS, Woolf CJ, Corey DP: TRPA1 contributes to cold, mechanical, and chemical nociception but is not essential for hair-cell transduction. Neuron 2006; 50:277–89
38. Vilar B, Tan CH, McNaughton PA: Heat detection by the TRPM2 ion channel. Nature 2020; 584:E5–E12
39. Basbaum AI, Bautista DM, Scherrer G, Julius D: Cellular and molecular mechanisms of pain. Cell 2009; 139:267–84
40. Park CK, Lü N, Xu ZZ, Liu T, Serhan CN, Ji RR: Resolving TRPV1- and TNF-α-mediated spinal cord synaptic plasticity and inflammatory pain with neuroprotectin D1. J Neurosci 2011; 31:15072–85
41. Szolcsányi J, Helyes Z, Oroszi G, Németh J, Pintér E: Release of somatostatin and its role in the mediation of the anti-inflammatory effect induced by antidromic stimulation of sensory fibres of rat sciatic nerve. Br J Pharmacol 1998; 123:936–42
42. Theodoropoulou M, Stalla GK: Somatostatin receptors: From signaling to clinical practice. Front Neuroendocrinol 2013; 34:228–52
43. Bowman BR, Bokiniec P, McMullan S, Goodchild AK, Burke PGR: Somatostatin 2 receptors in the spinal cord tonically restrain thermogenic, cardiac and other sympathetic outflows. Front Neurosci 2019; 13:121
44. Kardon AP, Polgár E, Hachisuka J, Snyder LM, Cameron D, Savage S, Cai X, Karnup S, Fan CR, Hemenway GM, Bernard CS, Schwartz ES, Nagase H, Schwarzer C, Watanabe M, Furuta T, Kaneko T, Koerber HR, Todd AJ, Ross SE: Dynorphin acts as a neuromodulator to inhibit itch in the dorsal horn of the spinal cord. Neuron 2014; 82:573–86
45. Koch SC, Acton D, Goulding M: Spinal circuits for touch, pain, and itch. Annu Rev Physiol 2018; 80:189–217
46. Chen XJ, Sun YG: Central circuit mechanisms of itch. Nat Commun 2020; 11:3052
47. Ross SE, Mardinly AR, McCord AE, Zurawski J, Cohen S, Jung C, Hu L, Mok SI, Shah A, Savner EM, Tolias C, Corfas R, Chen S, Inquimbert P, Xu Y, McInnes RR, Rice FL, Corfas G, Ma Q, Woolf CJ, Greenberg ME: Loss of inhibitory interneurons in the dorsal spinal cord and elevated itch in Bhlhb5 mutant mice. Neuron 2010; 65:886–98
48. Hachisuka J, Baumbauer KM, Omori Y, Snyder LM, Koerber HR, Ross SE: Semi-intact *ex vivo* approach to investigate spinal somatosensory circuits. Elife 2016; 5:e22866
49. Liu Y, Abdel Samad O, Zhang L, Duan B, Tong Q, Lopes C, Ji RR, Lowell BB, Ma Q: VGLUT2-dependent glutamate release from nociceptors is required to sense pain and suppress itch. Neuron 2010; 68:543–56

ANESTHESIOLOGY

Serendipity: Being in the Right Place at the Right Time

Lawrence J. Saidman, M.D.

ANESTHESIOLOGY 2022; 136:823–6

Effect of Nitrous Oxide and of Narcotic Premedication on the Alveolar Concentration Required for Anesthesia. By Saidman LJ, Eger EI II. ANESTHESIOLOGY 1964; 25:302–6.

Hyperthermia during Anesthesia. By Saidman LJ, Havard ES, Eger EI II. JAMA 1964; 190:1029–32.

Abstract

The minimum alveolar concentration (MAC) of an inhaled anesthetic preventing movement in response to a surgical incision as a measure of equipotency was "invented" in 1964 at the University of California, San Francisco. The principal advantage of MAC is that it allows the pharmacologic effects of inhaled anesthetics to be compared against each other at a similar anesthetic depth. Thus, if the hemodynamic effect (hypotension, decreased cardiac output) of anesthetic "A" is greater than that of anesthetic "B," the anesthesiologist may elect to use "A" in patients with myocardial dysfunction. A rare side effect of a volatile anesthetic is that in some patients, malignant hyperthermia may occur with or without succinylcholine use. This phenomenon was detected in a patient in whom halothane MAC was being measured. The availability of the Severinghaus blood gas device allowed for the first ever measurement of the metabolic and respiratory acidemia that accompanies malignant hyperthermia.

(ANESTHESIOLOGY 2022; 136:823–6)

I was introduced to anesthesiology as a third-year medical student at the University of Michigan (Ann Arbor, Michigan) in 1960, after which I chose the University of California, San Francisco (San Francisco, California) as the department in which to undertake residency training (fig. 1). I knew little of this department other than that it offered a third year of training (3 yr must be better than 2), and my wife, Arlene, and I (neither of whom had been west of the Mississippi) preferred San Francisco to Philadelphia or New York City.

Imagine my good fortune to have chosen University of California, San Francisco, wherein Edmond "Ted" Eger II, M.D., and John Severinghaus, M.D., were investigating all things related to inhaled anesthetic pharmacokinetics and pharmacodynamics (fig. 2). Ted Eger, at the time an assistant professor of anesthesia, had just published a paper with Giles Merkel, M.D., describing the minimum alveolar concentration (MAC) of halopropane needed to suppress a response to noxious stimulation in dogs.[1]

Several months after starting my training in 1962, I found myself being "grilled" by Ted, my faculty supervisor for the day, about my knowledge of gas laws (Boyle, Charles, Gay–Lussac, Dalton). Apparently I passed this test, for Ted subsequently invited me to participate in the first study to determine MAC in humans.[2] This study was performed in 68 surgical patients undergoing inhalation induction with halothane plus oxygen, oxygen with 70% nitrous oxide, or oxygen with opioid premedication. The end-tidal concentration of halothane that appeared to produce a light surgical plane of anesthesia was held constant for 10 to 15 min before surgical incision.

Neither intravenous induction agents nor muscle relaxants were used before incision. Each patient's response to the skin incision (movement *vs.* the absence of movement) was noted. The MAC of halothane in humans (0.74%) was determined as the transition point between responses of movement and nonmovement (fig. 3). Our study also demonstrated that 70% nitrous oxide and opioid premedication reduced the halothane alveolar concentration required to eliminate movement by 61% and 7%, respectively. The discovery of MAC in humans was revolutionary for clinical and research purposes in that it allowed the pharmacologic effects of inhaled anesthetics to be compared against each other at a similar anesthetic depth.

Ted and I then decided to determine MAC in each of four additional patients by a different method to validate our initial measurements. Rather than observing a response to a single skin incision occurring after a fixed concentration of halothane, we examined each of these four patients' responses to cutaneous electrical stimulation by increasing or decreasing the end-tidal halothane concentration. This process, which continued until the minimum concentration needed to eliminate movement was found, required several hours to accomplish! Remember that the early 1960s preceded the era of human study committees, and these patients had only been told that we would try to determine the precise amount of anesthetic needed for their surgery. These four latter patients' MAC determinations confirmed the data derived from the responses of the original 68 patients in whom a single surgical incision had occurred.[2]

In three of the four patients studied during the extended presurgical period, no untoward events occurred. The fourth patient, however, was very different.[3] The patient

The first paper (Saidman and Eger) was presented at the PostGraduate Assembly in Anesthesiology in New York, New York, in 1963. The second paper (Saidman, Havard, and Eger) was presented at the Anesthesia Section of the American Medical Association Meeting in San Francisco, California, in 1963.

Submitted for publication January 4, 2022. Accepted for publication January 6, 2022. Published online first on February 18, 2022. From the Department of Anesthesiology, Perioperative and Pain Medicine, Stanford University, Stanford, California.

 Anesthesiology 2022; 136:823–6. DOI: 10.1097/ALN.0000000000004140

<zdoi;. DOI: 10.1097/ALN.0000000000004140>

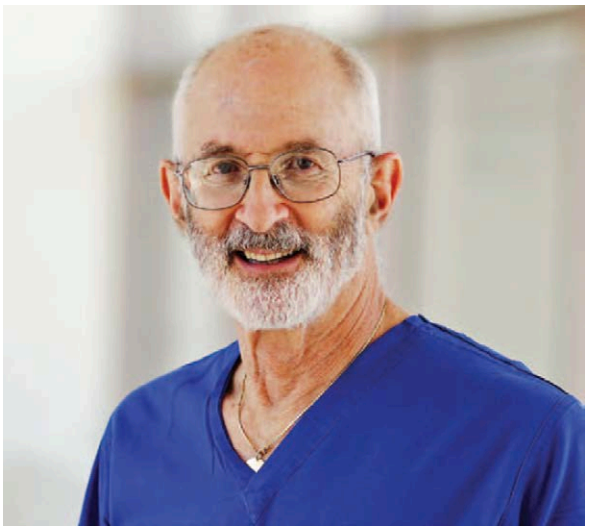

Fig. 1. Dr. Lawrence Saidman was Chairman of Anesthesia at the University of California, San Diego (San Diego, California) from 1973 to 1985; Editor-in-Chief of ANESTHESIOLOGY from 1986 to 1996; and President of the American Board of Anesthesiology from 1994 to 1995. Image courtesy of Stanford University (Stanford, California) and the International Anesthesia Research Society (San Francisco, California).

was a 47-yr-old man undergoing repair of a large ventral hernia. During the extended presurgical period described, he had been anesthetized with halothane–oxygen after premedication with 0.8 mg intramuscular atropine. After the MAC determination, surgery was started, and anesthesia was maintained with halothane, oxygen, and 65% nitrous oxide, along with a continuous infusion of succinylcholine for deep abdominal relaxation. Monitoring included a noninvasive blood pressure cuff, an esophageal temperature probe, and a continuous electrocardiogram.

One hour into surgery, the patient became diaphoretic, and his temperature had increased to 100°F. In order to maintain adequate muscle relaxation, it was necessary to increase the rate of the succinylcholine infusion. Alarmingly, the patient's temperature rapidly increased to 108.5°F, after which his blood pressure abruptly decreased from 100/70 mmHg to 40/0 mmHg. Fortuitously, we had access to John Severinghaus's apparatus (now called a blood gas machine),[4] and arterial blood gas analysis showed profound metabolic and respiratory acidosis (pH 6.8; P_{CO_2} 179 mmHg; base deficit 14.7). The surgeon was alerted to these events, and during the next 4 hr, the patient was packed in ice and given intravenous bicarbonate, vasopressors, prednisolone, and 3,000 ml cold lactated Ringer's solution. Gradually, his temperature decreased, his acidosis mostly resolved, and we were able to extubate his trachea. His subsequent recovery was uneventful.

I presented this case report to the Anesthesia Section of the American Medical Association meeting in San Francisco in 1963. At the end of my presentation, the moderator queried the audience if anyone had cared for a patient exhibiting similar events. To my surprise, several attendees described a similar combination of hyperthermia and hemodynamic instability occurring in patients to whom halothane and succinylcholine were given. However, they were unable to measure the metabolic derangement that is the hallmark of the condition.

We published this case report that presented the first-ever acid–base data associated with hyperthermia in a

Fig. 2. Personnel working in the Severinghaus Lab in 1962 to 1963. From left to right: Richard Shargel, Cedric Bainton, Lawrence Saidman, Robert Mitchell, Freeman Bradley, Ted Eger, Ed Munson, Dorothy Herbert, John Severinghaus, and Pat Bradley.

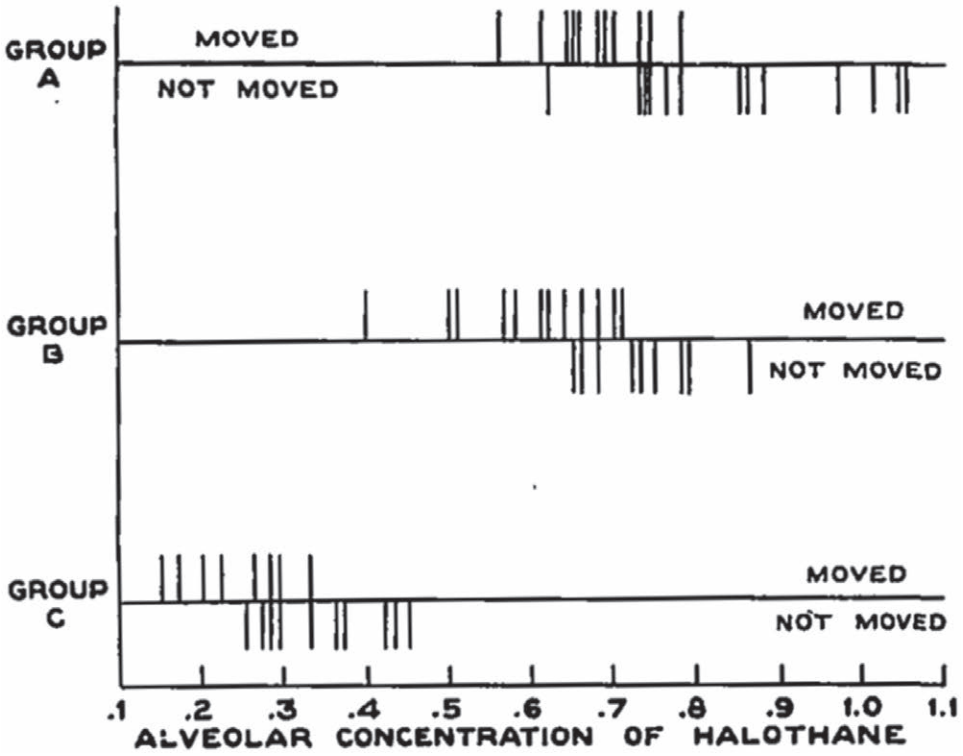

Fig. 3. Responses to skin incision in surgical patients in the first human minimum alveolar concentration study. Reprinted from Saidman and Eger[2] with permission.

patient anesthetized with halothane.[3] Denborough *et al.* had published a paper in 1962 describing deaths in a family who had received general anesthesia.[5] While these deaths may well have been related to malignant hyperthermia, no acid–base data had been readily available at the time.

The association between profound hyperthermia and severe acidosis had remained undescribed until our paper was published. I include "serendipity" in the title of this article because of the unusual set of circumstances that led to two separate papers, each of which included information from the same patient.[2,3] The serendipitous circumstances included the lengthy presurgical interval of halothane MAC measurement during which succinylcholine was not used, and body temperature remained normal[2,3]; the previously unknown association between halothane and malignant hyperthermia[3]; and the fortuitous availability of the Severinghaus blood gas machine—an early version of which now rests in the Smithsonian Institution (Washington, D.C.).

The second part of the MAC study during which four patients were anesthetized for several hours before surgery might not have been possible today due to the need for approval from an institutional human research committee. In addition, even if the study had been approved by a review board during that era, the cause of the hyperthermia would not have been properly diagnosed due to the lack of clinical experience with malignant hyperthermia. By contrast, PubMed citations of papers dealing with malignant hyperthermia now number in the thousands.

Our experience with this patient is a classic example of first observing a clinical phenomenon, then funding basic research to discover the mechanism underlying the problem, and finally applying this knowledge to clinical practice to prevent the problem from occurring. Personally, this experience left me in awe of how close our patient came to dying from a previously unknown phenomenon. He was rescued due to a device that had only recently become clinically available. This case also illustrates how what we do every day renders our patients susceptible to the vagaries of chance events. Most importantly, it affirmed the essential role of anesthesiologists in responding to these rare and unpredictable events.

Research Support

Support was provided solely from institutional and/or departmental sources.

Correspondence

Address correspondence to Dr. Saidman: 1850 Alice Street, Apartment 1215, Oakland, California 94612. lsaidman@stanford.edu. Anesthesiology's articles are made freely accessible to all readers, for personal use only, 6 months from the cover date of the issue.

References

1. Merkel G, Eger EI II: A comparative study of halothane and halopropane anesthesia including method for determining equipotency. Anesthesiology 1963; 24:346–57
2. Saidman LJ, Eger EI II: Effect of nitrous oxide and of narcotic premedication on the alveolar concentration of halothane required for anesthesia. Anesthesiology 1964; 25:302–6
3. Saidman LJ, Havard ES, Eger EI II: Hyperthermia during anesthesia. JAMA 1964; 190:1029–32
4. Severinghaus JW, Bradley AF: Electrodes for blood pO2 and pCO2 determination. J Appl Physiol 1958; 13:515–20
5. Denborough MA, Forster JF, Lovell RR, Maplestone PA, Villiers JD: Anaesthetic deaths in a family. Br J Anaesth 1962; 34:395–6

ANESTHESIOLOGY REFLECTIONS FROM THE WOOD LIBRARY-MUSEUM

Let the Record Show: McKesson's Automated Nargraf

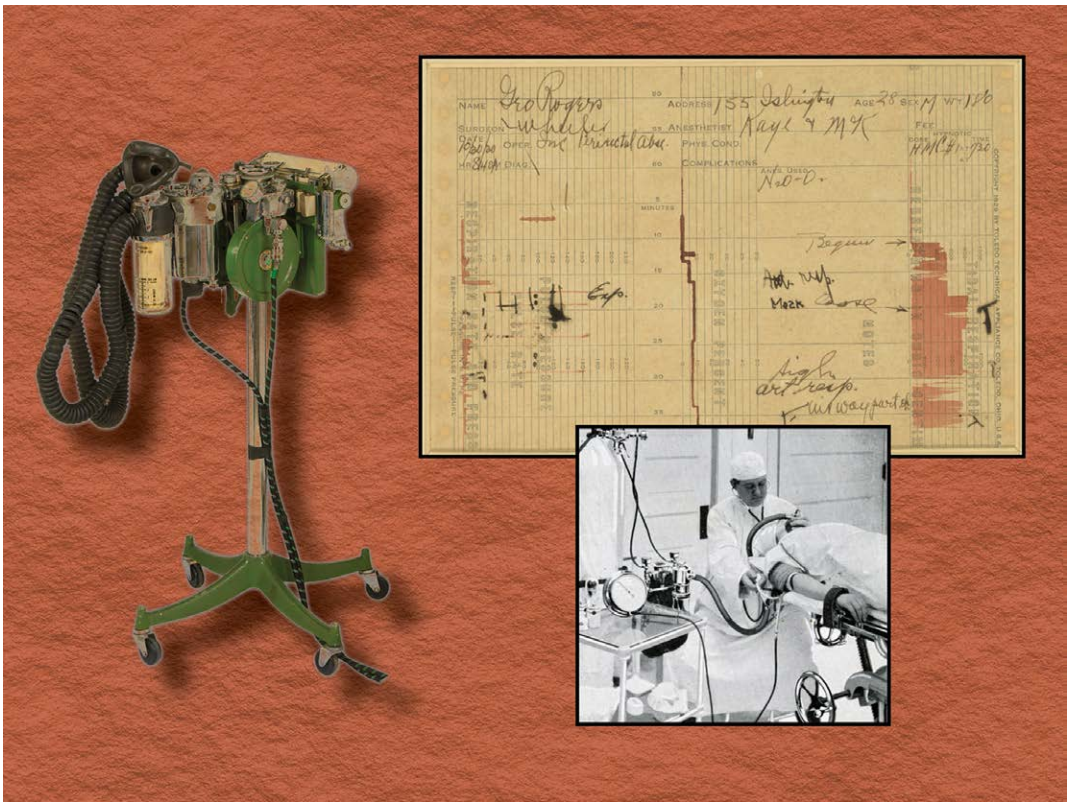

A high school principal who became a physician, inventor, and entrepreneur, Elmer McKesson, M.D. (1881 to 1935, *lower right*), championed technology to optimize physiology under anesthesia. Enchanted by nitrous oxide anesthesia as an intern, he designed his first gas apparatus and founded his successful McKesson Appliance Company a few years later. He also served as the first President of the International Anesthesia Research Society. Truly ahead of his time, McKesson invented the first semiautomated anesthesia record when intraoperative blood pressure measurement was only beginning to gain favor. His revolutionary Nargraf Model J (1930, *left*) fed a preprinted paper record through a machine that charted blood pressure, tidal volume, oxygen concentration, and inspiratory gas pressure (*red ink, upper right*). The anesthetist would document the patient's heart rate and respiratory rate by hand (*black ink, upper right*). While fully automated records would not be in vogue until the twenty-first century, McKesson's Nargraf was a harbinger of things to come. (Image of record from the Geoffrey Kaye Museum of Anaesthetic History, VGKM5042. Copyright © the American Society of Anesthesiologists' Wood Library-Museum of Anesthesiology.)

Jane S. Moon, M.D., Assistant Clinical Professor, Department of Anesthesiology and Perioperative Medicine, University of California, Los Angeles, California.

References

1. Merkel G, Eger EI II: A comparative study of halothane and halopropane anesthesia including method for determining equipotency. Anesthesiology 1963; 24:346–57
2. Saidman LJ, Eger EI II: Effect of nitrous oxide and of narcotic premedication on the alveolar concentration of halothane required for anesthesia. Anesthesiology 1964; 25:302–6
3. Saidman LJ, Havard ES, Eger EI II: Hyperthermia during anesthesia. JAMA 1964; 190:1029–32
4. Severinghaus JW, Bradley AF: Electrodes for blood pO2 and pCO2 determination. J Appl Physiol 1958; 13:515–20
5. Denborough MA, Forster JF, Lovell RR, Maplestone PA, Villiers JD: Anaesthetic deaths in a family. Br J Anaesth 1962; 34:395–6

ANESTHESIOLOGY REFLECTIONS FROM THE WOOD LIBRARY-MUSEUM

Let the Record Show: McKesson's Automated Nargraf

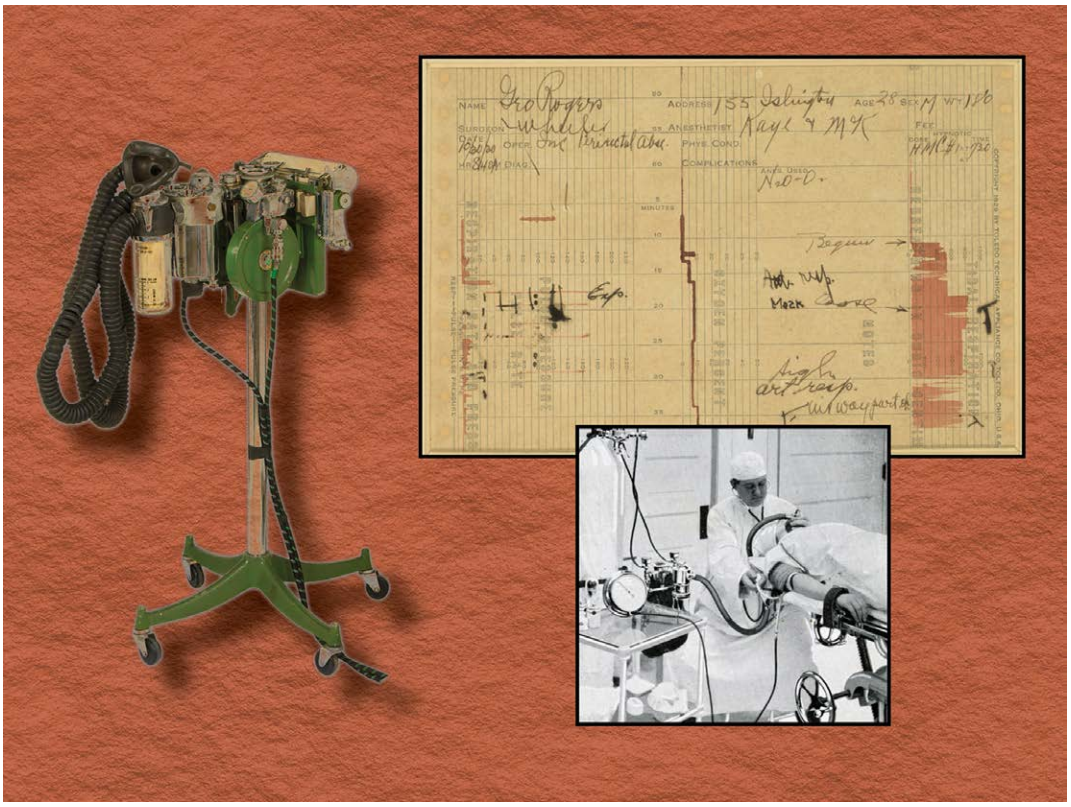

A high school principal who became a physician, inventor, and entrepreneur, Elmer McKesson, M.D. (1881 to 1935, *lower right*), championed technology to optimize physiology under anesthesia. Enchanted by nitrous oxide anesthesia as an intern, he designed his first gas apparatus and founded his successful McKesson Appliance Company a few years later. He also served as the first President of the International Anesthesia Research Society. Truly ahead of his time, McKesson invented the first semiautomated anesthesia record when intraoperative blood pressure measurement was only beginning to gain favor. His revolutionary Nargraf Model J (1930, *left*) fed a preprinted paper record through a machine that charted blood pressure, tidal volume, oxygen concentration, and inspiratory gas pressure (*red ink, upper right*). The anesthetist would document the patient's heart rate and respiratory rate by hand (*black ink, upper right*). While fully automated records would not be in vogue until the twenty-first century, McKesson's Nargraf was a harbinger of things to come. (Image of record from the Geoffrey Kaye Museum of Anaesthetic History, VGKM5042. Copyright © the American Society of Anesthesiologists' Wood Library-Museum of Anesthesiology.)

Jane S. Moon, M.D., Assistant Clinical Professor, Department of Anesthesiology and Perioperative Medicine, University of California, Los Angeles, California.

Facial Pressure Ulcers: Unsightly Complication of Prone Positioning

Eliane Varga, M.D., Sae-In Kay, D.O., Reine A. Zbeidy, M.D., Fouad G. Souki, M.D., M.S.

The image depicts a 67-yr-old man who had significant periorbital skin injury after 5 h of prone spine surgery using a foam headrest with standard taping of eyes. The patient underwent facial laser skin resurfacing 2 months before the event.

Facial pressure ulcers are a serious complication that may lead to pain, additional treatment, longer hospital stays, disfigurement or scarring, increased medical cost, and subsequent lawsuits.[1] Facial pressure ulcer has an incidence of 27% in prone spine surgery lasting more than 3 h and occurs most commonly over the bony prominence of the chin, maxilla, and forehead.[1] Skin damage is due to prolonged and excessive pressure and/or shear that blocks capillary blood flow.[2] Risk factors include operation duration, hyperthermia, hypotension, aggressive fluid replacement, and cervical hyperextension or hyperflexion.[1,2]

Patients with recent facial laser skin resurfacing are at greater risk of perioperative facial pressure ulcers due to increased skin fragility.[3] Laser skin resurfacing uses thermal damage of epidermis and parts of dermis to stimulate repair for ultimate facial rejuvenation.[3] Complete recovery could take up to 1 yr, particularly in older patients.[3] Perioperative considerations should include adequate healing of resurfaced skin, consultation with dermatologist, and communication about increased risk of skin injury.[3]

Preventive measures for facial pressure ulcers during prone position surgery include assessment of skin risk area, application of moisturizer barrier cream, using pressure redistribution support surfaces or positioning devices to offload pressure points (silicone-foam dressings, face-contoured prone device, Mayfield clamp, or Gardner–Wells tongs with traction), and minimizing risk factors.[1,2]

Published online first on March 14, 2022.

Eliane Varga, M.D.: Department of Anesthesiology, University of Miami, Jackson Memorial Hospital, Miami, Florida.

Sae-In Kay, D.O.: Department of Anesthesiology, University of Miami, Jackson Memorial Hospital, Miami, Florida.

Reine A. Zbeidy, M.D.: Department of Anesthesiology, University of Miami, Jackson Memorial Hospital, Miami, Florida.

Fouad G. Souki, M.D., M.S.: Department of Anesthesiology, University of Miami, Jackson Memorial Hospital, Miami, Florida.

 Anesthesiology 2022; 136:827–8. DOI: 10.1097/ALN.0000000000004188

<zdoi;. DOI: 10.1097/ALN.0000000000004188>

Competing Interests

The authors declare no competing interests.

Correspondence

Address correspondence to Dr. Souki: fsouki@med.miami.edu

References

1. Techanivate A, Athibai N, Siripongsaporn S, Singhatanadgige W: Risk factors for facial pressure ulcers in patients who underwent prolonged prone orthopedic spine surgery. Spine (Phila Pa 1976) 2021; 46:744–50
2. Atwater BI, Wahrenbrock E, Benumof JL, Mazzei WJ: Pressure on the face while in the prone position: ProneView versus Prone Positioner. J Clin Anesth 2004; 16:111–6
3. Li D, Lin SB, Cheng B: Complications and posttreatment care following invasive laser skin resurfacing: A review. J Cosmet Laser Ther 2018; 20:168–78

Perioperative Management of Patients Receiving Short-term Mechanical Circulatory Support with the Transvalvular Heart Pump

Isaac Y. Wu, M.D., Julie A. Wyrobek, M.D., Yoshifumi Naka, M.D., Ph.D., Marc L. Dickstein, M.D., Laurent G. Glance, M.D.

Cardiogenic shock continues to be an unresolved clinical challenge. The initial management of cardiogenic shock includes etiology-specific treatment (*e.g.*, coronary revascularization for acute myocardial infarction), optimization of volume and respiratory status, and administration of inotropic and vasopressor medications. However, inotropes may increase myocardial oxygen consumption, which may further worsen myocardial ischemia, can induce arrhythmias, and may not provide adequate circulatory support. Vasopressors may further decrease tissue perfusion and impair microcirculation.[1]

As a result, interest in the potential role of short-term mechanical circulatory support in cardiogenic shock has grown and clinical uptake of these devices continues to increase.[2,3] Use of the Impella (Abiomed Inc., USA) transvalvular heart pump in particular, has grown significantly.[3–5] As such, anesthesiologists are increasingly likely to care for patients receiving transvalvular heart pump support and should have a thorough understanding of the device and its hemodynamic effects and perioperative considerations. Recent publications have described other short-term mechanical circulatory support devices, including venoarterial extracorporeal membrane oxygenation and intraaortic balloon pump counterpulsation.[6,7] To provide clinicians with a comprehensive review, this article focuses on the perioperative management of a single device, the transvalvular heart pump.

Transvalvular Heart Pump

Device Overview

The Impella family of heart pumps are microaxial, transvalvular ventricular assist devices that provide continuous, antegrade flow. There are five left ventricular assist devices capable of providing various levels of circulatory support and one right ventricular assist device, the Impella RP (table 1). The Impella 2.5, CP, and RP are typically placed percutaneously, while the Impella 5.0, LD, and 5.5 are placed surgically. The surgically placed devices provide the highest levels of maximum pump flow, with the Impella 5.5 capable of flowing up to 6 l/min, and can be used in patients with unsuitable femoral and aorto-iliac anatomy.

The Impella catheter consists of a blood inlet area, cannula, placement sensor area, blood outlet area, and motor housing (fig. 1). Blood is aspirated from the blood inlet area and expelled through the outlet area. In the case of a left-sided transvalvular heart pump, the blood inlet and outlet areas reside in the left ventricle and ascending aorta, respectively; for the RP, they reside in the inferior vena cava and pulmonary artery, respectively. The placement sensor area, which is a fluid-filled pressure lumen in the 2.5 and CP, a differential pressure sensor in the 5.0, LD, and RP, and a fiber-optic sensor in the 5.5, generates a placement signal that is used to assist in proper device positioning. The Impella 2.5, CP, 5.0, and RP have a pigtail that is used to stabilize the device during placement.

The Automated Impella Controller (Abiomed Inc.) is used to monitor and control the Impella catheter. It contains a purge cassette, which delivers purge fluid to the catheter. The heparin-containing purge fluid prevents blood from entering the motor housing by pushing blood away from the motor housing and maintaining a pressure barrier between the blood and motor. The Automated Impella Controller monitor displays alarms, the P-level (flow rate) indicator, transvalvular heart pump flow rates, purge fluid flow rates, and battery power status. It also contains a central display area that changes depending on the "screen" selected. The placement screen, which is used to verify correct device positioning, is the most relevant screen for device placement and will

This article is featured in "This Month in Anesthesiology," page A1.

Submitted for publication August 30, 2021. Accepted for publication December 16, 2021. Published online first on February 4, 2022.

Isaac Y. Wu, M.D.: Department of Anesthesiology and Perioperative Medicine, University of Rochester School of Medicine and Dentistry, Rochester, New York.

Julie A. Wyrobek, M.D.: Department of Anesthesiology and Perioperative Medicine, University of Rochester School of Medicine and Dentistry, Rochester, New York.

Yoshifumi Naka, M.D., Ph.D.: Department of Cardiothoracic Surgery, Weill Cornell Medical College, Cornell University, Ithaca, New York; Department of Cardiothoracic Surgery, Columbia University College of Physicians and Surgeons, New York, New York.

Marc L. Dickstein, M.D.: Department of Anesthesiology at Columbia University Irving Medical Center, Columbia University College of Physicians and Surgeons, New York, New York.

Laurent G. Glance, M.D.: Department of Anesthesiology and Perioperative Medicine, University of Rochester School of Medicine and Dentistry, Rochester, New York; RAND Health, Boston, Massachusetts.

 Anesthesiology 2022; 136:829–42. DOI: 10.1097/ALN.0000000000004124

<zdoi;. DOI: 10.1097/ALN.0000000000004124>

Table 1. Impella Heart Pump Characteristics

	Impella 2.5	Impella CP	Impella LD	Impella 5.0	Impella 5.5	Impella RP
Supported ventricle	Left ventricle	Left ventricle	Left ventricle	Left ventricle	Left ventricle	Right ventricle
Insertion depth	3.5 cm into left ventricle from aortic valve annulus	3.5 cm into left ventricle from aortic valve annulus	3.5 cm into left ventricle from aortic valve annulus	3.5 cm into left ventricle from aortic valve annulus	5 cm into left ventricle from aortic valve annulus	4 cm into pulmonary artery from pulmonary valve annulus
Typical insertion technique	Percutaneous	Percutaneous	Surgical	Surgical	Surgical	Percutaneous
Typical insertion location	Femoral artery	Femoral artery	Ascending aorta	Axillary artery, femoral artery	Axillary artery, ascending aorta	Femoral vein
Catheter/motor housing size	9 Fr/12 Fr	9 Fr/14 Fr	9 Fr/21 Fr	9 Fr/21 Fr	9 Fr/19 Fr	11 Fr/22 Fr
Maximum flow rate	~2.5 l/min	~4.3 l/min	~5.0 l/min	~5.0 l/min	~6 l/min	~4.0 l/min
Placement signal	Fluid-filled pressure lumen	Fluid-filled pressure lumen*	Differential pressure sensor	Differential pressure sensor	Fiber-optic sensor	Differential pressure sensor
U.S. Food and Drug Administration–approved indications and emergency use authorizations	• Refractory cardiogenic shock • High-risk PCI • COVID-19 emergency use authorization	• Refractory cardiogenic shock • High-risk PCI • COVID-19 emergency use authorization	• Refractory cardiogenic shock	• Refractory cardiogenic shock • COVID-19 emergency use authorization	• Refractory cardiogenic shock • COVID-19 emergency use authorization	• Acute right heart failure • COVID-19 emergency use authorization

*Impella CP with SmartAssist (Abiomed Inc., USA) uses a fiber-optic sensor to determine the placement signal.

Fr, French; PCI, percutaneous coronary intervention.

be discussed here. When the placement screen is selected, the placement signal and motor current waveforms are displayed.

The placement signal is determined at the placement sensor area of the catheter and is used to confirm whether the device is appropriately positioned (fig. 2; fig. A1). In the Impella 2.5 and CP, the placement signal is a pressure waveform that is measured from the fluid-filled pressure lumen just proximal (closer to the insertion site) to the outlet area. The placement signal will display either a pulsatile aortic waveform (correct position) or pulsatile ventricular waveform (incorrect position) depending on the position of the fluid-filled pressure lumen. In the Impella 5.5, the placement signal is a pressure waveform measured from the fiber-optic sensor just distal (further from the insertion site) to the outlet area. The placement signal will display either an aortic pressure waveform (correct position) or ventricular pressure waveform (incorrect position) depending on the position of the fiber-optic sensor. In the Impella LD, 5.0, and RP, the placement signal is a differential pressure waveform that is measured from the differential pressure sensor. The differential pressure waveform displays the difference in pressure between the outside of the cannula and the inside of the cannula. In left-sided devices, when the Impella catheter is appropriately positioned across the aortic valve, the outside of the differential pressure sensor is exposed to aortic pressures, and the inside of the sensor is exposed to ventricular pressures. In this scenario, the difference in pressure should result in a pulsatile placement signal, with the maximum pressure difference occurring in diastole (when ventricular pressure is lowest relative to aortic pressure) and the minimum pressure difference occurring in systole (when ventricular pressure is closest to aortic pressure). If the blood inlet and outlet areas are in the same chamber, the outside and inside of the cannula will be exposed to the same pressures throughout the cardiac cycle leading to a nonpulsatile placement signal. In contrast to the left-sided devices, the differential pressure sensor on the RP is located by the blood inlet area. When the Impella catheter is appropriately positioned across the pulmonary valve, the outside of the differential pressure sensor is exposed to the inferior vena cava pressure, while the inside of the sensor is exposed to the pulmonary artery pressure. The placement signal will be pulsatile if the transvalvular heart pump is correctly positioned and will be nonpulsatile if the blood inlet and outlet areas are incorrectly located in the same chamber. Notably, the placement signal will also be pulsatile when the outlet is incorrectly positioned in the right ventricle, if the inlet is in the inferior vena cava. In this case, echocardiographic assessment will show the tip of the device in the right ventricle.

The motor current waveform displays the variation in energy use by the transvalvular heart pump motor (fig. 2; fig. A1). Energy use is affected by motor speed and by the pressure difference between the blood inlet and outlet areas. Because the pressure difference between the inlet and outlet changes throughout the cardiac cycle, the motor current waveform should be pulsatile if the device is appropriately positioned. This is particularly useful for left-sided devices to ensure that the device remains properly positioned. Notably, the motor current waveform will also be pulsatile even when the outlet of the RP is incorrectly positioned in the right ventricle, if the inlet is in the inferior vena cava.

Hemodynamic Effects

Transvalvular heart pump flow is directly related to rotations per minute of the device and inversely related to

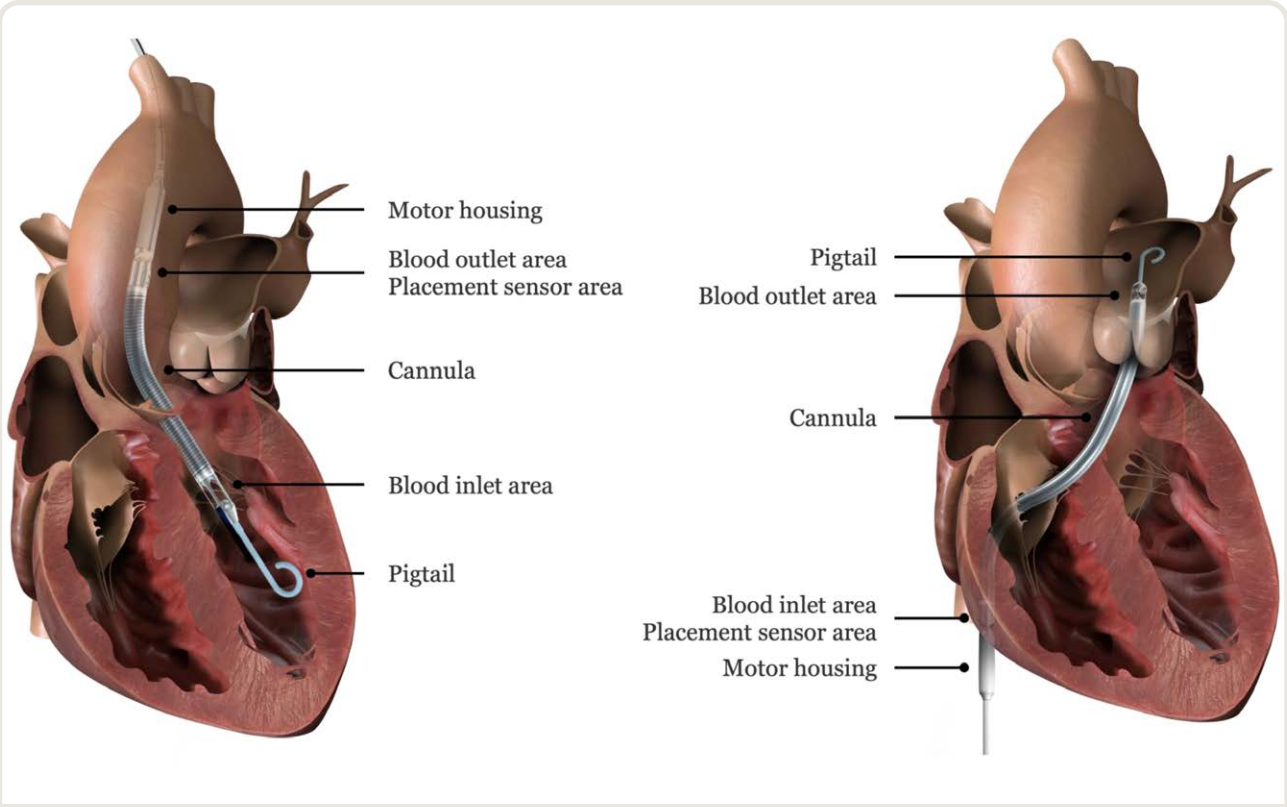

Fig. 1. Impella catheter. The Impella 5.0 (*left*) and Impella RP (*right*) are shown in their appropriate positions. Left-sided devices traverse the aortic valve, while the right-sided Impella RP traverses the tricuspid and pulmonary valves. Adapted and reproduced with permission from Abiomed Inc. (USA).

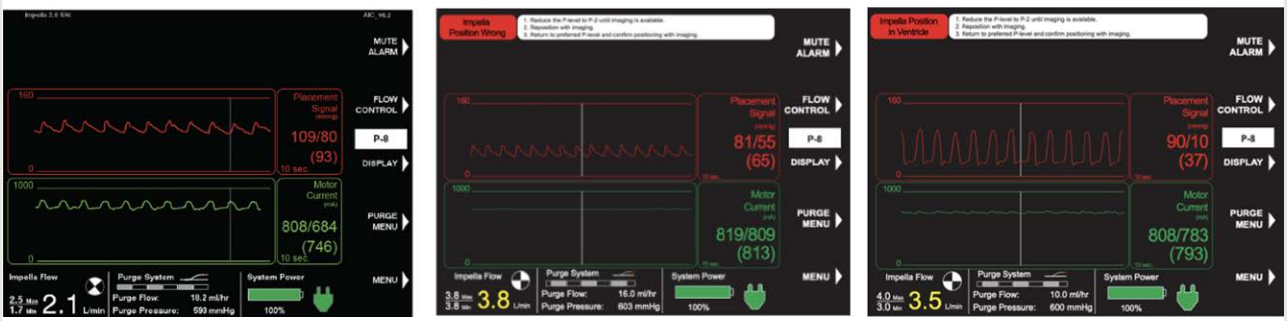

Fig. 2. Placement screen on the Automated Impella Controller. Placement screens generated by a fluid-filled pressure lumen (Impella 2.5 and CP) are shown. (*Left*) The transvalvular heart pump is appropriately positioned and shows an aortic waveform in the placement signal and a pulsatile motor current. (*Middle*) The blood inlet and outlet areas are both in the aorta (aortic waveform placement signal, flat motor current). (*Right*) Both the inlet and outlet areas are in the ventricle (ventricular waveform placement signal, flat motor current). Please see figure A1 for placement screens generated by a differential pressure sensor. Adapted and reproduced with permission from Abiomed Inc. (USA).

the pressure gradient between the blood inlet and outlet areas of the pump. The highest pump flow occurs when the gradient between the left ventricle and aorta (in the case of a left-sided device) or the inferior vena cava and pulmonary artery (in the case of the RP) is minimized. Variation in flow throughout the cardiac cycle is typically more pronounced in a left-sided device compared to the RP because there is greater pressure variation in the left ventricle than in the inferior vena cava and pulmonary artery.[8] Pump flows will decrease with vasopressor administration because the pressure gradient will increase as the systemic pressure (for left-sided devices) and pulmonary

arterial pressure (for the RP) increase. Unlike the intraaortic balloon pump, the transvalvular heart pump functions independently of cardiac rhythm and is not reliant upon on a consistent EKG signal or arterial pressure waveform to function properly.[9]

In left ventricular failure, the transvalvular heart pump is placed retrograde across the aortic valve and pumps blood from the left ventricle into the ascending aorta. This unloads the left ventricle, improves cardiac output, and increases systemic blood pressure.[9,10] Left ventricular unloading decreases peak left ventricular pressure, left ventricular end-diastolic pressure, and left ventricular wall tension, leading to a reduction in stroke work and myocardial oxygen demand. These hemodynamic effects are illustrated by the left ventricular pressure–volume loops in figure 3. Greater ventricular unloading is achieved with increasing pump flow rates, shown by a leftward shift in the pressure–volume loop. A decrease in the area enclosed by the loop reflects a reduction in left ventricular stroke work, while a decrease in the pressure–volume area reflects a reduction in myocardial oxygen consumption. Because the pump continuously unloads the ventricle throughout the cardiac cycle, isovolumic phases are absent, and the pressure–volume loop becomes triangular in shape. Left ventricular unloading also decreases left atrial and pulmonary capillary wedge pressure, which in turn may reduce cardiogenic pulmonary edema and right ventricular afterload.[9,11]

Escalating transvalvular heart pump flow rates induce a widening dissociation between arterial pressure, which increases, and peak left ventricular pressure, which decreases (fig. 3).[11] An increase in arterial diastolic pressure along with a decrease in left ventricular end-diastolic pressure leads to improved coronary perfusion pressure.[12]

In right ventricular failure, the transvalvular heart pump is placed antegrade across the tricuspid and pulmonary valves. Blood is pumped from the inferior vena cava into the pulmonary artery, bypassing the right ventricle. This decreases right atrial pressure while increasing mean pulmonary artery pressure and left ventricular preload.[8] If left ventricular function is normal, right-sided transvalvular heart pump support will result in increased or unchanged left ventricular pressures and improved cardiac output. However, in the setting of concomitant left ventricular dysfunction, right-sided transvalvular heart pump support may lead to a significant increase in left ventricular pressures, worsening left ventricular function, and pulmonary edema, with little improvement in cardiac output.[8] Similarly, initiation of left-sided transvalvular heart pump support in the setting of concomitant right ventricular dysfunction may result in an abrupt increase in right ventricular pressure and size, further exacerbating right ventricular dysfunction and limiting left ventricular preload. These effects underscore the importance of evaluating biventricular function before initiating right- or left-sided transvalvular heart pump support.

Evidence and Clinical Use

An overview of the major studies evaluating transvalvular heart pump use in cardiogenic shock are shown in table A1. While transvalvular heart pump support has been found to provide improved hemodynamics compared to intraaortic balloon pump counterpulsation, randomized controlled trials have not shown a survival benefit.[13,14] However, these trials involve very small numbers of patients and are likely underpowered. Studies have also found higher rates of major bleeding and vascular complications with transvalvular heart pump therapy compared to intraaortic balloon pump counterpulsation.[14,17] Therefore, while transvalvular heart pump use has expanded rapidly in recent years, there is limited evidence to support such robust growth. Larger randomized controlled trials are needed to further clarify the appropriate clinical indications and patient populations that would benefit most from transvalvular heart pump therapy.

The Impella received U.S. Food and Drug Administration approval in 2008 and is currently approved for commercial use in cardiogenic shock and high-risk percutaneous coronary intervention (PCI; table A2). In clinical practice, it is most commonly used for the treatment of acute heart failure—cardiogenic shock after acute myocardial infarction, decompensated heart failure,[22] postcardiotomy cardiogenic shock,[23] myocarditis,[24–26] and peripartum cardiomyopathy[27]—and for ventricular support during high-risk PCI. It has also been placed during procedures with elevated risk for hemodynamic instability, including ventricular tachycardia ablation,[28,29] off-pump coronary artery bypass grafting,[30] high-risk balloon aortic valvuloplasty,[31] and high-risk transcathether aortic valve replacement.[32] In advanced heart failure patients, transvalvular heart pump support has bridged patients to recovery, durable left ventricular assist device, and heart transplantation.[33] Finally, transvalvular heart pump therapy has been used to unload the left ventricle during the increased afterload state of venoarterial extracorporeal membrane oxygenation (ECMO).[34] The transvalvular heart pump is contraindicated in patients with conditions that would preclude safe device placement or use, including the presence of mechanical valves (aortic position for left-sided devices, and tricuspid or pulmonary position for the Impella RP) or cardiac thrombus, and significant valvular stenosis or regurgitation (aortic for left-sided devices, and tricuspid or pulmonary for Impella RP; table A3).

There are a number of known complications associated with transvalvular heart pump support. In a meta-analysis of 671 patients, Vargas *et al.*[35] found that major bleeding was the most common complication (19.9%). Hemolysis (10.5%), limb ischemia (5.0%), and stroke (3.8%) were also common. Hemolysis, which is caused by shear stress from the axial pump, may be exacerbated by higher device flows or obstruction of the blood inlet or outlet areas from improper device positioning or hypovolemia. Hemolysis

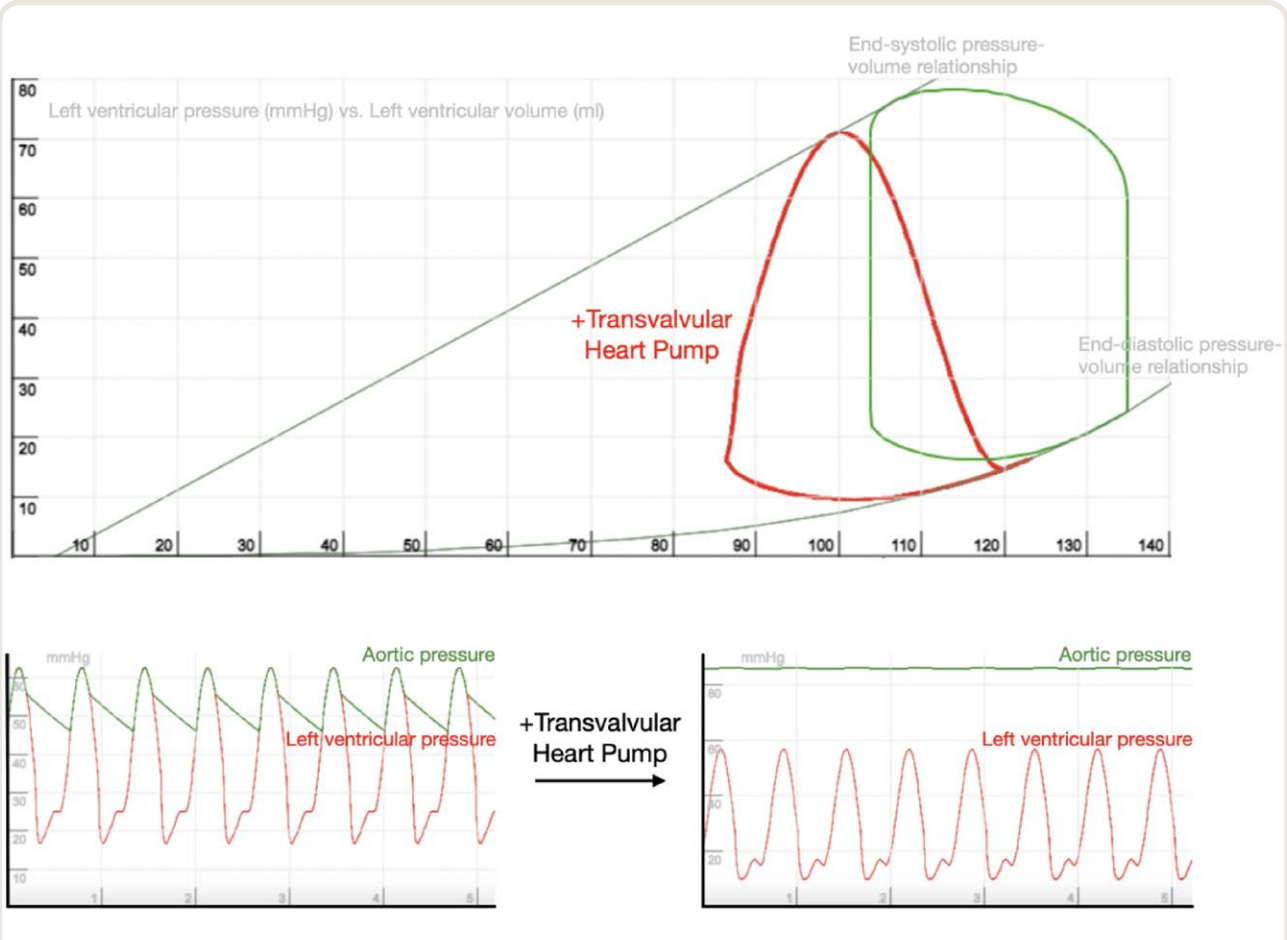

Fig. 3. Hemodynamic effects of the transvalvular heart pump. Pressure–volume relationships with (*red loop*) and without (*green loop*) transvalvular heart pump support are shown (*top*). The triangular-shaped pressure–volume loop reflects continuous left ventricular unloading performed by the pump. A reduction in pressure–volume area (the area enclosed by end-systolic pressure–volume relationship, end-diastolic pressure–volume relationship, and the systolic portion of the loop) with transvalvular heart pump support indicates a decrease in myocardial oxygen consumption. (*Bottom*) Uncoupling of arterial and left ventricular pressures after initiation of pump flow is illustrated. This uncoupling results in flattening of the arterial pressure waveform due to a loss of left ventricular ejection and native cardiac output. Figure created using Harvi.online with permission from PVLoops, Inc., USA (Burkhoff D, Dickstein ML, Schleicher T. Harvi – Online. Available at: https://harvi.online. Accessed December 15, 2021).

may also be an indicator of pump thrombosis. Persistent hemolysis despite proper device positioning and adequate volume is associated with acute kidney injury and may require device removal. In a meta-analysis comparing the transvalvular heart pump to intraaortic balloon pump counterpulsation, rates of major bleeding (relative risk, 3.11; 95% CI, 1.50 to 6.44; $P = 0.002$) and limb ischemia (relative risk, 2.58; 95% CI, 1.24 to 5.34; $P = 0.01$) were higher in the transvalvular heart pump population.[36] Infection, ventricular arrythmias, device migration, device malfunction from thrombosis, acute kidney injury, and thrombocytopenia are also known complications of transvalvular heart pump support.[14,37,38] Finally, aortic and mitral valve injury can occur during insertion or manipulation of left-sided devices, leading to clinically significant increases in aortic or mitral regurgitation.[39,40]

Perioperative Management

Device Placement and Initial Optimization

Standardized intraoperative monitoring requirements for patients who may require or are receiving transvalvular heart pump therapy have not been developed. However, it is appropriate to use standard American Society of Anesthesiologists monitors with continuous intraarterial blood pressure monitoring, pulmonary artery catheter monitoring, and echocardiography. In their analysis of registry data on 15,259 patients who received transvalvular heart pump support for cardiogenic shock, O'Neill *et al.*[16] found a higher survival rate in those who received hemodynamic monitoring with a pulmonary artery catheter than in those who did not (63% *vs.* 49%; $P < 0.0001$). In a separate registry analysis of 1,414 patients in cardiogenic shock, use

of complete pulmonary artery catheter-derived hemodynamic data before initiation of temporary mechanical circulatory support was found to be associated with improved survival.[41]

Anesthesiologists are most likely to encounter patients requiring transvalvular heart pump therapy for cardiogenic shock. The first line treatment for cardiogenic shock includes optimization of volume status and administration of vasopressors and inotropic medications. However, when medical therapy alone does not provide adequate circulatory support, temporary mechanical circulatory support should be considered. The specific mechanical circulatory support strategy will depend on patient factors, including the presence of any contraindications, as well as institutional experience and preference. The transvalvular heart pump is not commonly utilized in refractory cardiac arrest or when there is severe respiratory compromise; venoarterial ECMO should be considered in these situations.[42] Although not used in patients with severe primary pulmonary disease, transvalvular heart pump support may improve oxygenation by unloading the left heart and reducing pulmonary edema. The choice of left-sided transvalvular heart pump will depend in part on the level of support that is required; maximal flow rates range between 2.5 l/min for the Impella 2.5 and 6 l/min for the Impella 5.5 (table 1).

During transvalvular heart pump placement in the operating room, heparin should be administered to achieve an activated clotting time of 250 s or greater. Of note, while an activated clotting time of 250 s or greater is recommended for placement, the recommended activated clotting time for an indwelling device is 160 to 180 s. The optimal anticoagulation strategy for patients with heparin-induced thrombocytopenia is unknown. However, direct thrombin inhibitors have been used for both systemic anticoagulation and as a replacement for heparin in the purge solution.[9] The manufacturer notes that use of a purge solution without heparin has not been tested.[43]

Transesophageal echocardiography (TEE) can be used in combination with fluoroscopy to guide implantation. Successful implantation with TEE guidance alone has also been described when fluoroscopy is unavailable.[44] In the case of a left-sided transvalvular heart pump, the guidewire should be visualized in the lumen of the aorta, crossing the aortic valve and terminating in the left ventricle, with the tip directed toward the apex. The tip of the wire can be visualized crossing the aortic valve and terminating in the left ventricle using the midesophageal long-axis view. Worsening mitral regurgitation may occur with guidewire positioning because of interference with the mitral subvalvular apparatus. The midesophageal aortic valve long- and short-axis views can be used to verify normal aortic valve movement and rule out tethering or aortic valve injury. The descending aorta, aortic arch, and ascending aorta views should also be visualized to rule out aortic dissection. Once proper guidewire position is verified, the transvalvular heart pump is advanced over the wire under echocardiographic and fluoroscopic guidance. For the Impella 5.5, the device should be inserted 5 cm into the left ventricle from the aortic valve annulus (fig. 4). For the remaining left-sided devices, the inlet should terminate 3.5 cm into the ventricle (fig. 4). The tip of each device should be directed toward the left ventricular apex and sit in the middle of the ventricular cavity to prevent suction events. This should be verified using multiple two-dimensional views or a three-dimensional view of the left ventricle. A thorough examination of the aorta, mitral and aortic valves, and pericardial space should be performed after transvalvular heart pump implantation to promptly identify injuries to these structures. Transvalvular heart pump placement may also precipitate arrhythmias, which can often be managed by adjusting device position.

Echocardiographic guidance can also assist with Impella RP placement. The RP is inserted into the femoral vein and advanced antegrade over a guidewire, placed with the aid of a flow-directed catheter, across the tricuspid and pulmonary valves and into the pulmonary artery. As with left-sided device placement, the procedural steps can be visualized with echocardiography; correct positioning of the blood inlet (inferior vena cava) and outlet areas (4 cm into the pulmonary artery from the pulmonary valve annulus) should be confirmed; and surrounding structures, including the pericardial space, pulmonary artery, and tricuspid and pulmonary valves, should be examined to rule out injury.

For the sake of simplicity, we will primarily focus on the initial optimization of left-sided transvalvular heart pumps. Once a left-sided device is appropriately positioned, pump flow is initiated and increased gradually to allow the right ventricle to adapt to the increasing preload provided by the device and to allow for real-time hemodynamic and echocardiographic assessment. Color Doppler imaging should be used to confirm flow into the inlet (located in the left ventricle) and out of the outlet (located in the ascending aorta). Malpositioning of a left-sided transvalvular heart pump (inlet and outlet areas both within the left ventricle or both within the aorta) will cause recirculation and will not provide circulatory support. With correct positioning and optimization of pump flow rates, the interventricular septum should be in a neutral position when visualized in the midesophageal four-chamber view.

Deviation of the interventricular septum toward the right ventricular lateral wall may indicate inadequate left ventricular decompression, which may be due to malposition of the blood outlet area within the left ventricle. This will be associated with inadequate circulatory support and a lack of pulsatility (for devices with a differential pressure sensor) or increased pulsatility (left ventricular pressure waveform for devices with a fluid-filled or fiber-optic pressure sensor) on the placement screen of the Automated Impella Controller (fig. 2; fig. A1; table 1). If the transvalvular

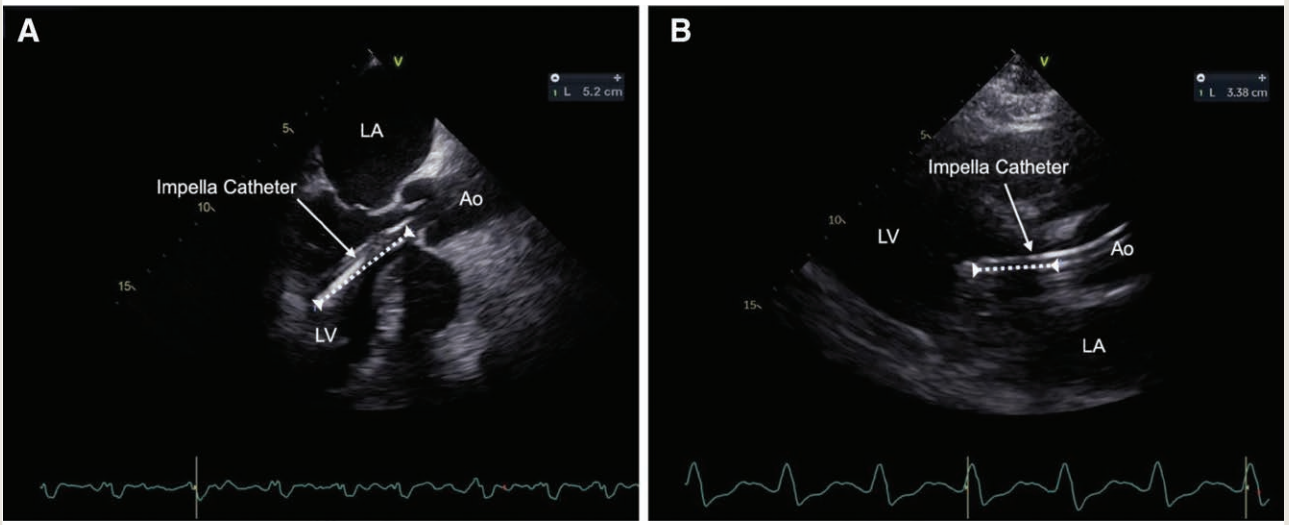

Fig. 4. Impella (Abiomed Inc., USA) placement. (*A*) The Impella 5.5 should be inserted 5.0 cm into the left ventricle, measured from the aortic valve annulus (*dashed line*). A midesophageal long-axis view is shown. (*B*) The Impella CP should be inserted 3.5 cm into the left ventricle (*dashed line*). A parasternal long-axis view is shown.

heart pump is noted to be inappropriately positioned, the device flow rate should be reduced, and the device should be repositioned under echocardiographic and fluoroscopic guidance. If rightward septal deviation remains despite appropriate device position, this can be managed by increasing transvalvular heart pump flows in the setting of inadequate cardiac output.

Deviation of the interventricular septum toward the left ventricular anterolateral wall as visualized in the midesophageal four-chamber view may indicate excessive left ventricular decompression due to pump flows that are too high, right heart failure causing inadequate left ventricular filling, or hypovolemia. Even if leftward septal shift is not caused by right ventricular failure, the resultant right ventricular distension will increase right ventricular wall stress and afterload and can lead to right ventricular decompensation. Device flow rates should be temporarily decreased, and the presence of right ventricular dysfunction or hypovolemia should be identified and treated.

Uriel *et al.*[45] have proposed a framework that can be used to evaluate the cardiovascular response to changing pump speeds after device implantation. This framework may be used to complement TEE evaluation. They propose monitoring the central venous pressure (CVP), pulmonary capillary wedge pressure (PCWP), and cardiac index as pump speeds are increased in a stepwise fashion. If achievable, the pump speed that normalizes PCWP, CVP, and cardiac index should be used.[11,45] As an example, patients with isolated left ventricular failure undergoing left-sided transvalvular heart pump placement may present with an elevated PCWP, normal CVP, and reduced cardiac index. As pump speeds are increased, PCWP should fall. If the right ventricle is able to increase right-sided output in response to the increase in venous return, CVP should remain within normal limits, and cardiac index should rise. A brisk rise in CVP and a greater-than-expected reduction in PCWP may indicate the need for additional right ventricular support.

Similarly, escalating pump speeds of a right-sided transvalvular heart pump in isolated right ventricular failure should reduce CVP and increase cardiac index with a minimal change in PCWP. A significant rise in PCWP may indicate the need for additional left ventricular support.

If additional left or right ventricular support is required, this may be achieved with escalation of inotropic support or initiation of pulmonary vasodilators, in the case of concomitant right ventricular failure. When this is inadequate, temporary mechanical circulatory support, including transvalvular heart pump placement, should be considered. In the case of BiPella (both left-sided Impella and Impella RP) support, it is critical to balance pulmonary and systemic blood flow.

If PCWP and CVP are both elevated despite increasing pump speeds and a normal cardiac index, the patient may be fluid overloaded and may benefit from diuretic therapy. On the other hand, if PCWP and CVP are both low, the patient may benefit from fluid administration.

Device Management

Patients receiving transvalvular heart pump support may require surgical intervention. Initial intraoperative management should include confirmation of appropriate device position and assessment of ventricular size and function by echocardiography. The adequacy of circulatory support

should also be continuously evaluated intraoperatively. Blood pressure, cardiac index, urine output, lactate, and mixed venous oxygen saturation are readily available indicators of tissue perfusion that should be monitored by the anesthesiologist. If there are signs of hypoperfusion, echocardiography and pulmonary artery catheter data can be used to elucidate the cause and to optimize pharmacologic and mechanical circulatory support. The potential causes of inadequate circulatory support and options for management are summarized in table 2 and described in the following paragraphs.

Hypoperfusion despite transvalvular heart pump support may be due to improper device positioning or device malfunction.[42] Device positioning was discussed in previous sections of this review and should be assessed when the expected pump flow cannot be achieved or when a suction event occurs. A suction event is a reduction in pump flow due to complete or partial obstruction of the blood inlet area. Suction events can be caused by incorrect device positioning (*i.e.*, blood inlet area abutting the ventricular wall), aspiration of thrombus, hypovolemia, or right ventricular failure leading to inadequate left ventricular preload. If a suction event occurs, device flow should be reduced until the etiology of the suction event is identified and addressed. Pump flows can then be returned to previous levels. Device malfunction is rare but often requires exchange or placement of an alternative mechanical circulatory support device. Malfunction is most frequently caused by aspiration of thrombus into the pump and typically presents with a motor current spike followed by motor current instability and hemolysis.[42]

Inadequate preload is a common cause of inadequate pump flow and may be due to hypovolemia or failure of the unsupported ventricle.[42] Hypovolemia should be suspected if filling pressures decrease in the setting of a constant pump speed, particularly in procedures with significant blood loss or coagulopathy. Assessment of ventricular size on echocardiography will also provide information on the etiology of inadequate preload. In particular, a low cardiac output associated with a reduction in both right and left end-diastolic volumes suggests that the patient is hypovolemic and will respond to volume administration. Fluid responsiveness can also often be assessed by passive leg raise, Trendelenburg positioning, or fluid challenge. In hypovolemia without concomitant dysfunction of the unsupported ventricle, a rapid fluid bolus should improve cardiac output without inducing a rapid significant rise in CVP or PCWP.

Failure of the unsupported ventricle may also cause inadequate preload to the supported ventricle, leading to low pump flow. Optimizing right ventricular function is one of the cornerstones of the management of left-sided transvalvular heart pumps. Poor right ventricular function often presents with an elevated CVP and reduced pulmonary artery pulsatility index.[46] Pulmonary artery pulsatility index is equal to pulmonary artery pulse pressure divided by CVP. A pulmonary artery pulsatility index less than 1.0 was found to be a highly sensitive marker for right ventricular failure in acute myocardial infarction,[47] while a pulmonary artery pulsatility index less than 1.85 was a sensitive predictor of right ventricular failure after left ventricular assist device implantation.[48] Echocardiographic signs of right ventricular dysfunction include worsening right ventricular dilation, a leftward shift in the interatrial or interventricular septum, and a reduction in parameters such as right ventricular fractional area change, tricuspid annular plane systolic excursion, and tissue Doppler-derived tricuspid lateral annular systolic velocity. Right ventricular output may be improved by reducing afterload with pulmonary vasodilators such as inhaled prostacyclin or nitric oxide and increasing contractility with inotropic agents such as epinephrine or milrinone. Right ventricular afterload may also be minimized by optimizing mechanical ventilation to achieve the lowest mean airway pressures and positive end-expiratory pressure that effectively avoids hypercarbia, atelectasis, and hypoxemia.[49] Left-sided transvalvular heart pump flows should also be adjusted to avoid leftward shift of the interventricular septum, with the goal of keeping the interventricular septum midline. Increasing systemic vascular resistance can reduce flattening of the interventricular septum by inducing a net increase in the pressure gradient between the device inlet and outlet areas. If this occurs, and rotations per minute are held constant, pump flow will be reduced, and left ventricular volumes will increase. In addition to decreasing leftward septal shift, increasing systemic vascular resistance can also be helpful in acutely reversing a suction event. Right-sided mechanical circulatory support, including use of the Impella RP should be considered in refractory right ventricular failure.

In the setting of an Impella RP, insufficient support may be caused by concomitant left ventricular failure. Under these conditions, cardiac output will remain unchanged or increase slightly with increasing RP flows, but the incremental improvement may not be enough to provide adequate circulatory support.[8] Left ventricular volumes and pressures may also increase significantly with escalating Impella RP flow rates, leading to pulmonary edema.[8] As such, biventricular failure must be identified and managed when initiating Impella RP support. Signs of left ventricular failure include an elevated PCWP, as well as worsening mitral regurgitation, left ventricular dilation, and poor ventricular contractility on echocardiography. Additionally, a cardiac power output less than 0.6 W is an indicator of ongoing cardiogenic shock.[50,51] Cardiac power output is equal to mean arterial pressure times cardiac output divided by 451. Management of left ventricular failure should include afterload optimization and consideration for additional inotropic or left ventricular mechanical support.

Table 2. Intraoperative Causes of Inadequate Circulatory Support in Transvalvular Heart Pump Therapy

Causes	Corroborating Findings	Treatment Options
Device-related complications		
Malposition	• Improper placement on echocardiography • Automated Impella Controller (Abiomed Inc., USA) showing inappropriate placement signal	• Reposition device
Malfunction	• Presence of thrombus on echocardiography • Motor current spike and instability • Abrupt cessation of pump flow	• Exchange device
Inadequate preload		
Hypovolemia	• Reduced biventricular filling on echocardiography • Improvement in systemic blood flow with fluid challenge • Reduction in CVP and PCWP • Presence of intraoperative bleeding	• Administer crystalloid, packed red blood cells • Treat coagulopathy
Dysfunction of unsupported ventricle	• Reduced ventricular function on echocardiography • No improvement in systemic blood flow with fluid challenge • *Right ventricular dysfunction*: elevated CVP and low/normal PCWP, reduced pulmonary artery pulsatility index • *Left ventricular dysfunction*: elevated PCWP and low/normal CVP, pulmonary edema	• Administer/escalate inotropic support • Optimize ventricular afterload* • Adjust device flows to optimize ventricular shape† • Place mechanical circulatory support device in unsupported ventricle • Rule out/treat arrhythmia, tamponade
Increased metabolic demand	• Inadequate depth of anesthesia • Hyperthermia	• Treat underlying cause • Increase depth of anesthesia • Avoid hyperthermia • Consider muscle paralysis, tracheal intubation
Insufficient maximum device flow	• Persistent hypoperfusion despite maximum device flow	• Place higher flow device • Place additional mechanical circulatory support device

*Pulmonary vasodilators/adjustment of ventilator settings to reduce right ventricular afterload. Reduction in vasopressor support to reduce left ventricular afterload. †Transvalvular heart pump flows should be adjusted to obtain a neutral interventricular septum (*e.g.*, reducing left-sided device flows can decrease flattening of the interventricular septum in the setting of excessive left ventricular decompression).

CVP, central venous pressure; PCWP, pulmonary capillary wedge pressure.

Ventricular function may be influenced by factors outside of intrinsic myocardial contractility, such as arrhythmia or cardiac tamponade. Depending on the hemodynamic status and precise rhythm abnormality, an arrhythmia may be managed medically or electrically, with pacing, cardioversion, or defibrillation. If cardiopulmonary resuscitation is indicated, device flow rates should be reduced while resuscitation is performed. After recovery of cardiac function to preresuscitation levels, pump flow rates may be restored. Because chest compressions may result in transvalvular heart pump displacement,[52] correct pump placement should be confirmed with imaging and assessment of the placement signal on the Automated Impella Controller. Tamponade in the setting of left-sided support presents with an elevated CVP without equalization of pressures,[42] and pericardial effusion with chamber collapse on echocardiography. The effusion should be drained to restore ventricular function and cardiac preload.

Inadequate circulatory support may also be due to increased metabolic demand,[42] which should be managed by treating the underlying cause. Intraoperatively, this may also require deeper levels of anesthesia, tracheal intubation, muscle paralysis, and avoidance of hyperthermia. Despite minimizing metabolic demand, confirming appropriate device function and position, and optimizing volume status and ventricular function, transvalvular heart pump therapy still may not provide sufficient support despite maximum pump flow. This should prompt consideration for escalation to a device capable of higher maximum flow or placement of an additional mechanical circulatory support device.

Weaning and Explantation

Due to a lack of standardized practice guidelines, the timing and management of weaning from transvalvular heart pump support is often determined by institution-specific protocols. In general, weaning should be considered once patient hemodynamics have stabilized (mean arterial pressure of at least 65 mmHg and heart rate less than 100 beats/min) on less than moderate doses of pharmacologic support, systemic arterial pulsatility (left-sided device), and pulmonary arterial pulsatility (right-sided device) have increased, indicators of tissue perfusion have improved (lactate less than 2 mmol/l), and end-organ dysfunction is resolving.[53] Under these conditions, transvalvular heart pump flows can be gradually reduced in a stepwise fashion while monitoring hemodynamics, mixed venous oxygen saturation, cardiac index, and ventricular function with echocardiography. Real-time calculated cardiac power output, which is available with SmartAssist (Abiomed Inc.) technology on the Impella CP and 5.5 devices, should not decrease

significantly during the weaning process.[53] If the transvalvular heart pump is removed in the operating room, the same monitors and parameters used during device implantation, including pulmonary artery catheterization and echocardiography, may be used to ensure adequate ventricular function and end-organ perfusion. Low doses of inotropes and vasopressors, including epinephrine and norepinephrine, are frequently administered to facilitate the weaning process and device explant. The transvalvular heart pump is typically removed once the activated clotting time is less than 150 to 160 s. In cases of inadequate myocardial recovery, a decision should be made regarding patient candidacy for escalation to durable ventricular assist device or heart transplantation. If irreversible multiorgan failure has occurred, withdrawal of mechanical circulatory support may also be considered.

Future Directions

With advancements in device technology,[54] the clinical uptake of transvalvular heart pump therapy will likely continue to grow. Larger, high-quality randomized controlled trials are needed to further clarify optimal clinical indications, patient selection criteria, and outcomes compared to standard therapy and alternative mechanical circulatory support devices. One such ongoing study is the Danish–German cardiogenic shock trial (ClinicalTrials.gov NCT01633502), a randomized controlled trial comparing Impella CP to conventional circulatory support in patients with acute myocardial infarction complicated by cardiogenic shock.[55] As use of the transvalvular heart pump in the treatment of cardiogenic shock increases, anesthesiologists will increasingly be called upon to care for patients who are receiving or may require mechanical support. A comprehensive understanding of the transvalvular heart pump, its mechanics, hemodynamic effects, and considerations for perioperative management will allow anesthesiologists to provide optimal patient care and contribute to the perioperative decision-making process.

Research Support

Support was provided solely from institutional and/or departmental sources.

Competing Interests

Dr. Naka is a consultant for Abbott (Abbott Park, Illinois), Biomet-Zimmer (Warsaw, Indiana), and CryoLife (Kennesaw, Georgia) and a speaker for Nipro (Osaka, Japan). Dr. Dickstein is a consultant for LivaNova (London, United Kingdom) and Abiomed (Danvers, Massachusetts) and is cofounder of PVLoops, Inc. (Remsenburg, New York). The other authors declare no competing interests.

Correspondence

Address correspondence to Dr. Wu: 601 Elmwood Avenue, Box 604, Rochester, New York 14642. isaac_wu@urmc.rochester.edu. ANESTHESIOLOGY's articles are made freely accessible to all readers on www.anesthesiology.org, for personal use only, 6 months from the cover date of the issue.

Appendix

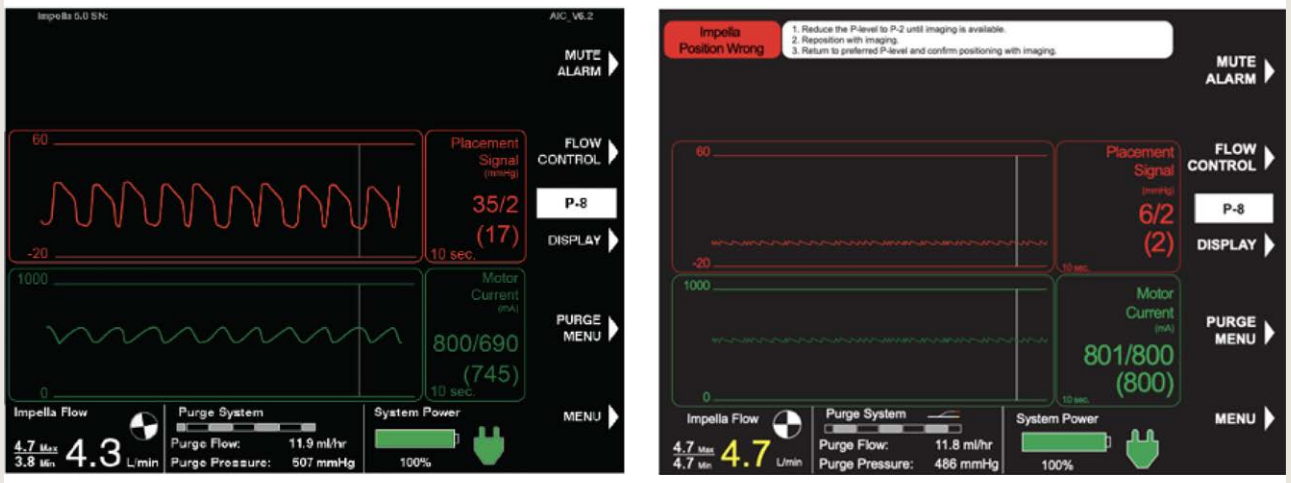

Fig. A1. Placement screen. Placement screens generated by a differential pressure sensor (Impella LD and 5.0) in an appropriately placed transvalvular heart pump (*left*) and inappropriately placed transvalvular heart pump (*right*) are shown. (*Right*) The inlet and outlet areas of the pump are in the same chamber (either the aorta or ventricle), resulting in no pulsatility in the placement signal or motor current. Adapted and reproduced with permission from Abiomed Inc. (USA).

Table A1. Overview of Major Studies

Reference	Design	Patient Population	N	Device(s)	Findings	Limitations
Seyfarth *et al.*[13]	Prospective, randomized	Cardiogenic shock after acute MI	26	Impella 2.5 (Abiomed Inc., USA) *vs.* intraaortic balloon pump	• Greater change in cardiac index from baseline at 30 minutes in Impella group: 0.49 ± 0.46 l/min/m^2 (Impella) *vs.* $0.11 \pm .31$ l/min/m^2 (intraaortic balloon pump), $P = 0.02$ • No difference in 30-day mortality: 46% in both groups	• Small N • Underpowered for mortality analysis
Ouweneel *et al.*[14]	Prospective, randomized	Cardiogenic shock after acute MI*	48	Impella CP *vs.* intraaortic balloon pump	• No difference in 30-day all-cause mortality: 46% (Impella) *vs.* 50% (intraaortic balloon pump), $P = 0.92$ • Major vascular/bleeding complications were higher in the Impella group	• Small N • Underpowered
Ouweneel *et al.*[15]	Meta-analysis	Cardiogenic shock after acute MI	95	Impella 2.5/CP *vs.* intraaortic balloon pump	• No difference in 30-day and 6-month all-cause mortality • No difference in follow-up left ventricular ejection fraction in subset of patients	• Retrospective • Small number of included studies/ total N • Included studies with different inclusion criteria
O'Neill *et al.*[16]	Retrospective analysis	Cardiogenic shock after acute MI	15,259	Impella 2.5/CP/5.0	• 51% survival to explantation • Wide variation in survival rates between institutions • Higher-volume centers, pre-PCI Impella implantation, use of right heart catheter associated with higher survival rate	• Retrospective • No control arm
Schrage *et al.*[17]	Retrospective, matched-pair analysis with Intraaortic Balloon Pump in Cardiogenic Shock II trial patients	Cardiogenic shock after acute MI	237 matched pairs	Impella 2.5/CP *vs.* intraaortic balloon pump or medical therapy	• No difference in 30-day mortality: 48.5% (Impella) *vs.* 46.4% (intraaortic balloon pump or medical therapy), $P = 0.64$ • Higher rates of major bleeding and peripheral vascular complications in Impella group	• Retrospective
Dhruva *et al.*[18]	Retrospective, propensity-matched analysis	Cardiogenic shock after acute MI	1,680 matched pairs	Impella device(s) not specified *vs.* intraaortic balloon pump	• Higher risk of in-hospital mortality in Impella group: absolute risk difference 10.9% (95% CI, 7.1 to 14.2%), $P < 0.001$ • Higher risk of in-hospital major bleeding in Impella group: absolute risk difference 15.4% (95% CI, 12.5 to 18.2), $P < 0.001$	• Retrospective
Griffith *et al.*[19]	Prospective, single-arm	Postcardiotomy shock	16	Impella 5.0/LD	• 94% survival until next therapy • 13% incidence of major adverse events • Improvement in cardiac index, MAP, pulmonary artery diastolic pressure	• Small N • No control arm
Anderson *et al.*[20]	Prospective, single-arm	Right ventricular failure after MI or cardiac surgery	30	Impella RP	• 73% survival to 30 days or hospital discharge • Improvement in cardiac index, reduction in CVP after device initiation	• Small N • No control arm
Anderson *et al.*[21]	Retrospective analysis	Right ventricular failure after MI or cardiac surgery	60	Impella RP	• 72% 30-day survival rate • Improvement in cardiac index, reduction in CVP after device initiation	• Retrospective • Small N • No control arm

*This study included only patients with ST-segment elevation myocardial infarction.

CVP, central venous pressure; MAP, mean arterial pressure; MI, myocardial infarction; PCI, percutaneous coronary intervention.

Table A2. U.S. Food and Drug Administration Approval Indications

Device	Approved Indications	Maximum Duration
Impella 2.5 (Abiomed Inc., USA)	High-risk PCI*	6 h
	Refractory cardiogenic shock†	4 days
	COVID-19 emergency use authorization‡	4 days
Impella CP	High-risk PCI*	6 h
	Refractory cardiogenic shock†	4 days
	COVID-19 emergency use authorization‡	4 days
Impella LD	Refractory cardiogenic shock†	14 days
Impella 5.0	Refractory cardiogenic shock†	14 days
	COVID-19 emergency use authorization‡	14 days
Impella 5.5	Refractory cardiogenic shock†	14 days
	COVID-19 emergency use authorization‡	14 days
Impella RP	Acute right heart failure§	14 days
	COVID-19 emergency use authorization‖	14 days

*Performed electively or urgently in hemodynamically stable patients with severe coronary artery disease. †Because of left ventricular failure in the setting of acute myocardial infarction, cardiac surgery, cardiomyopathy, and myocarditis. ‡In patients with COVID-19 and heart failure from myocarditis while on veno-venous ECMO or with pulmonary edema while on veno-arterial ECMO. §In the setting of acute myocardial infarction, heart transplantation, left ventricular assist device implantation, or cardiac surgery in patients with a body surface area greater than or equal to 1.5 m^2. ‖In patients with acute right ventricular failure caused by complications from COVID-19.

ECMO, extracorporeal membrane oxygenation; PCI, percutaneous coronary intervention.

Table A3. Contraindications

Contraindications to left-sided Impella (Abiomed Inc., USA)
- Presence of a mechanical aortic valve
- Presence of left ventricular thrombus
- Inability to tolerate anticoagulation
- Presence of an atrial or ventricular septal defect
- Severe peripheral arterial disease
- Severe aortic stenosis/≥2+ aortic regurgitation

Contraindications to Impella RP
- Presence of a mechanical tricuspid or pulmonary valve
- Presence of right-sided thrombus
- Presence of vena caval filter
- Severe tricuspid or pulmonary valve stenosis/regurgitation

References

1. Werdan K, Gielen S, Ebelt H, Hochman JS: Mechanical circulatory support in cardiogenic shock. Eur Heart J 2014; 35:156–67
2. Stretch R, Sauer CM, Yuh DD, Bonde P: National trends in the utilization of short-term mechanical circulatory support: Incidence, outcomes, and cost analysis. J Am Coll Cardiol 2014; 64:1407–15
3. Strom JB, Zhao Y, Shen C, Chung M, Pinto DS, Popma JJ, Yeh RW: National trends, predictors of use, and in-hospital outcomes in mechanical circulatory support for cardiogenic shock. EuroIntervention 2018; 13:e2152–9
4. Amin AP, Spertus JA, Curtis JP, Desai N, Masoudi FA, Bach RG, McNeely C, Al-Badarin F, House JA, Kulkarni H, Rao SV: The evolving landscape of Impella use in the United States among patients undergoing percutaneous coronary intervention with mechanical circulatory support. Circulation 2020; 141:273–84
5. Shah M, Patnaik S, Patel B, Ram P, Garg L, Agarwal M, Agrawal S, Arora S, Patel N, Wald J, Jorde UP: Trends in mechanical circulatory support use and hospital mortality among patients with acute myocardial infarction and non-infarction related cardiogenic shock in the United States. Clin Res Cardiol 2018; 107:287–303
6. Mazzeffi MA, Rao VK, Dodd-o J, Del Rio JM, Hernandez A, Chung M, Bardia A, Bauer RM, Meltzer JS, Satyapriya S, Rector R, Ramsay JG, Gutsche J: Intraoperative management of adult patients on extracorporeal membrane oxygenation: An expert consensus statement from the Society of Cardiovascular Anesthesiologists—Part II. Intraoperative management and troubleshooting. Anesth Analg 2021; 133:1478–93
7. González LS, Chaney MA: Intraaortic balloon pump counterpulsation. Part I: History, technical aspects, physiologic effects, contraindications, medical applications/outcomes. Anesth Analg 2020; 131:776–91
8. Kapur NK, Esposito ML, Bader Y, Morine KJ, Kiernan MS, Pham DT, Burkhoff D: Mechanical circulatory support devices for acute right ventricular failure. Circulation 2017; 136:314–26
9. Burzotta F, Trani C, Doshi SN, Townend J, van Geuns RJ, Hunziker P, Schieffer B, Karatolios K, Møller JE, Ribichini FL, Schäfer A, Henriques JP: Impella ventricular support in clinical practice: Collaborative viewpoint from a European expert user group. Int J Cardiol 2015; 201:684–91
10. Kar B, Gregoric ID, Basra SS, Idelchik GM, Loyalka P: The percutaneous ventricular assist device in severe refractory cardiogenic shock. J Am Coll Cardiol 2011; 57:688–96
11. Burkhoff D, Sayer G, Doshi D, Uriel N: Hemodynamics of mechanical circulatory support. J Am Coll Cardiol 2015; 66:2663–74
12. Alqarqaz M, Basir M, Alaswad K, O'Neill W: Effects of Impella on coronary perfusion in patients with critical coronary artery stenosis. Circ Cardiovasc Interv 2018; 11:e005870
13. Seyfarth M, Sibbing D, Bauer I, Fröhlich G, Bott-Flügel L, Byrne R, Dirschinger J, Kastrati A, Schömig A: A randomized clinical trial to evaluate the safety and efficacy of a percutaneous left ventricular assist device *versus* intra-aortic balloon pumping for treatment of cardiogenic shock caused by myocardial infarction. J Am Coll Cardiol 2008; 52:1584–8
14. Ouweneel DM, Eriksen E, Sjauw KD, van Dongen IM, Hirsch A, Packer EJ, Vis MM, Wykrzykowska JJ, Koch KT, Baan J, de Winter RJ, Piek JJ, Lagrand WK, de Mol BA, Tijssen JG, Henriques JP: Percutaneous mechanical circulatory support *versus* intra-aortic balloon pump in

cardiogenic shock after acute myocardial infarction. J Am Coll Cardiol 2017; 69:278–87
15. Ouweneel DM, Eriksen E, Seyfarth M, Henriques JP: Percutaneous mechanical circulatory support *versus* intra-aortic balloon pump for treating cardiogenic shock: Meta-analysis. J Am Coll Cardiol 2017; 69:358–60
16. O'Neill WW, Grines C, Schreiber T, Moses J, Maini B, Dixon SR, Ohman EM: Analysis of outcomes for 15,259 US patients with acute myocardial infarction cardiogenic shock (AMICS) supported with the Impella device. Am Heart J 2018; 202:33–8
17. Schrage B, Ibrahim K, Loehn T, Werner N, Sinning JM, Pappalardo F, Pieri M, Skurk C, Lauten A, Landmesser U, Westenfeld R, Horn P, Pauschinger M, Eckner D, Twerenbold R, Nordbeck P, Salinger T, Abel P, Empen K, Busch MC, Felix SB, Sieweke JT, Møller JE, Pareek N, Hill J, MacCarthy P, Bergmann MW, Henriques JPS, Möbius-Winkler S, Schulze PC, Ouarrak T, Zeymer U, Schneider S, Blankenberg S, Thiele H, Schäfer A, Westermann D: Impella support for acute myocardial infarction complicated by cardiogenic shock. Circulation 2019; 139:1249–58
18. Dhruva SS, Ross JS, Mortazavi BJ, Hurley NC, Krumholz HM, Curtis JP, Berkowitz A, Masoudi FA, Messenger JC, Parzynski CS, Ngufor C, Girotra S, Amin AP, Shah ND, Desai NR: Association of use of an intravascular microaxial left ventricular assist device *vs.* intra-aortic balloon pump with in-hospital mortality and major bleeding among patients with acute myocardial infarction complicated by cardiogenic shock. JAMA 2020; 323:734–45
19. Griffith BP, Anderson MB, Samuels LE, Pae WE Jr, Naka Y, Frazier OH: The RECOVER I: A multicenter prospective study of Impella 5.0/LD for postcardiotomy circulatory support. J Thorac Cardiovasc Surg 2013; 145:548–54
20. Anderson MB, Goldstein J, Milano C, Morris LD, Kormos RL, Bhama J, Kapur NK, Bansal A, Garcia J, Baker JN, Silvestry S, Holman WL, Douglas PS, O'Neill W: Benefits of a novel percutaneous ventricular assist device for right heart failure: The prospective RECOVER RIGHT study of the Impella RP device. J Heart Lung Transplant 2015; 34:1549–60
21. Anderson M, Morris DL, Tang D, Batsides G, Kirtane A, Hanson I, Meraj P, Kapur NK, O'Neill W: Outcomes of patients with right ventricular failure requiring short-term hemodynamic support with the Impella RP device. J Heart Lung Transplant 2018; 37:1448–58
22. Cena M, Karam F, Ramineni R, Khalife W, Barbagelata A: New Impella cardiac power device used in patient with cardiogenic shock due to nonischemic cardiomyopathy. Int J Angiol 2016; 25:258–62
23. Seliem A, Hall SA: The new era of cardiogenic shock: Progress in mechanical circulatory support. Curr Heart Fail Rep 2020; 17:325–32
24. Yastrebov K, Brunel L, Paterson HS, Williams ZA, Wise IK, Burrows CS, Bannon PG: Implantation of Impella CP left ventricular assist device under the guidance of three-dimensional intracardiac echocardiography. Sci Rep 2020; 10:17485
25. Fox H, Farr M, Horstkotte D, Flottmann C: Fulminant myocarditis managed by extracorporeal life support (Impella® CP): A rare case. Case Rep Cardiol 2017; 2017:9231959
26. Tschöpe C, Van Linthout S, Klein O, Mairinger T, Krackhardt F, Potapov EV, Schmidt G, Burkhoff D, Pieske B, Spillmann F: Mechanical unloading by fulminant myocarditis: LV-IMPELLA, ECMELLA, BI-PELLA, and PROPELLA Concepts. J Cardiovasc Transl Res 2019; 12:116–23
27. Schroeter MR, Unsold B, Holke K, Schillinger W: Pro-thrombotic condition in a woman with peripartum cardiomyopathy treated with bromocriptine and an Impella LP 2.5 heart pump. Clin Res Cardiol 2013; 102:155–7
28. Miller MA, Dukkipati SR, Chinitz JS, Koruth JS, Mittnacht AJ, Napolitano C, d'Avila A, Reddy VY: Percutaneous hemodynamic support with Impella 2.5 during scar-related ventricular tachycardia ablation (PERMIT 1). Circ Arrhythm Electrophysiol 2013; 6:151–9
29. Reddy YM, Chinitz L, Mansour M, Bunch TJ, Mahapatra S, Swarup V, Di Biase L, Bommana S, Atkins D, Tung R, Shivkumar K, Burkhardt JD, Ruskin J, Natale A, Lakkireddy D: Percutaneous left ventricular assist devices in ventricular tachycardia ablation: Multicenter experience. Circ Arrhythm Electrophysiol 2014; 7:244–50
30. Glazier JJ, Kaki A: The Impella device: Historical background, clinical applications and future directions. Int J Angiol 2019; 28:118–23
31. Ludeman DJ, Schwartz BG, Burstein S: Impella-assisted balloon aortic valvuloplasty. J Invasive Cardiol 2012; 24:E19–20
32. Singh V, Damluji AA, Mendirichaga R, Alfonso CE, Martinez CA, Williams D, Heldman AW, de Marchena EJ, O'Neill WW, Cohen MG: Elective or emergency use of mechanical circulatory support devices during transcatheter aortic valve replacement. J Interv Cardiol 2016; 29:513–22
33. Lima B, Kale P, Gonzalez-Stawinski GV, Kuiper JJ, Carey S, Hall SA: Effectiveness and safety of the Impella 5.0 as a bridge to cardiac transplantation or durable left ventricular assist device. Am J Cardiol 2016; 117:1622–8
34. Lim HS: The physiologic basis and clinical outcomes of combined Impella and veno-arterial extracorporeal membrane oxygenation support in cardiogenic shock. Cardiol Ther 2020; 9:245–55
35. Vargas KG, Jäger B, Kaufmann CC, Biagioli A, Watremez S, Gatto F, Özbek C, Razouk A, Geppert A, Huber K: Impella in cardiogenic shock following acute myocardial

infarction: A systematic review and meta-analysis. Wien Klin Wochenschr 2020; 132:716–25
36. Wernly B, Seelmaier C, Leistner D, Stähli BE, Pretsch I, Lichtenauer M, Jung C, Hoppe UC, Landmesser U, Thiele H, Lauten A: Mechanical circulatory support with Impella *versus* intra-aortic balloon pump or medical treatment in cardiogenic shock-a critical appraisal of current data. Clin Res Cardiol 2019; 108:1249–57
37. Wong ASK, Sin SWC: Short-term mechanical circulatory support (intra-aortic balloon pump, Impella, extracorporeal membrane oxygenation, TandemHeart): A review. Ann Transl Med 2020; 8:829
38. O'Neill WW, Schreiber T, Wohns DH, Rihal C, Naidu SS, Civitello AB, Dixon SR, Massaro JM, Maini B, Ohman EM: The current use of Impella 2.5 in acute myocardial infarction complicated by cardiogenic shock: Results from the USpella registry. J Interv Cardiol 2014; 27:1–11
39. Sef D, Kabir T, Lees NJ, Stock U: Valvular complications following the Impella device implantation. J Card Surg 2021; 36:1062–6
40. Hironaka CE, Ortoleva J, Zhan Y, Chen FY, Couper GS, Kapur NK, Kawabori M: The effects of percutaneous left ventricular assist device placement on native valve competency. ASAIO J 2021;1529
41. Garan AR, Kanwar M, Thayer KL, Whitehead E, Zweck E, Hernandez-Montfort J, Mahr C, Haywood JL, Harwani NM, Wencker D, Sinha SS, Vorovich E, Abraham J, O'Neill W, Burkhoff D, Kapur NK: Complete hemodynamic profiling with pulmonary artery catheters in cardiogenic shock is associated with lower in-hospital mortality. JACC Heart Fail 2020; 8:903–13
42. Balthazar T, Vandenbriele C, Verbrugge FH, Den Uil C, Engström A, Janssens S, Rex S, Meyns B, Van Mieghem N, Price S, Adriaenssens T: Managing patients with short-term mechanical circulatory support: JACC review topic of the week. J Am Coll Cardiol 2021; 77:1243–56
43. Abiomed. Impella Ventricular Support Systems for Use during Cardiogenic Shock and High-Risk PCI. Impella 2.5, Impella 5.0, Impella LD, and Impella CP (Shock): Impella 2.5 and Impella CP (HRPCI). Instructions for use and clinical reference manual. Danvers, Massachusetts, Abiomed, Inc., 2021
44. Pieri M, Pappalardo F: Bedside insertion of impella percutaneous ventricular assist device in patients with cardiogenic shock. Int J Cardiol 2020; 316:26–30
45. Uriel N, Sayer G, Addetia K, Fedson S, Kim GH, Rodgers D, Kruse E, Collins K, Adatya S, Sarswat N, Jorde UP, Juricek C, Ota T, Jeevanandam V, Burkhoff D, Lang RM: Hemodynamic ramp tests in patients with left ventricular assist devices. JACC Heart Fail 2016; 4:208–17
46. Gudejko MD, Gebhardt BR, Zahedi F, Jain A, Breeze JL, Lawrence MR, Shernan SK, Kapur NK, Kiernan MS, Couper G, Cobey FC: Intraoperative hemodynamic and echocardiographic measurements associated with severe right ventricular failure after left ventricular assist device implantation. Anesth Analg 2019; 128:25–32
47. Korabathina R, Heffernan KS, Paruchuri V, Patel AR, Mudd JO, Prutkin JM, Orr NM, Weintraub A, Kimmelstiel CD, Kapur NK: The pulmonary artery pulsatility index identifies severe right ventricular dysfunction in acute inferior myocardial infarction. Catheter Cardiovasc Interv 2012; 80:593–600
48. Morine KJ, Kiernan MS, Pham DT, Paruchuri V, Denofrio D, Kapur NK: Pulmonary artery pulsatility index is associated with right ventricular failure after left ventricular assist device surgery. J Card Fail 2016; 22:110–6
49. Alviar CL, Miller PE, McAreavey D, Katz JN, Lee B, Moriyama B, Soble J, van Diepen S, Solomon MA, Morrow DA; ACC Critical Care Cardiology Working Group: Positive pressure ventilation in the cardiac intensive care unit. J Am Coll Cardiol 2018; 72:1532–53
50. Rab T, Ratanapo S, Kern KB, Basir MB, McDaniel M, Meraj P, King SB III, O'Neill W: Cardiac shock care centers: JACC review topic of the week. J Am Coll Cardiol 2018; 72:1972–80
51. Fincke R, Hochman JS, Lowe AM, Menon V, Slater JN, Webb JG, LeJemtel TH, Cotter G; SHOCK Investigators: Cardiac power is the strongest hemodynamic correlate of mortality in cardiogenic shock: A report from the SHOCK trial registry. J Am Coll Cardiol 2004; 44:340–8
52. Aggarwal S, Bannon S: Displacement of impella post chest compressions. Heart Views 2014; 15:127–8
53. Randhawa VK, Al-Fares A, Tong MZY, Soltesz EG, Hernandez-Montfort J, Taimeh Z, Weiss AJ, Menon V, Campbell J, Cremer P, Estep JD. A pragmatic approach to weaning temporary mechanical circulatory support: A state-of-the-art review. JACC: Heart Failure 2021; 9:664–73
54. Karr S: FDA approves Abiomed's first-in-human trial of Impella ECP, world's smallest heart pump. Abiomed. Available at: https://investors.abiomed.com/news-releases/news-release-details/fda-approves-abiomeds-first-human-trial-impella-ecp-worlds. Accessed June 28, 2021.
55. Udesen NJ, Møller JE, Lindholm MG, Eiskjær H, Schäfer A, Werner N, Holmvang L, Terkelsen CJ, Jensen LO, Junker A, Schmidt H, Wachtell K, Thiele H, Engstrøm T, Hassager C; DanGer Shock investigators: Rationale and design of DanGer shock: Danish–German cardiogenic shock trial. Am Heart J 2019; 214:60–8

ANESTHESIOLOGY

Immune Modulatory Effects of Nonsteroidal Anti-inflammatory Drugs in the Perioperative Period and Their Consequence on Postoperative Outcome

Dirk J. Bosch, M.D., Ph.D.,
Gertrude J. Nieuwenhuijs-Moeke, M.D., Ph.D.,
Matijs van Meurs, M.D., Ph.D., Wayel H. Abdulahad, Ph.D.,
Michel M. R. F. Struys, M.D., Ph.D., F.R.C.A.

ANESTHESIOLOGY 2022; 136:843–60

ABSTRACT

Nonsteroidal anti-inflammatory drugs are among the most commonly administered drugs in the perioperative period due to their prominent role in pain management. However, they potentially have perioperative consequences due to immune-modulating effects through the inhibition of prostanoid synthesis, thereby affecting the levels of various cytokines. These effects may have a direct impact on the postoperative outcome of patients since the immune system aims to restore homeostasis and plays an indispensable role in regeneration and repair. By affecting the immune response, consequences can be expected on various organ systems. This narrative review aims to highlight these potential immune system–related consequences, which include systemic inflammatory response syndrome, acute respiratory distress syndrome, immediate and persistent postoperative pain, effects on oncological and neurologic outcome, and wound, anastomotic, and bone healing.

(ANESTHESIOLOGY 2022; 136:843–60)

Nonsteroidal anti-inflammatory drugs (NSAIDs) are widely used and are known for their analgesic, antipyretic, and immune-modulating properties. Their mechanism of action is though inhibition of cyclooxygenase, also known as prostaglandin–endoperoxide synthase, the key enzyme involved in prostaglandin synthesis. Cyclooxygenases (COX-1 and COX-2) catalyze the formation of prostaglandin (PS) H_2 (PGH_2) from arachidonic acid, upon which PGH_2 is metabolized by tissue-specific isomerases to other prostanoids such as prostaglandins (PGD_2, PGE_2, $PGF_{2\alpha}$), prostacycline (PGI_2), and thromboxane. Prostanoids are a subgroup of eicosanoids with distinct functions in health and disease. Their most important general and immunologic effects are summarized in table 1 and shown in figure 1.

Both cyclooxygenase isoenzymes have a similar molecular weight, a 65% amino acid sequence homology, and nearly identical catalytic sites, but differ in function, pattern, and location of expression.[17] COX-1 has predominantly homeostatic functions, such as maintaining normal gastric mucosa, regulating renal blood flow, and regulating coagulation by abetting platelet aggregation. It is present in most cells and is constitutively expressed, and various studies have shown that its messenger RNA and protein expression does not change upon inflammation.[18] In contrast, COX-2 is less widely expressed, but its expression is induced upon activation by proinflammatory mediators, like interleukin 1, tumor necrosis factor α, lipopolysaccharides, and tumor promotors.[19] Although it is generally stated that COX-1 is not involved upon immune activation, its role in inflammation should not be underestimated. Studies in animal models have shown that COX-1 serves an important role in the development of inflammatory sequelae like edema.[20,21] Nevertheless, COX-2–derived metabolites are considered to be responsible for mediating pain and inflammation. To minimize side effects, while maintaining their function, selective COX-2 inhibitors were developed and have been available since 2000 (fig. 2).

A specific category of NSAIDs, aspirin, not only inhibits cyclooxygenase but also stimulates the production of anti-inflammatory and proresolving mediators. These mediators are endogenous bioactive metabolites that are involved in the regulation and resolution of an effective innate immune response. Proresolving mediators stop the recruitment of leukocytes in inflamed

This article is featured in "This Month in Anesthesiology," page A1.

Submitted for publication June 4, 2021. Accepted for publication January 10, 2022. Published online first on February 18, 2022.

Dirk J. Bosch, M.D., Ph.D.: Department of Anesthesiology, University of Groningen, University Medical Center Groningen, Groningen, The Netherlands.

Gertrude J. Nieuwenhuijs-Moeke, M.D., Ph.D.: Department of Anesthesiology, University of Groningen, University Medical Center Groningen, Groningen, The Netherlands.

Matijs van Meurs, M.D., Ph.D.: Department of Critical Care, University of Groningen, University Medical Center Groningen, Groningen, The Netherlands.

Wayel H. Abdulahad, Ph.D.: Departments of Rheumatology and Clinical Immunology, University of Groningen, University Medical Center Groningen, Groningen, The Netherlands.

Michel M. R. F. Struys, M.D., Ph.D., F.R.C.A.: Department of Anesthesiology, University of Groningen, University Medical Center Groningen, Groningen, The Netherlands; Department of Basic and Applied Medical Sciences, Ghent University, Ghent, Belgium.

<zdoi;. DOI: 10.1097/ALN.0000000000004141>

Table 1. Short Outline of General and Immune Effects of Prostanoids

Prostanoids	Receptor	Function	Immunologic Effect
PGD_2	DP_{1-2}	• Platelet aggregation • Allergic reactions • Contraction of bronchial airway • Sensation of pain • Sleep–wake cycle	• Involved in type 2 immune responses, including T helper 2 cells, type 2 innate lymphoid cells, and eosinophils with a subsequent effect on asthmatic airways inflammation through increased inflammatory cell chemotaxis/cytokines and enhanced immunoglobulin E class switching in B cells.[1] • Elevated level of PGD_2 resulted in a defect in virus-specific T-cell responses due to impaired respiratory dendritic cells migration.[2] • PGD_2 also has anti-inflammatory effects upon multiple spontaneous dehydrations and conversion into 15-deoxy-Δ-prostaglandin J2, which in turn inhibits the activation of nuclear factor κB system resulting in reduction of interleukins 6, 1β, and 12 and tumor necrosis factor α from macrophages and decreases the production of inducible nitric oxide synthase.[3]
PGE_2	EP_{1-4}	• Contraction and relaxation of smooth muscle • Control of blood pressure • Sensation of pain • Proinflammatory response	• Serves as an important proinflammatory mediator, involved in development of all physical signs of inflammation such as rubor, tumor, and dolor. • Also has anti-inflammatory properties that are context-dependent; downregulation of interleukin 2 by T cells and phagocytosis by macrophages.[4] • Promotes dendritic cells migration and upregulates costimulatory molecule expression to promote T cell activation.[5] • Promotes T helper 2 cell response by impairing the ability of dendritic cells to produce interleukin 12 and shifts the balance away from a cellular T helper 1 cell to a humoral T helper 2 cell response with a decreased T helper 1/T helper 2 ratio.[6] • Involved in the activation of the T helper 17 cell responses that characterized by the production of the proinflammatory cytokine interleukin 17.[7] • Promotes the development and function of regulatory T cells.[8] • Inhibits the cytolytic function of natural killer cells and therefore reduces target cell lysis.[9] • Suppresses proliferation and induce apoptosis of immature B cells and enhances immunoglobulin class switching in mature B cells.[10,11]
PGI_2	P	• Platelet aggregation • Vasodilatation • Renin release	• Decreases the production of proinflammatory cytokines (tumor necrosis factor α and interleukins 12, 1β, and 6) and chemokines (MIP-1α and MCP-1) and increases the production of the anti-inflammatory cytokine interleukin 10 by bone marrow dendritic cells.[12] • Inhibits the ability of dendritic cells to stimulate antigen-specific T-cell proliferation.[12] • Inhibits T helper 1 cell and T helper 2 cell activation, differentiation, and cytokine production, while enhancing T helper 17 cell immune responses and interleukin 17 production.[13]
$PGF_2\alpha$	FP_{A-B}	• Stimulates the contraction of uterine and bronchial smooth muscle • Produces vasoconstriction	• Involved in cellular infiltration and early recruitment of neutrophils.[14]
Thromboxane	TPα,β	• Platelet aggregation • Vasoconstriction • Bronchoconstriction	• Acts as a general suppressor of a low-avidity interaction between dendritic cells and T cells and inhibits T cell activation.[15,16]

PG, prostaglandin.

tissue and increase the removal of apoptotic polymorphonuclear neutrophils. Polymorphonuclear neutrophils enhance microbial killing and clearance and are considered organ-protective.[22] This unique feature of aspirin involves acetylation rather than inhibition of the active site of COX-2 in endothelial or epithelial cells, which results in the conversion of arachidonic acid to proresolving mediators. Examples of proresolving mediators activated by aspirin, termed aspirin-triggered specialized proresolving mediators, are aspirin-triggered resolvins and lipoxins.[23] Lipoxins are known to regulate leukocyte traffic, interfere with the chemokine-cytokine axis, reduce edema, and block pain signals.

The immune-modulatory consequences of NSAIDs are considered to be relevant in the perioperative period, since surgical injury elicits an inflammatory response associated with postoperative outcome.[24] Several reviews and meta-analyses have focused on the adverse effects of NSAIDs on multiple organ systems like the kidney and heart, which are beyond the scope of this review, whereas the immune-modulating effects of NSAIDs are poorly described.[25–29] Therefore, the aim of this narrative review is to describe the immunologic effects of NSAIDs in the perioperative period and their consequence on different postoperative outcomes. When possible, a distinction will be made between selective and nonselective cyclooxygenase inhibitors.

Beneficial Immune-modulating Effects of NSAIDs

Effects on the Surgical Stress Response

Surgical injury activates the immune system in a direct manner by the binding of danger-associated molecular patterns to pattern recognition receptors of the innate immune system and indirectly *via* surgical injury induced activation of the neuroendocrine system, through the hypothalamic–pituitary–adrenal axis. Activation then involves the release of

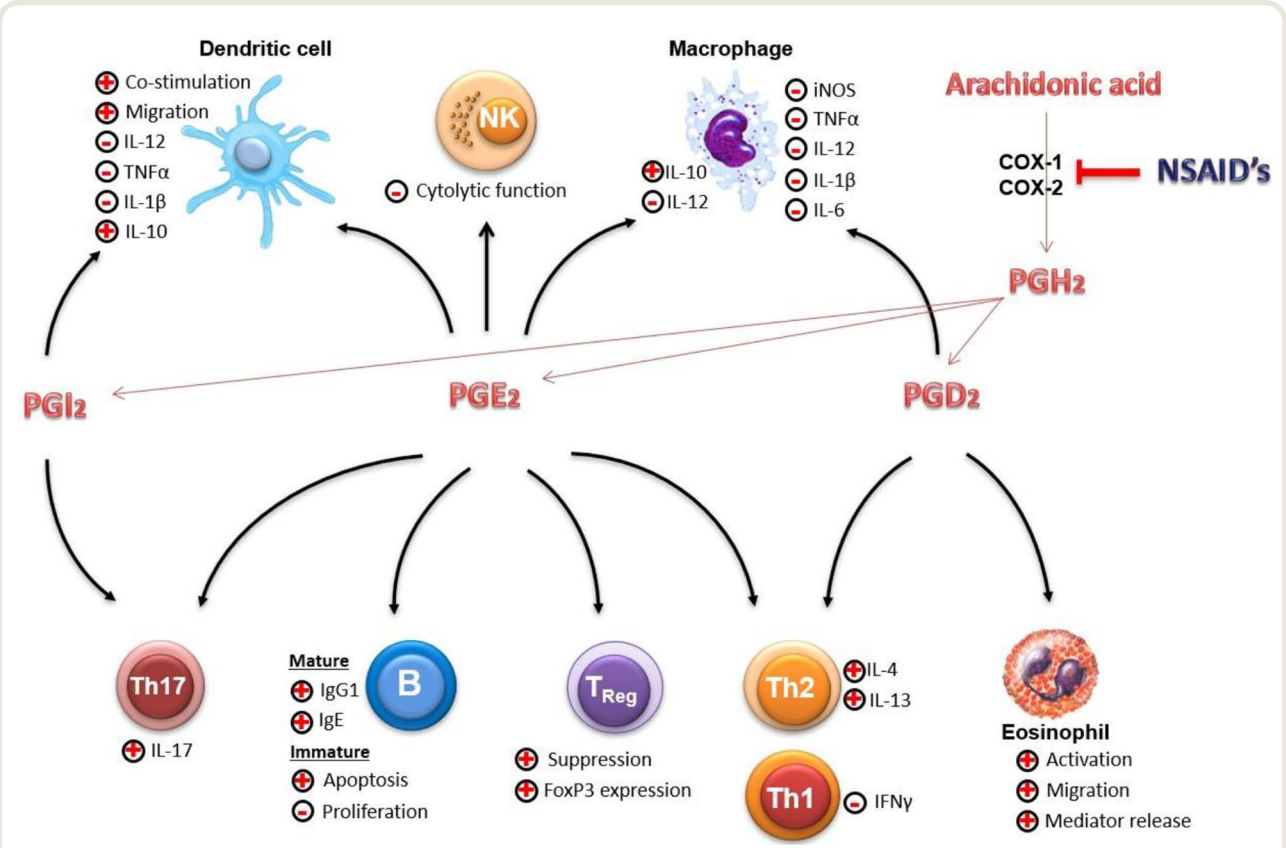

Fig. 1. Effects of the most important immune active prostanoids: prostaglandin (PG) I_2, PGE_2, and PGD_2. PGI_2 increases the level of anti-inflammatory cytokines, while the proinflammatory cytokines tumor necrosis factor α (TNF-α), interleukin (IL)-1β, and interleukin 12 decrease *in vitro*. Depending on the stage of inflammation, PGE_2 has a profound effect on the production of cytokines by T cells. Particularly at later stages of immune responses, PGE_2 has immune suppressive properties, resulting in the inhibition of T helper (Th) 1 cell cytokines (interferon γ [IFN-γ] and IL-2), which results in the suppression of Th1 cell–dependent antimetastatic immunity. Furthermore, PGE_2 is a potent inhibitor of the cytolytic effector function of natural killer cells and therefore reduces target cell lysis. In contrast, PGE_2 promotes the production of cytokines produced by Th2 (IL-4, IL-5, IL-10, and IL-13), although these cytokines can also be mediated indirectly by PGE_2 through cyclic adenosine monophosphate (cAMP). Thus, PGE_2 promotes Th2 cell differentiation and shifts the balance away from a cellular Th1 cell to a humeral Th2 cell response, with a decreased Th1/Th2 ratio. PGD_2 is a prostaglandin produced mainly by mast cells but also by other leukocytes, including dendritic cells and Th2 cells. Production of PGD_2 by mast cells is an important initiator of immunoglobulin E (IgE) mediated type 1 acute allergic reactions. PGD_2 has anti-inflammatory effects through inhibition of the production of inducible nitric oxide synthase (iNOS), TNF-α, and IL-1β by mouse and human macrophages.

hormones, cytokines, chemokines, and prostanoids, which are essential to restore homeostasis and are involved in tissue repair and the host's response against invading pathogens.[24] An exaggerated surgical stress response may lead to a systemic inflammatory response syndrome, is associated with postoperative morbidity and a higher risk of infections and organ failure, and may be detrimental to long-term survival after oncological surgery.[30] In response to surgical injury, the T helper 1/T helper 2 balance (between T helper 1 cells and T helper 2 cells) shifts toward T helper 2 cells, suggesting that cell-mediated immunity is downregulated and antibody/humoral-mediated immunity is upregulated.[31] This also affects the cytolytic function of natural killer cells, which is enhanced by a T helper 1 cell response. In a study examining the immunologic effects of parecoxib (a selective COX-2 inhibitor) in adults undergoing laparoscopic cholecystectomy, the balance between T helper 1 cells, T helper 2 cells, T helper 17 cells, and regulatory T cell cytokines was restored after administration of parecoxib, suggesting an important role for prostanoids in the polarization of T helper cells.[32]

In two randomized controlled trials, the effect of intravenous ibuprofen on the surgical stress response during cholecystectomy was assessed.[33,34] Although administration strategies were different (500 mg ibuprofen, 12 and 2 h before surgery and every 8 h until the third postoperative day *vs.* a single preoperative dose of 800 mg ibuprofen), a reduced endocrine response and cytokine release were observed in both studies in patients receiving ibuprofen. Both trials, however, observed increased intraoperative levels of tumor necrosis factor α, which the authors

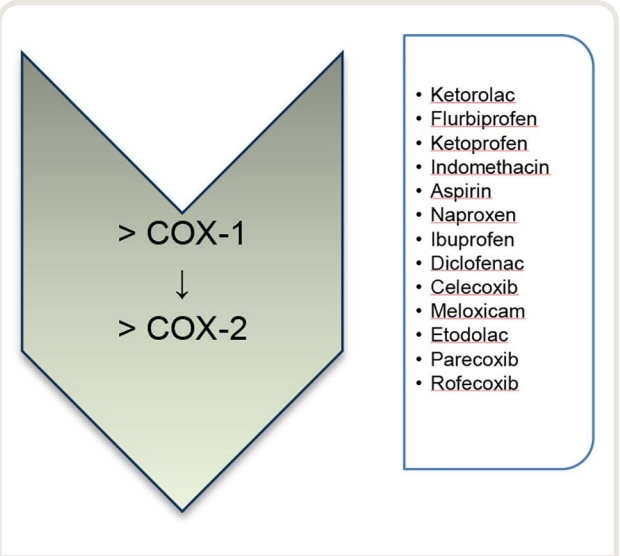

Fig. 2. Cyclooxygenase (COX) 1/2 selectivity of different nonsteroidal anti-inflammatory drugs ordered from mainly COX-1 selectivity to mainly COX-2 selectivity.

ascribe to the direct stimulation of mononuclear cells and the release of tumor necrosis factor α by NSAIDs, thereby causing a subsequent short-term intraoperative increase.[34] Ibuprofen attenuated postoperative anti-inflammatory interleukin 10 release, suggesting a reduction of the proinflammatory response, requiring less interleukin 10 modulation.[18] Although the study of Le *et al.*[34] could not demonstrate a difference in perioperative interleukin 6 levels, several other studies, administering ibuprofen, diclofenac, and parecoxib perioperatively, demonstrated an association between the use of NSAIDs and lower interleukin 6 levels.[33,35,36] Moreover, high perioperative levels of interleukin 6 are associated with postoperative complications in different types of surgery.[37,38] According to clinicaltrials.gov (accessed January 2, 2021), there are no current randomized controlled trials assessing the effect of NSAIDs on the surgical stress response.

The effects of NSAIDs in septic patients undergoing surgery has not been investigated. In (animal) sepsis models, however, aspirin and other NSAIDs are associated with improved hemodynamic parameters, organ function, and survival.[39,40] There are several hypotheses about the potential beneficial effect of NSAIDs or aspirin in systemic inflammatory response syndrome/sepsis patients. The immune response in systemic inflammatory response syndrome/sepsis is a dynamic process and differs between an immune-activated state and a paralyzed state. Effects will therefore depend on the time of administration and the current immunologic state of the patient. During an exaggerated immune response, one could hypothesize that it might be beneficial to have NSAIDs mitigating this response. The positive effect of aspirin might be explained by the ability of aspirin to stimulate the production of anti-inflammatory and proresolving mediators, a feature that is not shared by other NSAIDs. On the other hand, aspirin has been shown to potentiate leukocytic cytokine production in human endotoxemia trials.[41,42] This proinflammatory response might be beneficial in a sepsis-induced immunoparalysis and could contribute to the improved survival found in a meta-analysis that included 17,065 patients from observational studies: aspirin use before the onset of sepsis resulted in a 7% decrease in mortality.[43] In a recent double-blind, placebo-controlled follow-up study, in which 16,703 patients aged above 70 yr were randomized to receive either 100 mg aspirin or placebo, these beneficial effects could not be confirmed. After follow-up with a median of 4.6 yr, a total of 203 deaths were considered to be associated with sepsis, with no differences between the two groups.[44] These studies, however, have a different design (meta-analysis of observational studies *vs.* randomized controlled trial), which may explain the difference in outcome. In a randomized, double-blind, placebo-controlled trial that included 455 septic patients, treatment with ibuprofen (10 mg/kg given every 6 h for eight doses) decreased fever, tachycardia, oxygen consumption, and lactic acidosis but was not associated with improved survival or development of shock.[45] With a maximum of eight doses of ibuprofen, longer-lasting therapy might have produced different results. Comparing these studies is difficult due to major methodologic differences such as duration and start of treatment and type of NSAID. Administration of NSAIDs might even have negative consequences, since the use of NSAIDs in patients with septic shock led to a delayed administration of antibiotic therapy by masking the signs of sepsis.[46] Moreover, various case reports have suggested that NSAIDs in septic patients might increase the severity of infection, which might be due to the immune suppression seen in these patients.[47,48] According to clinicaltrials.gov (accessed January 2, 2021), there is currently one randomized controlled trial (NCT01784159) in septic patients assessing the effect of aspirin on the reduction of intensity of organ dysfunction, measured by the variation of the Sequential Organ Failure Assessment score, starting from the day of admission to day 7.

Taken together, there is no beneficial effect of NSAIDs in patients with sepsis and in those with an exaggerated surgical stress response. These responses are highly dynamic, not only changing over time but also differing between subjects. In addition, prostaglandins possess pro- and anti-inflammatory properties, again dependent on type, time of release, and context (table 1). The ultimate effect, tempering or enhancing the immune response, therefore, most likely depends on the cause of sepsis, patient characteristics (immune status, comorbidity), type of NSAID (COX-1 and/or COX-2, aspirin), dosage, and time point of administration (studies are summarized in table 2).

Acute Respiratory Distress Syndrome

Aspirin and, to a lesser extent, other NSAIDs might have beneficial effects on patients with acute respiratory distress

Table 2. Overview of Described Literature and Their Conclusions about the Effect of Nonsteroidal Anti-inflammatory Drugs on Different Postoperative Outcomes

Outcome	Randomized Controlled Trial	(Systemic) Review	Meta-analysis
Immune response			
Surgical stress response	• Decreased[33–36]		
Systemic inflammatory distress syndrome/sepsis	• Improved[45] • No effect[44]		• Improved[43]
Pulmonary effects			
ARDS	• No effect[49]	• Unknown[50]	• Improved (animal)[51]
Aspirin-exacerbated respiratory disease	• No effect (COX-2)[52]	• No effect (COX-2)[53]	
Inflammation and pain			
Preemptive		• Moderate effect[54]	• Improved (COX-2)[55,56]
Perioperative		• Improved[57]	• Improved[58,59]
Persistent pain	• No effect[60–63]		• No effect[64]
Oncology			
Outcome	• Improved[65]	• Unknown[66]	• Improved (animal studies)[67]
Neurology			
Postoperative cognitive dysfunction			• Improved[68]
Aneurysmal subarachnoid hemorrhage	• No effect[69]		
Healing processes			
Wound healing	• No effect[70]		
Anastomotic healing	• Impaired (animal study)[71]		• Impaired[72–74] • No effect[75]
Bone healing	• No effect[76]	• No effect[77]	• Impaired[78] • No effect in high-quality studies[79]

ARDS, acute respiratory distress syndrome; COX, cyclooxygenase.

syndrome (ARDS) due to their effect on platelet activation and anti-inflammatory properties. Aspirin covalently and irreversibly binds to platelet cyclooxygenase, whereas other NSAIDs reversibly inhibit platelet cyclooxygenase. Platelets are activated in the presence of lipopolysaccharides and thrombin, both sepsis mediators, resulting in pulmonary microcirculatory thrombosis, increasing pulmonary vascular dead space, ventilation perfusion mismatch, and worse outcomes in patients with ARDS.[80] The interaction between activated platelets and leukocytes results in production of proinflammatory cytokines (interleukins 1β and 8 and tumor necrosis factor α) and pulmonary edema.[81] Aspirin has the ability to modify these pathways and might be used both preventively and therapeutically. Furthermore, aspirin-triggered specialized proresolving mediators can potentially contribute to regulation of the immune response during ARDS. These effects are further enhanced by the fact that aspirin has the ability to regulate leukocyte traffic by aspirin-triggered lipoxins.[82] In different *in vitro*, animal, and observational studies, the administration of aspirin was related to the prevention of or an improvement in patients with ARDS.[50] In a review of preclinical models and a meta-analysis of clinical studies, the authors concluded that the administration of aspirin in animal studies was associated with improved survival and attenuated inflammation and pulmonary edema. In clinical trials, there was an association with a reduced incidence of ARDS.[51] The differences between preclinical and clinical studies may be explained by differences in dosage and timing of administration. In preclinical studies, higher doses of aspirin have generally been administered compared to clinical studies in which lower doses were used. A higher dose provides a greater COX-2 blockade, while a lower dose provides a greater COX-1 blockade. A 2015 review by Toner *et al.*[50] concluded that ongoing randomized controlled trials would elucidate the role of aspirin in treating ARDS. Afterward, a multicenter double-blind, placebo-controlled, randomized controlled trial including 390 patients at risk of ARDS was performed: in contrast to former research, the use of aspirin compared with placebo did not reduce the risk of ARDS at 7 days, nor were there any differences in secondary outcomes or adverse events.[49] Patients in this study were administered a loading dose of 325 mg aspirin, followed by 81 mg/day for up to 7 days after admission. Although, or perhaps because, patients were enrolled in the emergency department, the incidence of ARDS was lower than expected (9.5% *vs.* 18%), resulting in an insufficient power. Another randomized controlled trial (NCT02326350), investigating the effect of 75 mg aspirin on oxygenation index at day 7 in patients diagnosed with ARDS, was terminated prematurely due to slow recruitment (clinicaltrials.gov). Recently, Chow *et al.*[83] examined the relationship between aspirin and clinical outcomes in patients with ARDS due to COVID-19. In this retrospective study of 412 patients, patients who received aspirin (N = 98) were less likely to need mechanical ventilation (35.7% *vs.* 48.4%) and intensive care unit admission (38.8% *vs.* 41.0%), despite a higher rate of comorbidities in the aspirin group. These results, however, should be interpreted with caution, since COVID-19 patients display a hypercoagulatory state, the study only concerns a small number of patients, and the differences are

small, making the clinical relevance minimal. Currently, the Effect of Aspirin on REducing iNflammation in Human *in vivo* Model of Acute Lung Injury (ARENA) trial is including patients (according to clinicaltrials.gov accessed January 2, 2021; 33 patients after 8 yr of inclusion) and examines the effect of aspirin on inflammation in acute lung injury (NCT01659307). In conclusion, despite a pathophysiologic explanation for a beneficial effect of aspirin or other NSAIDs in patients with ARDS, the only performed randomized controlled trial does not show a protective effect (the studies are summarized in table 2).

Inflammation and Pain

Surgical injury leads to activation and sensitization of the nociceptive system through the release of different mediators, like bradykinin, prostanoids, and cytokines. Activated prostanoids, in particular PGE_2 and PGI_2, are involved in peripheral and central sensitization and in (neuro)inflammatory pain. PGE_2 serves as an important proinflammatory mediator and is involved in development of all physical signs of inflammation. Peripheral sensitization by PGE_2 involves the activation of E-prostanoid receptors (EP1, EP2, and EP4), which mediate pain responses from noxious and innocuous stimuli.[84] These receptors are also found in the spinal cord, highlighting the central sensitization activity of PGE_2, where it is considered the dominant prostaglandin in the spinal nociceptive system.[85] PGI_2 causes hyperalgesia by activating the prostacyclin (IP) receptor, which acts directly on the peripheral afferent nociceptors.[85] In addition, PGE_2 and PGI_2 also have sensitizing properties through other mechanisms. For instance, PGE_2 enhances the sensitization of nociceptors by lowering the threshold of the tetrodoxin-resistant sodium channels (found in the cell bodies of many peripheral nervous systems).[84] Second, the transient receptor potential vanilloid 1 channel, which is involved in heat sensation, is potentiated severalfold by PGE_2 and PGI_2 in afferent neurons.[84] Finally, PGE_2 sensitizes afferent neurons to produce bradykinin, which is involved in lowering the heat threshold of bradykinin 2 receptors and is therefore responsible for long-lasting pain associated with inflammation.[84] In addition to activated prostanoids, proinflammatory cytokines, like tumor necrosis factor α and interleukins 1β, 6, and 17, secreted at and recruited to the site of injury, have the ability to activate and to increase the sensitivity to pain stimuli.[86] Receptors for these specific cytokines are located on the nociceptive neurons and, together with other noxious stimuli, stimulate the primary afferent A-delta and C-nerve fibers and synapse with neurons in the dorsal horn of the spinal cord.[87] Neutralization of these cytokines results in a quick reduction of pain. In addition, these cytokines not only play a role in mechanical pain stimulation but also are involved in the development of neuropathic pain.[84]

NSAIDs as Preemptive Analgesics

NSAIDs are widely used in the treatment of acute (perioperative) or chronic pain but are also used as a preemptive analgesic agent. NSAIDs might be ideal for this purpose due to their anti-inflammatory effects and by preventing the establishment of peripheral and central sensitization in nociceptive pathways. In a systematic review, the authors concluded that some aspects of postoperative pain control were improved by preemptive treatment in 4 of the 20 randomized controlled trials, but overall, the effect was moderate.[54] Moreover, there was no analgesic benefit to preemptive administration of NSAIDs compared with postincisional administration. Despite including only randomized controlled trials, the studies displayed a wide heterogeneity, ranging from abdominal to orthopedic surgery, and many different NSAIDs (for example, ibuprofen, diclofenac, ketorolac, naproxen, and flurbiprofen) were used. In a more recent systemic review and meta-analysis, the authors examined the effect of preemptive drug administration on postoperative analgesic consumption during the 24 h postsurgery. A significant reduction of postoperative analgesic consumption was observed using COX-2 inhibitors but not for nonselective NSAIDs.[55] Comparable results were found in a meta-analysis that examined the efficiency of selective COX-2 inhibitors in patients undergoing total knee arthroplasty. The authors found a beneficial effect on the visual analog scale score (24 and 72 h postoperatively) and a decreased opioid consumption.[56] The clinical relevance, however, of both meta-analyses is not clear, since there were no statements about the reduction in the visual analog scale or opioid consumption. Based on the included studies in these meta-analyses, it is also unclear whether preemptive administration has advantages over postincisional administration. This question, however, is not about the efficacy of NSAIDs but about the most ideal time to administer them. This most likely will remain difficult to answer due to small differences in direct clinical outcome measures and many different covariates. Furthermore, interpretation of current literature is hampered by a high degree of heterogeneity with differences in dose and timing, type of postoperative rescue analgesic, postoperative analgesia therapy, type of surgery, and reported outcomes.

NSAIDs in Multimodal Management of Acute Postoperative Pain

While it is uncertain whether preemptive administration of NSAIDs is beneficial over postincisional administration, these drugs have been given an important role in the multimodal management of acute postoperative pain. The American Society of Anesthesiologists (ASA; Schaumburg, Illinois) recommend administration, unless contraindicated, of multimodal pain management consisting of acetaminophen combined with an NSAID or selective COX-2 inhibitor during the perioperative period.[88] In contrast to opioids, which mainly act in the central nervous system, NSAIDs alleviate pain by reducing the inflammatory response caused by tissue damage and by preventing peripheral and central sensitization. The effects of NSAIDs are predictable and suitable for most surgical procedures and have, in contrast to

opioids, no risk of addiction. Moreover, the administration of NSAIDs leads to a shorter recovery period, higher patient satisfaction, and a reduction in postoperative morbidity.[89]

Several meta-analyses have been performed to demonstrate the efficiency of NSAIDs or COX-2 inhibitors. In a meta-analysis from 2005, four conclusions emerge regarding the perioperative use of NSAIDs: nonopioid analgesics are opioid-sparing, the visual analog scale score is significantly decreased, and their use is associated with a reduction of opioid-related adverse effects.[58] However, there was also an increased risk of rare but important adverse effects related to the use of nonselective NSAIDs/selective COX-2 inhibitors, such as renal failure in cardiac patients (odds ratio, 4.86; 95% CI, 1.01 to 23.4; nonselective NSAIDs/COX-2 inhibitors) and increased surgical bleeding (odds ratio, 4.54; 95% CI, 1.54 to 13.42; nonselective NSAIDs). To determine which class of nonopioid analgesic is the most effective in reducing morphine consumption and morphine-related adverse effects, a systematic review was conducted by Maund *et al.*[57] The authors concluded that, in combination with a patient-controlled analgesia with morphine, NSAIDs (mean difference, −10.18 mg) and COX-2 inhibitors (mean difference, −10.92 mg) were related to a reduced morphine consumption. Furthermore, nausea and postoperative vomiting were significantly reduced by adding NSAIDs to a multimodal management.[57] In another meta-analysis, the authors focused on the effect of NSAIDs on opioid-related adverse effects. They observed a reduction in nausea (12%), vomiting (32%), and sedation (29%).[59] There was no reduction in pruritus, urinary retention, and respiratory depression. The authors tried to limit the degree of heterogeneity as much as possible but still included different NSAIDs and type of surgeries. In addition, their primary endpoints were scored differently throughout the included studies. In conclusion, these meta-analyses demonstrate a reduction in the visual analog scale score, opioid consumption, and various opioid-related adverse effects when administered in a multimodal regimen. It is, however, important to realize that studies investigating the effect of multimodal analgesic regiments all suffer from the same weakness: namely, if something changes in the model, it is nearly impossible to conclude whether this is due to one drug *versus* another drug, which makes it difficult to draw firm conclusions.

NSAIDs in Preventing Chronic Pain after Surgery

Persistent postoperative pain is a major problem and affects health-related quality of life. The exact pathophysiology is not fully understood but has recently been discussed in several reviews.[90–92] In summary, it is a multifactorial disorder involving (neuro)inflammation, which is characterized by the activation of glial cells and results in the release of cytokines and chemokines, and peripheral and central sensitization due to persistent noxious signaling, leading to nociceptive and neuropathic pain. Under normal circumstances, the immune response, elicited by surgical injury, resolves after several days, resulting in baseline nociceptive receptor sensitivity. In patients with persistent postoperative pain, these receptors remain overstimulated. Prolonged augmented action potentials will lead to central sensitization and results in allodynia and hyperalgesia. In addition, proinflammatory cytokines and chemokines in the central nervous system, released by glial cells, also play a role in the development of central sensitization. Moreover, this neuroinflammatory condition will contribute to allodynia, hyperalgesia, and widespread pain throughout the body.[92] The importance of prostaglandins in persistent pain has been confirmed in a mouse model in which hyperalgesic doses of PGE_2 induced long-lasting sensitization of afferent nociceptors.[93] Since NSAIDs interfere with these processes, there is a theoretical basis for a beneficial effect in preventing chronic pain after surgery. Nevertheless, studies examining the long-lasting effects of perioperative NSAID administration could not demonstrate a positive effect on persistent postoperative pain.[60–63] In a recent meta-analysis and systematic review, the effects of various perioperative pharmacologic strategies to prevent chronic pain after surgery were assessed. The included studies differed in type of NSAID, duration of administration, type of surgery, but also outcome measures such as reported time endpoints to score the prevalence of pain ranged from 3 to 12 months.[64] The authors concluded that none of the examined pharmacologic interventions could be recommended to prevent chronic pain after surgery.

Tumor Growth and Metastasis

In various epidemiologic studies, it has been shown that the long-term use of aspirin or other NSAIDs is associated with a reduction in the incidence of cancer.[94,95] In a large systemic review of epidemiologic studies, the relative risk was decreased by 43% for colon cancer, 25% for breast cancer, 28% for lung cancer, and 27% for prostate cancer.[96] Of the two cyclooxygenase isoforms, COX-2 expression is dysregulated in many types of cancer and is associated with carcinogenesis, invasiveness, and angiogenesis.[97] With elevated levels of COX-2, the metastatic potential also seems to increase. Of the prostanoids, PGE_2 seems to be the most important prooncogenic prostanoid.[97] PGE_2 is involved in tumor angiogenesis, cell migration or invasion, and inhibition of apoptosis.[97] In addition to its effect on prostanoids, aspirin activates aspirin-triggered specialized proresolving mediators, including resolvins and lipoxins. These anti-inflammatory mediators inhibit primary tumor growth and metastasis by enhancing endogenous macrophage clearance and cytokine response.[23] In addition to the long-term protective properties of NSAIDs against certain cancer types, these drugs also interfere with the immune response against circulating tumor cells during the surgical resection of a solid tumor. The likelihood of circulating tumor cells is dependent on several factors, including the immune response of the patient. Local inflammation increases the level of circulating tumor cells in the bloodstream, and an adequate functioning

immune response is pivotal for the first-line defense against circulating tumor cells.[98] The elimination of cancer cells takes place through natural killer cells, cytotoxic T cells, and dendritic cells. Their activity is inhibited by PGE_2, which is overexpressed by many tumors, such as colorectal, breast, cervical, bladder, and ovarian.[99] In addition, surgical injury increases a number of proinflammatory cytokines such as interleukins 1β and 6 and tumor necrosis factor α, which also suppress the activity of immune cells necessary for the elimination of circulating tumor cells.[100] Theoretically, NSAIDs have the ability to reduce these effects. The inhibition of PGE_2 synthesis in tumor cells leads directly to an impaired capacity to survive and proliferate and leads indirectly to an increased cytotoxic activity of natural killer and T cells.[101] Brunda *et al.*[102] showed that *in vivo* administration of indomethacin or aspirin resulted in a marked restoration of natural killer activity in tumor-bearing animals. In a meta-analysis of animal studies, the authors concluded that treatment with analgesics significantly decreased the number and risk of metastases, which was mainly the consequence of NSAIDs.[67]

Recently, five randomized controlled trials (NCT00888797, NCT02141139, NCT00502684, NCT01806259, and NCT03172988; clinicaltrials.gov) were conducted to assess the effect of perioperative NSAIDs on cancer recurrence. These trials differed in the type of cancer, the duration of NSAID administration, whether administration started preoperatively, the coadministration of a β-adrenergic antagonist, and the NSAID type (COX-1 and/or COX-2). The status of four of these randomized controlled trials (NCT00888797, NCT02141139, NCT01806259, and NCT03172988) is either unknown or lacking in sufficient power due to early termination, protocol violation, or a lower recurrence rate than anticipated.[103] The positive effect of NSAIDs in the perioperative period was shown in a randomized controlled trial (NCT00502684) that combined a COX-2 inhibitor with a β-adrenergic antagonist (propranolol), using study outcome points of cellular and molecular responses related to metastasis and disease recurrence.[65] Cata *et al.*[66] conducted a systemic review and found mainly observational and retrospective studies, all dealing with a high degree of heterogeneity, and concluded that the current evidence was equivocal regarding the effects of short-term NSAIDs on cancer recurrence after major cancer surgery. However, these observational and retrospective studies claim a reduced recurrence rate, longer disease-free survival, or overall survival due to the effects of perioperative NSAIDs.[104–112] In conclusion, despite the positive effect of NSAIDs in epidemiologic studies, immune-based perioperative antitumor effects, and positive observational and retrospective studies, there is insufficient or inconclusive evidence from high-quality clinical studies to support the experimental data (studies are summarized in table 2).

Neurologic Effects

Neuroinflammation is an important underlying mechanism in several neurologic disorders. Affecting this pathophysiologic process through the anti-inflammatory effects of NSAIDs is of general interest. Regarding the perioperative period, postoperative cognitive dysfunction is a common complication, particularly affecting the elderly population. Postoperative elevated levels of proinflammatory cytokines are associated with the development of postoperative cognitive dysfunction in both animal and human studies.[113–120] The hypothesis is that proinflammatory cytokines disrupt the blood–brain barrier *via* upregulation of COX-2 and matrix metalloproteinases, upon which these cytokines can enter the central nervous system.[121] After surgical injury, increased inflammatory activity was found in plasma and in human cerebrospinal fluid.[122] In a study by Peng *et al.*,[123] administration of parecoxib, a selective COX-2 inhibitor thought to have good central nervous system distribution, resulted in reduced surgery-induced levels of interleukin 1β and tumor necrosis factor α in the hippocampus in aged rats. Improvements in memory function in mice were demonstrated by Kamer *et al.*,[124] who administered meloxicam 24 h after surgical splenectomy. A recent meta-analysis included eight randomized controlled trials assessing the effect of parecoxib on the incidence of postoperative cognitive dysfunction in geriatric patients undergoing orthopedic surgery.[68] The authors concluded that perioperative administration of parecoxib was effective in reducing the incidence of postoperative cognitive dysfunction and improving the score on the Mini-Mental State Examination. The methodologic quality of the included studies was assessed as moderate to good. Nevertheless, only one of the eight randomized controlled trials was sufficiently powered, parecoxib was administered pre- or postoperatively, and postoperative cognitive dysfunction definitions were different between studies. Furthermore, it is unclear whether these results can be extrapolated to other surgical interventions.

NSAIDs are also associated with reduced cerebral ischemic injury in patients with aneurysmal subarachnoid hemorrhage.[125,126] Encouraging results of NSAIDs were found in animal models of aneurysmal subarachnoid hemorrhage, which showed an overall better control of cerebral vasospasm.[127–132] After propensity score matching of 178 patients, positive effects were observed by Nassiri *et al.*,[133] who concluded that administration of NSAIDs after aneurysmal subarachnoid hemorrhage was associated with reduced mortality and improved functional outcome. In this study, no distinction was made between the different types of NSAIDs, nor is it clear how long NSAIDs were administered. An important limitation, however, concerns the indication for administration of NSAIDs. Patients with a better neurologic status are more likely to report pain and therefore receive more NSAIDs than patients with a poorer neurologic status. A randomized controlled trial by Ghodsi *et al.*,[69] however, could not demonstrate significant differences in cerebral vasospasm, hospital stay, or mortality after administration of meloxicam (7.5 mg for 7 days) in patients

with subarachnoid hemorrhage. This study may have been underpowered (N = 81), since no sample size calculation was made. Regarding the safety of NSAIDs, several studies have shown that there is no association with higher rates of rebleed in aneurysmal subarachnoid hemorrhage patients.[125]

Neuroinflammation is an important underlying mechanism in the pathophysiology of various neurologic disorders. NSAIDs might have additional value in the multimodal treatment approach in patients at risk of postoperative cognitive dysfunction, but well-designed clinical trials are needed to determine whether these effects are clinically relevant. Encouraging results of NSAIDs in patients with aneurysmal subarachnoid hemorrhage are not yet sufficiently substantiated to justify any advice (studies are summarized in table 2).

Unfavorable Immune-modulating Effects of NSAIDs

Wound, Anastomotic, and Bone Healing

Wound Healing

NSAIDs might have immune-modifying properties that are detrimental in the process of normal wound healing. There are a number of crucial steps in the process of normal wound healing, including the acute phase response, proliferation, and remodeling of tissue. The acute phase is characterized by homeostasis and inflammation. Neutrophils are involved at an early stage and stimulate the migration of fibroblasts, epithelial cells, and vascular endothelial cells.[134] In a later stage, macrophages become the predominant cells and form an important barrier against bacteria.[134] In response to cytokines, released upon (surgical) injury, nitric oxide is produced, which is essential for angiogenesis and mediation of inflammation.[135] In an animal study in which nitric oxide was bound to ibuprofen, wound contraction increased, and epithelialization improved; the authors concluded that the results indicated that the esterification of ibuprofen with nitric oxide reverses the healing-suppressant effect of ibuprofen.[136] During the proliferation step, fibroblasts are the most important cells and are involved in wound contraction, collagen synthesis, and angiogenesis.[137] NSAIDs might impair the acute and proliferation phase of wound healing by their inhibitory effects on PGE_2.[138–140] Inhibition of PGE_2 is related to impaired wound healing; therefore, the use of NSAIDs in the proliferative phase of wound healing may result in increased scar formation.[140] PGE_2 has shown to be essential for neutrophil removal *via* the promotion of reverse migration.[141] Although the negative effects of NSAIDs on wound healing are well documented in animal studies, large clinical trials describing the effects of NSAIDs in wound healing are lacking. During a phase 3 randomized, placebo-controlled trial to evaluate the safety of intravenous meloxicam (30 mg) after major surgery, no differences were observed regarding wound healing.[70] The authors, however, pointed out the relatively healthy study population, in which patients with a history of cardiovascular, renal, hepatic, and bleeding events were excluded.

Anastomotic Healing

The hypothesis of impaired wound healing also applies to an intraabdominal bowel anastomosis, in which NSAIDs may increase the risk of anastomotic leakage. COX-2 is essential for gastrointestinal homeostasis, and the subsequent prostaglandin PGE_2 is involved in mucosal repair.[142,143] Moreover, anastomotic healing benefits from a proinflammatory response, leading to proliferation, angiogenesis, and granulation.[144] Reduced prostaglandin expression has been shown to reduce measured hydroxyproline levels and collagen repair in fresh anastomosis.[145] However, no information has been provided about the subtype of collagen, and therefore, the quality of the collagen cannot be determined.[144] An association between the perioperative use of NSAIDs and an increased risk of anastomotic leakage is demonstrated in various animal experiments and human clinical trials.[143,146] A randomized controlled trial in 24 rats assessed the effect of parecoxib on abdominal wound healing, both clinically and histologically.[71] There were no differences in clinical outcome; however, histological differences, on which the study was powered, were observed, such as decreased epithelization and increased necrosis in the parecoxib group.[71] The results, however, are not generalizable to humans, as the authors chose an intraperitoneal route of administration. Interestingly, the risk of anastomotic leakage caused by NSAIDs seemed to be location-dependent, with a higher risk in small bowel anastomosis compared to colon anastomosis.[147–149] Three meta-analyses, one published in 2018, 2019, and 2020, all concluded that caution must be taken when prescribing NSAIDs after gastrointestinal anastomosis.[72–74] A subgroup analysis in the meta-analysis of Jamjittrong *et al.*[72] showed that nonselective NSAIDs, but not selective COX-2 inhibitors, were significantly associated with anastomotic leakage. However, according to the authors, the safety of selective COX-2 inhibitors was inconclusive. In another subgroup analysis of randomized controlled trials by the same authors, no significant association was observed.[72] Finally, a fourth meta-analysis has recently been published, in which the authors pointed to important methodologic concerns regarding the previous meta-analyses, such as the inclusion of different types of gastrointestinal anastomoses and the underlying surgical pathology.[75] In this latest meta-analysis, only patients with colorectal cancer were included (N = 10,868). The authors concluded that perioperative NSAID administration does not increase the overall anastomotic leakage rate and that these findings were consistent throughout subgroup analyses for low anterior resections and both NSAID classes. Nevertheless, this latest meta-analysis also has important

methodologic limitations: like most studies, there are no data on dosage and duration of administration. In addition, it is unclear when administration was started, as later dosing during the postoperative phase is associated with a lower risk of anastomotic leakage. There are currently no registered studies (accessed January 2, 2021, clinicaltrials.gov) examining the effects of NSAIDs on anastomotic leakage.

Bone Healing

In addition to the potential negative effects on wound and anastomotic healing, the use of NSAIDs perioperative might also affect bone healing, since inflammation is an essential part of the early stage of bone fracture healing. Although the contribution of NSAIDs is controversial with respect to other risk factors (comorbidities, medications, oncology interventions, and lifestyle habits), the inhibition of COX-1 and COX-2 might result in an impaired bone turnover.[150] COX-2 is involved in the differentiation of mesenchymal cells into osteoblasts.[151] In COX-2 knockout animals, bone density was significantly decreased, whereas parathyroid hormone levels were increased, implicating a compensatory mechanism for the lack of COX-2 expression.[152] In a meta-analysis from 2010, the authors reviewed all available evidence regarding the effect of NSAIDs exposure on bone healing.[79] Lower-quality reports showed a significant association between NSAID exposure and nonunion, while this association disappeared when only higher-quality studies were included in the analysis.[79] A more recent meta-analysis from 2019, however, observed a negative effect of NSAIDs on bone healing, which may be dose- and/or duration-dependent, since low dose or short duration was not associated with nonunion.[78] Low dose or short duration was, however, not defined in this study and could only be analyzed in 4 of 16 evaluable studies, of which 2 found no effect and 2 found an increased risk. Moreover, it should be noted that no randomized studies were included in either meta-analysis. A systematic review including 3 randomized controlled trials and 13 retrospective studies concluded that there was no strong evidence that NSAIDs led to an increased rate of nonunion.[77] In all of these analyses, the authors had to deal with heterogeneity and conflicting data among the included studies. Important differences between long bones and vertebral bones, with variation in reported nonunion rates between both, and lifestyle habits, such as smoking, should be taken into account. Furthermore, there was a significant difference in the definition of nonunion between studies, ranging from a radiographic score to the need for reoperation. Finally, these studies also showed a large variation in dosage, type of NSAID, and duration of administration. A recent randomized trial examined the effect of different ibuprofen regimens (3×600 mg ibuprofen for 7 days *vs.* 3×600 mg ibuprofen for 4 days *vs.* placebo) on bone healing in Colles' fracture patients.[76] The authors concluded that there were no differences in bone mineral density, histomorphometric estimations, and changes in bone biomarkers between the treatment groups.[76] Although confounding variables were equally distributed between groups, the start of treatment could differ substantially between patients. According to clinicaltrials.gov, this study was initially registered under NCT01606540, with a power calculation of 192 participants. The final study is registered under NCT01567072, with the same power calculation, but only 95 patients were included. A forthcoming randomized controlled trial (NCT03880981) will study the effect of NSAIDs on the healing of tibia fractures and Achilles tendon ruptures (accessed January 2, 2021).

In conclusion, based on histological and animal studies, there appears to be an association between NSAIDs, in particular COX-2 inhibition, and impaired wound, anastomotic, and bone healing after surgery. However, high-quality clinical trials are lacking, and many questions are unanswered, such as the duration of use, type of NSAID, and, for anastomotic healing, whether underlying pathology and the location of the anastomosis influences the outcome. The potentially negative consequences that have emerged in histological and animal studies have therefore not been sufficiently substantiated in clinical studies. Administration must be individually weighed against the other known risk factors and benefits of NSAIDs (studies are summarized in table 2).

Aspirin-exacerbated Respiratory Disease

The pulmonary effects of NSAIDs in the perioperative period are considered to be minimal. Nevertheless, the administration of NSAIDs should be carefully considered in specific circumstances, and detrimental effects may occur in patients with a history of asthma. In 2% of patients with mild asthma up to 25% of patients with severe asthma, the inhibition of COX-1 may trigger aspirin-exacerbated respiratory disease, a condition characterized by eosinophilic rhinosinusitis with humoral T helper 2 cell inflammation, bronchospasm, and acute asthma exacerbation.[153] Bronchospasm can be severe and life-threatening, developing within 1 to 3 h of administration.[153] The underlying pathophysiologic mechanism is related to inhibition of the cyclooxygenase pathway, resulting in activated lipoxygenase, which leads to increased leukotriene synthesis. Leukotriene provokes the constriction of smooth muscle and the stimulation of airway mucus production.[154] The prostanoids PGD_2 and PGE_2 also have pulmonary effects, but their role in the development of aspirin-exacerbated respiratory disease is not fully understood. PGE_2 causes bronchodilation, while PGD_2 causes bronchoconstriction.[155] It is generally assumed that all nonselective cyclooxygenase inhibitors pose a risk for patients with a history of asthma and that highly selective COX-2 inhibitors are safe. This assumption is based on previous data suggesting that the release of both prostanoids (PGD_2 and PGE_2) is

only COX-1–dependent. Although two cases of aspirin-exacerbated respiratory disease were described in a case report after administration of a highly selective COX-2 inhibitor, this observation was not supported by a randomized crossover study in which 16 subjects with mild asthma received etoricoxib, and none developed pulmonary symptoms.[52,156] These results are consistent with a meta-analysis performed by Morales *et al.*,[53] who concluded that acute exposure to COX-2 inhibitors is safe in patients with stable mild-to-moderate asthma with aspirin-exacerbated respiratory disease. In conclusion, nonselective NSAIDs should be avoided during the perioperative period in patients with a history of asthma. Highly selective COX-2 inhibitors are most likely safe.

Conclusions

In this narrative review, we have summarized the immune-modulating effects of NSAIDs in the perioperative period and their effect on various postoperative outcomes. The body's response to surgical injury, and the accompanying release of subsequent cytokines, chemokines, and prostanoids, affects the postoperative course in various organ systems and regeneration processes. NSAIDs interfere with this response through the inhibition of cyclooxygenase, leading to a reduction in the synthesis of several of the prostanoids involved. Aspirin also stimulates the production of anti-inflammatory and proresolving mediators, but the consequences of this additional effect, to date, are unclear in clinical practice.

NSAIDs have been shown to have immune modulatory effects in cellular and animal models and significantly affect various outcome in these models. In randomized clinical studies, however, the immune-modulatory effects are much less evident, potentially due to a high degree of heterogeneity, genetic variances among patients, the use of various comedications, and the presence of several comorbidities. The risks and benefits of NSAID administration should be weighed individually, taking into account that the dosage and duration of administration often play important roles. To date, there is insufficient or inconclusive evidence from high-quality clinical studies to support the administration of NSAIDs to control the surgical stress response or sepsis, to prevent or improve ARDS, to improve postoperative neurologic outcome, or to minimize the risk of metastatic disease after oncological surgery. On the other hand, there is also insufficient evidence that NSAIDs are related to an impaired wound healing, increased risk of anastomotic leakage, and impaired bone regeneration. Their role in the multimodal treatment of acute pain has been sufficiently demonstrated and is associated with an opioid-sparing effect. It is not yet sufficiently clear whether preemptive administration of NSAIDs also has beneficial effects on postoperative pain perception. There does not, however, appear to be a beneficial effect on the development of chronic pain after surgery.

Search Strategy

We searched PubMed, Google, and clinical guidelines and screened the reference lists of studies retrieved by the searches. Most up-to-date studies and/or those with high impact were selected. Thereafter, a selection was made based on randomized controlled trials, reviews, and systematic reviews, or meta-analyses. We used the following terms: "nonsteroidal anti-inflammatory drugs" OR "NSAID" OR "aspirin" AND:

- "surgical stress response" OR "cytokine" OR "SIRS" OR "sepsis"
- "ARDS" OR "acute respiratory distress syndrome"
- "AERD" OR "aspirin-exacerbated respiratory disease"
- "surgery" AND "preemptive" OR "preoperative"
- "surgery" AND "perioperative"
- "surgery" AND "chronic pain" OR "persistent pain"
- "surgery" AND "oncology"
- "surgery AND "postoperative cognitive dysfunction" OR "POCD"
- "aneurysmal subarachnoid hemorrhage" OR "aSAH"
- "surgery" AND "wound healing" OR "tissue healing"
- "surgery" AND "anastomotic leakage" OR "anastomotic dehiscence"
- "surgery" AND "bone healing" OR "nonunion"

Research Support

Support was provided solely from institutional and/or departmental sources.

Competing Interests

Dr. Struys' research group/department received (over the last 3 yr) research grants and consultancy fees from The Medicines Company (Parsippany, New Jersey), Masimo (Irvine, California), Becton Dickinson (Eysins, Switzerland), Fresenius (Bad Homburg, Germany), Dräger (Lübeck, Germany), Paion (Aachen, Germany), Medtronic (Dublin, Ireland), and Medcaptain Europe (Andelst, The Netherlands). He receives royalties on intellectual property from Demed Medical (Temse, Belgium) and the Ghent University (Ghent, Belgium). He is an editorial board member and Director for the *British Journal of Anaesthesia* and associate editor for Anesthesiology. The other authors declare no competing interests.

Correspondence

Address correspondence to Dr. Bosch: Hanzeplein 1, P.O. Box 30001, 9700 RB Groningen, The Netherlands. d.j.bosch@umcg.nl.

References

1. Domingo C, Palomares O, Sandham DA, Erpenbeck VJ, Altman P: The prostaglandin D2 receptor 2 pathway in asthma: A key player in airway inflammation. Respir Res 2018; 19:189
2. Zhao J, Zhao J, Legge K, Perlman S: Age-related increases in PGD(2) expression impair respiratory DC migration, resulting in diminished T cell responses upon respiratory virus infection in mice. J Clin Invest 2011; 121:4921–30
3. Scher JU, Pillinger MH: The anti-inflammatory effects of prostaglandins. J Investig Med 2009; 57:703–8
4. Fink MP: Prostaglandins and sepsis: Still a fascinating topic despite almost 40 years of research. Am J Physiol Lung Cell Mol Physiol 2001; 281:L534–6
5. Kabashima K, Sakata D, Nagamachi M, Miyachi Y, Inaba K, Narumiya S: Prostaglandin E2-EP4 signaling initiates skin immune responses by promoting migration and maturation of Langerhans cells. Nat Med 2003; 9:744–9
6. Kaliński P, Hilkens CM, Snijders A, Snijdewint FG, Kapsenberg ML: IL-12-deficient dendritic cells, generated in the presence of prostaglandin E2, promote type 2 cytokine production in maturing human naive T helper cells. J Immunol 1997; 159:28–35
7. Boniface K, Bak-Jensen KS, Li Y, Blumenschein WM, McGeachy MJ, McClanahan TK, McKenzie BS, Kastelein RA, Cua DJ, de Waal Malefyt R: Prostaglandin E2 regulates Th17 cell differentiation and function through cyclic AMP and EP2/EP4 receptor signaling. J Exp Med 2009; 206:535–48
8. Baratelli F, Lin Y, Zhu L, Yang SC, Heuzé-Vourc'h N, Zeng G, Reckamp K, Dohadwala M, Sharma S, Dubinett SM: Prostaglandin E2 induces FOXP3 gene expression and T regulatory cell function in human CD4+ T cells. J Immunol 2005; 175:1483–90
9. Holt D, Ma X, Kundu N, Fulton A: Prostaglandin E(2) (PGE (2)) suppresses natural killer cell function primarily through the PGE(2) receptor EP4. Cancer Immunol Immunother 2011; 60:1577–86
10. Roper RL, Brown DM, Phipps RP: Prostaglandin E2 promotes B lymphocyte Ig isotype switching to IgE. J Immunol 1995; 154:162–70
11. Brown DM, Warner GL, Alés-Martínez JE, Scott DW, Phipps RP: Prostaglandin E2 induces apoptosis in immature normal and malignant B lymphocytes. Clin Immunol Immunopathol 1992; 63:221–9
12. Zhou W, HASHIMOTO K, Goleniewska K, O'Neal JF, Ji S, Blackwell TS, Fitzgerald GA, Egan KM, Geraci MW, Peebles RS Jr: Prostaglandin I2 analogs inhibit proinflammatory cytokine production and T cell stimulatory function of dendritic cells. J Immunol 2007; 178:702–10
13. Boswell MG, Zhou W, Newcomb DC, Peebles RS Jr: PGI2 as a regulator of CD4+ subset differentiation and function. Prostaglandins Other Lipid Mediat 2011; 96:21–6
14. de Menezes GB, dos Reis WG, Santos JM, Duarte ID, de Francischi JN: Inhibition of prostaglandin F(2alpha) by selective cyclooxygenase 2 inhibitors accounts for reduced rat leukocyte migration. Inflammation 2005; 29:163–9
15. Kabashima K, Murata T, Tanaka H, Matsuoka T, Sakata D, Yoshida N, Katagiri K, Kinashi T, Tanaka T, Miyasaka M, Nagai H, Ushikubi F, Narumiya S: Thromboxane A2 modulates interaction of dendritic cells and T cells and regulates acquired immunity. Nat Immunol 2003; 4:694–701
16. Moalli F, Cupovic J, Thelen F, Halbherr P, Fukui Y, Narumiya S, Ludewig B, Stein JV: Thromboxane A2 acts as tonic immunoregulator by preferential disruption of low-avidity CD4+ T cell-dendritic cell interactions. J Exp Med 2014; 211:2507–17
17. Nina M, Bernèche S, Roux B: Anchoring of a monotopic membrane protein: The binding of prostaglandin H2 synthase-1 to the surface of a phospholipid bilayer. Eur Biophys J 2000; 29:439–54
18. Smith CJ, Zhang Y, Koboldt CM, Muhammad J, Zweifel BS, Shaffer A, Talley JJ, Masferrer JL, Seibert K, Isakson PC: Pharmacological analysis of cyclooxygenase-1 in inflammation. Proc Natl Acad Sci U S A 1998; 95:13313–8
19. Barrios-Rodiles M, Tiraloche G, Chadee K: Lipopolysaccharide modulates cyclooxygenase-2 transcriptionally and posttranscriptionally in human macrophages independently from endogenous IL-1beta and TNF-alpha. J Immunol 1999; 163:963–9
20. Dinchuk JE, Car BD, Focht RJ, Johnston JJ, Jaffee BD, Covington MB, Contel NR, Eng VM, Collins RJ, Czerniak PM: Renal abnormalities and an altered inflammatory response in mice lacking cyclooxygenase II. Nature 1995; 378:406–9
21. Langenbach R, Loftin CD, Lee C, Tiano H: Cyclooxygenase-deficient mice: A summary of their characteristics and susceptibilities to inflammation and carcinogenesis. Ann N Y Acad Sci 1999; 889:52–61
22. Serhan CN, Levy BD: Resolvins in inflammation: Emergence of the pro-resolving superfamily of mediators. J Clin Invest 2018; 128:2657–69
23. Gilligan MM, Gartung A, Sulciner ML, Norris PC, Sukhatme VP, Bielenberg DR, Huang S, Kieran MW, Serhan CN, Panigrahy D: Aspirin-triggered proresolving mediators stimulate resolution in cancer. Proc Natl Acad Sci U S A 2019; 116:6292–7
24. Desborough JP: The stress response to trauma and surgery. Br J Anaesth 2000; 85:109–17
25. Bally M, Dendukuri N, Rich B, Nadeau L, Helin-Salmivaara A, Garbe E, Brophy JM: Risk of acute myocardial infarction with NSAIDs in real world use: Bayesian meta-analysis of individual patient data. BMJ 2017; 357:j1909
26. Harirforoosh S, Asghar W, Jamali F: Adverse effects of nonsteroidal antiinflammatory drugs: An update of

gastrointestinal, cardiovascular and renal complications. J Pharm Pharm Sci 2013; 16:821–47
27. Pepine CJ, Gurbel PA: Cardiovascular safety of NSAIDs: Additional insights after PRECISION and point of view. Clin Cardiol 2017; 40:1352–6
28. Sheth KR, Bernthal NM, Ho HS, Bergese SD, Apfel CC, Stoicea N, Jahr JS: Perioperative bleeding and non-steroidal anti-inflammatory drugs: An evidence-based literature review, and current clinical appraisal. Medicine (Baltimore) 2020; 99:e20042
29. Day RO, Graham GG: Non-steroidal anti-inflammatory drugs (NSAIDs). BMJ 2013; 346:f3195
30. Wall T, Sherwin A, Ma D, Buggy DJ: Influence of perioperative anaesthetic and analgesic interventions on oncological outcomes: A narrative review. Br J Anaesth 2019; 123:135–50
31. Decker D, Schondorf M, Bidlingmaier F, Hirner A, von Ruecker AA: Surgical stress induces a shift in the type-1/type-2 T-helper cell balance, suggesting down-regulation of cell-mediated and up-regulation of antibody-mediated immunity commensurate to the trauma. Surgery 1996; 119:316–25
32. Ma W, Wang K, Du J, Luan J, Lou G: Multi-dose parecoxib provides an immunoprotective effect by balancing T helper 1 (Th1), Th2, Th17 and regulatory T cytokines following laparoscopy in patients with cervical cancer. Mol Med Rep 2015; 11:2999–3008
33. Chambrier C, Chassard D, Bienvenu J, Saudin F, Paturel B, Garrigue C, Barbier Y, Boulétreau P: Cytokine and hormonal changes after cholecystectomy. Effect of ibuprofen pretreatment. Ann Surg 1996; 224:178–82
34. Le V, Kurnutala L, SchianodiCola J, Ahmed K, Yarmush J, Daniel Eloy J, Shapiro M, Haile M, Bekker A: Premedication with intravenous ibuprofen improves recovery characteristics and stress response in adults undergoing laparoscopic cholecystectomy: A randomized controlled trial. Pain Med 2016; 17:1163–73
35. Mahdy AM, Galley HF, Abdel-Wahed MA, el-Korny KF, Sheta SA, Webster NR: Differential modulation of interleukin-6 and interleukin-10 by diclofenac in patients undergoing major surgery. Br J Anaesth 2002; 88:797–802
36. Pandazi A, Kapota E, Matsota P, Paraskevopoulou P, Dervenis C, Kostopanagiotou G: Preincisional *versus* postincisional administration of parecoxib in colorectal surgery: Effect on postoperative pain control and cytokine response. A randomized clinical trial. World J Surg 2010; 34:2463–9
37. Rettig TC, Verwijmeren L, Dijkstra IM, Boerma D, van de Garde EM, Noordzij PG: Postoperative interleukin-6 level and early detection of complications after elective major abdominal surgery. Ann Surg 2016; 263:1207–12
38. Kaufmann KB, Heinrich S, Staehle HF, Bogatyreva L, Buerkle H, Goebel U: Perioperative cytokine profile during lung surgery predicts patients at risk for postoperative complications: A prospective, clinical study. PLoS One 2018; 13:e0199807
39. Reddy RC, Chen GH, Tateda K, Tsai WC, Phare SM, Mancuso P, Peters-Golden M, Standiford TJ: Selective inhibition of COX-2 improves early survival in murine endotoxemia but not in bacterial peritonitis. Am J Physiol Lung Cell Mol Physiol 2001; 281:L537–43
40. Aronoff DM: Cyclooxygenase inhibition in sepsis: Is there life after death? Mediators Inflamm 2012; 2012:696897
41. Leijte GP, Kiers D, van der Heijden W, Jansen A, Gerretsen J, Boerrigter V, Netea MG, Kox M, Pickkers P: Treatment with acetylsalicylic acid reverses endotoxin tolerance in humans *in vivo*: A randomized placebo-controlled study. Crit Care Med 2019; 47:508–16
42. Kiers D, van der Heijden WA, van Ede L, Gerretsen J, de Mast Q, van der Ven AJ, El Messaoudi S, Rongen GA, Gomes M, Kox M, Pickkers P, Riksen NP: A randomised trial on the effect of anti-platelet therapy on the systemic inflammatory response in human endotoxaemia. Thromb Haemost 2017; 117:1798–807
43. Trauer J, Muhi S, McBryde ES, Al Harbi SA, Arabi YM, Boyle AJ, Cartin-Ceba R, Chen W, Chen YT, Falcone M, Gajic O, Godsell J, Gong MN, Kor D, Lösche W, McAuley DF, O'Neal HR Jr, Osthoff M, Otto GP, Sossdorf M, Tsai MJ, Valerio-Rojas JC, van der Poll T, Violi F, Ware L, Widmer AF, Wiewel MA, Winning J, Eisen DP: Quantifying the effects of prior acetyl-salicylic acid on sepsis-related deaths: An individual patient data meta-analysis using propensity matching. Crit Care Med 2017; 45:1871–9
44. Eisen DP, Leder K, Woods RL, Lockery JE, McGuinness SL, Wolfe R, Pilcher D, Moore EM, Shastry A, Nelson MR, Reid CM, McNeil JJ, McBryde ES: Effect of aspirin on deaths associated with sepsis in healthy older people (ANTISEPSIS): A randomised, double-blind, placebo-controlled primary prevention trial. Lancet Respir Med 2021; 9:186–95
45. Bernard GR, Wheeler AP, Russell JA, Schein R, Summer WR, Steinberg KP, Fulkerson WJ, Wright PE, Christman BW, Dupont WD, Higgins SB, Swindell BB, Ibuprofen in Sepsis Study Group: The effects of ibuprofen on the physiology and survival of patients with sepsis. N Engl J Med 1997; 336:912–8
46. Legras A, Giraudeau B, Jonville-Bera AP, Camus C, François B, Runge I, Kouatchet A, Veinstein A, Tayoro J, Villers D, Autret-Leca E: A multicentre case-control study of nonsteroidal anti-inflammatory drugs as a risk factor for severe sepsis and septic shock. Crit Care 2009; 13:R43
47. Veenstra RP, Manson WE, van der Werf TS, Fijen JW, Tulleken JE, Zijlstra JG, Ligtenberg JJ: Fulminant necrotizing fasciitis and nonsteroidal anti-inflammatory drugs. Intensive Care Med 2001; 27:1831

48. Schummer W, Schummer C: Nonsteroidal anti-inflammatory drugs and streptococcal toxic shock syndrome. Intensive Care Med 2002; 28:1194
49. Kor DJ, Carter RE, Park PK, Festic E, Banner-Goodspeed VM, Hinds R, Talmor D, Gajic O, Ware LB, Gong MN; US Critical Illness and Injury Trials Group: Lung Injury Prevention with Aspirin Study Group (USCIITG: LIPS-A): Effect of aspirin on development of ARDS in at-risk patients presenting to the emergency department: The LIPS–A randomized clinical trial. JAMA 2016; 315:2406–14
50. Toner P, McAuley DF, Shyamsundar M: Aspirin as a potential treatment in sepsis or acute respiratory distress syndrome. Crit Care 2015; 19:374
51. Panka BA, de Grooth HJ, Spoelstra-de Man AM, Looney MR, Tuinman PR: Prevention or treatment of ARDS with aspirin: A review of preclinical models and meta-analysis of clinical studies. Shock 2017; 47:13–21
52. Daham K, James A, Balgoma D, Kupczyk M, Billing B, Lindeberg A, Henriksson E, FitzGerald GA, Wheelock CE, Dahlén SE, Dahlén B: Effects of selective COX-2 inhibition on allergen-induced bronchoconstriction and airway inflammation in asthma. J Allergy Clin Immunol 2014; 134:306–13
53. Morales DR, Lipworth BJ, Guthrie B, Jackson C, Donnan PT, Santiago VH: Safety risks for patients with aspirin-exacerbated respiratory disease after acute exposure to selective nonsteroidal anti-inflammatory drugs and COX-2 inhibitors: Meta-analysis of controlled clinical trials. J Allergy Clin Immunol 2014; 134:40–5
54. Møiniche S, Kehlet H, Dahl JB: A qualitative and quantitative systematic review of preemptive analgesia for postoperative pain relief: The role of timing of analgesia. Anesthesiology 2002; 96:725–41
55. Nir RR, Nahman-Averbuch H, Moont R, Sprecher E, Yarnitsky D: Preoperative preemptive drug administration for acute postoperative pain: A systematic review and meta-analysis. Eur J Pain 2016; 20:1025–43
56. Wang C, Fu H, Wang J, Huang F, Cao X: Preemptive analgesia using selective cyclooxygenase-2 inhibitors alleviates postoperative pain in patients undergoing total knee arthroplasty: A protocol for PRISMA guided meta-analysis of randomized controlled trials. Medicine (Baltimore) 2021; 100:e24512
57. Maund E, McDaid C, Rice S, Wright K, Jenkins B, Woolacott N: Paracetamol and selective and non-selective non-steroidal anti-inflammatory drugs for the reduction in morphine-related side-effects after major surgery: A systematic review. Br J Anaesth 2011; 106:292–7
58. Elia N, Lysakowski C, Tramèr MR: Does multimodal analgesia with acetaminophen, nonsteroidal antiinflammatory drugs, or selective cyclooxygenase-2 inhibitors and patient-controlled analgesia morphine offer advantages over morphine alone?: Meta-analyses of randomized trials. Anesthesiology 2005; 103:1296–304
59. Marret E, Kurdi O, Zufferey P, Bonnet F: Effects of nonsteroidal antiinflammatory drugs on patient-controlled analgesia morphine side effects: Meta-analysis of randomized controlled trials. Anesthesiology 2005; 102:1249–60
60. Meunier A, Lisander B, Good L: Effects of celecoxib on blood loss, pain, and recovery of function after total knee replacement: A randomized placebo-controlled trial. Acta Orthop 2007; 78:661–7
61. Fransen M, Anderson C, Douglas J, MacMahon S, Neal B, Norton R, Woodward M, Cameron ID, Crawford R, Lo SK, Tregonning G, Windolf M; HIPAID Collaborative Group: Safety and efficacy of routine postoperative ibuprofen for pain and disability related to ectopic bone formation after hip replacement surgery (HIPAID): Randomised controlled trial. BMJ 2006; 333:519
62. Lakdja F, Dixmérias F, Bussières E, Fonrouge JM, Lobéra A: [Preventive analgesic effect of intraoperative administration of ibuprofen-arginine on postmastectomy pain syndrome]. Bull Cancer 1997; 84:259–63
63. Romundstad L, Breivik H, Roald H, Skolleborg K, Romundstad PR, Stubhaug A: Chronic pain and sensory changes after augmentation mammoplasty: Long term effects of preincisional administration of methylprednisolone. Pain 2006; 124:92–9
64. Carley ME, Chaparro LE, Choinière M, Kehlet H, Moore RA, Van Den Kerkhof E, Gilron I: Pharmacotherapy for the prevention of chronic pain after surgery in adults: An updated systematic review and meta-analysis. Anesthesiology 2021; 135:304–25
65. Shaashua L, Shabat-Simon M, Haldar R, Matzner P, Zmora O, Shabtai M, Sharon E, Allweis T, Barshack I, Hayman L, Arevalo J, Ma J, Horowitz M, Cole S, Ben-Eliyahu S: Perioperative COX-2 and β-adrenergic blockade improves metastatic biomarkers in breast cancer patients in a phase-II randomized trial. Clin Cancer Res 2017; 23:4651–61
66. Cata JP, Guerra CE, Chang GJ, Gottumukkala V, Joshi GP: Non-steroidal anti-inflammatory drugs in the oncological surgical population: Beneficial or harmful?: A systematic review of the literature. Br J Anaesth 2017; 119:750–64
67. Hooijmans CR, Geessink FJ, Ritskes-Hoitinga M, Scheffer GJ: A systematic review and meta-analysis of the ability of analgesic drugs to reduce metastasis in experimental cancer models. Pain 2015; 156:1835–44
68. Huang JM, Lv ZT, Zhang B, Jiang WX, Nie MB: Intravenous parecoxib for early postoperative cognitive dysfunction in elderly patients: Evidence from a meta-analysis. Expert Rev Clin Pharmacol 2020; 13:451–60

69. Ghodsi SM, Mohebbi N, Naderi S, Anbarloie M, Aoude A, Habibi Pasdar SS: Comparative efficacy of meloxicam and placebo in vasospasm of patients with subarachnoid hemorrhage. Iran J Pharm Res 2015; 14:125–30
70. Bergese SD, Melson TI, Candiotti KA, Ayad SS, Mack RJ, McCallum SW, Du W, Gomez A, Marcet JE: A phase 3, randomized, placebo-controlled evaluation of the safety of intravenous meloxicam following major surgery. Clin Pharmacol Drug Dev 2019; 8:1062–72
71. Martinou E, Drakopoulou S, Aravidou E, Sergentanis T, Kondi-Pafiti A, Argyra E, Voros D, Fragulidis GP: Parecoxib's effects on anastomotic and abdominal wound healing: A randomized controlled trial. J Surg Res 2018; 223:165–73
72. Jamjittrong S, Matsuda A, Matsumoto S, Kamonvarapitak T, Sakurazawa N, Kawano Y, Yamada T, Suzuki H, Miyashita M, Yoshida H: Postoperative non-steroidal anti-inflammatory drugs and anastomotic leakage after gastrointestinal anastomoses: Systematic review and meta-analysis. Ann Gastroenterol Surg 2020; 4:64–75
73. Modasi A, Pace D, Godwin M, Smith C, Curtis B: NSAID administration post colorectal surgery increases anastomotic leak rate: Systematic review/meta-analysis. Surg Endosc 2019; 33:879–85
74. Huang Y, Tang SR, Young CJ: Nonsteroidal anti-inflammatory drugs and anastomotic dehiscence after colorectal surgery: A meta-analysis. ANZ J Surg 2018; 88:959–65
75. Arron MNN, Lier EJ, de Wilt JHW, Stommel MWJ, van Goor H, Ten Broek RPG: Postoperative administration of non-steroidal anti-inflammatory drugs in colorectal cancer surgery does not increase anastomotic leak rate: A systematic review and meta-analysis. Eur J Surg Oncol 2020; 46:2167–73
76. Aliuskevicius M, Østgaard SE, Hauge EM, Vestergaard P, Rasmussen S: Influence of ibuprofen on bone healing after Colles' fracture: A randomized controlled clinical trial. J Orthop Res 2020; 38:545–54
77. Borgeat A, Ofner C, Saporito A, Farshad M, Aguirre J: The effect of nonsteroidal anti-inflammatory drugs on bone healing in humans: A qualitative, systematic review. J Clin Anesth 2018; 49:92–100
78. Wheatley BM, Nappo KE, Christensen DL, Holman AM, Brooks DI, Potter BK: Effect of NSAIDs on bone healing rates: A meta-analysis. J Am Acad Orthop Surg 2019; 27:e330–6
79. Dodwell ER, Latorre JG, Parisini E, Zwettler E, Chandra D, Mulpuri K, Snyder B: NSAID exposure and risk of nonunion: A meta-analysis of case-control and cohort studies. Calcif Tissue Int 2010; 87:193–202
80. Mendez JL, Hubmayr RD: New insights into the pathology of acute respiratory failure. Curr Opin Crit Care 2005; 11:29–36
81. Chen CM, Lu HC, Tung YT, Chen W: Antiplatelet therapy for acute respiratory distress syndrome. Biomedicines 2020; 8:E230
82. Yang A, Wu Y, Yu G, Wang H: Role of specialized pro-resolving lipid mediators in pulmonary inflammation diseases: Mechanisms and development. Respir Res 2021; 22:204
83. Chow JH, Khanna AK, Kethireddy S, Yamane D, Levine A, Jackson AM, McCurdy MT, Tabatabai A, Kumar G, Park P, Benjenk I, Menaker J, Ahmed N, Glidewell E, Presutto E, Cain S, Haridasa N, Field W, Fowler JG, Trinh D, Johnson KN, Kaur A, Lee A, Sebastian K, Ulrich A, Pena S, Carpenter R, Sudhakar S, Uppal P, Fedeles BT, Sachs A, Dahbour L, Teeter W, Tanaka K, Galvagno SM, Herr DL, Scalea TM, Mazzeffi MA: Aspirin use is associated with decreased mechanical ventilation, ICU admission, and in-hospital mortality in hospitalized patients with COVID-19. Anesth Analg 2021; 132:930–41
84. Ronchetti S, Migliorati G, Delfino DV: Association of inflammatory mediators with pain perception. Biomed Pharmacother 2017; 96:1445–52
85. Zeilhofer HU: Prostanoids in nociception and pain. Biochem Pharmacol 2007; 73:165–74
86. Sommer C, Kress M: Recent findings on how proinflammatory cytokines cause pain: Peripheral mechanisms in inflammatory and neuropathic hyperalgesia. Neurosci Lett 2004; 361:184–7
87. Vanderwall AG, Milligan ED: Cytokines in pain: Harnessing endogenous anti-inflammatory signaling for improved pain management. Front Immunol 2019; 10:3009
88. American Society of Anesthesiologists Task Force on Acute Pain Management: Practice guidelines for acute pain management in the perioperative setting: An updated report by the American Society of Anesthesiologists Task Force on Acute Pain Management. Anesthesiology 2012; 116:248–73
89. Mathiesen O, Wetterslev J, Kontinen VK, Pommergaard HC, Nikolajsen L, Rosenberg J, Hansen MS, Hamunen K, Kjer JJ, Dahl JB. Scandinavian Postoperative Pain Alliance (ScaPAlli): Adverse effects of perioperative paracetamol, NSAIDs, glucocorticoids, gabapentinoids and their combinations: A topical review. Acta Anaesthesiol Scand 2014; 58: 1182–98
90. Richebé P, Capdevila X, Rivat C: Persistent postsurgical pain: Pathophysiology and preventative pharmacologic considerations. Anesthesiology 2018; 129:590–607
91. Gulur P, Nelli A: Persistent postoperative pain: Mechanisms and modulators. Curr Opin Anaesthesiol 2019; 32:668–73
92. Ji RR, Nackley A, Huh Y, Terrando N, Maixner W: Neuroinflammation and central sensitization in chronic and widespread pain. Anesthesiology 2018; 129:343–66

93. Villarreal CF, Funez MI, Cunha Fde Q, Parada CA, Ferreira SH: The long-lasting sensitization of primary afferent nociceptors induced by inflammation involves prostanoid and dopaminergic systems in mice. Pharmacol Biochem Behav 2013; 103:678–83
94. Seufert BL, Poole EM, Whitton J, Xiao L, Makar KW, Campbell PT, Kulmacz RJ, Baron JA, Newcomb PA, Slattery ML, Potter JD, Ulrich CM: IκBKβ and NFκB1, NSAID use and risk of colorectal cancer in the colon cancer family registry. Carcinogenesis 2013; 34:79–85
95. Chan AT, Giovannucci EL, Meyerhardt JA, Schernhammer ES, Curhan GC, Fuchs CS: Long-term use of aspirin and nonsteroidal anti-inflammatory drugs and risk of colorectal cancer. JAMA 2005; 294:914–23
96. Harris RE: Cyclooxygenase-2 (cox-2) blockade in the chemoprevention of cancers of the colon, breast, prostate, and lung. Inflammopharmacology 2009; 17:55–67
97. Hashemi Goradel N, Najafi M, Salehi E, Farhood B, Mortezaee K: Cyclooxygenase-2 in cancer: A review. J Cell Physiol 2019; 234:5683–99
98. Mohme M, Riethdorf S, Pantel K: Circulating and disseminated tumour cells: Mechanisms of immune surveillance and escape. Nat Rev Clin Oncol 2017; 14:155–67
99. Liu B, Qu L, Yan S: Cyclooxygenase-2 promotes tumor growth and suppresses tumor immunity. Cancer Cell Int 2015; 15:106
100. Chen Z, Zhang P, Xu Y, Yan J, Liu Z, Lau WB, Lau B, Li Y, Zhao X, Wei Y, Zhou S: Surgical stress and cancer progression: The twisted tango. Mol Cancer 2019; 18:132
101. Harizi H: Reciprocal crosstalk between dendritic cells and natural killer cells under the effects of PGE2 in immunity and immunopathology. Cell Mol Immunol 2013; 10:213–21
102. Brunda MJ, Herberman RB, Holden HT: Inhibition of murine natural killer cell activity by prostaglandins. J Immunol 1980; 124:2682–7
103. Forget P, Bouche G, Duhoux FP, Coulie PG, Decloedt J, Dekleermaker A, Guillaume JE, Ledent M, Machiels JP, Mustin V, Swinnen W, van Maanen A, Vander Essen L, Verougstraete JC, De Kock M, Berliere M: Intraoperative ketorolac in high-risk breast cancer patients: A prospective, randomized, placebo-controlled clinical trial. PLoS One 2019; 14:e0225748
104. Forget P, Bentin C, Machiels JP, Berliere M, Coulie PG, De Kock M: Intraoperative use of ketorolac or diclofenac is associated with improved disease-free survival and overall survival in conservative breast cancer surgery. Br J Anaesth 2014; 113:i82–7
105. Forget P, Vandenhende J, Berliere M, Machiels JP, Nussbaum B, Legrand C, De Kock M: Do intraoperative analgesics influence breast cancer recurrence after mastectomy?: A retrospective analysis. Anesth Analg 2010; 110:1630–5
106. Forget P, Machiels JP, Coulie PG, Berliere M, Poncelet AJ, Tombal B, Stainier A, Legrand C, Canon JL, Kremer Y, De Kock M: Neutrophil:lymphocyte ratio and intraoperative use of ketorolac or diclofenac are prognostic factors in different cohorts of patients undergoing breast, lung, and kidney cancer surgery. Ann Surg Oncol 2013; 20:S650–60
107. Choi JE, Villarreal J, Lasala J, Gottumukkala V, Mehran RJ, Rice D, Yu J, Feng L, Cata JP: Perioperative neutrophil:lymphocyte ratio and postoperative NSAID use as predictors of survival after lung cancer surgery: A retrospective study. Cancer Med 2015; 4:825–33
108. Yeh CC, Lin JT, Jeng LB, Ho HJ, Yang HR, Wu MS, Kuo KN, Wu CY: Nonsteroidal anti-inflammatory drugs are associated with reduced risk of early hepatocellular carcinoma recurrence after curative liver resection: A nationwide cohort study. Ann Surg 2015; 261:521–6
109. Jiang W, Wang L, Zhang J, Shen H, Dong W, Zhang T, Li X, Wang K, Du J: Effects of postoperative non-steroidal anti-inflammatory drugs on long-term survival and recurrence of patients with non-small cell lung cancer. Medicine (Baltimore) 2018; 97:e12442
110. Schack A, Fransgaard T, Klein MF, Gögenur I: Perioperative use of nonsteroidal anti-inflammatory drugs decreases the risk of recurrence of cancer after colorectal resection: A cohort study based on prospective data. Ann Surg Oncol 2019; 26:3826–37
111. Desmedt C, Demicheli R, Fornili M, Bachir I, Duca M, Viglietti G, Berlière M, Piccart M, Sotiriou C, Sosnowski M, Forget P, Biganzoli E: Potential benefit of intra-operative administration of ketorolac on breast cancer recurrence according to the patient's body mass index. J Natl Cancer Inst 2018; 110:1115–22
112. Huang Z, Wang X, Zou Q, Zhuang Z, Xie Y, Cai D, Bai L, Tang G, Huang M, Luo Y, Yu H: High platelet-to-lymphocyte ratio predicts improved survival outcome for perioperative NSAID use in patients with rectal cancer. Int J Colorectal Dis 2020; 35:695–704
113. Terrando N, Monaco C, Ma D, Foxwell BM, Feldmann M, Maze M: Tumor necrosis factor-alpha triggers a cytokine cascade yielding postoperative cognitive decline. Proc Natl Acad Sci U S A 2010; 107:20518-22
114. Fidalgo AR, Cibelli M, White JP, Nagy I, Maze M, Ma D: Systemic inflammation enhances surgery-induced cognitive dysfunction in mice. Neurosci Lett 2011; 498:63–6
115. Wang P, Cao J, Liu N, Ma L, Zhou X, Zhang H, Wang Y: Protective effects of edaravone in adult rats with surgery and lipopolysaccharide administration-induced cognitive function impairment. PLoS One 2016; 11:e0153708

116. Buvanendran A, Kroin JS, Berger RA, Hallab NJ, Saha C, Negrescu C, Moric M, Caicedo MS, Tuman KJ: Upregulation of prostaglandin E2 and interleukins in the central nervous system and peripheral tissue during and after surgery in humans. Anesthesiology 2006; 104:403–10
117. van Harten AE, Scheeren TW, Absalom AR: A review of postoperative cognitive dysfunction and neuroinflammation associated with cardiac surgery and anaesthesia. Anaesthesia 2012; 67:280–93
118. Ji MH, Yuan HM, Zhang GF, Li XM, Dong L, Li WY, Zhou ZQ, Yang JJ: Changes in plasma and cerebrospinal fluid biomarkers in aged patients with early postoperative cognitive dysfunction following total hip-replacement surgery. J Anesth 2013; 27:236–42
119. Peng L, Xu L, Ouyang W: Role of peripheral inflammatory markers in postoperative cognitive dysfunction (POCD): A meta-analysis. PLoS One 2013; 8:e79624
120. Liu X, Yu Y, Zhu S: Inflammatory markers in postoperative delirium (POD) and cognitive dysfunction (POCD): A meta-analysis of observational studies. PLoS One 2018; 13:e0195659
121. Safavynia SA, Goldstein PA: The role of neuroinflammation in postoperative cognitive dysfunction: Moving from hypothesis to treatment. Front Psychiatry 2018; 9:752
122. Hirsch J, Vacas S, Terrando N, Yuan M, Sands LP, Kramer J, Bozic K, Maze MM, Leung JM: Perioperative cerebrospinal fluid and plasma inflammatory markers after orthopedic surgery. J Neuroinflammation 2016; 13:211
123. Peng M, Wang YL, Wang FF, Chen C, Wang CY: The cyclooxygenase-2 inhibitor parecoxib inhibits surgery-induced proinflammatory cytokine expression in the hippocampus in aged rats. J Surg Res 2012; 178:e1–8
124. Kamer AR, Galoyan SM, Haile M, Kline R, Boutajangout A, LiYS, Bekker A: Meloxicam improves object recognition memory and modulates glial activation after splenectomy in mice. Eur J Anaesthesiol 2012; 29:332–7
125. Solar P, Mackerle Z, Joukal M, Jancalek R: Nonsteroidal anti-inflammatory drugs in the pathophysiology of vasospasms and delayed cerebral ischemia following subarachnoid hemorrhage: A critical review. Neurosurg Rev 2021; 44:649–58
126. Khansari PS, Halliwell RF: Mechanisms underlying neuroprotection by the NSAID mefenamic acid in an experimental model of stroke. Front Neurosci 2019; 13:64
127. Çelik Ö, Bilginer B, Korkmaz A, Gürgör PN, Bavbek M, Özgen T, Ziyal İ: Effects of intramuscular parecoxib administration on vasospasm in an experimental subarachnoid hemorrhage model. Int J Neurosci 2011; 121:316–22
128. Mani BK, Brueggemann LI, Cribbs LL, Byron KL: Activation of vascular KCNQ (Kv7) potassium channels reverses spasmogen-induced constrictor responses in rat basilar artery. Br J Pharmacol 2011; 164:237–49
129. Mani BK, O'Dowd J, Kumar L, Brueggemann LI, Ross M, Byron KL: Vascular KCNQ (Kv7) potassium channels as common signaling intermediates and therapeutic targets in cerebral vasospasm. J Cardiovasc Pharmacol 2013; 61:51–62
130. Ji X, Wang A, Trandafir CC, Kurahashi K: Influence of experimental subarachnoid hemorrhage on nicotine-induced contraction of the rat basilar artery in relation to arachidonic acid metabolites signaling pathway. J Stroke Cerebrovasc Dis 2013; 22:951–8
131. Munakata A, Naraoka M, Katagai T, Shimamura N, Ohkuma H: Role of cyclooxygenase-2 in relation to nitric oxide and endothelin-1 on pathogenesis of cerebral vasospasm after subarachnoid hemorrhage in rabbit. Transl Stroke Res 2016; 7:220–7
132. Silav G, Ergün H, Dolgun H, Sancak T, Sargon MF, Egemen N: Dipyrone attenuates cerebral vasospasm after experimental subarachnoid hemorrhage in rabbits. J Neurosurg Sci 2017; 61:380–7
133. Nassiri F, Ibrahim GM, Badhiwala JH, Witiw CD, Mansouri A, Alotaibi NM, Macdonald RL: A propensity score-matched study of the use of non-steroidal anti-inflammatory agents following aneurysmal subarachnoid hemorrhage. Neurocrit Care 2016; 25:351–8
134. Cañedo-Dorantes L, Cañedo-Ayala M: Skin acute wound healing: A comprehensive review. Int J Inflam 2019; 2019:3706315
135. Schwentker A, Vodovotz Y, Weller R, Billiar TR: Nitric oxide and wound repair: Role of cytokines? Nitric Oxide 2002; 7:1–10
136. Kaushal M, Kutty NG, Rao CM: Nitrooxyethylation reverses the healing-suppressant effect of Ibuprofen. Mediators Inflamm 2006; 2006:24396
137. Gonzalez AC, Costa TF, Andrade ZA, Medrado AR: Wound healing: A literature review. An Bras Dermatol 2016; 91:614–20
138. Krischak GD, Augat P, Claes L, Kinzl L, Beck A: The effects of non-steroidal anti-inflammatory drug application on incisional wound healing in rats. J Wound Care 2007; 16:76–8
139. Anderson K, Hamm RL: Factors that impair wound healing. J Am Coll Clin Wound Spec 2012; 4:84–91
140. Wilgus TA, Bergdall VK, Tober KL, Hill KJ, Mitra S, Flavahan NA, Oberyszyn TM: The impact of cyclooxygenase-2 mediated inflammation on scarless fetal wound healing. Am J Pathol 2004; 165:753–61
141. Loynes CA, Lee JA, Robertson AL, Steel MJ, Ellett F, Feng Y, Levy BD, Whyte MKB, Renshaw SA: PGE2

production at sites of tissue injury promotes an anti-inflammatory neutrophil phenotype and determines the outcome of inflammation resolution *in vivo*. Sci Adv 2018; 4:eaar8320
142. Manieri NA, Drylewicz MR, Miyoshi H, Stappenbeck TS: Igf2bp1 is required for full induction of Ptgs2 mRNA in colonic mesenchymal stem cells in mice. Gastroenterology 2012; 143:110–21.e10
143. Reisinger KW, Schellekens DH, Bosmans JW, Boonen B, Hulsewé KW, Sastrowijoto P, Derikx JP, Grootjans J, Poeze M: Cyclooxygenase-2 is essential for colorectal anastomotic healing. Ann Surg 2017; 265:547–54
144. Bosmans JW, Jongen AC, Bouvy ND, Derikx JP: Colorectal anastomotic healing: Why the biological processes that lead to anastomotic leakage should be revealed prior to conducting intervention studies. BMC Gastroenterol 2015; 15:180
145. Inan A, Koca C, Sen M: Effects of diclofenac sodium on bursting pressures of anastomoses and hydroxyproline contents of perianastomotic tissues in a laboratory study. Int J Surg 2006; 4:222–7
146. Martinou E, Drakopoulou S, Aravidou E, Sergentanis T, Kondi-Pafiti A, Argyra E, Voros D, Fragulidis GP: Parecoxib's effects on anastomotic and abdominal wound healing: A randomized controlled trial. J Surg Res 2018; 223:165–73
147. de Hingh IH, van Goor H, de Man BM, Lomme RM, Bleichrodt RP, Hendriks T: Selective cyclo-oxygenase 2 inhibition affects ileal but not colonic anastomotic healing in the early postoperative period. Br J Surg 2006; 93:489–97
148. Yauw ST, Lomme RM, van der Vijver RJ, Hendriks T, van Laarhoven KJ, van Goor H: Diclofenac causes anastomotic leakage in the proximal colon but not in the distal colon of the rat. Am J Surg 2015; 210:382–8
149. van der Vijver RJ, van Laarhoven CJ, de Man BM, Lomme RM, Hendriks T: Perioperative pain relief by a COX-2 inhibitor affects ileal repair and provides a model for anastomotic leakage in the intestine. Surg Innov 2013; 20:113–8
150. Pountos I, Georgouli T, Calori GM, Giannoudis PV: Do nonsteroidal anti-inflammatory drugs affect bone healing?: A critical analysis. ScientificWorldJournal 2012; 2012:606404
151. Zhang X, Schwarz EM, Young DA, Puzas JE, Rosier RN, O'Keefe RJ: Cyclooxygenase-2 regulates mesenchymal cell differentiation into the osteoblast lineage and is critically involved in bone repair. J Clin Invest 2002; 109:1405–15
152. Myers LK, Bhattacharya SD, Herring PA, Xing Z, Goorha S, Smith RA, Bhattacharya SK, Carbone L, Faccio R, Kang AH, Ballou LR: The isozyme-specific effects of cyclooxygenase-deficiency on bone in mice. Bone 2006; 39:1048–52
153. Ledford DK, Wenzel SE, Lockey RF: Aspirin or other nonsteroidal inflammatory agent exacerbated asthma. J Allergy Clin Immunol Pract 2014; 2:653–7
154. Szczeklik A: Mechanism of aspirin-induced asthma. Allergy 1997; 52:613–9
155. Claar D, Hartert TV, Peebles RS Jr: The role of prostaglandins in allergic lung inflammation and asthma. Expert Rev Respir Med 2015; 9:55–72
156. Looney Y, O'Shea A, O'Dwyer R: Severe bronchospasm after parenteral parecoxib: Cyclooxygenase-2 inhibitors: Not the answer yet. Anesthesiology 2005; 102:473–5

MIND TO MIND

Creative writing that explores the abstract side of our profession and our lives

Stephen T. Harvey, M.D., Editor

Dyspnea

Jefferson Dryden, D.O.

Through panes I watch
the trade of purple to red
halt.
Monitors darken
preceding terminal liberation.

Stiff
stoic.
The hour and minute recorded.
I shamble away.

Alone.

Just as he was.
Caring strangers no proxy
for family.

Our compliant connections once allowing
free exchange
now inhibited.
Fibrotic.

I heave
a burdensome breath.

Accepted for publication September 7, 2021. Published online first on October 5, 2021.

Jefferson Dryden, D.O.: Department of Anesthesiology, Critical Care Division, The Ohio State University, Columbus, Ohio. jefferson.dryden@osumc.edu.

 Anesthesiology 2022; 136:861. DOI: 10.1097/ALN.0000000000004014

MIND TO MIND

Creative writing that explores the abstract side of our profession and our lives

Stephen T. Harvey, M.D., Editor

The ICU: Ants in the Forest

Jennifer M. Connell, B.S.

During a break between clinical rotations in medical school, I was 6 miles into a hike in Kings Canyon National Park. Surrounded by stunning scenery—expansive mountain vistas, towering forests of redwoods, and the first streams of sunlight shining on the valley dirt path—I found myself staring at a rock. Not a particularly notable rock, except for the vibrant, neon green moss growing on its side. As I leaned in to get a closer look, I watched tiny ants navigating their way through the stalks of the moss forest. Tiny step after tiny step, each fork in the road a new critical decision point in reaching their destination. They navigate their moss as I navigate the redwood forest.

"Silly ants," I thought, "they don't even know how much more moss there is on this rock. They don't even know that this rock is just a single rock in a whole pile of rocks set atop a mountain, which itself is a giant rock."

Flashback to my first week on my intensive care unit elective: I too felt lost in the forest that was patient care in the ICU. Surrounded by very different scenery—peaks and valleys scrolling on the ventilator screen with each patient breath, tangles of IV tubing spilling from towering poles above the bed, bands of fluorescent light reflecting on tile illuminating the path down the hall.

The following series of pictures depicts my progression in thinking about patient care.

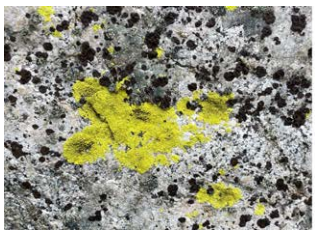

Accepted for publication October 14, 2021. Published online first on November 8, 2021.

Jennifer M. Connell, B.S.: Vanderbilt University School of Medicine, Nashville, Tennessee. jennifer.m.connell@vanderbilt.edu

 Anesthesiology 2022; 136:862–3. DOI: 10.1097/ALN.0000000000004058

Left: *Feeling like the ant in the moss of day-to-day decisions:* Can we decrease positive end-expiratory pressure from 10 to 8 today? Is the arterial line giving us the accurate blood pressure or should we titrate pressors based off the cuff? Should we give fluids? Or are they already volume overloaded?

Center: *Stepping back to their current illness trajectory:* Once we get them off continuous renal replacement therapy, will they need dialysis indefinitely? How much longer will they stay in the ICU? Should we start talking about a tracheostomy at this point? What sort of cognitive recovery can they expect?

Right: *Seeing their life as a whole, not limited to their illness:* What matters to them in life? What makes life worth living to them? Will we be able to get them home to enjoy a Sunday afternoon ice cream cone with their grandchildren? What were they looking forward to before this admission?

As students/clinicians/ants, let us all humbly aspire to escape the forest within the moss to see the magnitude of scope in caring for each patient.

Acknowledgments

The author thanks Pratik Pandharipande, M.D., M.S.C.I., professor of anesthesiology and surgery (Vanderbilt University Medical Center, Nashville, Tennessee), for his incredible teaching and thoughtful reflections during the author's time in the intensive care unit.

Review of the ASA Physical Status Classification: Comment

To the Editor:

We read with great interest the review article on the American Society of Anesthesiologists (ASA; Schaumburg, Illinois) Physical Status Classification System by Horvath *et al.*[1] The review presents in excellent detail the origin, evolution, and current state of the ASA Physical Status system. Further, the authors describe the recent addition of clinical examples to help clarify the classifications. These examples have been useful to provide some consistency in the assignment of ASA Physical Status classifications by anesthesia-trained and non–anesthesia-trained clinicians[2] and have been demonstrated to improve communication about patient status to anesthesia providers when assessments are performed by anesthesiologists in preanesthesia clinic settings and before the day of surgery.[3]

As an extension of the historical perspective they have given, the authors also consider whether further refinements or more granular categories might be of value. In proposing that the ASA and anesthesia community revise the ASA Physical Status system, we want to provide some additional background information about the current status of the system and its implications. Although the ASA Physical Status system is used by many anesthesia and nonanesthesia clinicians in the United States and around the world for purposes unrelated to the initial purpose for which it was created, in the United States, physical status modifiers based on (and identical to) the ASA classification system are part of the Current Procedural Terminology, which is a product of the American Medical Association (Chicago, Illinois).[4] These billing modifiers are used to justify additional payment by some payers based on the physical status of patients receiving anesthesia care. If the ASA determined that modifications to the current system were warranted, the society would have the ability to make changes to it. However, any changes proposed by the ASA will not impact payment unless the ASA requested revisions to the Current Procedural Terminology–defined physical status modifiers. To do so, the ASA would have to submit an application for a code change at the Current Procedural Terminology level and then a valuation through the American Medical Association Relative Value System Update Committee.[5] Although ASA can give input, the Current Procedural Terminology Editorial Board and the American Medical Association Relative Value System Update Committee would make final decisions on the physical status billing modifiers (the definitions, categories, and valuation). This request and approval process takes at least 3 yr to be implemented.

Based on this historical background, the ASA, through the House of Delegates and with support and recommendations provided by the ASA Committee on Economics, chose to provide additional examples to better illustrate the application of the definitions and the determination of appropriate ASA Physical Status assignment rather than propose revisions to the categories and definitions. As noted in the review, the initial examples were adopted in 2014 specifically for adult patients. In 2020, examples for pediatric patients and obstetric patients were added with input from the ASA Committees on Pediatric Anesthesia and on Obstetric Anesthesia.

Competing Interests

The authors are all members of the American Society of Anesthesiologists (ASA) Committee on Economics (Schaumburg, Illinois). S. Merrick is the ASA staff member on the committee.

Amr E. Abouleish, M.D., M.B.A., Jonathan Gal, M.D., M.B.A., M.S., Christopher Troianos, M.D., Sharon Merrick, M.S., Neal Cohen, M.D., M.P.H., M.S., Stanley Stead, M.D., M.B.A.
University of Texas Medical Branch, Galveston, Texas (A.E.A.).
aaboulei@utmb.edu

DOI: 10.1097/ALN.0000000000004145

References

1. Horvath B, Kloesel B, Todd MM, Cole DJ, Prielipp RC: The evolution, current value, and future of the American Society of Anesthesiologists Physical Status Classification System. Anesthesiology 2021; 135:904–19
2. Hurwitz EE, Simon M, Vinta SR, Zehm CF, Shabot SM, Minhajuddin A, Abouleish AE: Adding examples to the ASA-Physical Status classification improves correct assignment to patients. Anesthesiology 2017; 126:614–22
3. Abouleish AE, Vinta SR, Shabot SM, Patel NV, Hurwitz EE, Krishnamurthy P, Simon M: Improving communication between pre-anesthesia screening and day of anesthesia evaluations by increasing agreement of ASA Physical Status Class with addition of

institutional-specific and ASA-approved examples. Perioper Med 2020; 9:34
4. American Medical Association: CPT® 2021 Professional Edition. Chicago, American Medical Association, 2021
5. American Medical Association: Lifecycle of a code: How the CPT and RUC process works. Available at: https://www.ama-assn.org/about/cpt-editorial-panel/lifecycle-code-how-cpt-and-ruc-process-works. Accessed September 14, 2021.

(Accepted for publication January 14, 2022. Published online first on February 7, 2022.)

Review of the ASA Physical Status Classification: Comment

To the Editor:

We read with interest the review of the American Society of Anesthesiologists (ASA; Schaumburg, Illinois) Physical Status Classification System by Horvath *et al.*[1] The authors provided an overview of the ASA Physical Status system; however, one use of the ASA Physical Status system is not mentioned that we believe warrants attention due to its impact on hospital finances and quality ratings.

The ASA Physical Status score is a key variable in mathematical models used by the Centers for Disease Control and Prevention (Atlanta, Georgia) National Healthcare Safety Network to risk-adjust surgical site infection rates at U.S. acute care hospitals.[2] For each hospital, a standardized infection ratio is calculated for colon surgery and abdominal hysterectomy. The standardized infection ratio is calculated by dividing the observed number of infections for each procedure by the expected number of infections. A standardized infection ratio greater than 1 indicates better than expected performance, whereas a standardized infection ratio less than 1 indicates worse than expected performance. The probability of infection for each patient is calculated using logistic regression equations that incorporate patient, procedural, and facility factors that have been found to predict surgical site infection incidence (table 1). The total number of expected infections is equal to the sum of the probabilities for all patients over a given period.[2] The ASA Physical Status score is the only variable that is subjective and therefore prone to misclassification. Systematic underreporting of ASA Physical Status will adversely impact a hospital's risk-adjusted surgical site infection performance, whereas overreporting (up-coding) will artificially improve a hospital's performance.

Table 1. Centers for Disease Control and Prevention National Healthcare Safety Network Surgical Site Infection Logistic Regression Equations[2]

Variable	Coefficient	Variable Coding	Odds Ratio
Abdominal hysterectomy surgical site infection (30-day model)			
Intercept	–5.1801		
Diabetes	0.3247	Yes = 1 No = 0	1.38
ASA score	0.4414	1 = 1 2 = 2 3 = 3 4/5 = 4	1.55
Body mass index	0.1106	≥ 30 = 1 < 30 = 0	1.12
Age	–0.1501	Patient age ÷ 10	0.86
Oncology hospital	0.5474	Oncology hospital = 1 Nononcology hospital = 0	1.73
Colon surgery (30-day model)			
Intercept	–3.6601		
Diabetes	0.0821	Yes = 1 No = 0	1.09
ASA score	0.3028	1 = 1 2 = 2 3/4/5 = 3	1.35
Body mass index	0.1249	≥ 30 = 1 < 30 = 0	1.13
Age	–0.1396	Patient age ÷ 10	0.87
Sex	0.1036	Male = 1 Female = 0	1.11
Closure technique	0.2383	Primary = 0 Other = 1	1.27
Oncology hospital	0.5437	Oncology hospital = 1 Nononcology hospital = 0	1.72

Odds ratios calculated by authors.
ASA, American Society of Anesthesiologists.

The surgical site infection standardized infection ratio is an important quality metric with both financial and reputational implications for hospitals. It is one of six quality measures evaluated by the Centers for Medicare & Medicaid Services (Baltimore, Maryland) for the Healthcare Acquired Conditions Reduction Program, through which the bottom 25% of hospitals are penalized 1% of their Medicare inpatient revenue.[3] Surgical site infection rates also constitute two of the six measures in the safety domain of the Centers for Medicare & Medicaid Services Hospital Value-Based Purchasing Program, which places another 2% of Medicare revenue at risk and provides bonuses to high-performing hospitals.[4] Moreover, surgical site infection performance is reported by the Leapfrog Group (Washington, D.C.),[5] displayed on the Centers for Medicare & Medicaid Services Care Compare website,[6] and incorporated into calculations for Centers for Medicare & Medicaid Services Overall Hospital Quality Star Ratings.[7] Each of these programs uses the Centers for Disease Control and Prevention

institutional-specific and ASA-approved examples. Perioper Med 2020; 9:34
4. American Medical Association: CPT® 2021 Professional Edition. Chicago, American Medical Association, 2021
5. American Medical Association: Lifecycle of a code: How the CPT and RUC process works. Available at: https://www.ama-assn.org/about/cpt-editorial-panel/lifecycle-code-how-cpt-and-ruc-process-works. Accessed September 14, 2021.

(Accepted for publication January 14, 2022. Published online first on February 7, 2022.)

Review of the ASA Physical Status Classification: Comment

To the Editor:

We read with interest the review of the American Society of Anesthesiologists (ASA; Schaumburg, Illinois) Physical Status Classification System by Horvath *et al.*[1] The authors provided an overview of the ASA Physical Status system; however, one use of the ASA Physical Status system is not mentioned that we believe warrants attention due to its impact on hospital finances and quality ratings.

The ASA Physical Status score is a key variable in mathematical models used by the Centers for Disease Control and Prevention (Atlanta, Georgia) National Healthcare Safety Network to risk-adjust surgical site infection rates at U.S. acute care hospitals.[2] For each hospital, a standardized infection ratio is calculated for colon surgery and abdominal hysterectomy. The standardized infection ratio is calculated by dividing the observed number of infections for each procedure by the expected number of infections. A standardized infection ratio greater than 1 indicates better than expected performance, whereas a standardized infection ratio less than 1 indicates worse than expected performance. The probability of infection for each patient is calculated using logistic regression equations that incorporate patient, procedural, and facility factors that have been found to predict surgical site infection incidence (table 1). The total number of expected infections is equal to the sum of the probabilities for all patients over a given period.[2] The ASA Physical Status score is the only variable that is subjective and therefore prone to misclassification. Systematic underreporting of ASA Physical Status will adversely impact a hospital's risk-adjusted surgical site infection performance, whereas overreporting (up-coding) will artificially improve a hospital's performance.

Table 1. Centers for Disease Control and Prevention National Healthcare Safety Network Surgical Site Infection Logistic Regression Equations[2]

Variable	Coefficient	Variable Coding	Odds Ratio
Abdominal hysterectomy surgical site infection (30-day model)			
Intercept	–5.1801		
Diabetes	0.3247	Yes = 1 No = 0	1.38
ASA score	0.4414	1 = 1 2 = 2 3 = 3 4/5 = 4	1.55
Body mass index	0.1106	≥ 30 = 1 < 30 = 0	1.12
Age	–0.1501	Patient age ÷ 10	0.86
Oncology hospital	0.5474	Oncology hospital = 1 Nononcology hospital = 0	1.73
Colon surgery (30-day model)			
Intercept	–3.6601		
Diabetes	0.0821	Yes = 1 No = 0	1.09
ASA score	0.3028	1 = 1 2 = 2 3/4/5 = 3	1.35
Body mass index	0.1249	≥ 30 = 1 < 30 = 0	1.13
Age	–0.1396	Patient age ÷ 10	0.87
Sex	0.1036	Male = 1 Female = 0	1.11
Closure technique	0.2383	Primary = 0 Other = 1	1.27
Oncology hospital	0.5437	Oncology hospital = 1 Nononcology hospital = 0	1.72

Odds ratios calculated by authors.
ASA, American Society of Anesthesiologists.

The surgical site infection standardized infection ratio is an important quality metric with both financial and reputational implications for hospitals. It is one of six quality measures evaluated by the Centers for Medicare & Medicaid Services (Baltimore, Maryland) for the Healthcare Acquired Conditions Reduction Program, through which the bottom 25% of hospitals are penalized 1% of their Medicare inpatient revenue.[3] Surgical site infection rates also constitute two of the six measures in the safety domain of the Centers for Medicare & Medicaid Services Hospital Value-Based Purchasing Program, which places another 2% of Medicare revenue at risk and provides bonuses to high-performing hospitals.[4] Moreover, surgical site infection performance is reported by the Leapfrog Group (Washington, D.C.),[5] displayed on the Centers for Medicare & Medicaid Services Care Compare website,[6] and incorporated into calculations for Centers for Medicare & Medicaid Services Overall Hospital Quality Star Ratings.[7] Each of these programs uses the Centers for Disease Control and Prevention

National Healthcare Safety Network standardized infection ratios for colon surgery and abdominal hysterectomy; thus, ASA Physical Status misclassification by anesthesiologists will impact hospital performance across these programs.

Competing Interests

Dr. Flynn is a Medical Advisor for Psychable, Inc. (Hawthorne, California), a privately held company, and owns shares in MedCrypt, Inc. (Encinitas, California), a privately held company. Dr. Grant is the principal investigator on an institutionally funded research grant from SPR Therapeutics (Cleveland, Ohio), receives royalty payments from Oxford University Press (Oxford, United Kingdom), serves on the Board of Directors of the American Society for Regional Anesthesia and Pain Medicine (Pittsburgh, Pennsylvania), and previously served on the Advisory Board for B. Braun Medical, Inc. (Bethlehem, Pennsylvania). Dr. Lund declares no competing interests.

David N. Flynn, M.D., M.B.A., Elisa T. Lund, M.D., Stuart A. Grant, M.B., Ch.B. University of North Carolina at Chapel Hill School of Medicine, Chapel Hill, North Carolina (D.N.F.). david_flynn@med.unc.edu

DOI: 10.1097/ALN.0000000000004146

References

1. Horvath B, Kloesel B, Todd MM, Cole DJ, Prielipp RC: The evolution, current value, and future of the American Society of Anesthesiologists Physical Status Classification System. Anesthesiology 2021; 135:904–19
2. Centers for Disease Control and Prevention: The NHSN standardized infection ratio (SIR). Available at: https://www.cdc.gov/nhsn/pdfs/ps-analysis-resources/nhsn-sir-guide.pdf. Accessed November 2, 2021.
3. The Center for Medicare & Medicaid Services: Hospital-acquired condition (HAC) reduction program: scoring methodology. Available at: https://www.cms.gov/files/document/fy-2022-hac-reduction-program-fact-sheet.pdf. Accessed November 2, 2021.
4. The Center for Medicare & Medicaid Services: FY 2023 Hospital Value-Based Purchasing Program quick reference guide. Available at: https://qualitynet.cms.gov/files/5fa4da92ca7c850025cd3748?filename=VBP_FY2023_Summary_PurchaseGde.pdf. Accessed November 2, 2021.
5. The Leapfrog Group: Leapfrog Hospital Safety Grade. Scoring methodology. Available at: https://www.hospitalsafetygrade.org/media/file/Safety-Grade-Scoring-Methodology-Spring-2021_2.pdf. Accessed November 2, 2021.
6. The Center for Medicare & Medicaid Services: Medicare.gov. Available at: https://www.medicare.gov/care-compare/. Accessed November 5, 2021.
7. The Center for Medicare & Medicaid Services: Overall Hospital Quality Star Rating on Care Compare Methodology report (v4.0). Available at: https://qualitynet.cms.gov/files/603966dda413b400224ddf50?filename=Star_Rtngs_CompMthdlgy_v4.1.pdf. Accessed November 2, 2021.

(Accepted for publication January 14, 2022. Published online first on February 7, 2022.)

Review of the ASA Physical Status Classification: Reply

In Reply:

We sincerely thank Abouleish *et al.*[1] and Flynn *et al.*[2] for their interest in and comments on our review article.[3] Whereas our manuscript emphasized the virtually universal, multidisciplinary application of the American Society of Anesthesiologists (ASA; Schaumburg, Illinois) Physical Status Classification System to patient care and research, Abouleish *et al.* and Flynn *et al.* highlight the fact that it is also used for purposes that go far beyond the original intent of its developers. Indeed, we agree with the thoughtful insights of both letters noting the considerable economic implications of the ASA Physical Status Classification System to both clinicians and medical facilities.

The authors[1,2] provide vivid illustrations with specific examples of the potential financial impact of misclassification of ASA Physical Status—perhaps far greater than we suggested in our original review.[3] Although economics was not the primary focus of our article, the financial impact of the ASA Physical Status system is real, and any future changes to the classification system involve a complex set of stakeholders (ASA members and leadership, Centers for Medicare & Medicaid Services [Baltimore, Maryland], the Current Procedural Terminology, which is a product of the American Medical Association [Chicago, Illinois], and the AMA Relative Value Unit Update Committee). As noted by Flynn *et al.*,[2] "The ASA Physical Status score is a key variable in mathematical models used by the Centers for Disease Control and Prevention [Atlanta, Georgia] National Healthcare Safety Network to risk-adjust surgical site infection rates at U.S. acute care hospitals." Because it is considered a "key variable" in models with profound impact on both quality assessment and billing, we believe that minimizing the variability behind this key variable should be a high priority.

National Healthcare Safety Network standardized infection ratios for colon surgery and abdominal hysterectomy; thus, ASA Physical Status misclassification by anesthesiologists will impact hospital performance across these programs.

Competing Interests

Dr. Flynn is a Medical Advisor for Psychable, Inc. (Hawthorne, California), a privately held company, and owns shares in MedCrypt, Inc. (Encinitas, California), a privately held company. Dr. Grant is the principal investigator on an institutionally funded research grant from SPR Therapeutics (Cleveland, Ohio), receives royalty payments from Oxford University Press (Oxford, United Kingdom), serves on the Board of Directors of the American Society for Regional Anesthesia and Pain Medicine (Pittsburgh, Pennsylvania), and previously served on the Advisory Board for B. Braun Medical, Inc. (Bethlehem, Pennsylvania). Dr. Lund declares no competing interests.

David N. Flynn, M.D., M.B.A., Elisa T. Lund, M.D., Stuart A. Grant, M.B., Ch.B. University of North Carolina at Chapel Hill School of Medicine, Chapel Hill, North Carolina (D.N.F.). david_flynn@med.unc.edu

DOI: 10.1097/ALN.0000000000004146

References

1. Horvath B, Kloesel B, Todd MM, Cole DJ, Prielipp RC: The evolution, current value, and future of the American Society of Anesthesiologists Physical Status Classification System. Anesthesiology 2021; 135:904–19
2. Centers for Disease Control and Prevention: The NHSN standardized infection ratio (SIR). Available at: https://www.cdc.gov/nhsn/pdfs/ps-analysis-resources/nhsn-sir-guide.pdf. Accessed November 2, 2021.
3. The Center for Medicare & Medicaid Services: Hospital-acquired condition (HAC) reduction program: scoring methodology. Available at: https://www.cms.gov/files/document/fy-2022-hac-reduction-program-fact-sheet.pdf. Accessed November 2, 2021.
4. The Center for Medicare & Medicaid Services: FY 2023 Hospital Value-Based Purchasing Program quick reference guide. Available at: https://qualitynet.cms.gov/files/5fa4da92ca7c850025cd3748?filename=VBP_FY2023_Summary_PurchaseGde.pdf. Accessed November 2, 2021.
5. The Leapfrog Group: Leapfrog Hospital Safety Grade. Scoring methodology. Available at: https://www.hospitalsafetygrade.org/media/file/Safety-Grade-Scoring-Methodology-Spring-2021_2.pdf. Accessed November 2, 2021.
6. The Center for Medicare & Medicaid Services: Medicare.gov. Available at: https://www.medicare.gov/care-compare/. Accessed November 5, 2021.
7. The Center for Medicare & Medicaid Services: Overall Hospital Quality Star Rating on Care Compare Methodology report (v4.0). Available at: https://qualitynet.cms.gov/files/603966dda413b400224ddf50?filename=Star_Rtngs_CompMthdlgy_v4.1.pdf. Accessed November 2, 2021.

(Accepted for publication January 14, 2022. Published online first on February 7, 2022.)

Review of the ASA Physical Status Classification: Reply

In Reply:

We sincerely thank Abouleish *et al.*[1] and Flynn *et al.*[2] for their interest in and comments on our review article.[3] Whereas our manuscript emphasized the virtually universal, multidisciplinary application of the American Society of Anesthesiologists (ASA; Schaumburg, Illinois) Physical Status Classification System to patient care and research, Abouleish *et al.* and Flynn *et al.* highlight the fact that it is also used for purposes that go far beyond the original intent of its developers. Indeed, we agree with the thoughtful insights of both letters noting the considerable economic implications of the ASA Physical Status Classification System to both clinicians and medical facilities.

The authors[1,2] provide vivid illustrations with specific examples of the potential financial impact of misclassification of ASA Physical Status—perhaps far greater than we suggested in our original review.[3] Although economics was not the primary focus of our article, the financial impact of the ASA Physical Status system is real, and any future changes to the classification system involve a complex set of stakeholders (ASA members and leadership, Centers for Medicare & Medicaid Services [Baltimore, Maryland], the Current Procedural Terminology, which is a product of the American Medical Association [Chicago, Illinois], and the AMA Relative Value Unit Update Committee). As noted by Flynn *et al.*,[2] "The ASA Physical Status score is a key variable in mathematical models used by the Centers for Disease Control and Prevention [Atlanta, Georgia] National Healthcare Safety Network to risk-adjust surgical site infection rates at U.S. acute care hospitals." Because it is considered a "key variable" in models with profound impact on both quality assessment and billing, we believe that minimizing the variability behind this key variable should be a high priority.

Thus, the best route to appropriate and fair compensation for services for both clinicians and medical facilities is to embrace education and adopt future processes (*e.g.*, technology assist[3]) that optimize the accuracy and reproducibility of the ASA Physical Status classification by all providers, and efforts to optimize interrater reliability should continue or even be enhanced by the ASA and other leading organizations.

However, given the long-term design and intent of the ASA Physical Status system, it is not clear that any changes to this system that aim to directly impact economics—as distinct from the society's 80-yr-long (and continuing) efforts to improve accuracy and reproducibility and provide a valuable tool for its clinicians—are desirable. We should make changes based on a need for clinical improvement and let the economic process evolve in parallel. That effort is best led by the ASA with other key stakeholders as we consider any future refinements to our classic ASA Physical Status system.

Competing Interests

Dr. Todd was the Editor-in-Chief of Anesthesiology, the Official Journal of the American Society of Anesthesiologists (ASA; Schaumburg, Illinois), from 1997 to 2006. Dr. Todd was also the awarded the 2016 Excellence in Research Award by the ASA. Dr. Cole is vice president of the Anesthesia Patient Safety Foundation (Rochester, Minnesota), a foundation of the ASA, and is a past president of the ASA. Dr. Prielipp is a former member of the Board of Directors of the Anesthesia Patient Safety Foundation and serves on the speakers' bureau for Merck Co., Inc. (Kenilworth, New Jersey) and as an opinion leader for 3M (Minneapolis, Minnesota). The other authors declare no competing interests.

Balazs Horvath, M.D., F.A.S.A., Benjamin Kloesel, M.D., M.S.B.S., Michael M. Todd, M.D., Daniel J. Cole, M.D., F.A.S.A., Richard C. Prielipp, M.D., M.B.A., F.C.C.M. University of Minnesota School of Medicine, Minneapolis, Minnesota (B.H.). bhorvath@umn.edu

DOI: 10.1097/ALN.0000000000004147

References

1. Abouleish AE, Gal J, Troianos C, Merrick S, Cohen N, Stead S: Review of the ASA Physical Status Classification: Comment. Anesthesiology 2022; 136:864–5
2. Flynn DN, Lund ET, Grant SA: Review of the ASA Physical Status Classification: Comment. Anesthesiology 2022; 136:865–6
3. Horvath B, Kloesel B, Todd MM, Cole DJ, Prielipp RC: The evolution, current value, and future of the American Society of Anesthesiologists Physical Status Classification System. Anesthesiology 2021; 135:904–19

(Accepted for publication January 14, 2022. Published online first on February 7, 2022.)

Vasopressor Effects on Cerebral Microcirculation: Comment

To the Editor:

We read with great interest the study by Koch *et al.*,[1] which concluded that "ephedrine results in better brain microcirculation and oxygen delivery than phenylephrine" and raised "concerns regarding phenylephrine for blood pressure augmentation in patients with cerebral pathology." The results of this prospective, randomized trial are similar to those of a network meta-analysis[2] of 399 patients from nine randomized trials comparing various inotropes/vasopressors used to treat intraoperative hypotension in patients mostly without cerebral pathology. That analysis found that dopamine, ephedrine, and norepinephrine had the lowest probability of adversely affecting cerebral oxygen saturation as measured by cerebral oximetry and that phenylephrine, compared with the other inotropes/vasopressors, decreased cerebral oxygen saturation. Koch *et al.*'s findings on the deterioration of microcirculation after phenylephrine administration on the side of the brain not affected by brain pathology highlight the importance of considering the cerebrovascular effect of vasopressors in every patient, not only the ones with cerebral pathologies. Phenylephrine is very effective in restoring systemic blood pressure to normal values. Clinicians tend to favor what has been described by Thiele *et al.*[3] as the "tangible bias," which is our tendency to fix what we can see and understand, that is, systemic blood pressure, over what we cannot: macro- and microscopic cerebral perfusion. Koch *et al.*'s results should prompt clinicians to choose the appropriate vasopressor to maintain optimal cerebral microcirculation.

Competing Interests

The authors declare no competing interests.

Anna Maria Bombardieri, M.D., Ph.D., Ban C. H. Tsui, M.D., M.Sc. Stanford University School of Medicine, Stanford, California (A.M.B.). abomba@stanford.edu

DOI: 10.1097/ALN.0000000000004149

References

1. Koch KU, Mikkelsen IK, Espelund US, Angleys H, Tietze A, Oettingen GV, Juul N, Østergaard L, Rasmussen M: Cerebral macro- and microcirculation during ephedrine *versus* phenylephrine treatment in anesthetized brain tumor patients: A randomized

Thus, the best route to appropriate and fair compensation for services for both clinicians and medical facilities is to embrace education and adopt future processes (*e.g.*, technology assist[3]) that optimize the accuracy and reproducibility of the ASA Physical Status classification by all providers, and efforts to optimize interrater reliability should continue or even be enhanced by the ASA and other leading organizations.

However, given the long-term design and intent of the ASA Physical Status system, it is not clear that any changes to this system that aim to directly impact economics—as distinct from the society's 80-yr-long (and continuing) efforts to improve accuracy and reproducibility and provide a valuable tool for its clinicians—are desirable. We should make changes based on a need for clinical improvement and let the economic process evolve in parallel. That effort is best led by the ASA with other key stakeholders as we consider any future refinements to our classic ASA Physical Status system.

Competing Interests

Dr. Todd was the Editor-in-Chief of Anesthesiology, the Official Journal of the American Society of Anesthesiologists (ASA; Schaumburg, Illinois), from 1997 to 2006. Dr. Todd was also the awarded the 2016 Excellence in Research Award by the ASA. Dr. Cole is vice president of the Anesthesia Patient Safety Foundation (Rochester, Minnesota), a foundation of the ASA, and is a past president of the ASA. Dr. Prielipp is a former member of the Board of Directors of the Anesthesia Patient Safety Foundation and serves on the speakers' bureau for Merck Co., Inc. (Kenilworth, New Jersey) and as an opinion leader for 3M (Minneapolis, Minnesota). The other authors declare no competing interests.

Balazs Horvath, M.D., F.A.S.A., Benjamin Kloesel, M.D., M.S.B.S., Michael M. Todd, M.D., Daniel J. Cole, M.D., F.A.S.A., Richard C. Prielipp, M.D., M.B.A., F.C.C.M. University of Minnesota School of Medicine, Minneapolis, Minnesota (B.H.). bhorvath@umn.edu

DOI: 10.1097/ALN.0000000000004147

References

1. Abouleish AE, Gal J, Troianos C, Merrick S, Cohen N, Stead S: Review of the ASA Physical Status Classification: Comment. Anesthesiology 2022; 136:864–5
2. Flynn DN, Lund ET, Grant SA: Review of the ASA Physical Status Classification: Comment. Anesthesiology 2022; 136:865–6
3. Horvath B, Kloesel B, Todd MM, Cole DJ, Prielipp RC: The evolution, current value, and future of the American Society of Anesthesiologists Physical Status Classification System. Anesthesiology 2021; 135:904–19

(Accepted for publication January 14, 2022. Published online first on February 7, 2022.)

Vasopressor Effects on Cerebral Microcirculation: Comment

To the Editor:

We read with great interest the study by Koch *et al.*,[1] which concluded that "ephedrine results in better brain microcirculation and oxygen delivery than phenylephrine" and raised "concerns regarding phenylephrine for blood pressure augmentation in patients with cerebral pathology." The results of this prospective, randomized trial are similar to those of a network meta-analysis[2] of 399 patients from nine randomized trials comparing various inotropes/vasopressors used to treat intraoperative hypotension in patients mostly without cerebral pathology. That analysis found that dopamine, ephedrine, and norepinephrine had the lowest probability of adversely affecting cerebral oxygen saturation as measured by cerebral oximetry and that phenylephrine, compared with the other inotropes/vasopressors, decreased cerebral oxygen saturation. Koch *et al.*'s findings on the deterioration of microcirculation after phenylephrine administration on the side of the brain not affected by brain pathology highlight the importance of considering the cerebrovascular effect of vasopressors in every patient, not only the ones with cerebral pathologies. Phenylephrine is very effective in restoring systemic blood pressure to normal values. Clinicians tend to favor what has been described by Thiele *et al.*[3] as the "tangible bias," which is our tendency to fix what we can see and understand, that is, systemic blood pressure, over what we cannot: macro- and microscopic cerebral perfusion. Koch *et al.*'s results should prompt clinicians to choose the appropriate vasopressor to maintain optimal cerebral microcirculation.

Competing Interests

The authors declare no competing interests.

Anna Maria Bombardieri, M.D., Ph.D., Ban C. H. Tsui, M.D., M.Sc. Stanford University School of Medicine, Stanford, California (A.M.B.). abomba@stanford.edu

DOI: 10.1097/ALN.0000000000004149

References

1. Koch KU, Mikkelsen IK, Espelund US, Angleys H, Tietze A, Oettingen GV, Juul N, Østergaard L, Rasmussen M: Cerebral macro- and microcirculation during ephedrine *versus* phenylephrine treatment in anesthetized brain tumor patients: A randomized

clinical trial using magnetic resonance imaging. Anesthesiology 2021; 135:788–803
2. Bombardieri AM, Singh NP, Yaeger L, Athiraman U, Tsui BCH, Singh PM: The regional cerebral oxygen saturation effect of inotropes/vasopressors administered to treat intraoperative hypotension: A Bayesian network meta-analysis. J Neurosurg Anesthesiol 2021 [Epub ahead of print]
3. Thiele RH, Nemergut EC, Lynch C III: The physiologic implications of isolated alpha(1) adrenergic stimulation. Anesth Analg 2011; 113:284–96

(Accepted for publication January 20, 2022. Published online first on February 14, 2022.)

Vasopressor Effects on Cerebral Microcirculation: Reply

In Reply:

We thank Bombardieri and Tsui[1] for their excellent comments and interest in our study.[2] We agree with Bombardieri and Tsui that the deterioration of microperfusion and possibly tissue oxygenation after phenylephrine administration in the "healthy" brain hemisphere[2] indicates that different vasopressors may also have a different influence on microperfusion and tissue oxygenation in the healthy anesthetized brain and should be further explored.[3] In our opinion, future studies on the effects of different vasopressors on the cerebral macro- and microcirculation should be considered in the context of their different effects on the systemic circulation to provide a fully integrated picture of their influence on organ perfusion and oxygenation.[4] Due to current difficulties in monitoring brain microcirculation and cerebral tissue oxygenation, we tend to rely on systemic parameters such as heart rate and blood pressure when treating patients with inotropes/vasopressors. However, a recent publication suggests that brain tissue oxygen saturation, as measured by near-infrared spectroscopy, may reflect cerebral metabolic supply–demand balance during vasopressor therapy.[4] Although the use of near-infrared spectroscopy is associated with limitations, such as extracranial signal contamination, it may currently be the only way to provide a continuous indicium of brain microperfusion and tissue oxygenation.

Competing Interests

Dr. Rasmussen declares a financial relationship with the Health Research Foundation of the Central Denmark Region (Aarhus, Denmark). Dr. Koch declares no competing interests.

Klaus Ulrik Koch, M.D., Ph.D., Mads Rasmussen, M.D., Ph.D.
Aarhus University Hospital, Aarhus, Denmark (K.U.K.).
klaukoch@rm.dk

DOI: 10.1097/ALN.0000000000004150

References

1. Bombardieri AM, Tsui BCH: Vasopressor effects on cerebral microcirculation: Comment. Anesthesiology 2022; 136:867–8
2. Koch KU, Mikkelsen IK, Espelund US, Angleys H, Tietze A, Oettingen GV, Juul N, Østergaard L, Rasmussen M: Cerebral macro- and microcirculation during ephedrine versus phenylephrine treatment in anesthetized brain tumor patients: A randomized clinical trial using magnetic resonance imaging. Anesthesiology 2021; 135:788–803
3. Bombardieri AM, Singh NP, Yaeger L, Athiraman U, Tsui BCH, Singh PM: The regional cerebral oxygen saturation effect of inotropes/vasopressors administered to treat intraoperative hypotension: A Bayesian network meta-analysis. J Neurosurg Anesthesiol 2021 [Epub ahead of print]
4. Koch KU, Zhao X, Mikkelsen IK, Espelund US, Aanerud J, Rasmussen M, Meng L: Correlation between cerebral tissue oxygen saturation and oxygen extraction fraction during anesthesia: Monitoring cerebral metabolic demand-supply balance during vasopressor administration. J Neurosurg Anesthesiol 2021 [Epub ahead of print]

(Accepted for publication January 20, 2022. Published online first on February 14, 2022.)

Recent U.S. Food and Drug Administration Labeling Changes for Hydroxyethyl Starch Products Due to Concerns about Mortality, Kidney Injury, and Excess Bleeding

To the Editor:

The U.S. Food and Drug Administration (Silver Spring, Maryland) is requiring safety labeling changes to the

clinical trial using magnetic resonance imaging. Anesthesiology 2021; 135:788–803
2. Bombardieri AM, Singh NP, Yaeger L, Athiraman U, Tsui BCH, Singh PM: The regional cerebral oxygen saturation effect of inotropes/vasopressors administered to treat intraoperative hypotension: A Bayesian network meta-analysis. J Neurosurg Anesthesiol 2021 [Epub ahead of print]
3. Thiele RH, Nemergut EC, Lynch C III: The physiologic implications of isolated alpha(1) adrenergic stimulation. Anesth Analg 2011; 113:284–96

(Accepted for publication January 20, 2022. Published online first on February 14, 2022.)

Vasopressor Effects on Cerebral Microcirculation: Reply

In Reply:

We thank Bombardieri and Tsui[1] for their excellent comments and interest in our study.[2] We agree with Bombardieri and Tsui that the deterioration of microperfusion and possibly tissue oxygenation after phenylephrine administration in the "healthy" brain hemisphere[2] indicates that different vasopressors may also have a different influence on microperfusion and tissue oxygenation in the healthy anesthetized brain and should be further explored.[3] In our opinion, future studies on the effects of different vasopressors on the cerebral macro- and microcirculation should be considered in the context of their different effects on the systemic circulation to provide a fully integrated picture of their influence on organ perfusion and oxygenation.[4] Due to current difficulties in monitoring brain microcirculation and cerebral tissue oxygenation, we tend to rely on systemic parameters such as heart rate and blood pressure when treating patients with inotropes/vasopressors. However, a recent publication suggests that brain tissue oxygen saturation, as measured by near-infrared spectroscopy, may reflect cerebral metabolic supply–demand balance during vasopressor therapy.[4] Although the use of near-infrared spectroscopy is associated with limitations, such as extracranial signal contamination, it may currently be the only way to provide a continuous indicium of brain microperfusion and tissue oxygenation.

Competing Interests

Dr. Rasmussen declares a financial relationship with the Health Research Foundation of the Central Denmark Region (Aarhus, Denmark). Dr. Koch declares no competing interests.

Klaus Ulrik Koch, M.D., Ph.D., Mads Rasmussen, M.D., Ph.D.
Aarhus University Hospital, Aarhus, Denmark (K.U.K.).
klaukoch@rm.dk

DOI: 10.1097/ALN.0000000000004150

References

1. Bombardieri AM, Tsui BCH: Vasopressor effects on cerebral microcirculation: Comment. Anesthesiology 2022; 136:867–8
2. Koch KU, Mikkelsen IK, Espelund US, Angleys H, Tietze A, Oettingen GV, Juul N, Østergaard L, Rasmussen M: Cerebral macro- and microcirculation during ephedrine versus phenylephrine treatment in anesthetized brain tumor patients: A randomized clinical trial using magnetic resonance imaging. Anesthesiology 2021; 135:788–803
3. Bombardieri AM, Singh NP, Yaeger L, Athiraman U, Tsui BCH, Singh PM: The regional cerebral oxygen saturation effect of inotropes/vasopressors administered to treat intraoperative hypotension: A Bayesian network meta-analysis. J Neurosurg Anesthesiol 2021 [Epub ahead of print]
4. Koch KU, Zhao X, Mikkelsen IK, Espelund US, Aanerud J, Rasmussen M, Meng L: Correlation between cerebral tissue oxygen saturation and oxygen extraction fraction during anesthesia: Monitoring cerebral metabolic demand-supply balance during vasopressor administration. J Neurosurg Anesthesiol 2021 [Epub ahead of print]

(Accepted for publication January 20, 2022. Published online first on February 14, 2022.)

Recent U.S. Food and Drug Administration Labeling Changes for Hydroxyethyl Starch Products Due to Concerns about Mortality, Kidney Injury, and Excess Bleeding

To the Editor:

The U.S. Food and Drug Administration (Silver Spring, Maryland) is requiring safety labeling changes to the

clinical trial using magnetic resonance imaging. Anesthesiology 2021; 135:788–803
2. Bombardieri AM, Singh NP, Yaeger L, Athiraman U, Tsui BCH, Singh PM: The regional cerebral oxygen saturation effect of inotropes/vasopressors administered to treat intraoperative hypotension: A Bayesian network meta-analysis. J Neurosurg Anesthesiol 2021 [Epub ahead of print]
3. Thiele RH, Nemergut EC, Lynch C III: The physiologic implications of isolated alpha(1) adrenergic stimulation. Anesth Analg 2011; 113:284–96

(Accepted for publication January 20, 2022. Published online first on February 14, 2022.)

Vasopressor Effects on Cerebral Microcirculation: Reply

In Reply:

We thank Bombardieri and Tsui[1] for their excellent comments and interest in our study.[2] We agree with Bombardieri and Tsui that the deterioration of microperfusion and possibly tissue oxygenation after phenylephrine administration in the "healthy" brain hemisphere[2] indicates that different vasopressors may also have a different influence on microperfusion and tissue oxygenation in the healthy anesthetized brain and should be further explored.[3] In our opinion, future studies on the effects of different vasopressors on the cerebral macro- and microcirculation should be considered in the context of their different effects on the systemic circulation to provide a fully integrated picture of their influence on organ perfusion and oxygenation.[4] Due to current difficulties in monitoring brain microcirculation and cerebral tissue oxygenation, we tend to rely on systemic parameters such as heart rate and blood pressure when treating patients with inotropes/vasopressors. However, a recent publication suggests that brain tissue oxygen saturation, as measured by near-infrared spectroscopy, may reflect cerebral metabolic supply–demand balance during vasopressor therapy.[4] Although the use of near-infrared spectroscopy is associated with limitations, such as extracranial signal contamination, it may currently be the only way to provide a continuous indicium of brain microperfusion and tissue oxygenation.

Competing Interests

Dr. Rasmussen declares a financial relationship with the Health Research Foundation of the Central Denmark Region (Aarhus, Denmark). Dr. Koch declares no competing interests.

Klaus Ulrik Koch, M.D., Ph.D., Mads Rasmussen, M.D., Ph.D.
Aarhus University Hospital, Aarhus, Denmark (K.U.K.).
klaukoch@rm.dk

DOI: 10.1097/ALN.0000000000004150

References

1. Bombardieri AM, Tsui BCH: Vasopressor effects on cerebral microcirculation: Comment. Anesthesiology 2022; 136:867–8
2. Koch KU, Mikkelsen IK, Espelund US, Angleys H, Tietze A, Oettingen GV, Juul N, Østergaard L, Rasmussen M: Cerebral macro- and microcirculation during ephedrine versus phenylephrine treatment in anesthetized brain tumor patients: A randomized clinical trial using magnetic resonance imaging. Anesthesiology 2021; 135:788–803
3. Bombardieri AM, Singh NP, Yaeger L, Athiraman U, Tsui BCH, Singh PM: The regional cerebral oxygen saturation effect of inotropes/vasopressors administered to treat intraoperative hypotension: A Bayesian network meta-analysis. J Neurosurg Anesthesiol 2021 [Epub ahead of print]
4. Koch KU, Zhao X, Mikkelsen IK, Espelund US, Aanerud J, Rasmussen M, Meng L: Correlation between cerebral tissue oxygen saturation and oxygen extraction fraction during anesthesia: Monitoring cerebral metabolic demand-supply balance during vasopressor administration. J Neurosurg Anesthesiol 2021 [Epub ahead of print]

(Accepted for publication January 20, 2022. Published online first on February 14, 2022.)

Recent U.S. Food and Drug Administration Labeling Changes for Hydroxyethyl Starch Products Due to Concerns about Mortality, Kidney Injury, and Excess Bleeding

To the Editor:

The U.S. Food and Drug Administration (Silver Spring, Maryland) is requiring safety labeling changes to the

prescribing information for hydroxyethyl starch products to warn about the risk of mortality, acute kidney injury (AKI), and coagulopathy in all patient populations. The changes contraindicate use of hydroxyethyl starch products for treatment of hypovolemia unless adequate alternative treatment is unavailable and update the Boxed Warning, Indications and Usage, Warnings and Precautions, and Adverse Reactions sections of the prescribing information to reflect new safety information (note: the indication for leukocytapheresis using Hespan [B. Braun Medical, Inc., USA] remains unchanged).

The Food and Drug Administration first mandated a safety labeling change for hydroxyethyl starch products in 2013. Changes made at that time included the addition of a Boxed Warning to the prescribing information and contraindications to their use in critically ill patients, including patients with sepsis. This action was prompted by publication of clinical studies, including randomized controlled trials, which showed that infusion of hydroxyethyl starch products increased mortality, AKI, and coagulopathy in the intensive care unit population. An increasing number of studies published subsequently have shown a similar safety risk profile in the surgery and blunt trauma populations.

In early 2017, the Food and Drug Administration received a citizen petition from the watchdog organization Public Citizen (Washington, D.C.) requesting that hydroxyethyl starch products be removed from the market. Public Citizen argued that all patient populations were at risk from hydroxyethyl starch products and that safer alternative resuscitation fluids were widely available.

The Food and Drug Administration assembled an internal, multidisciplinary review team to evaluate the available scientific literature, with special attention directed at clinical studies performed in surgery and trauma patients published after 2012. Prespecified clinical and statistical criteria were used to assess whether each study was "informative" or "less informative" for the purposes of addressing this issue.

A statistical threshold of $P < 0.05$, usually reserved for evaluating efficacy, was prespecified to define hydroxyethyl starch safety signals (*i.e.*, an adverse event possibly or definitely related to product administration). "Informative" studies were defined as those that (1) found a statistically significant (lower bound of the 95% CI ≥ 1.0) change in the relative risk of one or more clinical safety signals associated with hydroxyethyl starch products—death, AKI including need for renal replacement therapy, and coagulopathy; and (2) did not have major methodologic limitations. "Less informative" studies were defined as those that either (1) failed to find a statistically significant change in the incidence of one or more clinical safety signals described above or (2) were determined to have major methodologic limitations.

Failure to achieve statistical significance for an hydroxyethyl starch–associated safety signal was often due to weaknesses in study design or execution. These included a study size too small to detect a safety signal had one been present (*i.e.*, inadequate power); inappropriately low control event rates; limited exposure to the product; presence of heterogeneity (I^2) that could confound the analysis (*e.g.*, data from elective surgery and critically ill surgery patients enrolled in the same study without a prespecified subgroup analysis); a comparator whose safety profile overlapped with that of the hydroxyethyl starch product under review (*e.g.*, a different hydroxyethyl starch product); changes in comparator/adjunctive therapy once the study already had begun; an incomplete description of the randomization and allocation concealment procedure, where applicable; and short duration of follow-up (typically 7 to 10 days). Less informative studies did not permit the Food and Drug Administration to draw any conclusions about product safety.

Of 37 post-2012 studies identified by the Food and Drug Administration review team, 10 were classified as informative. Results of these studies provided the basis for requiring the labeling changes.

1. In a meta-analysis of 15 randomized controlled trials and 6 observational studies in patients undergoing elective surgery, hydroxyethyl starch was associated with increased risk of mortality and AKI. The study populations included both noncardiac surgery (hepatic, renal transplant, vascular, thoracic, gastrointestinal) and cardiac surgery in association with cardiopulmonary bypass.[1–7]
2. In two observational trauma studies, hydroxyethyl starch was associated with increased mortality and AKI in patients with blunt[8,9] (but not penetrating) trauma.
3. In a randomized controlled trial and an observational study among patients undergoing elective surgery, hydroxyethyl starch was associated with excess bleeding.[5,10]

In many cases, demonstration of a dose–response and/or temporal relationship between exposure to hydroxyethyl starch and excess risk provided additional support for implementing the labeling changes, which, along with additional information about the studies, were posted online at https://www.fda.gov/vaccines-blood-biologics/safety-availability-biologics/labeling-changes-mortality-kidney-injury-and-excess-bleeding-hydroxyethyl-starch-products on July 7, 2021.

Acknowledgments

The authors thank Salim Haddad, M.D., and Victor Baum, M.D. (U.S. Food and Drug Administration, Silver Spring, Maryland), for their suggestions and review of the manuscript.

Research Support

Support for this study was provided solely from institutional and/or departmental sources.

Competing Interests

The authors declare no competing interests. This free-standing letter is an informal communication that reflects the views of the authors. It should not be construed to represent U.S. Food and Drug Administration (Silver Spring, Maryland) views or policies.

Laurence Landow, M.D., Shaokui Wei, M.D., M.P.H., Linye Song, Ph.D., Ravi Goud, M.D., Katherine Cooper, J.D.
U.S. Food and Drug Administration, Silver Spring, Maryland (L.L.). laurence.landow@fda.hhs.gov

DOI: 10.1097/ALN.0000000000004164

References

1. Wilkes MM, Navickis RJ: Postoperative renal replacement therapy after hydroxyethyl starch infusion: A meta-analysis of randomized trials. Neth J Crit Care 2014; 18:4–9
2. Green RS, Butler MB, Hicks SD, Erdogan M: Effect of hydroxyethyl starch on outcomes in high-risk vascular surgery patients: A retrospective analysis. J Cardiothorac Vasc Anesth 2016; 30:967–72
3. Ahn HJ, Kim JA, Lee AR, Yang M, Jung HJ, Heo B: The risk of acute kidney injury from fluid restriction and hydroxyethyl starch in thoracic surgery. Anesth Analg 2016; 122:186–93
4. Kashy BK, Podolyak A, Makarova N, Dalton JE, Sessler DI, Kurz A: Effect of hydroxyethyl starch on postoperative kidney function in patients having noncardiac surgery. Anesthesiology 2014; 121:730–9
5. Lagny MG, Roediger L, Koch JN, Dubois F, Senard M, Donneau AF, Hubert MB, Hans GA: Hydroxyethyl starch 130/0.4 and the risk of acute kidney injury after cardiopulmonary bypass: A single-center retrospective study. J Cardiothorac Vasc Anesth 2016; 30:869–75
6. Patel MS, Niemann CU, Sally MB, De La Cruz S, Zatarain J, Ewing T, Crutchfield M, Enestvedt CK, Malinoski DJ: The impact of hydroxyethyl starch use in deceased organ donors on the development of delayed graft function in kidney transplant recipients: A propensity-adjusted analysis. Am J Transplant 2015; 15:2152–8
7. Bayer O, Schwarzkopf D, Doenst T, Cook D, Kabisch B, Schelenz C, Bauer M, Riedemann NC, Sakr Y, Kohl M, Reinhart K, Hartog CS: Perioperative fluid therapy with tetrastarch and gelatin in cardiac surgery–A prospective sequential analysis. Crit Care Med 2013; 41:2532–42
8. Allen CJ, Valle EJ, Jouria JM, Schulman CI, Namias N, Livingstone AS, Proctor KG: Differences between blunt and penetrating trauma after resuscitation with hydroxyethyl starch. J Trauma Acute Care Surg 2014; 77:859–64; discussion 864
9. Eriksson M, Brattström O, Mårtensson J, Larsson E, Oldner A: Acute kidney injury following severe trauma: Risk factors and long-term outcome. J Trauma Acute Care Surg 2015; 79:407–12
10. Rasmussen KC, Johansson PI, Højskov M, Kridina I, Kistorp T, Thind P, Nielsen HB, Ruhnau B, Pedersen T, Secher NH: Hydroxyethyl starch reduces coagulation competence and increases blood loss during major surgery: Results from a randomized controlled trial. Ann Surg 2014; 259:249–54

(Accepted for publication January 14, 2022. Published online first on March 8, 2022.)

Smith's Anesthesia for Infants and Children, 10th Edition

Edited by Peter J. Davis, M.D., and Franklyn P. Cladis, M.D., F.A.A.P. Philadelphia, Elsevier, 2022. Pages: 1,561. ISBN-13: 978-0323698252. Price: $259.99 (Hardcover with accompanying eBook; Elsevier); $215.99 (Hardcover with accompanying eBook; Amazon); $207.99 (eBook only; Elsevier).

Smith's Anesthesia for Infants and Children is regarded by many as one of the classic textbooks of pediatric anesthesia. Dr. Robert M. Smith, a distinguished clinician and scholar and former Chief of Anesthesia at the Children's Hospital in Boston, wrote the first edition of the book in 1959. From a modest 400-page text, the 10th edition of this classic has grown into a 1,500-page multiplatform reference with 156 contributors. Lead editors Peter J. Davis and Franklyn P. Cladis have done remarkable work in preserving Dr. Smith's vision. This edition is truly an homage to his legacy.

In this age of instant information, the role of traditional textbooks is often contested. However, reference texts can remain eminent and relevant if they continuously innovate to changing technology and learning styles. The new 10th edition of *Smith's Anesthesia for Infants and Children* is timely, up-to-date, and ingenious, coming just 4 yr after the last edition. An enhanced eBook version is included with the purchase of the hardcover. The eBook can also be purchased without the printed version through the Elsevier Expert Consult Inkling Platform.

The 10th edition carries over the basic structure from the previous edition. Content is better organized than ever before and divided into eight main parts. Pain management gets its own well-deserved updated section. The chapter on regional anesthesia has been expanded with new graphics. The last section of the book brings together special topics like medical ethics and patient safety. The section on the history of pediatric anesthesia is enlightening and gratifying.

The book adopts a conventional and instructive approach to presenting information. The first two parts are dedicated exclusively to comparative anatomy and physiology, behavioral development, fluid management, and clinical pharmacology. The material presented is detailed and refined. Basic science topics can come across as dull and unexciting to read, but I don't see them as redundant. The authors have made an earnest effort to highlight differences vis-à-vis adults based on available evidence. The chapter on thermoregulation is both concise and relatable to clinical practice. Similarly, the chapter on behavioral development includes a plethora of graphics and photos highlighting growth and developmental metrics. It was refreshing to see updated chapters on inhalation anesthetics, opioids, and muscle relaxants. Commentary on newer drugs like sugammadex is adequate and clinically pertinent.

Airway management is a fundamental aspect of anesthesia. A dedicated chapter on normal and difficult pediatric airway management is a welcome addition. Clinical aspects of normal airway management were conspicuous by their absence in previous editions. The information was dispersed across various sections of the book and not easy to collate. The new chapter is well written and covers the most essential elements. Video laryngoscopy gets its due place under management techniques.

Contemporary practice of pediatric anesthesia demands in-depth knowledge of neonatal medicine and pediatric critical care. Pediatric anesthesiologists routinely find themselves tasked with providing anesthetic care to smaller and younger neonates. The editors appreciate this knowledge gap and have rightfully dedicated almost 100 pages of this textbook to comprehensive understanding of neonatology for anesthesiologists. One of the positive changes I noticed in this edition is an attempt to incorporate topics that would generally have fallen under the domain of general pediatric medicine.

Parts V, VI, and VII of this textbook are dedicated to clinical management. Chapters in Part V are organized by surgical subspecialities, whereas Part VI is organized by organ systems and associated disorders. Part VII is dedicated to pediatric critical care for anesthesiologists. Pediatric cardiopulmonary resuscitation gets a comprehensive review. Pediatric anesthesiologists practicing in North America will relate quite easily to anesthetic management techniques and pearls described in Parts V, VI, and VII. I could find information on most pediatric surgical case scenarios likely to be encountered in primary and tertiary pediatric anesthesia practice. Most narratives are very detailed, giving useful practical guidance. As an example, the section on adenotonsillectomy and obstructive sleep apnea is impressive. In the same chapter, however, anesthetic management of choanal atresia is brief and may not provide sufficient instruction to a novice practitioner. Color information boxes summarizing perioperative management are informative. Perhaps practical perioperative management guidance standardized along the lines found in *Anesthesiologist's Manual of Surgical Procedures* (6th edition, edited by Jaffe R.A., Schmiesing C.A., Golianu B., Wolters Kluwer, 2020) can be considered in future editions. Having said that, reference textbooks such as Smith's are not intended to be

 Anesthesiology 2022; 136:871–2. DOI: 10.1097/ALN.0000000000004166

<zdoi;. DOI: 10.1097/ALN.0000000000004166>

a substitute for supervised hands-on clinical experience and mentoring.

The accompanying eBook version is available on the Elsevier Inkling multimedia platform. It is quite intuitive and easy to navigate. The interface is clean, simple, and visually appealing. Mobile and tablet versions of the app are available to download on iOS and Android platforms. The online accompanying video library is extensive, covering a wide range of topics. A sizeable percentage is dedicated to ultrasound-guided regional anesthesia techniques and congenital heart disease. It was illuminating to see new content added on practical aspects of pediatric anesthesia such as videos on airway management, sleep endoscopy, single-lung ventilation techniques, and video laryngoscopy. Like the previous edition, the eBook includes updated multiple-choice questions with answers and explanations. References used in the text are only available in the online version.

Like any other reference textbook, some chapters are better written than others. With more than 150 contributing authors, this is quite inevitable. Nonetheless, I feel that the 10th edition of this modern classic is a definitive step up from the previous edition. The text covers the subject matter in extraordinary depth and scale. Existing content has been logically reorganized and thoroughly revised. New chapters reflect new advances and improve on the deficiencies of past editions. The addition of new color graphics and imagery enhances the overall readability and presentation of the book. The lead authors show mature understanding of changing times, learning styles, and technology. The book will appeal to all categories of learners. For the advanced practitioner, the 10th edition of *Smith's Anesthesia for Infants and Children* provides a solid repository of up-to-date peer-reviewed subject matter, whereas the budding pediatric anesthesiologist will find this an invaluable and dependable reference covering all aspects of perioperative pediatric anesthesia practice.

Aman Kalra, M.D., Tufts Medical Center, Boston, Massachusetts. akalra1@tuftsmedicalcenter.org

(Accepted for publication February 2, 2022. Published online first on February 28, 2022.)

Pregnancy and Labor Epidural Effects on Gastric Emptying: A Prospective Comparative Study: Erratum

The gastric emptying rate referenced throughout the article is not a true "rate," but is rather a fraction. Accordingly, gastric emptying "rate" has been changed to gastric emptying "fraction" throughout the article.

The authors regret this error. The online version and PDF of the article have been corrected.

DOI: 10.1097/ALN.0000000000004190

Reference

Bouvet L, Schulz T, Piana F, Desgranges F-P, Chassard D: Pregnancy and labor epidural effects on gastric emptying: A prospective comparative study. ANESTHESIOLOGY 2022; 136:542–50

<zdoi;DOI:10.1097/ALN.0000000000004190>